Proceedings of CMS WORKSHOP

Cracking of massive concrete structures

March 17, 2015, ENS Cachan
Cachan, Île-de-France, FRANCE

ENS CACHAN

LMT CACHAN

Editors:
Eduardo FAIRBAIRN
Miguel AZENHA
Farid BENBOUDJEMA
Aveline DARQUENNES
Agnieszka KNOPPIK-WRÓBEL

ECOLE FRANCAISE DU BETON
www.efbeton.com

CMS Workshop

The workshop on „Cracking of massive concrete structures”, held on 17 March 2015 in Cachan, France, was organised by École normale supérieure de Cachan (ENS-Cachan), supported by Ecole Française du Béton. It was dedicated to the problems of early-age cracking in massive concrete structures.

The aim of the workshop was to establish an international forum of experts and promote discussion as well as exchange of knowledge in the domain of early-age behaviour of concrete structures.

Hereby we present the proceedings of the CMS Workshop.

Table of contents

Table of contents (c.d.)

CMS Workshop “Cracking of massive concrete structures”

March 17, 2015, ENS-Cachan

Cachan, Île-de-France, FRANCE

Case studies of massive concrete constructions: hydroelectric and nuclear power plants

Eduardo M. R. Fairbairn[1]

[1]COPPE/UFRJ – The Post-Graduate Institute of the Federal University of Rio de Janeiro

Methodologies

Thermo-chemo-mechanical model

Chemo-mechanical coupling

$$d\boldsymbol{\sigma} = \boldsymbol{C}(\xi):(d\boldsymbol{\varepsilon} - d\boldsymbol{\varepsilon}^p - d\boldsymbol{\varepsilon}^f - d\boldsymbol{\varepsilon}^v - \alpha(\xi)\boldsymbol{I}dT - \beta(\xi)\boldsymbol{I}d\xi)$$

$\boldsymbol{\sigma}$	– stress tensor
C(*x*)	– tensor of elastic properties(*n* Constante) **C**(x)=**C**(*E*(x))
$\boldsymbol{\varepsilon}$	– total strain tensor
$\boldsymbol{\varepsilon}^p$	– plastic strain tensor
$\boldsymbol{\varepsilon}^f$	– long-tern strain tensor
$\boldsymbol{\varepsilon}^v$	– short-term strain tensor
α(x)	– coefficient of thermal dilation
β(x)	– coefficient of autogenous shrinkage

Thermo-chemical coupling

$$c\gamma\dot{T} = L\dot{\xi} + k\nabla^2 T$$

c	– specific heat
γ	– density
L	– latent heat
k	– thermal conductivity

$$\dot{\xi} = \tilde{A}(\xi) exp\left(-\frac{E_a}{RT}\right)$$

$0<\xi<1$	– hydration degree
$\tilde{A}$	– normalized affinity
E_a	– activation energy
R	– universal gas constant
T	– temperature

Methodologies

Thermo-chemo-mechanical experimental facilities

Experimental framework

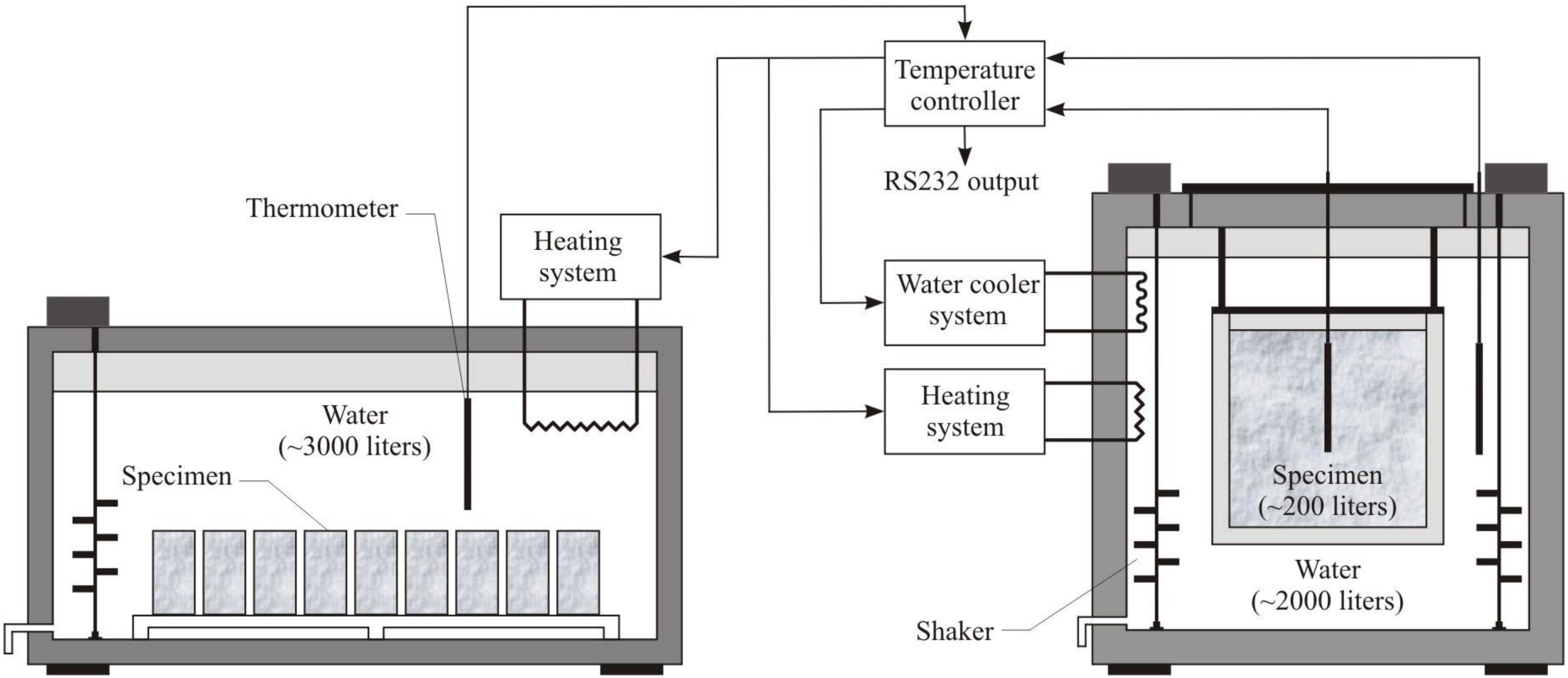

Materials and Structures Laboratory @ COPPE/UFRJ

Materials and Structures Laboratory @ COPPE/UFRJ

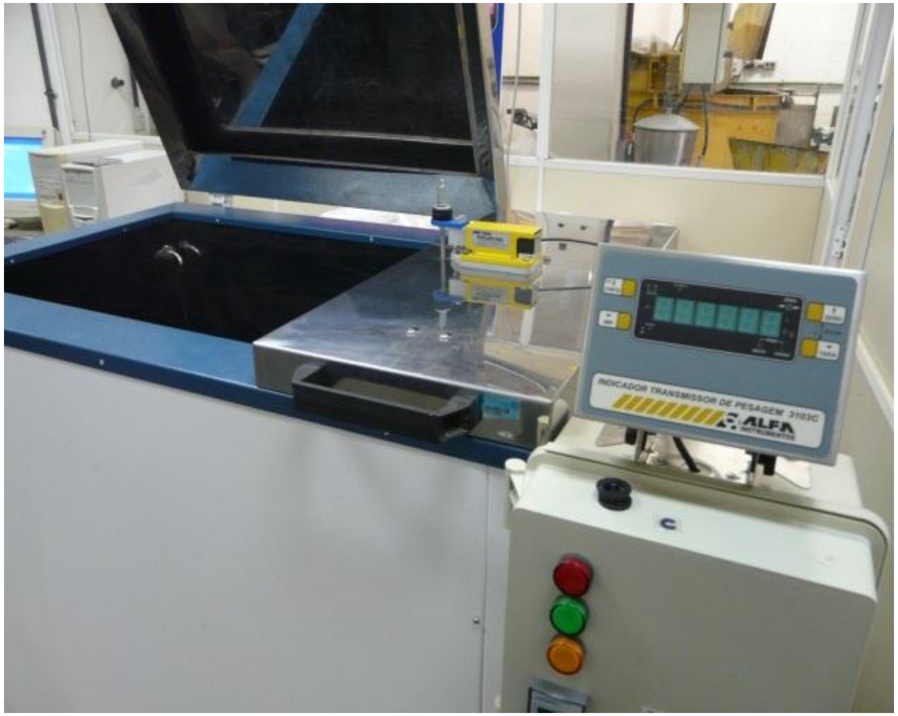

Materials and Structures Laboratory @ COPPE/UFRJ

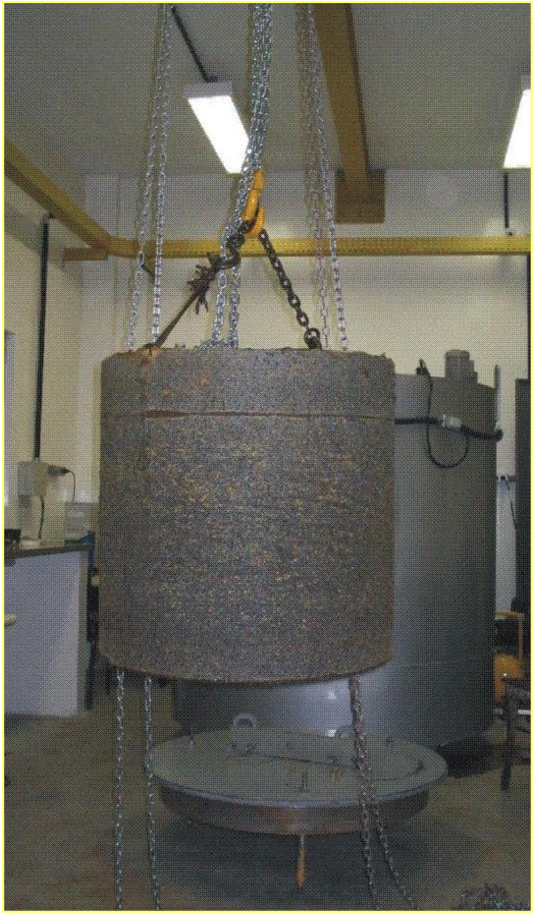

Materials and Structures Laboratory @ COPPE/UFRJ

Specific heat

Thermal diffusivity and thermal expansion coefficient

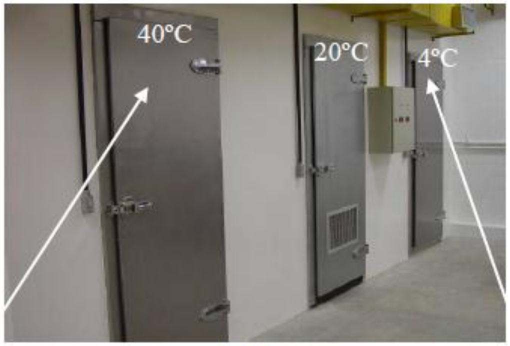

(a)

Materials and Structures Laboratory @ COPPE/UFRJ

Materials and Structures Laboratory @ COPPE/UFRJ

Materials and Structures Laboratory @ COPPE/UFRJ

Ambient temperature variation of 700°C

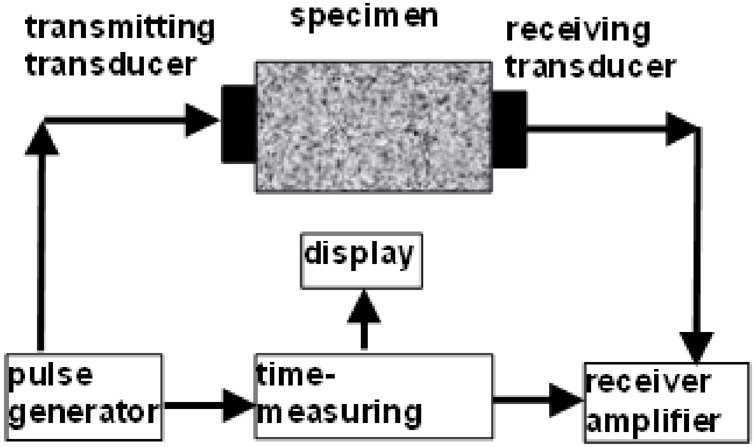

a) scheme

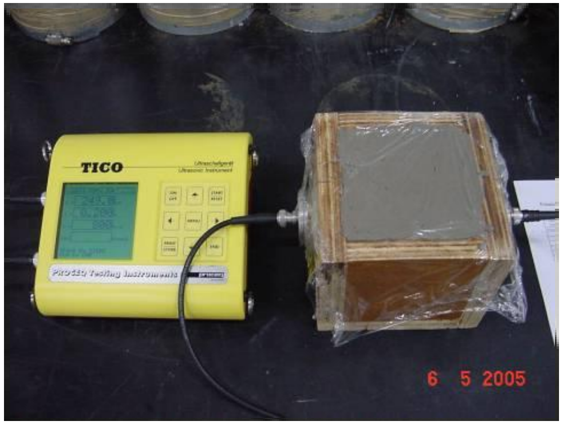

b) photograph

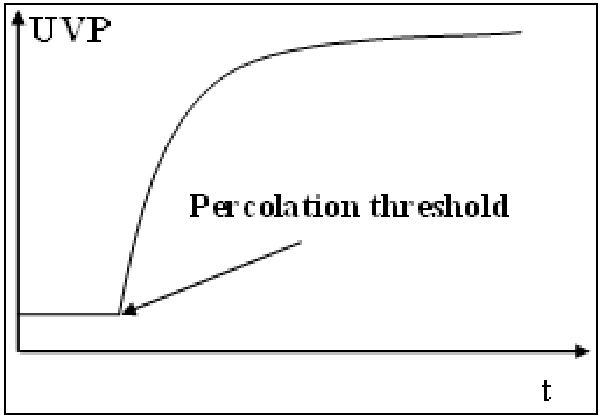

c)typical response

UVP device used to determine the percolation threshold ξ_0.

Methodologies

Data mining techniques

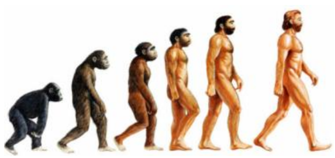

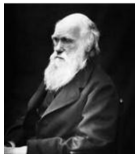

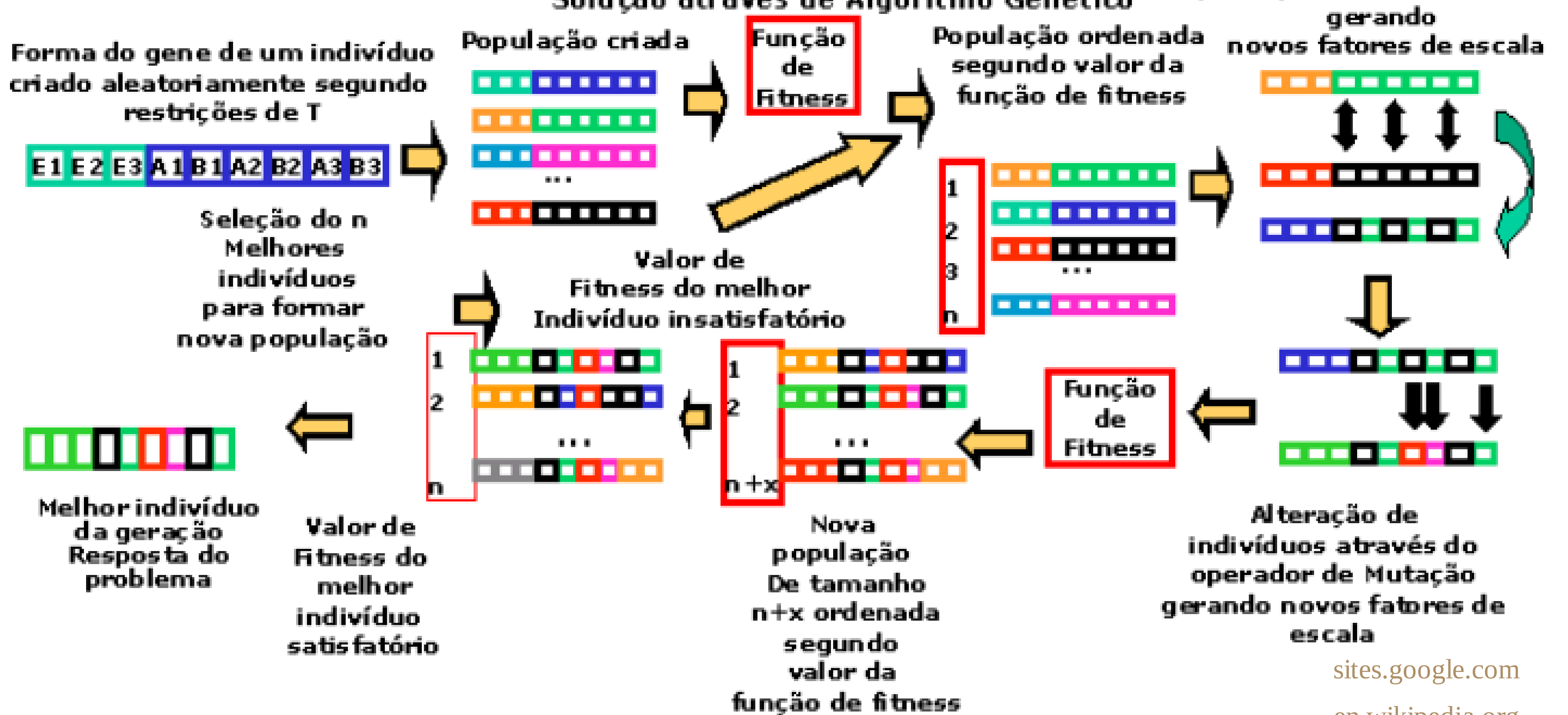

sites.google.com

en.wikipedia.org

https://linux.ime.usp.br

Esquema geral de um algoritmo genético

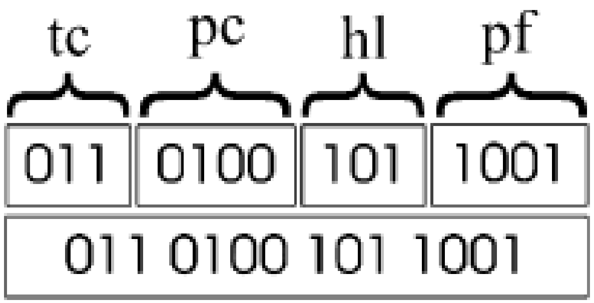

Binary representation of an individual: chromosome

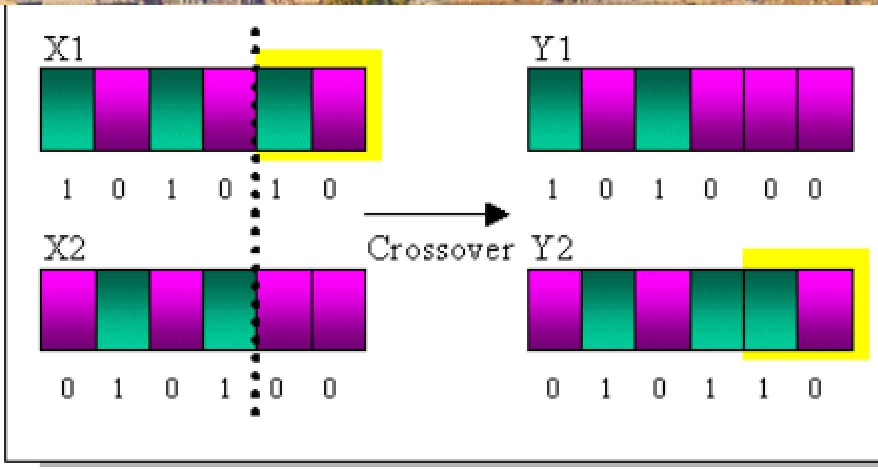

“crossover”

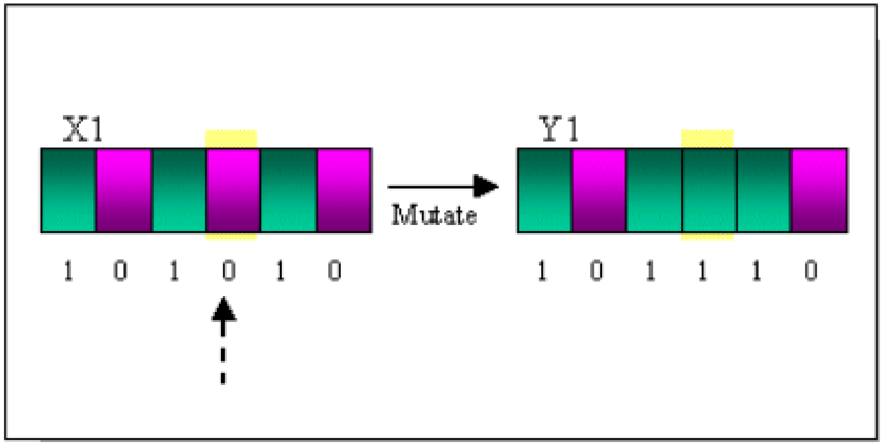

mutation

http://www.ewh.ieee.org/

E.M.R. Fairbairn et al. / Computers and Structures 82 (2004) 281–299

Methodologies

Computational implementation

- Parallel architecture.
- Computer code DAMTHE/COPPE allows the simulation of layered construction.

Cluster 32 dual nodes

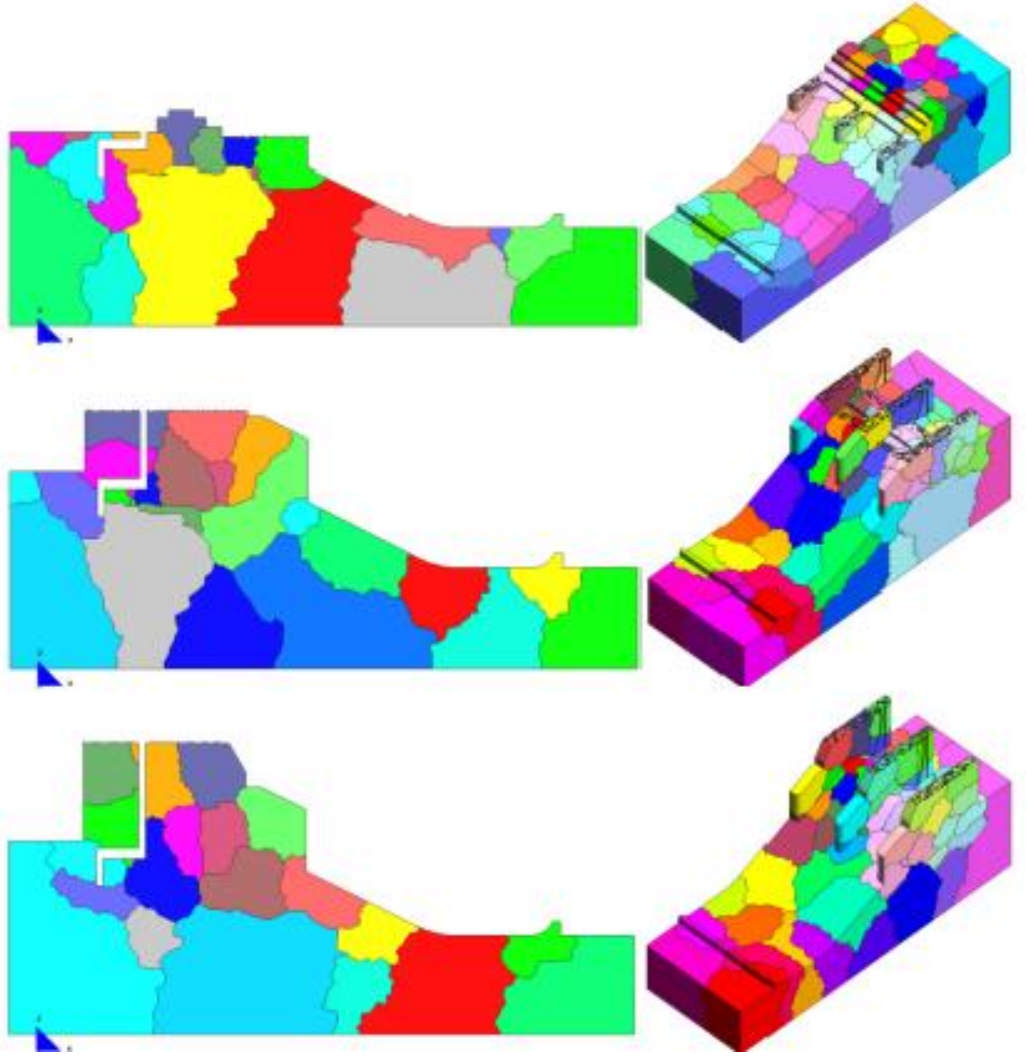

DAMTHE/COPPE: Dynamic partitioning of domains for parallel computing of layered construction

High speed-ups

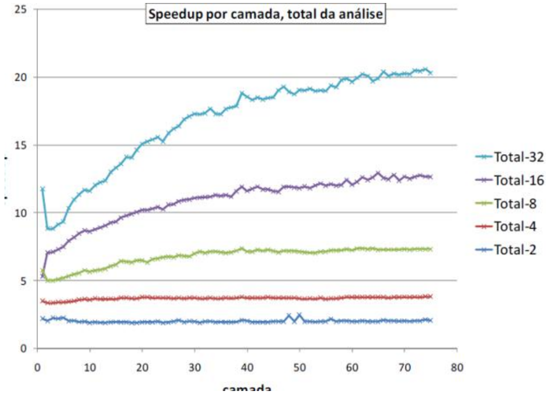

Case study 1 (academics)

Optimization of the construction of a small dam

GIVEN: the geometry of the structure

DETERMINE X^T = {*Hc, Fl, Tc, Tl)*} :

- The height of the lifts (*Hc*)
- The placing frequency (*Fl*)
- The type of concrete (*Tc*)
- The placing temnperature (*Tl*)

Minimizing :

- The cost C(*X*) = C(*Hc, Fl, Tc, Tl*)

Avoiding cracking : *ECr*(*X*) = *ECr*(*Hc, Fl, Tc, Tl*) = 0

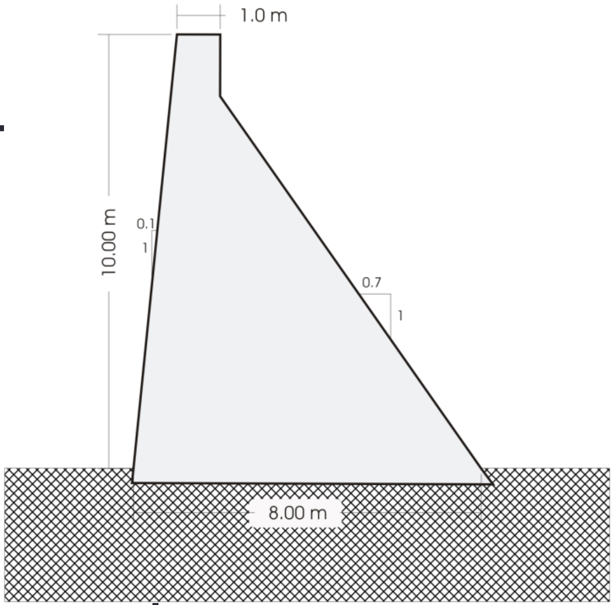

Optimization flowchart

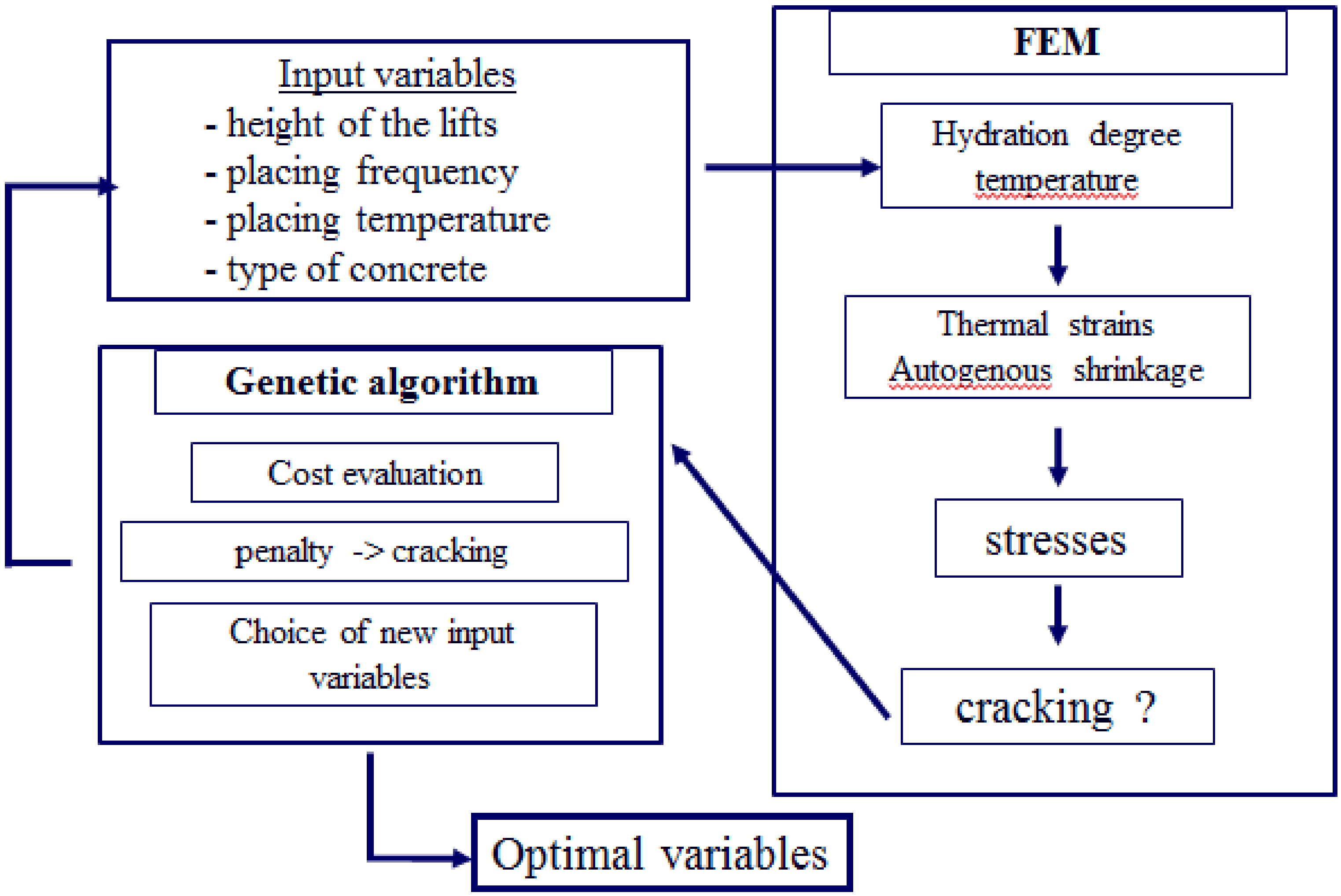

$$Custo_t/V_{Con,tot} = c_t = (c_{Fixo} + c_{comp}(Tc) + c_{RC}(Tl) + c_{Op}(Hc,Fl))$$

Normalized cost: $$\tilde{c}(X) = \frac{c_{comp}(Tc) + c_{RC}(Tl) + c_{Op}(Hc,Fl)}{c_{t,\max}}, \qquad \tilde{c}(X) \in [\tilde{c}_{\min}, 1]$$

Objective function: $$f(X) = \tilde{c}(X)$$

Fitness function: $$F(X,t) = f(X) + P(X,t_g)$$

Cracking extension: $$ECr = \frac{\sum_{iel=1}^{nplast} V_{iel}}{\sum_{iel=1}^{nel} V_{iel}} \; ; \; ECr \in [0,1]$$

Penalty:

$$P\left(ECr(X), t_g\right) = \begin{cases} 1-\tilde{c}_{min} & , se\ ECr(X) > ECr_{lim}(t_g) \\ ECr(X)\dfrac{1-\tilde{c}_{min}}{ECr_{lim}(t_g)} & , se\ ECr(X) \le ECr_{lim}(t_g) \end{cases}$$

$$ECr_{lim}(t_g) = \begin{cases} ECr_{lim,0} - t_g \dfrac{ECr_{lim,0}}{Ng/2} & , se\ 0 \le t \le Ng/2 \\ 0 & , se\ Ng/2 \le t_g \le Ng \end{cases}$$

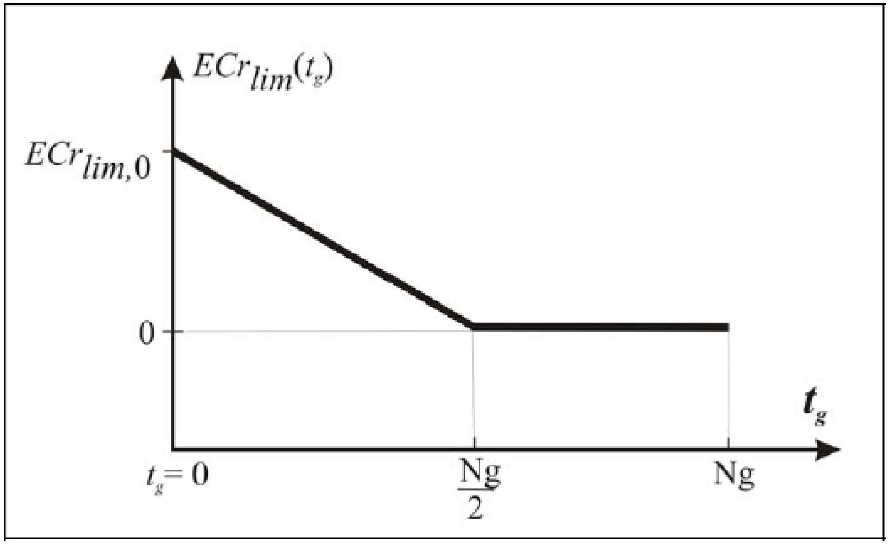

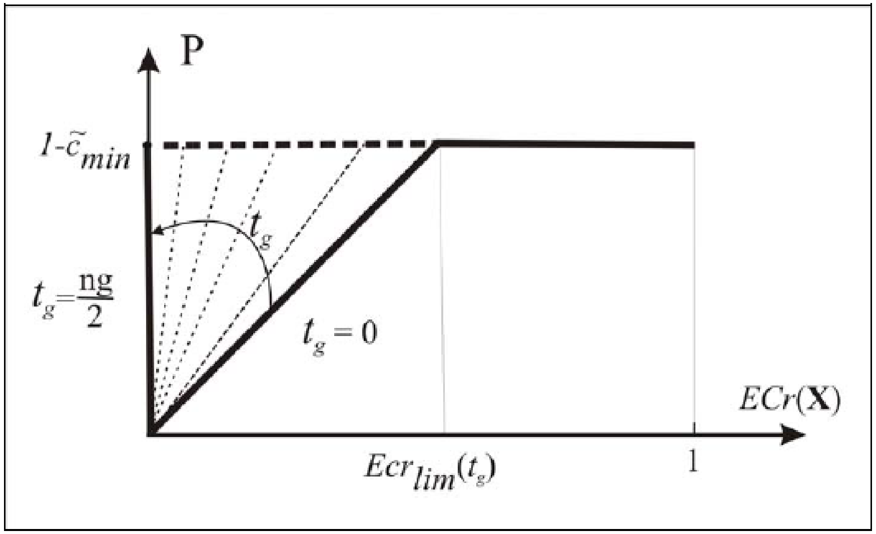

Fitness function

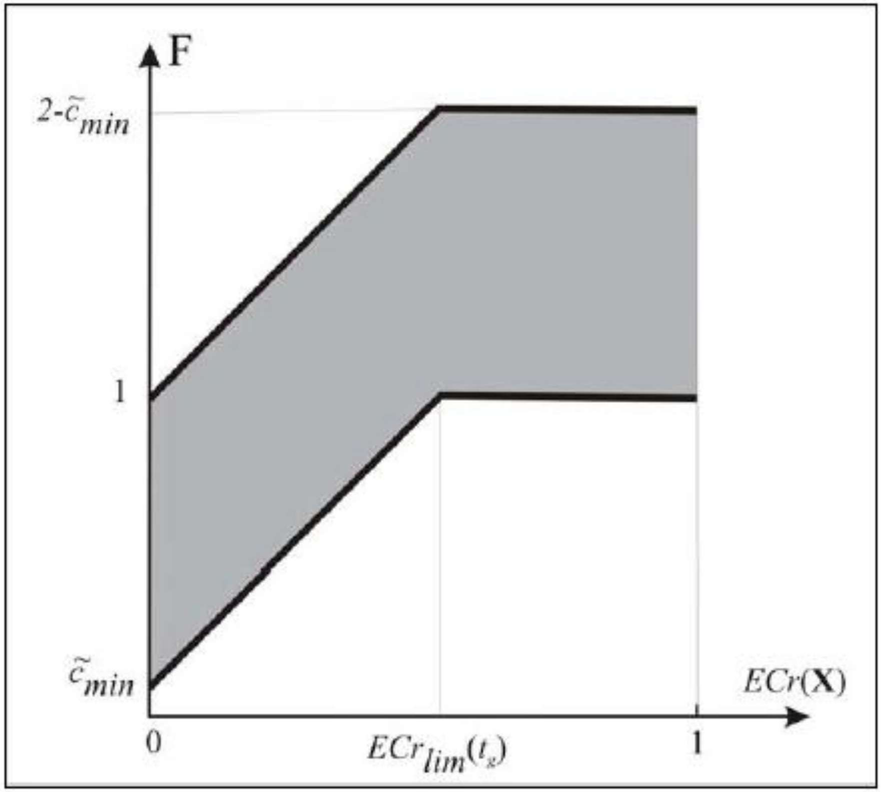

GA flowchart

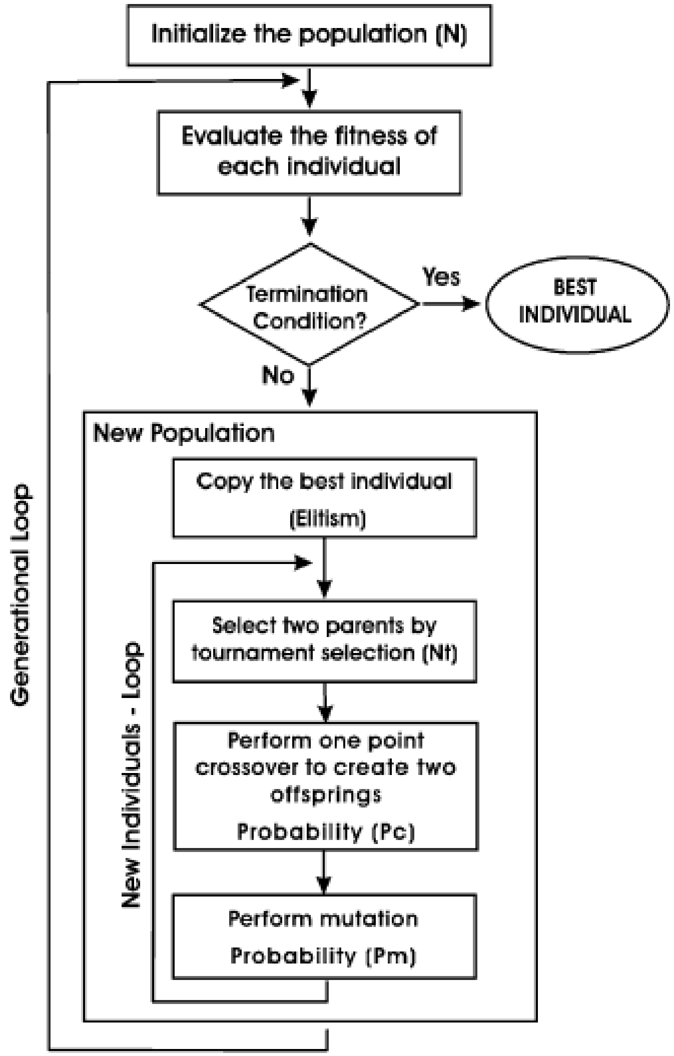

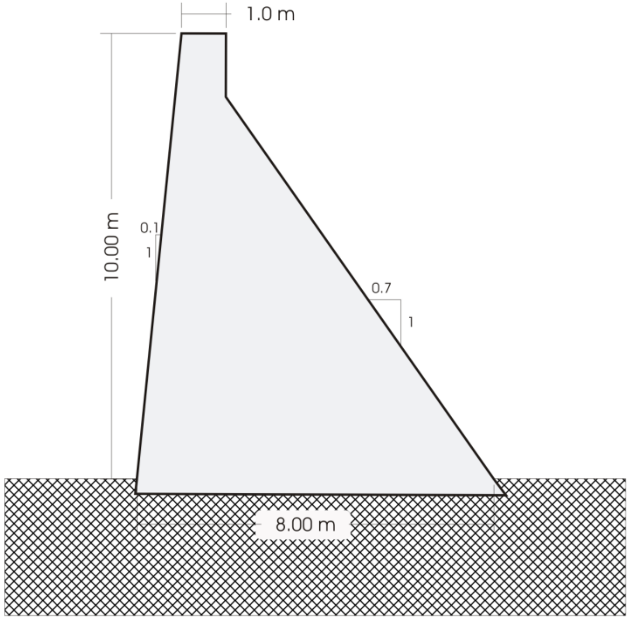

Geometry

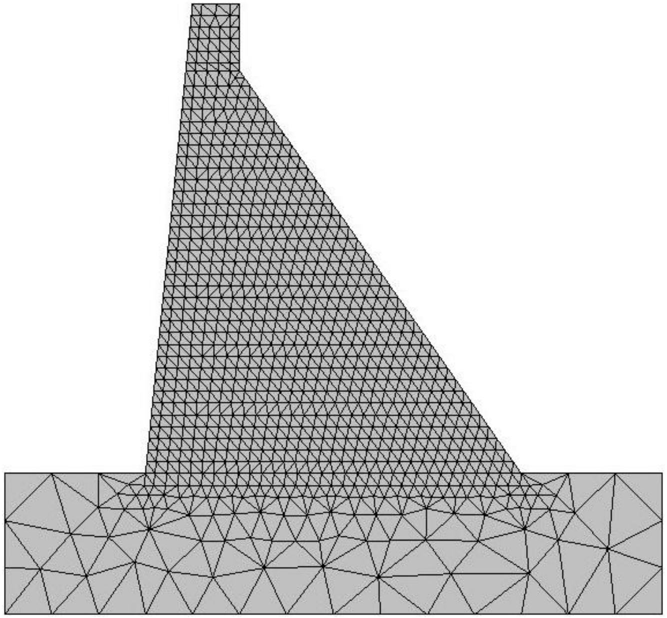

FE Mesh

$$Hc(\mathrm{m}) \in \{\ 0{,}50\ ;\ 0{,}75\ ;\ 1{,}0\ ;\ 1{,}25\ ;\ 1{,}50\ ;\ 1{,}75\ ;\ 2{,}00\ ;\ 2{,}5\ \}$$

$$Fl(\mathrm{dias}) \in \{\ 6\ ;\ 7\ ;\ 8\ ;\ \ldots\ ;\ 20\ ;\ 21\ \}$$

$$Tc \in \{\ 1\ ;\ 2\ ;\ 3\ ;\ 4\ ;\ 5\ ;\ 6\ ;\ 7\ ;\ 8\ \}$$ Concretes from FURNAS database

$$Tl(^{\circ}\mathrm{C}) \in \{\ 10\ ;\ 11\ ;\ \ldots\ ;\ 20\ ;\ 25\ \}$$

Costs

$Hc(\mathrm{m}) \in \{\ 0{,}50\ ;\ 0{,}75\ ;\ 1{,}0\ ;\ 1{,}25\ ;\ 1{,}50\ ;\ 1{,}75\ ;\ 2{,}00\ ;\ 2{,}5\ \}$

$Fl(\mathrm{dias}) \in \{\ 6\ ;\ 7\ ;\ 8\ ;\ \ldots\ ;\ 20\ ;\ 21\ \}$

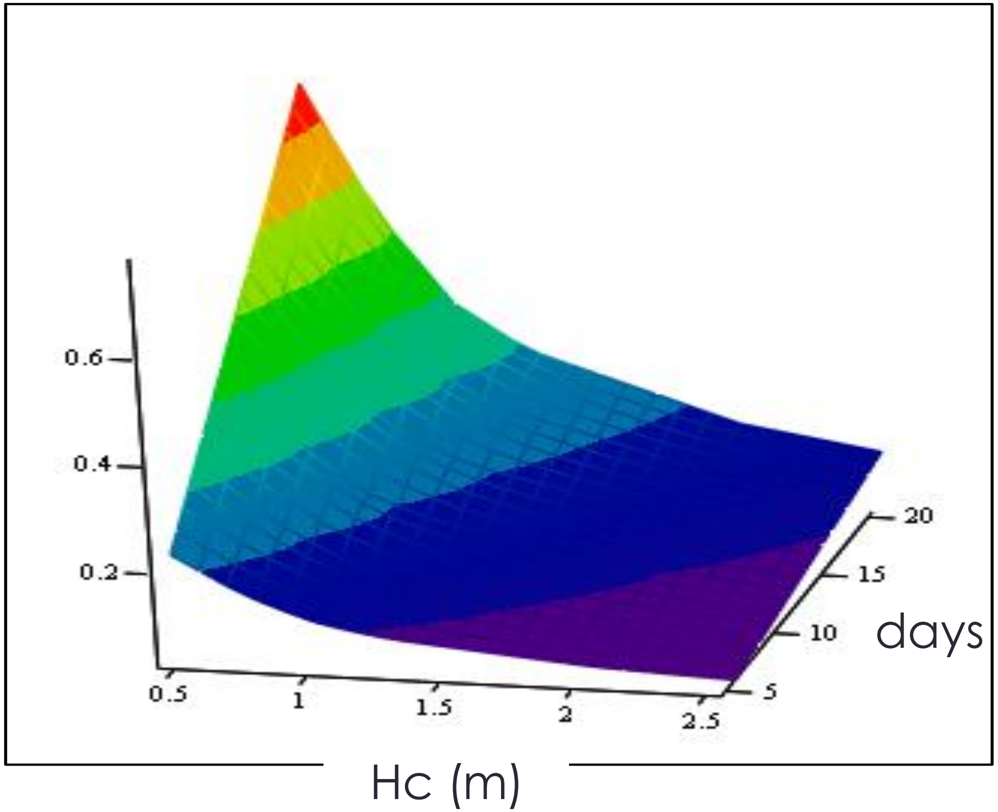

Tc	C_ε (J.kg/K)	k W/(m.K)	α (10^{-6})	$f_{c,\infty}$ (MPa)	E_∞ (MPa)	$\varepsilon^{RA,Max}$ (μs)*
1	1017	2,65	13,02	29,9	21,7	23,46
2	1109	2,64	10,78	28,9	30,6	21,09
3	1134	2,64	10,37	24,8	25,9	11,37
4	1084	2,64	10,62	30,2	26,0	24,17
5	1059	2,64	12,03	27,3	22,4	17,30
6	1092	2,24	9,93	23,9	23,2	10,05
7	1063	2,26	12,58	25,4	24,0	12,79
8	1050	2,49	12,09	25,2	17,1	12,32

Costs

$$Tc \in \{1;2;3;4;5;6;7;8\}$$

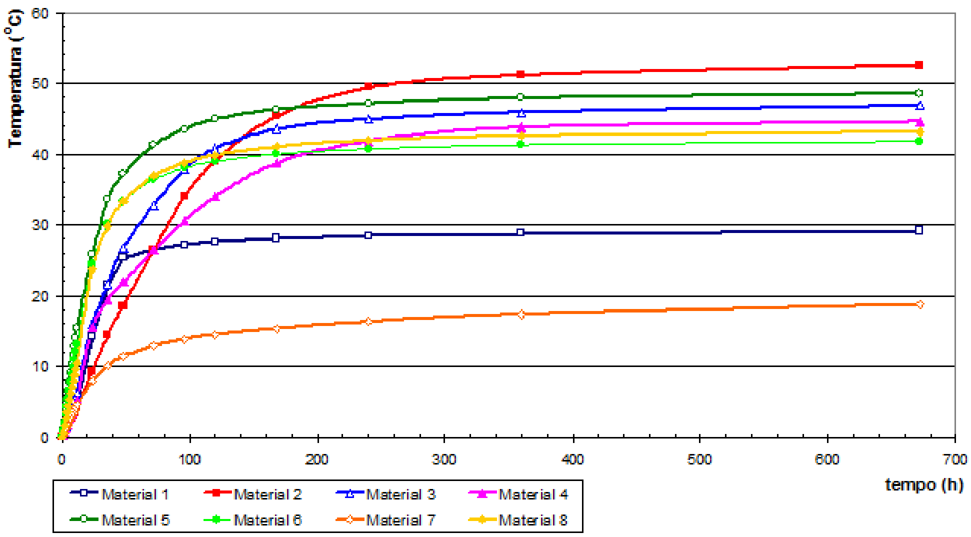

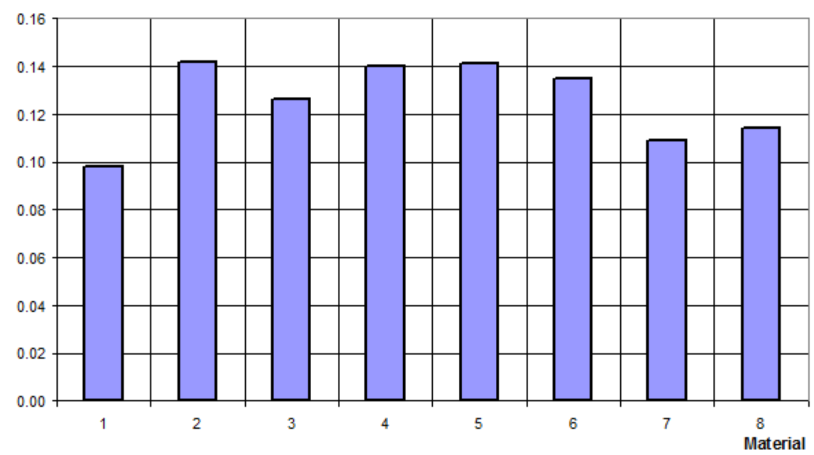

Costs

$Tl(^{o}C) \in \{\ 10\ ;\ 11\ ;\ ...\ ;\ 20\ ;\ 25\ \}$

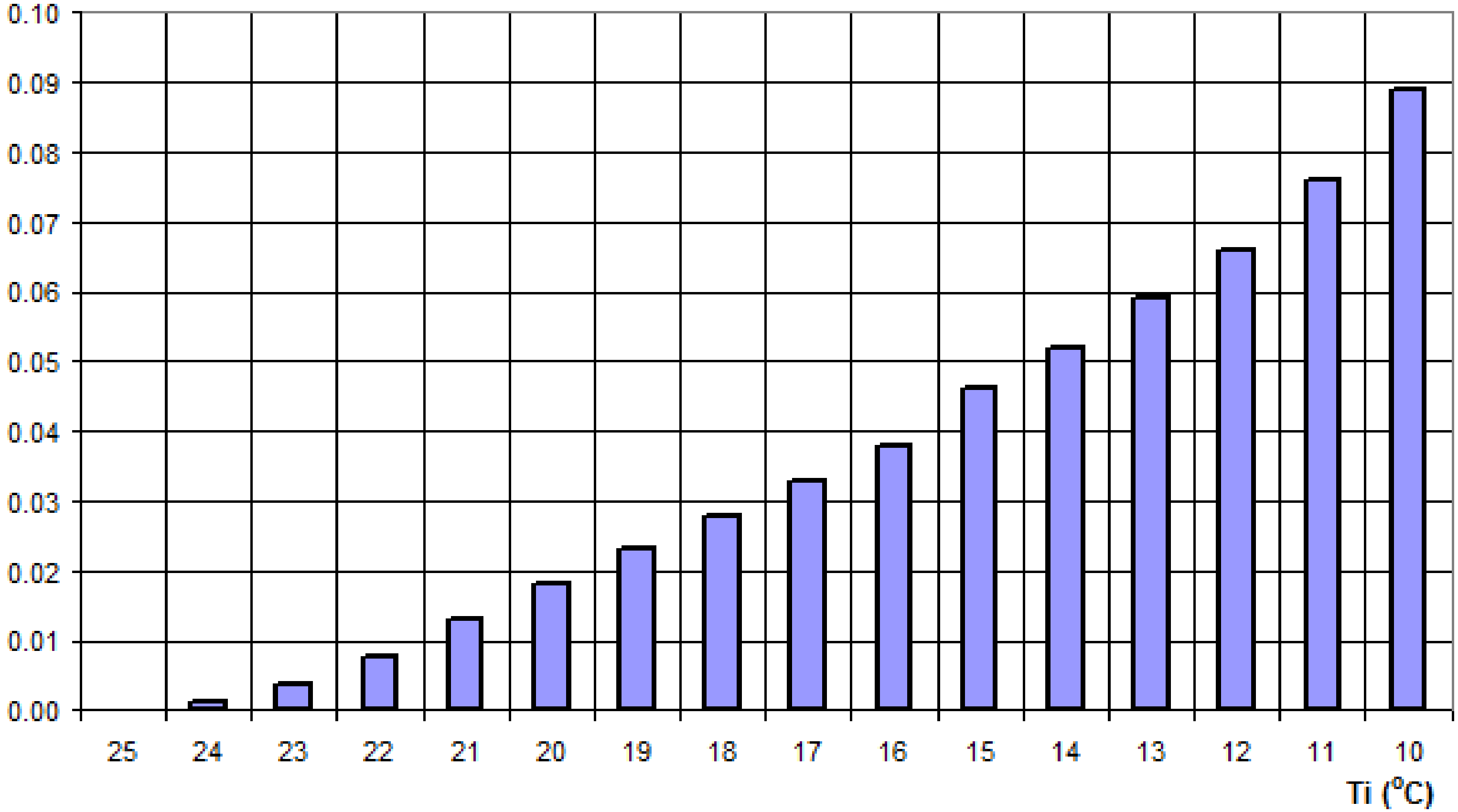

Evolution of the algorithm

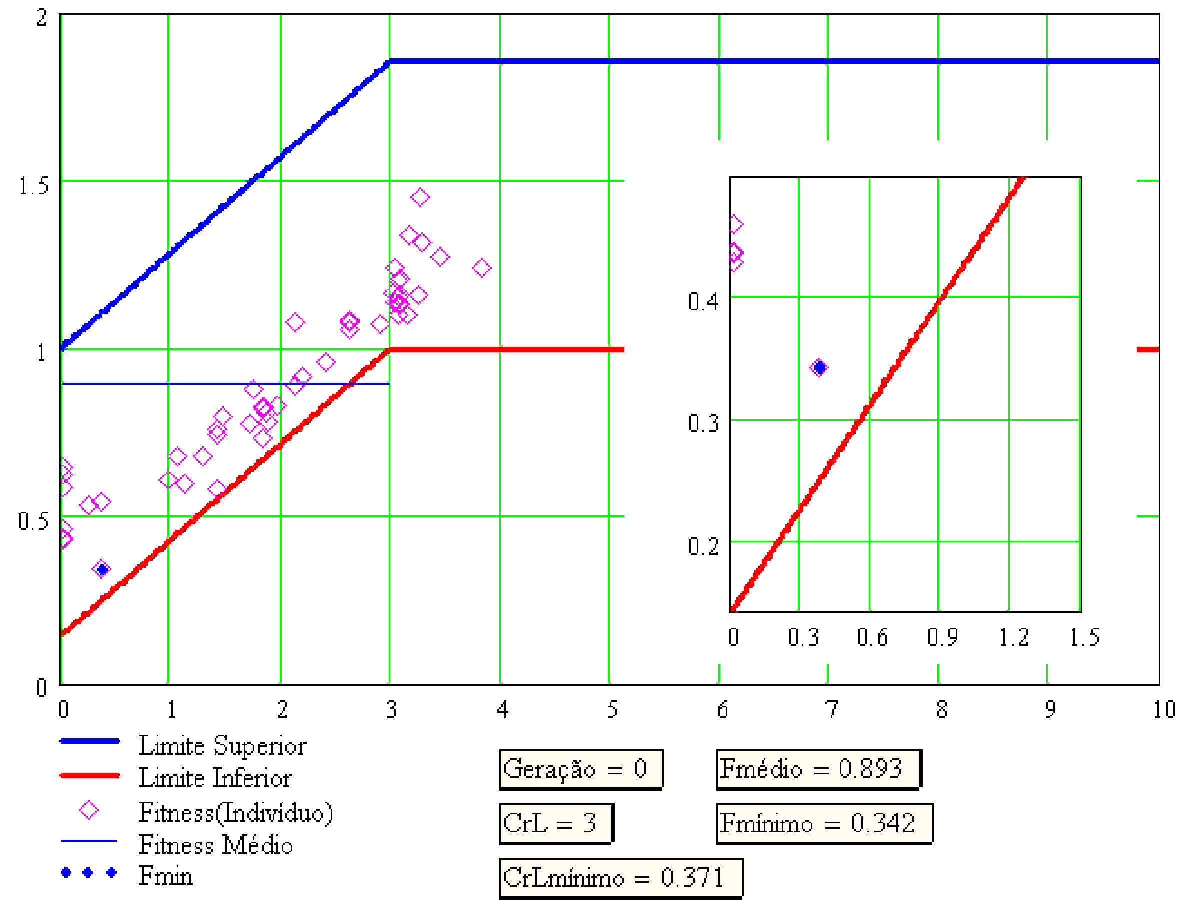

Optimum construction scheme

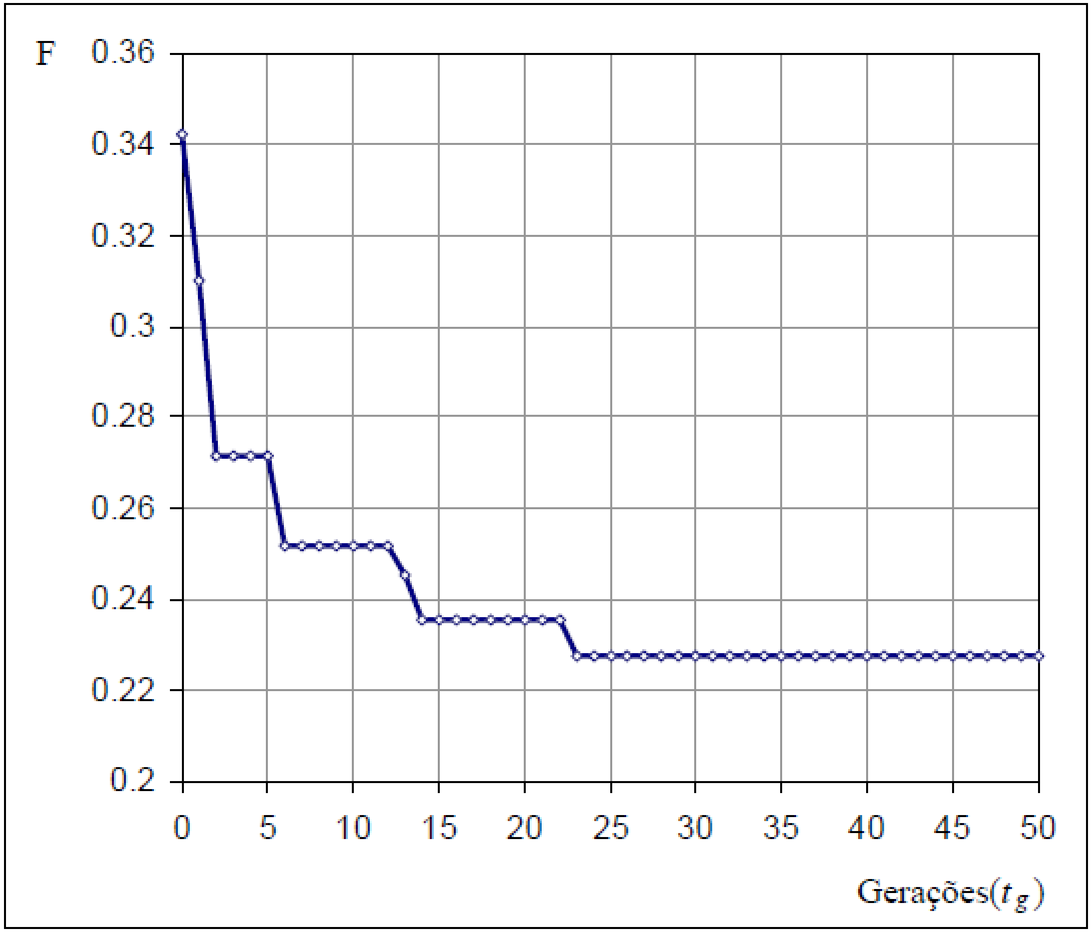

Optimal variables: {*Hc = 1,25m, Fl = 6 days, Tc = 8, Tl= 19°C*}

Optimal variables: **{***Hc = 1,25m, Fl = 6 days, Tc = 8, Tl= 19°C***}**

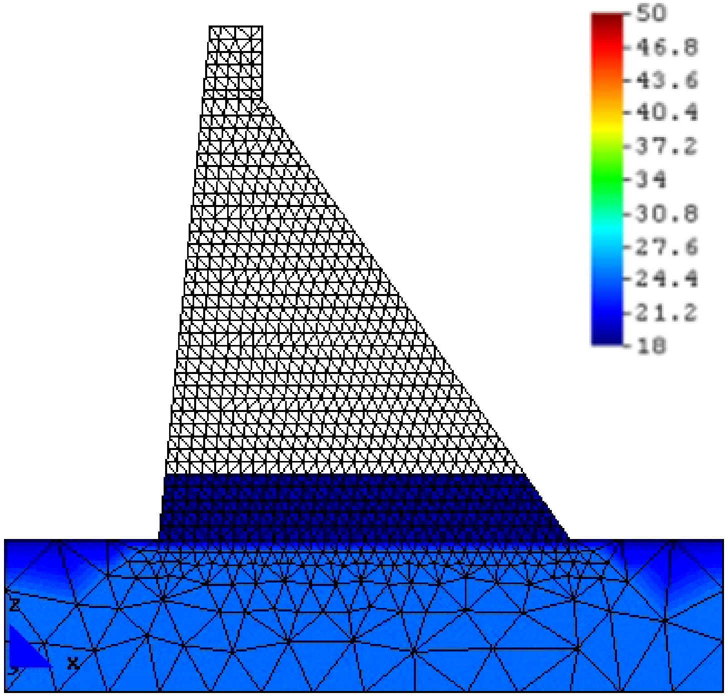

Temperatures (°C)

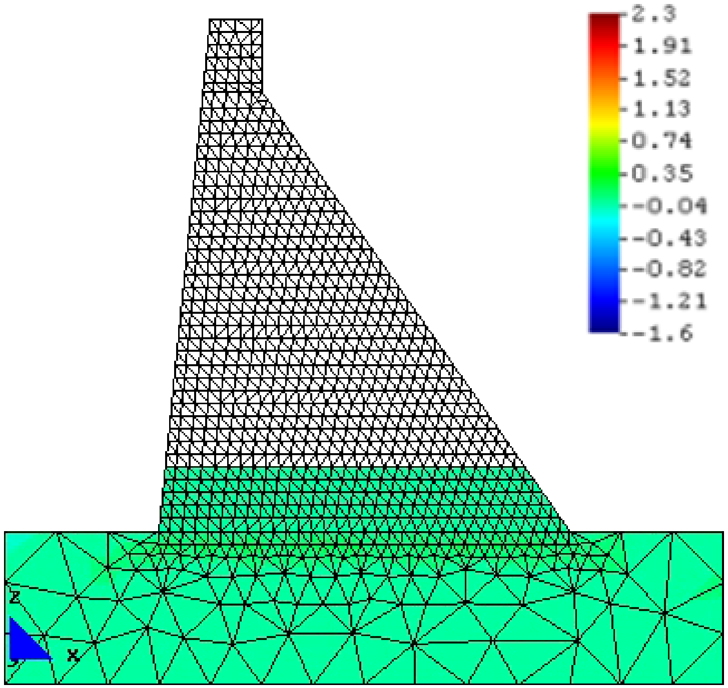

stresses σ_1 (MPa)

Case study 2
Tocoma dam Venezuela

Analysis of two construction schemes

Tocoma hydroelectric power plant

Tocoma hydroelectric power plant

Tocoma hydroelectric power plant: power house

Tocoma hydroelectric power plant: power house

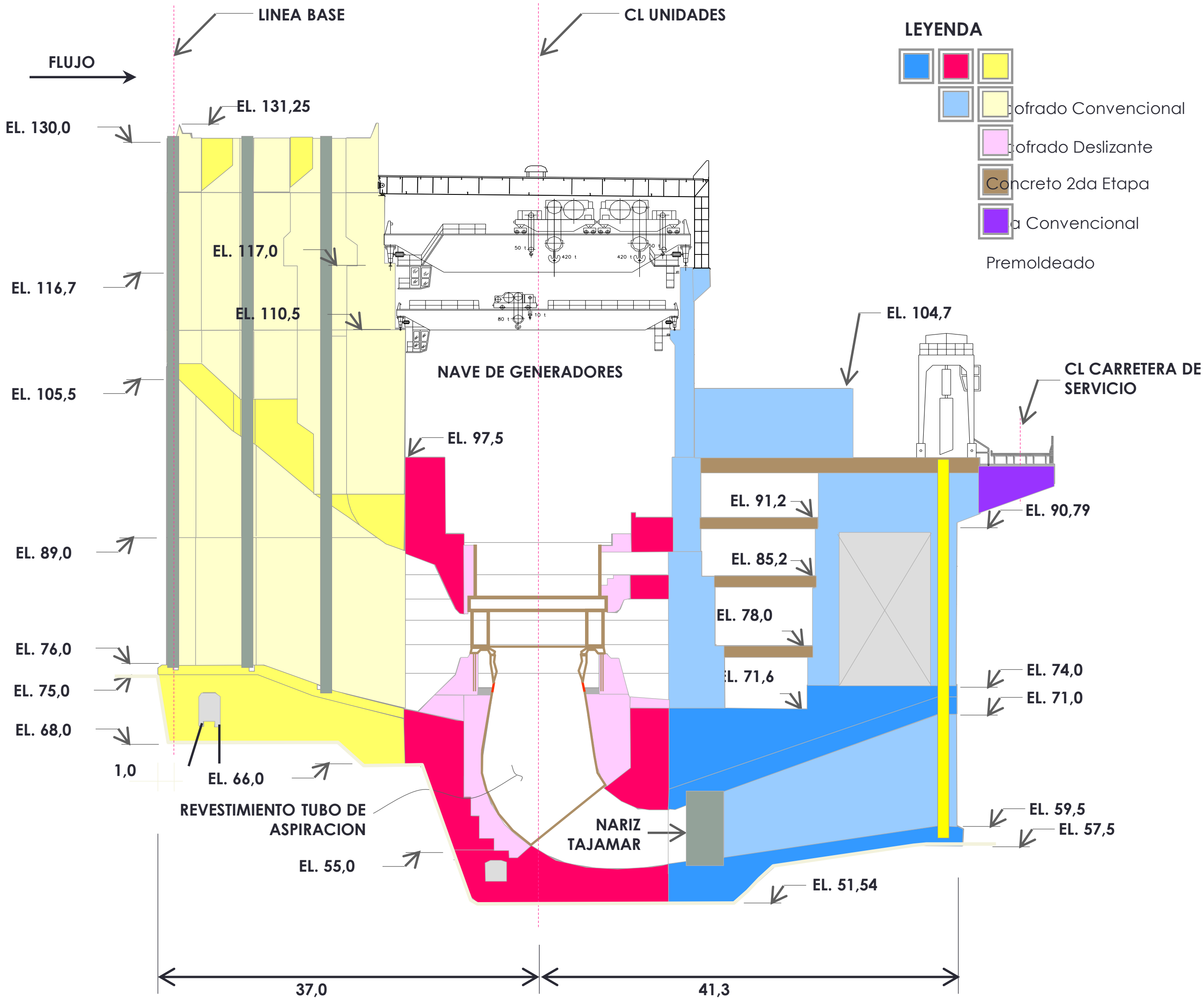
LINEA BASE
CL UNIDADES
LEYENDA
ofrado Convencional
ofrado Deslizante
Concreto 2da Etapa
a Convencional
Premoldeado
FLUJO
EL. 131,25
EL. 130,0
EL. 117,0
EL. 116,7
EL. 110,5
EL. 105,5
EL. 104,7
NAVE DE GENERADORES
CL CARRETERA DE SERVICIO
EL. 97,5
EL. 91,2
EL. 90,79
EL. 89,0
EL. 85,2
EL. 78,0
EL. 76,0
EL. 75,0
EL. 74,0
EL. 71,6
EL. 71,0
EL. 68,0
1,0
EL. 66,0
REVESTIMIENTO TUBO DE ASPIRACION
NARIZ TAJAMAR
EL. 59,5
EL. 57,5
EL. 55,0
EL. 51,54
37,0
41,3

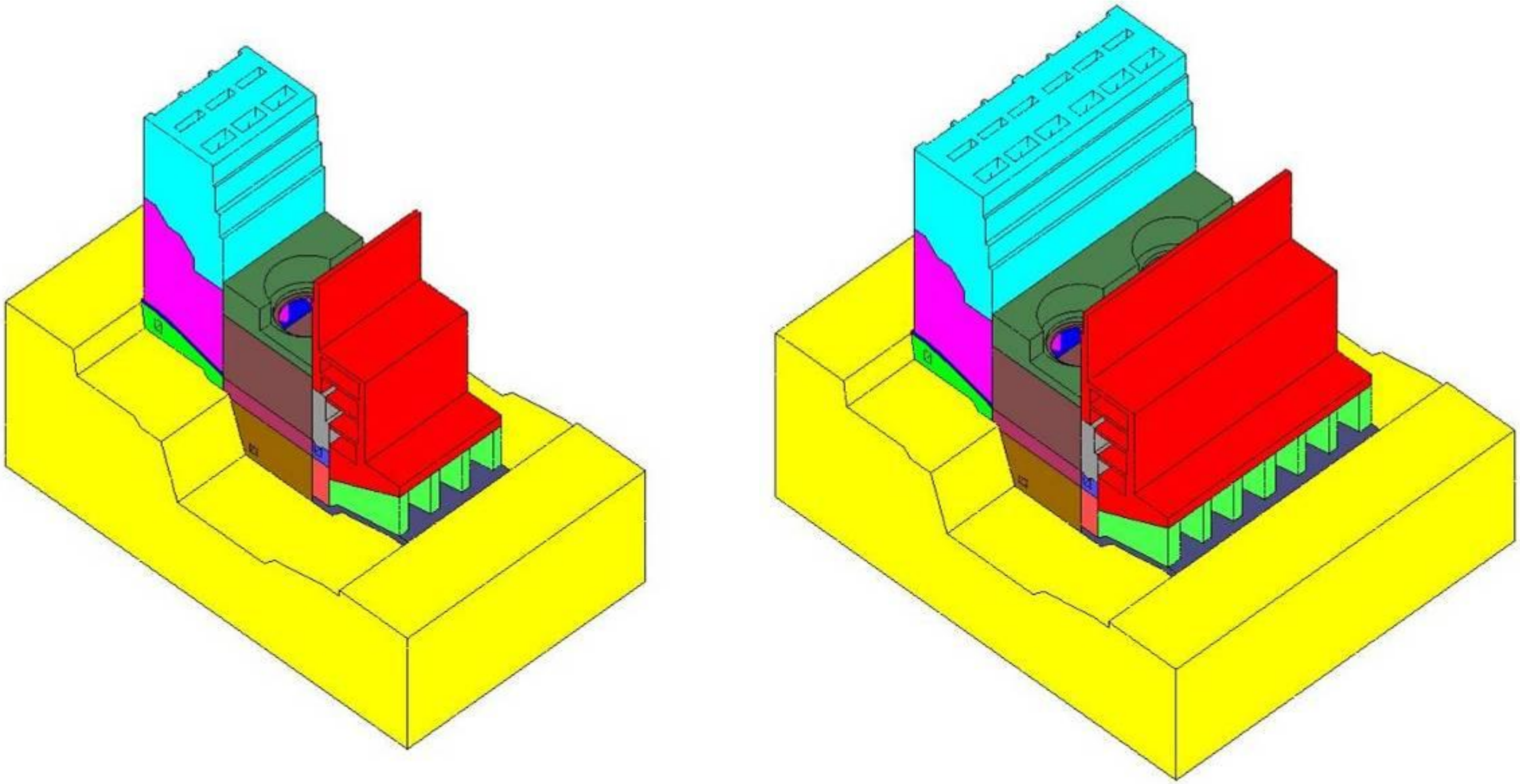

Study of two solutions

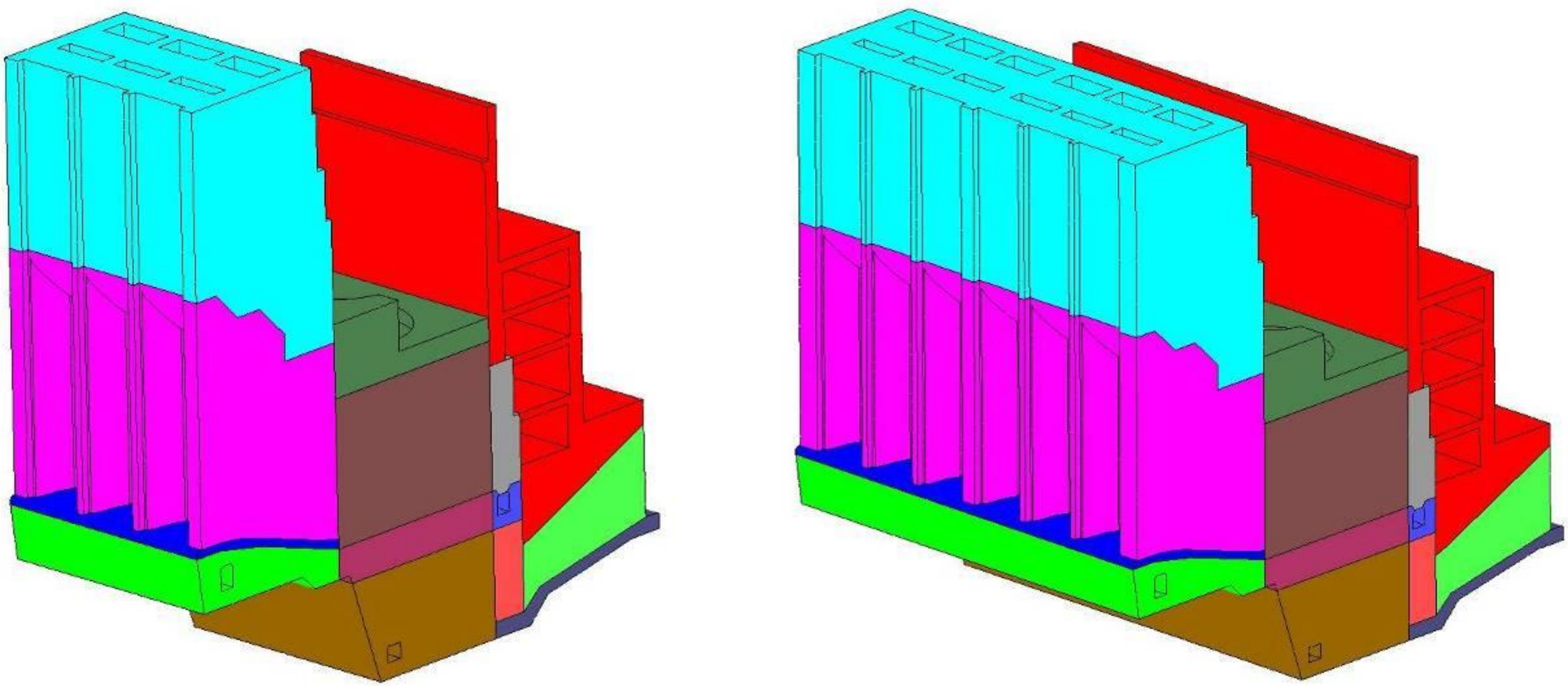

Study of two solutions

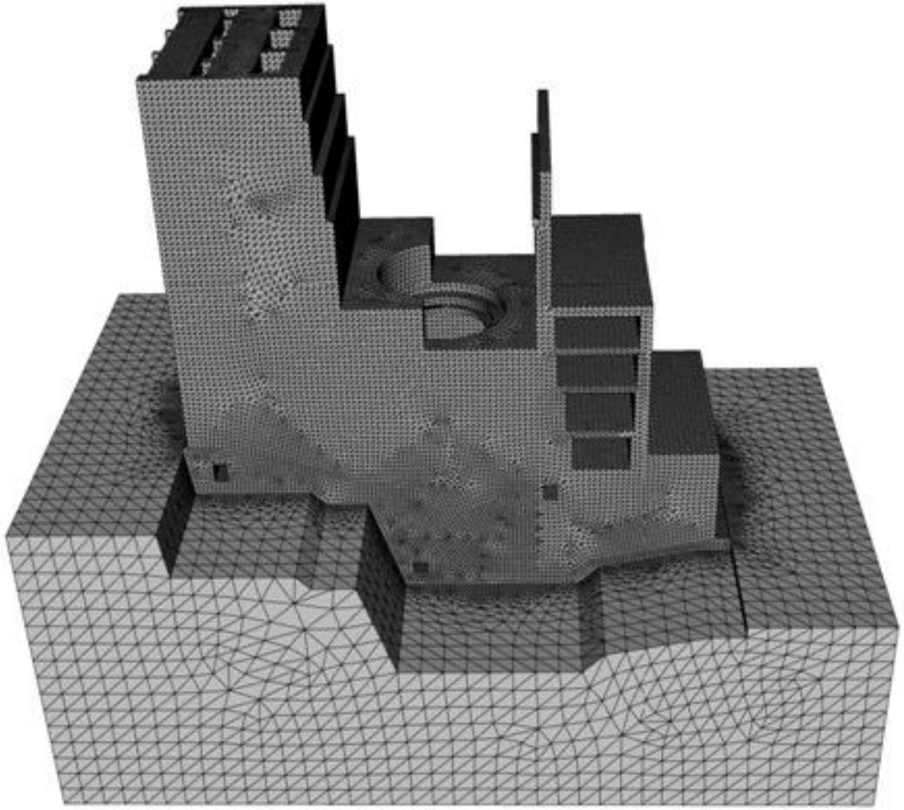

2.256.511 tetrahedral linear elements
419.262 nodes

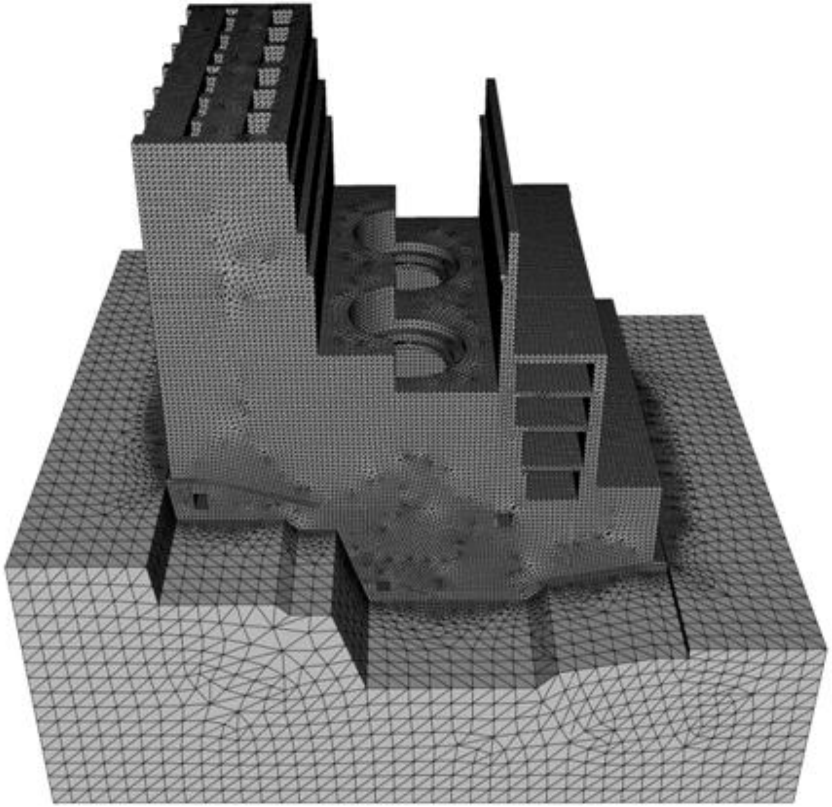

4.445.325 tetrahedral linear elements
816.189 nodes

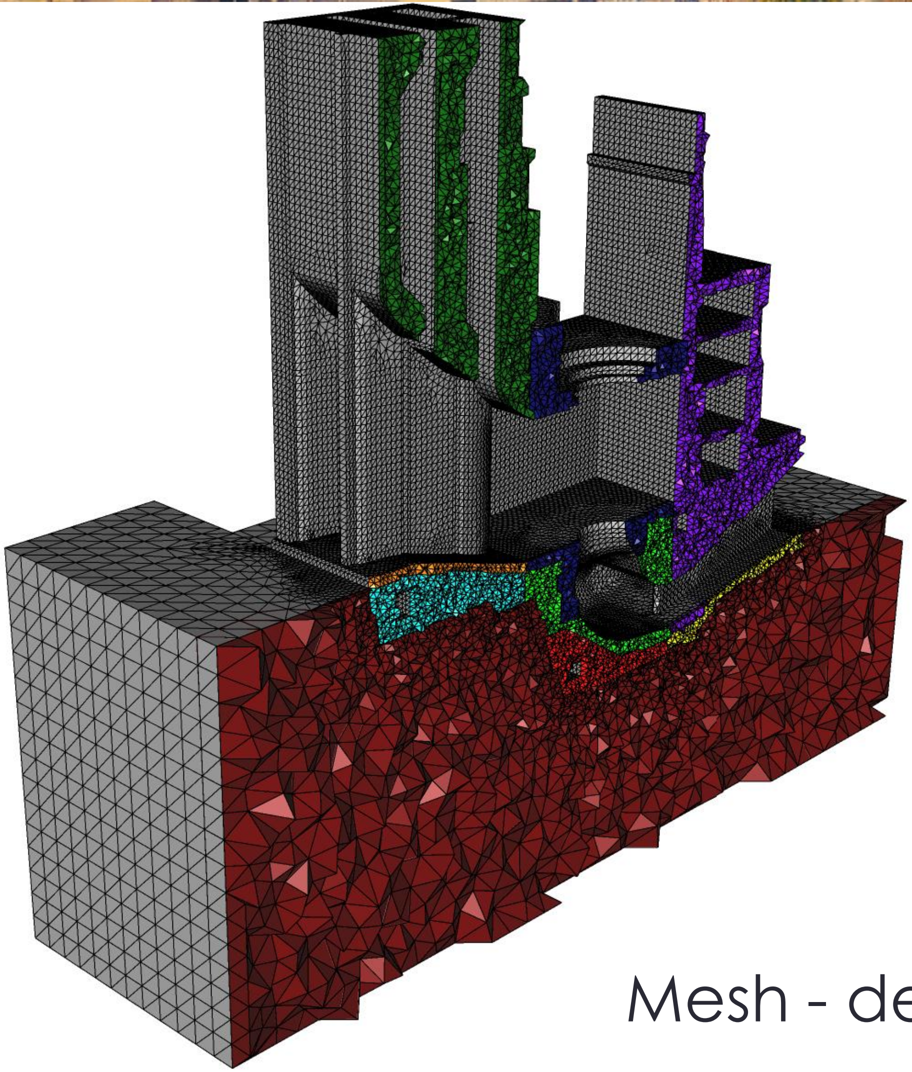

Mesh - detail

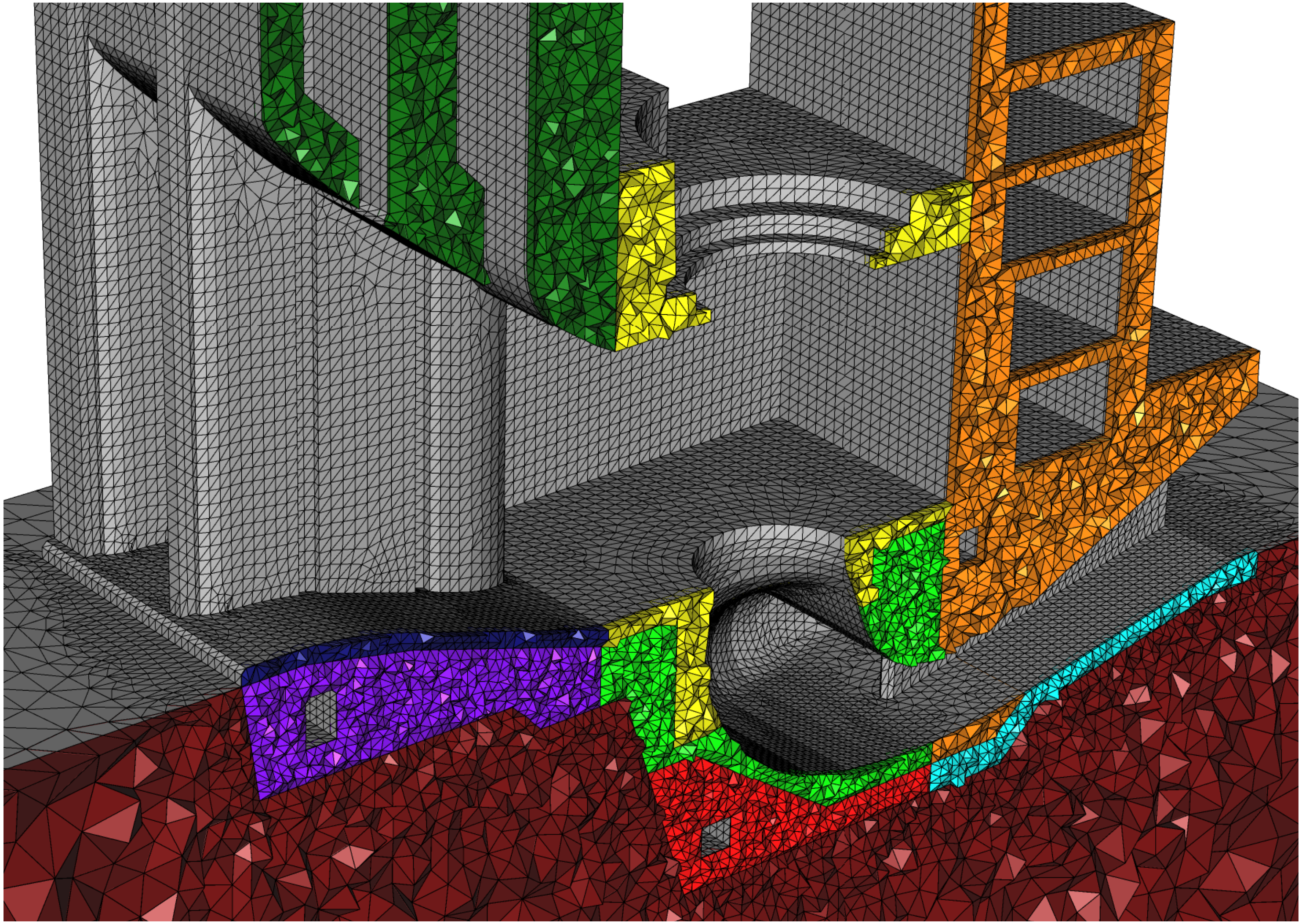

Mesh detail

	Montante				
	Etapa	Altura da Camada (m)	Idade de Lançamento (dias)	Temperatura de Lançamento (^oC)	Material
Volume 01	Etapa 01	3.7	0	12.00	M. 4
	Etapa 02	2.3	7	12.00	M. 4
	Etapa 03	1.0	14	12.00	M. 4
	Etapa 04	2.0	21	12.00	M. 4
Volume 02	Etapa 05	1.0	28	12.00	M. 4
Volume 03	Etapa 06	5.0	35	12.00	M. 4
	Etapa 07	7.0	42	12.00	M. 4
	Etapa 08	6.5	49	12.00	M. 4
	Etapa 09	2.5	56	12.00	M. 4
	Etapa 10	2.5	63	12.00	M. 4
	Etapa 11	2.5	70	12.00	M. 4
	Etapa 12	2.5	77	12.00	M. 4
	Etapa 13	2.5	84	12.00	M. 4
	Etapa 14	2.8	91	12.00	M. 4
	Etapa 15	3.2	98	12.00	M. 4
Volume 04	Etapa 12	2.5	77	15.00	M. 4
	Etapa 13	2.5	84	15.00	M. 4
	Etapa 14	2.8	91	15.00	M. 4
	Etapa 15	2.8	98	15.00	M. 4
	Etapa 16	2.4	105	15.00	M. 4
	Etapa 17	2.5	112	15.00	M. 4
	Etapa 18	2.5	119	15.00	M. 4
	Etapa 19	2.2	126	15.00	M. 4
	Etapa 20	2.8	133	15.00	M. 4
	Etapa 21	2.5	140	15.00	M. 4
	Etapa 22	2.5	147	15.00	M. 4
	Etapa 23	2.5	154	15.00	M. 4
	Etapa 24	1.5	161	15.00	M. 4
	Etapa 25	2.5	168	15.00	M. 4

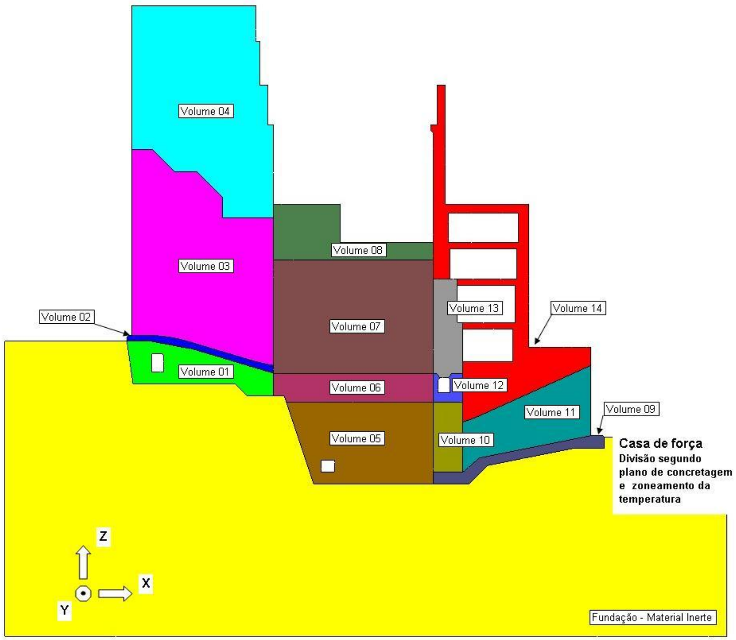

construction schedule

	Parte Central				
	Etapa	Altura da Camada (m)	Idade de Lançamento (dias)	Temperatura de Lançamento (°C)	Material
Volume 05	Etapa 26	2.0	198	12.00	M. 4
	Etapa 27	2.8	205	12.00	M. 4
	Etapa 28	2.0	212	12.00	M. 4
	Etapa 29	2.0	219	12.00	M. 4
	Etapa 30	2.0	226	12.00	M. 4
	Etapa 31	2.0	233	12.00	M. 4
Volume 06	Etapa 32	2.3	240	12.00	M. 4
	Etapa 33	1.7	247	12.00	M. 4
	Etapa 34	1.5	254	12.00	M. 4
Volume 07	Etapa 35	1.4	261	10.00	M. 4
	Etapa 36	1.4	268	10.00	M. 4
	Etapa 37	1.5	275	10.00	M. 4
	Etapa 38	1.3	282	10.00	M. 4
	Etapa 39	3.0	289	10.00	M. 4
	Etapa 40	2.4	296	10.00	M. 4
	Etapa 41	2.4	303	10.00	M. 4
	Etapa 42	2.4	310	10.00	M. 4
	Etapa 43	3.1	317	10.00	M. 4
Volume 08	Etapa 44	1.0	324	15.00	M. 4
	Etapa 45	1.9	331	15.00	M. 4
	Etapa 46	3.1	338	15.00	M. 4
	Etapa 47	3.0	345	15.00	M. 4

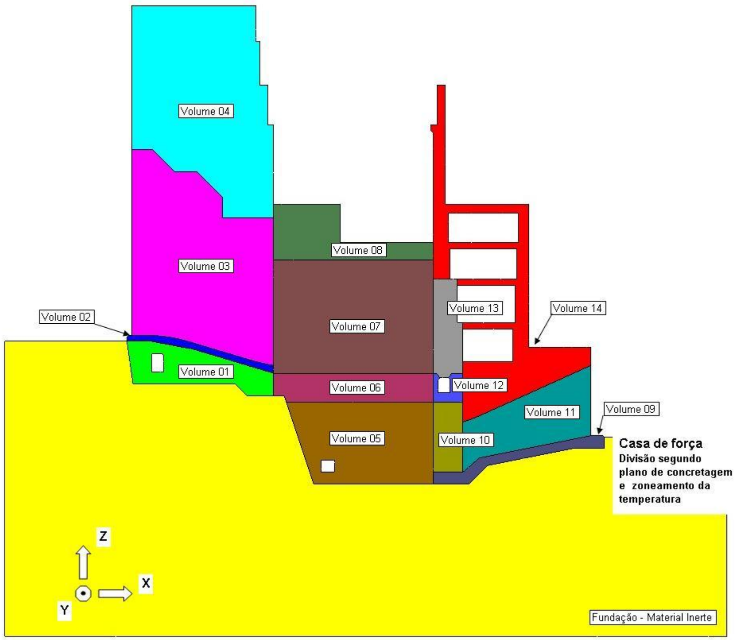

construction schedule

	Jusante				
Volume 14	Etapa 56	2.0	431	15.00	M. 4
	Etapa 57	3.0	438	15.00	M. 4
	Etapa 58	2.1	445	15.00	M. 4
	Etapa 59	2.4	452	15.00	M. 4
	Etapa 60	3.0	459	15.00	M. 4
	Etapa 61	3.6	466	15.00	M. 4
	Etapa 62	3.6	473	15.00	M. 4
	Etapa 63	3.0	480	15.00	M. 4
	Etapa 64	3.0	487	15.00	M. 4
	Etapa 65	2.9	494	15.00	M. 4
	Etapa 66	2.9	501	15.00	M. 4
	Etapa 67	1.5	508	15.00	M. 4
	Etapa 68	3.5	515	15.00	M. 4
	Etapa 69	3.7	522	15.00	M. 4
	Etapa 70	2.9	529	15.00	M. 4
	Etapa 71	2.9	536	15.00	M. 5
	Etapa 72	3.0	543	15.00	M. 4
	Etapa 73	3.5	550	15.00	M. 4

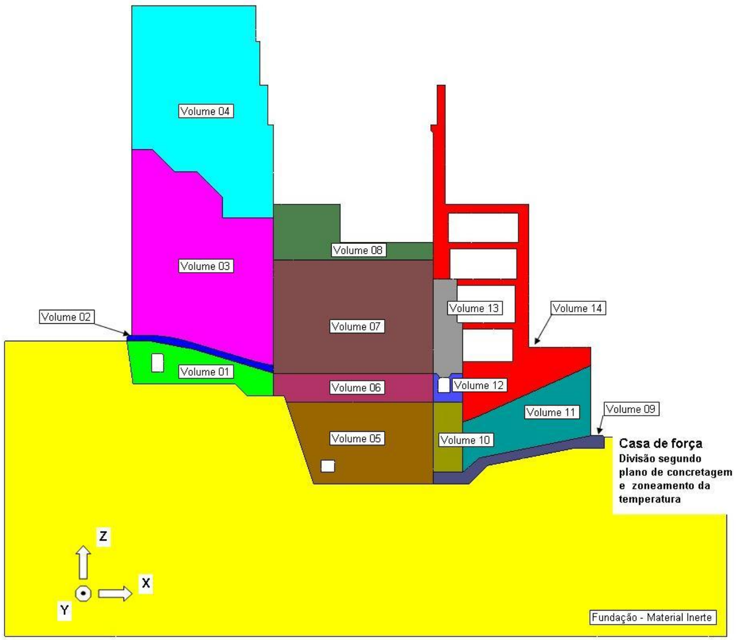

construction schedule

Step 47 – 368 days

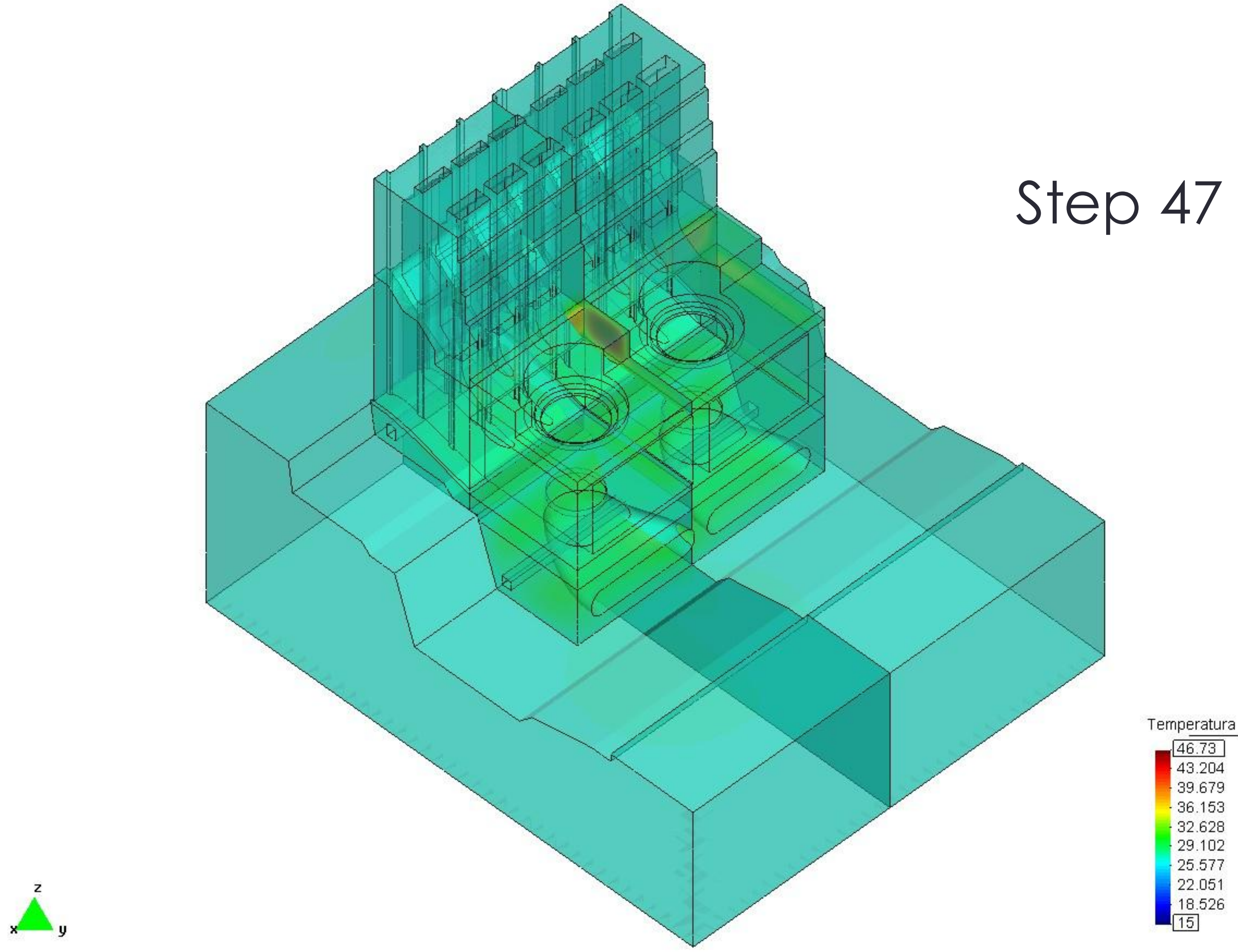

Step 47 – 368 days

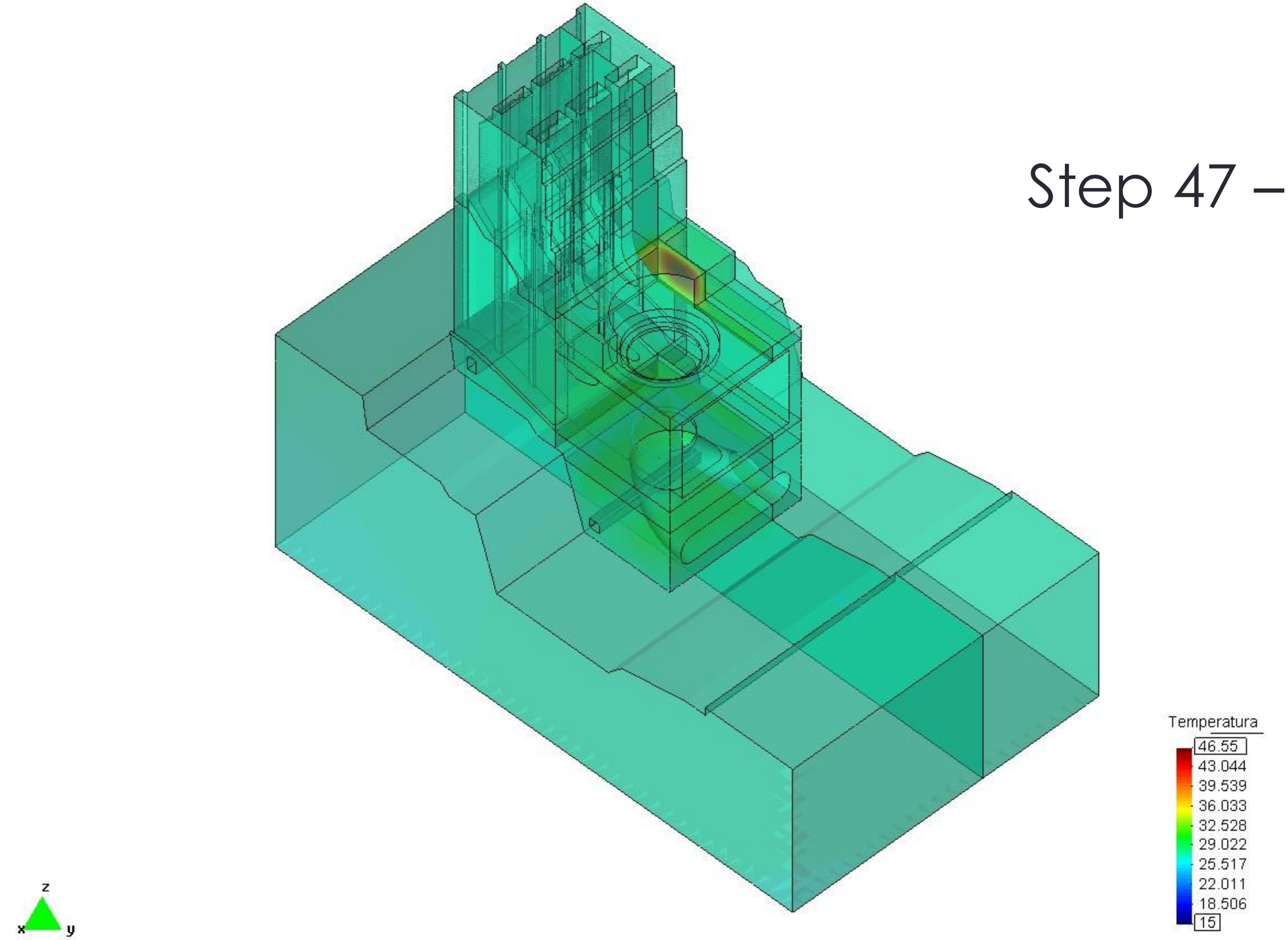

Comparison of the maximum temperatures

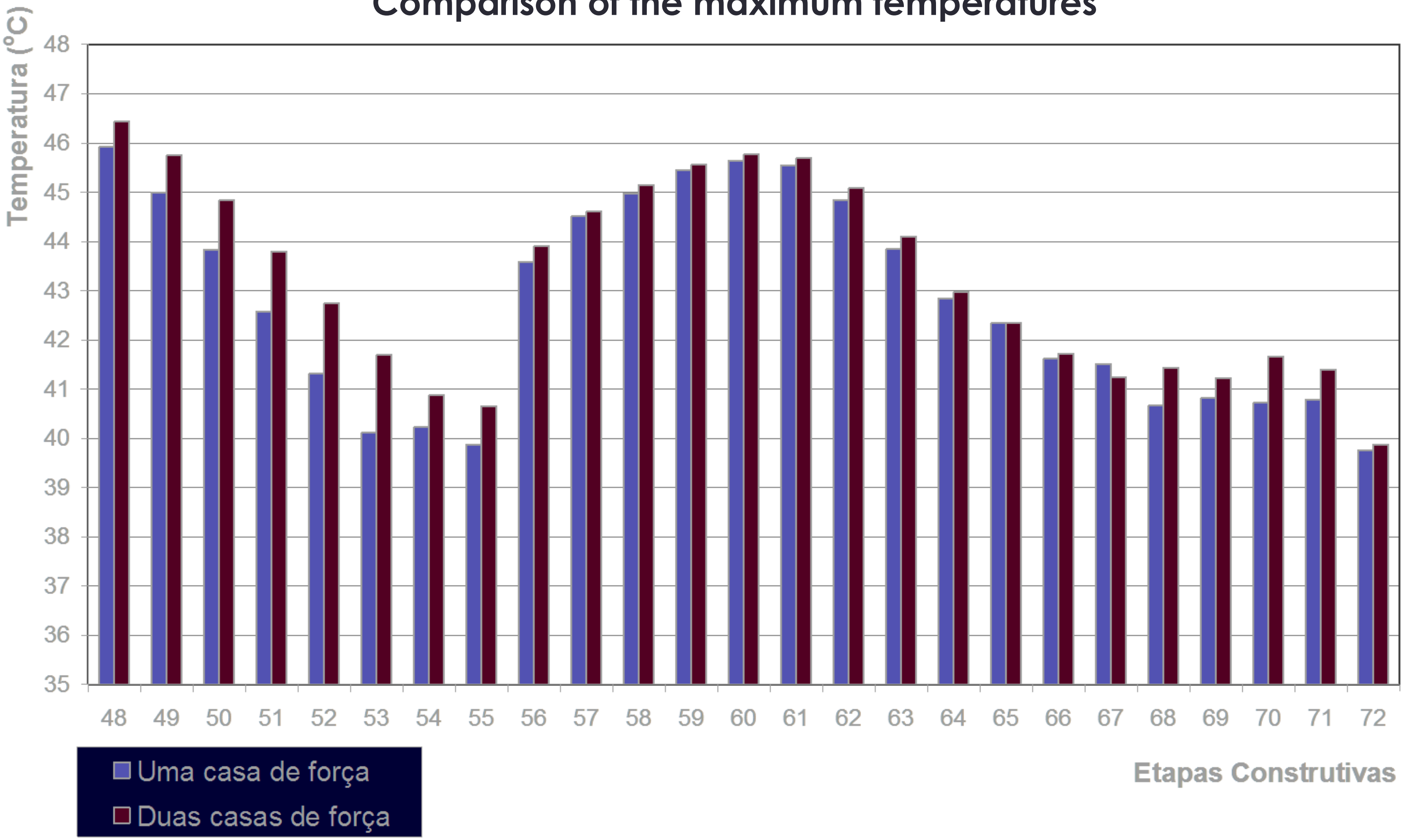

Cracking index, t = 198 days

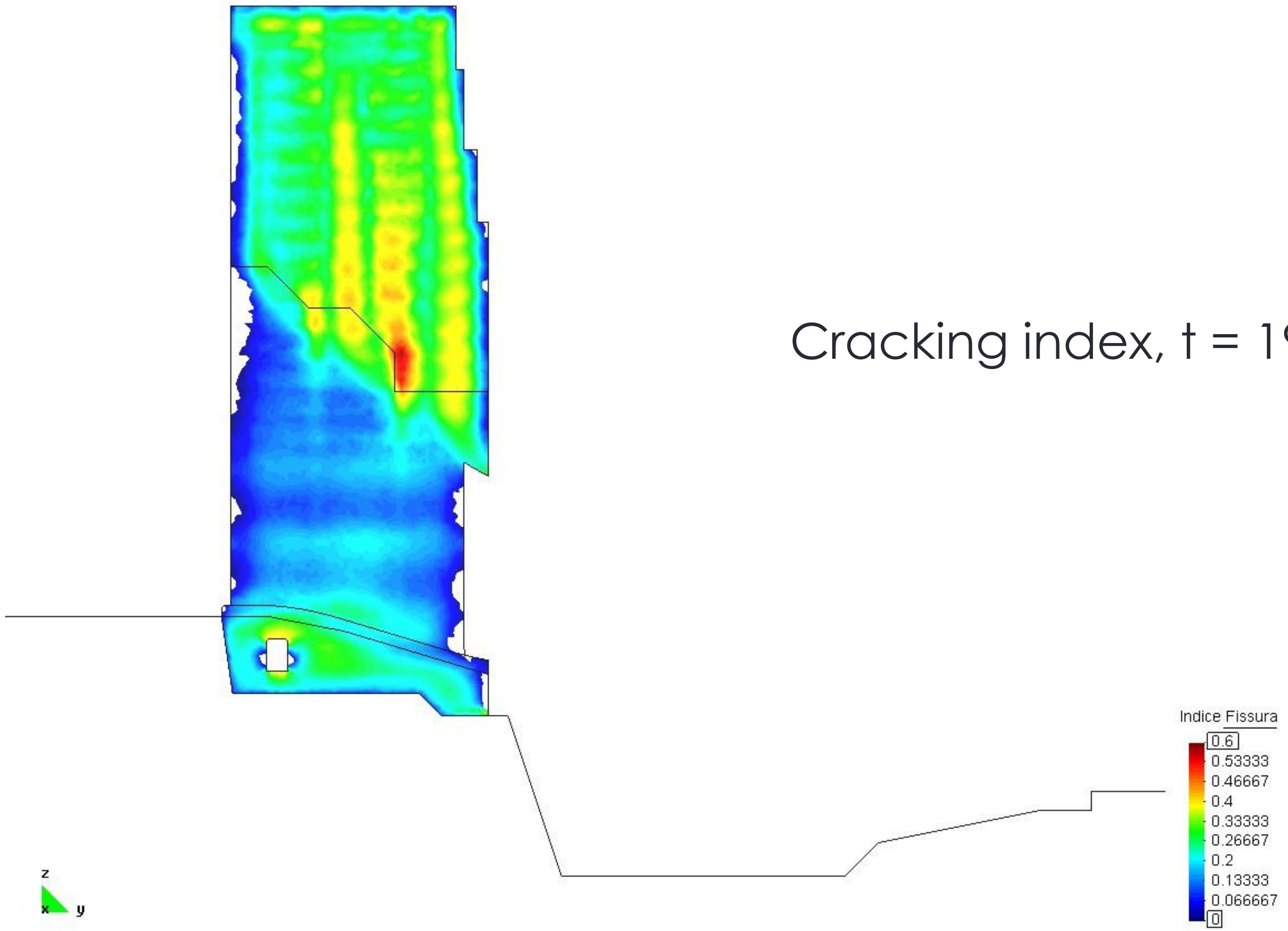

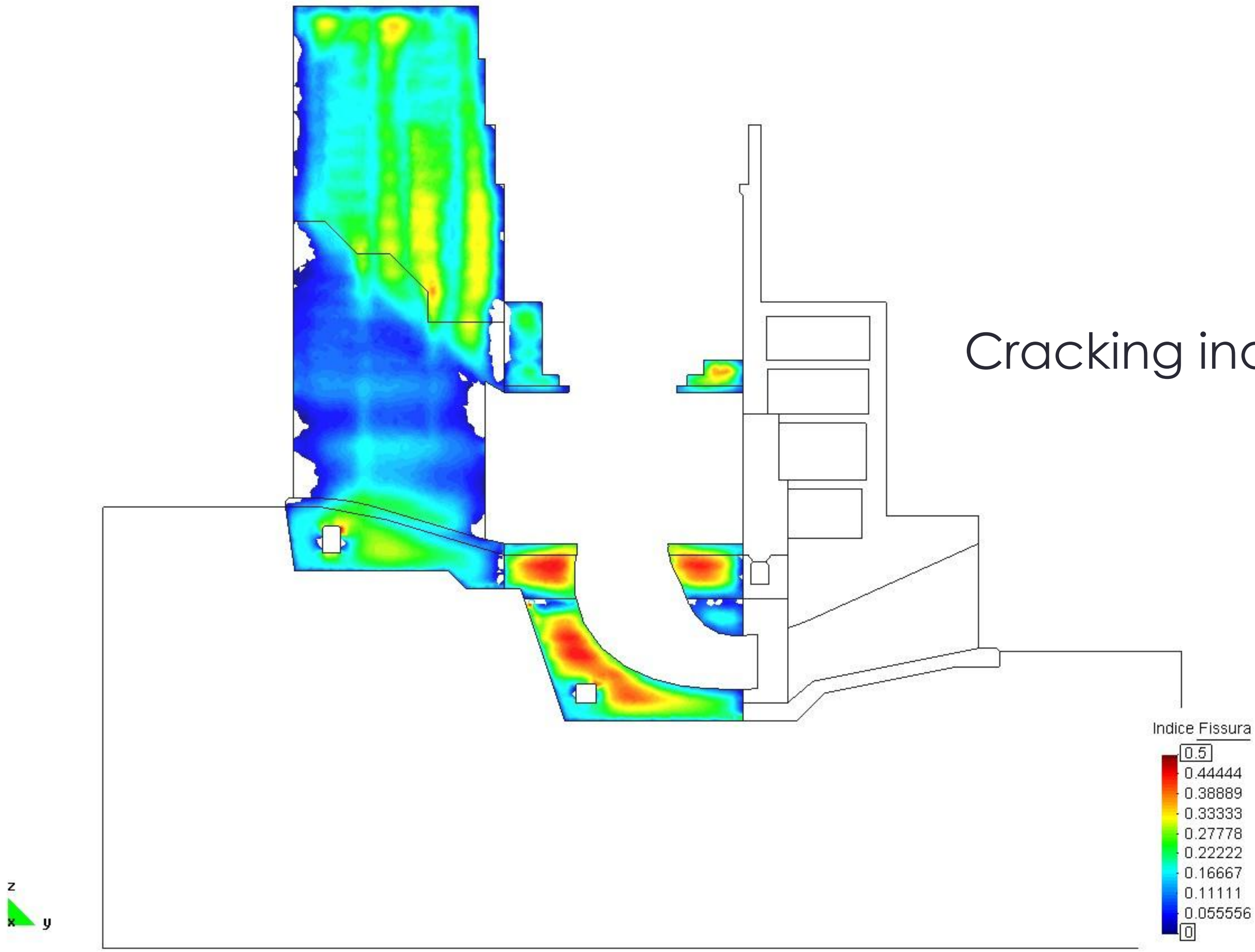

Cracking index, t = 375 days

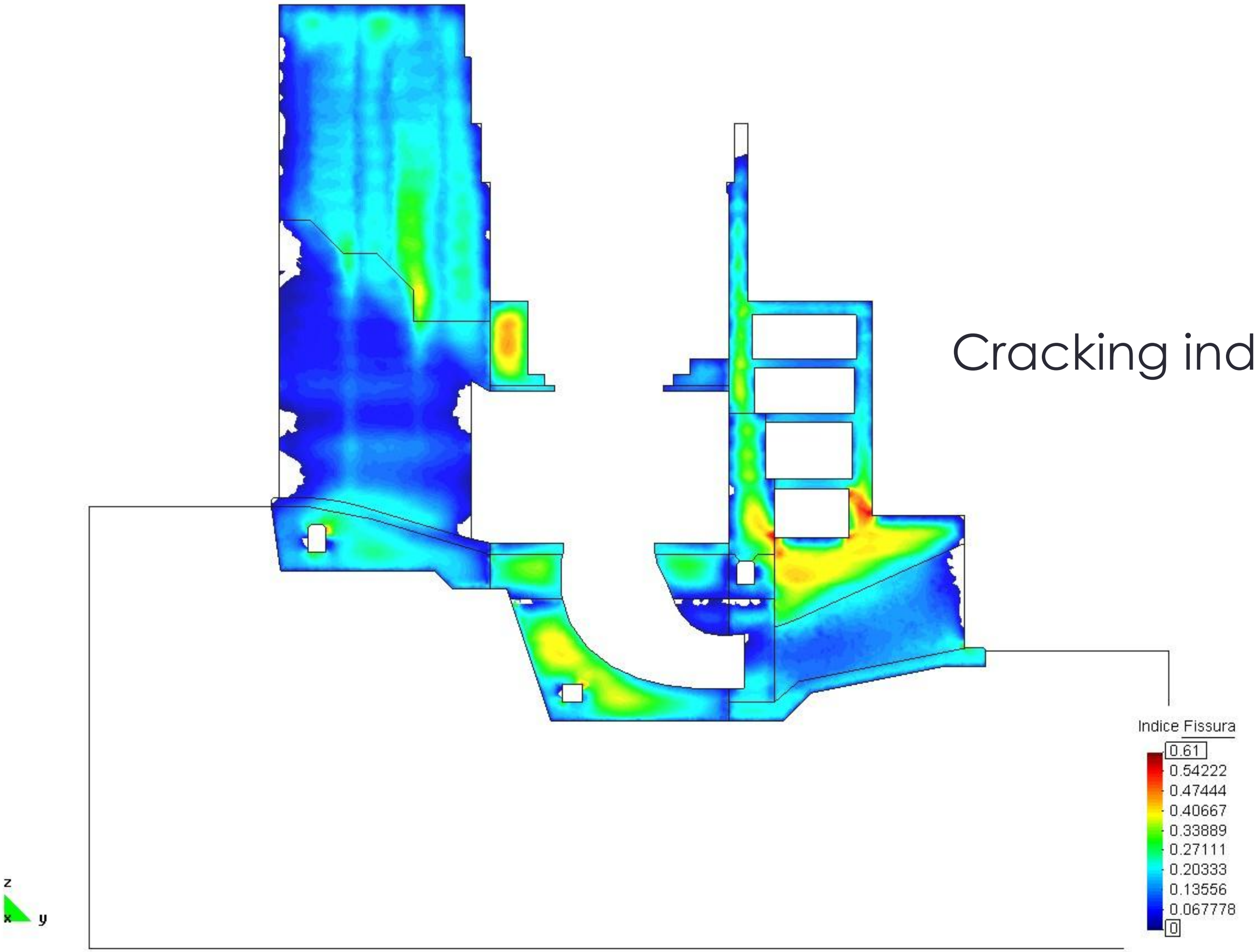

Cracking index, t = 550 days

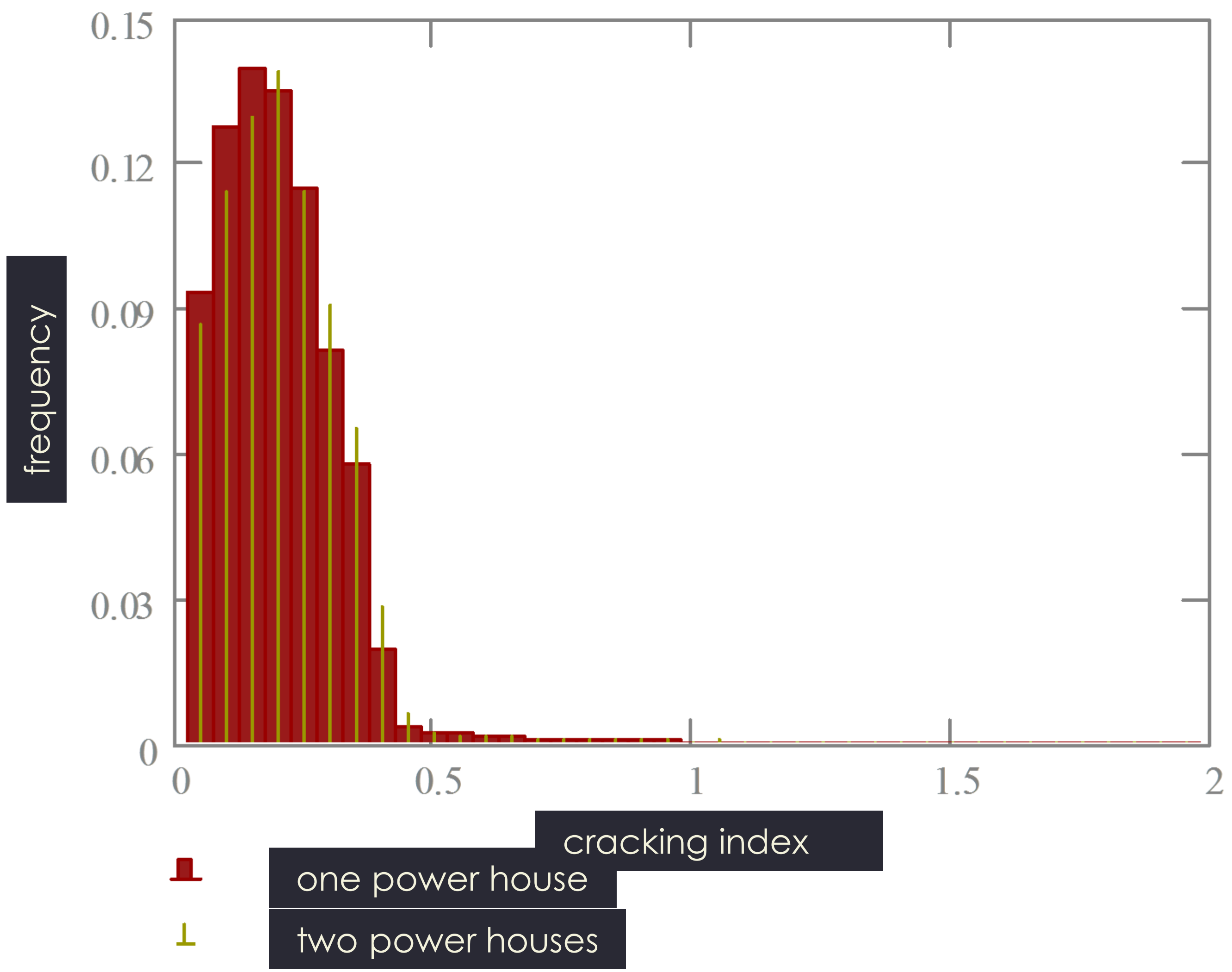
0.15
0.12
0.09
0.06
0.03
0
frequency
0
0.5
1
1.5
2
cracking index
one power house
two power houses

Case study 3
Tocoma dam Venezuela

Analysis of a spillway – complete analysis

Tocoma hydroelectric power plant: spillway

Tocoma hydroelectric power plant: spillway

Tocoma hydroelectric power plant: spillway

Tocoma hydroelectric power plant: spillway

Tocoma hydroelectric power plant: spillway

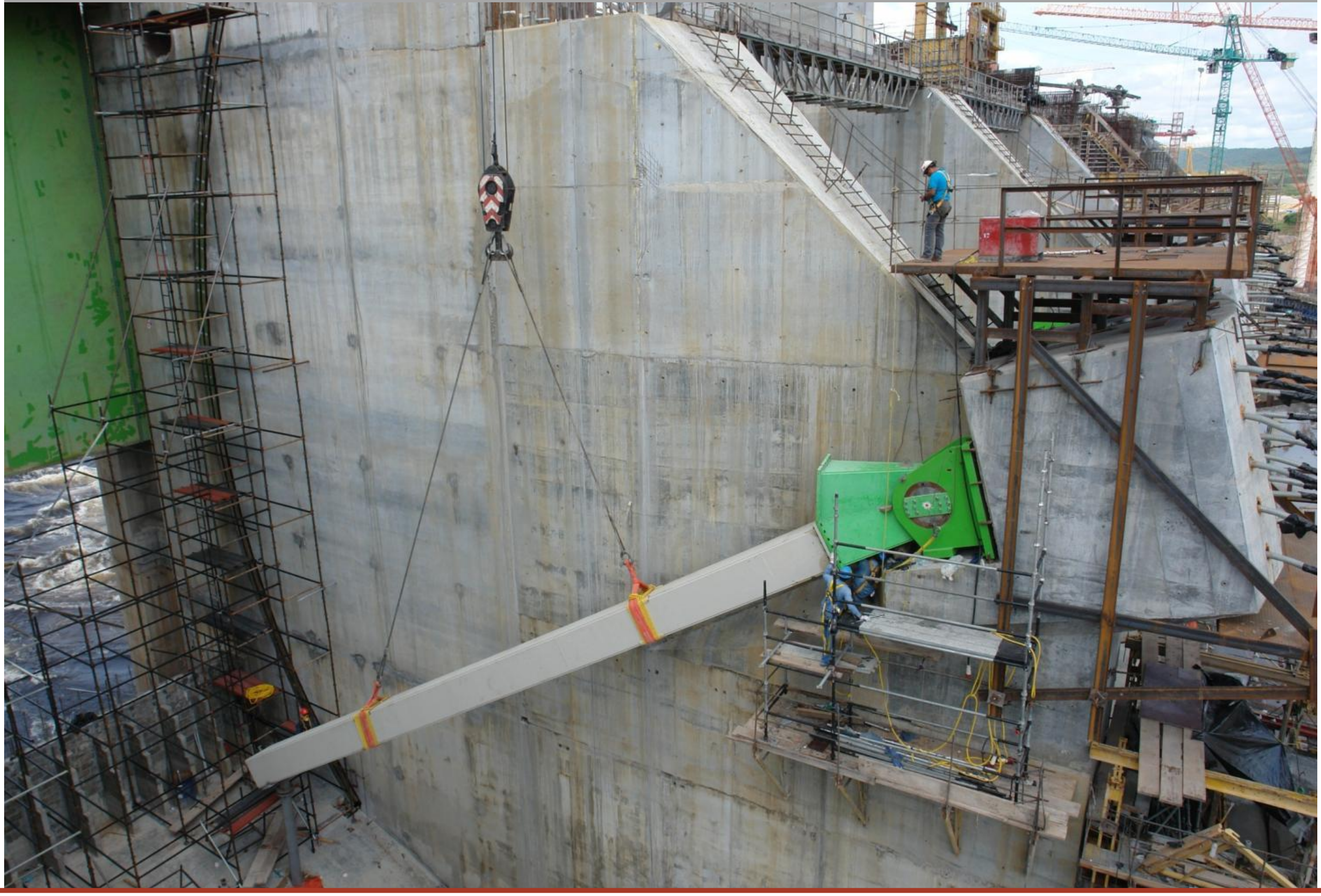

Layered construction:
complete analysis,
traditional formwork

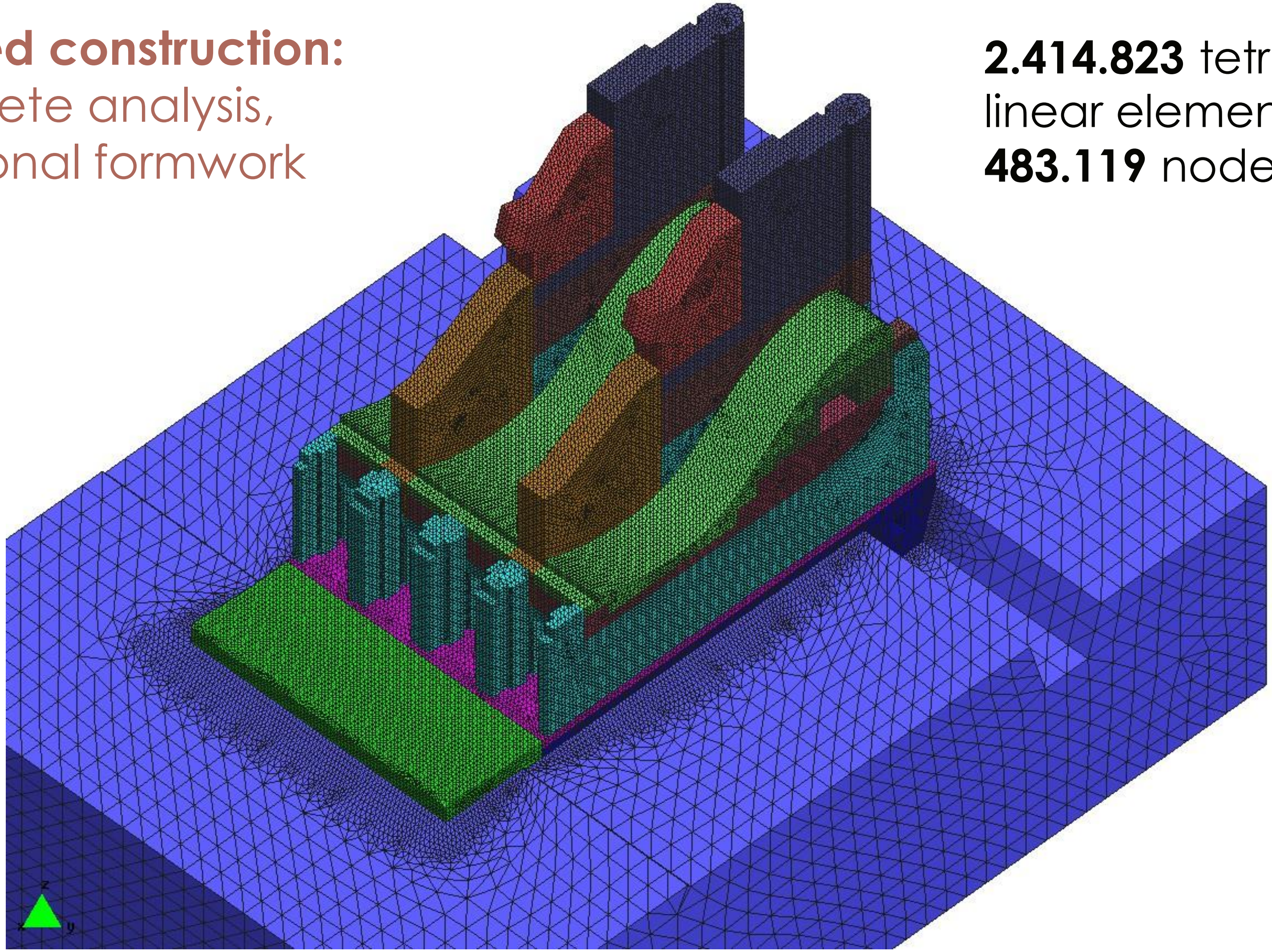

2.414.823 tetrahedral linear elements
483.119 nodes

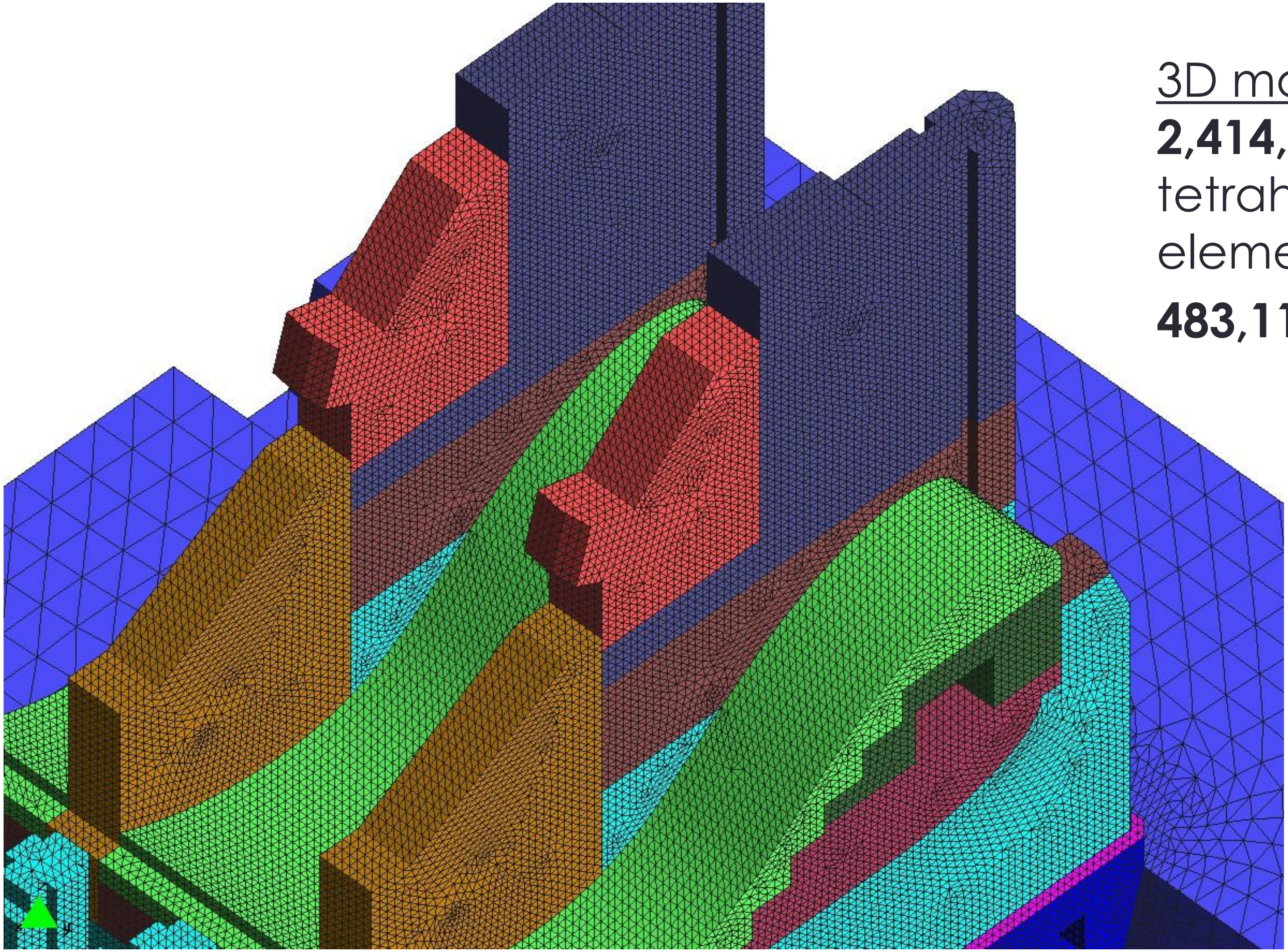

3D model :

2,414,823 linear tetrahedral elements

483,119 nodes

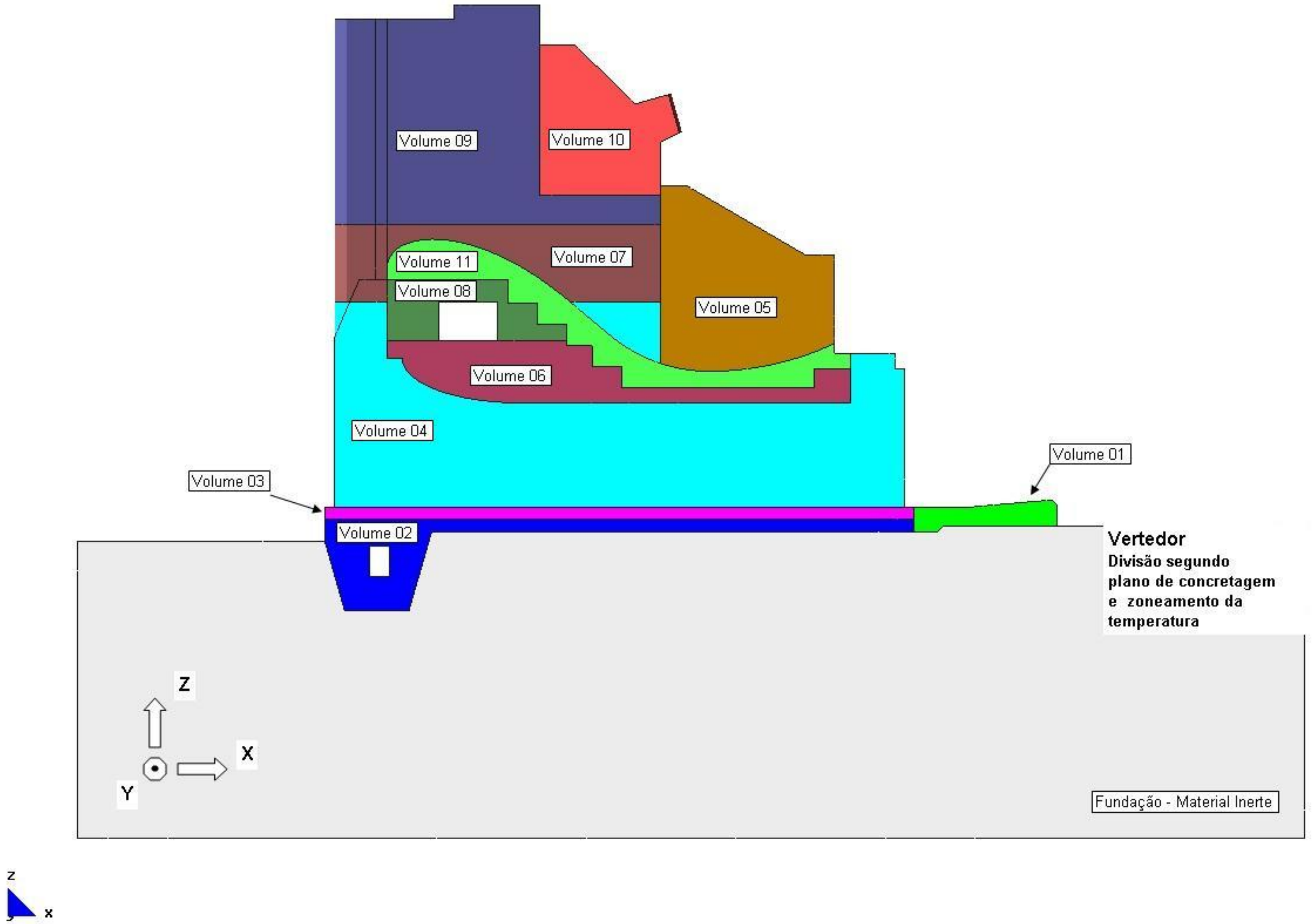
Volume 09
Volume 10
Volume 11
Volume 07
Volume 08
Volume 05
Volume 06
Volume 04
Volume 03
Volume 01
Volume 02
Vertedor
Divisão segundo
plano de concretagem
e zoneamento da
temperatura
Z
X
Y
Fundação - Material Inerte

3D model : construction scheme

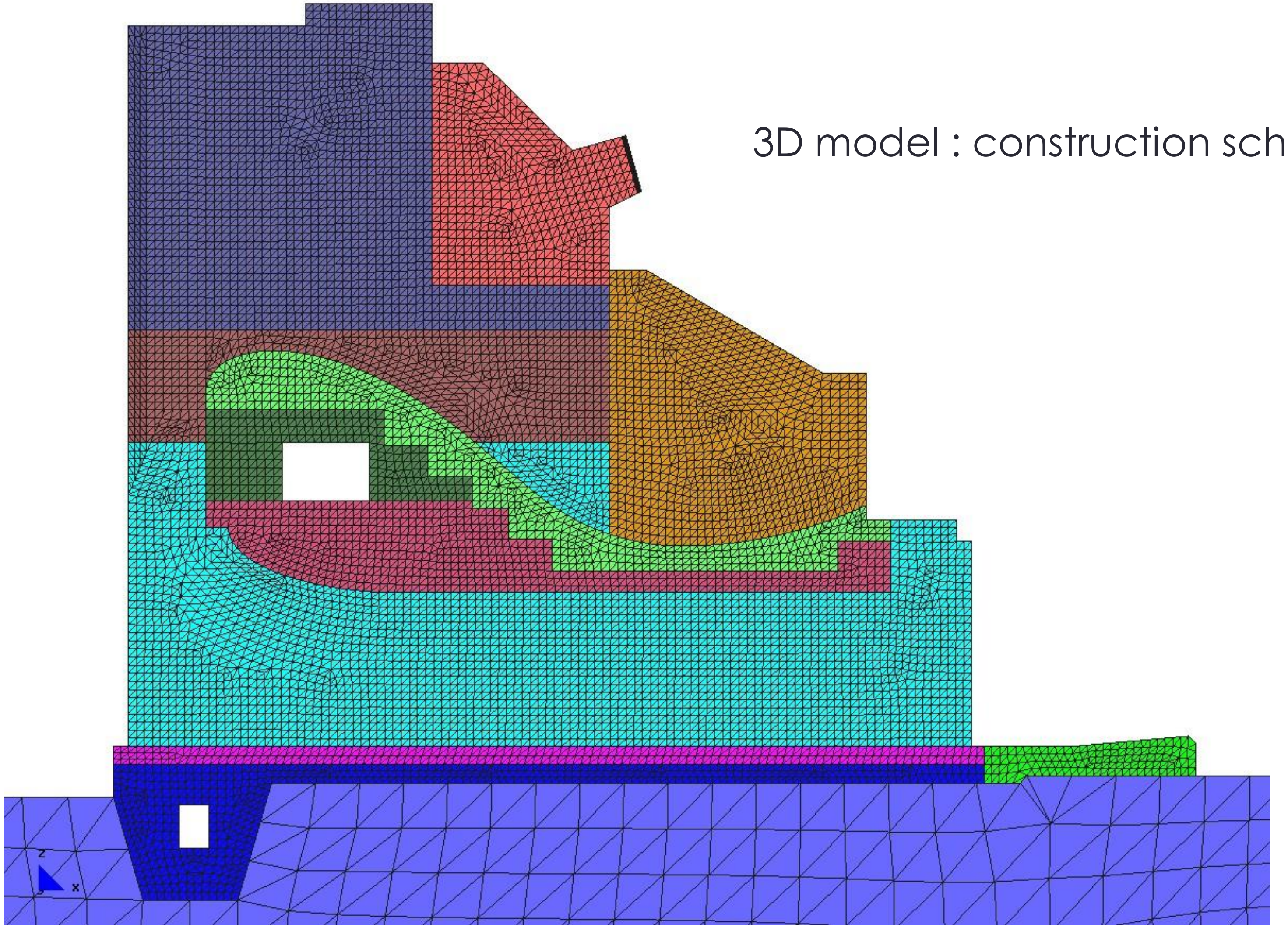

construction schedule

	Vertedor				
	Etapa	Altura da Camada (m)	Idade de Lançamento (dias)	Temperatura de Lançamento (°C)	Material
Volume 02	Etapa 01	9.3	0	15.00	M. 4
Volume 03	Etapa 02	1.3	7	10.00	M. 4
Volume 04	Etapa 03	4.2	14	10.00	M. 4
	Etapa 04	4.2	21	10.00	M. 4
	Etapa 05	4.2	28	10.00	M. 4
	Etapa 06	4.2	35	15.00	M. 4
	Etapa 07	4.0	42	15.00	M. 4
Volume 06	Etapa 08	2.1	49	15.00	M. 3
	Etapa 09	4.2	56	15.00	M. 3
Volume 07	Etapa 10	3.0	63	15.00	M. 4
	Etapa 11	2.4	70	15.00	M. 4
	Etapa 12	2.4	77	15.00	M. 4
Volume 08	Etapa 13	4.0	84	15.00	M. 3
	Etapa 14	2.3	91	15.00	M. 3
Volume 09	Etapa 15	3.0	98	15.00	M. 4
	Etapa 16	3.0	105	15.00	M. 4
	Etapa 17	4.0	112	15.00	M. 4
	Etapa 18	4.0	119	15.00	M. 4
	Etapa 19	4.3	126	15.00	M. 4
	Etapa 20	5.3	133	15.00	M. 4
Volume 05	Etapa 05	4.2	28	15.00	M. 4
	Etapa 06	4.2	35	15.00	M. 4
	Etapa 07	4.0	42	15.00	M. 4
	Etapa 10	3.0	63	15.00	M. 4
	Etapa 11	2.4	70	15.00	M. 4
	Etapa 12	2.4	77	15.00	M. 4
	Etapa 15	3.0	98	15.00	M. 4
	Etapa 16	3.0	105	15.00	M. 4
Volume 10	Etapa 21	3.0	140	12.00	M. 5 *
	Etapa 22	6.6	147	12.00	M. 5 *
	Etapa 23	1.4	154	12.00	M. 5 *
	Etapa 24	4.3	161	12.00	M. 5 *
Volume 11	Etapa 25	2.3	168	12.00	M. 4
Volume 12	Etapa 26	2.7	175	15.00	M. 3

* Adotado Material 5 = Material 3

t = 021 days

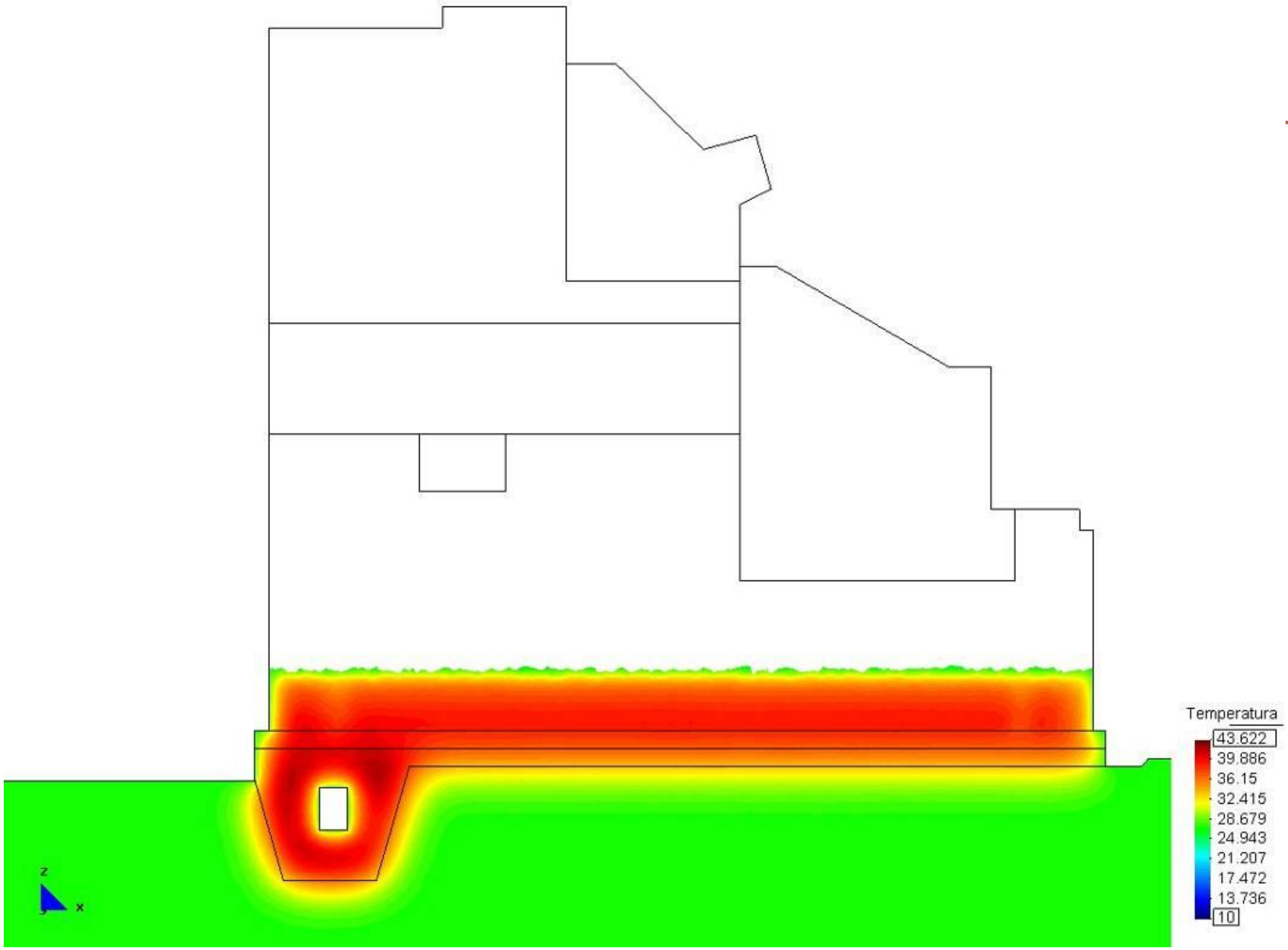
Temperatura
43.622
39.886
36.15
32.415
28.679
24.943
21.207
17.472
13.736
10
z
x

t = 028 days

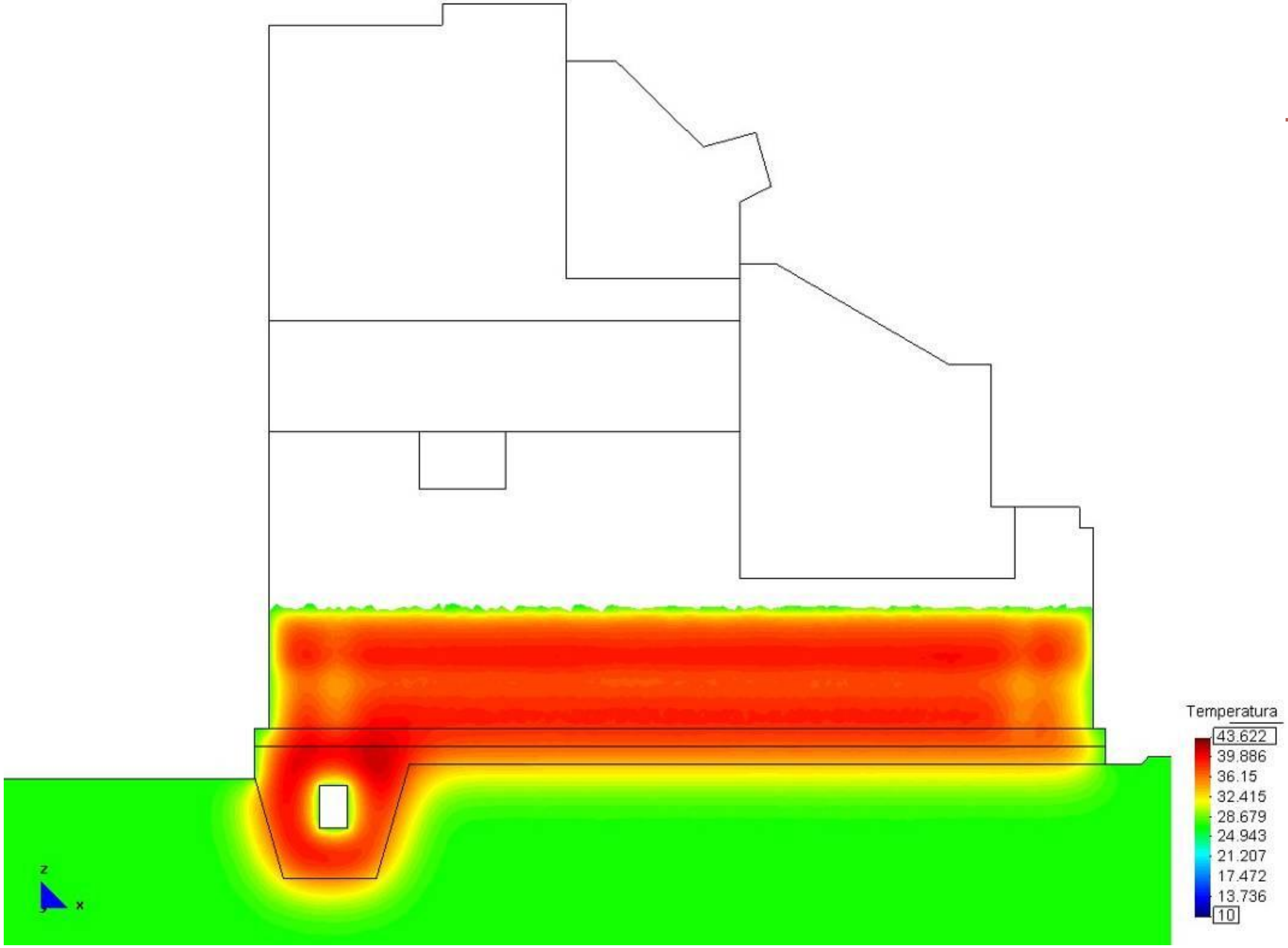
Temperatura
43.622
39.886
36.15
32.415
28.679
24.943
21.207
17.472
13.736
10
z
x

t = 035 days

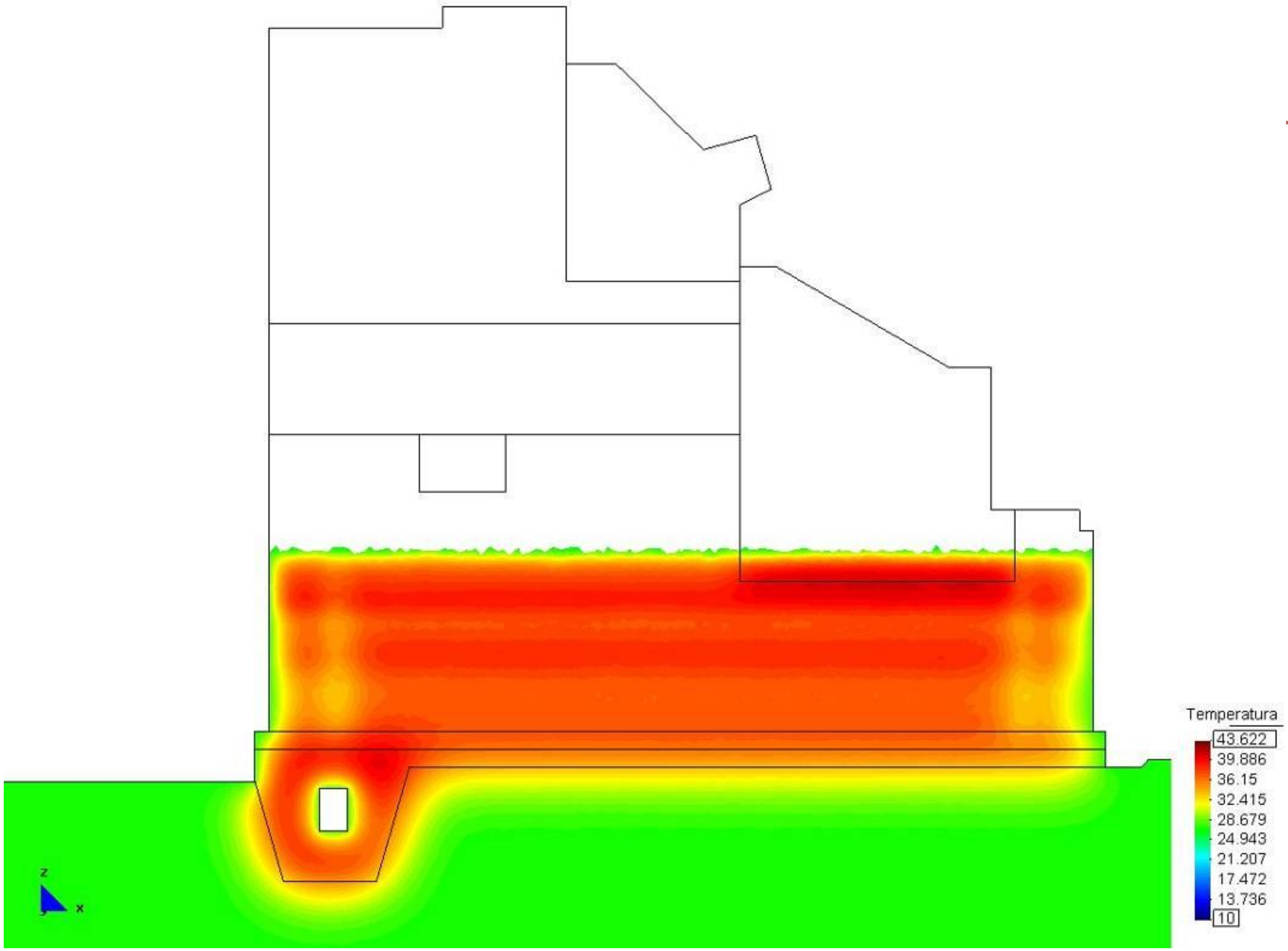
Temperatura
43.622
39.886
36.15
32.415
28.679
24.943
21.207
17.472
13.736
10
z
x

t = 042 days

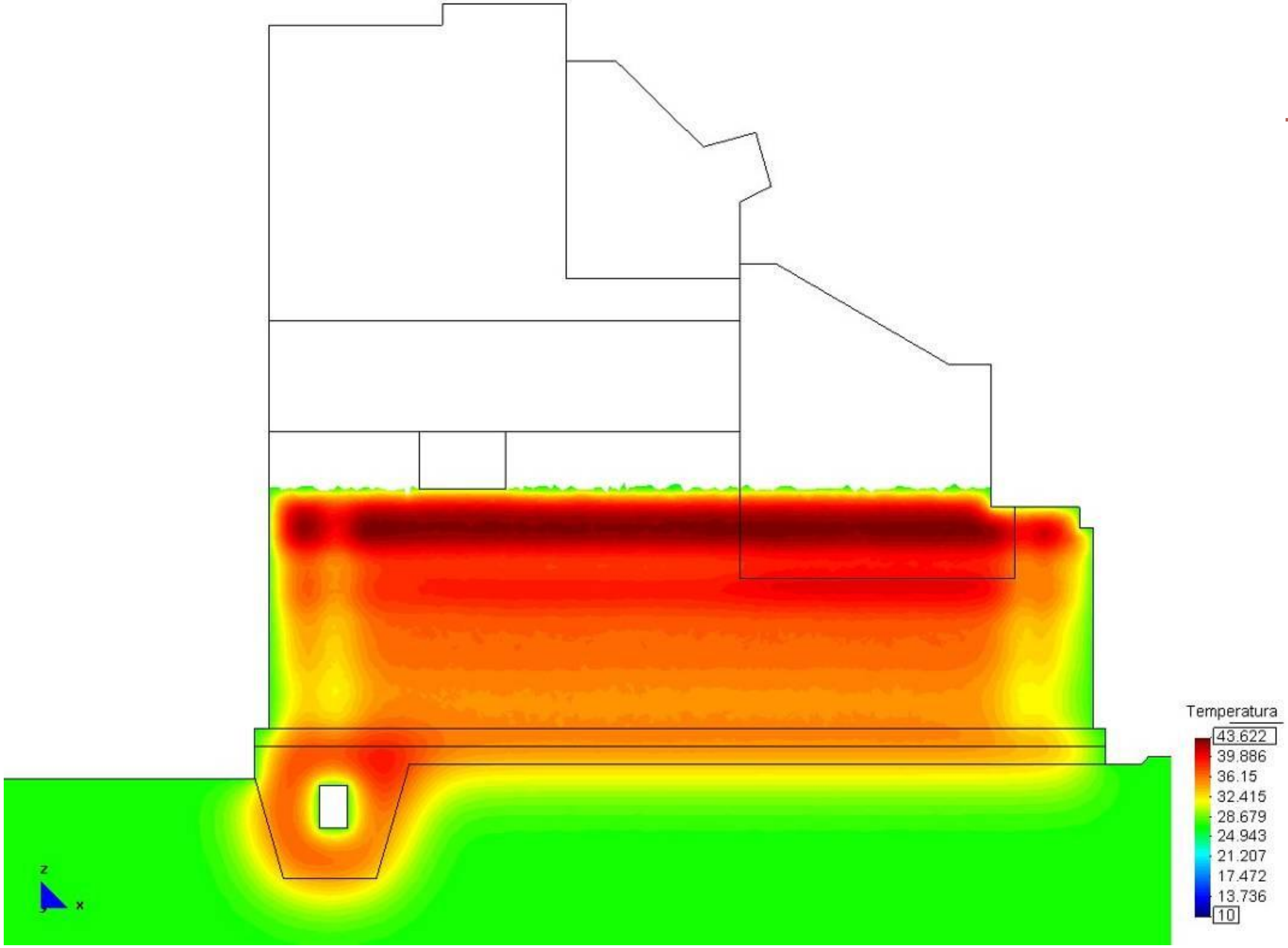
Temperatura
43.622
39.886
36.15
32.415
28.679
24.943
21.207
17.472
13.736
10
z
x

t = 049 days

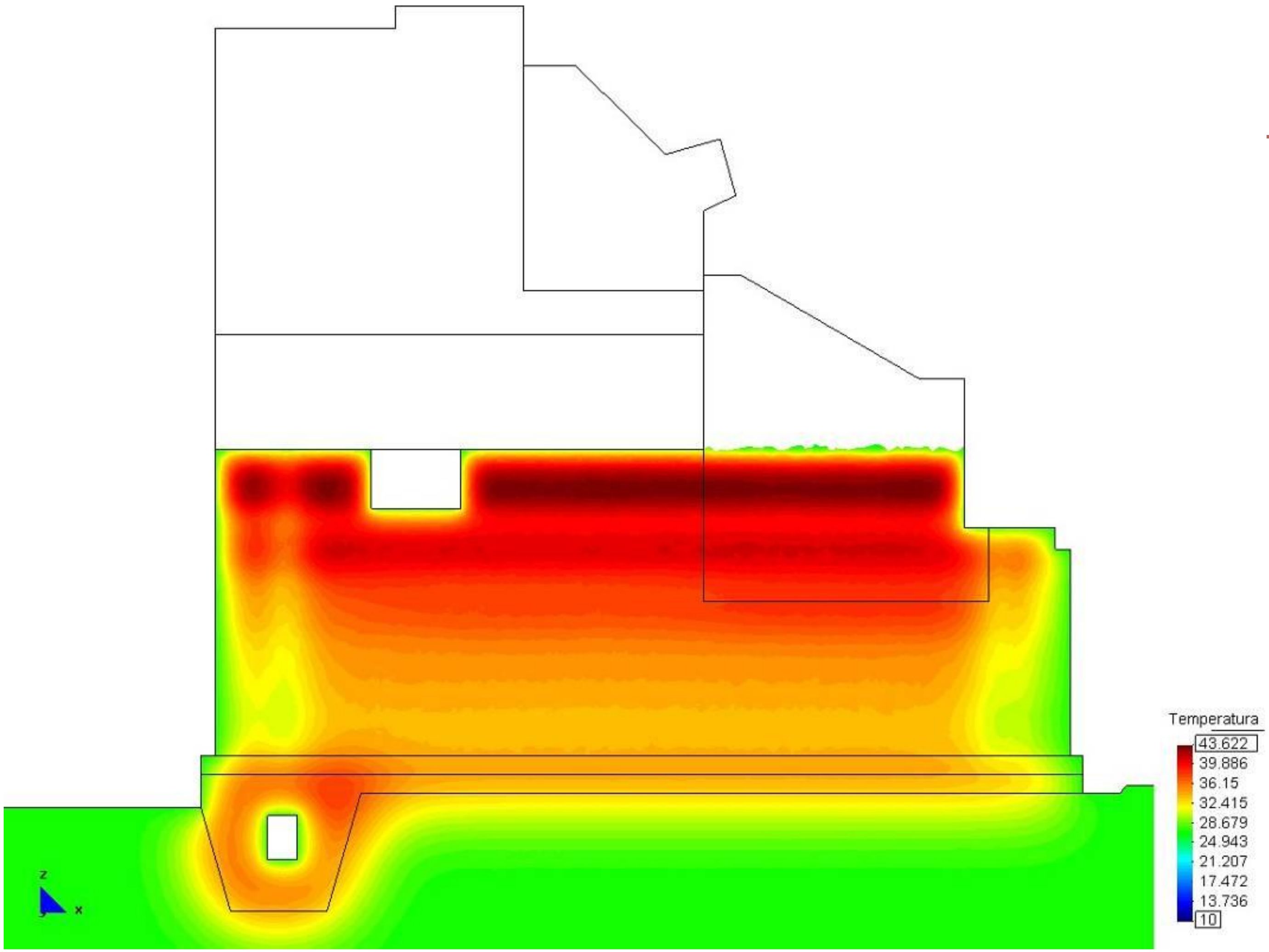
Temperatura
43.622
39.886
36.15
32.415
28.679
24.943
21.207
17.472
13.736
10
z
x

t = 063 days

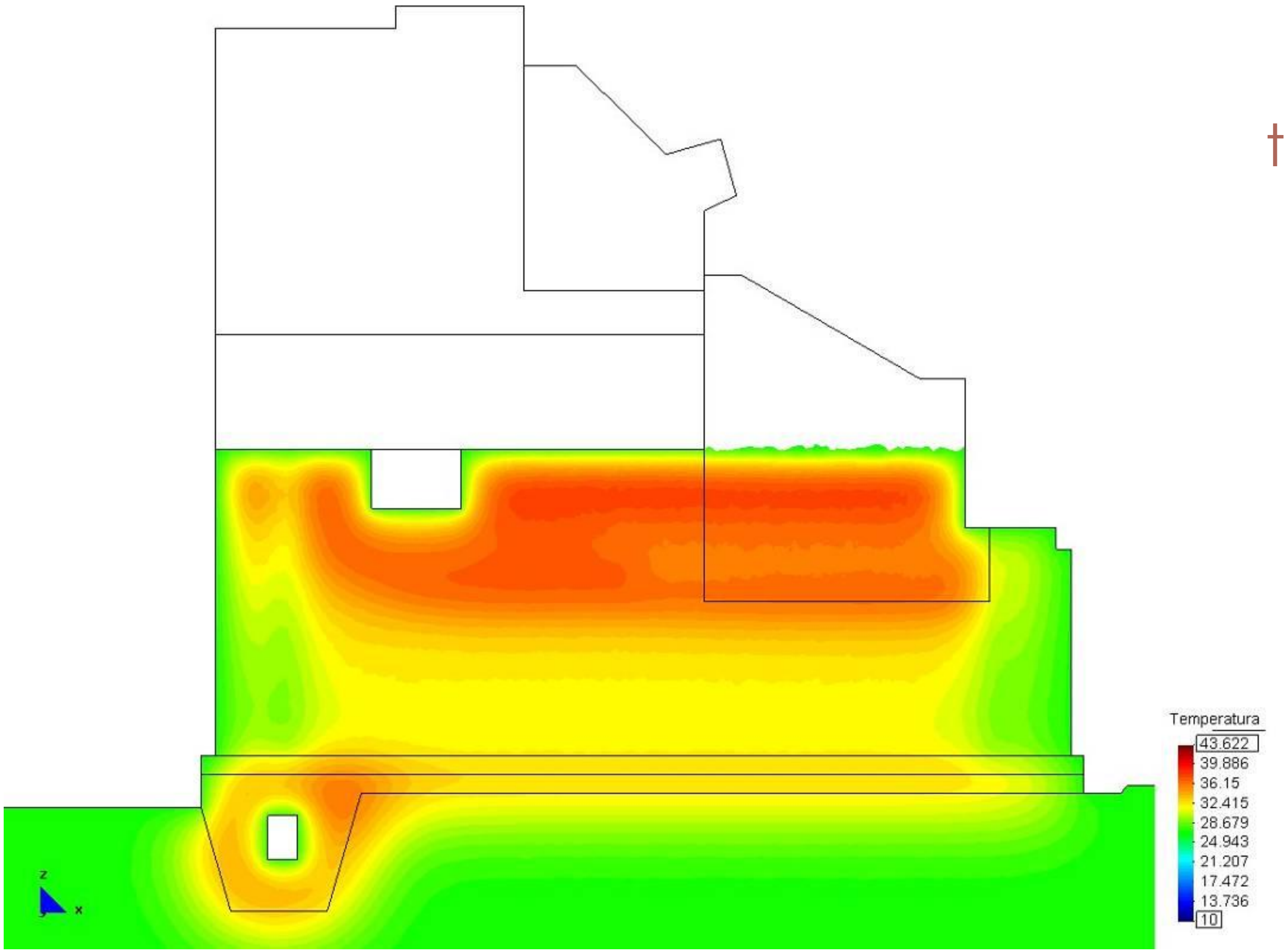
Temperatura
43.622
39.886
36.15
32.415
28.679
24.943
21.207
17.472
13.736
10
z
x

t = 098 days

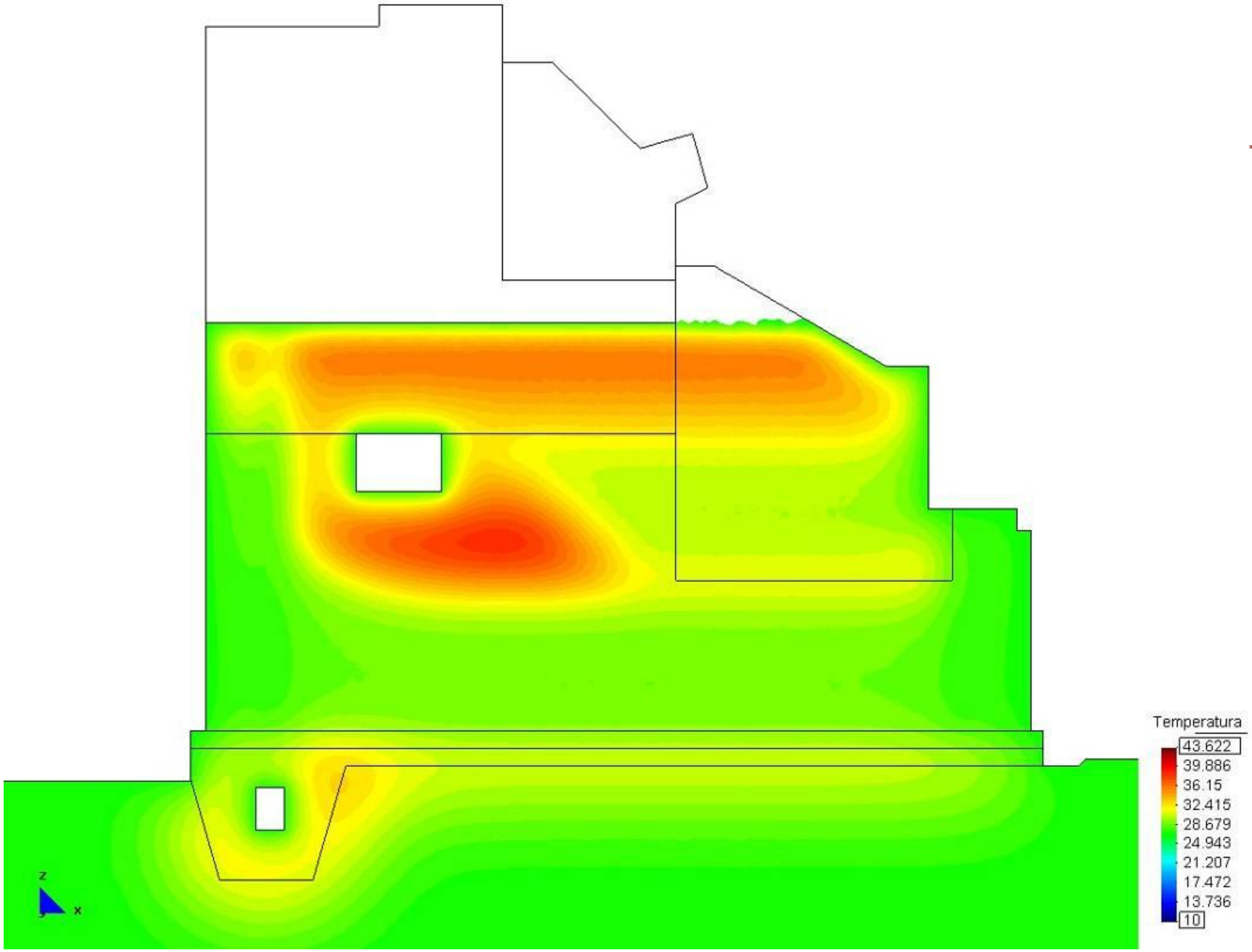
Temperatura
43.622
39.886
36.15
32.415
28.679
24.943
21.207
17.472
13.736
10
z
x

t = 112 days

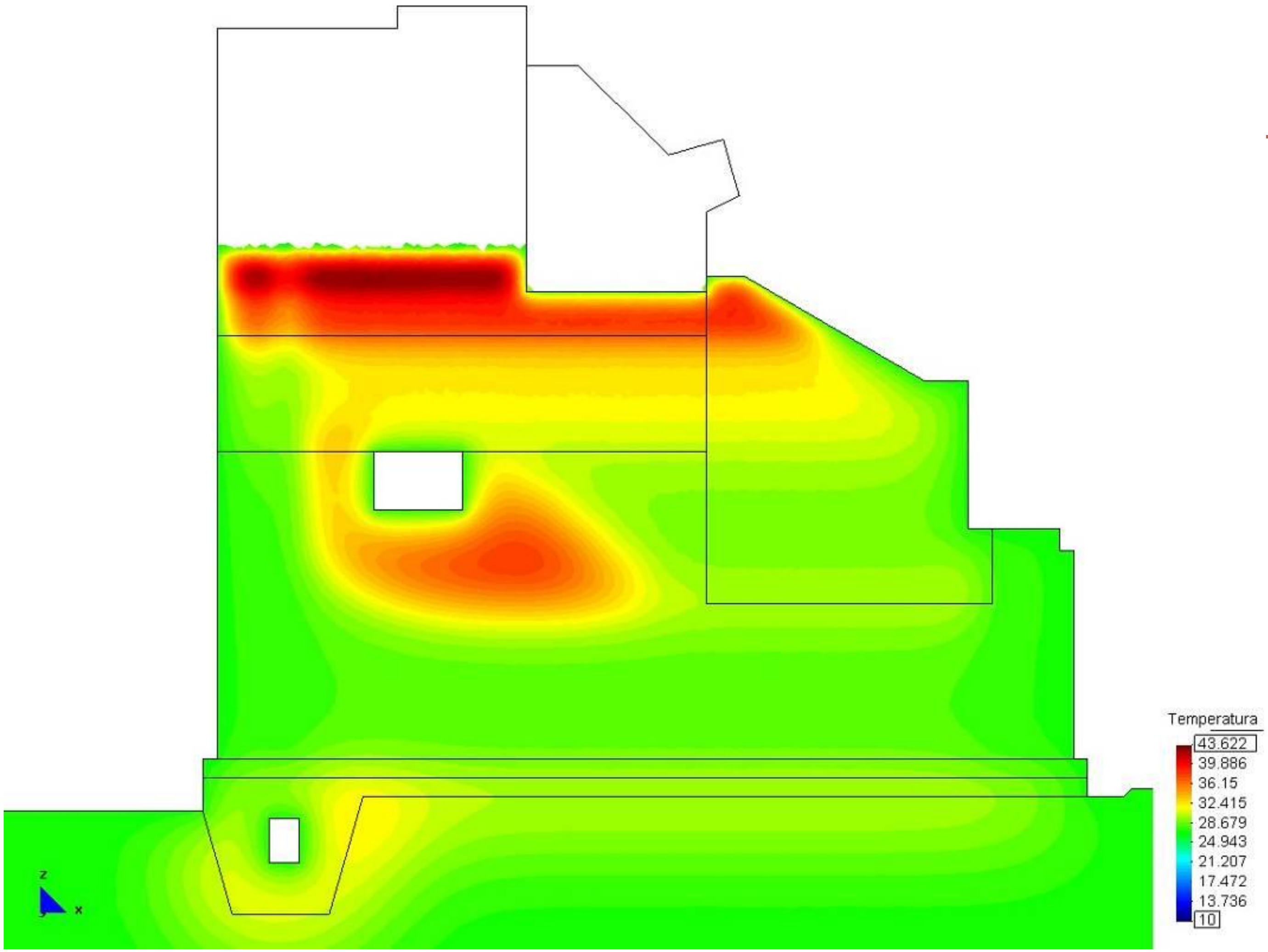
Temperatura
43.622
39.886
36.15
32.415
28.679
24.943
21.207
17.472
13.736
10
z
x

t = 119 days

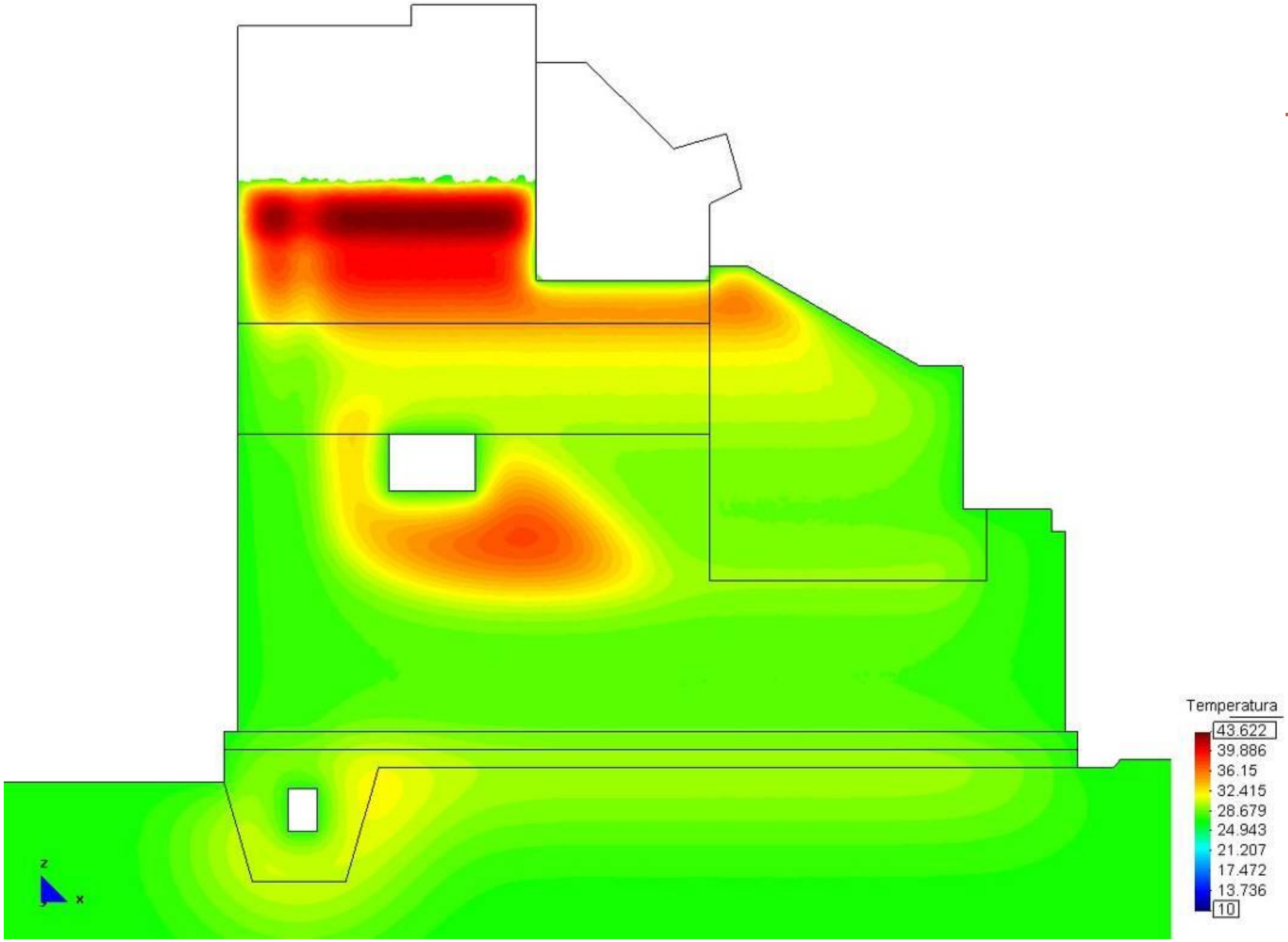
Temperatura
43.622
39.886
36.15
32.415
28.679
24.943
21.207
17.472
13.736
10
z
x

t = 126 days

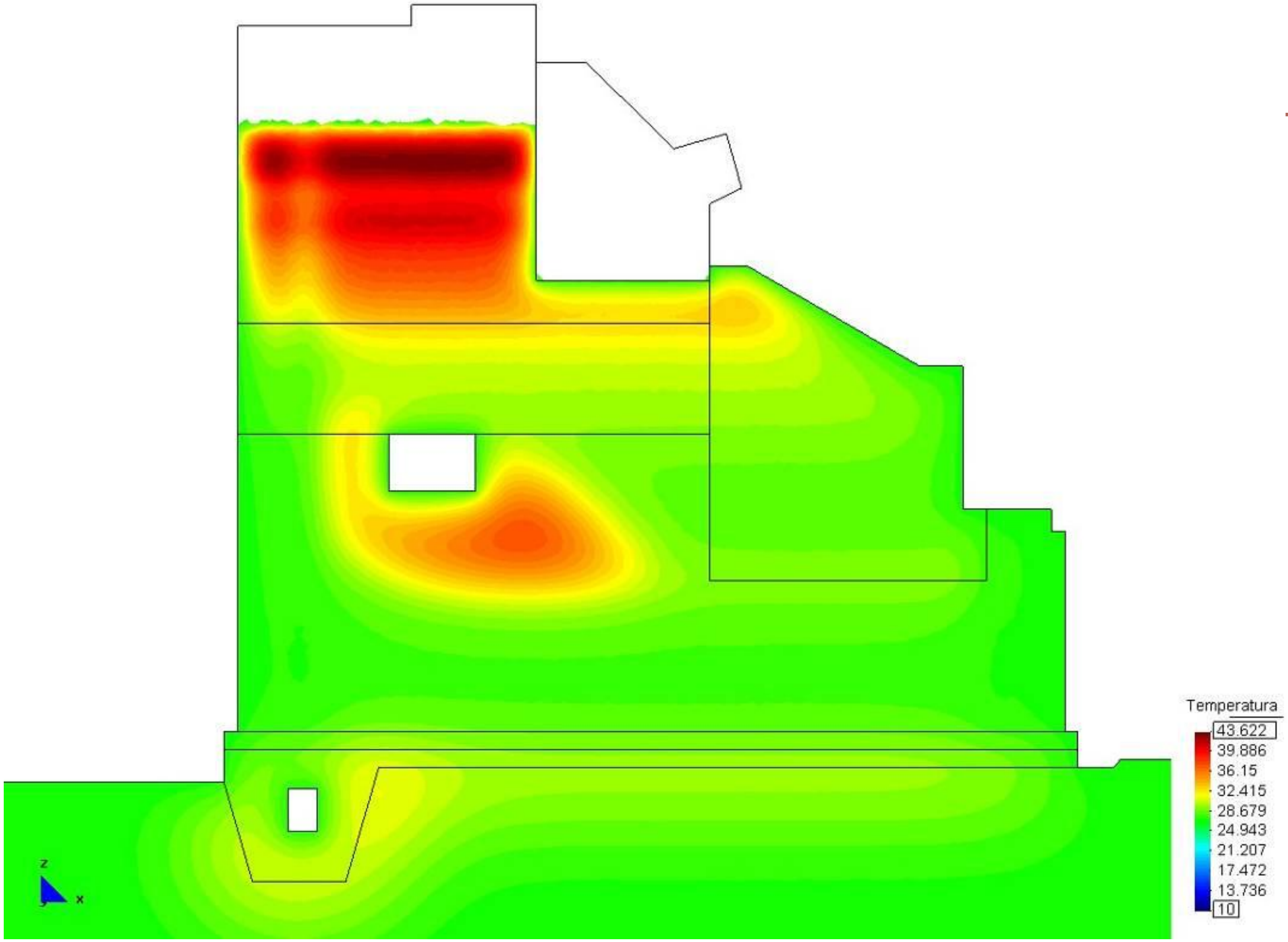
Temperatura
43.622
39.886
36.15
32.415
28.679
24.943
21.207
17.472
13.736
10
z
x

t = 140 days

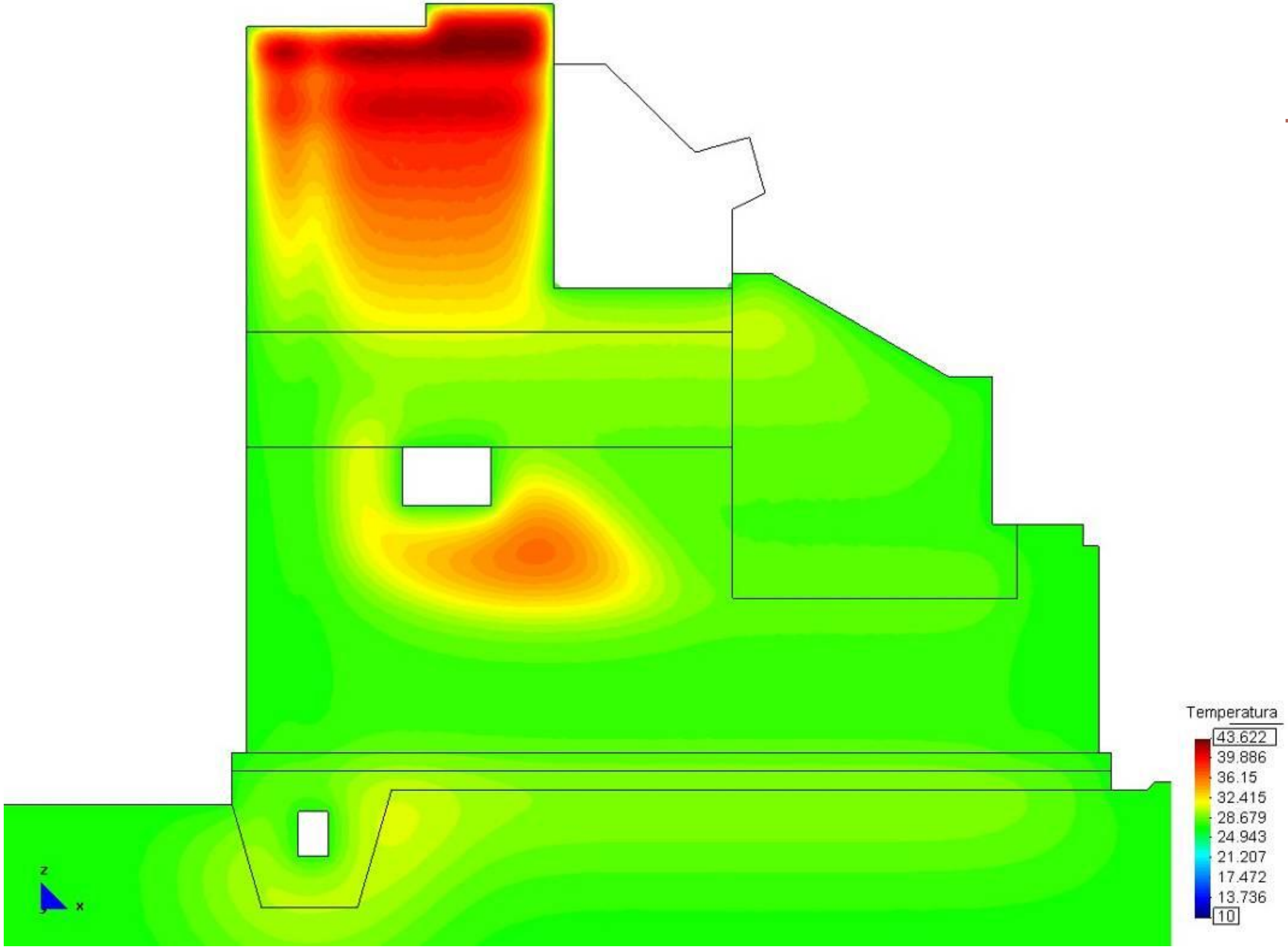
Temperatura
43.622
39.886
36.15
32.415
28.679
24.943
21.207
17.472
13.736
10
z
x

t = 200 days

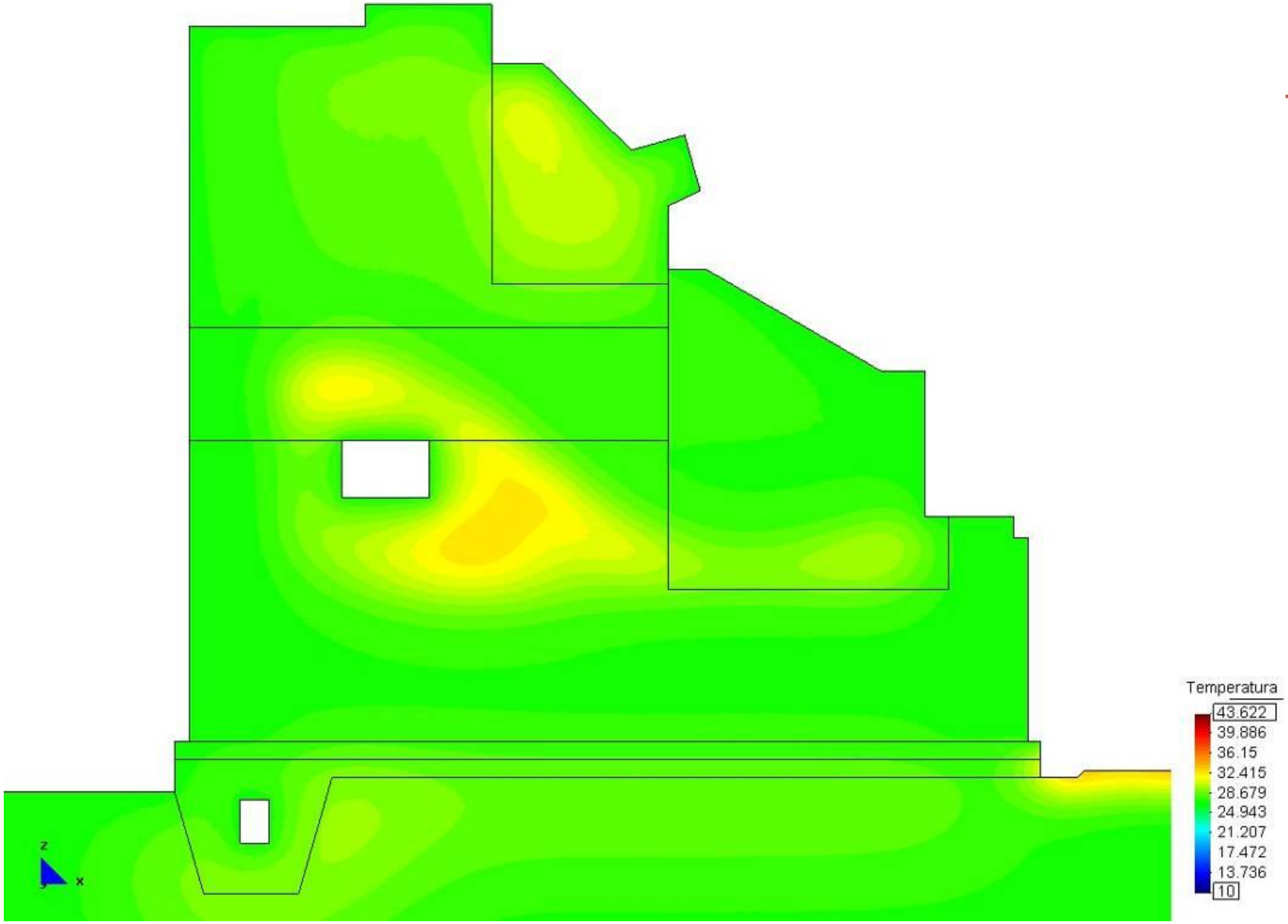
Temperatura
43.622
39.886
36.15
32.415
28.679
24.943
21.207
17.472
13.736
10
z
x

Cracking index
t = 140 days

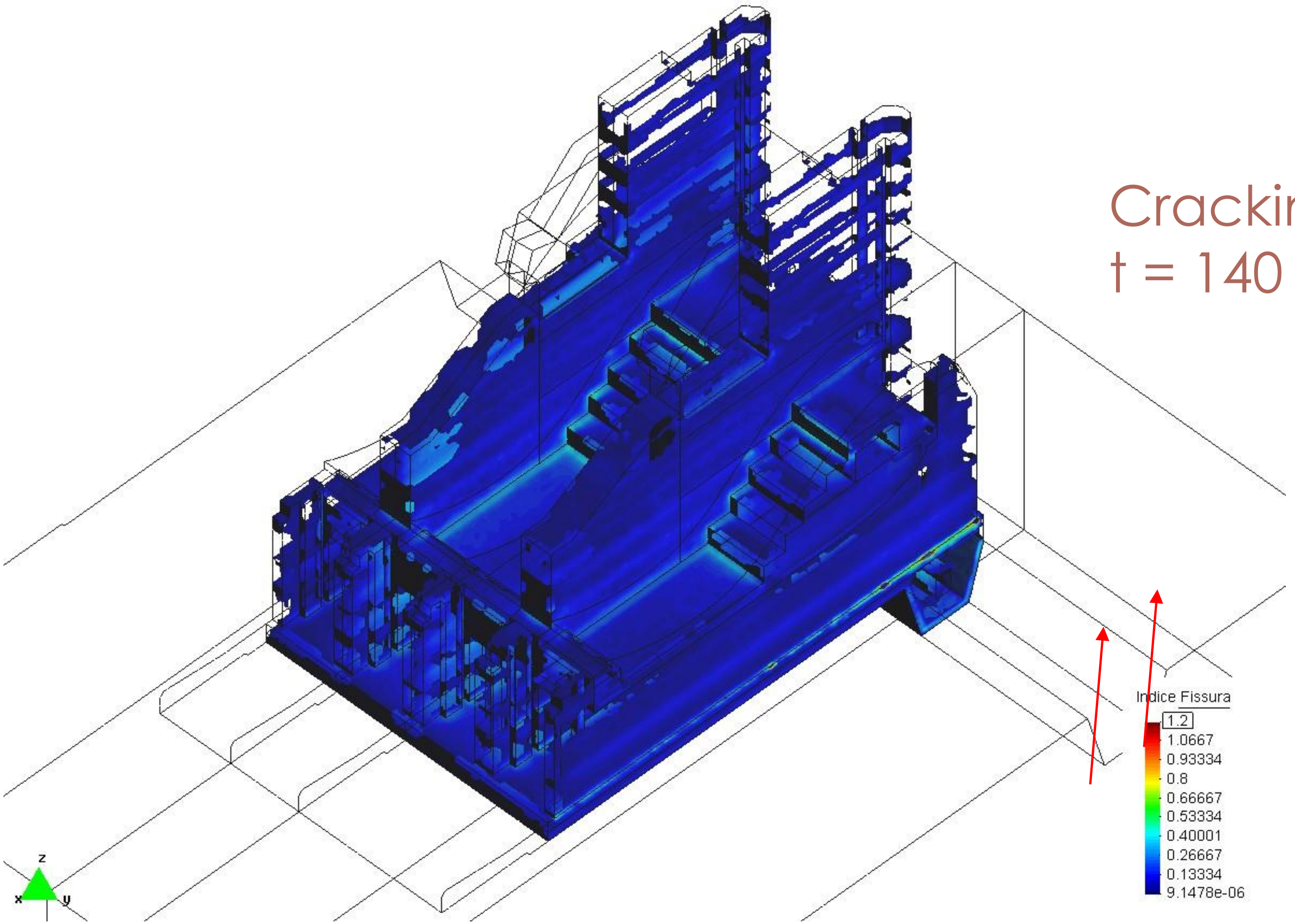

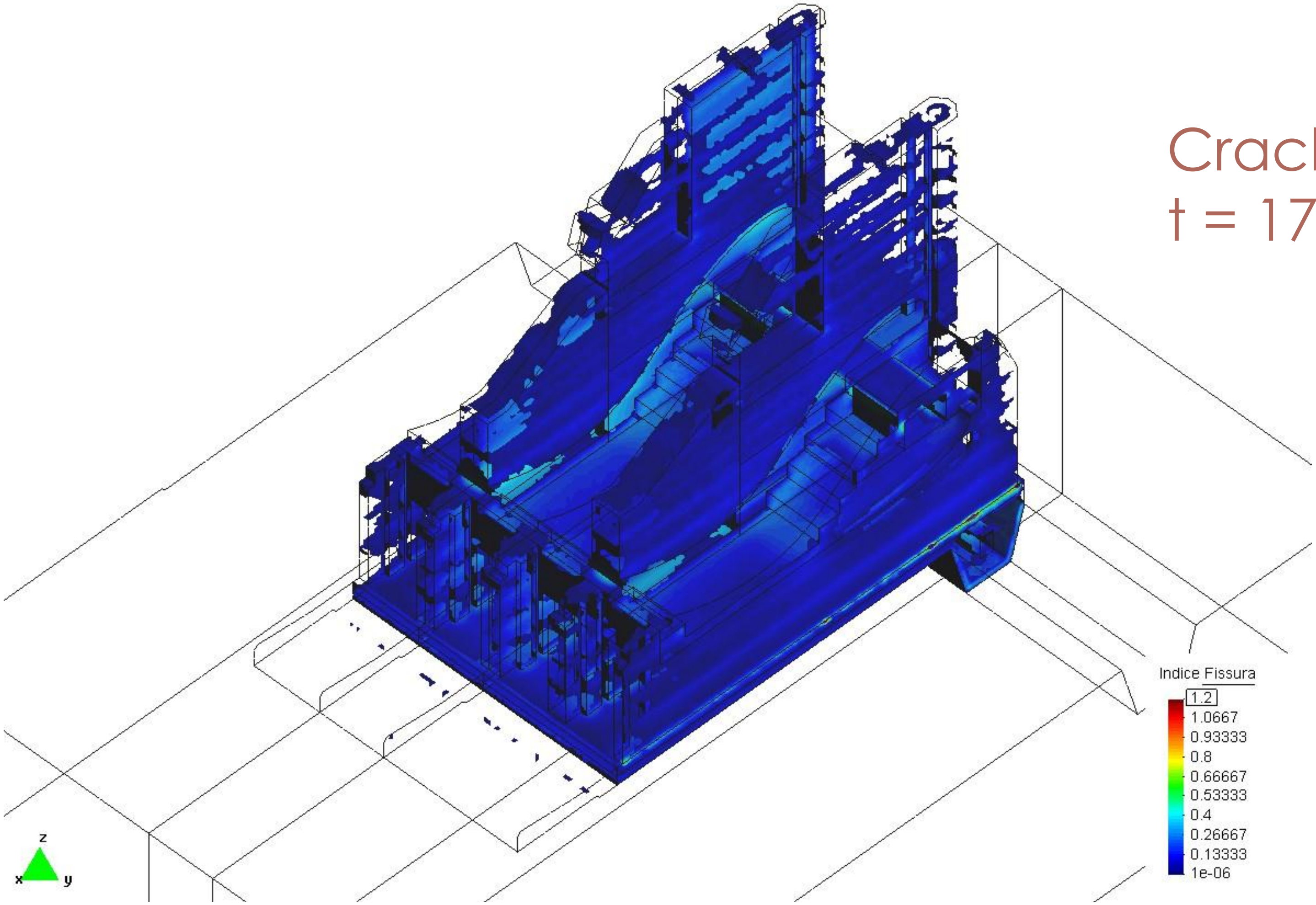

Cracking index
t = 175 days

Histogram of cracking index

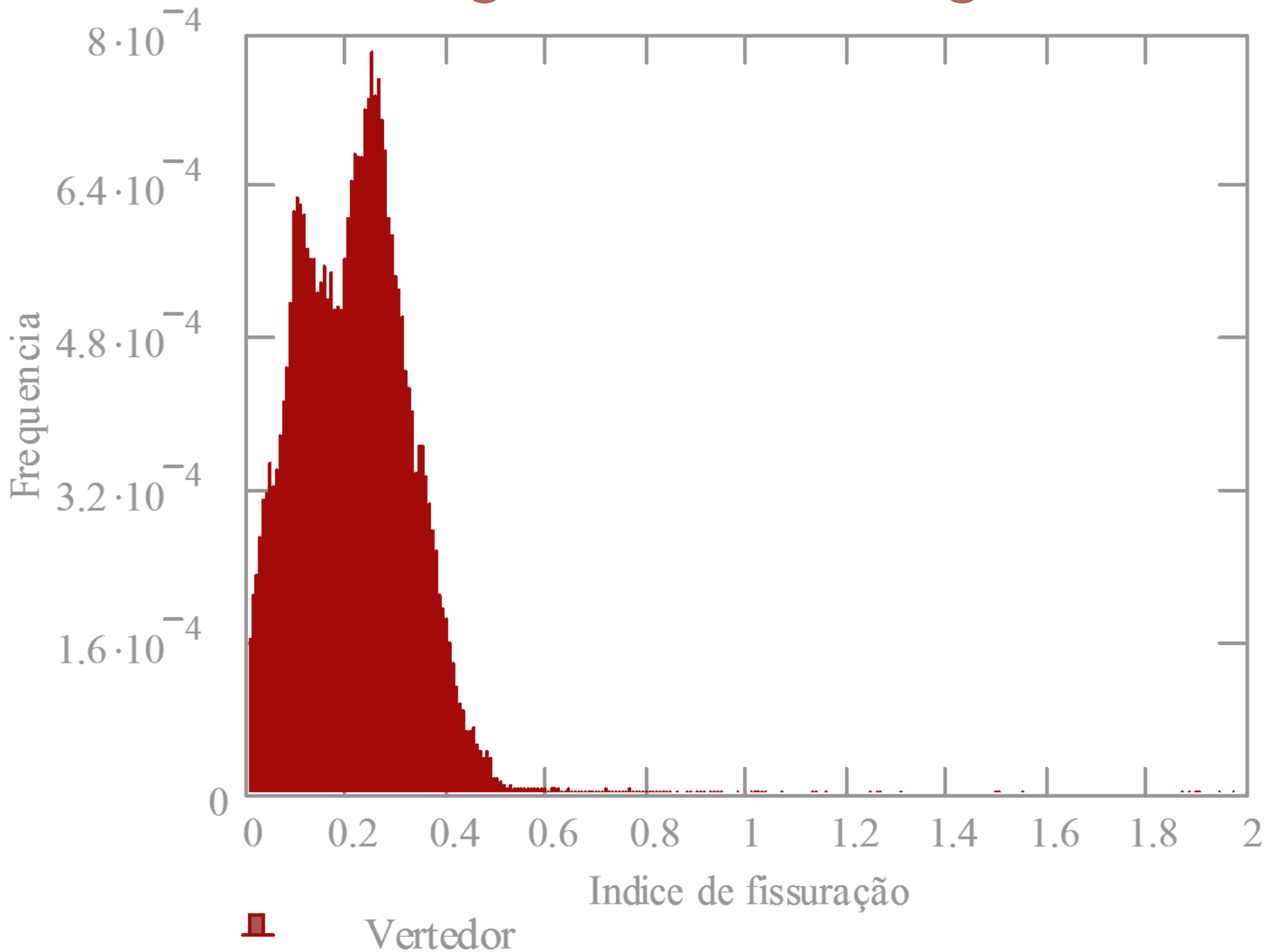

Case study 4
Tocoma dam Venezuela

Determination of the adiabatic temperature rising by inverse analysis

Fitting of adiabatic temperature rising curves

$$\Delta T^{ad} = \Delta T^{ad}_{max} \frac{t^n}{k^n + t^n}$$

Variables: $\mathbf{x}^T = \{x_1, x_2, x_3\} = \{T^\infty, k, n\}$

Fitness function: $F(\mathbf{x}) = ET(\mathbf{x})$

$$ET(\tilde{\mathbf{x}}) = \frac{\sum_{p=1}^{np} E_p(\tilde{\mathbf{x}})}{np} \qquad E_p(\tilde{\mathbf{x}}) = \frac{\sum_{i=1}^{n} \left| T_{p,meas}(t_i) - T_{p,comp}(\tilde{\mathbf{x}}, t_i) \right|}{nt}$$

Optimization problem:

Find **x** that minimizes F(**x**)

FEM analysis
temperatures measured in the field

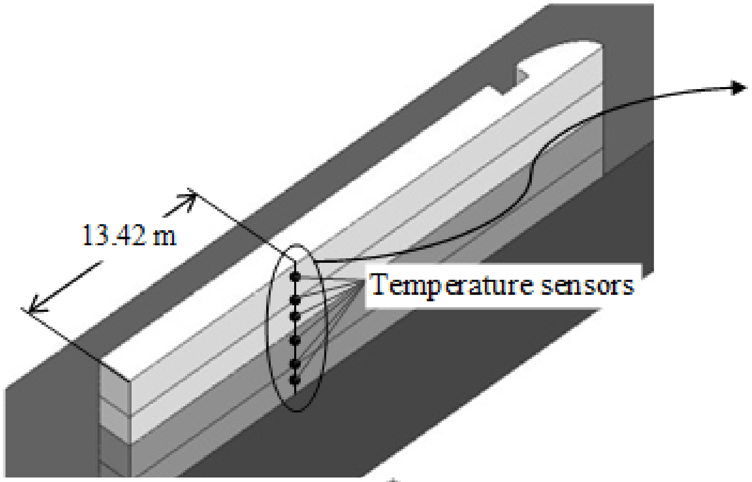

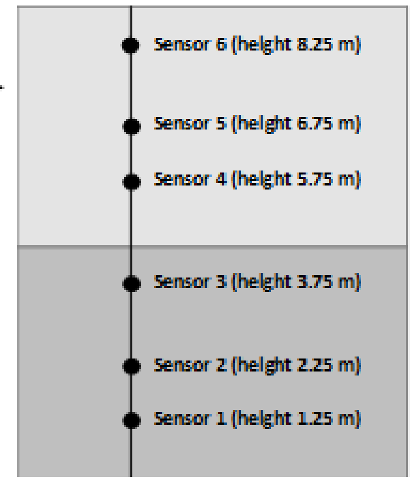

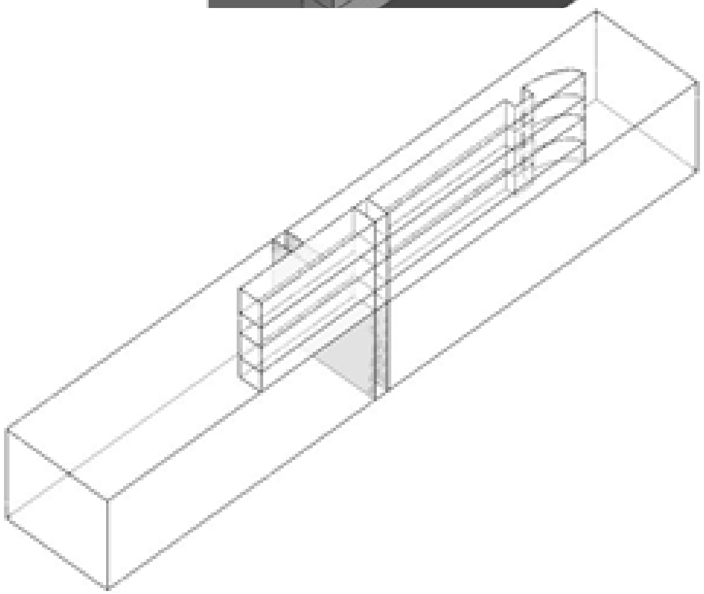

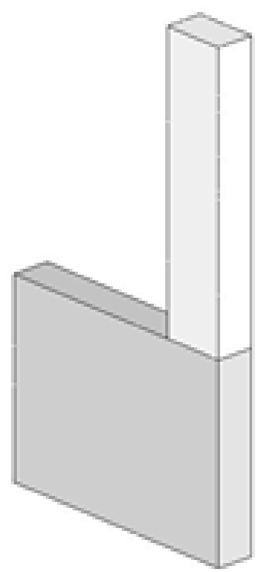

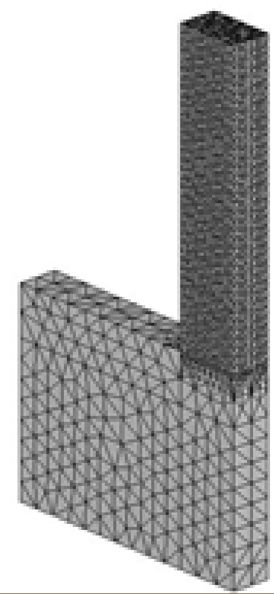

Determination of adiabatic temperature rise curve

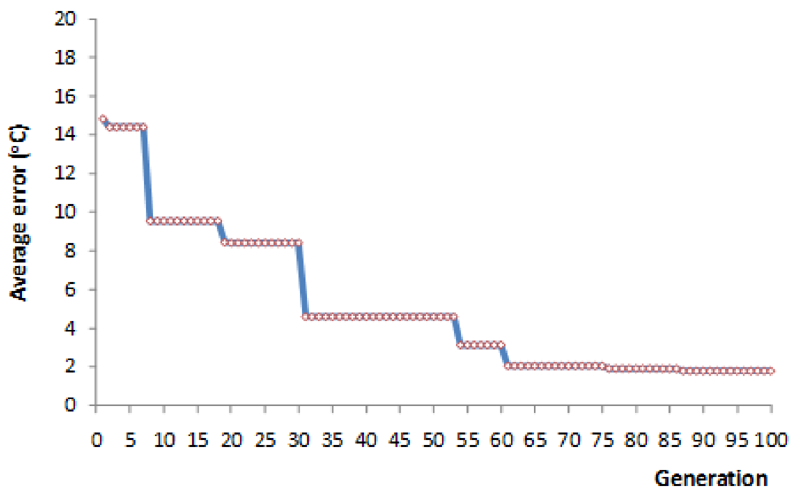

Evolution of algorithm

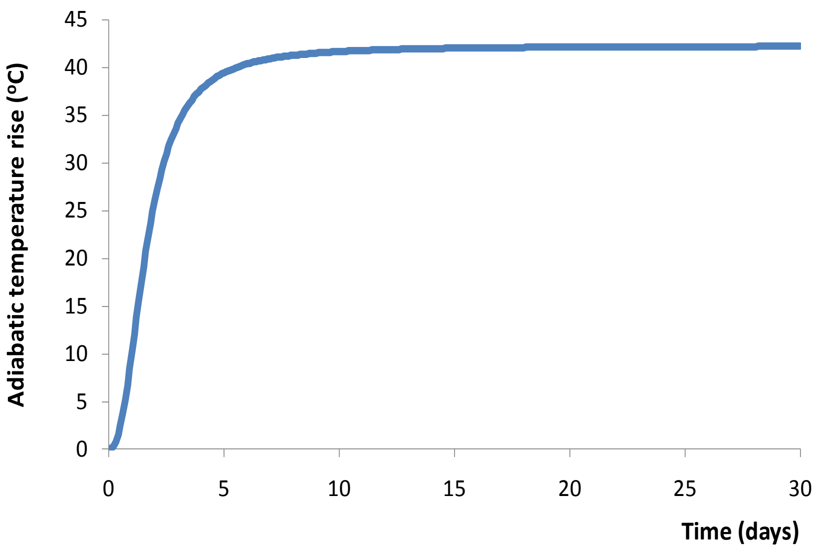

Adiabatic temperature rise curve

Comparison of measured and calculated temperatures, P1

Verification

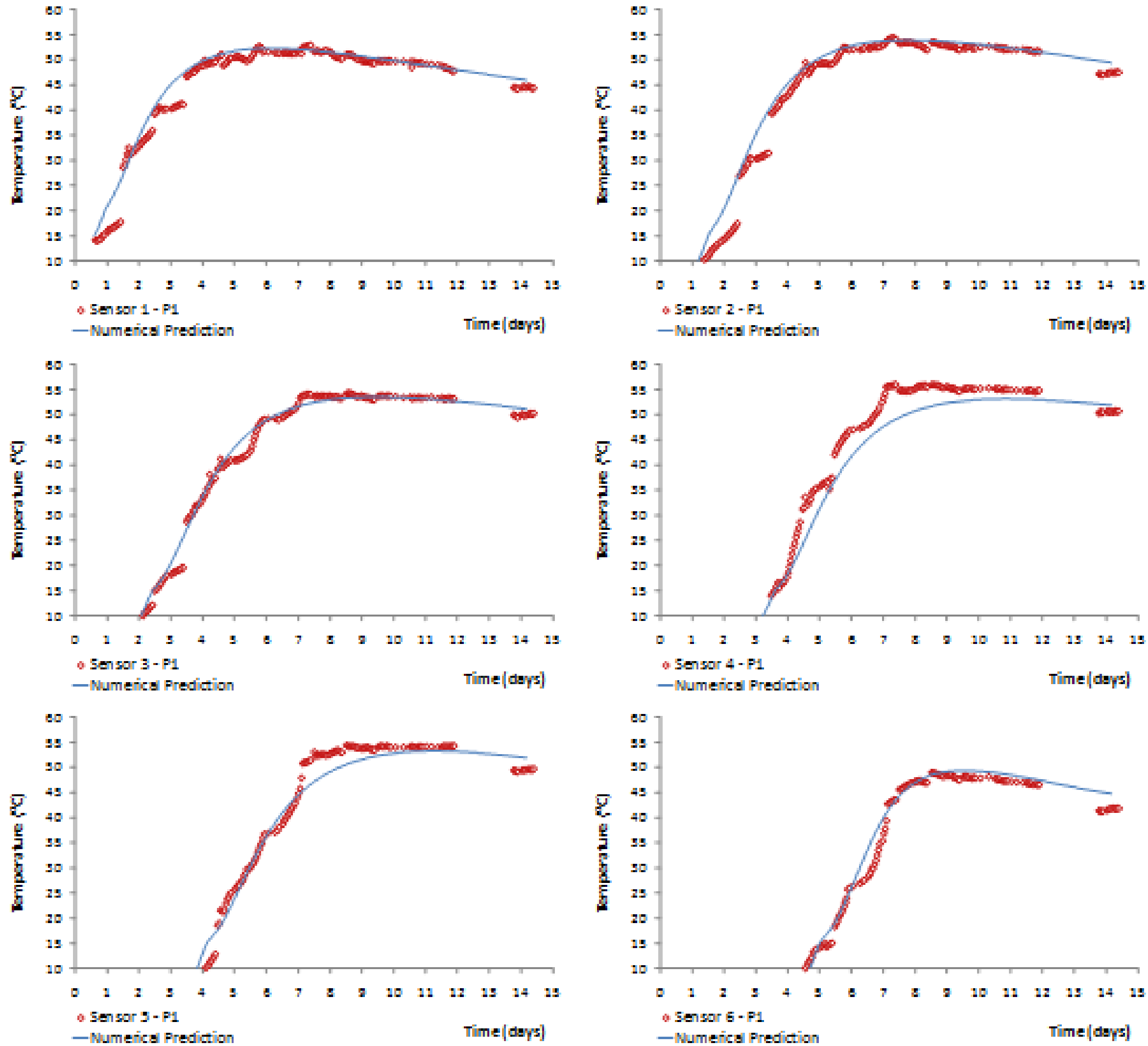

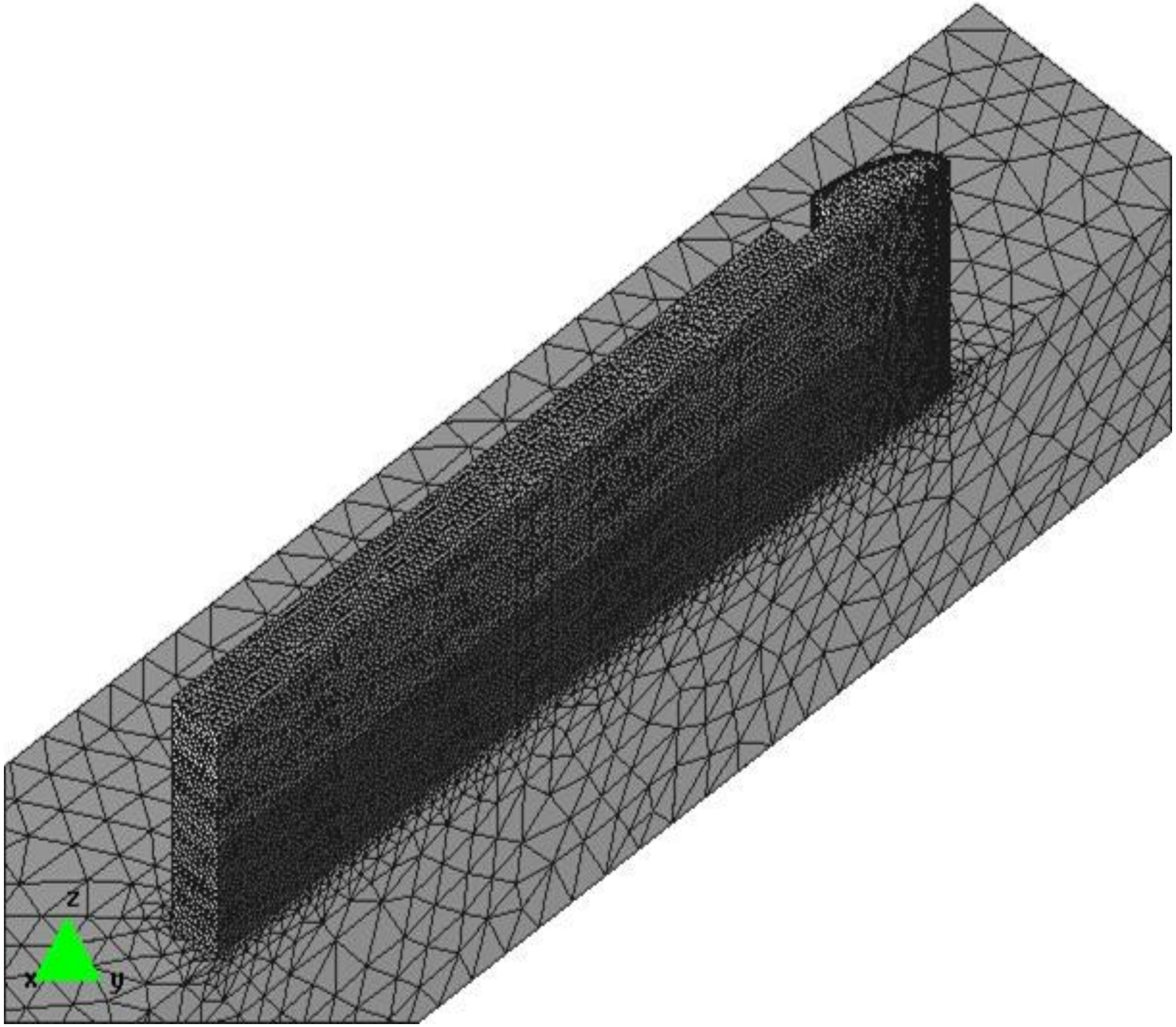

Construction of P2 with different pace than P1

Forecasting

Comparison of measured and calculated temperatures, P2

Forecasting

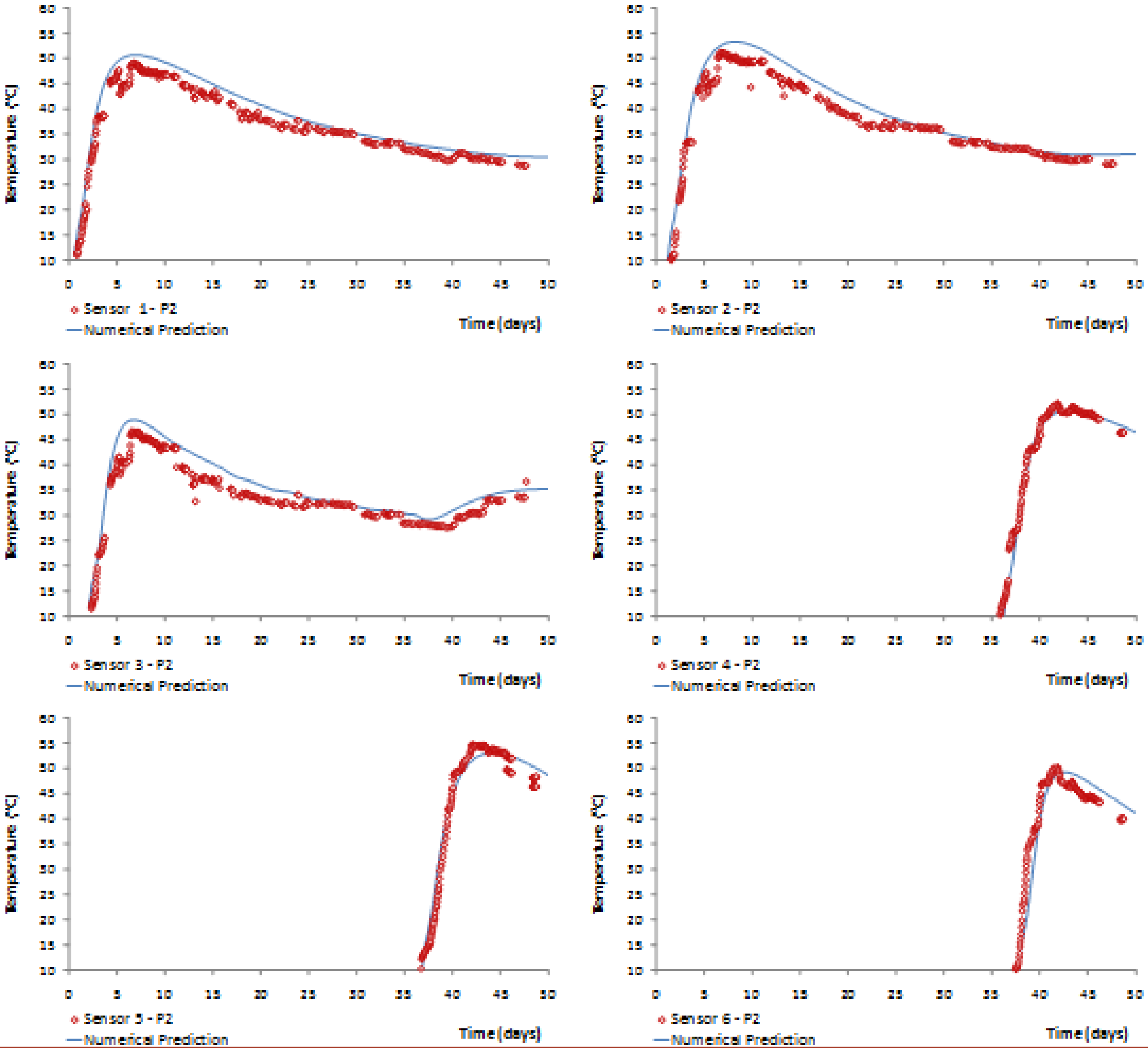

Case study 5
Tocoma dam Venezuela

Analysis of post cooling system and sliding formwork

Tocoma – Spillway gate pier

approximately 33 m height

Simplified model of the gate pier:

114.943 nodes

610.931 elements

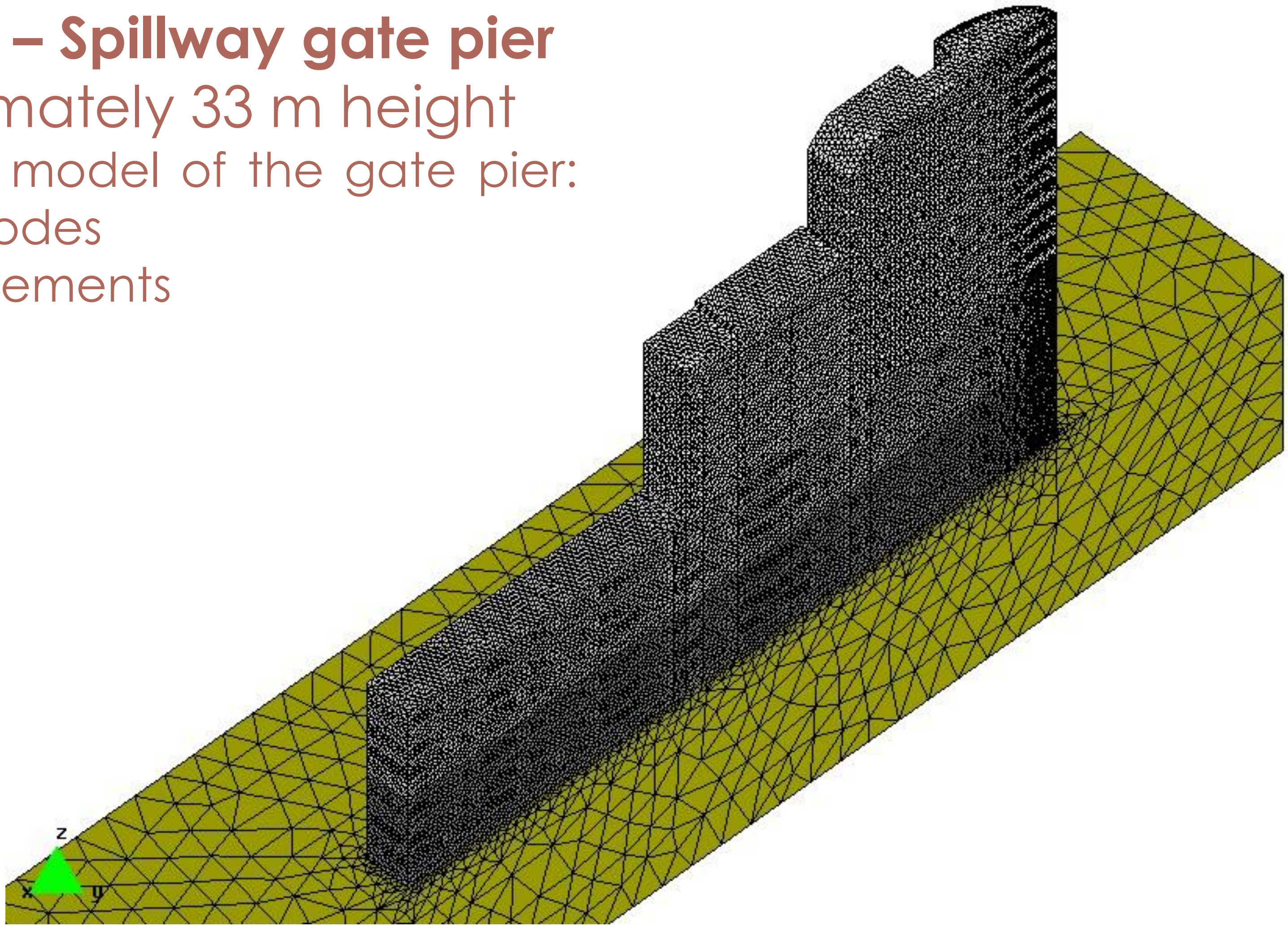

Materials properties

Property	Concrete
k (J /(m.s.K))	2,700
C_ε (J/(kg.K))	1140
Ea/R (K)	4000
γ (kg/m^3)	2330
α (K^{-1})	$9{,}06 \cdot 10^{-6}$
ξ_0	0,15
ε^{RA}	$0 \text{ se } 0 \le \xi < \xi_0$ $50 \cdot 10^{-6} \frac{\xi - 0{,}1}{1 - 0{,}1} \text{ if } \xi_0 \le \xi \le 1$
E (MPa)	$0 \text{ se } 0 \le \xi < \xi_0$ $33.672 \left(\frac{\xi - \xi_0}{1 - \xi_0} \right)^1 \text{ if } \xi_0 \le \xi \le 1$
f_{ct}(MPa)	$0 \text{ se } 0 \le \xi < \xi_0$ $3{,}4 \left(\frac{\xi - \xi_0}{1 - \xi_0} \right)^1 \text{ if } \xi_0 \le \xi \le 1$
ν	$0 \text{ se } 0 \le \xi < \xi_0$ $0{,}2 \text{ se } \xi_0 \le \xi \le 1$

Age (days)	Compressive strength fc (MPa)	Tension strength fct (MPa)	Young´s modulus E (MPa)
3	12.1	1.9	15,200
7	17.6	2.3	26,900
28	30.1	3.1	30,700
90	33.9	3.4	33,700

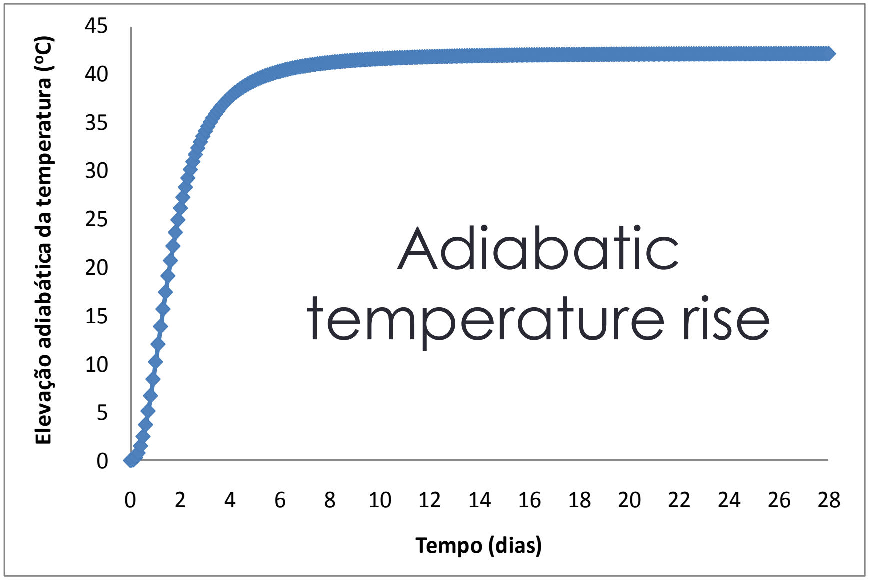

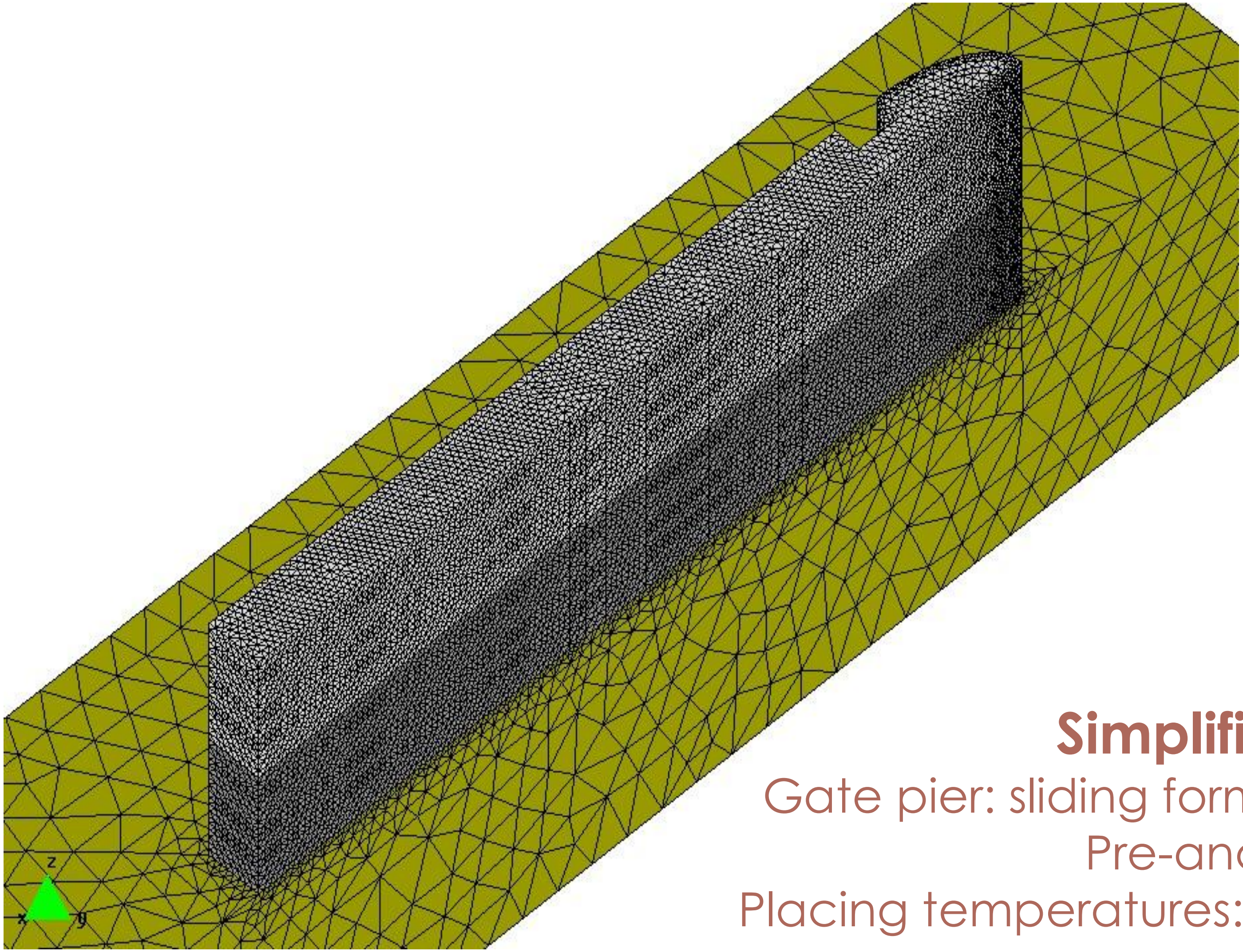

Simplified FEM model

Gate pier: sliding formwork 10cm/hour

Pre-analysis: initial 9.0 m

Placing temperatures: 20°C; 15°C; 10°C

Simplified FEM model

Gate pier : sliding formwork 10cm/hour
Pre-analysis: initial 9.0 m
Placing temperatures: 20°C; 15°C; 10°C

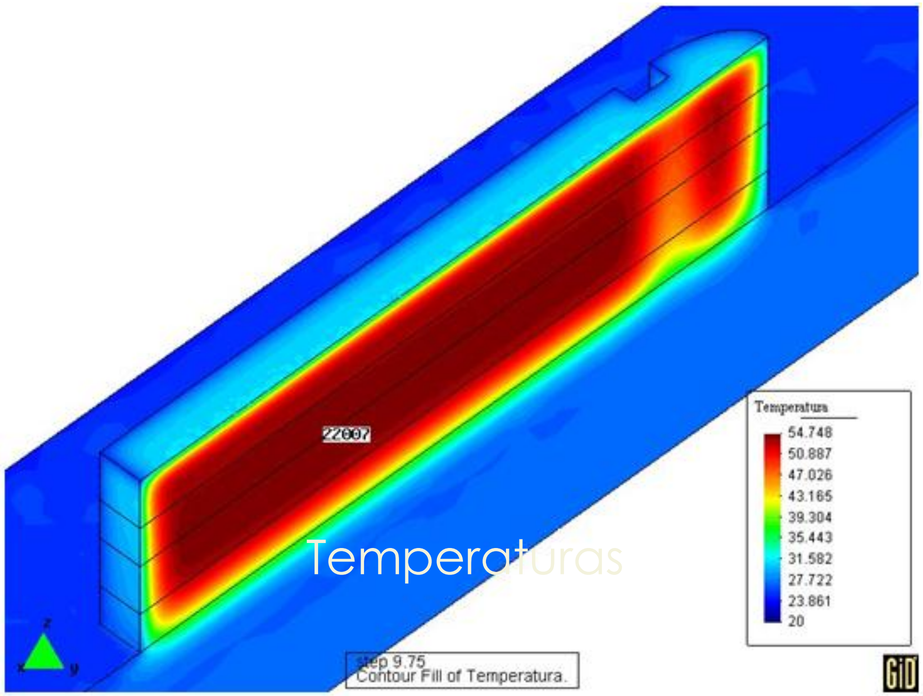

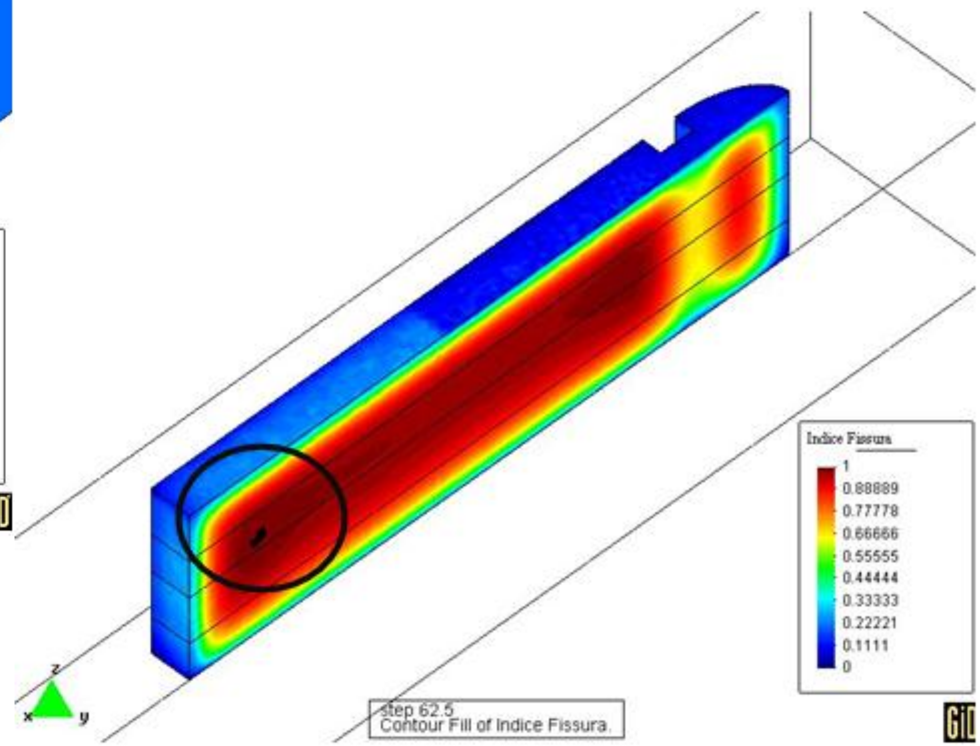

Indice de fissuração

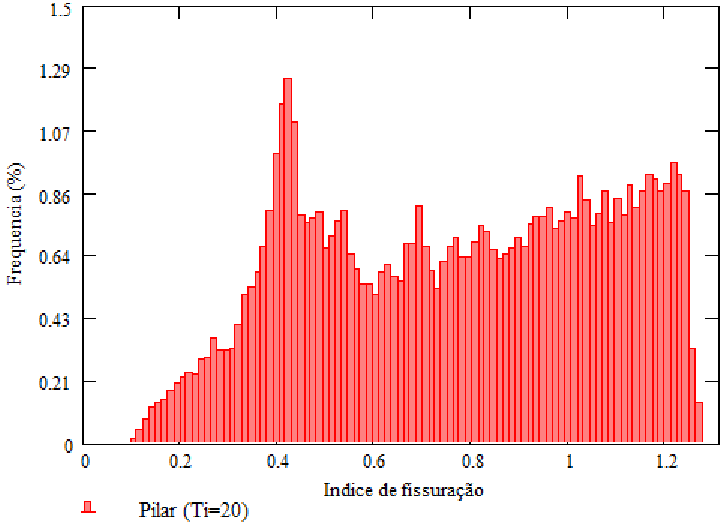

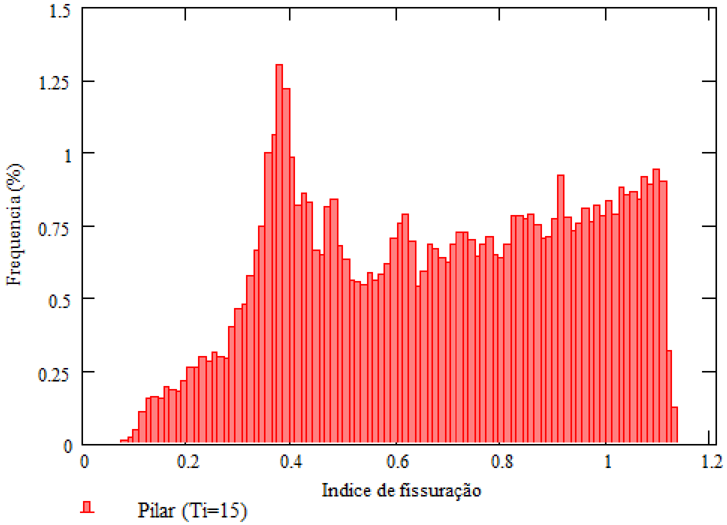

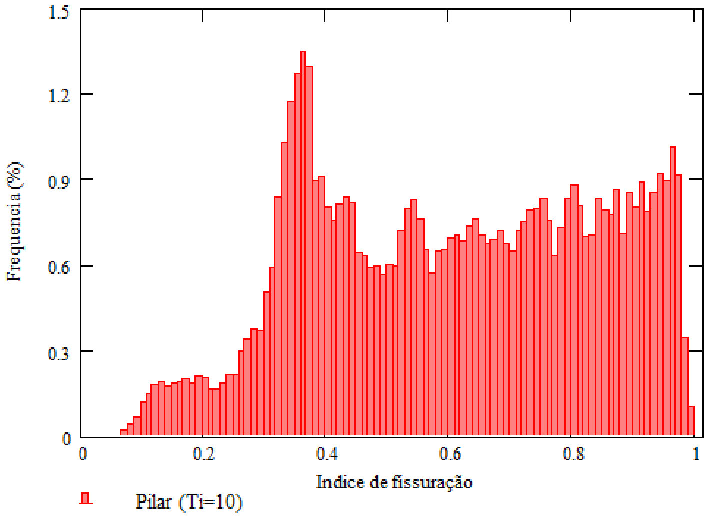

Cracking index histograms

Post-cooling system

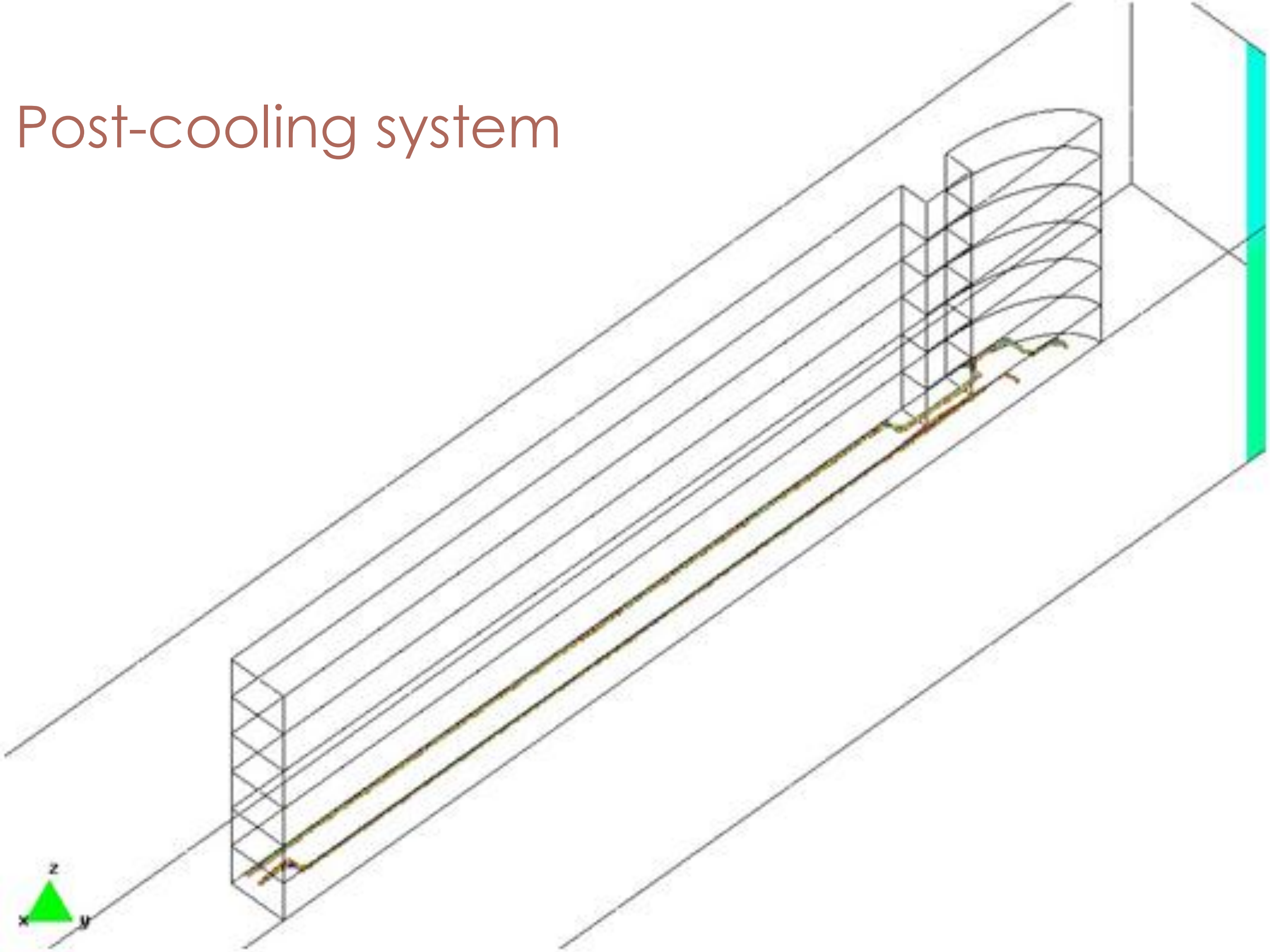

Post-cooling system

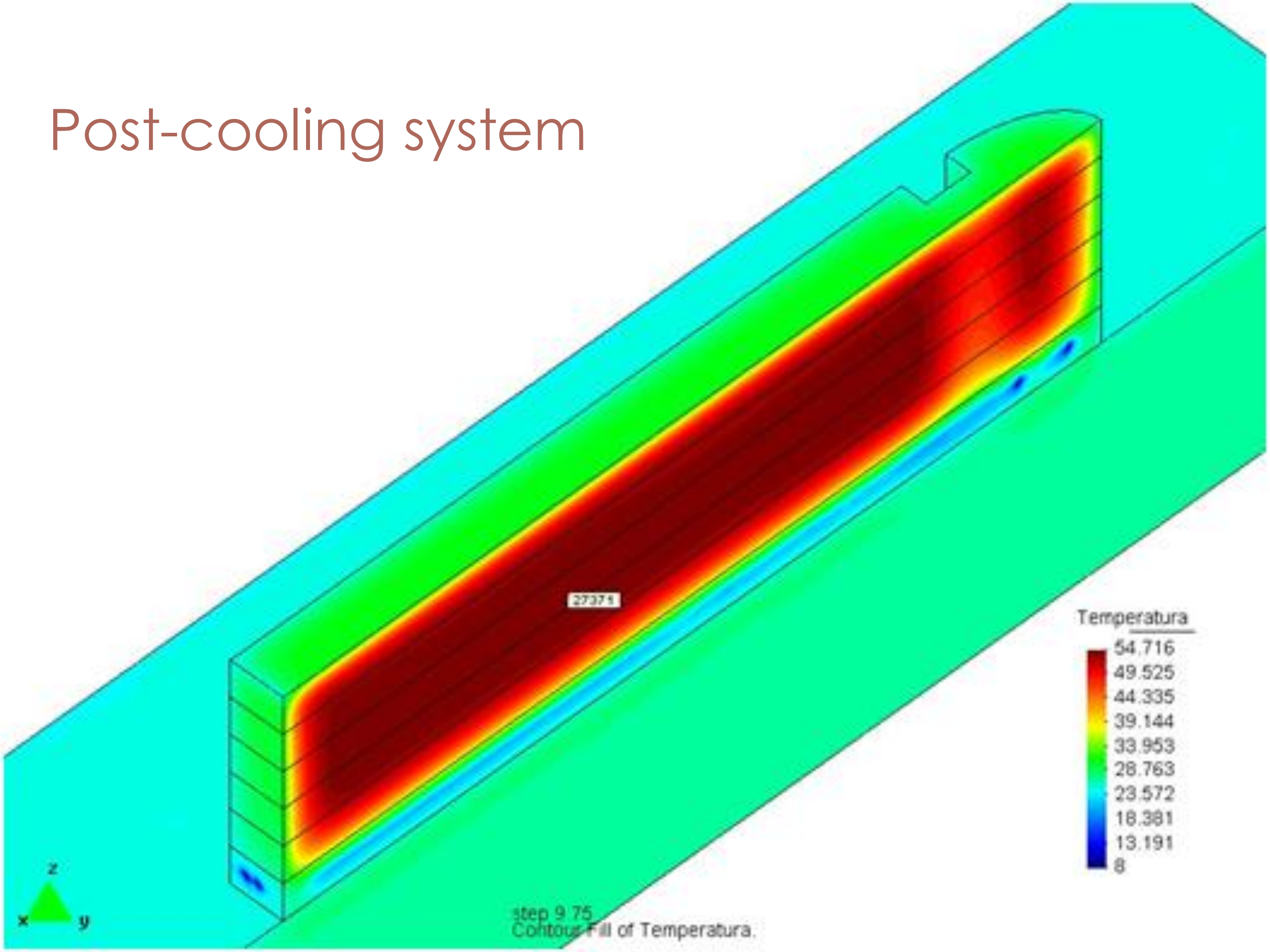

Case studies

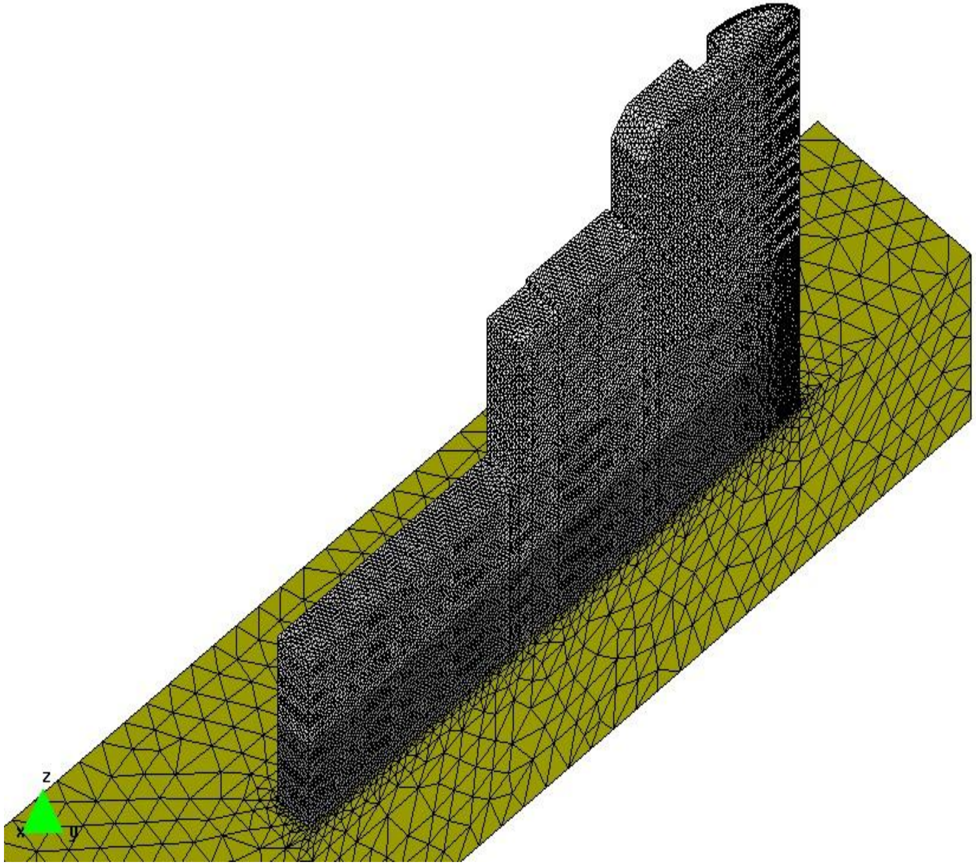

Placing temperature (°C)	Post-cooling temperature (°C)
10	10
10	20
15	10
15	20
20	10
20	20

Principal tensile stresses at control nodes: PT=10°C; PCT=10°C

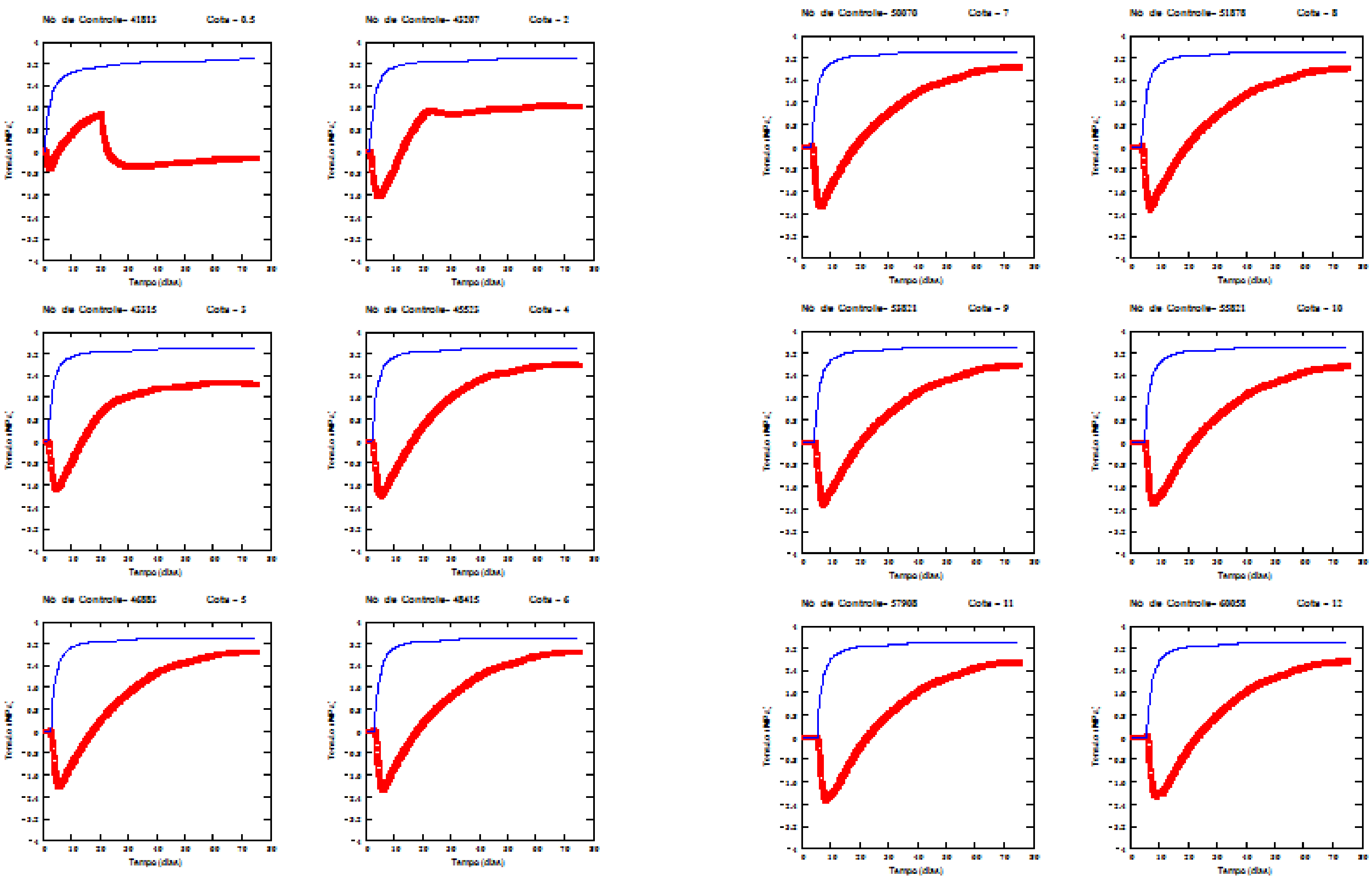

Principal tensile stresses at control nodes: PT=20°C; PCT=20°C

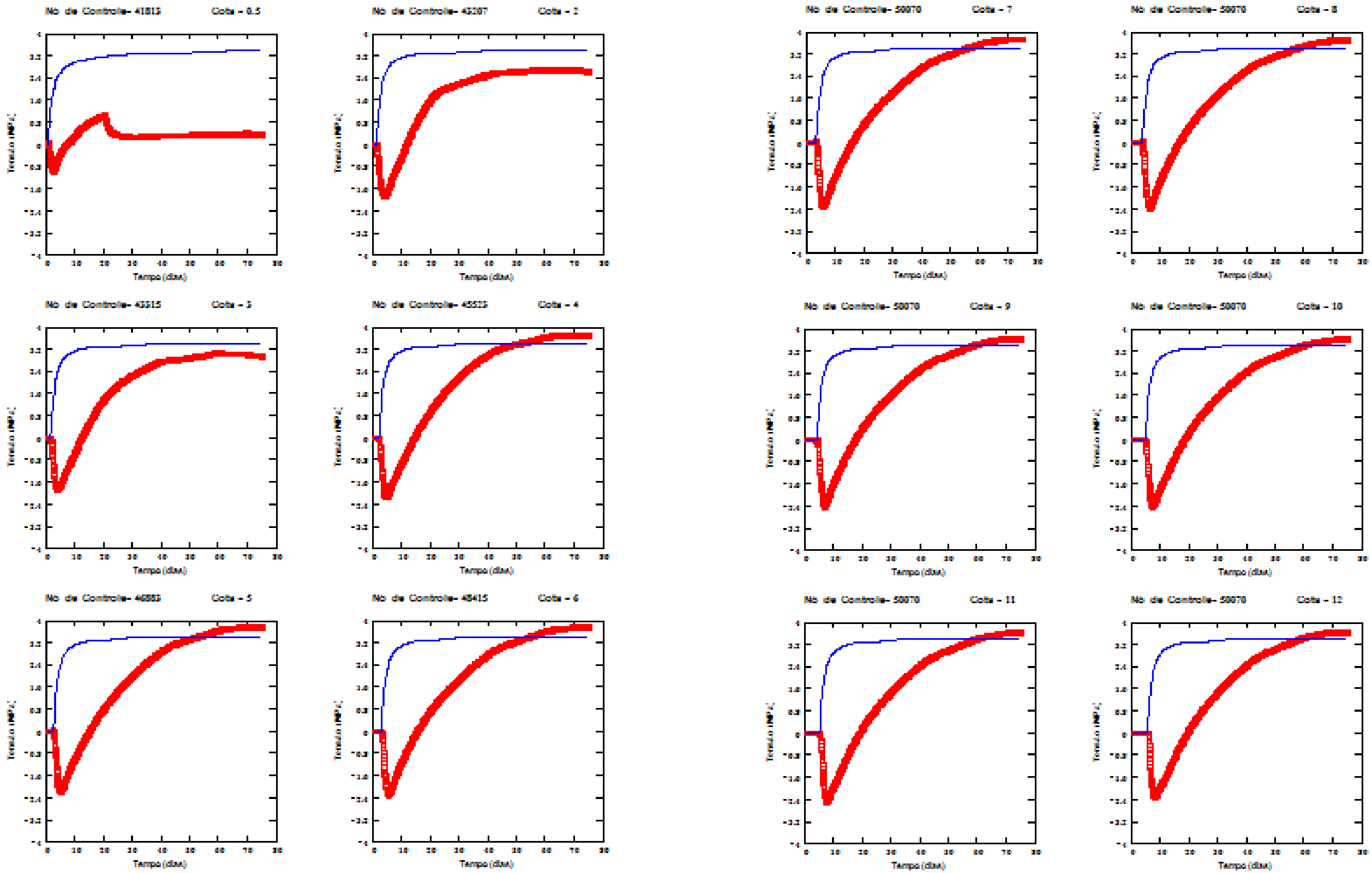

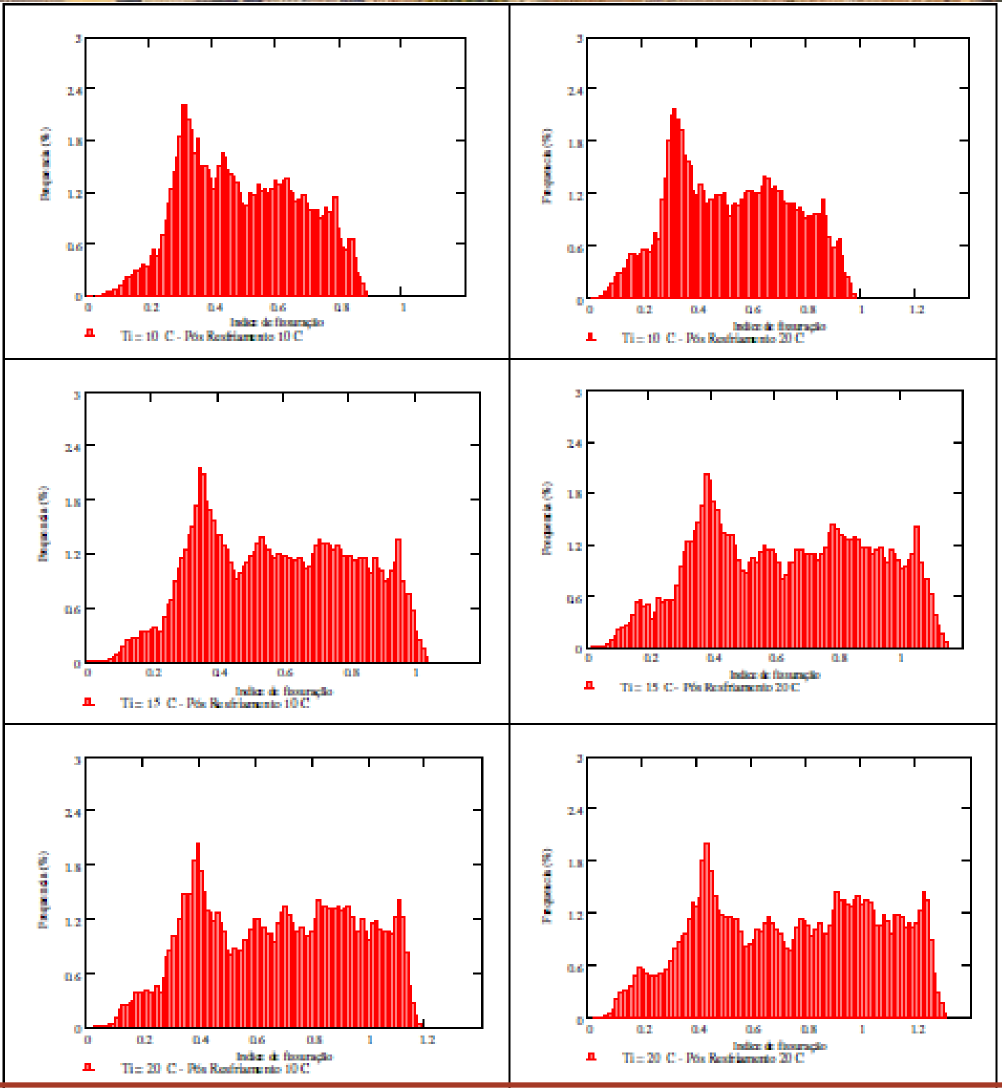

Histograms of cracking indexes

The post-cooling system implemented in Tocoma: 35 days for the cosntruction of the pier instead of 118 days with the traditional formwork.

Geominas, vol. 37, no. 8, 2009

Case study 5
Tocoma dam Venezuela

Other studies

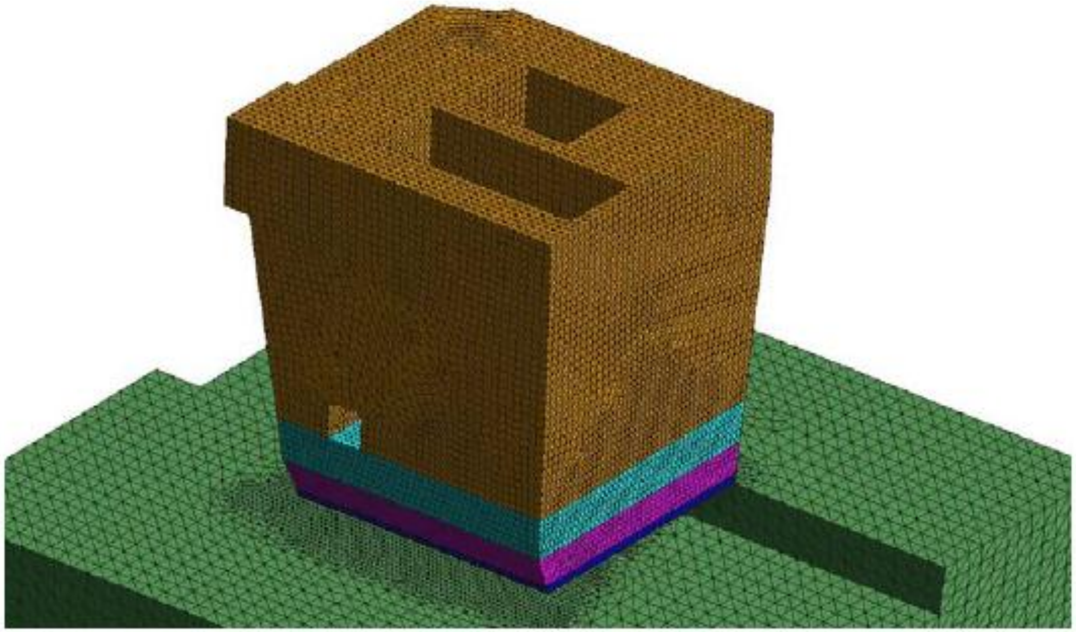

Sink:
1.007.194 elements
178.660 nodes

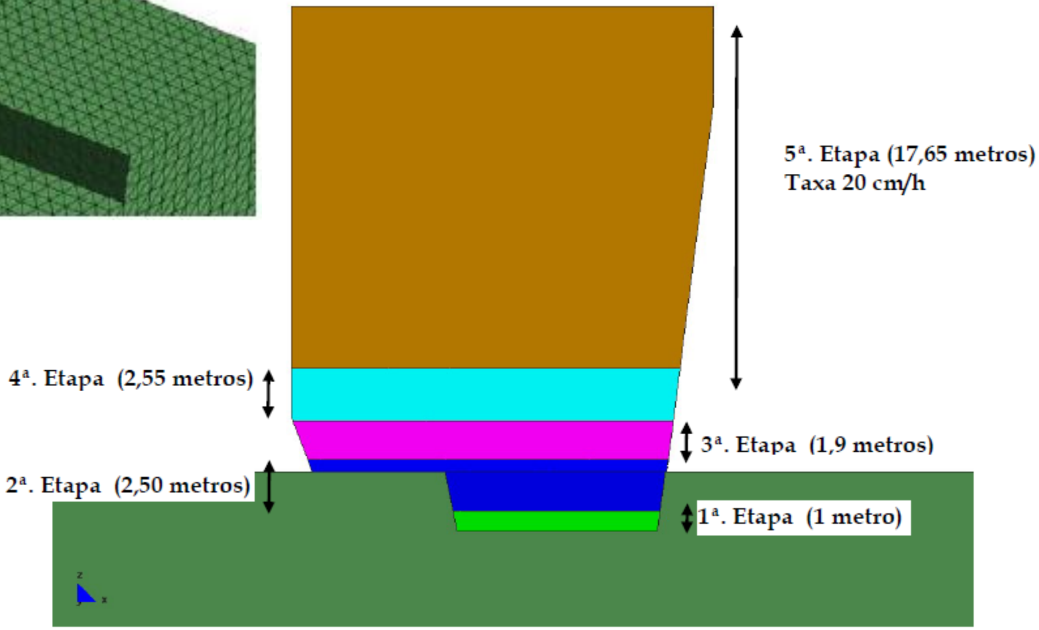

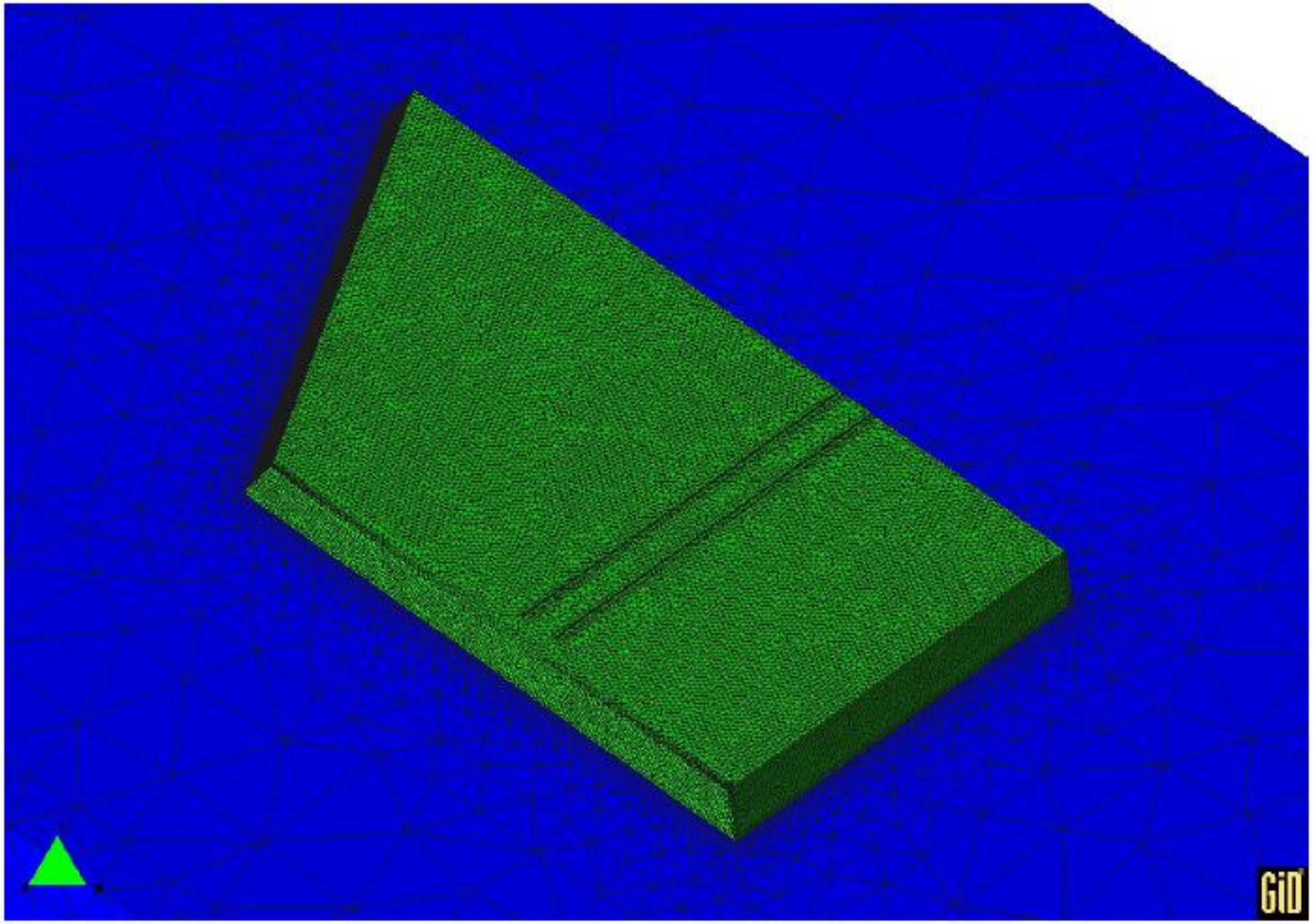

Monolith #02
3 initial layers
1.893.713 el.
331.693 nodes

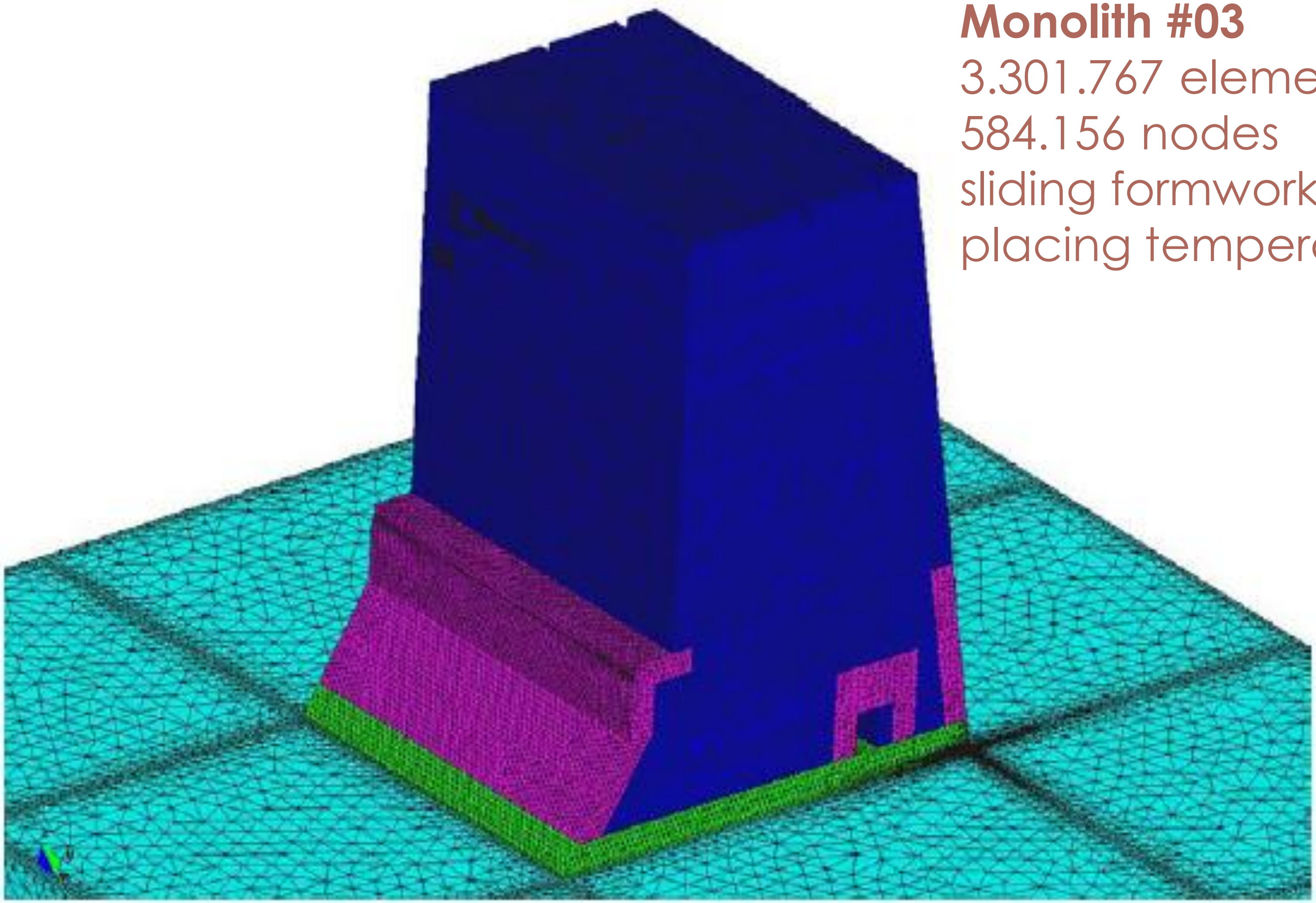

Monolith #03

3.301.767 elements

584.156 nodes

sliding formworks (20 cm/hour)

placing temperature 25°C

Case study 6
Angra III nuclear power plant
Rio de Janeiro, Brazil

Foundation of auxiliary building

Agra III nuclear power plant

Agra III nuclear power plant

Agra III nuclear power plant
Slab foundation h = 1.80 m

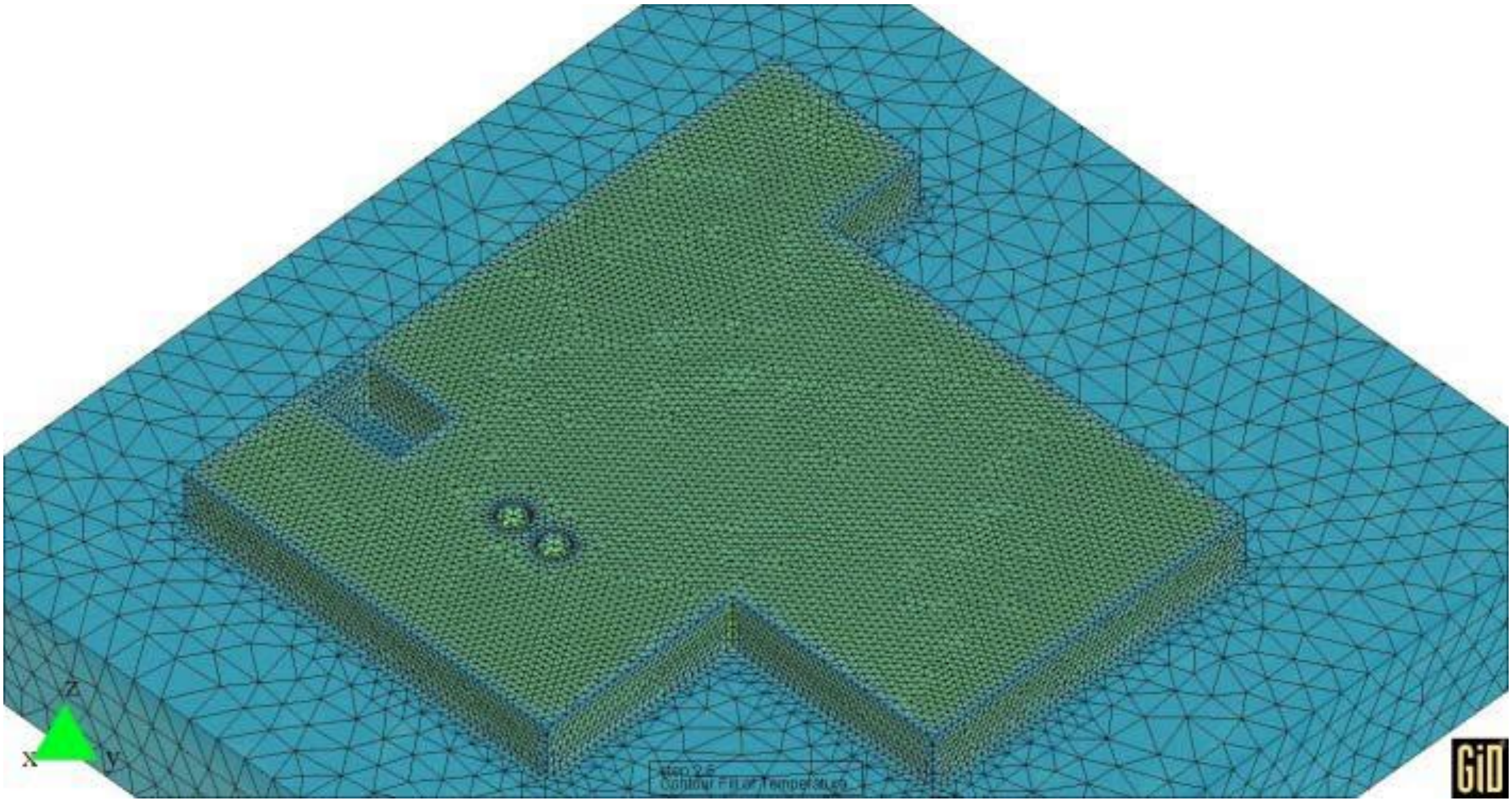

Slab foundation h = 1.80 m

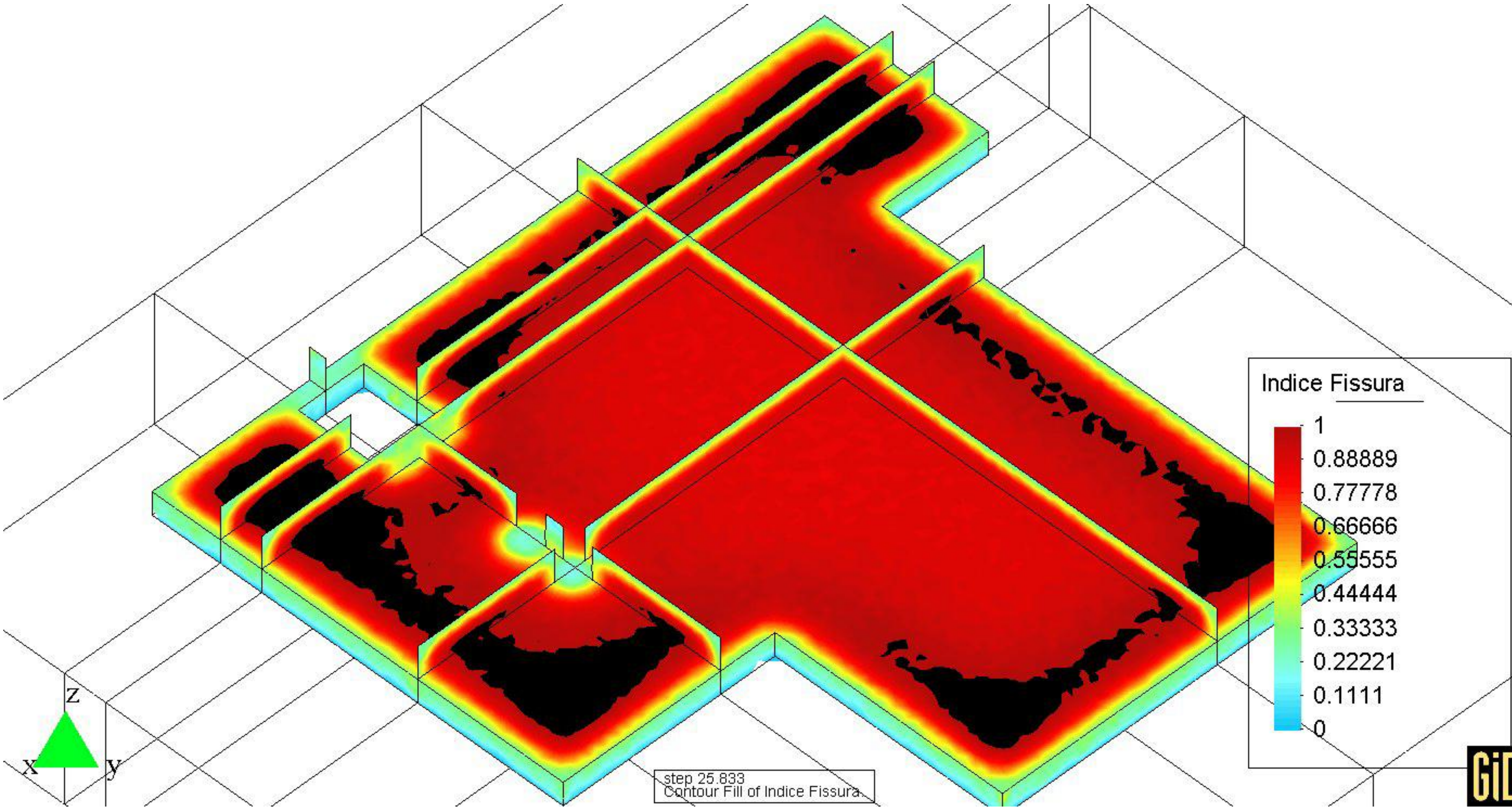

Cracking index for placing temperature = 12°C

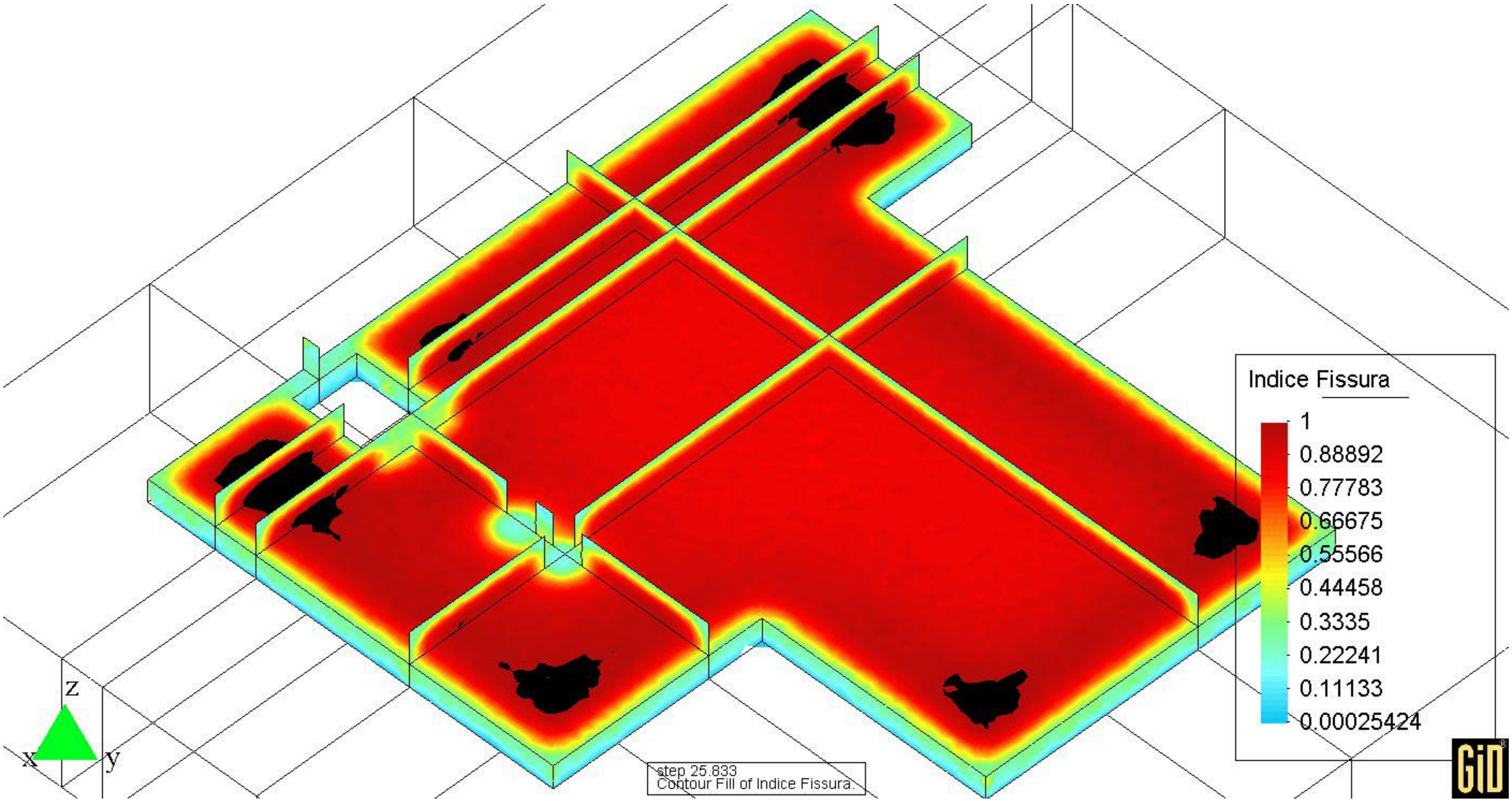

Cracking index for placing temperature = 11°C

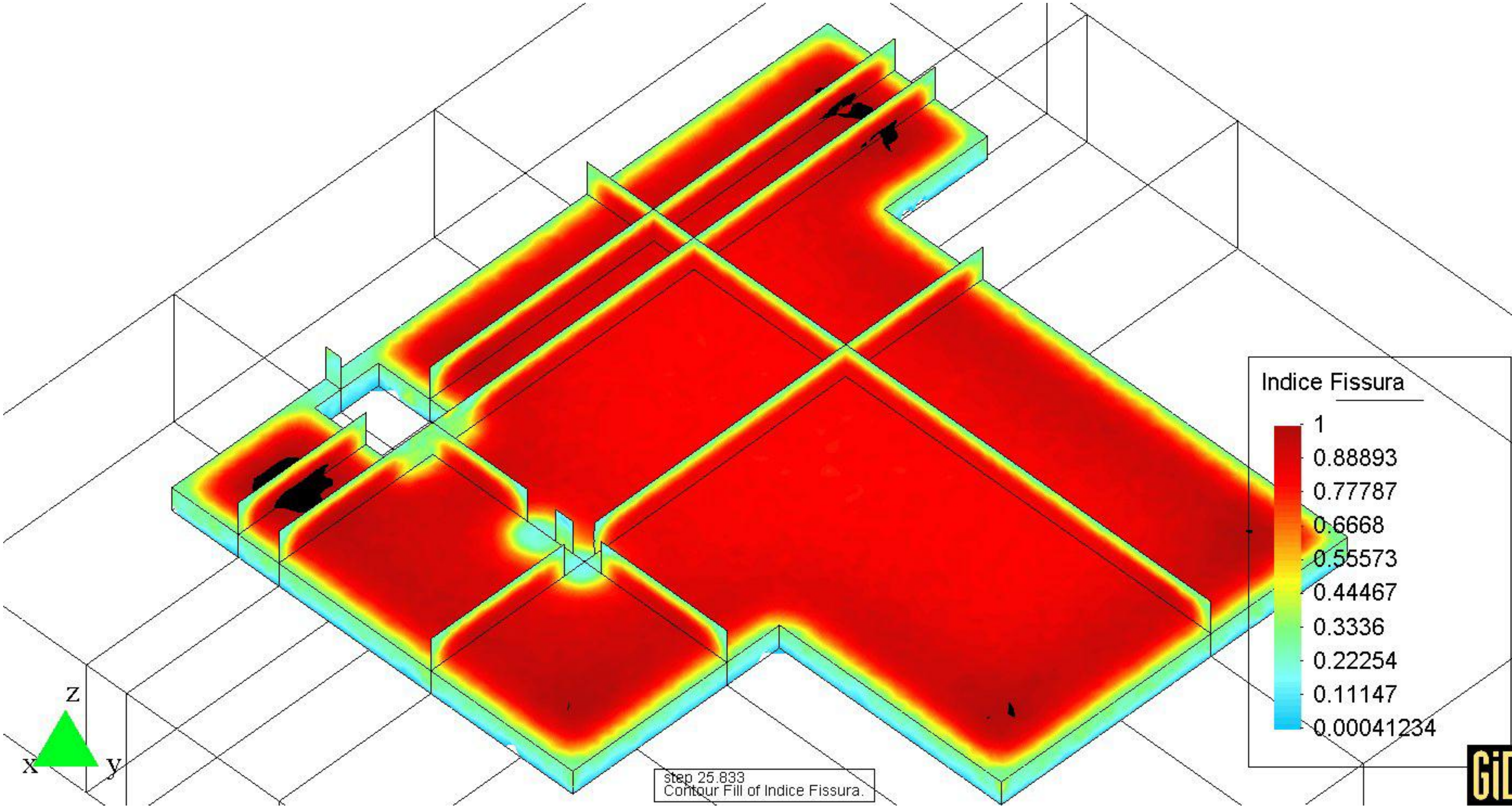

Cracking index for placing temperature = 10°C

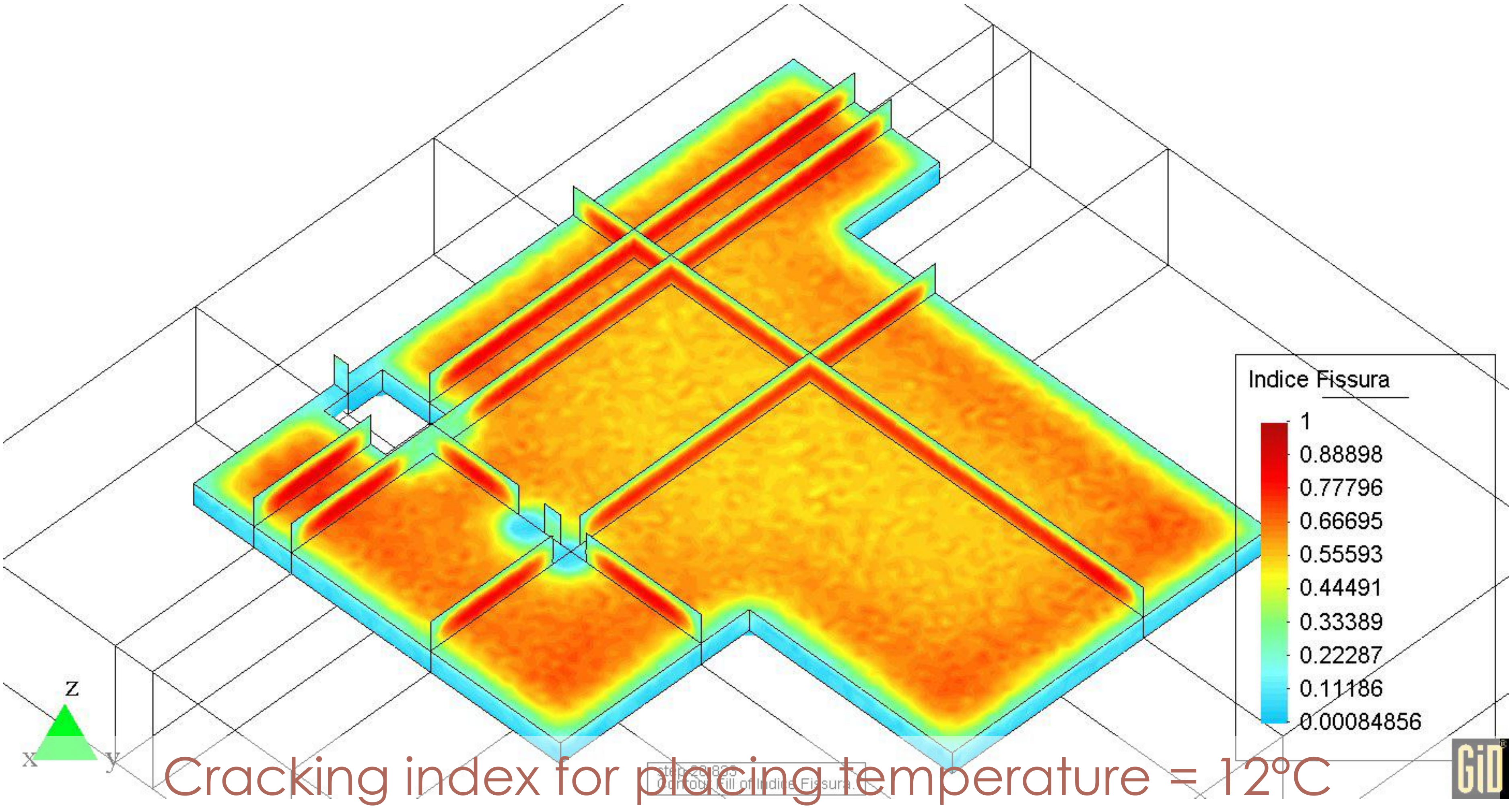

Cracking index for placing temperature = 12°C

in 2 layers, 3days delay between layers

Case study 7
Angra III nuclear power plant
Rio de Janeiro, Brazil

Reactor dome

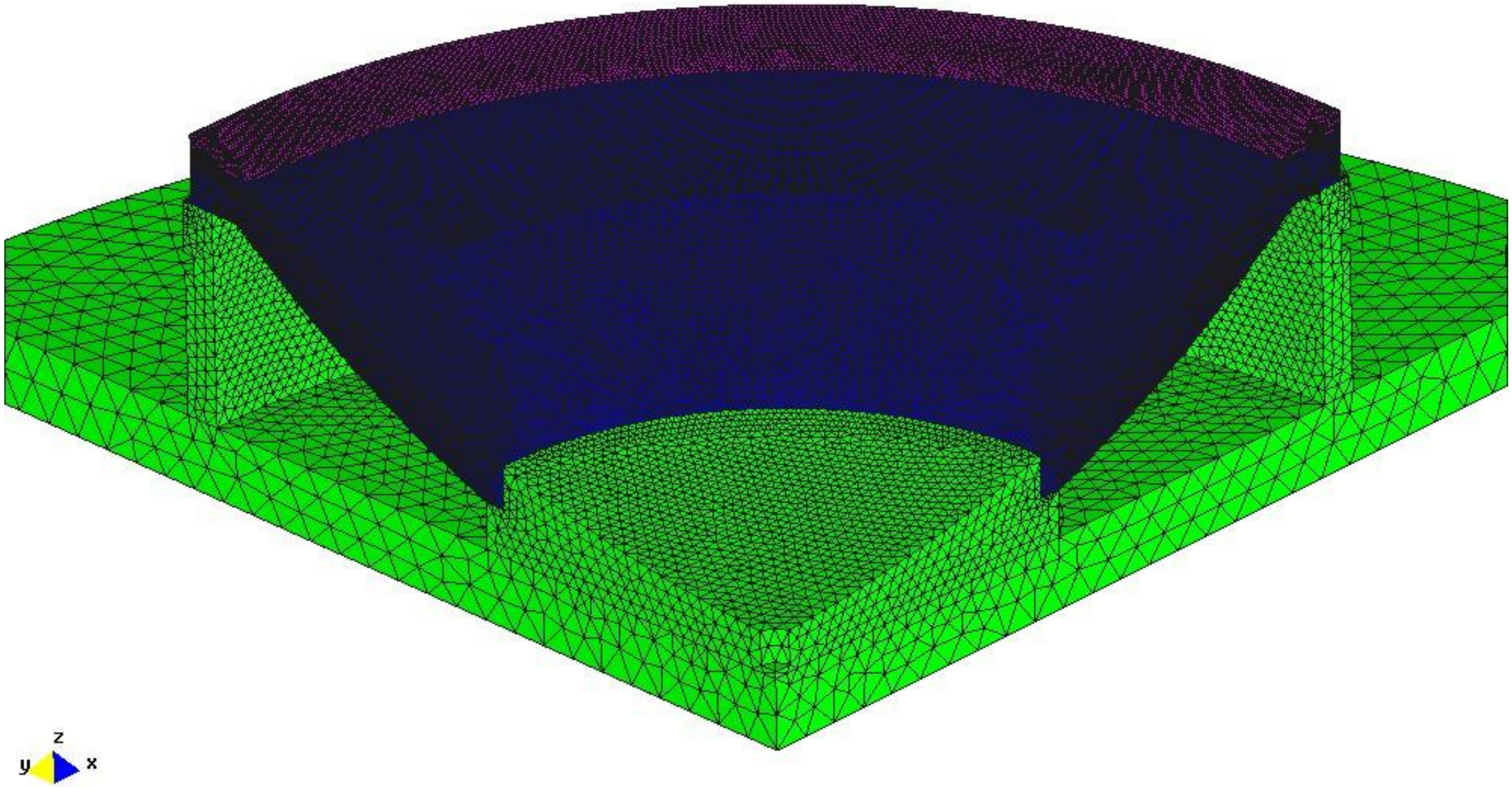

Mesh: 2.233.880 elements e 404.129 nodes

Construction with 2 layers

Mesh - detail

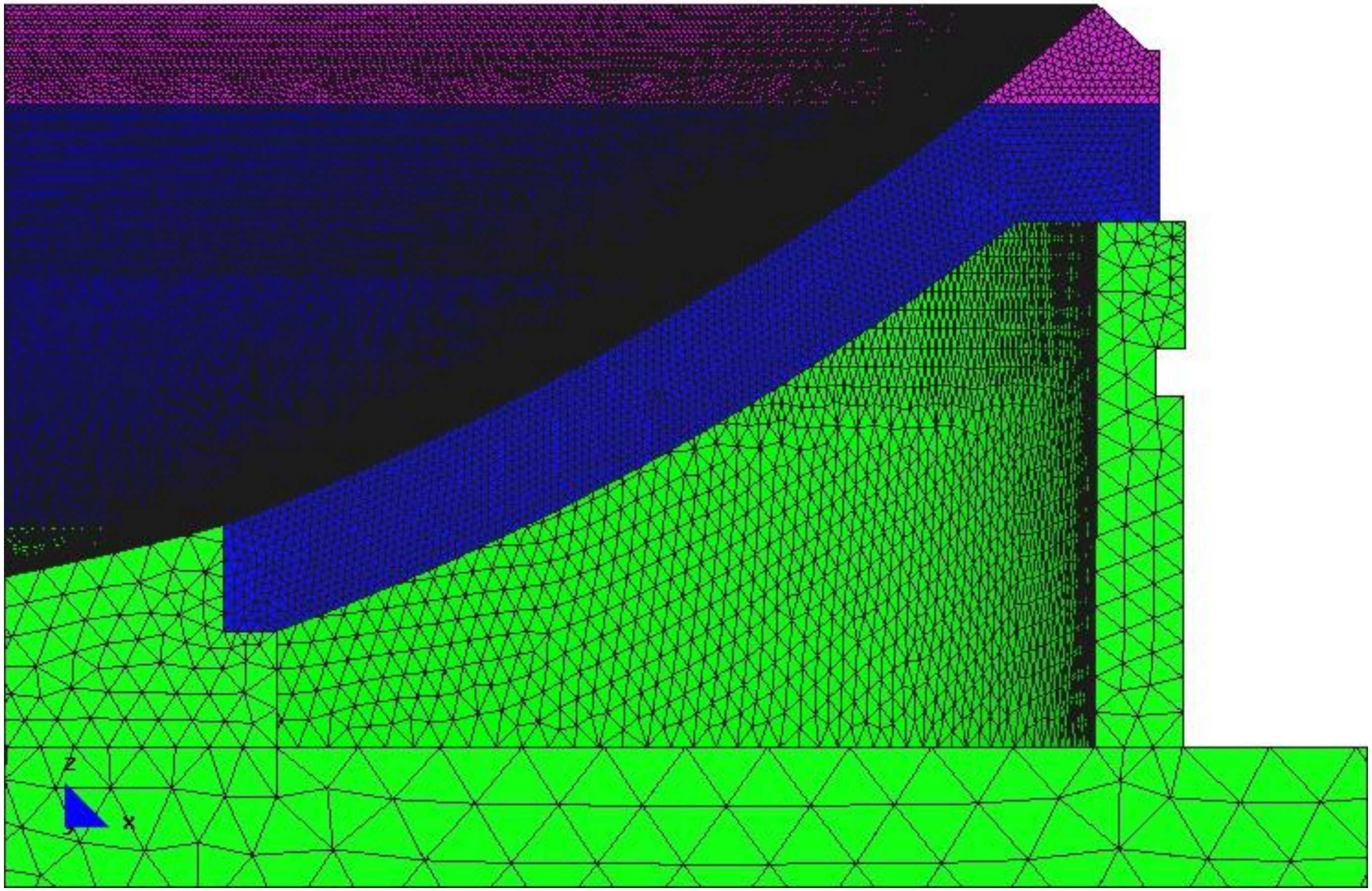

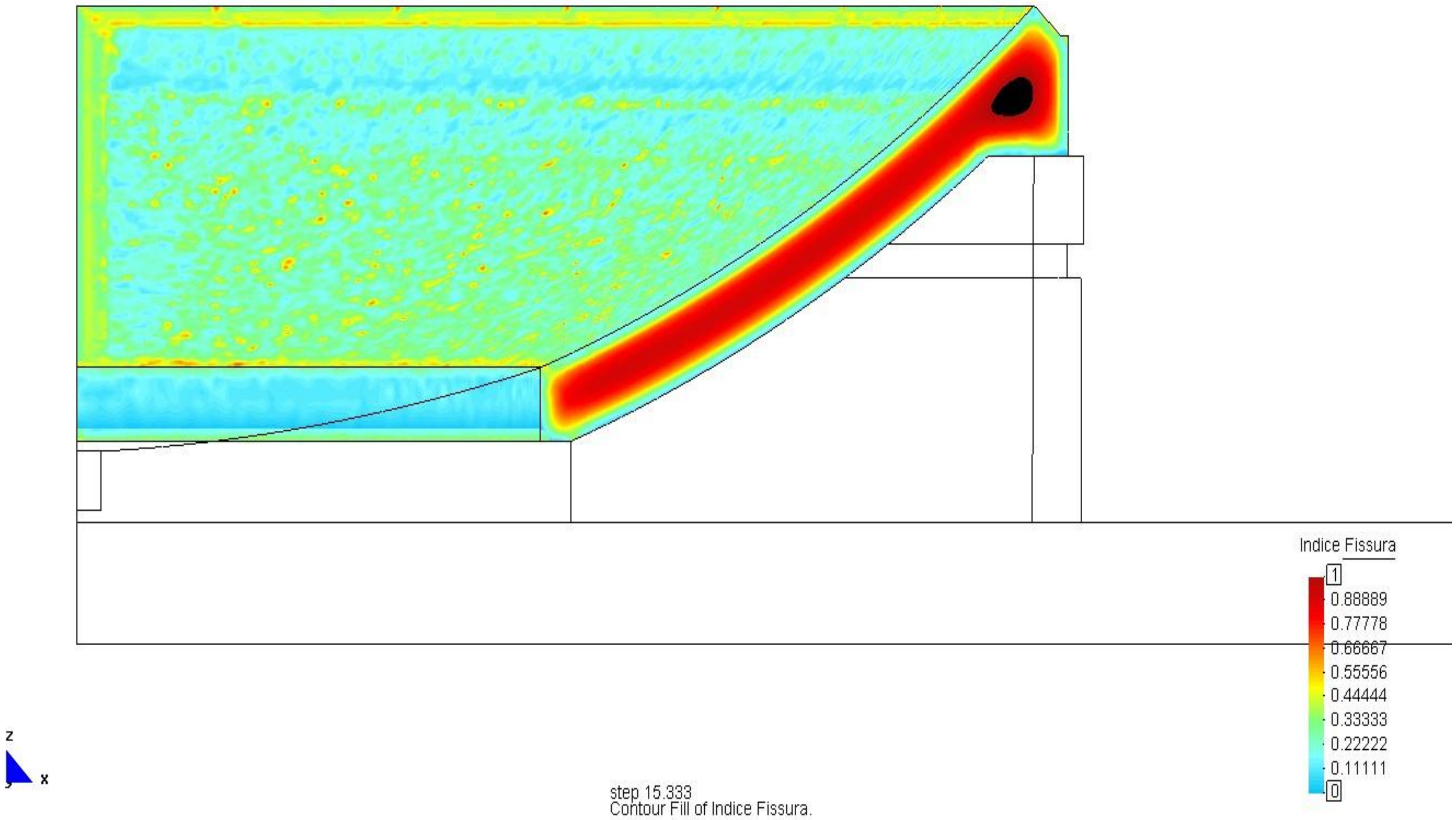

Cracking index for placing temperature = 10ºC

Cracking index: 16 days

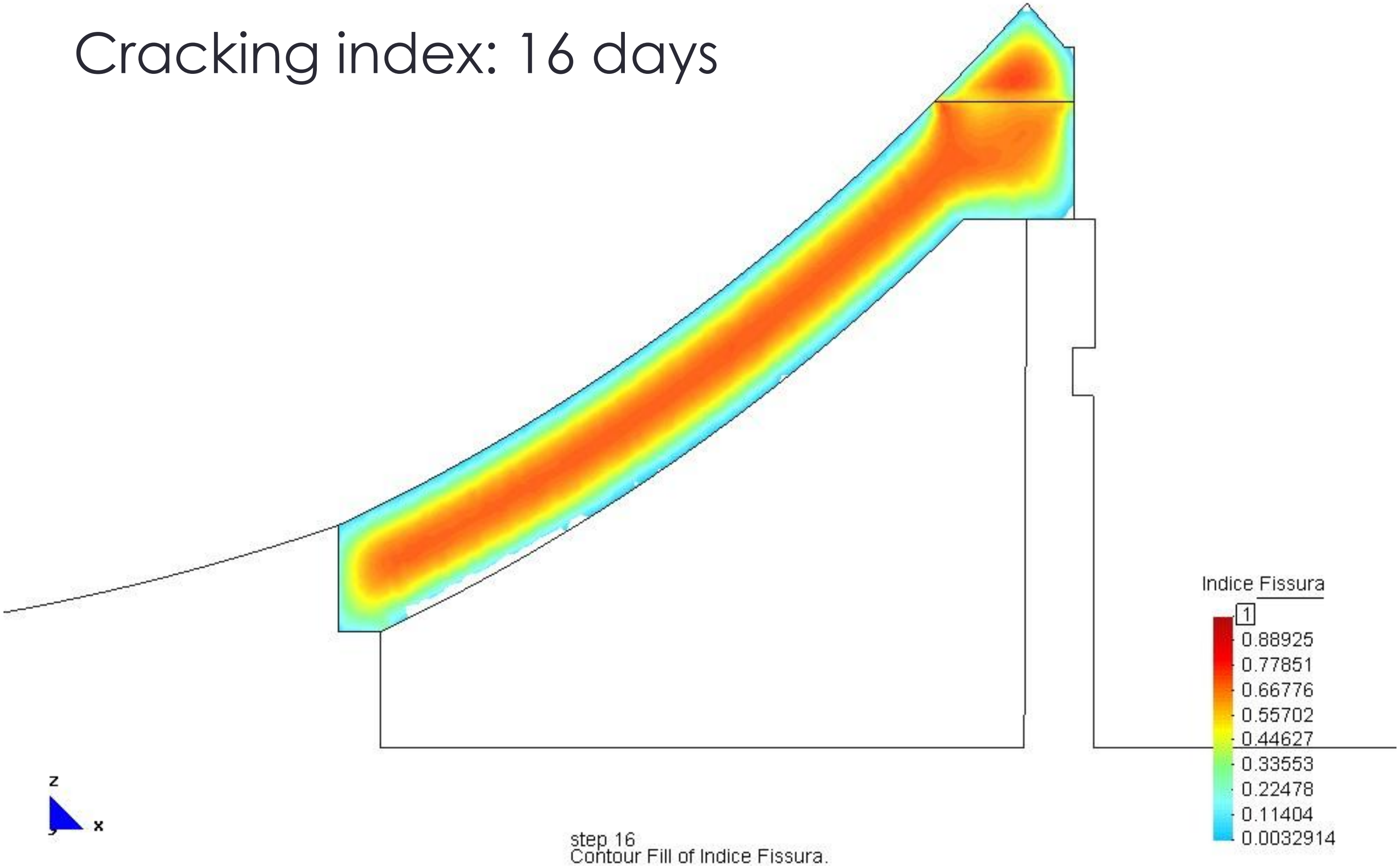

Cracking index for placing temperature = 12°C, 2 layers

Agra III power plant: reactor dome

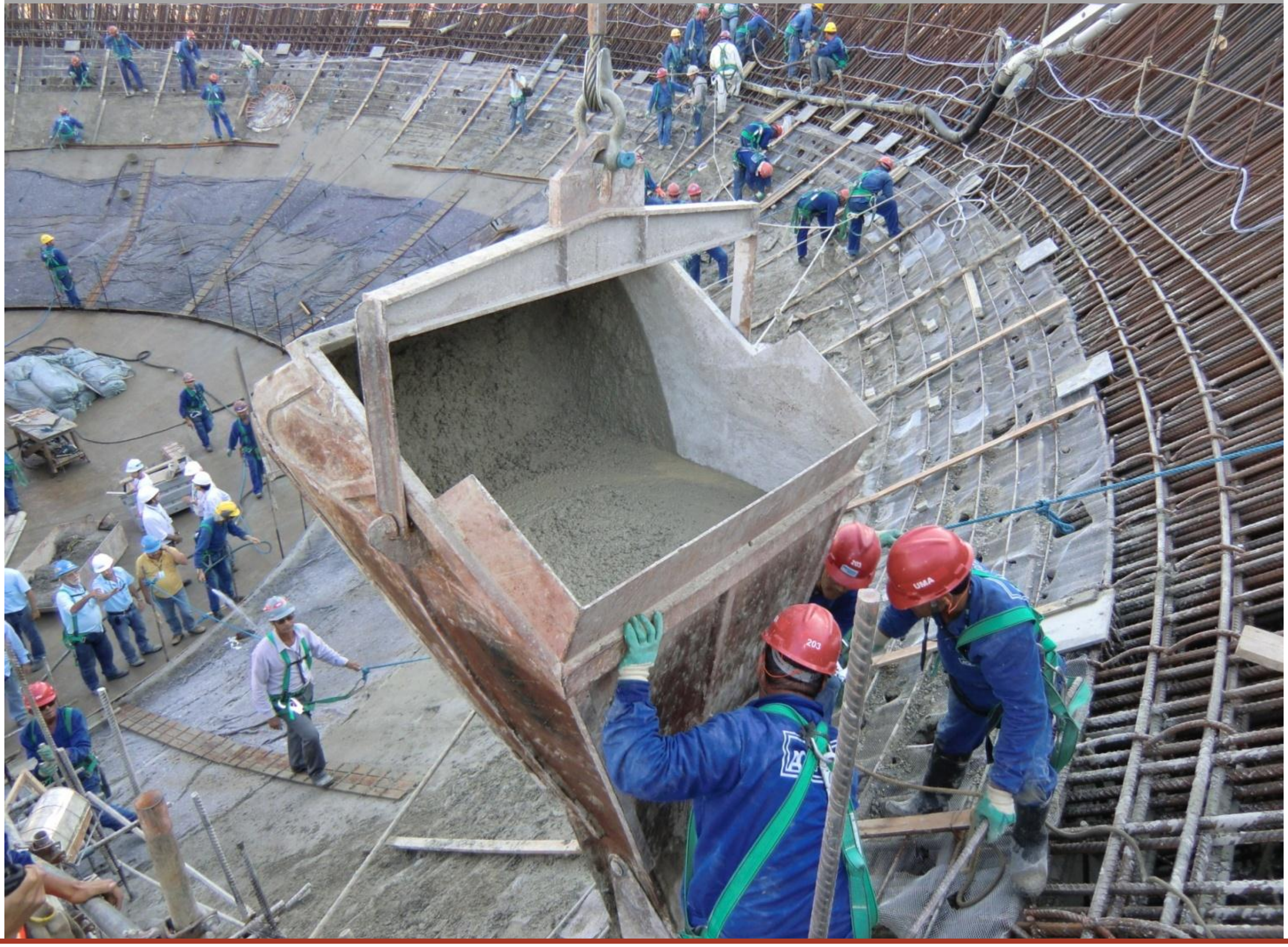

Agra III power plant: reactor dome

Case study 8
Angra III nuclear power plant
Rio de Janeiro, Brazil

Foundations of auxiliary building

Plan of building UPC

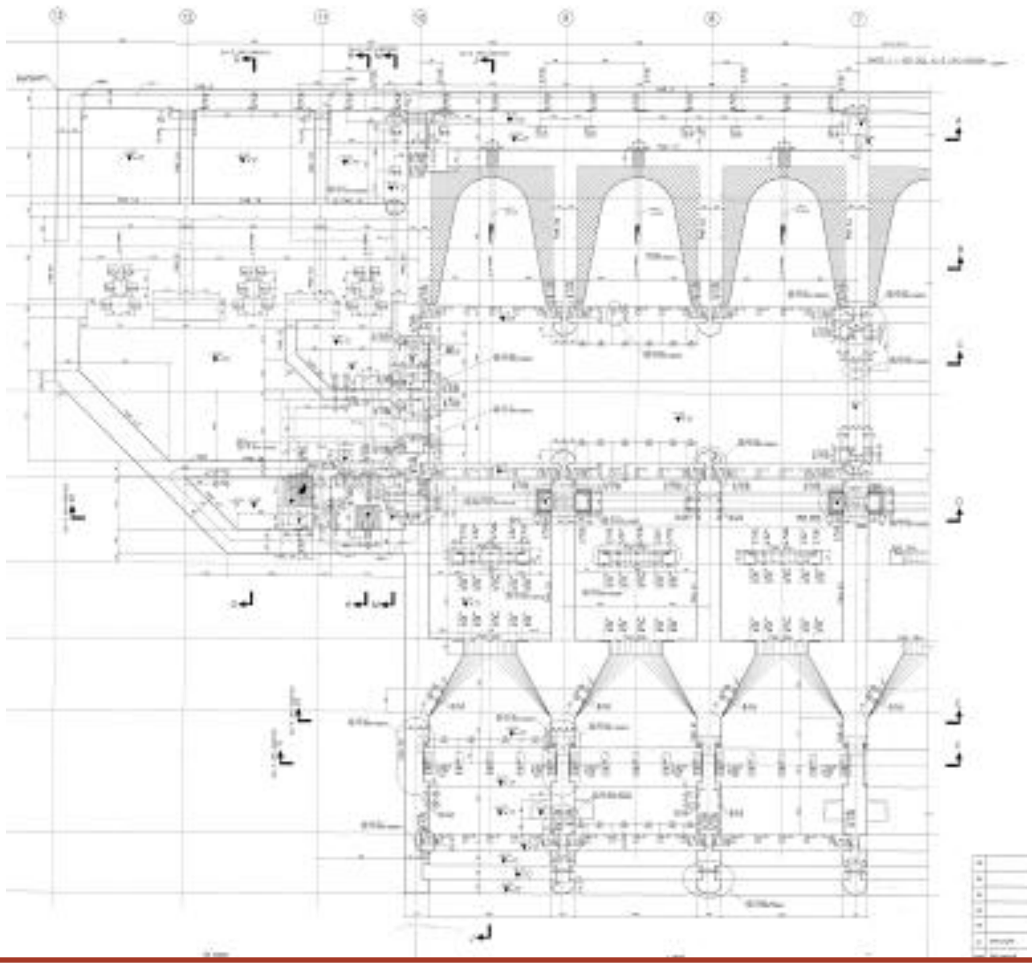

Executive plan for concrete pouring

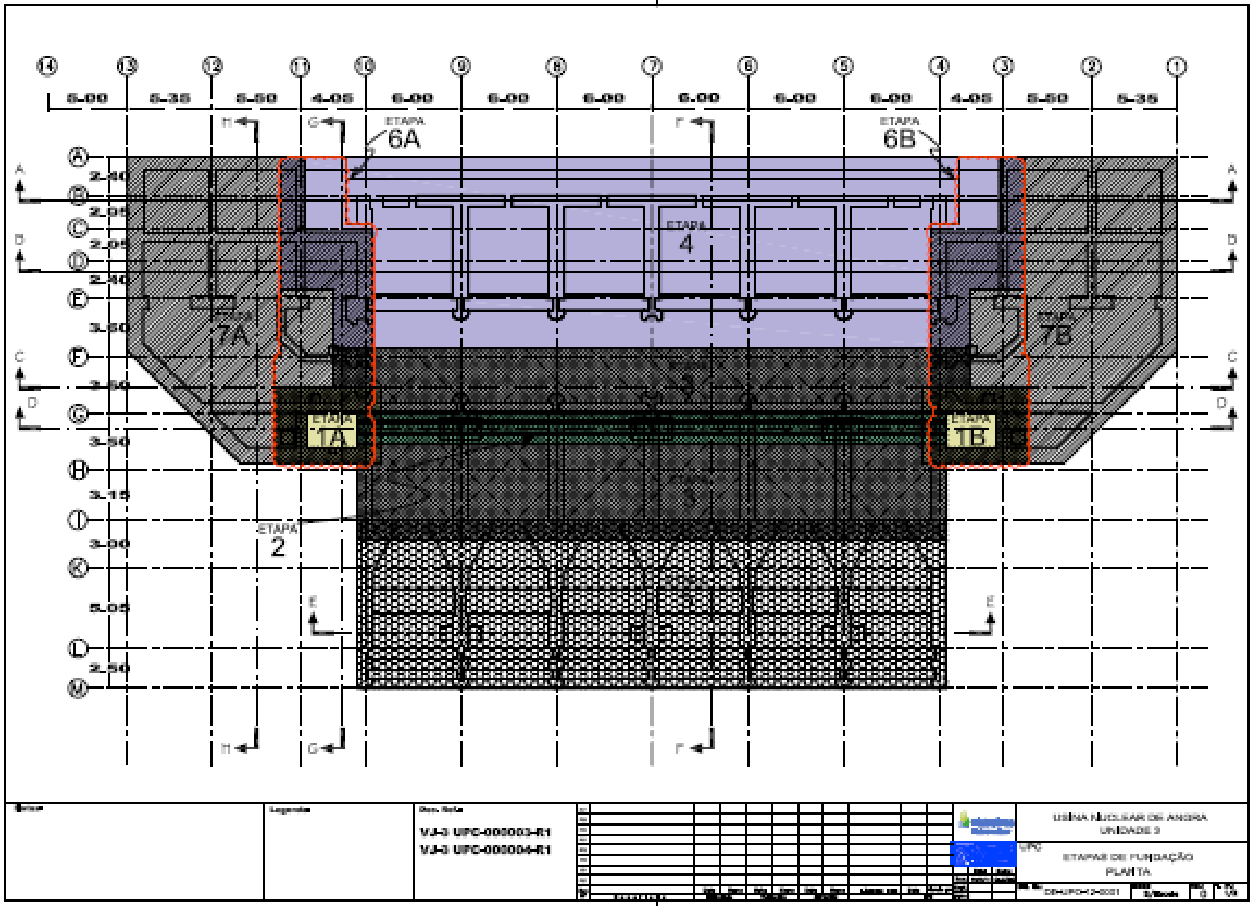

Executive plan for concrete pouring

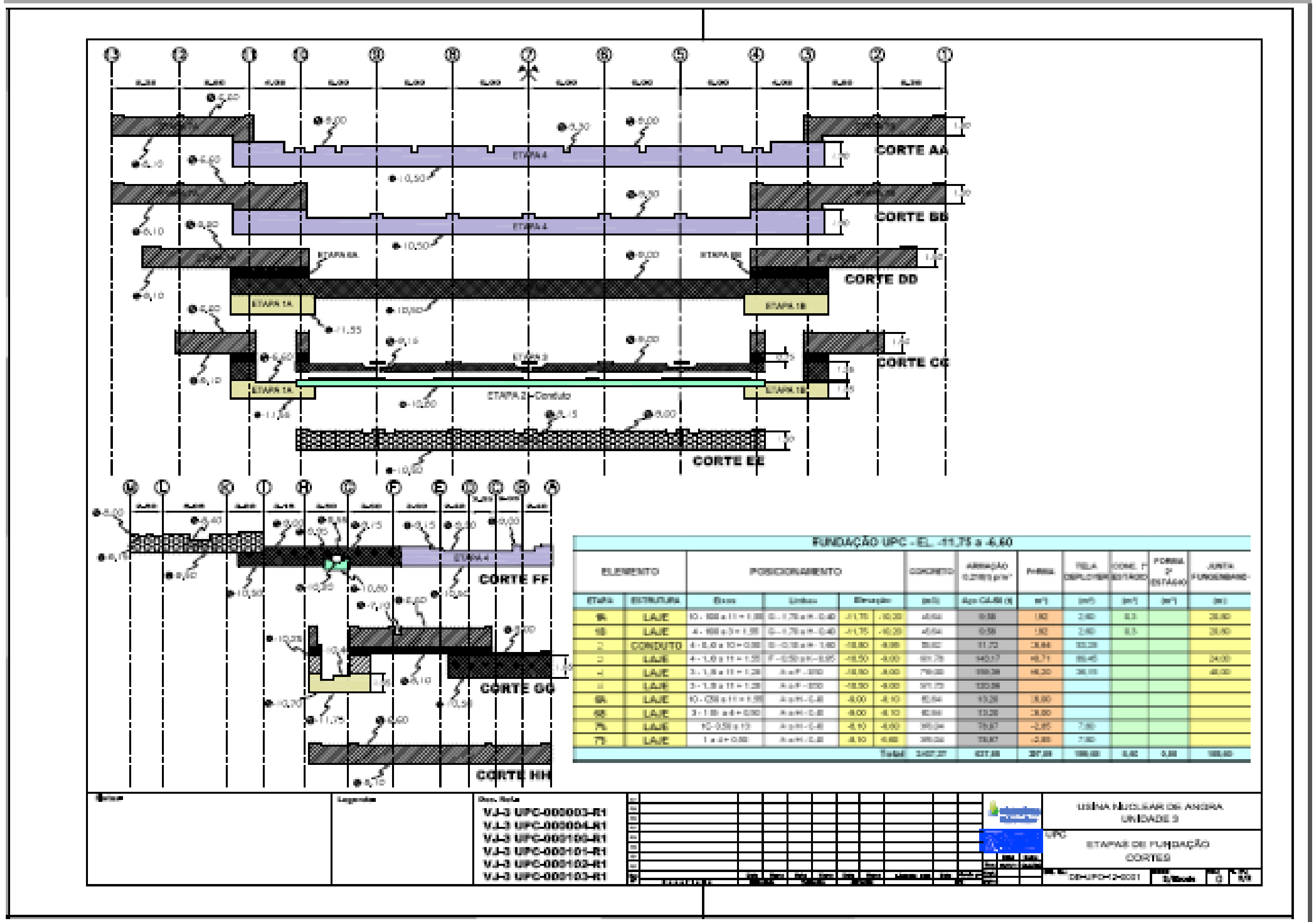

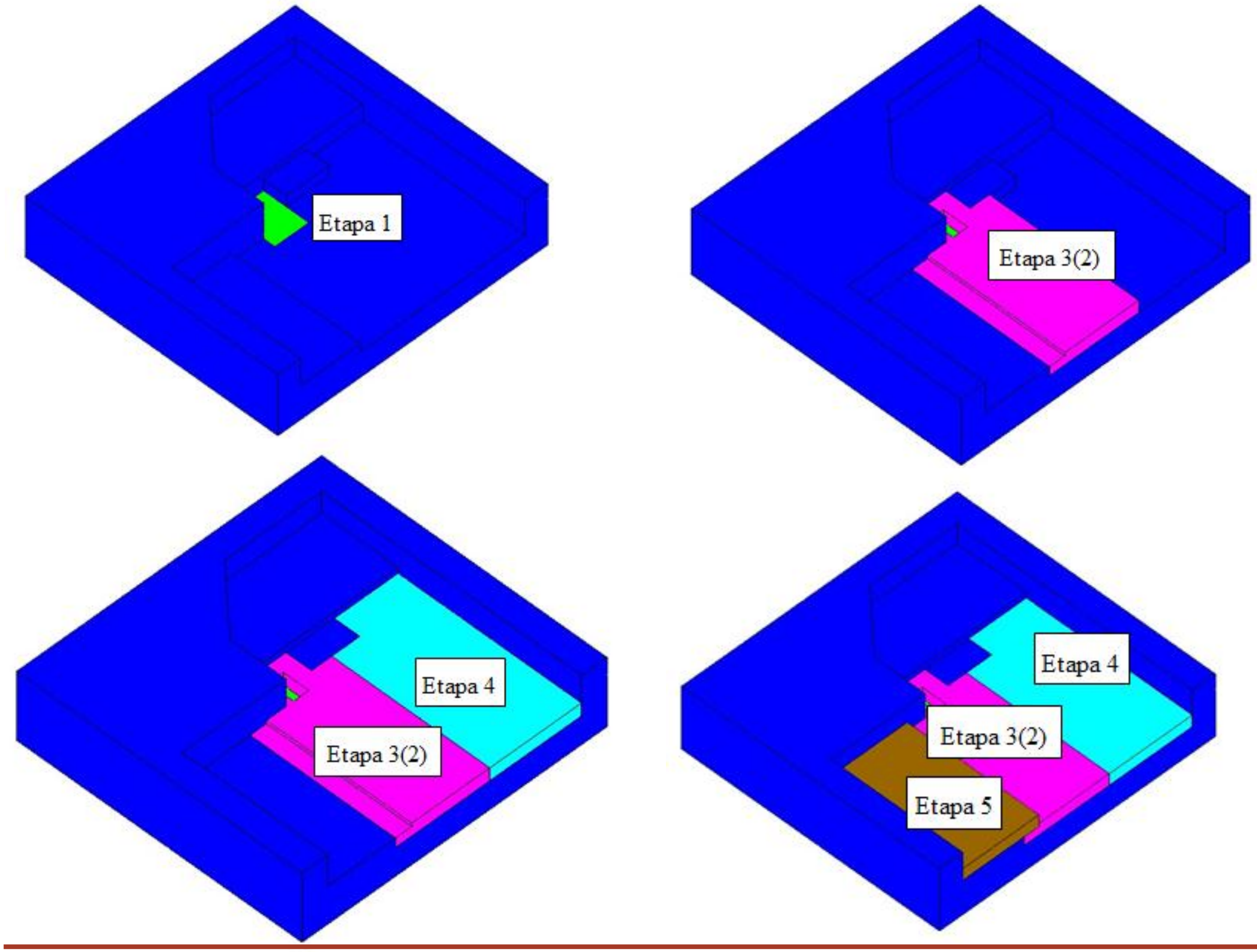

Logistics for construction of the several volumes

Logistics for the construction of the several volumes

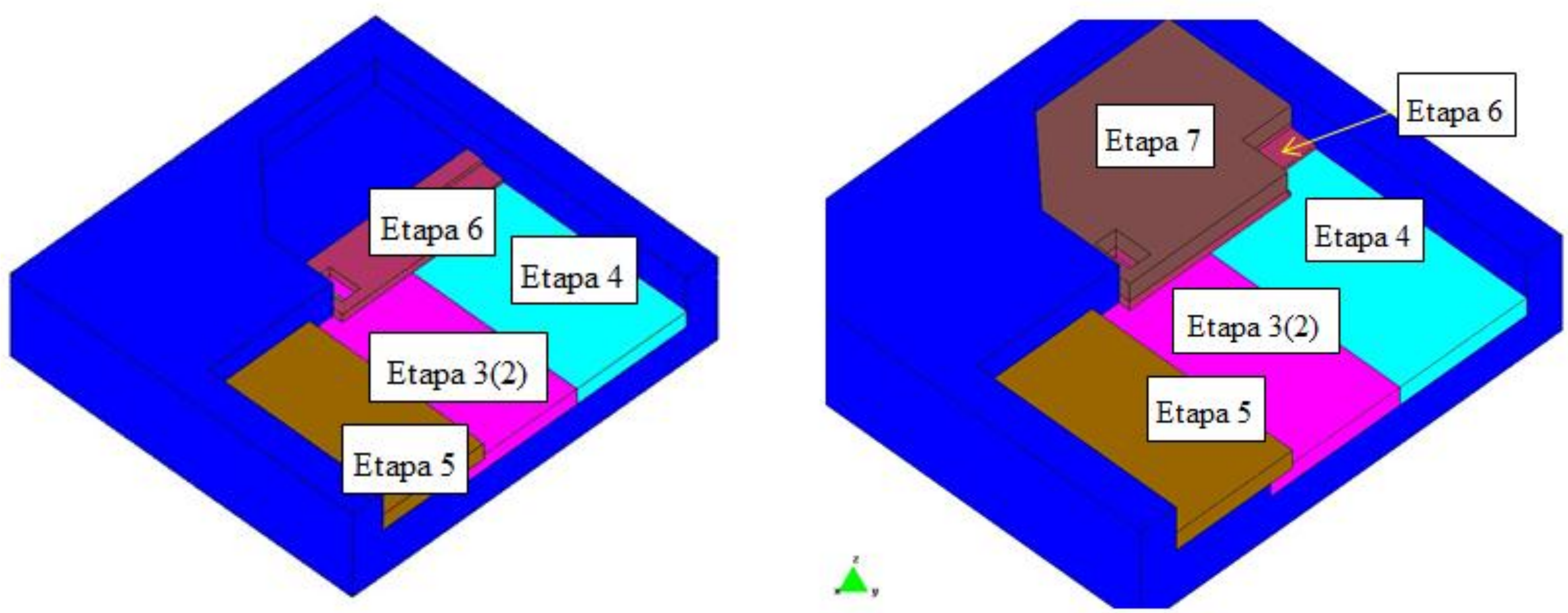

Cracking index

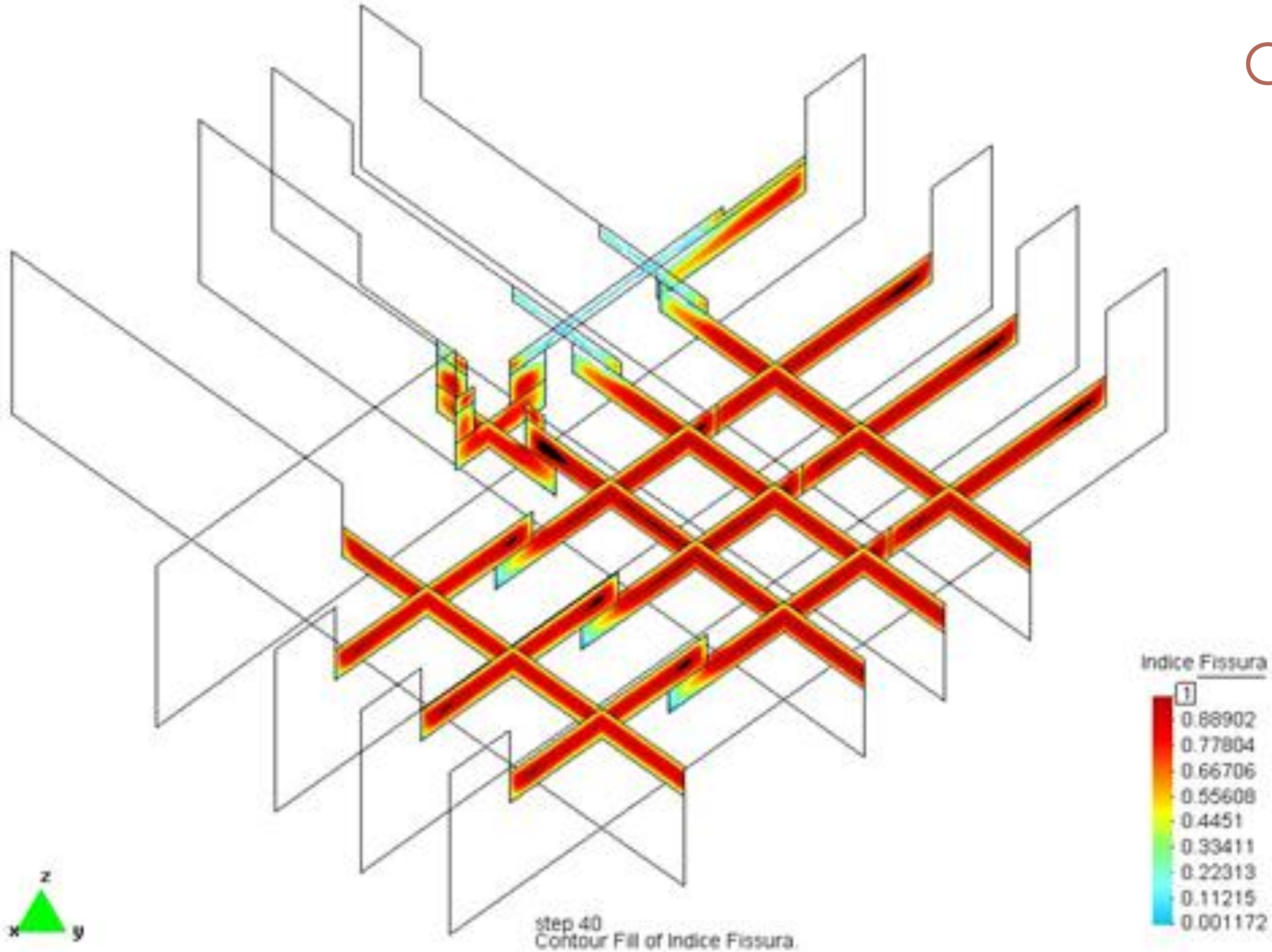

Case study 9
Angra III nuclear power plant
Rio de Janeiro, Brazil

Other studies

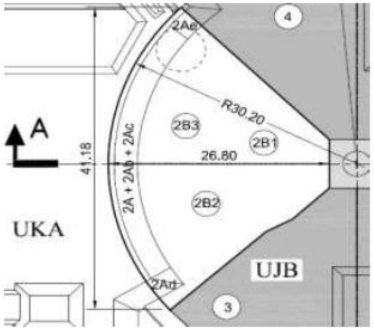
2Ae
4
R30.20
A
41.18
2A + 2Ab + 2Ac
2B3
2B1
26.80
2B2
UKA
UJB
2Ad
3

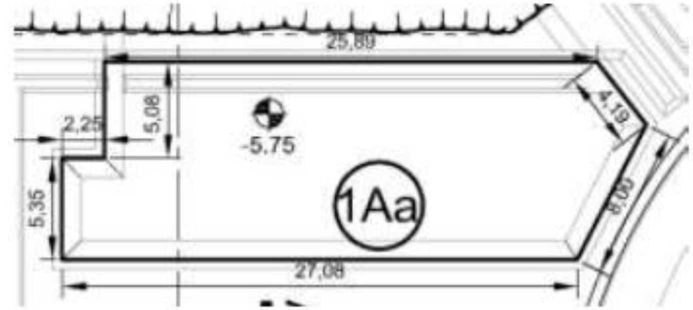
25,89
2,25
5,08
4,19
-5,75
1Aa
5,35
27,08

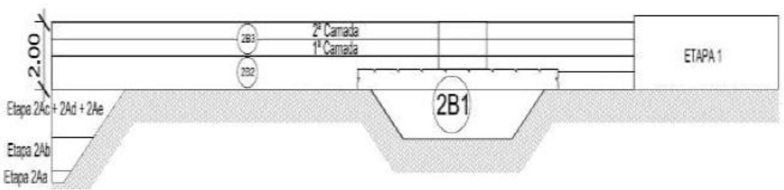
2.00
2B3
2ª Camada
1ª Camada
2B2
ETAPA 1
2B1
Etapa 2Ac + 2Ad + 2Ae
Etapa 2Ab
Etapa 2Aa

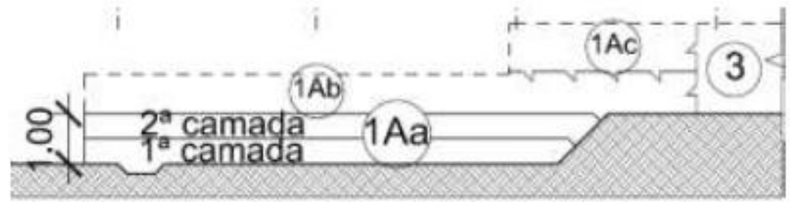
1Ac
3
1Ab
1.00
2ª camada
1ª camada
1Aa

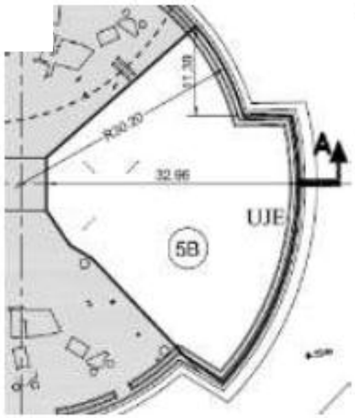
R30.20
32.96
A
UJE
5B

Angra III


2.00
0.50
0.50
0.50
0.50
0.50
4ª Camada
3ª Camada
2ª Camada
1ª Camada
5B

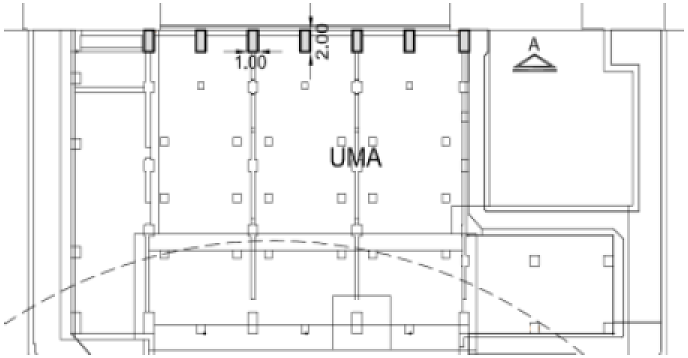
1,00
2,00
A
UMA


31,33
PAR 1156

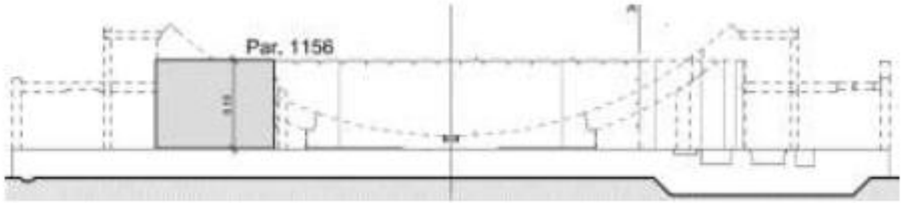
Par. 1156

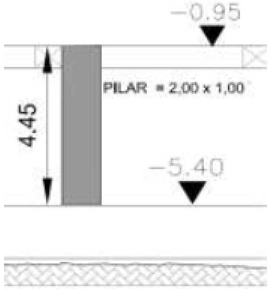
-0,95
PILAR = 2,00 x 1,00
4,45
-5,40

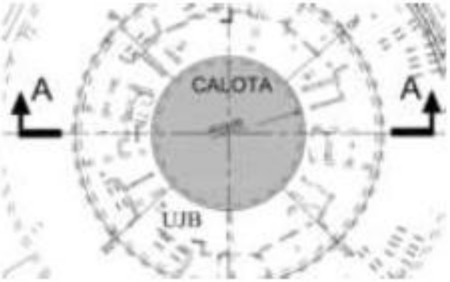
CALOTA
A
A

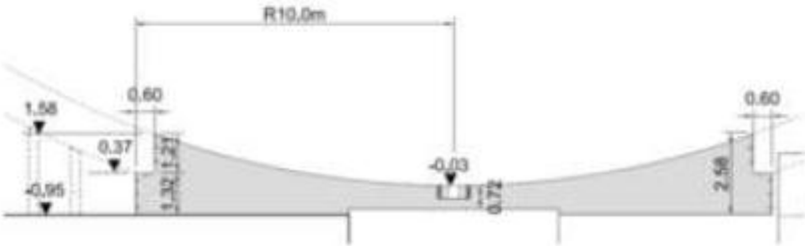
R10,0m
0,60
0,60
1,58
0,37
-0,95
-0,03

Angra III

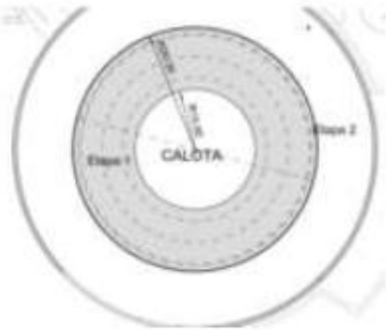
CALOTA

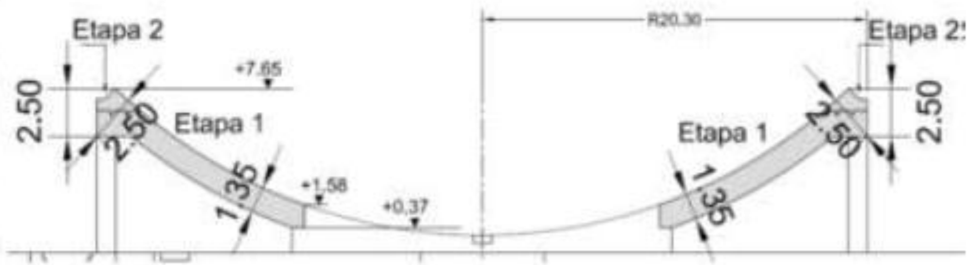
Etapa 2
R20.30
Etapa 2
+7.65
2.50
2.50
Etapa 1
Etapa 1
2.50
2.50
1.35
1.35
+1.58
+0.37


6b
2.00

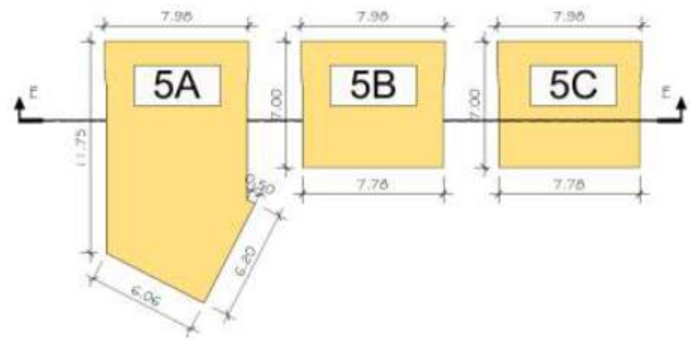
7.98
7.98
7.98
5A
5B
5C
7.00
7.00
7.78
7.78
6.20
6.06

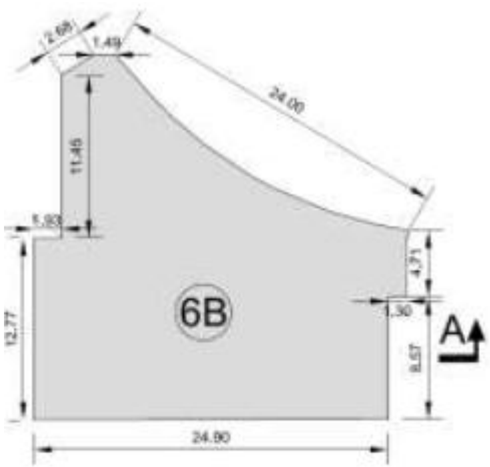
24.00
11.46
6B
A
24.90

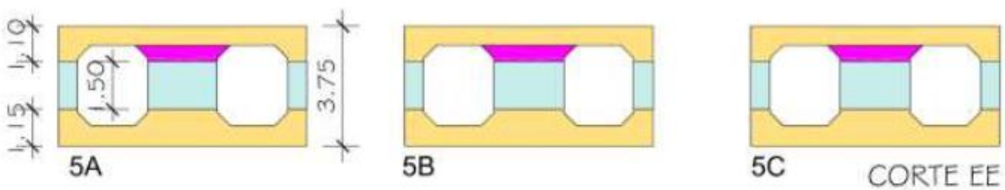
1.10
1.50
1.15
3.75
5A
5B
5C
CORTE EE

References

1. Fairbairn, E. M. R., Silvoso, M. M., Toledo Filho, R. D., Alves, J. L. D. & Ebecken, N. F. F. (2004). Optimization of mass concrete construction using genetic algorithms. *Computers & Structures*, 82, 281-299.
2. Fairbairn, E. M. R., Silvoso, M. M., Ribeiro, F. L. B., & Toledo Filho, R. D. (2011). *Industrial applications of the thermo-chemo-mechanical model*, in MPPS 2011, Symposium on Mechanics and Physics of Porous Solids: a tribute to Pr. Olivier Coussy, IFSTTAR, Paris, (2011), 353-370.
3. Fairbairn, E. M. R., Silvoso, M. M., Koenders, E. A. B., Ribeiro, F. L. B., & Toledo-Filho, R. D. (2012). , Thermo-chemo-mechanical cracking assessment for early-age mass concrete structures,. *Concrete International*, 34 (2012), 30-35.

CMS Workshop “Cracking of massive concrete structures”

March 17, 2015, ENS-Cachan

Cachan, Île-de-France, FRANCE

Degree of restraint concept for analysis of early-age stresses in concrete walls

Agnieszka Knoppik-Wróbel[1,*]

[1]Silesian University of Technology, Department of Structural Engineering, Gliwice, Poland

*Agnieszka Knoppik-Wróbel is a scholar under the project „DoktoRIS” co-financed by EU – European Social Fund.

Introduction

early-age stresses in concrete walls

Concrete structures subjected to early-age cracking

massive internally-restrained

- thick slabs,
- blocks,
- gravity dams

medium-thick externally-restrained

- tank walls,
- nuclear containment walls,
- bridge abutments,
- retaining walls

Early-age stresses in walls

self-induced and restraint

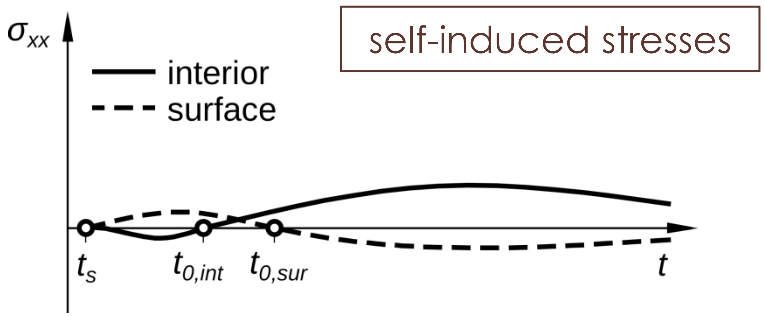

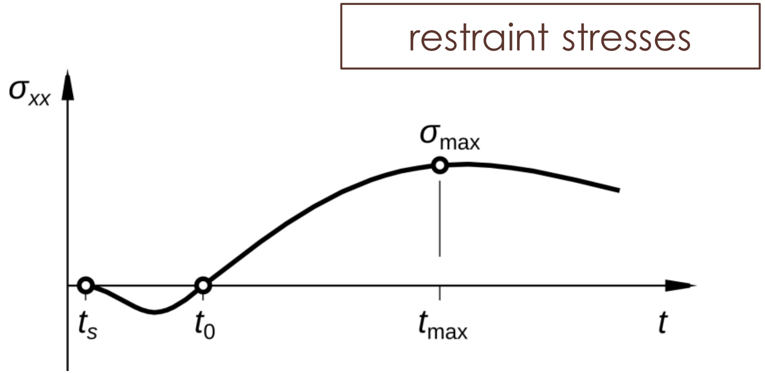

origin of cracking

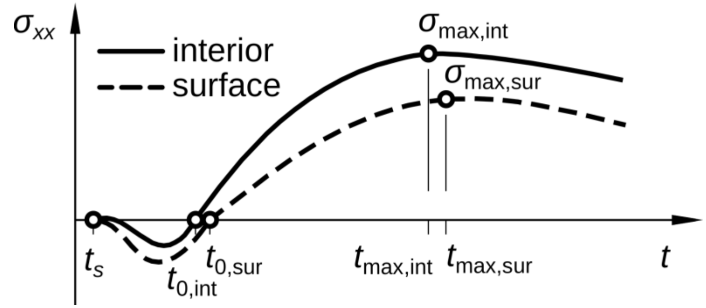

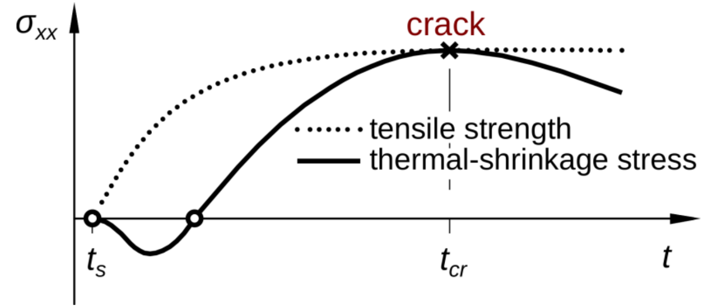

Early-age stresses in walls

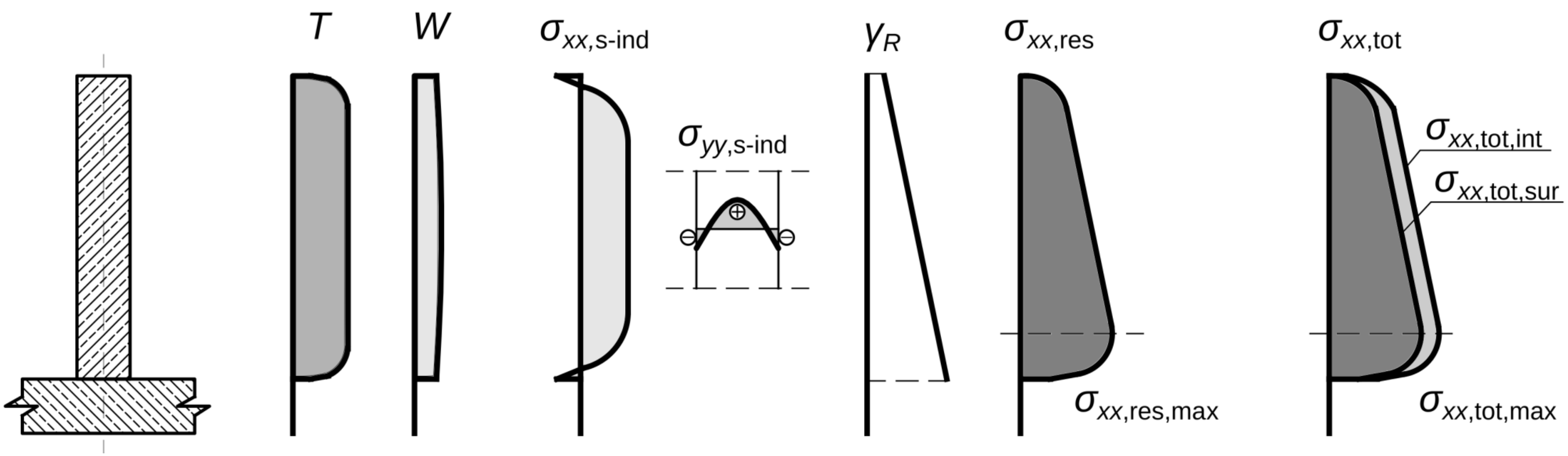

Dominating influence of the thermal restraint stresses.

Cracking pattern vs. mode of restraint

base- and end-restraint

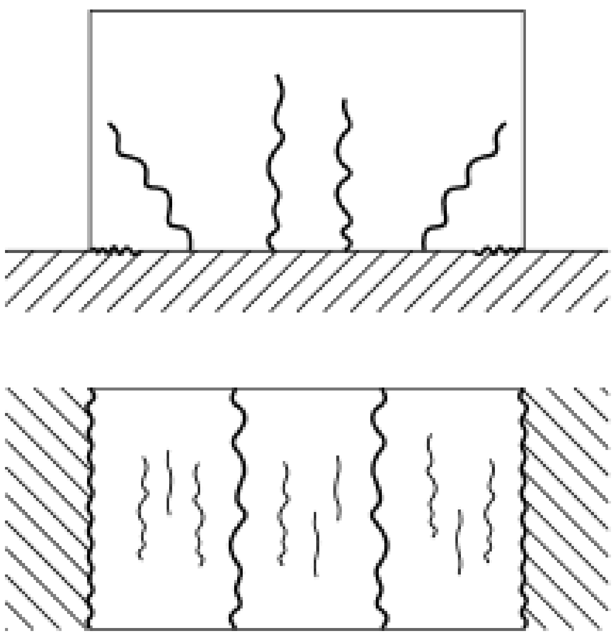

mixed modes

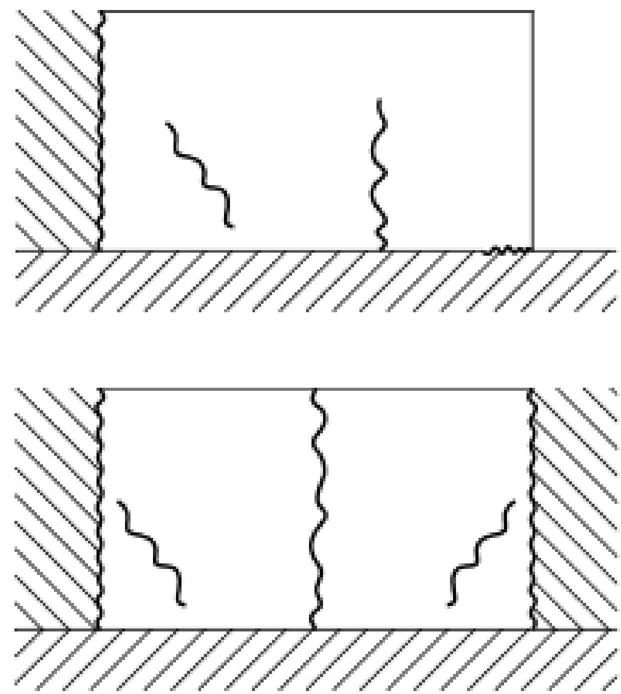

Theoretical background

degree of restraint concept

Compensation Plane Method

total stress

[JSCE standard, 2011]

due to internal restraint

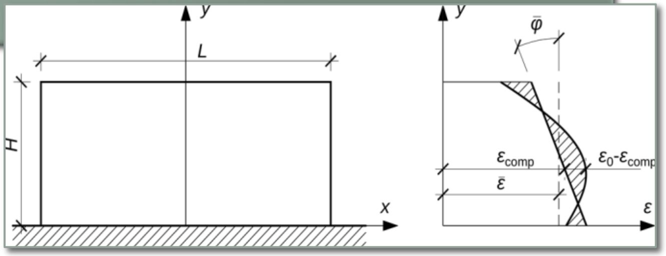

due to external restraint

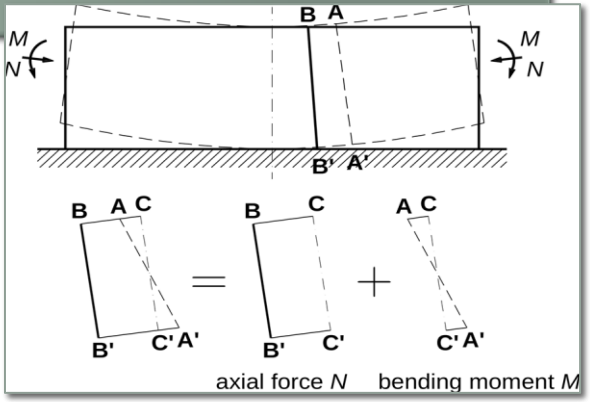

CPM – self-induced stress

Stress due to internal restraint – unbalanced strain due to gradients of temperature and humidity

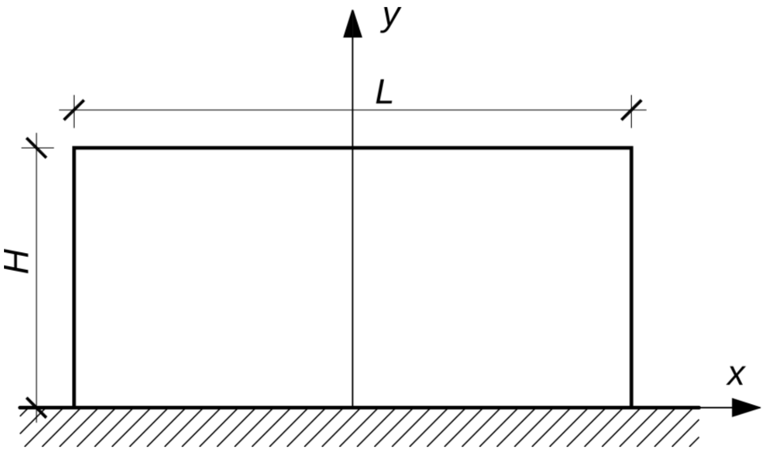

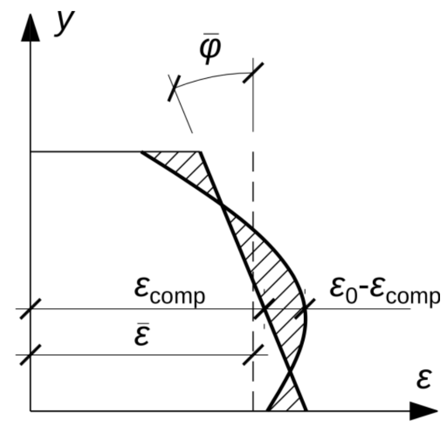

$$\sigma_{int} = E_{c,eff}\left(\varepsilon_0 - \varepsilon_{comp}\right)$$

$$\varepsilon_0 = \varepsilon_T + \varepsilon_{sh}$$

$$E_{c,eff} = \frac{E_c}{1+\varphi}$$

free axial strain $\bar{\boldsymbol{\varepsilon}}$

change of curvature $\bar{\boldsymbol{\varphi}}$

CPM – restraint stress

Stress due to external restraint – translational and rotational

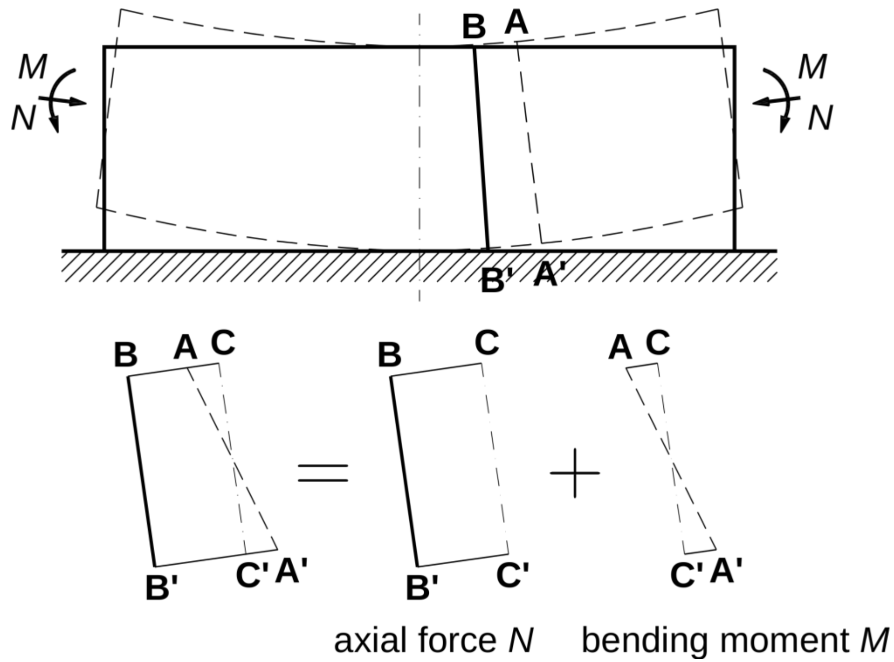

$$\sigma_{ext} = \frac{N}{A_c} + \frac{M}{I_c}(y - y_{cen})$$

$$N = R_N \cdot E_c \cdot A_c \cdot \bar{\varepsilon} \qquad M = R_M \cdot E_c \cdot I_c \cdot \bar{\varphi}$$

Degree of restraint

Models using the concept of the restraint factor as representation of the degree of restraint:

1. **standards**
   - Japan: JSCE Guidelines for Concrete, JCI Guidelines;
   - USA: ACI Report 207.2;
   - Europe: Eurocode 2 Part 3 + CIRIA C660;
2. **other methods**
   - Sweden: Luleå University of Technology [Nilsson, 2003];
   - Poland: Cracow University of Technology [Flaga, 1990].

Restraint coefficient
[Nilsson, 2003]

$$\sigma = \gamma_R \cdot \sigma_{fix}$$

$$\gamma_R(y) = \delta_{slip} \cdot \left[\delta_{res}(y) - \left({\gamma^t}_R(y) + {\gamma^{ry}}_R(y) + {\gamma^{rz}}_R(y)\right)\right]$$

$$\delta_{res} = \delta_{res}(L/H)$$

$$\delta_{slip} = \delta_{slip}(L/H)$$

$${\gamma^t}_R = {\gamma^t}_R\left(\frac{L}{H}, \frac{A_F E_F}{A_c E_c}\right)$$

$${\gamma^{ry}}_R = {\gamma^{ry}}_R(H_c, H_F)$$

$${\gamma^{rz}}_R = {\gamma^{rz}}_R(B_c, B_F)$$

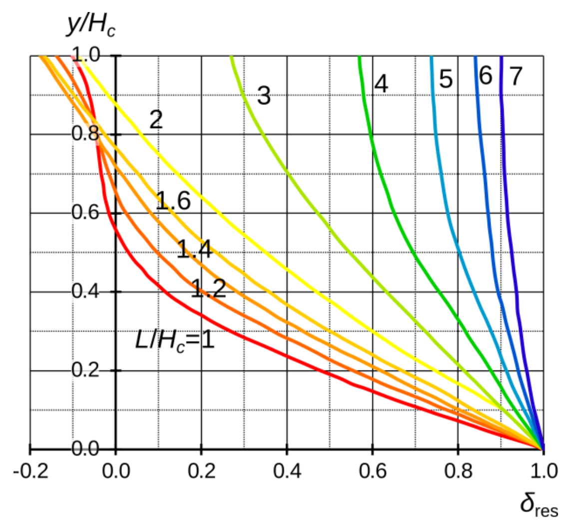

resilience factor, δ_{res}

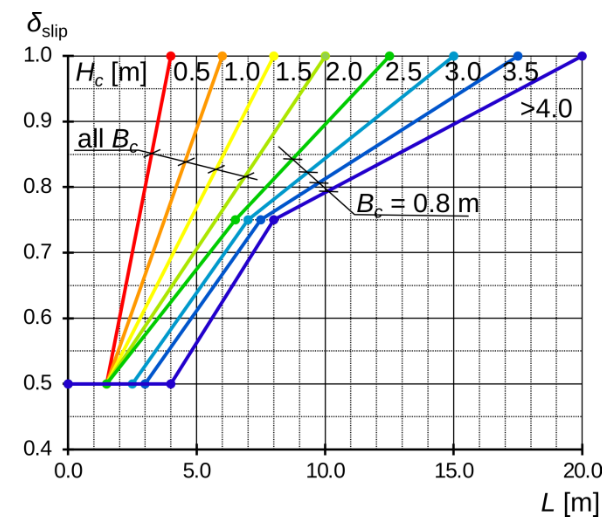

slip factor, δ_{slip}

Strategy for analysis

modelling

Aim of the study

To **analyse** the character and magnitude of **early-age stresses occurring in concrete walls** due to thermal–shrinkage effects and to **investigate the influence of restraint conditions** including the soil–structure interaction.

Degree of restraint in numerical analysis

Luleå Technical University (LTU)
Sweden

Anders Hösthagen

Majid Al-Gburi

Local Restraint Method (LRM)
Equivalent Restraint Method (ERM)

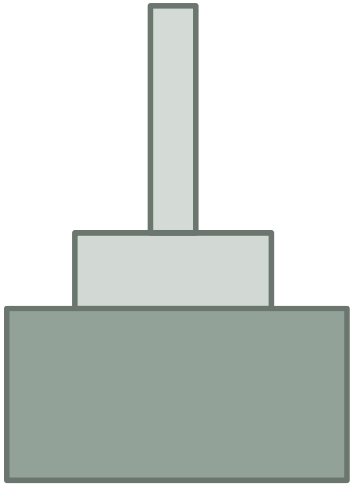

analysis of cross-section

self-induced stress, σ_{fix}

LRM or **ERM** (general-purpose 3D FEM software)

γ_R

total stress
$\sigma = \gamma_R \cdot \sigma_{fix}$

Numerical model

Strategy: reverse of LRM/ERM

$$\gamma_R = \frac{\sigma}{\sigma_{fix}}$$

Phenomenological model for simulation of thermo–hydro–mechanical behaviour of concrete structures taking into account construction sequence and soil–structure interaction.

Thermal–moisture analysis

- **concrete:** coupled thermal–moisture equations [Klemczak, 2011]
- **soil:** partially coupled equations; moisture diffusion dependent on temperature [Clapp and Hornberger, 1978]
- **initial conditions:** initial temperature and moisture content
- **boundary conditions:** 3rd type
- **concrete source function** in thermal equation and **sink function** in humidity equation – <u>hydration heat rate</u>
  - $q = \dot{Q}$, Q(*t*) - approximation with exponential function,
  - based on cement composition [Schindler and Folliard, 2005]

Stress analysis – concrete

- **viscoelasto–viscoplastic** material model with consistent conception [Klemczak, 2014]
- yield surface and boundary surface are rate-dependent
- modified 3-parameter Willam–Warnke (**MWW3**) failure criterion [Majewski, 2004; Klemczak, 2007]
- **creep** function acc. to Model Code 1990 [Guénot et al., 1994]
- **maturity development** expressed with time development of mechanical properties [Model Code 2010]
- equivalent age of concrete

Stress analysis – soil

- **elasto–plastic** material model [Majewski, 1995]
- Drucker–Prager failure criterion [Majewski, 1995]
- **Mechanical parameters** acc. to Duncan and Chang [Dunkan and Chang, 1970] modified by Majewski [Majewski, 1995]
- Soil–structure interaction by application of contact elements [Majewski, 1995]

Influence of restraint conditions

external restraint, geometry and dimensions, support conditions, soil–structure interaction

Influence of external restraint

Verification and comparison on the benchmark tunnel wall in Sweden [Hösthagen, 2014]

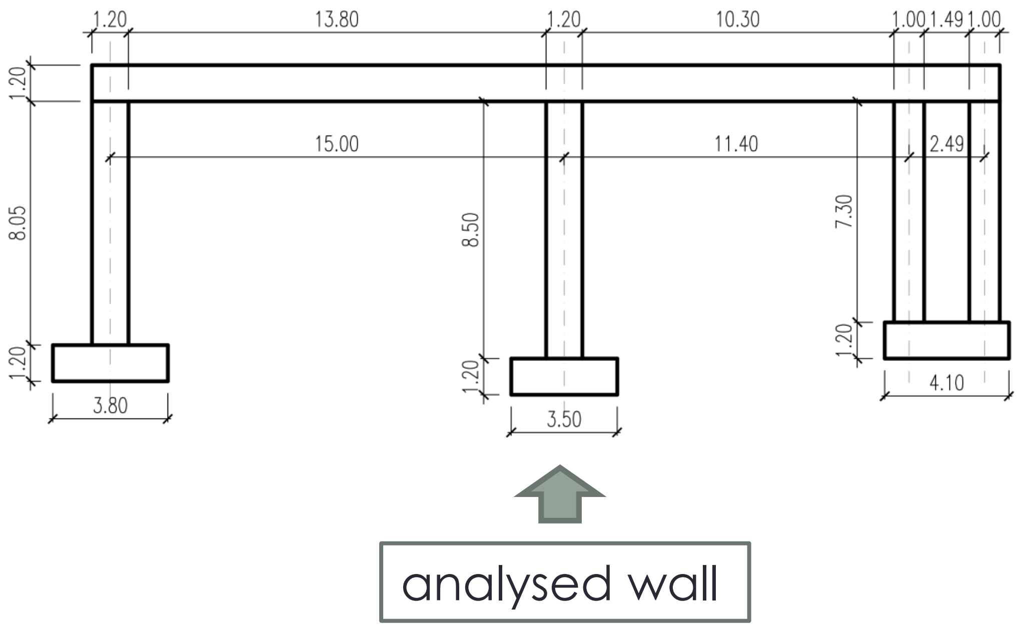

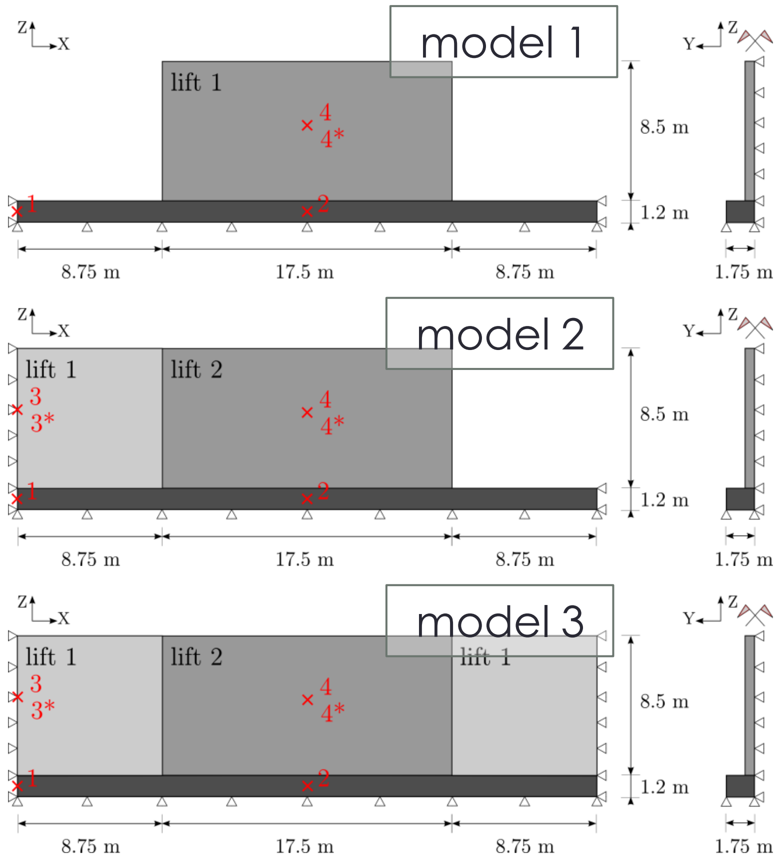

Stresses in different wall segments

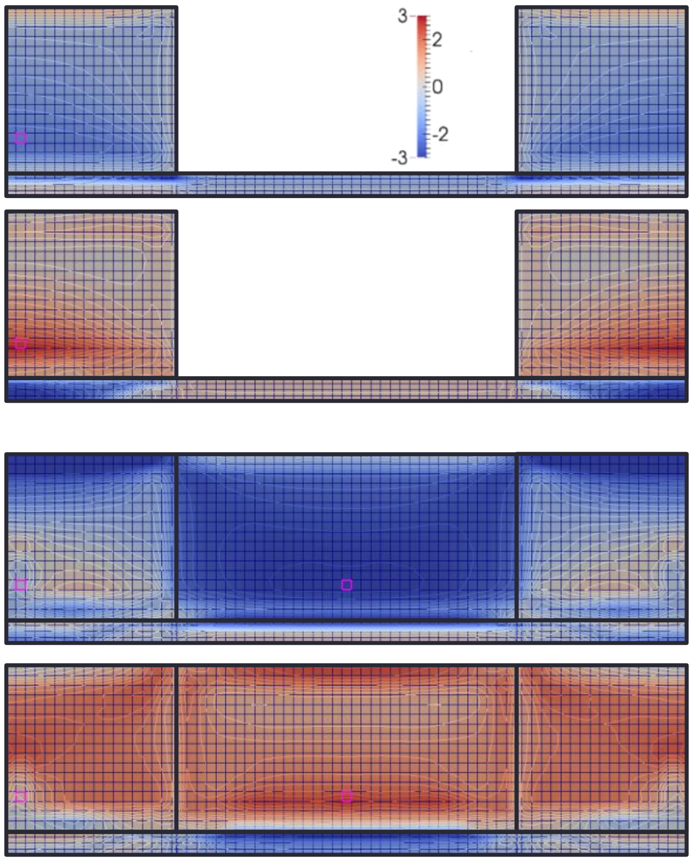

1st lift

heating

cooling

2nd lift

heating

cooling

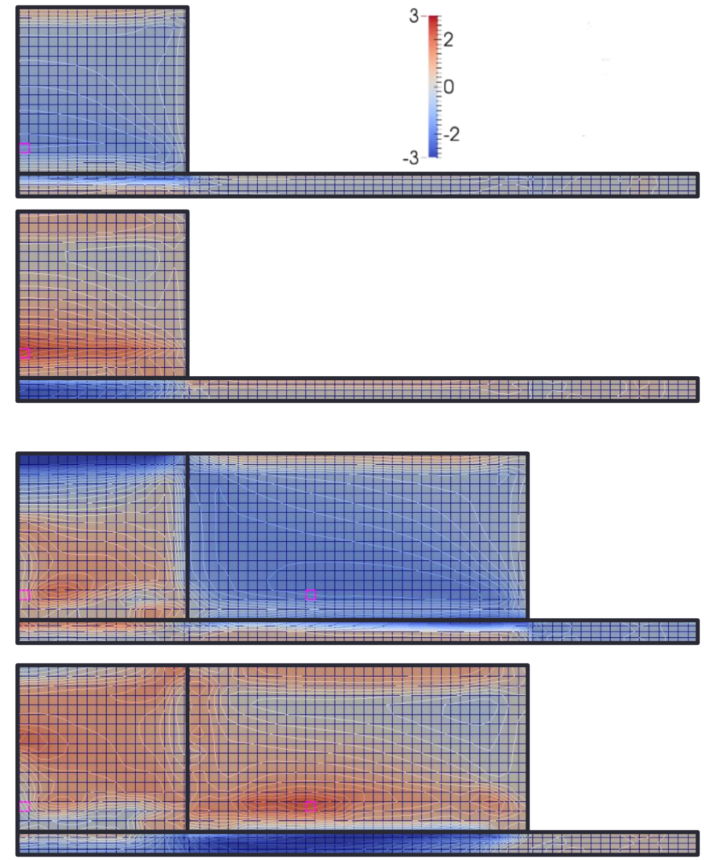

Cracking in different wall segments

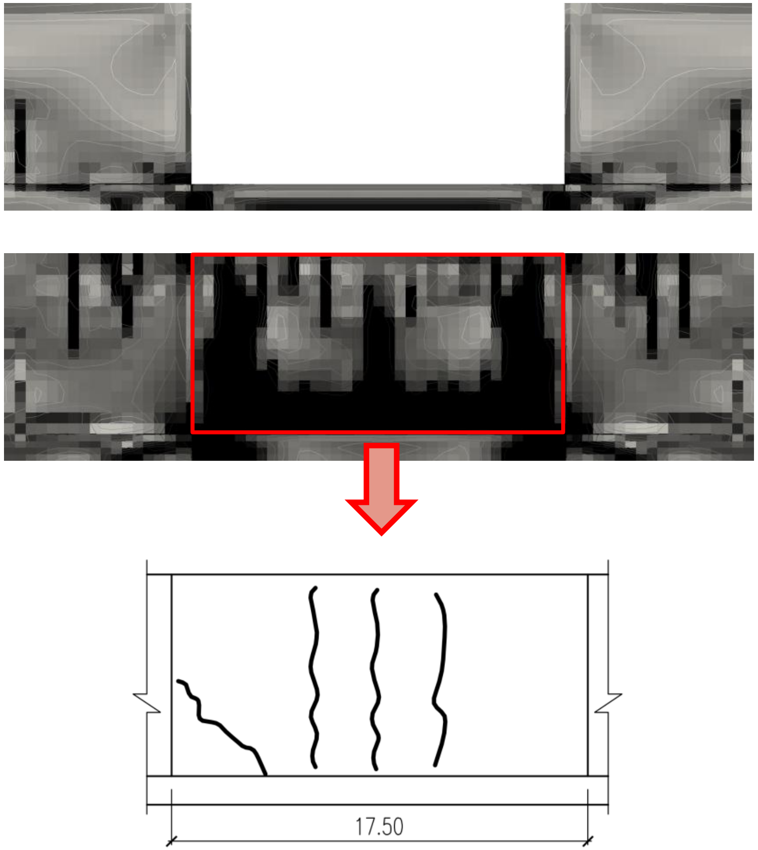

1st lift

2nd lift

real cracking image

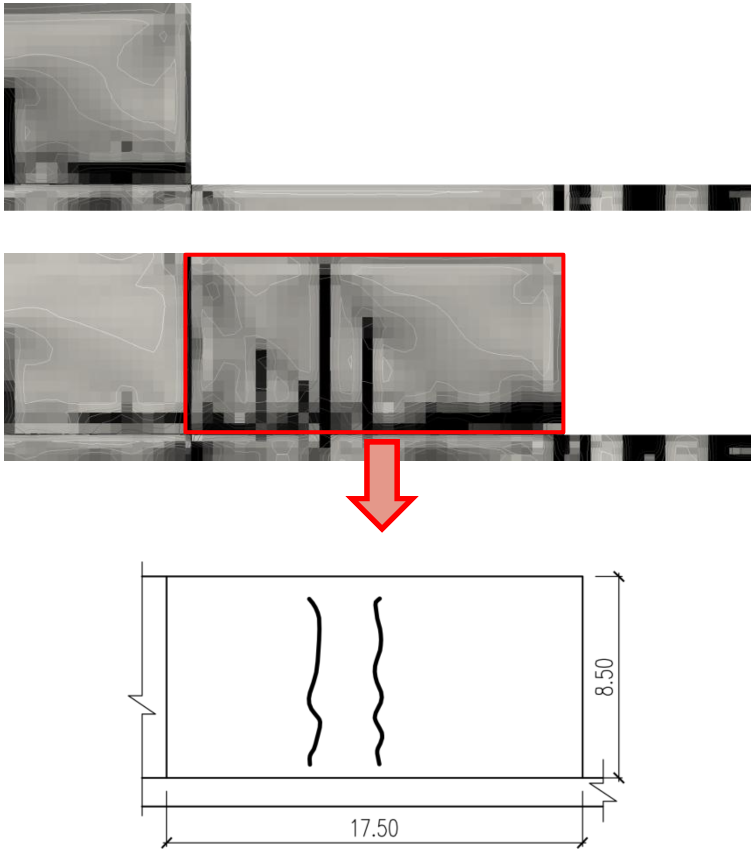

Influence of walls dimensions

- 12 walls with *L/H* from **1.4** to **10**
- several walls with **equal *L/H*** but **different *L* and *H***
- $A_C = A_F$ and $I_C = I_F$

  ⇓

  $H_C = H_F$ and $B_C = B_F$

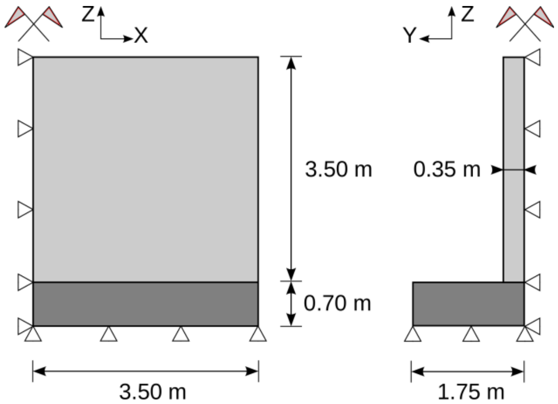

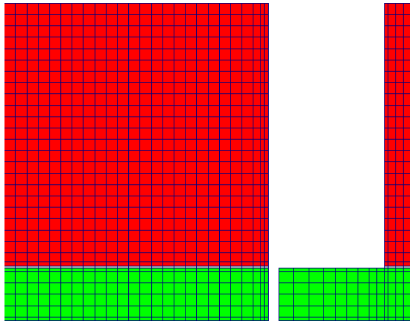

Influence of walls dimensions

Numerical calculations

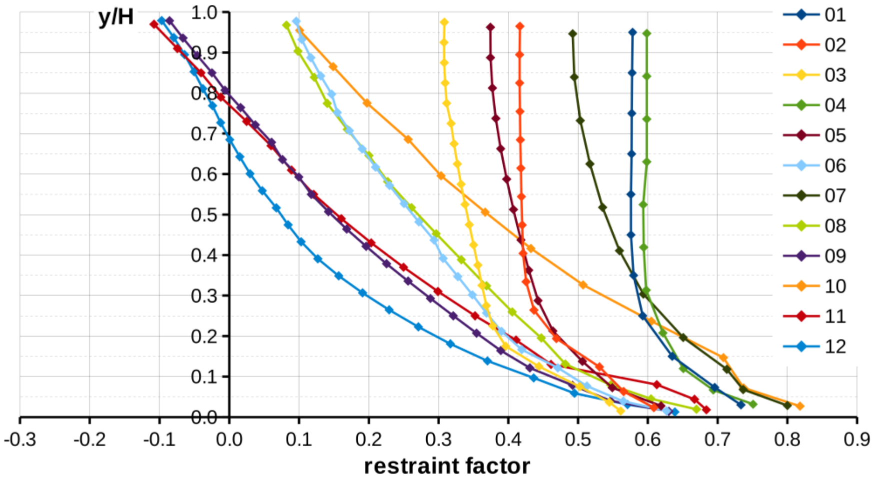

Analytic approach

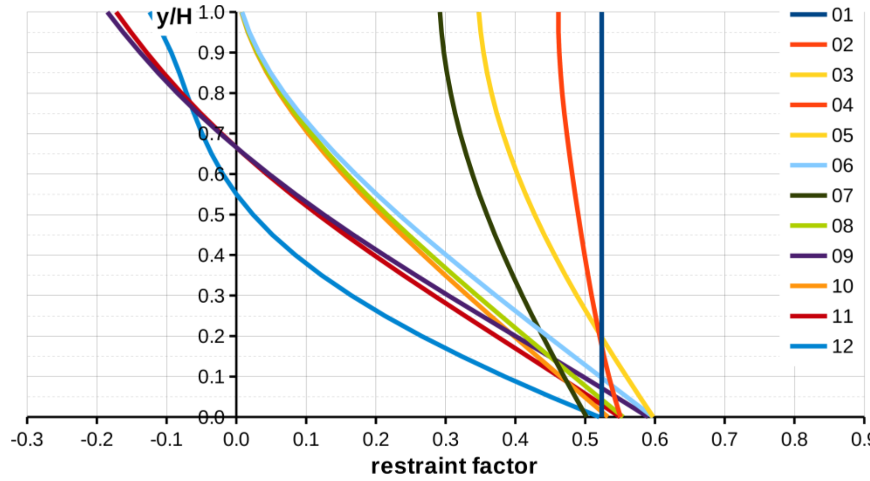

Conclusion: results comply to some extent only. In walls with equal *L*/*H* ratio the degree of restraint is not the same.

Walls with equal lengths

„Normalised” restraint factor

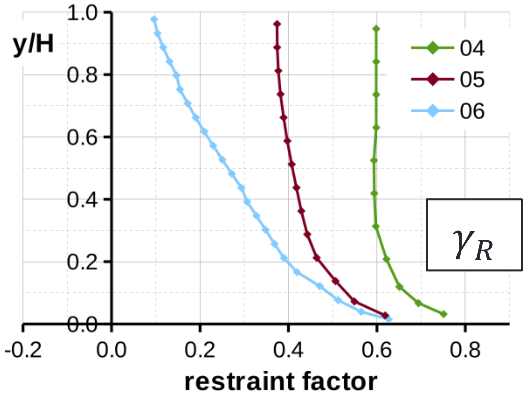

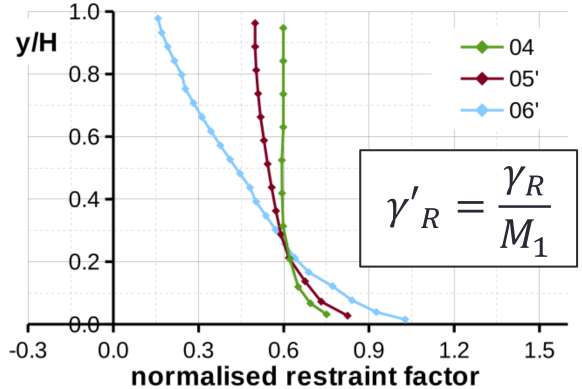

Influence of walls height

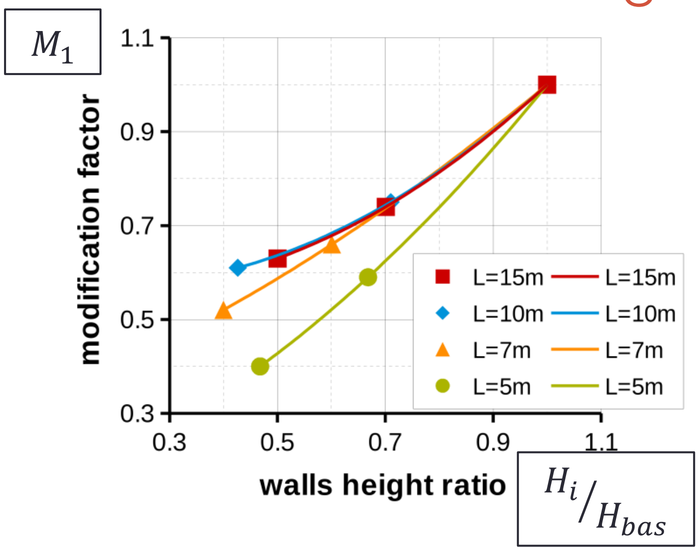

Conclusion: with the increasing height of the wall the magnitude of the restraint decreases. This relationship becomes more pronounced as the length of the wall increases.

Walls with equal *L/H* ratios

„Normalised" restraint factor

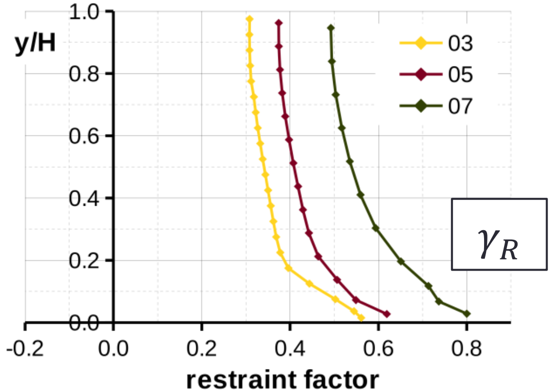

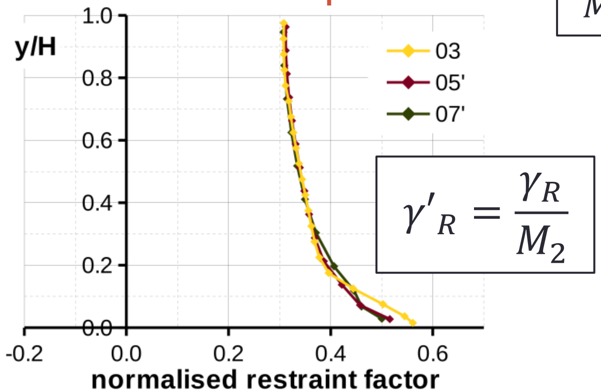

Influence of walls area

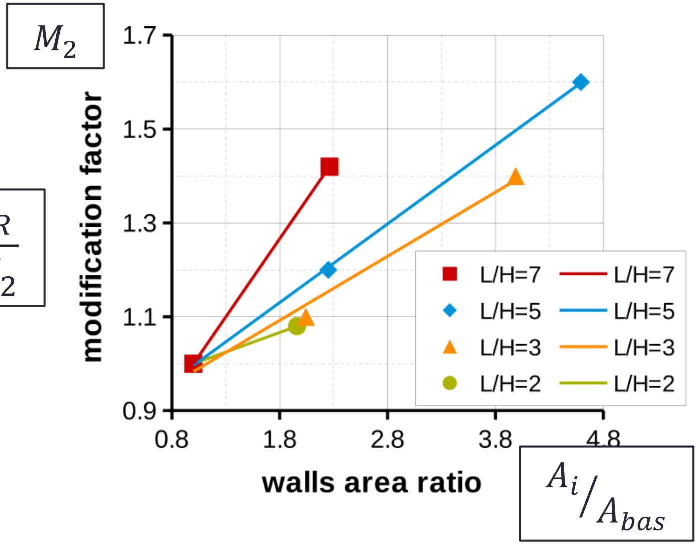

Conclusion: with the increasing area of the wall (increasing length, increasing height) the magnitude of the restraint decreases. The influence of the walls area increases with the increasing *L/H* ratio.

Influence of support conditions

Two walls:
- **short** (L/H = 1.4)
- **long** (L/H = 7)

Two types of soil:
- **soft**
- **hard**

$K_{hard} >> K_{soft}$
$G_{hard} >> G_{soft}$

~ x100

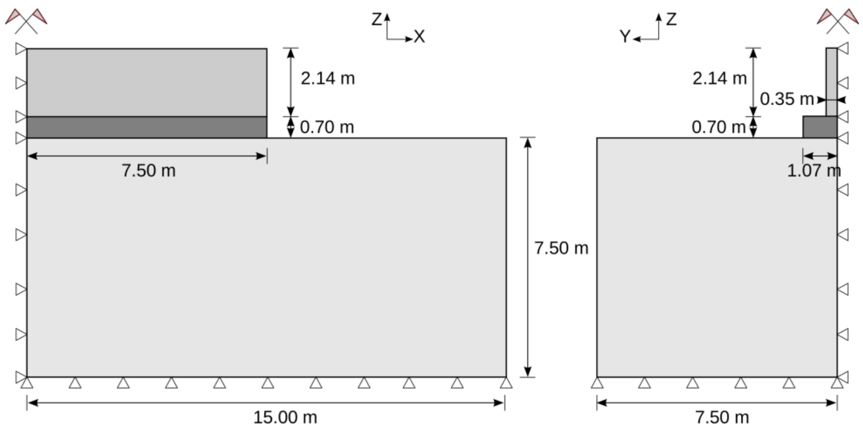

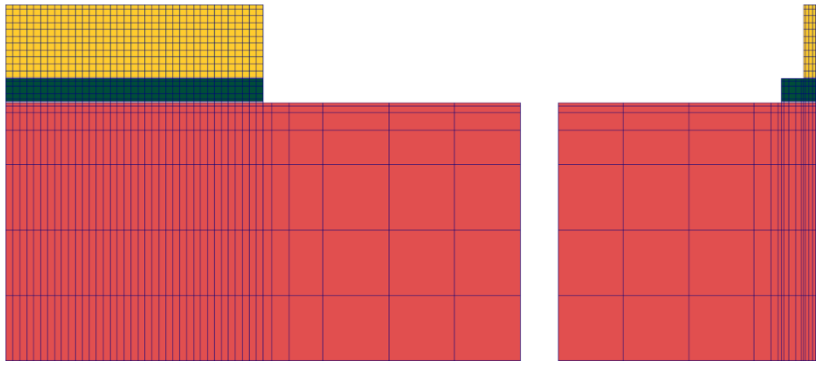

Influence of support conditions

Long wall

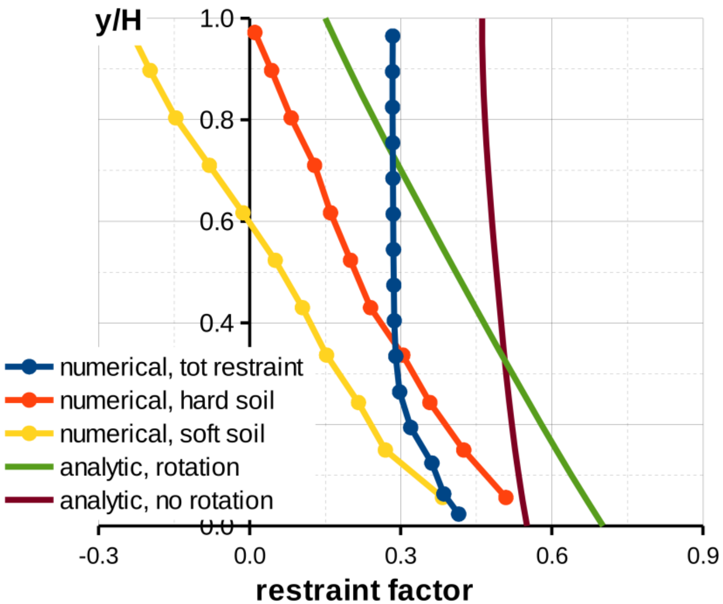

Short wall

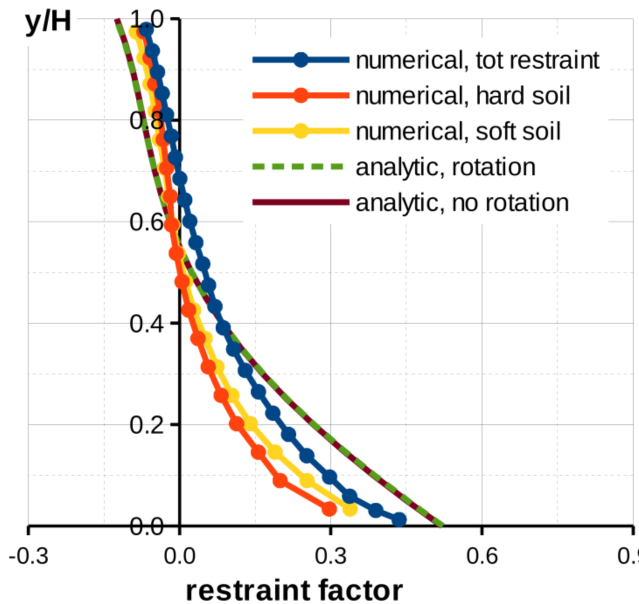

Conclusion: effect of support conditions visible in long wall; effect of soil: occurrence of rotation + translational restraint

Influence of support conditions

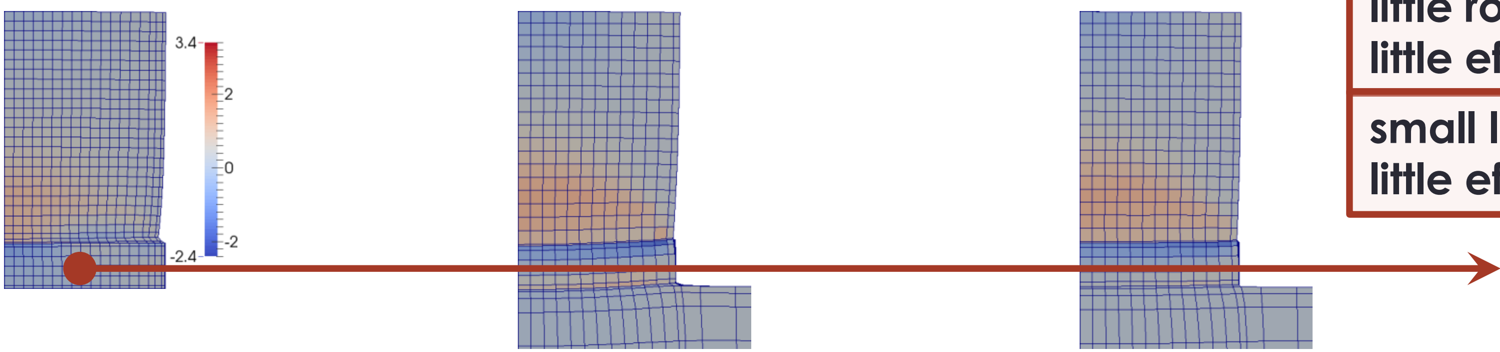

little rotation → little effect on γ^{ry}_R

small length → little effect on γ^{t}_R

total rotational restraint

hard soil

soft soil

stress redistribution due to cracking

large rotation → large effect on γ^{ry}_R

great length → huge effect on γ^{t}_R

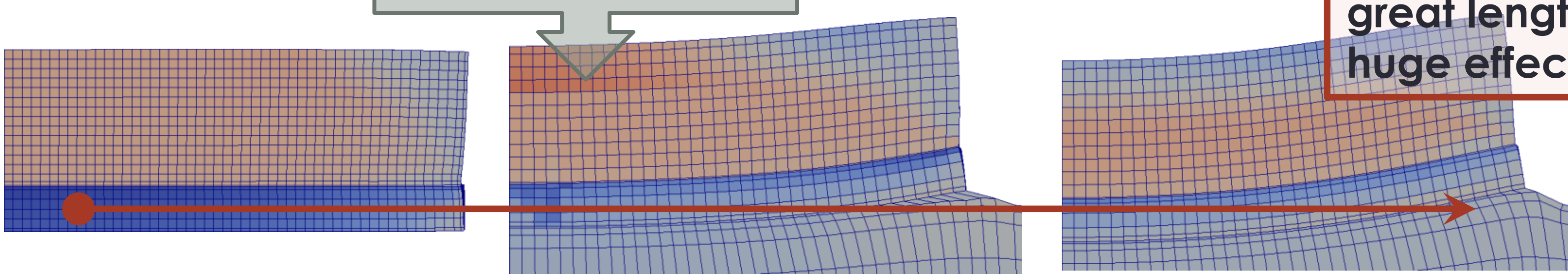

Conclusions

1. In determination of the degree of restraint **not only the *L/H* ratio but also** the individual dimensions of the wall (***L* and *H***) must be taken into account – scale effect.
2. Real support conditions must be provided in analysis of walls which means **introduction of the soil block** to simulate:
   - the founding soil with its real properties (stiffness)
   - the possibility of loss of contact between the foundation and the soil as a result of ends lifting due to rotation of the structure.

References

Early-age stresses in concrete structures – modelling and analysis

1. **Klemczak B.;** *Adapting of the Willam–Warnke failure criteria for young concrete*. Archives of Civil Engineering 53(2), 2007
2. **Klemczak B.;** *Prediction of coupled heat and moisture transfer in early-age massive concrete structures*. Numerical Heat Transfer, Part A: Applications 60(3), 2011
3. **Klemczak B.;** *Modeling thermal–shrinkage stresses in early age massive concrete structures – Comparative study of basic models*. Archives of Civil and Mechanical Engineering 14(4), 2014
4. **Klemczak B., Knoppik-Wróbel A.;** *Analysis of early-age thermal and shrinkage stresses in reinforced concrete walls*. ACI Structural Journal 111(2), 2014
5. **Klemczak B., Knoppik-Wróbel A.;** *Reinforced concrete tank walls and bridge abutments: early-age behaviour, analytic approaches and numerical models*. Engineering Structures 84, 2015
6. **Knoppik-Wróbel A.;** *Analysis od early-age thermal–shrinkage stresses in reinforced concrete walls*. PhD thesis (in review, expected publication date 05.2015)
7. **Majewski S.;** *Sprężysto–plastyczny model współpracującego układu budynek—podłoże poddanego wpływom górniczych deformacji terenu (Elasto–plastic model of soil –sutructure interaction system undet mining-induced deformations of terrain)*. Gliwice, 1995 [in Polish]
8. **Majewski S.;** *MWW3 — Elasto–plastic model for concrete*. Archives of Civil Engineering 50(1), 2004

References

Degree of restraint

9. **Nilsson M.**; *Restraint factors and partial coefficients for crack risk analyses of early age concrete structures*. PhD thesis, 2003
10. **Hösthagen A. et al.**; *Thermal crack risk estimations of concrete tunnel segments - Equivalent Restraint Method correlated to empirical observations*. Nordic Concrete Research 49, 2014
11. **Al-Gburi M. et al.**; *Simplified methods for crack risk analyses of early age concrete*. Part 1 & 2. Nordic Concrete Research 46, 2012
12. **American Concrete Institute**; ACI 207.2R-07: *Report on thermal and volume change effects on cracking of mass concrete*, 2007
13. **Eurocode 2** – Design of concrete structures. Part 3: Liquid retaining and containment structures
14. **Japanese Concrete Institute**; *JCI Guidelines for control of cracking of mass concrete*, 2008
15. **Japanese Society of Civil Engineers**; *JSCE Guidelines for Concrete. No. 15: Standard specifications for concrete structures. Design*, 2011
16. **Bamforth P. B.**; *CIRIA C660: Early-age thermal crack control in concrete*, 2007

Internal visco-elastic modulus for stress analysis of early-age concrete

E.A.B. Koenders[1], W. Hansen[2]
[1]Technical University of Darmstadt, [2]University of Michigan

Introduction

Photo courtesy of O.M. Jensen

Introduction

Photo EAB Koenders, San Francisco Airport, 2014

Introduction

Classical approach for early age stresses

$$\Delta\sigma(t) = \Delta\left[\varepsilon_{T(\alpha)} + \varepsilon_{cs(\alpha)} + \varepsilon_{as(\alpha)}\right] \cdot E(t)_{(\alpha)} \cdot R$$

$$\Delta\sigma(t,\tau) = \Delta\sigma(t) \cdot \psi(t,\tau)$$

$$\sigma(t) = \sum_{i=0}^{j} \Delta\sigma(t,\tau)$$

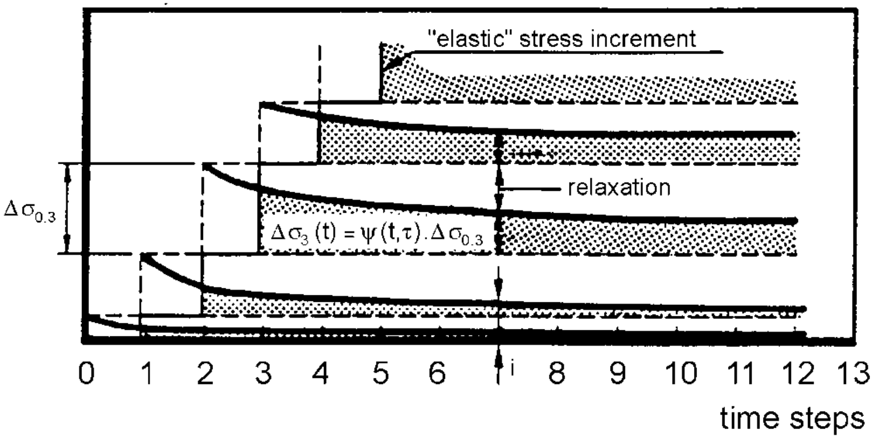

Introduction

Relaxation factor

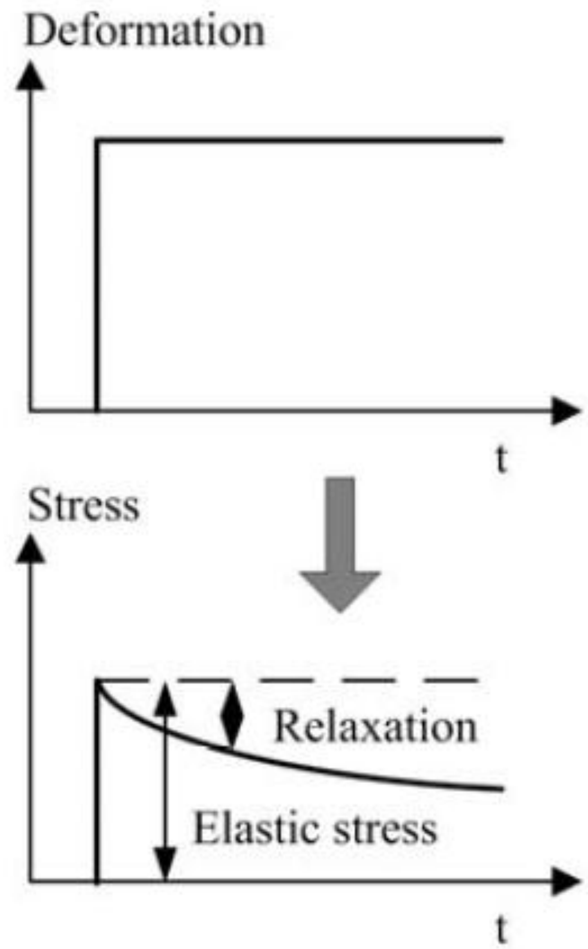

Introduction

Classical approach for early age stresses

Breugel (1985)

$$\psi(\tau_i, t, \alpha_{\tau,i}, \alpha_t) = \exp(-[\frac{\alpha_h(t)}{\alpha_h(\tau_i)} - 1 + 1.34 \cdot \omega^{1.65} \cdot \tau_i^{-d} \cdot (t - \tau_i)^n \cdot \frac{\alpha_h(t)}{\alpha_h(\tau_i)}])$$

Other approach (Schlangen (2006):

$$\psi(t) = E_{factor}(t) \cdot t_{factor}(t)$$

$$E_{factor}(t_i) = \frac{E_{t_i}}{E_{t=168h}}$$

$$t_{factor}(t_i) = -0.05 \cdot \ln(t_i - t_{i-1}) + 1$$

τ	= time when the stress increases
wcr	= w/c-ratio
α	= degree of hydration
d	= constant depending on the hydration rate of cement, slow cement: d = 0.3
n	= constant factor = 0.3

Introduction

Concept of Early-Age Self-Induced Tensile Stresses due to Restrained Deformation Assuming Stress Relaxation

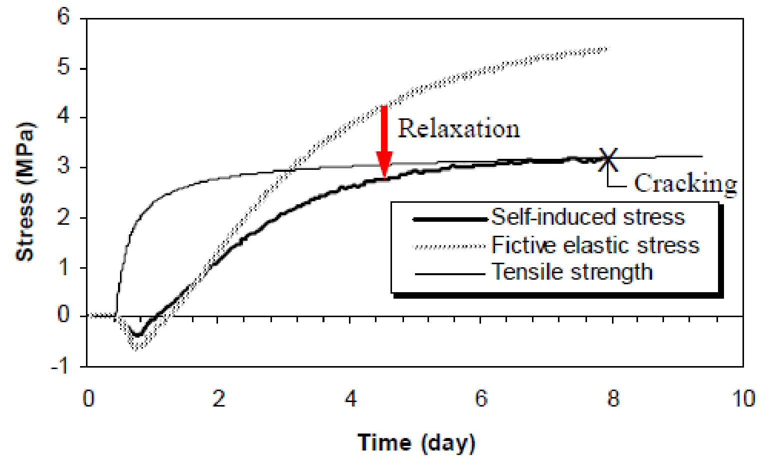

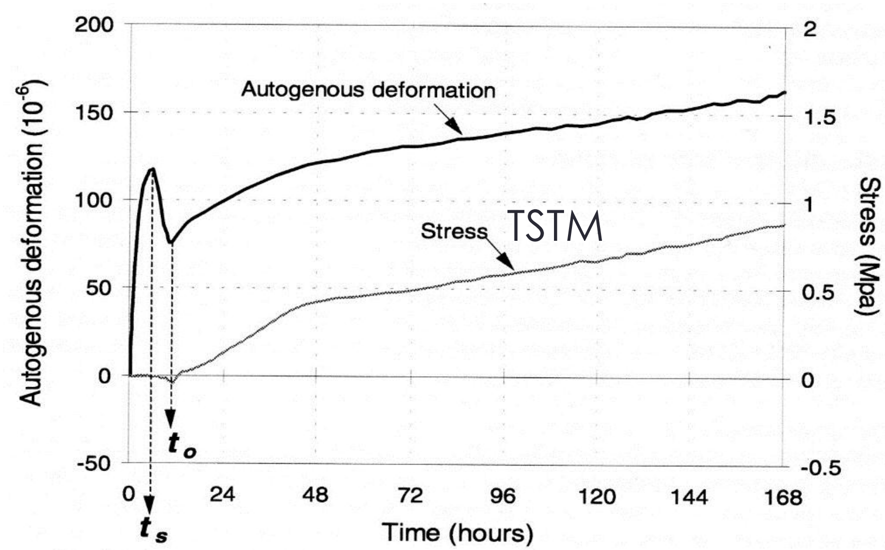

Bjøntegaard, Ø., “Thermal Dilation and Autogenous Deformation as Driving Forces to Self-induced Stresses in High Performance Concrete”, PhD Thesis, NTNU, 1999, 255 pp.

Introduction

TSTM Testing Principle

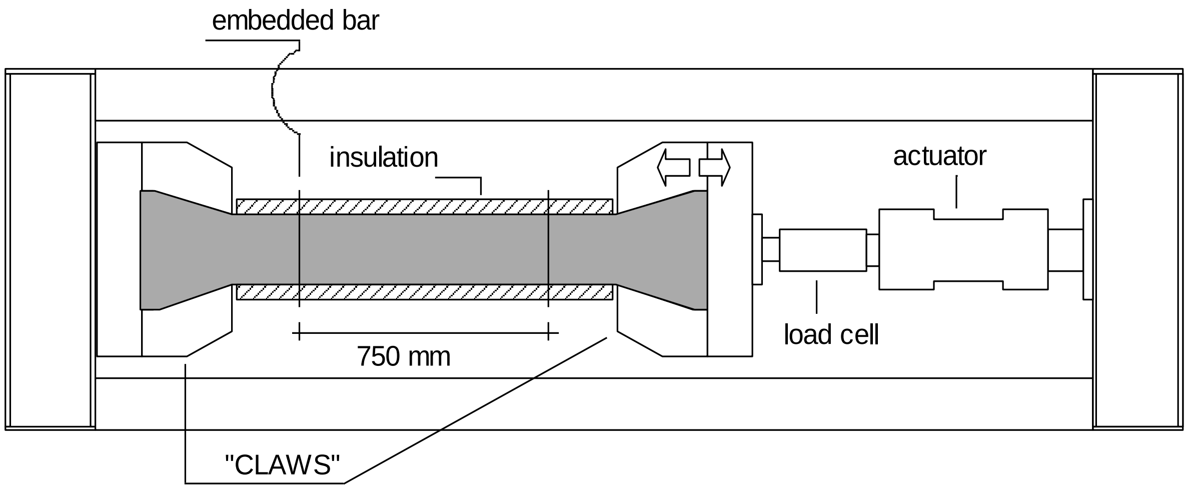

Lokhorst
TU Delft
1995

To measure early age stresses and deformations

Introduction

TSTM Testing Principle

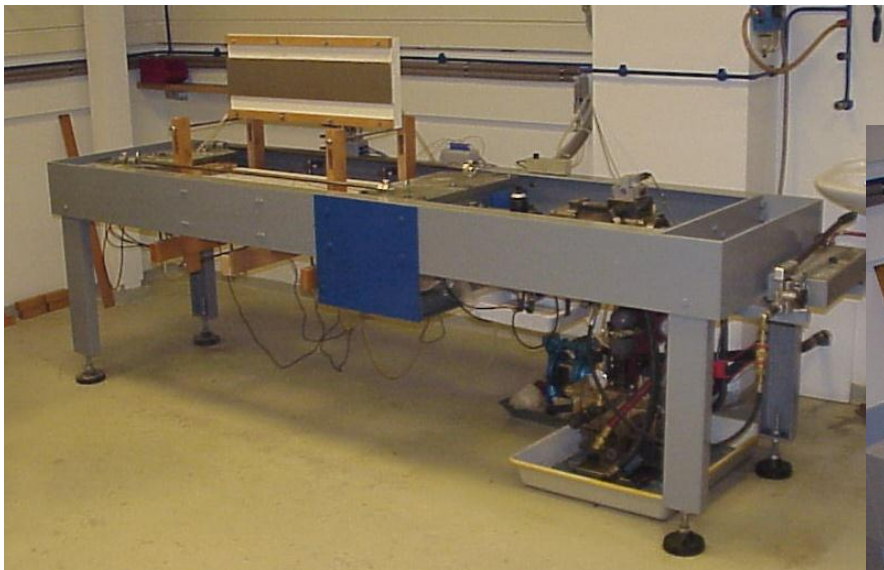

Early age stress measurements

Lokhorst
TU Delft
1995

Introduction

TSTM Testing Principle

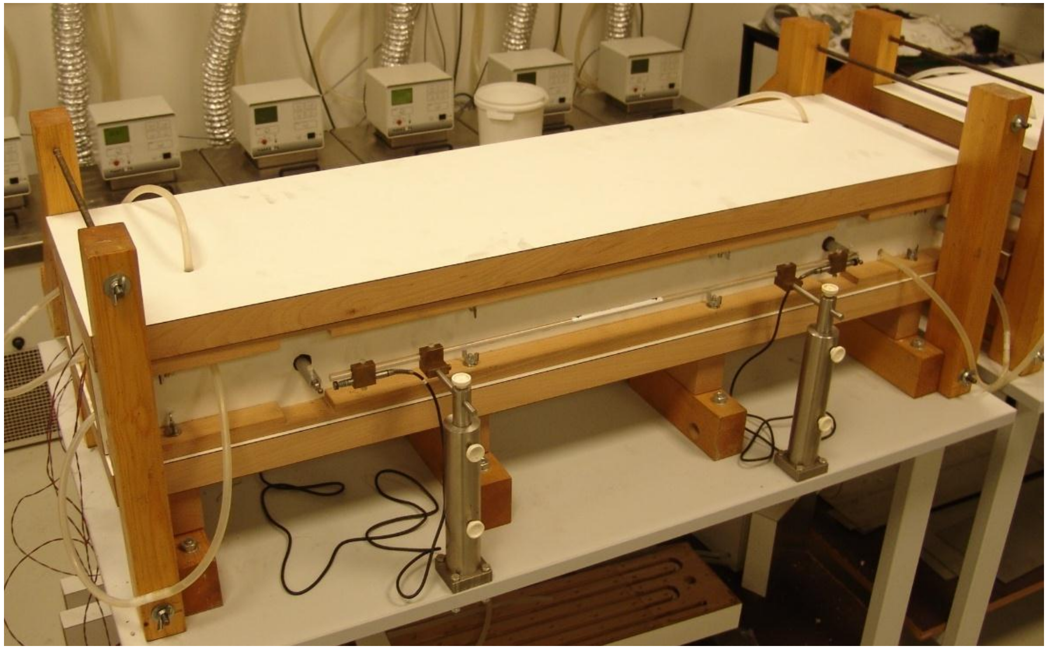

Lokhorst
TU Delft
1995

Early age deformation measurements

Introduction

TSTM Testing Principle

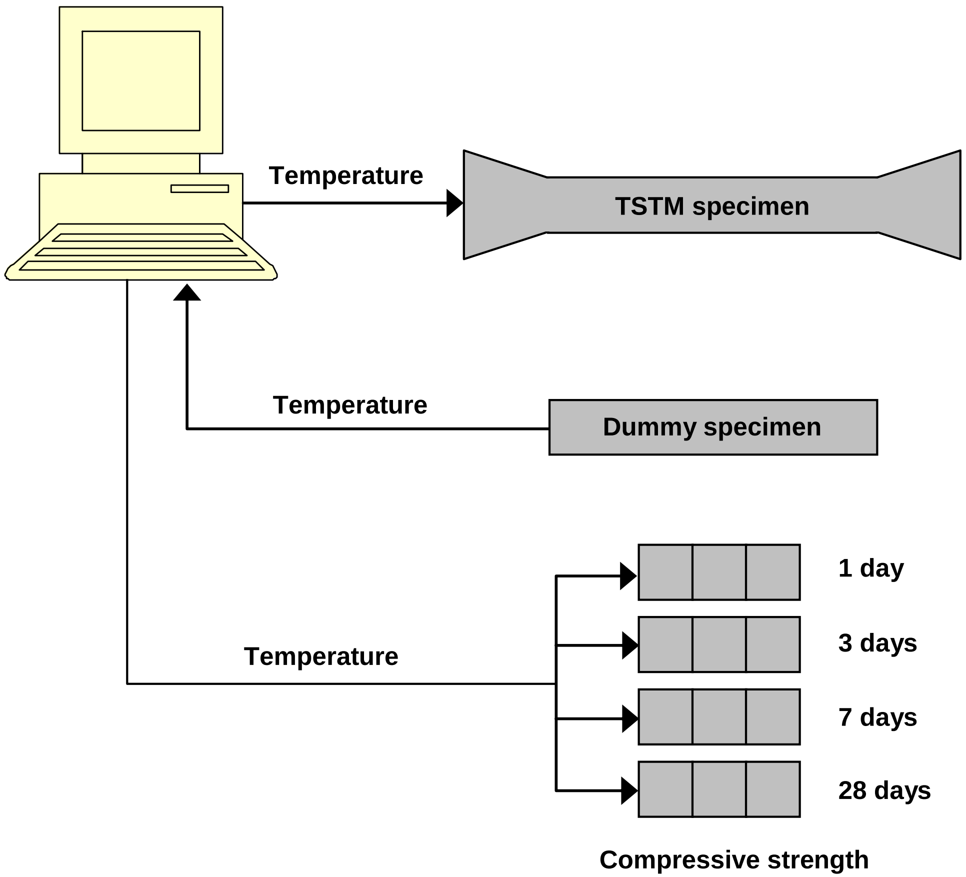

Lokhorst
TU Delft
1995

Internal and External Drying

Hydration of cementitious materials in concrete is affecting its autogenous shrinkage and the associated viscoelastic stress development

Autogenous shrinkage

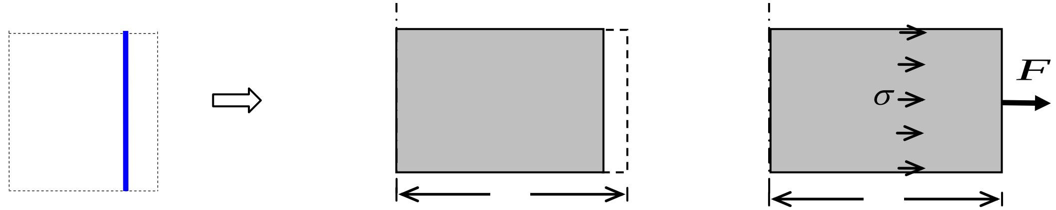

Uniform moisture gradient due to self desiccation — Free autogenous shrinkage — Stress status if autogenous shrinkage is restrained

Drying shrinkage

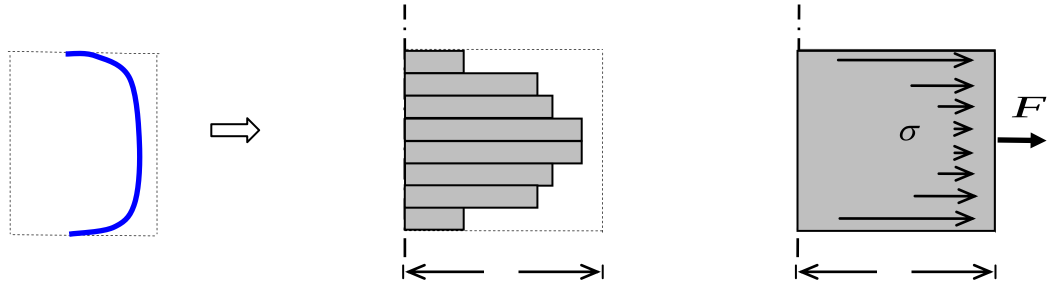

Differential moisture gradient due to external drying — Free drying shrinkage — Stress status if drying shrinkage is restrained

Introduction

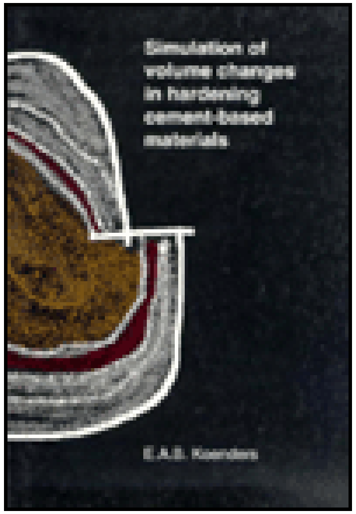

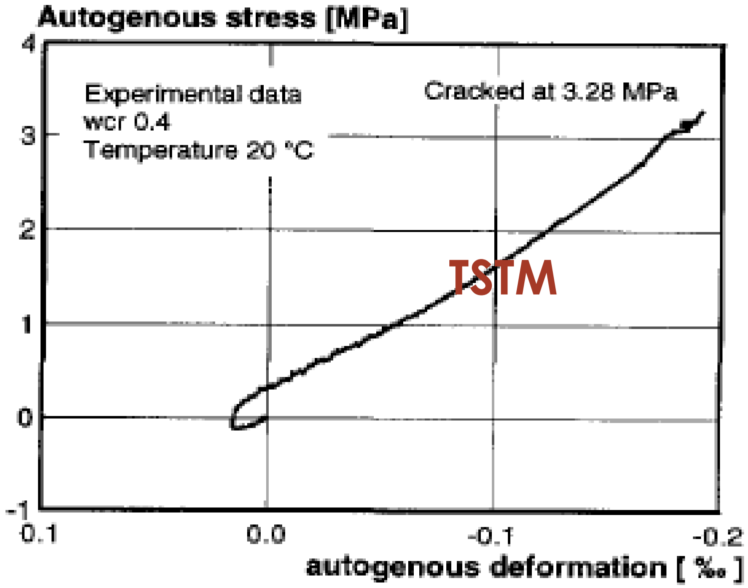

Autogenous stress versus deformation

Free and Restrained Autogenous Shrinkage

Free shrinkage

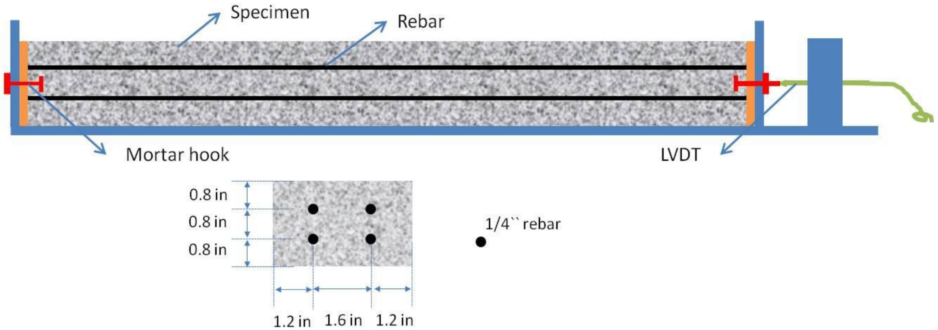

Rebar restrained shrinkage

Sealed curing by double layer plastic

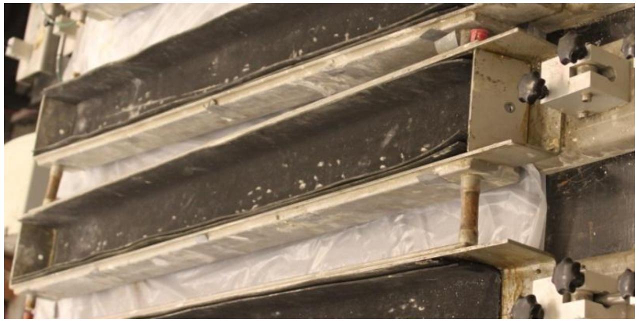

Friction control by rubber pad lining

Movable end plate with LVDT attachment

Free and Restrained Autogenous Shrinkage

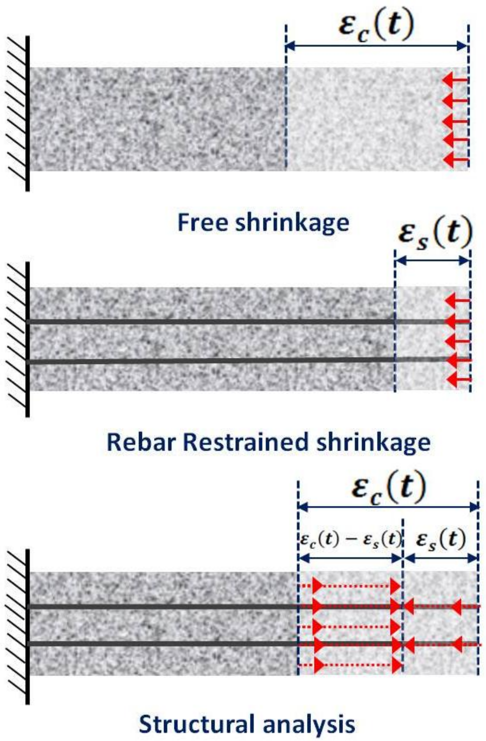

⇨ Rebar in compression
Concrete in tension

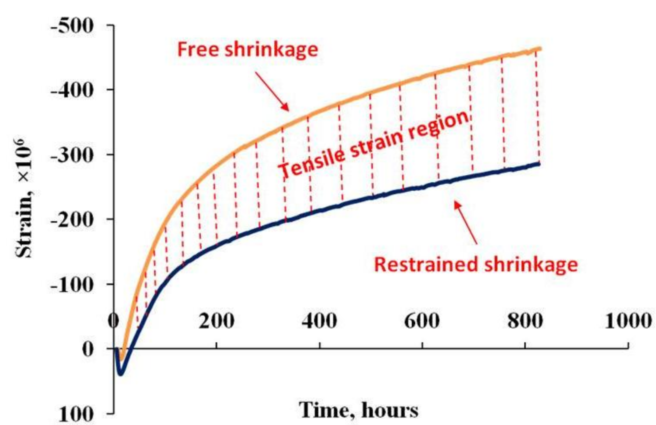

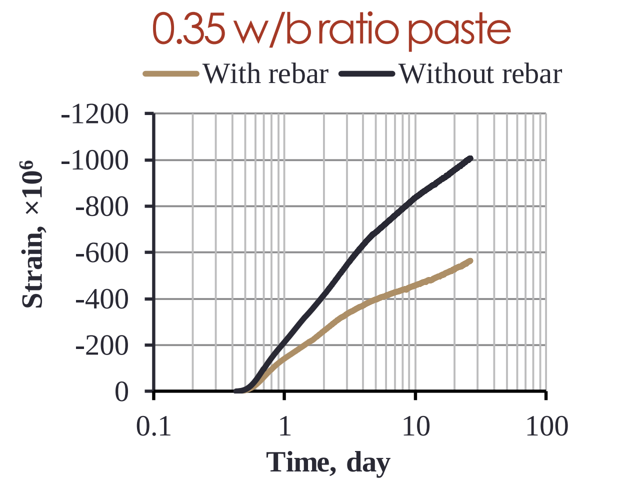

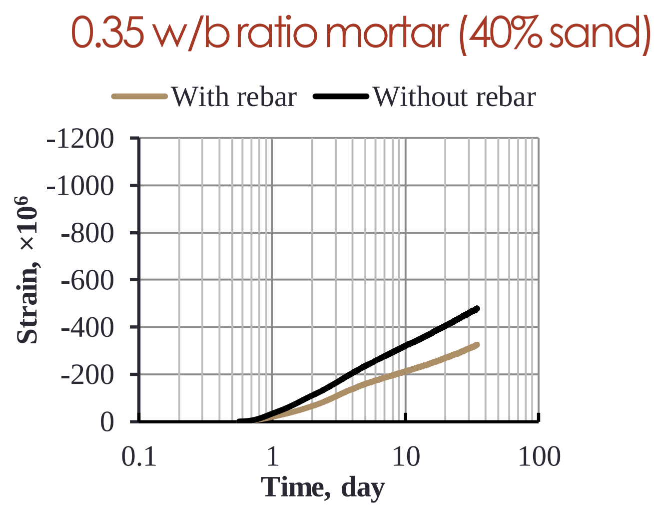

Free and Restrained Autogenous Shrinkage

Bond-slip relationship

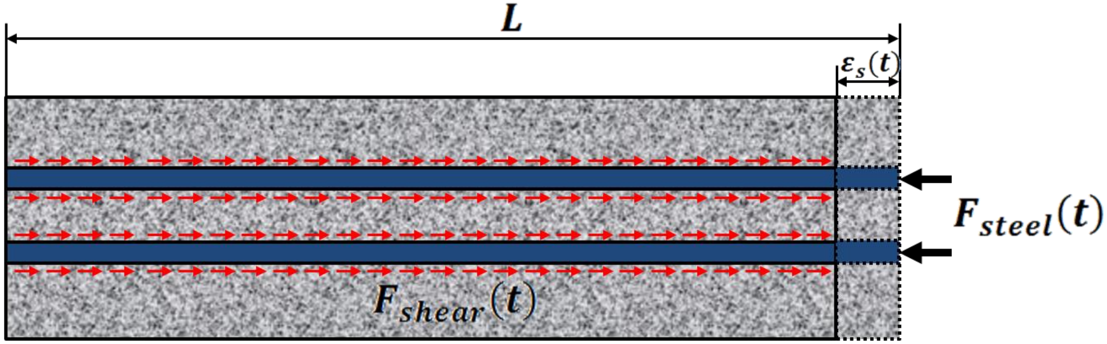

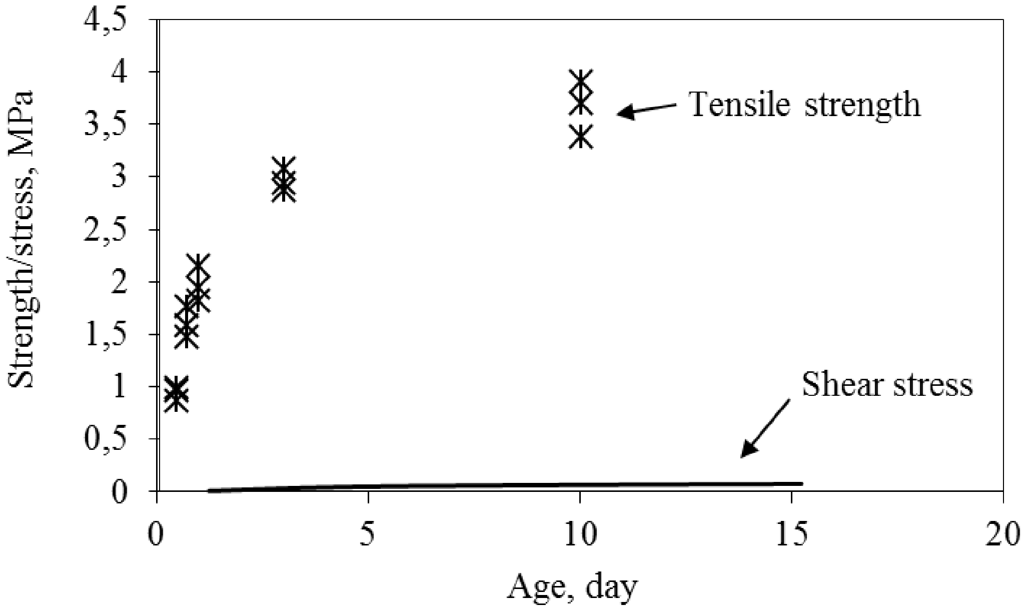

Shear stress in rebars

Free and Restrained Autogenous Shrinkage

$$E_v = E_s n_s / (\frac{\varepsilon_{sh}(t)}{\varepsilon_s(t)} - 1)$$

Where:

$\varepsilon_{sh}(t)$= free shrinkage of plain mix, $\varepsilon_s(t)$= steel deformation in RC mix

A_c= area of concrete,

A_s= area of steel,

n_s= steel ratio,

E_s= steel modulus,

E_v= viscoelastic hydration modulus.

0.35 w/b ratio paste

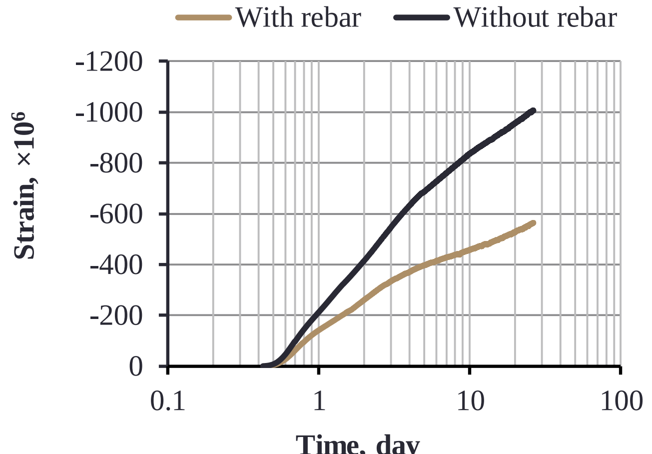

0.35 w/b ratio mortar (40% sand)

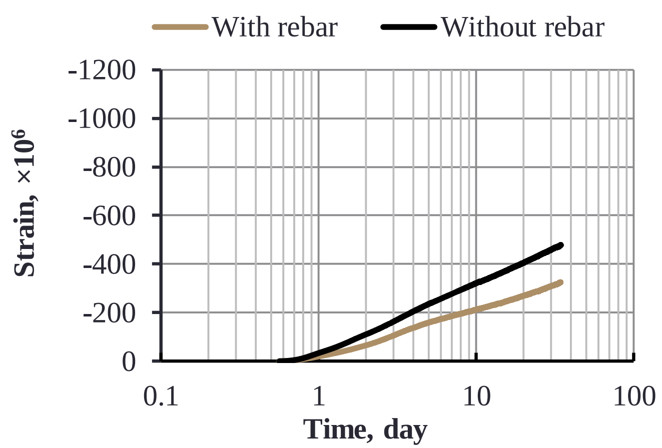

Hydration Modulus E_V and Young’s Modulus E_C

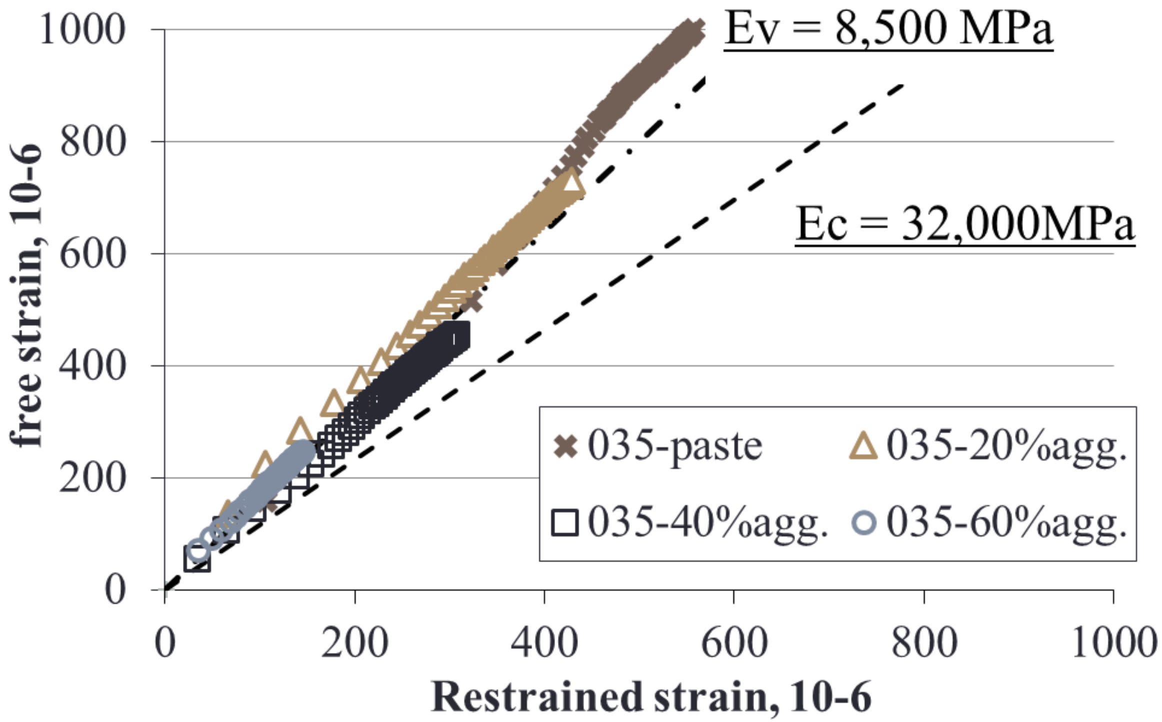

•Low Hydration Modulus due to High Internal Deformation Capacity (Interlayer & Capillary Pores)

• Young’s Modulus controlled by Aggregate Stiffness and High Volume Fraction

Components for total Tensile Stress Prediction

The Pickett shrinkage model: $\varepsilon_c = \varepsilon_p(1 - V_a)^n$

V_a Agg. content

ε_c Concrete shrinkage

ε_p Paste shrinkage

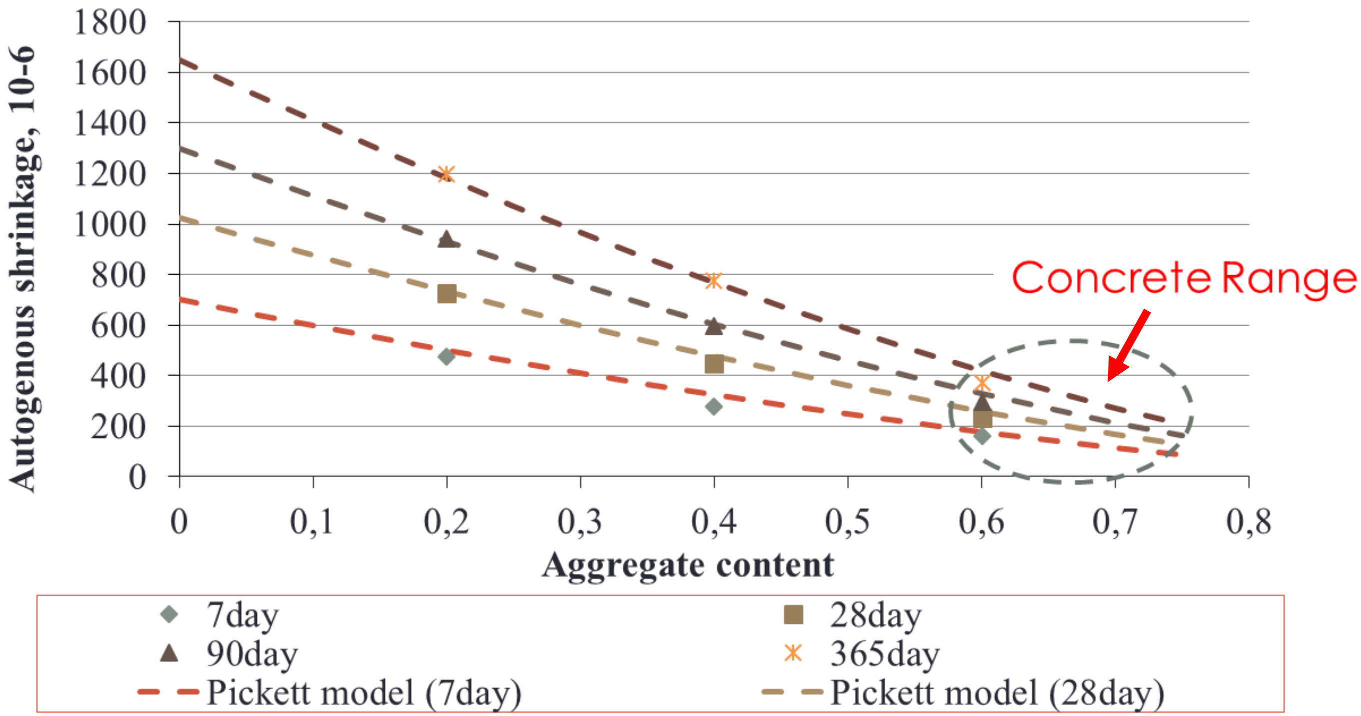

The Pickett shrinkage model is ideally suited for modeling autogenous shrinkage as it is developed for a uniform paste shrinkage stress within a cross section.

Mechanical Components for Total Tensile Stress Prediction

Static modulus development

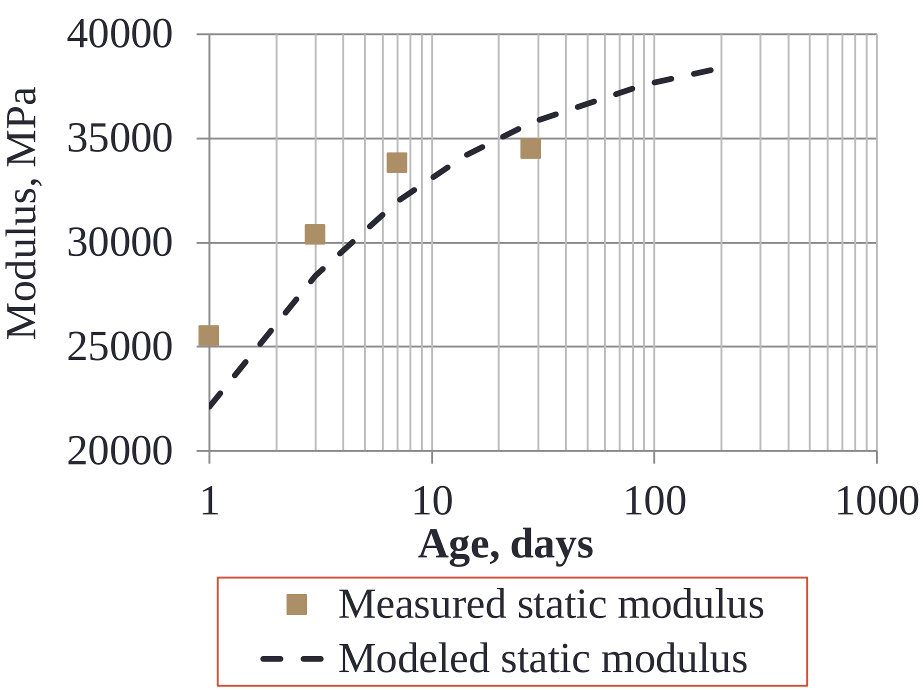

Strength development

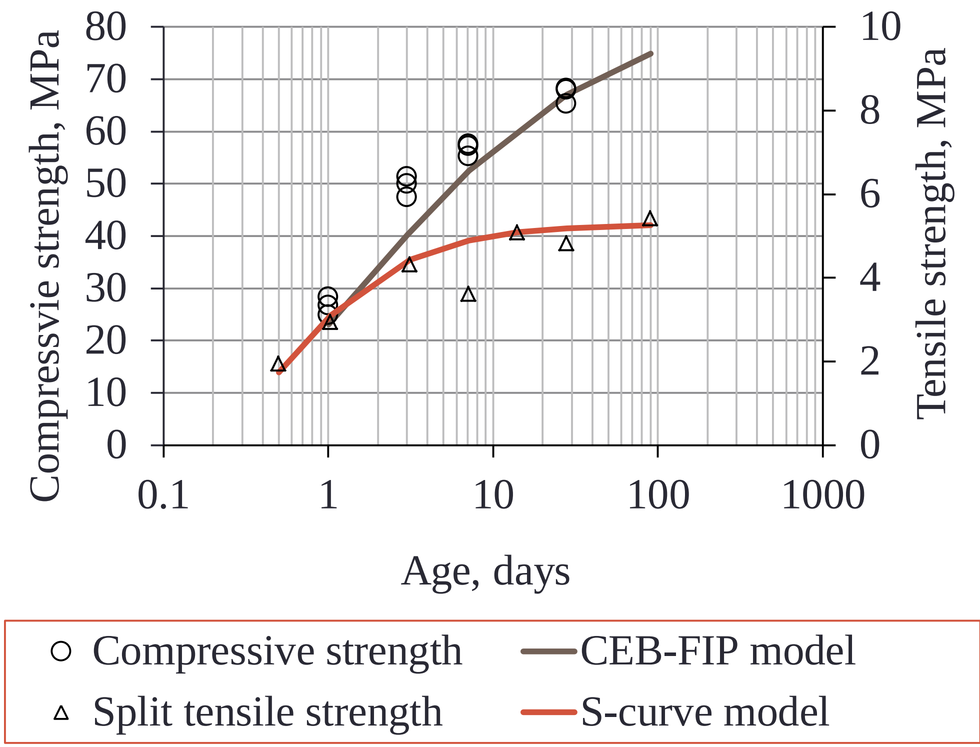

Early-Age Tensile Stress Prediction Methodology

Tensile stress

$$\sigma_{tensile}(t) = \sigma_{thermal}(t) + \sigma_{shrinkage}(t)$$

Thermal stress from TSTM

$$\sigma_{thermal}(t) = (T_{zero} - T_c) \times CTE \times E_t \times R_f$$

Shrinkage stress

$$\sigma_{shrinkage}(t) = E_v \times \varepsilon_{sh}(t) \times R_f$$

R_f : Restraint factor (0-1)

CTE : Coefficient of thermal expansion

E_t : Elastic tension modulus

E_v : Internal visco-elastic modulus

Early-Age Tensile Stress Prediction Methodology

Stress from autogenous $\sigma_{shrinkage}(t) = E_v \times \varepsilon_{sh}(t) \times R_f$

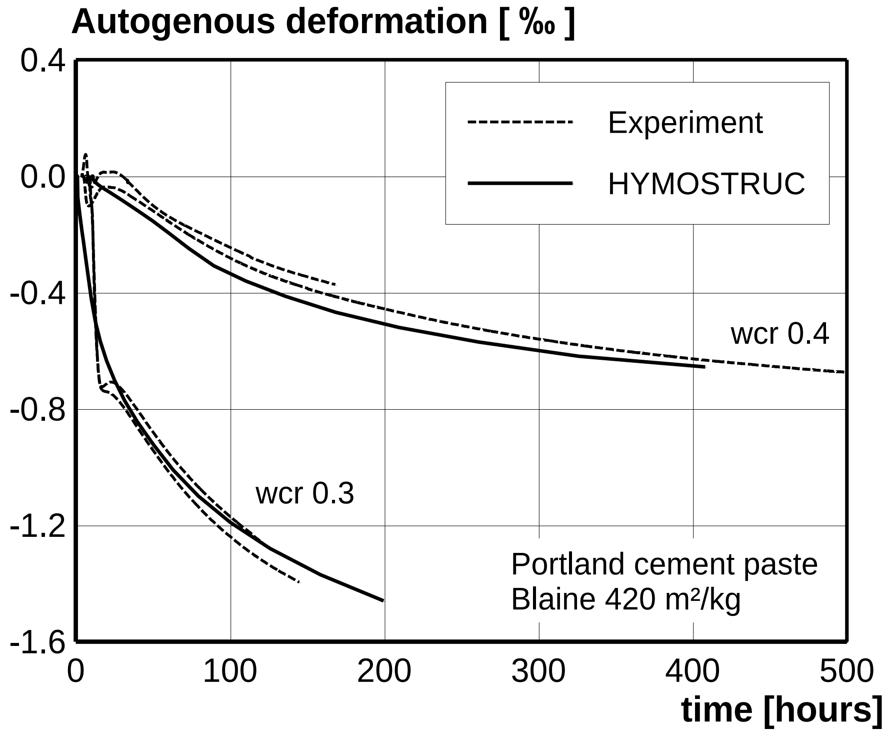

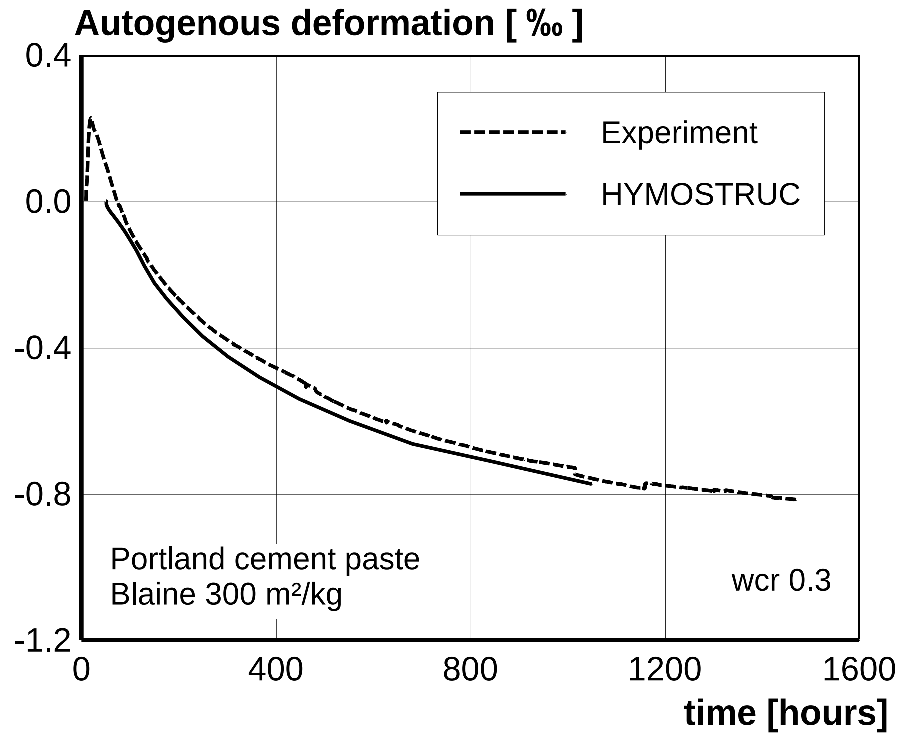

Early-Age Tensile Stress Prediction Methodology

Stress from autogenous

$$\sigma_{shrinkage}(t) = E_v \times \varepsilon_{sh}(t) \times R_f$$

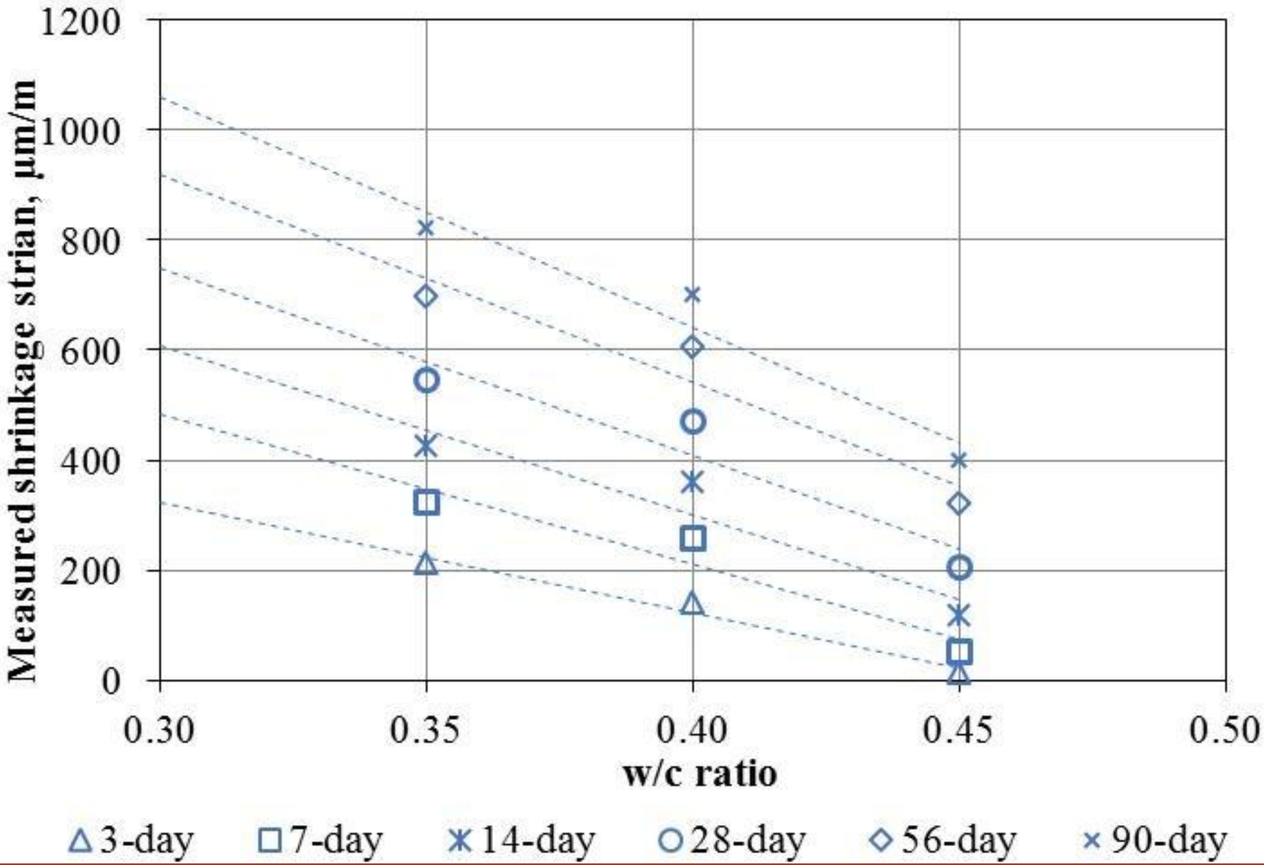

Early-Age Tensile Stress Prediction Methodology

Stress from temperature $\sigma_{thermal}(t) = (T_{zero} - T_c) \times CTE \times E_c^t$

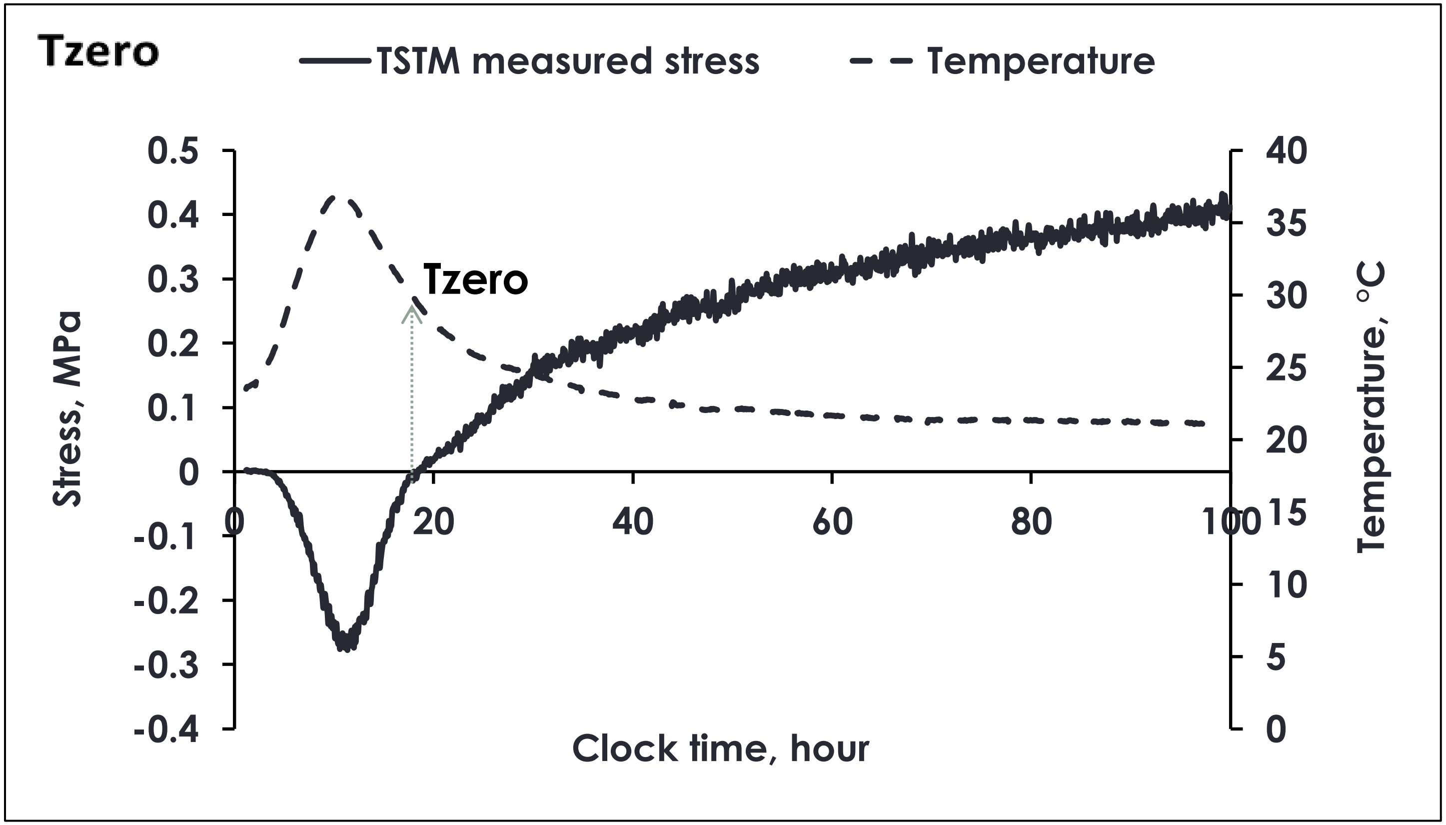

Probability method for tensile failure (Lokhorst)

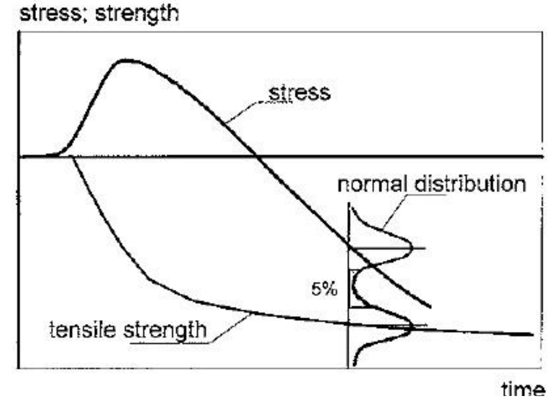

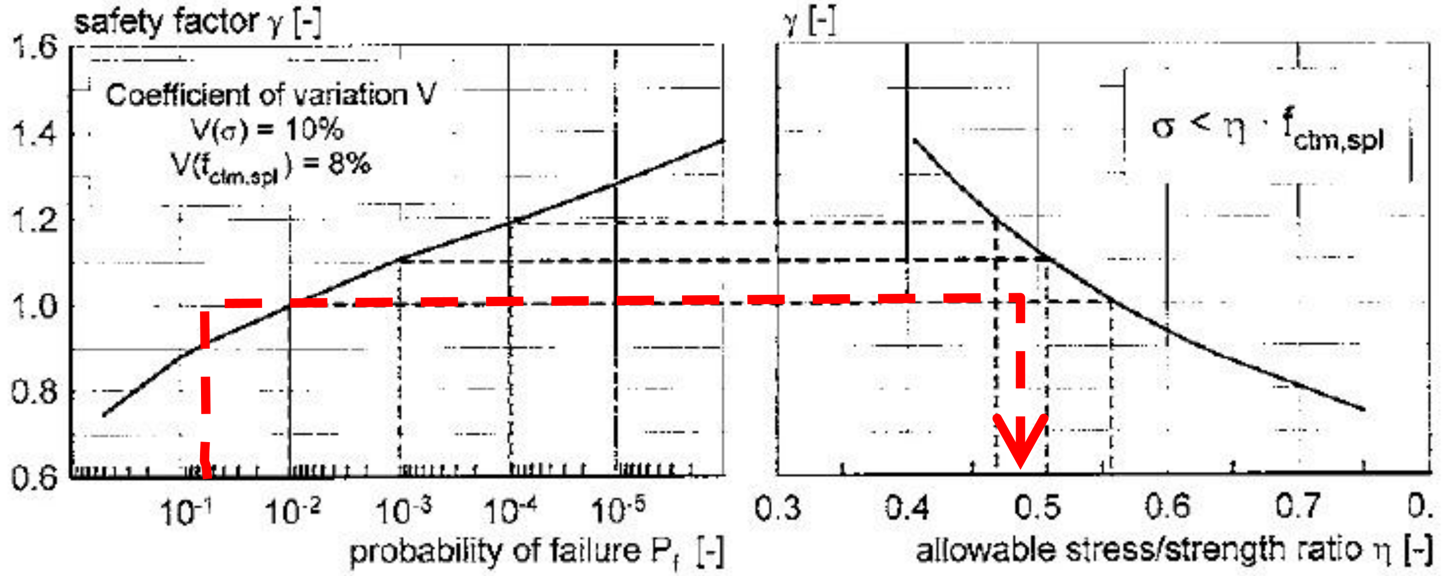

1% probability of failure ~ 0.56 stress/strength ratio

Early-Age Tensile Stress Prediction Without Thermal Effects

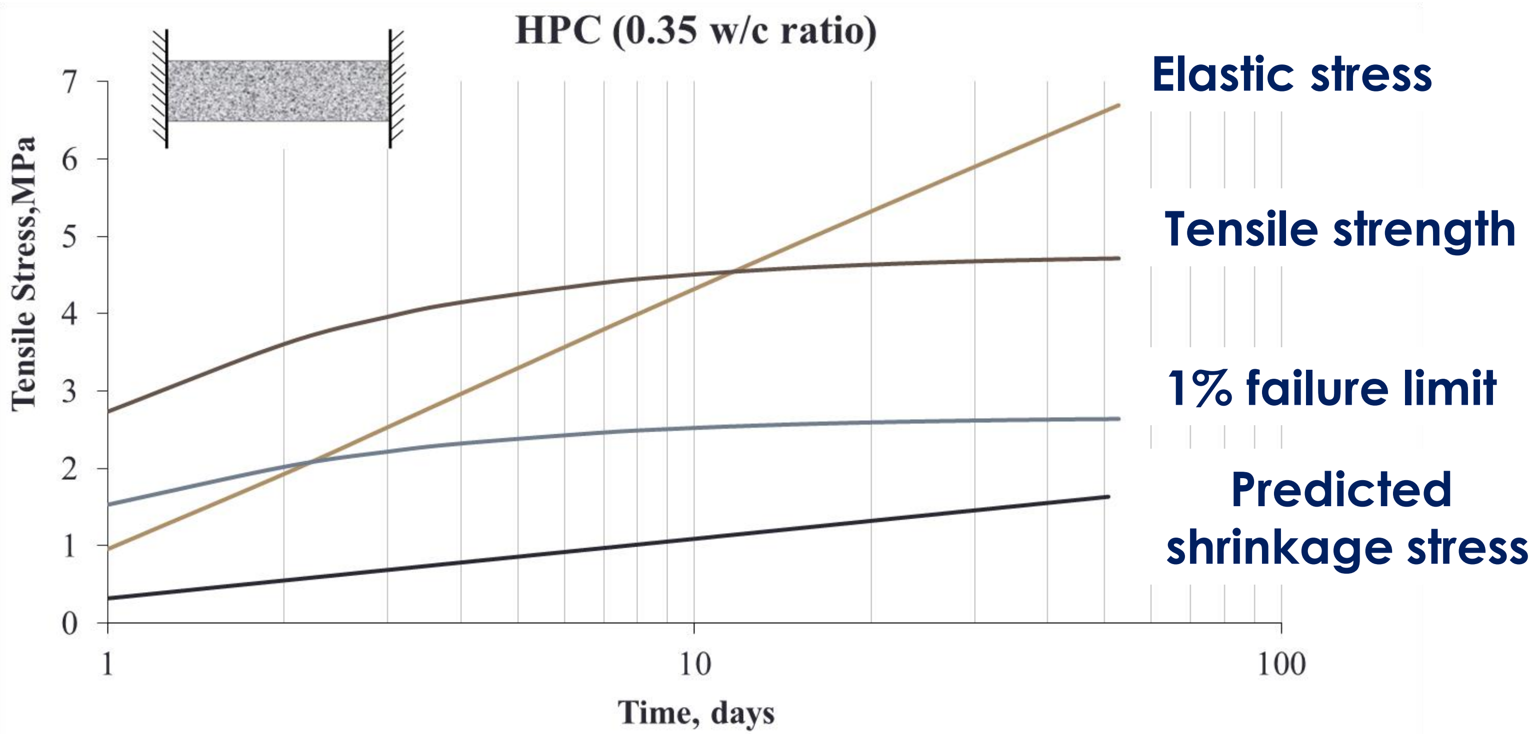

Shrinkage stress prediction for 28-day autogenous shrinkage (~ 172 x 10^{-6})

28-day shrinkage stress is significant

Important parameters

So: What are now the important parameters?

Pore structure model

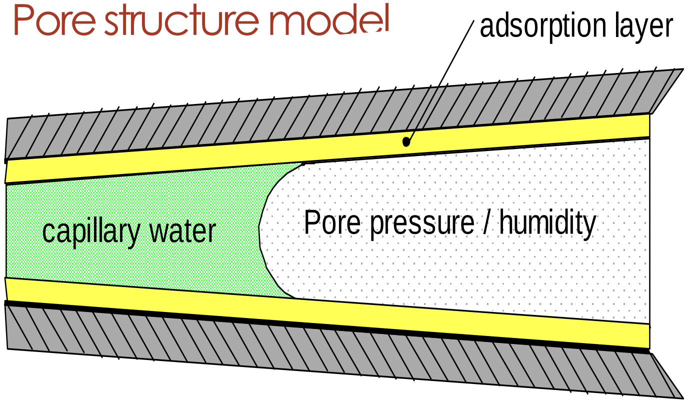

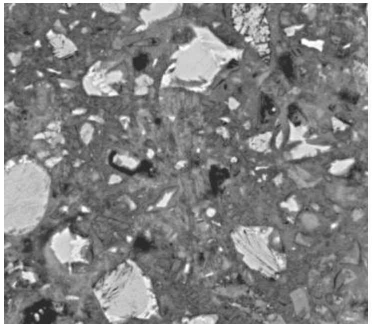

microstructure

Paste:

- Relative Humidity: RH
- Pore size distribution: φ
- Blaine: [m^2/kg]
- w/c ratio

Concrete:

- Aggregate ratio
- Reinforcement ratio

Pore structure in microstructure dependent

Conclusions

- The internal Shrinkage Modulus E_v is obtained from Autogenous Shrinkage Measurements

- Total Stress Analysis of High Performance (low w/c ratio) Cementitious Materials incorporate significant contribution from restrained Autogenous Shrinkage

References

1. W. Hansen, Z. Liu, and E.A.B. Koenders, Internal Viscoelastic Modulus Associated with Autogenous Shrinkage in Cementitious Materials, Journal of Advanced Concrete Technology Vol. 12, 496-502, November 2014, http://dx.doi.org/10.3151/jact.12.496
2. Will Hansen, Eduard A.B. Koenders, Zhichao Liu, Bo Meng and Ya Wei, (2014), "Shrinkage Stress Development in Cementitious Materials", Proceedings International ConMod2014 conference, Beijing, China, pp 204-211.
3. Hansen W, Zhichao Liu and Koenders E.A.B., (2014), "Viscoelastic Stress Modeling in Cementitious Materials Using Constant Viscoelastic Hydration Modulus", Proc. Int. conference on Ageing of Materials and Structures, Delft, The Netherlands, pp 509-515.

CMS Workshop "Cracking of massive concrete structures"

March 17, 2015, ENS-Cachan

Cachan, Île-de-France, FRANCE

Progress in the consideration of the microstructure effects on the aging behaviour of concrete

Frédéric Grondin[1], Ahmed Loukili[1]

[1]Institut de Recherche en Génie Civil et Mécanique (GeM), Ecole Centrale de Nantes, France

Introduction

Structures made with cast concrete are submitted to high loads at early ages. Their effects, particularly the creep strains, are significant.

Structures made with reinforced concrete (shrinkage induces creep)

⇩

Evolving applied loading

Undergroud structures (soil pressure effect)

⇩

Constant applied loading

How the creep develops in reinforced concrete at early ages?

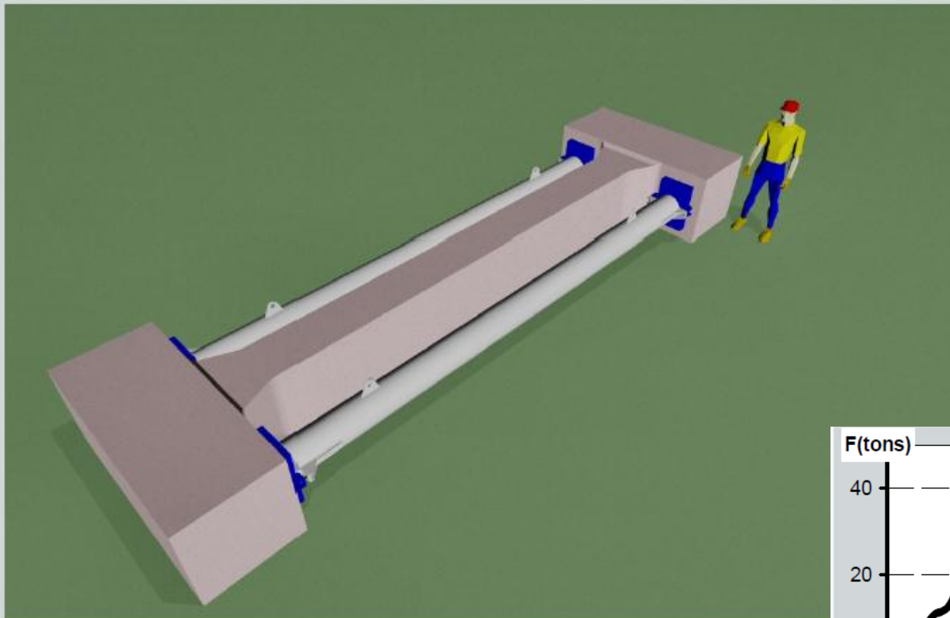

Restrained shrinkage (6.10m x 0.80m x 0.50m)
RG8b: reference concrete and reinforcement

CEOS.FR
Projet National de R&D

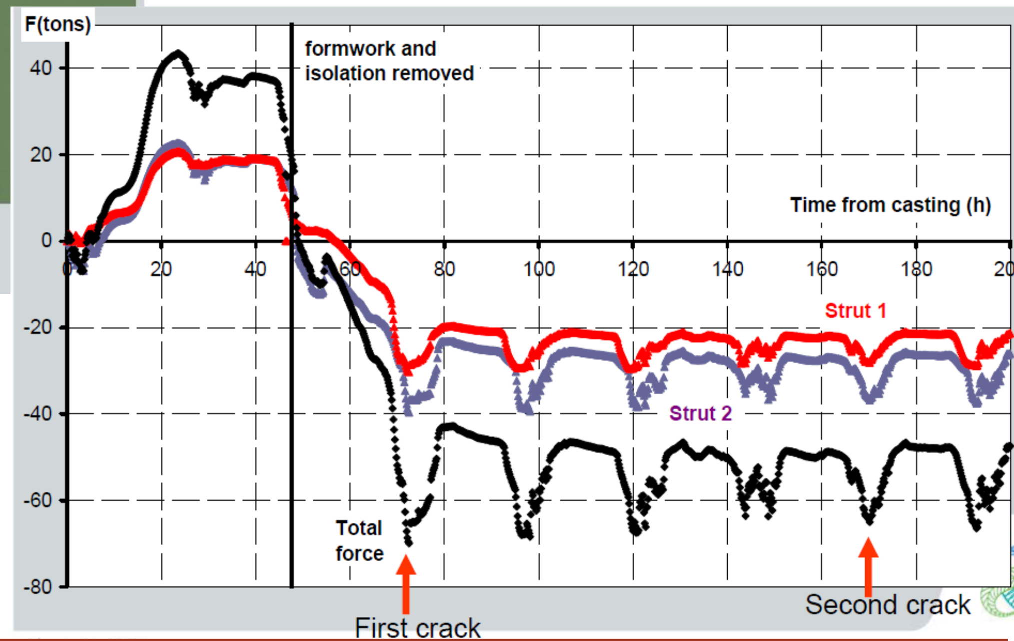

Restrained solidification in concrete

At early ages, local stresses occur on reinforcement in reinforced concrete due to shrinkage.
This implies creep which can lead to microcracking.

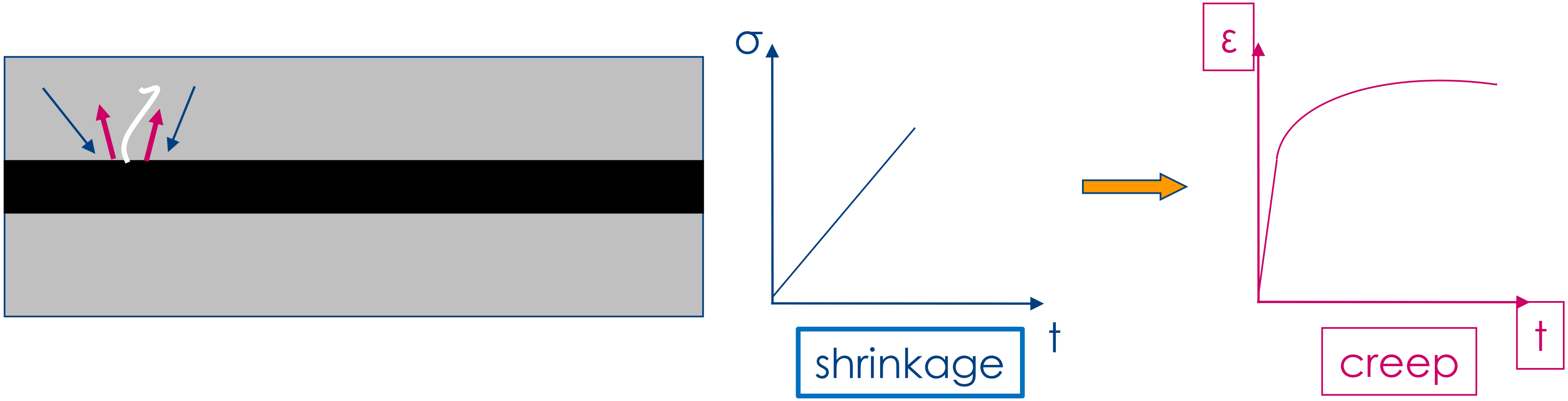

Concrete: a heterogeneous complex material

Concrete is formed by a chemical process between cement and water and aggregates are used for the consolidation. Many chemical reactions occur and give a lot of different phases with different properties.

Infrastructure

Concrete

Mortar

Hydrates

Macro | Meso | Micro

How to model its mechanical behaviour?

- Macro: Standards; Mechanical behaviour law
- Meso: Poro-mechanical behaviour law
- Micro: Chemo-poro-mechanical behaviour law

What is the interest in the development of multiscale models for concrete?

For standard and macroscopic models, laboratory experiments are expected to characterize material properties and some coefficients which are used to define micromechanisms (interactions between components)!

In case of new materials or complex conditions, laboratory investigations are long and difficult to analyze without a good comprehension of the micromechanisms.

Experiments need to be assisted by micromechanical models: multi-scale methods are expected!

Goal

- Study of the coupling between creep and damage at early ages (a)
- Understand the micro-mechanisms which induce creep (b)

New experimental device for creep tests

Creep of ***mature*** concrete has been studied by many authors (Bazant et al., 88; Sanahuja et al., 09; Omar, 04; Reviron, 09; Saliba, 2012)

The creep study of young concrete has been studied by compressive and tensile tests (Briffaut, 10; Jiang, 14…)

Lack of flexural creep tests on concrete

Why a new creep device?

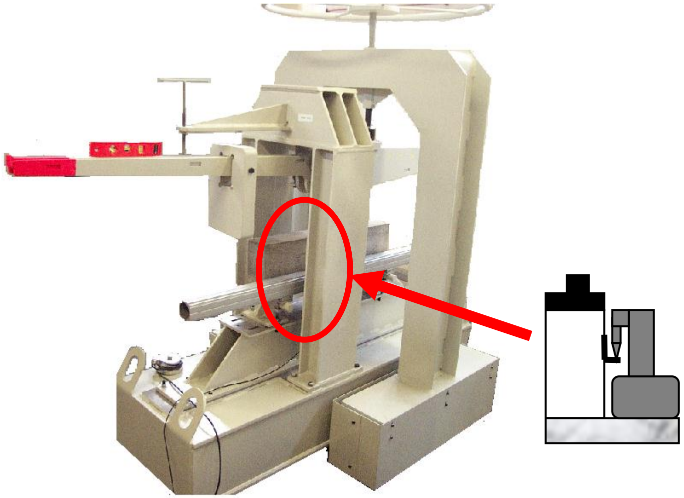

Omar et al.,, 2009.

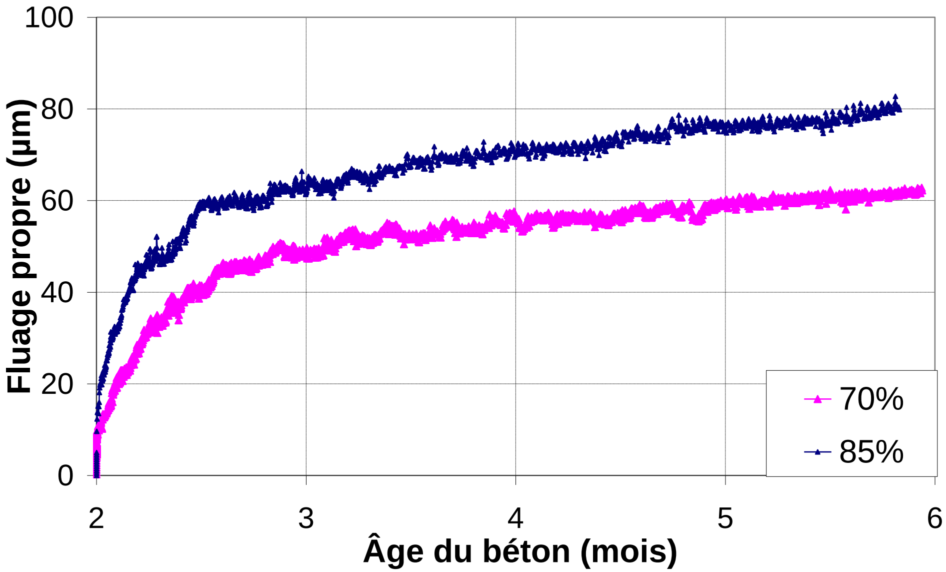

Saliba et al., 2012

- Device developed at GeM Institute

Limitations of this device?

☹ Failure tests (stress relaxation + can not measure the crack opening)

☹ Only one control mode (by force load)

Presentation of the new device

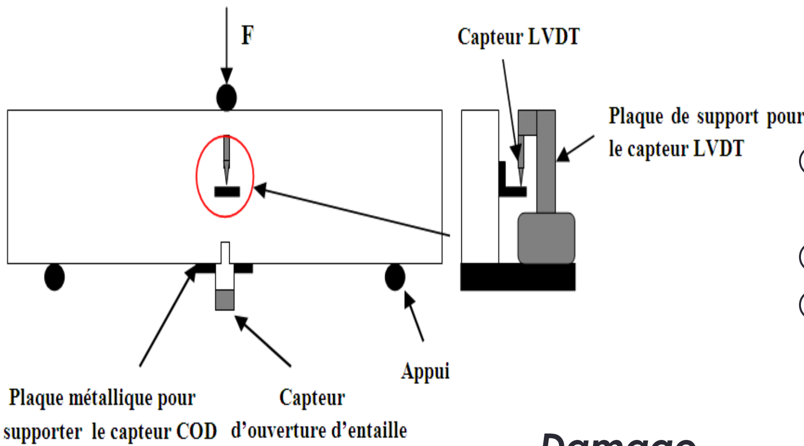

Advantages

- ☺ Failure tests (no stress relaxation + measurement of the crack opening)
- ☺ Two control modes (by CMOD and by force load)
- ☺ Creep tests on cracked concrete beam

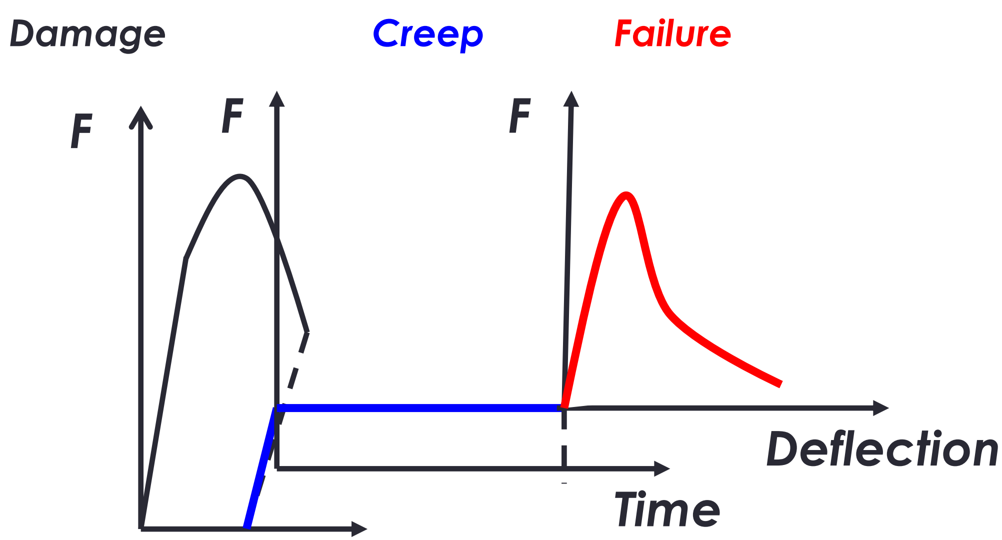

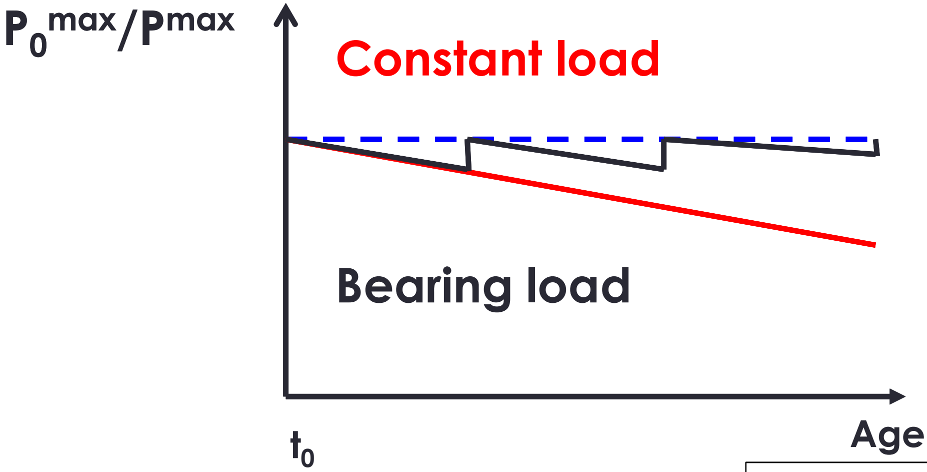

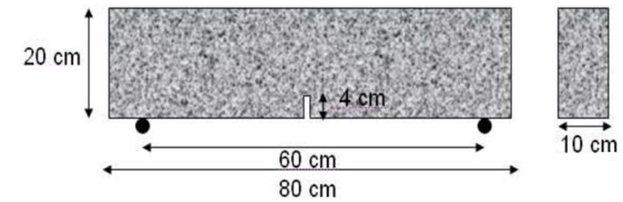

The bearing load gives much larger displacements than those obtained by a constant load

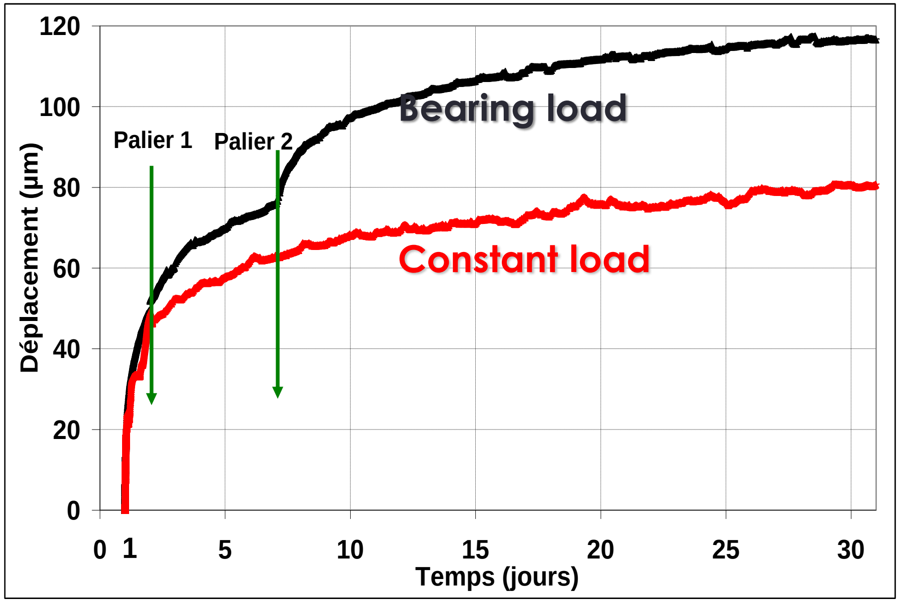

Complex creep loads

Failure behaviour after creep

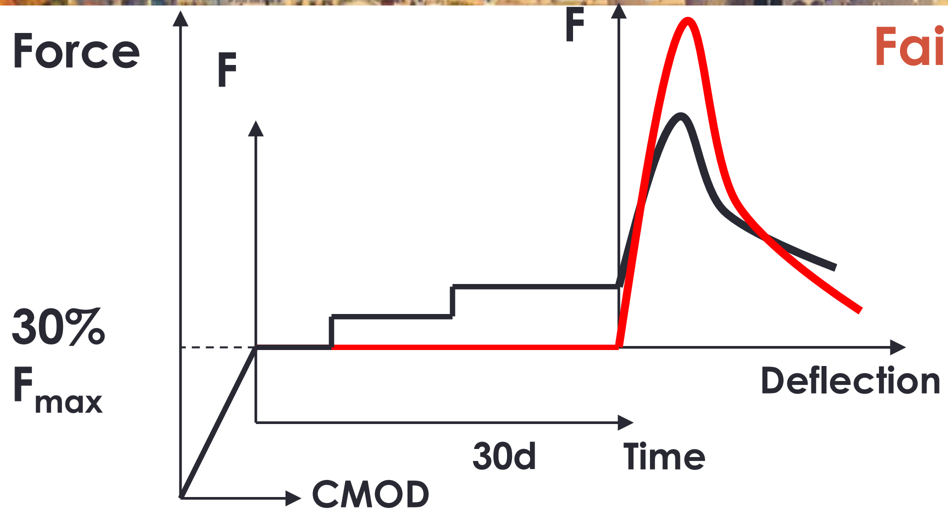

The bearing load most contributes to the loss of rigidity with a small decrease in the flexural strength

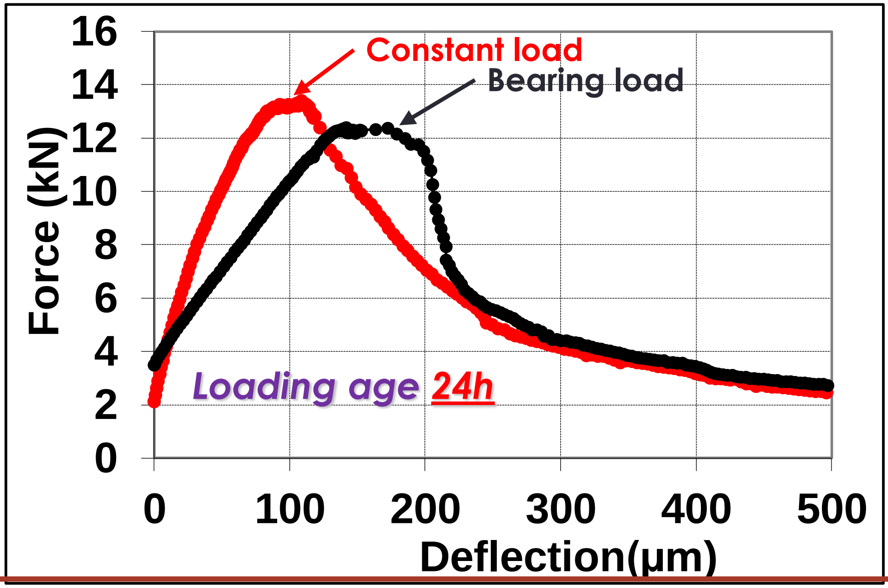

Failure behaviour after creep on pre-damaged beams

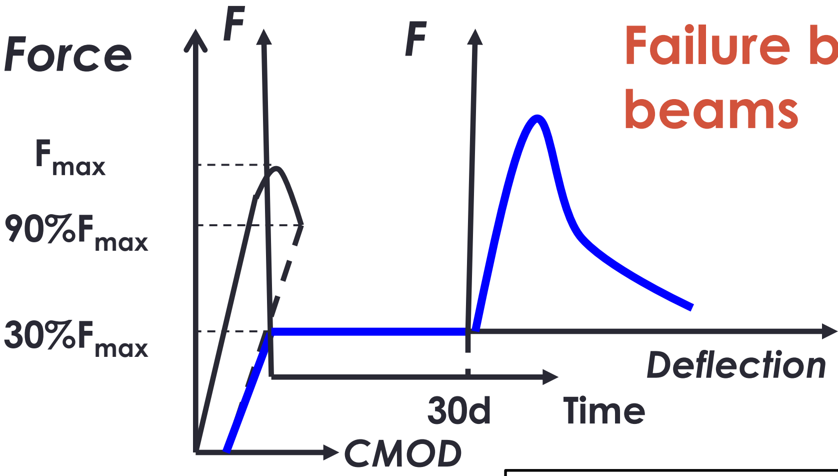

Loss of rigidity and significant decrease in the flexural strength for the pre-damaged beams

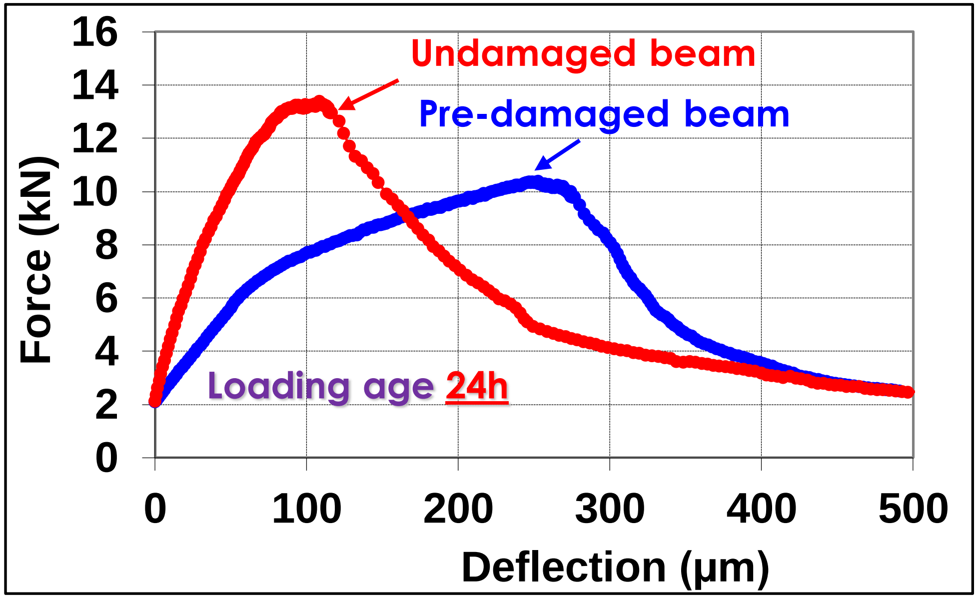

In brief

- **Developpement of a new device to perform flexural tests:**
  - Of creep at early ages
  - Of failure after a creep period without stress relaxation
  - Of creep on pre-damaged beams

- **Characterization of the delayed behaviour**
  - Amplitude of the basic creep is important in the case of a bearing load

- **Characterization of the mechanical behaviour after creep**
  - **Undamaged beams under a constant load**
    - Negligible effect of creep
  - **Undamaged beams under a bearing load**
    - Loss of rigidity with a low decrease of the flexural strength
  - **Pre-damaged beams under a constant load**
    - Loss of rigidity with an important decrease of the flexural strength

Does microcracking occur at low loading?

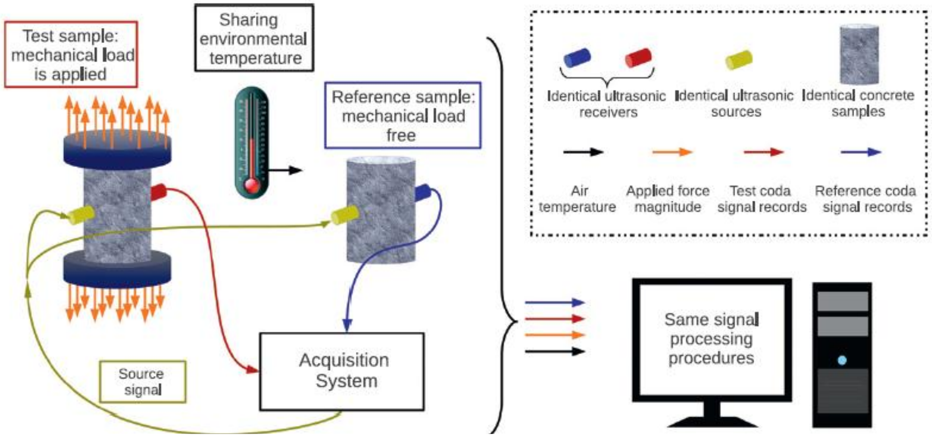

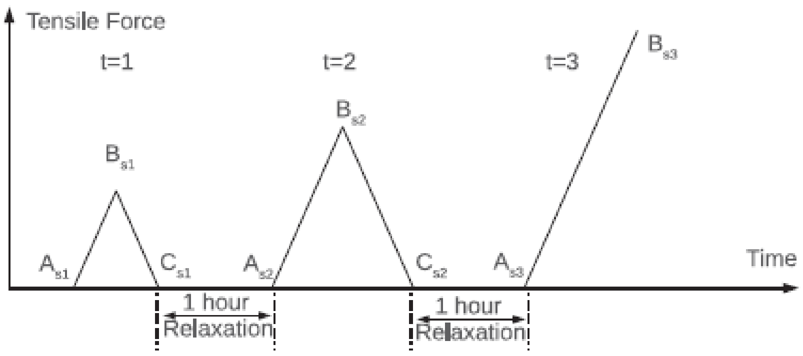

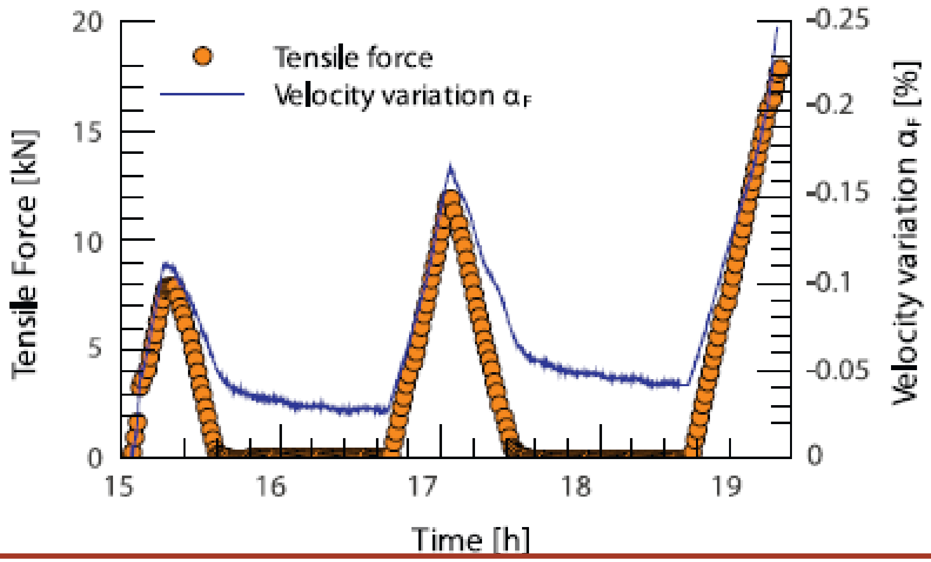

A portion of the velocity reduction remains within the concrete body and accumulates after each loading test.

Modelling of early-age creep

What is the interest in the development of multi-scales creep models for concrete?

At the mesoscopic scale, we make some assumptions on the visco-elasticity of the matrix but we do not consider explicitly the viscous behaviour of C-S-H as recommanded by many authors.

The influence of C-S-H on creep of concrete is more important at early ages. Because the volume fraction of C-S-H increases significantly and its viscous behaviour plays an important role. It allows limiting the micro-cracking due to early-age shrinkage. But it leads to a redistribution of local stresses and can cause new micro-cracking.

Theory: focus on the secondary creep

The main theory adopted to explain the secondary creep is the sliding of the calcium silicate hydrates (C-S-H)

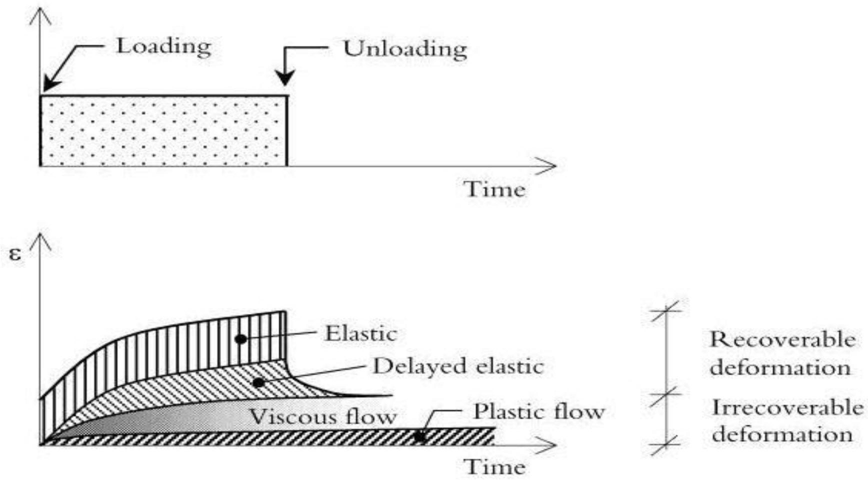

[Emborg, 89]

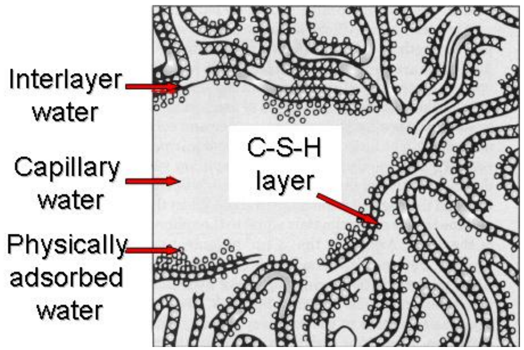

Bazant and Prasannan (1988) have introduced the solidification theory to explain the creep of concrete: *The aging is treated as a consequence of volume growth of the load-bearing solidified matter (hydrated cement) whose properties are nonaging and are described by a Kelvin chain with age-independent moduli and viscosities.*

Presentation of the multiscale model

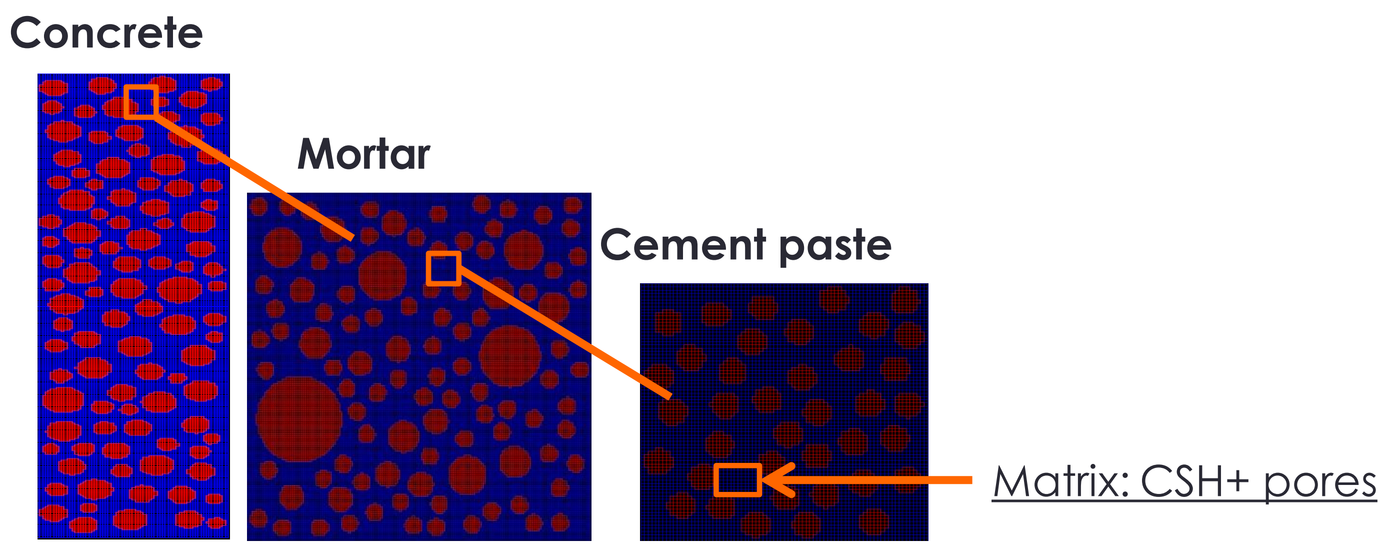

Step 1: Inverse approach to determine the viscoelastic paramters of the matrix at the lowest scale (CSH in this study) without evolution of the volume fractions.

Step 2: Study of the age influence and the evolution of the porosity on the creep of concrete

Step 3: Validation of the model by experiments

Presentation of the multiscale model

Homogeneization of the cement paste and the mortar (Tran et al., 2011) :

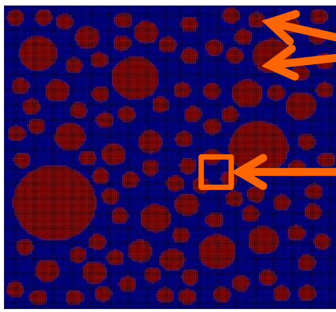

Rigid inclusions

Viscoelastic matrix

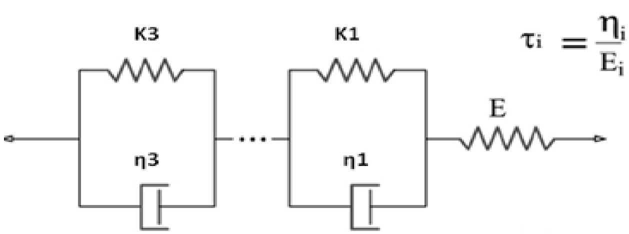

$$J_{matrix}(t) = \frac{1}{E_{matrix}} + \sum_{i=1}^{i=3} \frac{1}{k_i}\left(1 - e^{\frac{-t}{\tau_i}}\right)$$

$$\langle \underline{\varepsilon} \rangle V = \underline{\underline{\underline{\underline{J}}}}^{hom} : \langle \underline{\sigma} \rangle V$$

Effect of the pores quantity on the coefficients of the cement paste matrix (Ricaud et al., 2009):

For each Kelvin-Voigt chain

$$k_{bc}^{i} = \frac{4.\frac{\zeta^{i}}{\tau^{i}}}{3.A(f_p)} = \frac{4.k_{int}^{i}}{3.A(f_p)}$$

Characteristic coeff. defined for an unvolving material

Porosity

Chemical relations

$$C_3S + 5.3H \rightarrow CSH + 1.3CH$$
$$C_2S + 4.3H \rightarrow CSH + 0.3CH$$
$$C_3A + 6H \rightarrow C_3(A,F)H_6$$
$$C_4AF + 10H \rightarrow C_3(A,F)H_6 + FH_3 + CH$$
$$C_3A + 3C\bar{S}H_2 + 26H \rightarrow C_6A\bar{S}_3H_{32}$$
$$C_4AF + 3C\bar{S}H_2 + 30H \rightarrow C_6A\bar{S}_3H_{32} + FH_3 + CH$$
$$2C_3A + C_6A\bar{S}_3H_{32} + 4H \rightarrow 3C_4A\bar{S}H_{12}$$
$$2C_4AF + C_6A\bar{S}_3H_{32} + 12H \rightarrow 3C_4A\bar{S}H_{12} + 2FH_3 + 2CH$$

Residual clinkers $V_X(t) = V_{C0} f_X (1 - \xi_X(t))$

Residual water $V_E(t) = V_{E0} - \sum V_E^X \xi_X(t)$

with $V_E^X = V_{C0} \dfrac{n_E \rho_C f_X / M_X}{n_X \rho_E / M_E}$

Hydrates

$$V_i^P(t) = \sum_{j=1}^{n} C_i^j \xi_j(t)$$

with $C_i^j = V_{C0} \dfrac{n_i^R \rho_C f_j / M_j}{n_j^P \rho_i / M_i}$

Gypsum

$$V_{gyp}(t) = V_{C0} . f_{gyp} (1 - \beta.(3\xi_{C_3A}(t) - 3\xi_{C_4AF}(t)))$$

Ettringite

$$V_{ett}(t) = V_{ett}(t_g)(1 - 0.5\xi_{C_3A}(t) - 0.5\xi_{C_4AF}(t))$$

Inverse approach

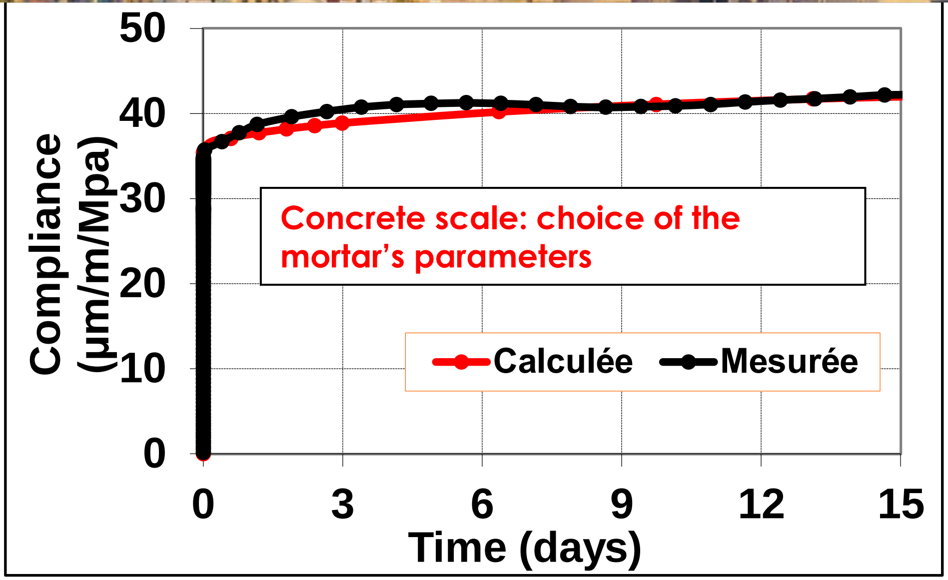

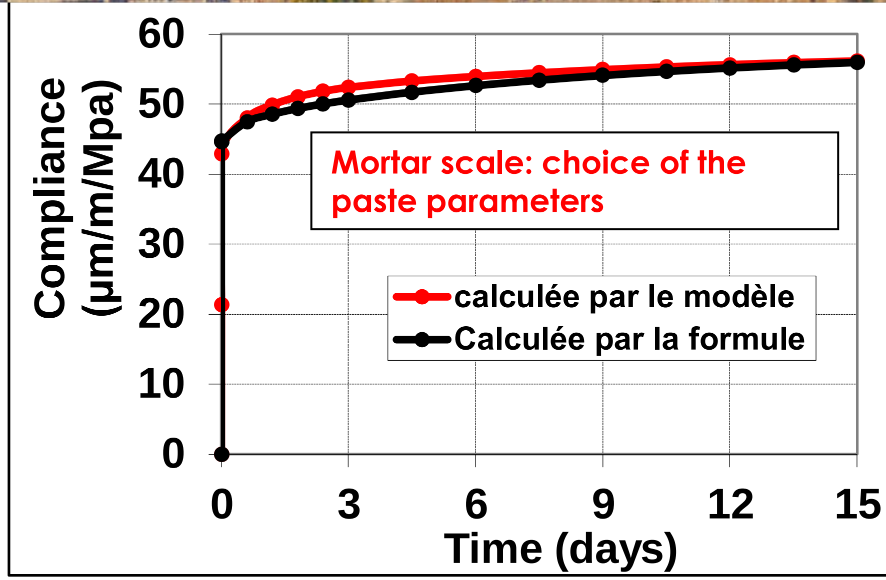

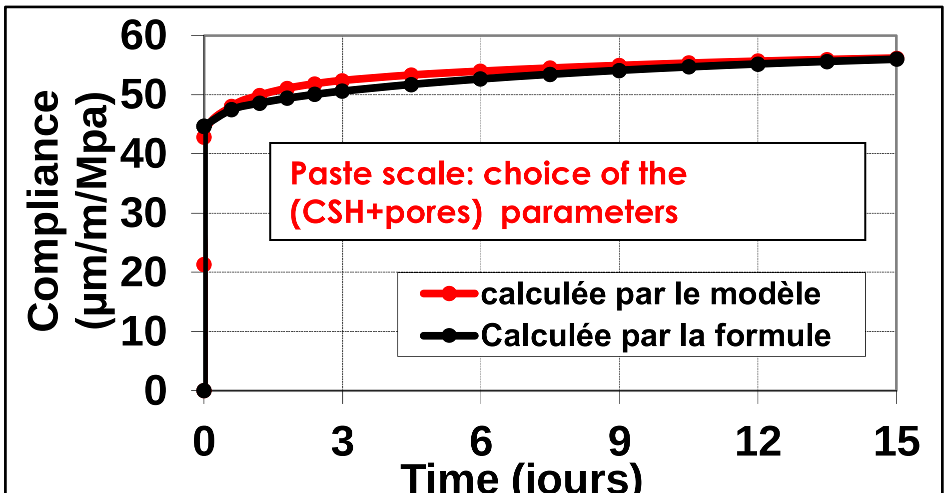

	E(GPa)	k^1_{fp} (GPa)	k^2_{fp}(GPa)	k^3_{fp}(GPa)
Mortar	22.4	776.7	472	98.1
Aggregate	60	-	-	-
Cement paste	18	300	100	90
Sand grains	80	-	-	-
CP matrix	12	*150*	*80*	*65*
CP inclusions	45	-	-	-

Inverse approach

The characteristic viscoelastic parameters of the cement paste matrix were derived from previous results by using the analytical formula of Ricaud and Masson (2009):

$$k_{bc}^{i} = \frac{4.\frac{\varsigma^{i}}{\tau^{i}}}{3.A(f_p)} = \frac{4.k_{\text{int}}^{i}}{3.A(f_p)}$$

k^1_{int} (GPa)	K^2_{int} (GPa)	K^3_{int} (GPa)	Age (h)	fp (%)	k^1_{bc} (GPa)	K^2_{bc} (GPa)	K^3_{bc} (GPa)
107	57	46.4	16	58	103	55	45
			24	50	142	76	62
			48	48.8	150	80	65

Basic coefficients of the cement paste matrix

Homogeneization

	Age (h)	E(GPa)	k^1_{bc} (GPa)	k^2_{bc}(GPa)	k^3_{bc}(GPa)
(CSH+pores)	16	9.5	103	55	45
	24	10.5	142	76	62
	>48	12	150	80	65
Cement paste	16	13.1	170.4	56.8	51.1
	24	15.9	286.2	95.4	85.9
	>48	16.7	300	100	90
Mortar	16	17	483.9	294.1	61.1
	24	21	745.5	453	94.2
	>48	24	777	472	98

Creep-damage coupling

Non-linear viscoelastic behaviour law: $\underline{\underline{\sigma}}(\underline{y}) = \underset{\sim}{C}(\underline{y}, \underline{\underline{\varepsilon}}(\underline{y})) : (\underline{\underline{\varepsilon}}(\underline{y}) - \underline{\underline{\varepsilon}}^{fp}(\underline{y}))$

Damage model linking the total stress to the effective stress [Fichant et al., 99] :

$\underline{\underline{\tilde{\sigma}}}(\underline{y}) = \underset{\sim}{C}^{0}(\underline{y}) : \underline{\underline{\varepsilon}}^{e}(\underline{y})$ and $\underline{\underline{\sigma}}(\underline{y}) = \underset{\sim}{C}(\underline{y}, \underline{\underline{\varepsilon}}(\underline{y})) : \left(\underset{\sim}{C}^{0}(\underline{y})\right)^{-1} : \underline{\underline{\tilde{\sigma}}}(y)$

Damage evolution: $d = 1 - \frac{\varepsilon_{d0}}{\varepsilon_{eq}} \exp\left[B_t(\varepsilon_{d0} - \varepsilon_{eq}\right]$ $\qquad \varepsilon_{eq} = \sqrt{\langle \varepsilon^{e} \rangle_{+} : \langle \varepsilon^{e} \rangle_{+}}$

Simulation of the failure tests

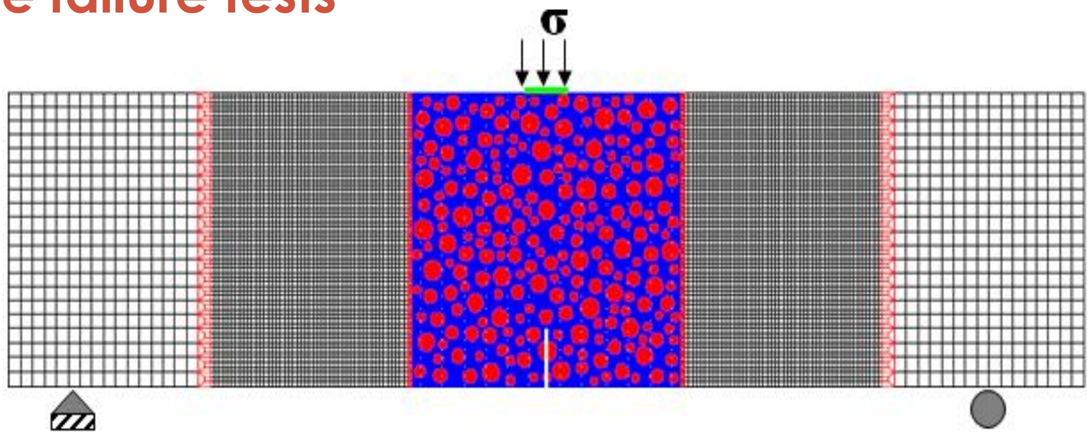

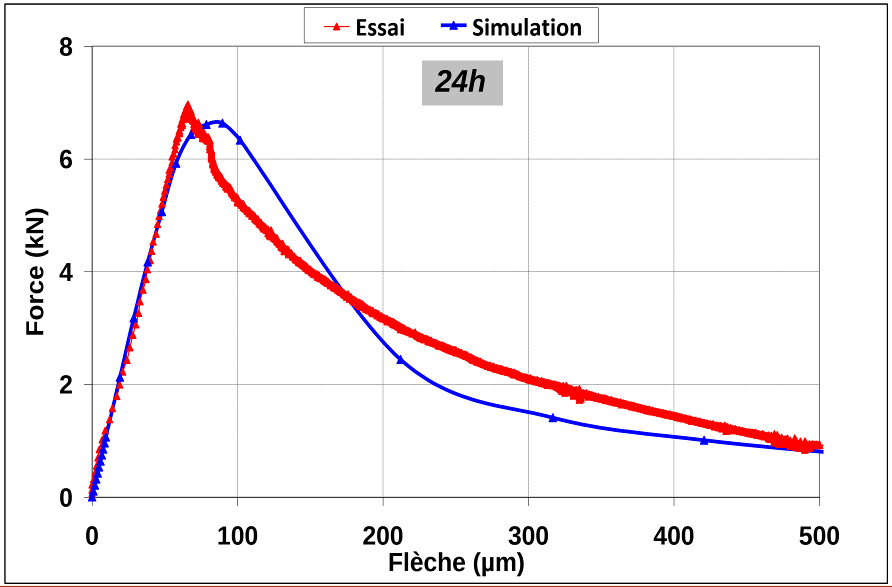

Simulation of the creep tests

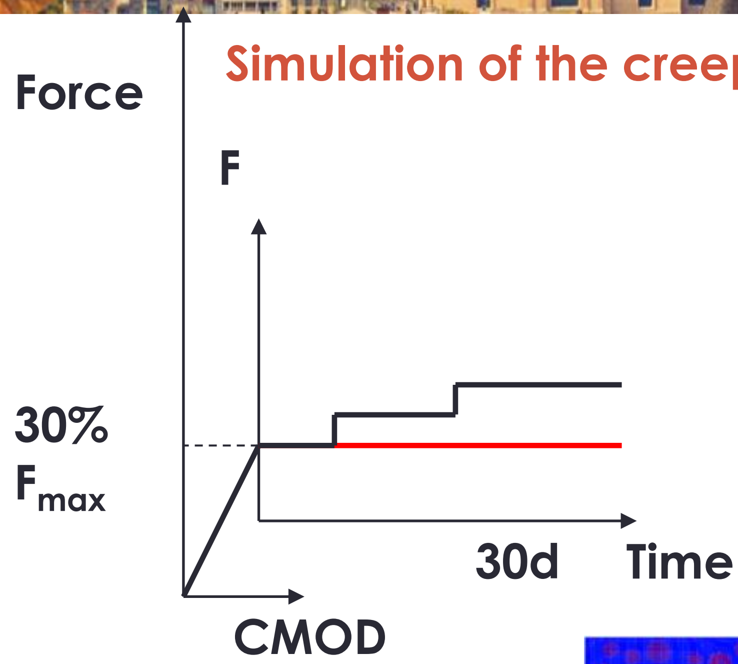

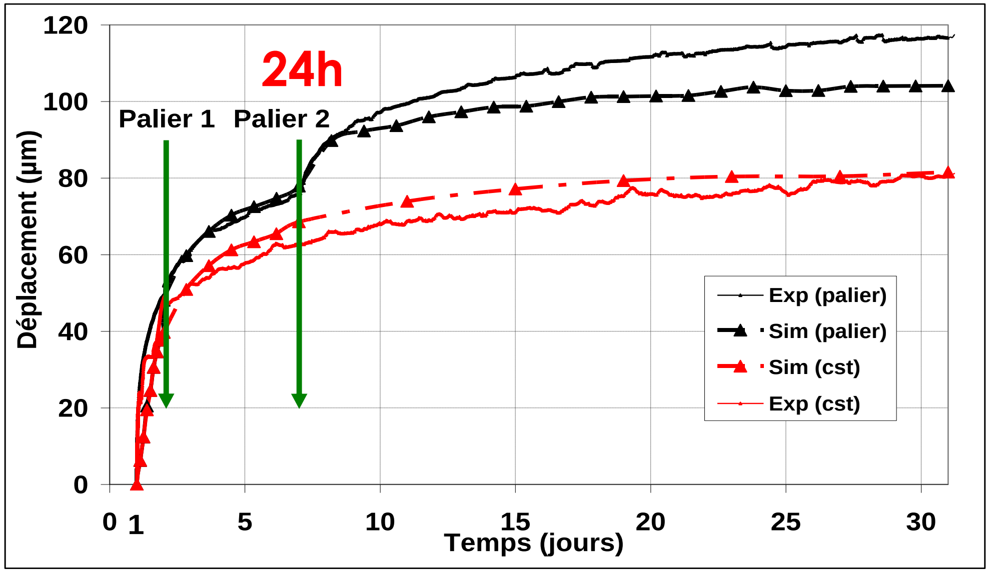

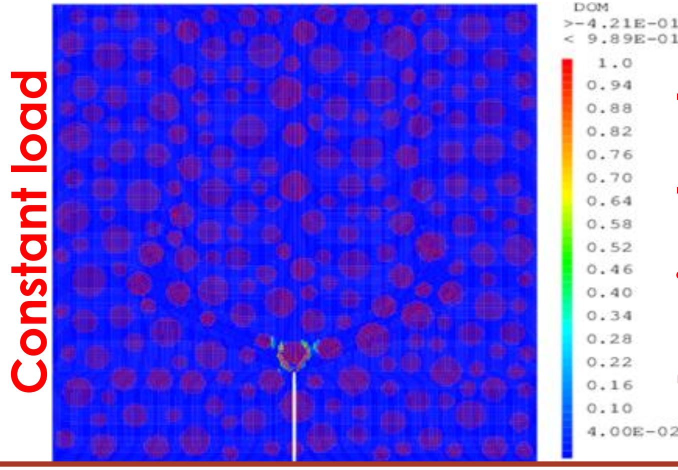

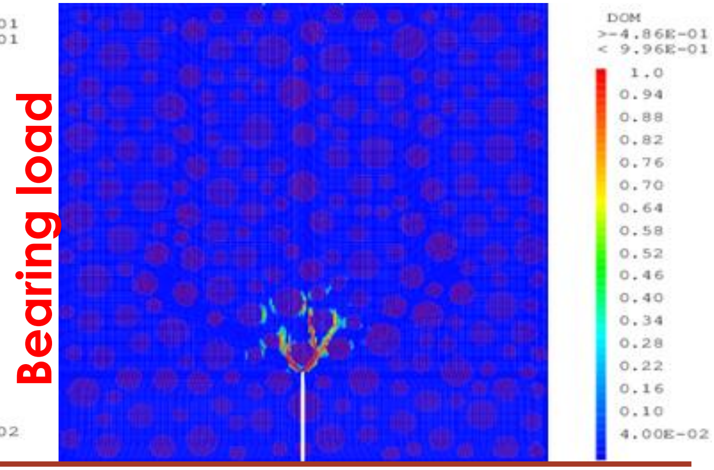

A little gap is observed between simulation and the measurement for the bearing load

Future couplings

Consideration of the shrinkage

The micromechanical approach

The local hydro-mechanical problem

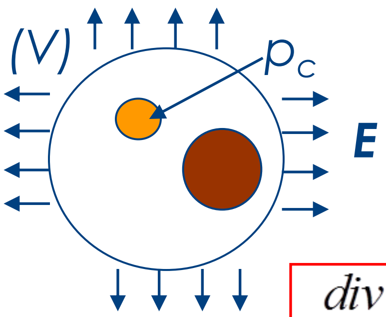

Micro

$$\underline{div}\ \underline{\underline{\sigma}} = \underline{0} \quad \text{in } V$$

$$\underline{\underline{\sigma}} = \underset{\sim}{C}_1 : \underline{\underline{\varepsilon}} \quad \text{in } V_1$$

$$\underline{\underline{\sigma}} = \underset{\sim}{C}_2 : \underline{\underline{\varepsilon}} - p_c \underline{\underline{\delta}} \quad \text{in } V_2$$

$$\underline{\underline{\varepsilon}} = \frac{1}{2}(\underline{\underline{\nabla}}\underline{u} + {}^t\underline{\underline{\nabla}}\underline{u})$$

$$\left\| \underline{\underline{\sigma}}.\underline{n} \right\| = 0 \text{ and } \left\| \underline{u} \right\| = 0 \quad \text{on } \partial V$$

$$\underline{u} = \underline{\underline{E}}.\underline{y} \quad \text{on } \Gamma_{mi}$$

Macro

$$\underline{\underline{\Sigma}} = \underset{\sim}{C}^{\text{hom}} : \underline{\underline{E}} + \underline{\underline{\Sigma}}^p$$

Changing of the capillary pressure (Coussy et al., 2004)

$$p_c(S) = M(S^{-1/m} - 1)^{(1-m)}$$

M = 37,55 MPa and m = 0,46 are material constant parameters which define the liquid saturation of the cement paste.

The micromechanical approach

The homogenized strain of the cement paste

$$dE^{cp} = \frac{1}{k^{\text{hom}}}\left[\frac{p_c(k^{\text{hom}} - k_s^{\text{hom}})}{k_w - k_s^{\text{hom}}}\right]$$

Calculation of the chemical shrinkage (Mounanga et al., 2004)

$$\Delta\varepsilon(t) = \Delta\varepsilon_{Gy} M_{Gy} + \Delta\varepsilon_{C3S} M_{C3S}(t) + \Delta\varepsilon_{C2S} M_{C2S}(t) + \Delta\varepsilon_{C3A} M_{C3A}(t) + \Delta\varepsilon_{C4AF} M_{C4AF}(t) + \Delta\varepsilon_{Ett} M_{Ett}(t)$$

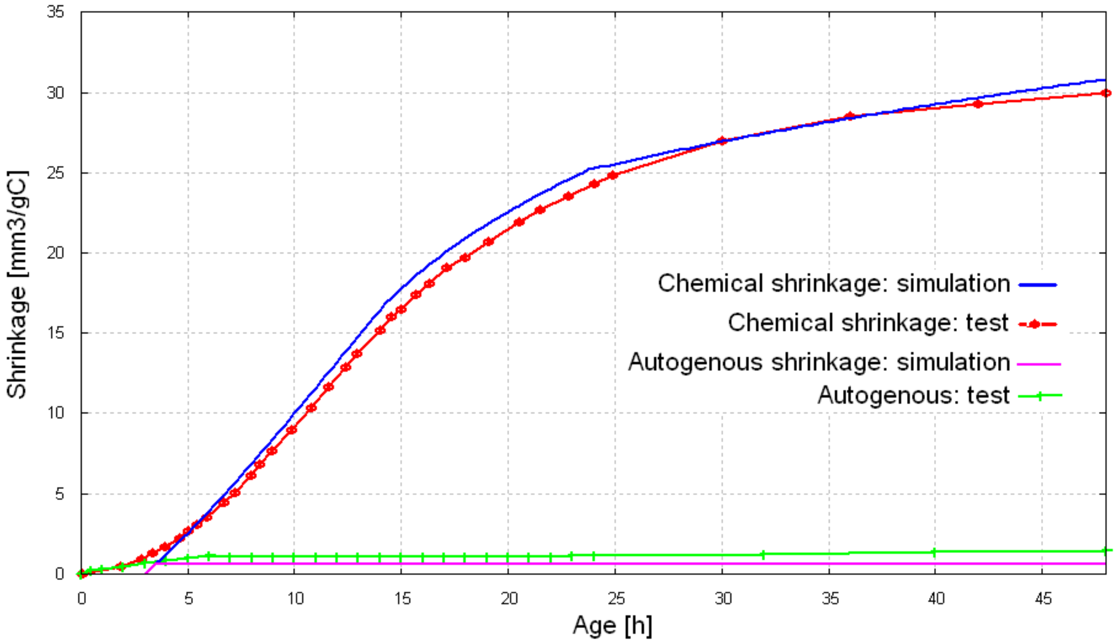

Cracking due to shrinkage

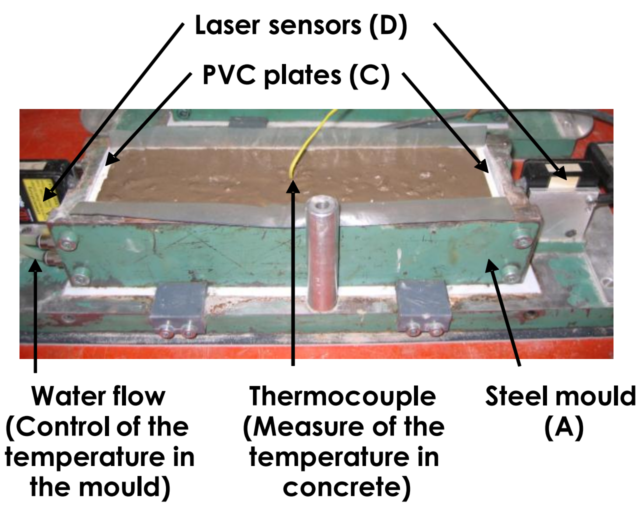

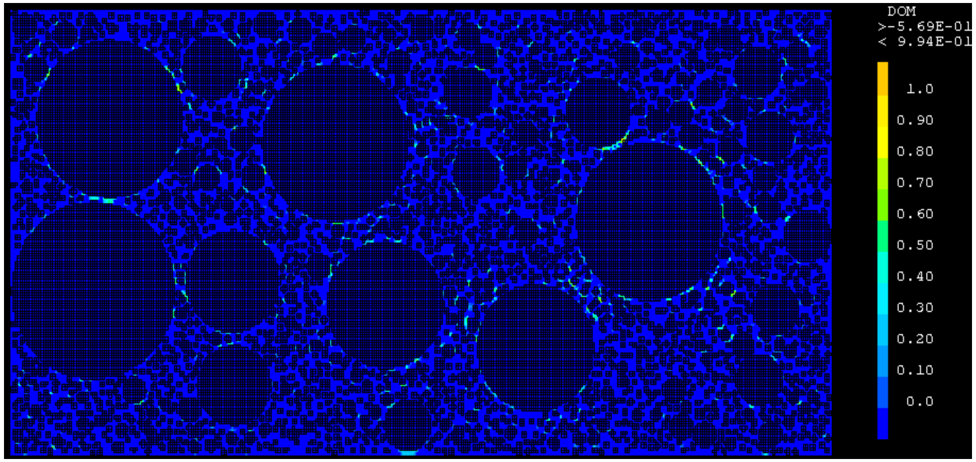

Future couplings

Modelling of ITZ

ITZ properties

Thickness between 20 and 50 µm!

Finite element modelling:

If ITZ is represented the REV dimension to element size ratio is oversize

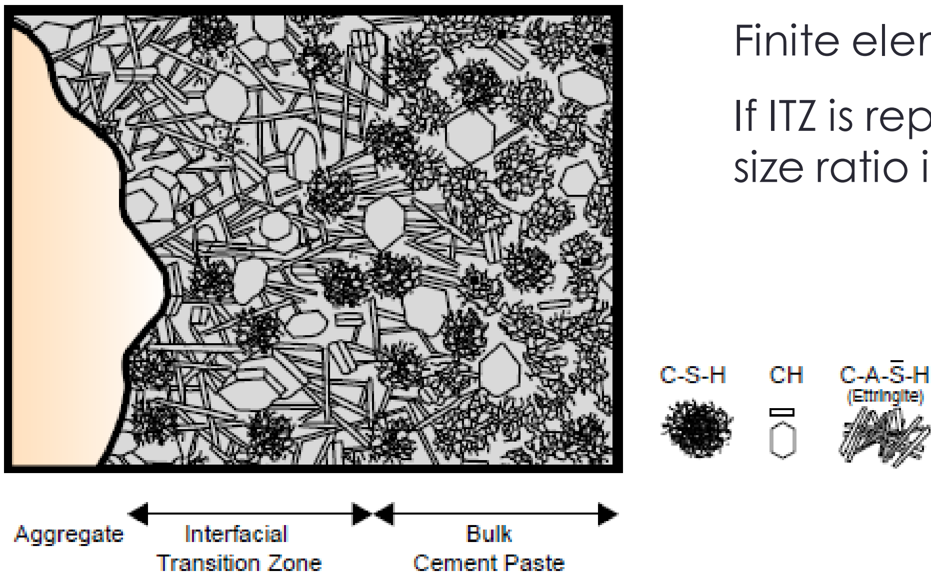

(radius r_a) **(thickness δ)**

(Mehta and Monteiro, « Concrete: microstructure, properties and materials »)

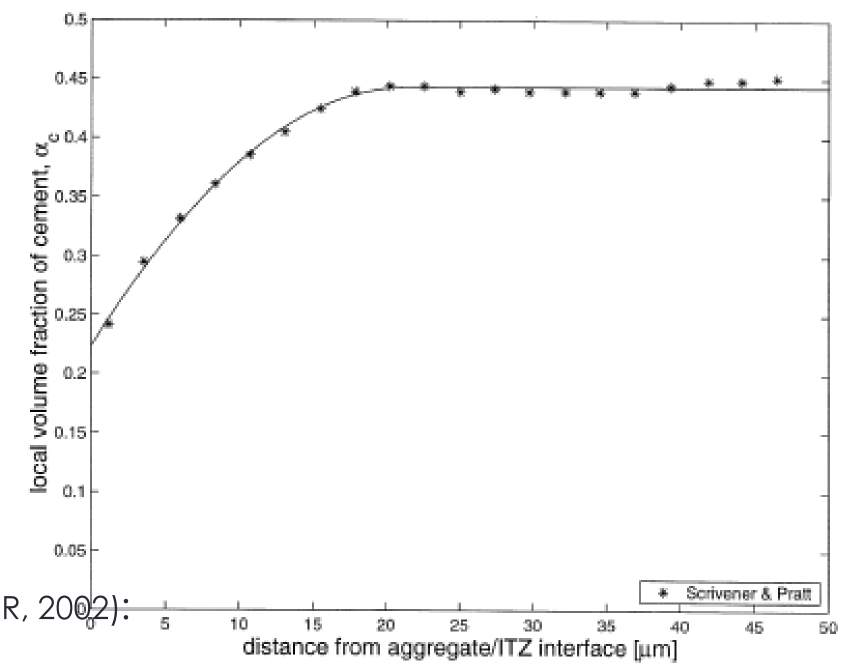

(Scrivener et Pratt, 1996)

Cement volume fraction in the cement paste (Nadeau, CCR, 2002):

$$\alpha_c(r) = \begin{cases} \bar{\alpha}_c\left[1 + a_c\left(\frac{r - r_a - \delta}{\delta}\right)^2\right] & r_a \leq r \leq r_a + \delta \\ \bar{\alpha}_c & r \geq r_a + \delta \end{cases}$$

Definition of a new interphase

Grondin and Matallah, 2014

Interphase properties = Average (layers of ITZ + a bulk fraction)

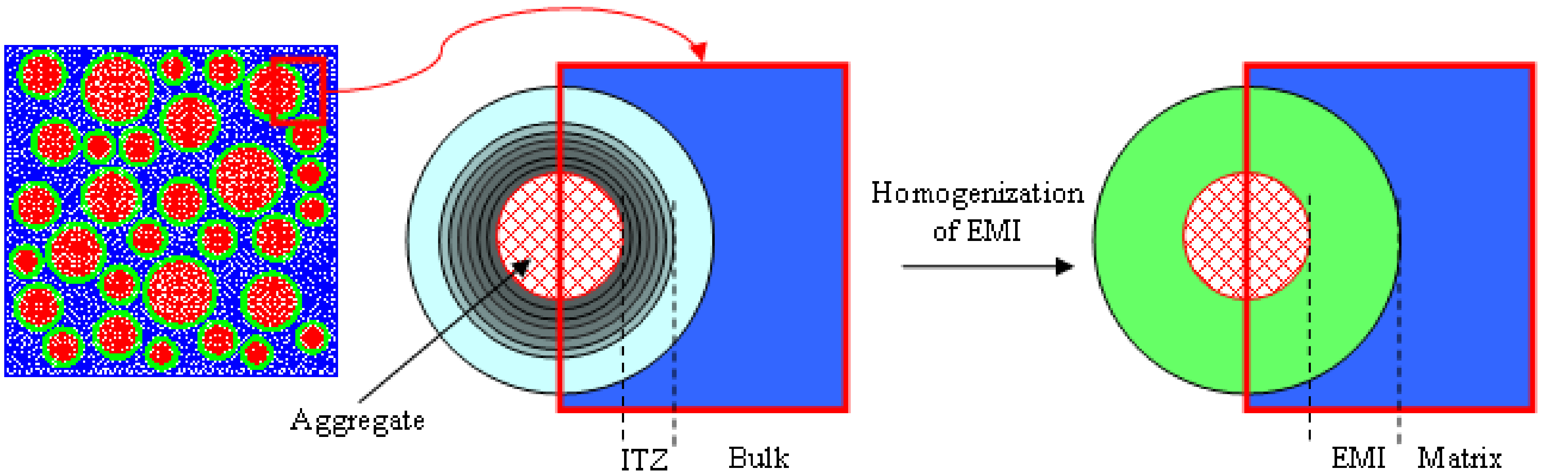

Cement volume:

$$V_c = V_c^{ITZ} + V_c^{nonITZ} = \frac{3c_a\bar{\alpha}_c V}{r_a^3}\int_{r_a}^{r_a+\delta}\left[1 + a_c\left(\frac{r-r_a-\delta}{\delta}\right)^2\right] r^2\,dr + \bar{\alpha}_c\left[V - \frac{4}{3}n_a\pi(r_a+\delta)^3\right]$$

Modelling of the direct tensile load

Grondin and Matallah, 2014

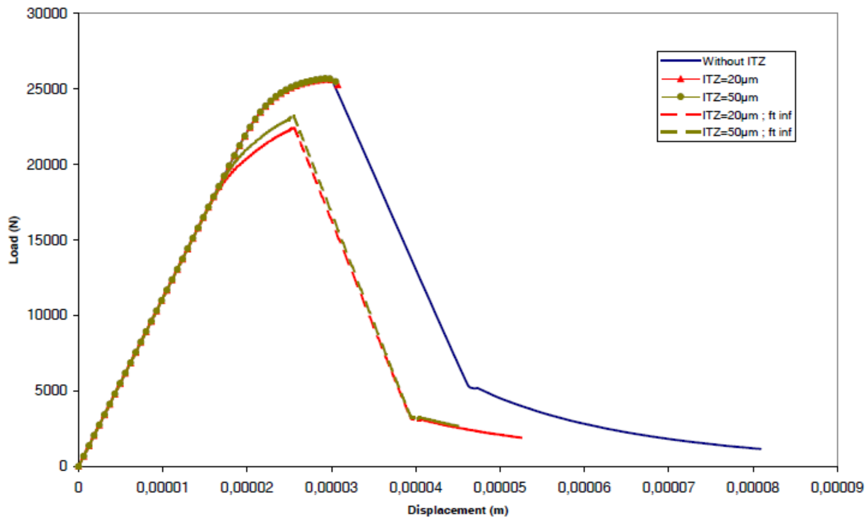

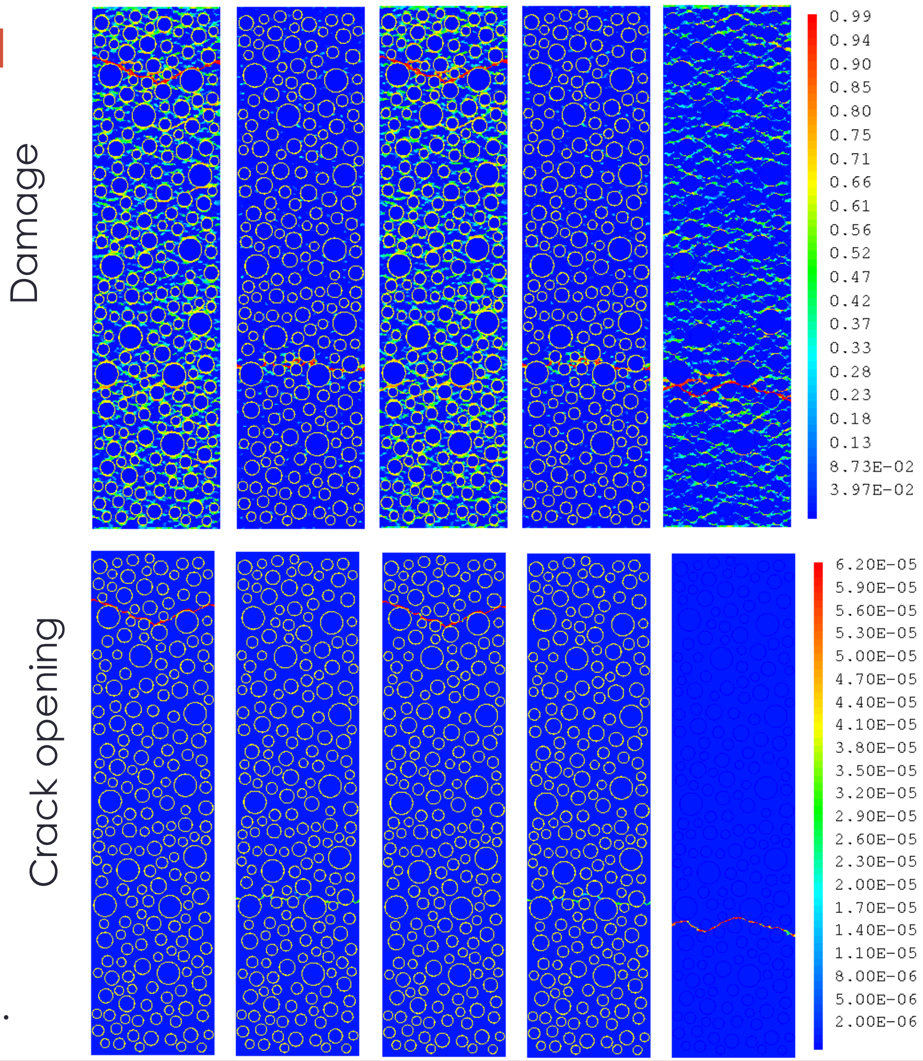

Note: More the hydration is advanced, more the difference between ITZ and bulk decreases.

References

1. Omar, Loukili, Pijaudier-Cabot, Le Pape, J. Mater. Civ. Eng., vol. 21, 2009.
2. Saliba, Loukili, Grondin, Regoin, Mater. & Struc., vol. 45, 2012
3. Tran, Yvonnet, He, Toulemonde, Sanahuja, Comp. Meth. Applied Mech. Eng, vol. 200, 2011.
4. Ricaud, Masson, Int. J. Solids Struc., vol. 46, 2009.
5. Grondin, Bouasker, Mounanga, Khelidj, Perronnet, Materials and Structures, 2010.
6. Zhang, Abraham, Grondin, Loukili, Tournat, Le Duff, Lascoup, Durand, Ultrasonics, 2012
7. Grondin, Matallah, Cement and Concrete Research, 2014.

CMS Workshop "Cracking of massive concrete structures"

March 17, 2015, ENS-Cachan

Cachan, Île-de-France, FRANCE

Characterisation of concrete properties at early ages: Case studies of the University of Minho

Miguel Azenha[1], José Granja[1]

[1]ISISE, University of Minho, Portugal

isise Institute for Sustainability and Innovation in Structural Engineering

University of Minho School of Engineering

POPH QUALIFICAR É CRESCER.

QREN QUADRO DE REFERÊNCIA ESTRATÉGICO NACIONAL PORTUGAL 2007.2013

GOVERNO DA REPÚBLICA PORTUGUESA

UNIÃO EUROPEIA Fundo Social Europeu

Index

- Assessing the thermal dilation of concrete since early ages
- Continous monitoring of concrete E-modulus (EMM-ARM) in the context of the construction of a bridge
- Other recent works and further ongoing research of interest for TC-CMS

Assessing the thermal dilation of concrete

since early ages

Scope / Motivation

- Early ages of concrete -> hydration heat -> stresses;
- Limited knowledge about thermal dilation coefficient (TDC);
- Need for new experimental approaches applied to concrete.

Objectives / Organization

- Development of new method to measure TDC;
- Possibility of measuring TDC since early ages;
- Very short temperature cycles and internal cooling;
- Pilot experiment.

Techniques for measurement of the thermal dilation coefficient (TDC)

Volumetric techniques

Loser *et. al.*, 2010

Limitations:
- ✓ Sample size
- ✓ Material suitability

Techniques based on the longitudinal length variation of a specimen

AASHTO-T336, 2011

Only applicable to hardened concrete

↓

TDC not measured at early ages

New method for TDC measurement: requirements and considerations

- Temperature cycles to which the specimen is subjected
  - Short enough to maximize the number of measurements of TDC;
  - With enough amplitude to generate measurable volumetric variations.
- Applicable to concrete specimens
  - 150mm diameter and 300mm length (standard size);
  - Internal pipes to accelerate thermal equilibrium state (12mm);
  - Internal strain monitoring with vibrating wire strain gauge.
- Average temperature of 20°C, avoiding maturity corrections
  - Cycles between ~17.5°C e 22.5°C;
  - 180 minutes of duration for each complete cycle (2 measurements per cycle).

Proposal of a new methodology for TDC measurement
Geometry and study of internal pipes

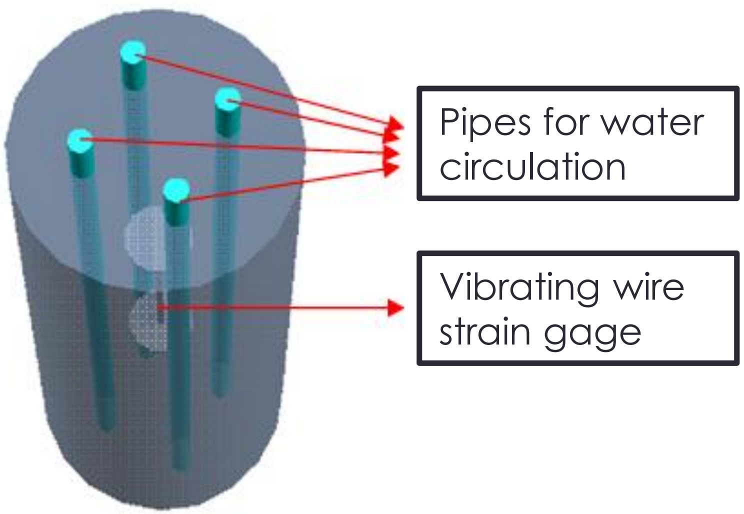

150mm diameter
300mm length

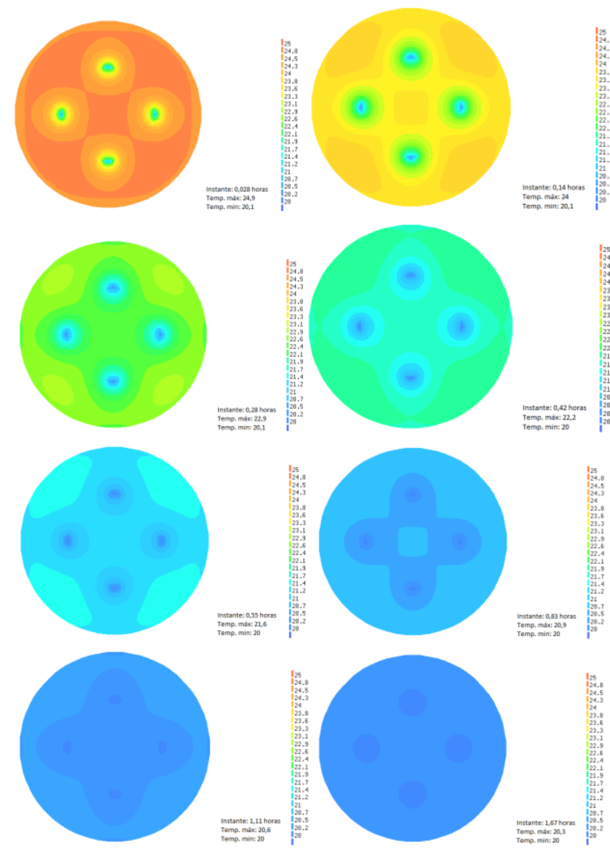

FEM Thermal simulation

Proposal of a new methodology for TDC measurement
Specimen and surrounding bath

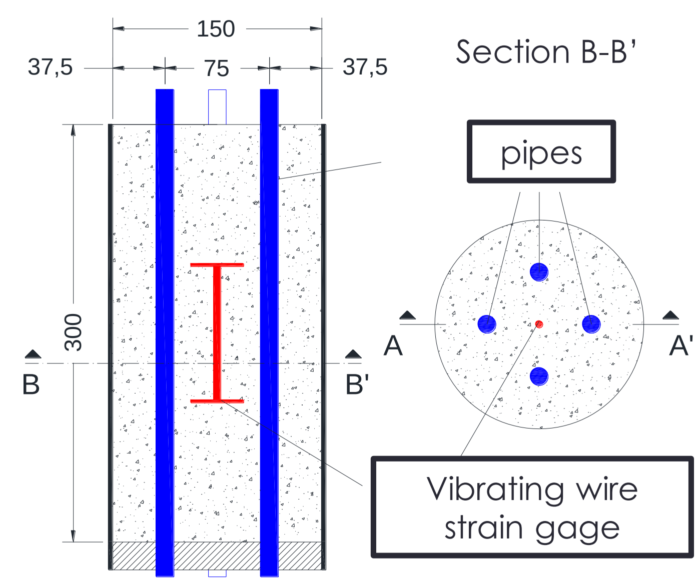

Specimen

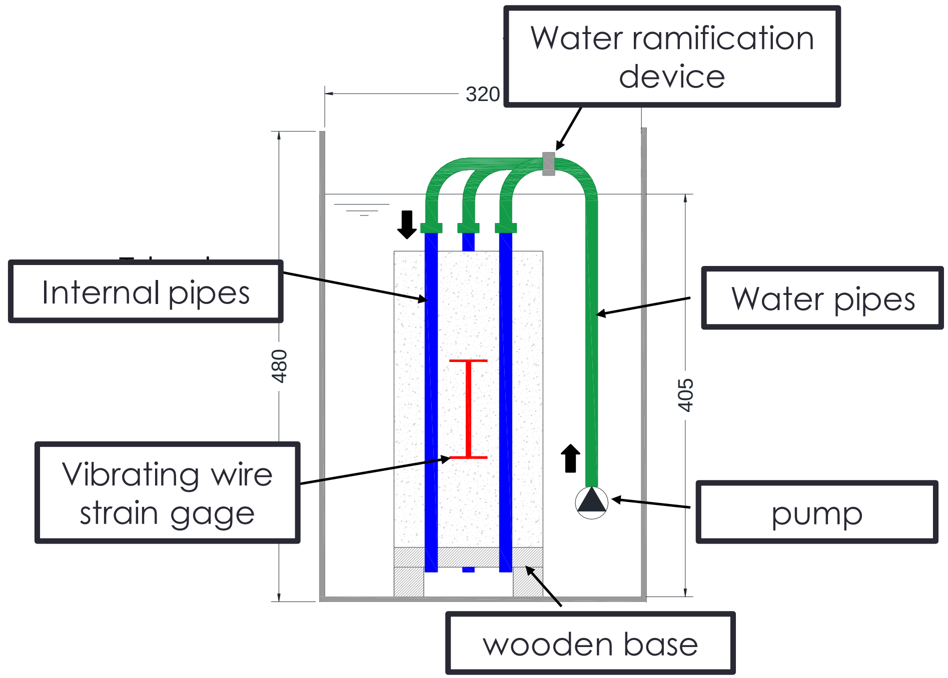

Positioning of specimen within surrounding bath

Proposal of a new methodology for TDC measurement
System for heating/cooling the bath

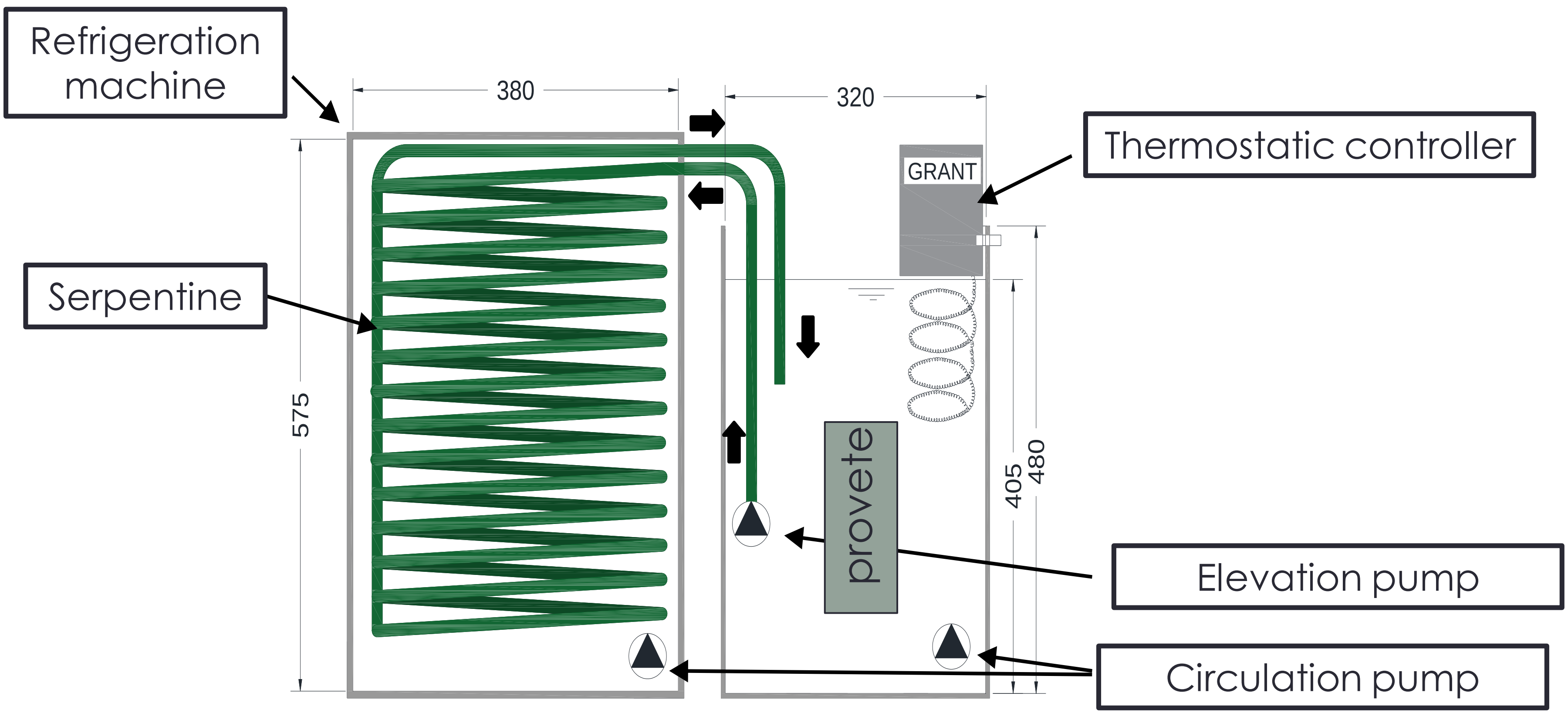

Pilot experiment – General information

- Cycles 17.5°C-22.5°C with 180 min duration;
- Test starts 40 min after casting;
- Concrete composition:

Material	Quantity (kg) per m^3 of concrete
Cement (kg)	500,0
Sand (0-4) (kg)	851,6
Gravel (4-8) (kg)	822,9
Superplasticizer (kg)	10,0
Water (kg)	181,6

Pilot experiment – Practical implementation

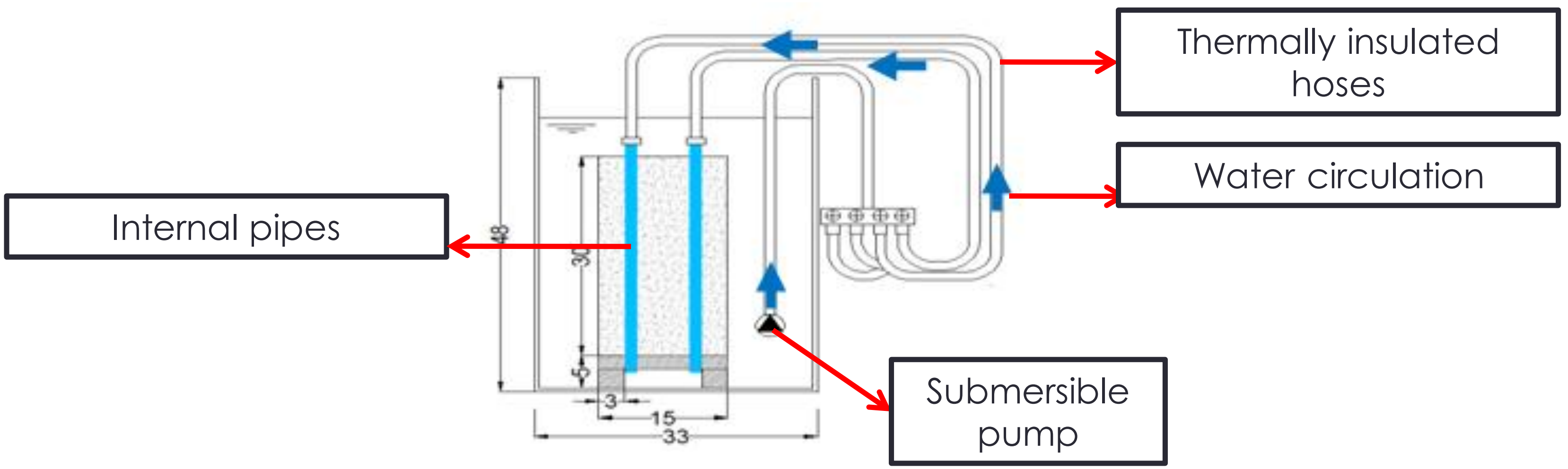

Pilot experiment – Practical implementation

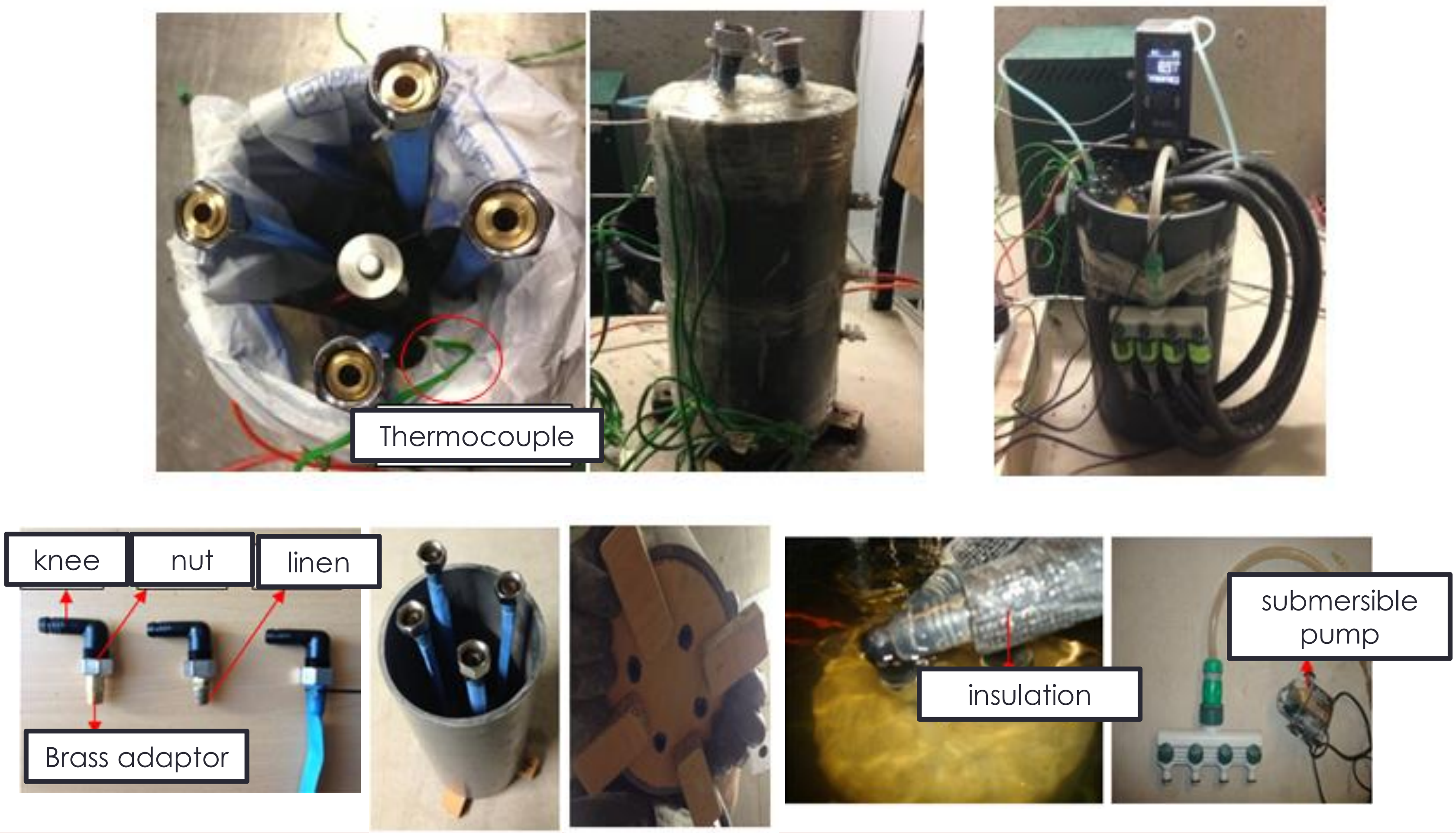

Pilot experiment – main results

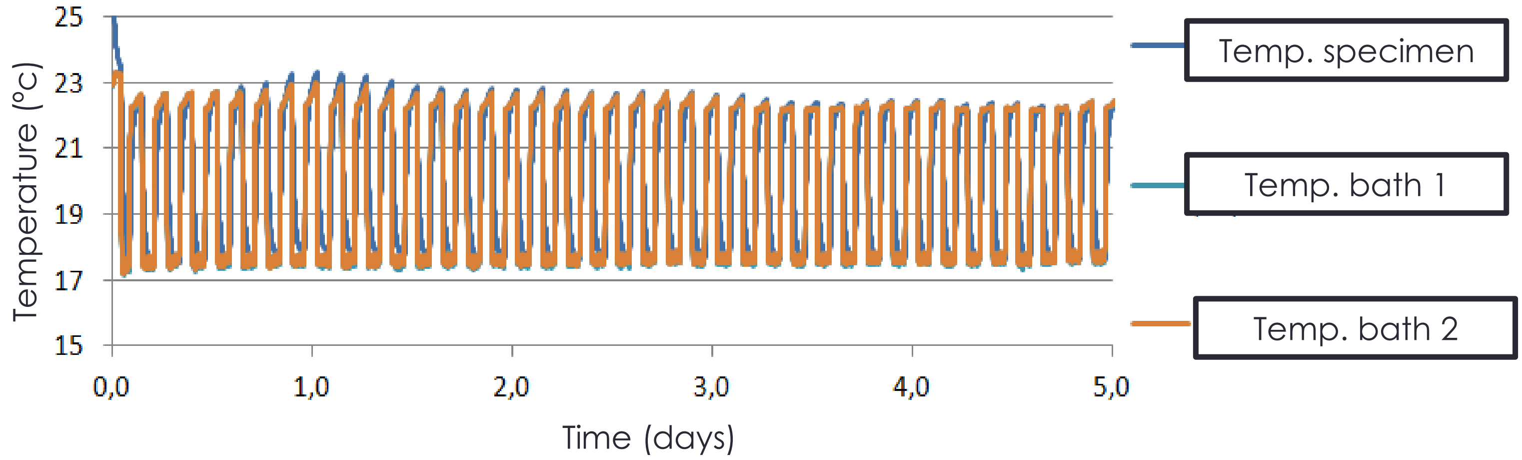

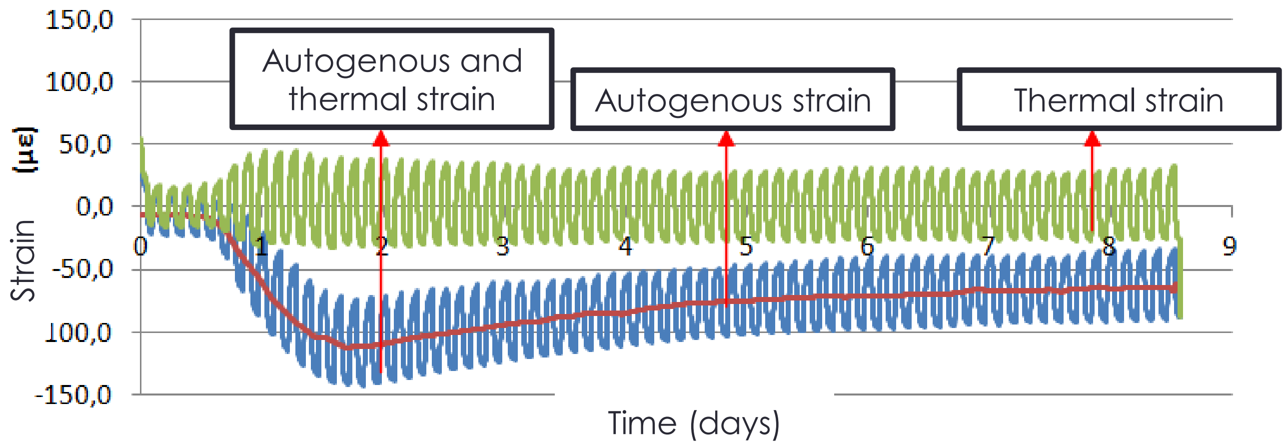

Pilot experiment – main results

- Evolution of the thermal dilation coefficient

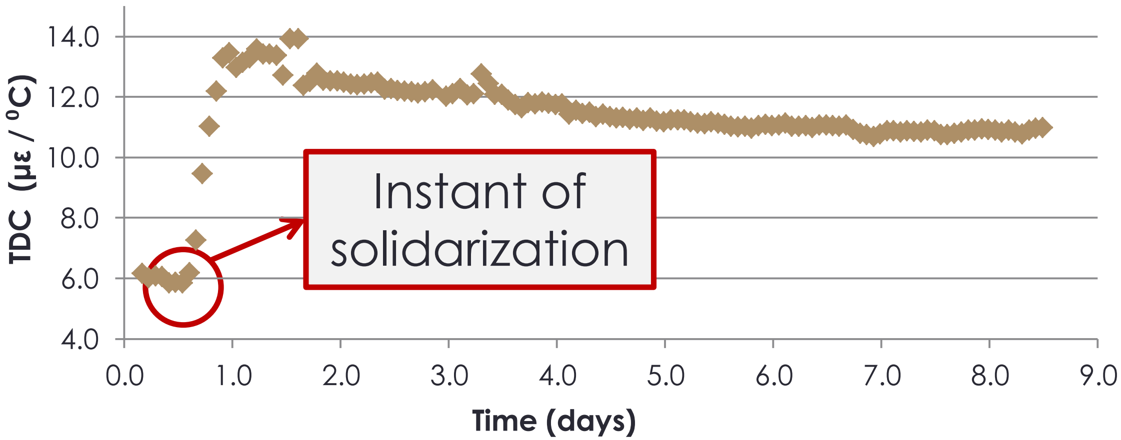

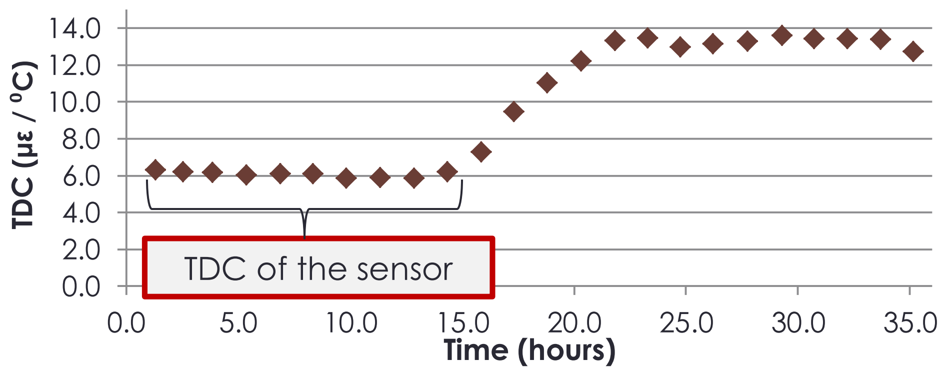

Conclusions

- Proposal of an innovative methodology for measurement of concrete TDC since early ages;
- Main originality: internal pipes (accelerated equilibrium states);
- Pilot experiment with cycles of 180 min, starting shortly after setting;
- Good performance of strain monitoring;
- Values/evolution of TDC plausible in view of the literature.

Continous monitoring of concrete E-modulus (EMM-ARM)

in the context of the construction of a bridge

EMM-ARM - **E-M**odulus **M**easurement through **A**mbient **R**esponse **M**ethod

- Continuous monitoring of the elastic modulus of cementitious materials from the moment of casting;
- General principles of the technique (Azenha et al., 2009):

Cylindrical mould

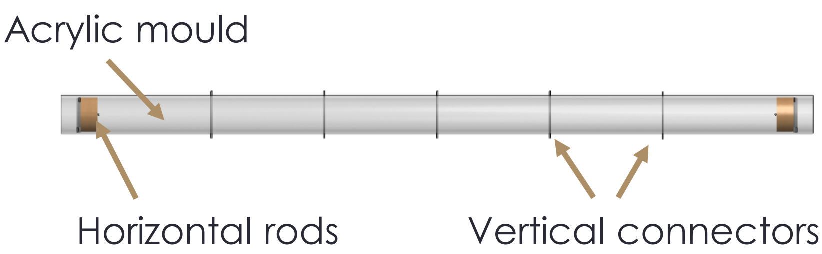

Casting a mould with the material to be tested

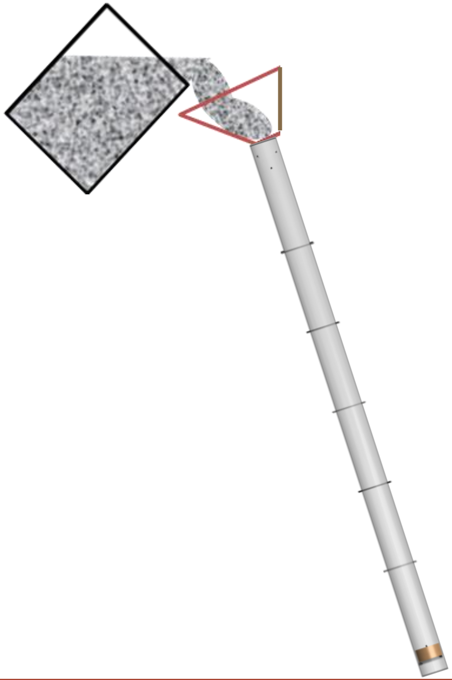

EMM-ARM

- Placing the mould in a simply supported condition and monitoring the accelerations at mid-span;

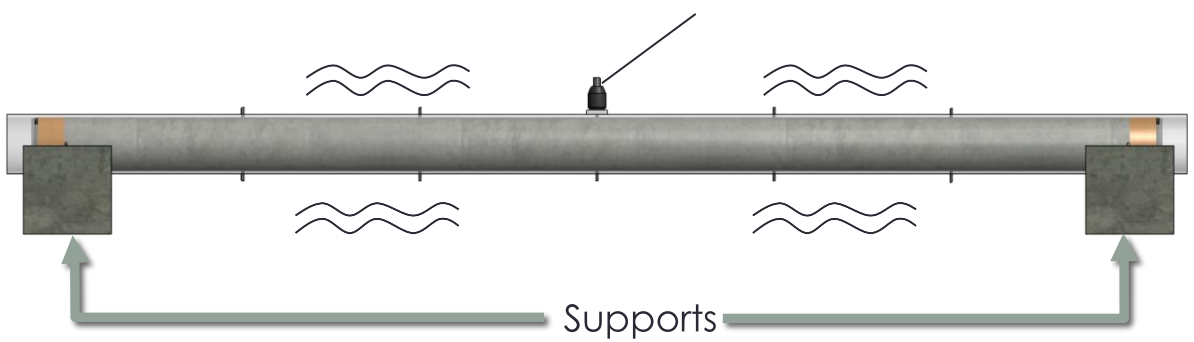

- Identification of the first resonant frequency of the composite beam at each instant while the curing of the material occurs inside the mould.

EMM-ARM – Frequency Identification

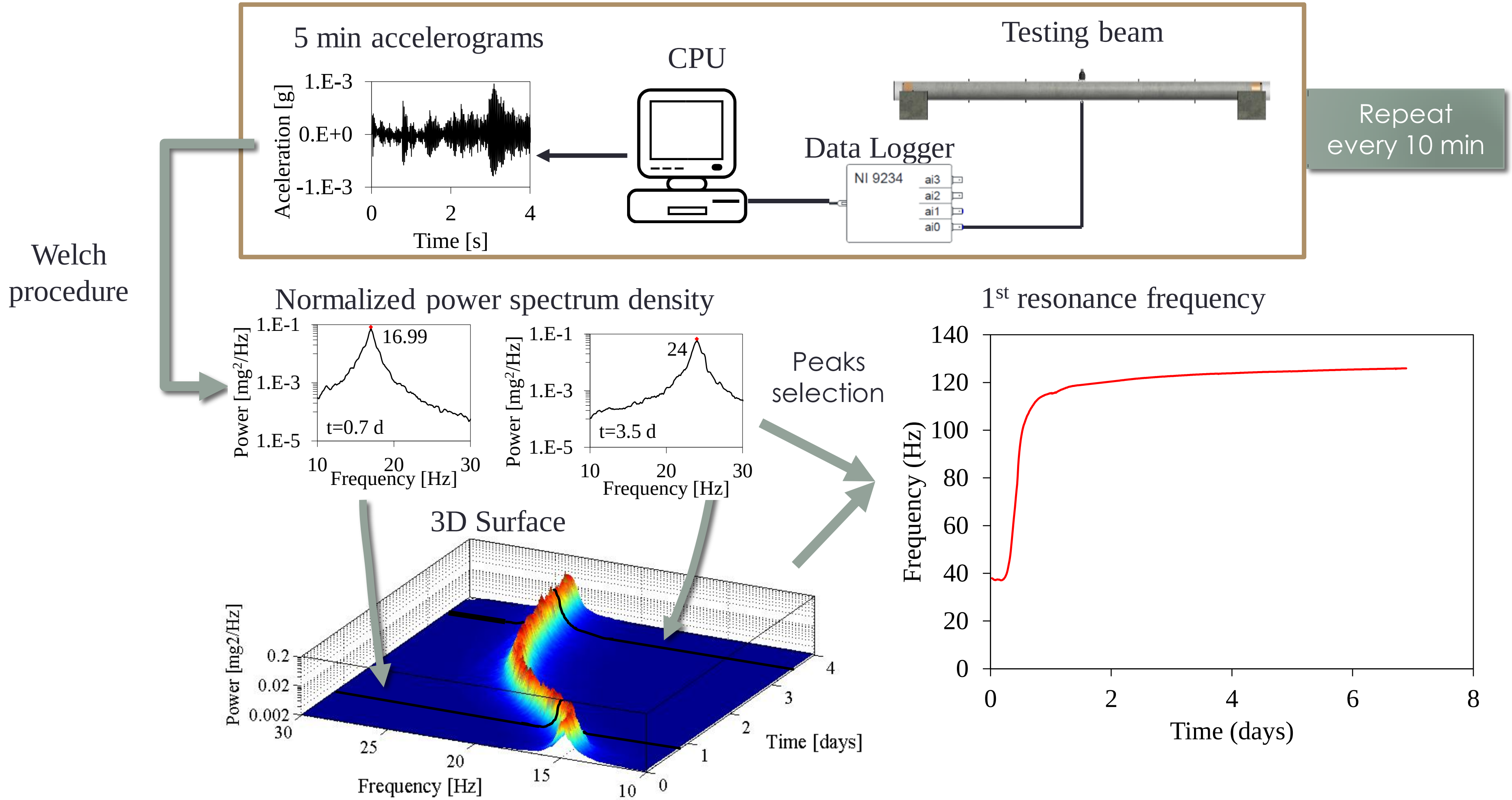

Evaluation of Concrete E-Modulus (Based on Modal ID)

Based on the equations of free motion of a simply supported beam with a concentrated load at mid-span

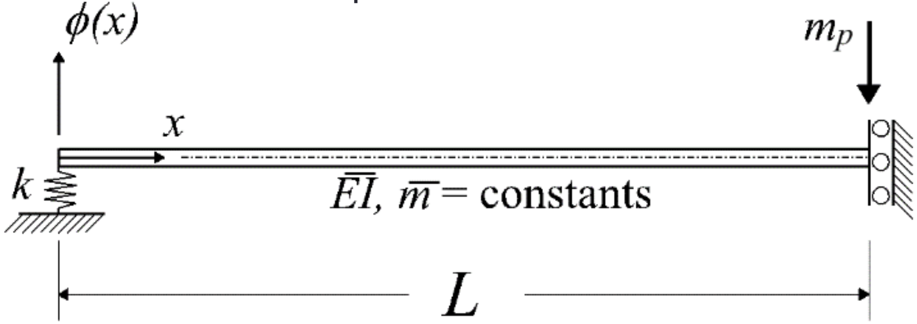

it is possible to relate the 1st resonant frequency of the composite beam w with its stiffness $\overline{EI}$ (which is the only unknown in the following equation):

$$-1/(2k)\Big[\ \overline{EI}\,a^3\sin(aL)^2 w^2 m_p + 2\cosh(aL)k\,w^2 m_p\sin(aL) + \cosh(aL)^2 w^2 m_p\,\overline{EI}\,a^3$$
$$+2\left(\overline{EI}\right)^2 a^6\sin(aL)\cosh(aL) - \overline{EI}\,a^3\sinh(aL)^2 w^2 m_p + 2\cos(aL)\left(\overline{EI}\right)^2 a^6\sinh(aL) -$$
$$4\cos(aL)k\,\overline{EI}\,a^3\cosh(aL) + \cos(aL)^2 w^2 m_p\,\overline{EI}\,a^3 + 2\cos(aL)w^2 m_p\,\overline{EI}\,a^3\cosh(aL) -$$
$$2\cos(aL)k\,w^2 m_p\sinh(aL)\ \Big] = 0 \quad \text{with} \quad a = \sqrt[4]{\frac{w^2\overline{m}}{\overline{EI}}}$$

$$\overline{EI} = E_a I_a + E_c I_c$$

Concrete E-modulus is obtained.

EMM-ARM
Orignal mould

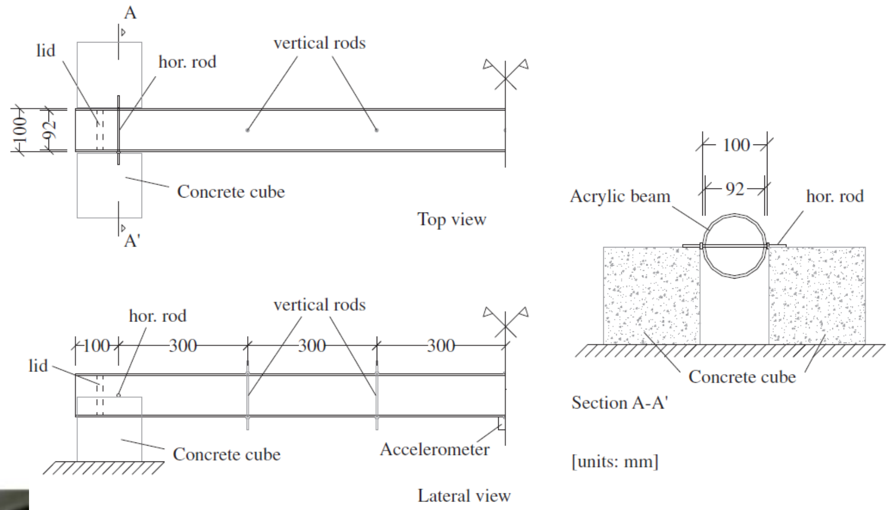

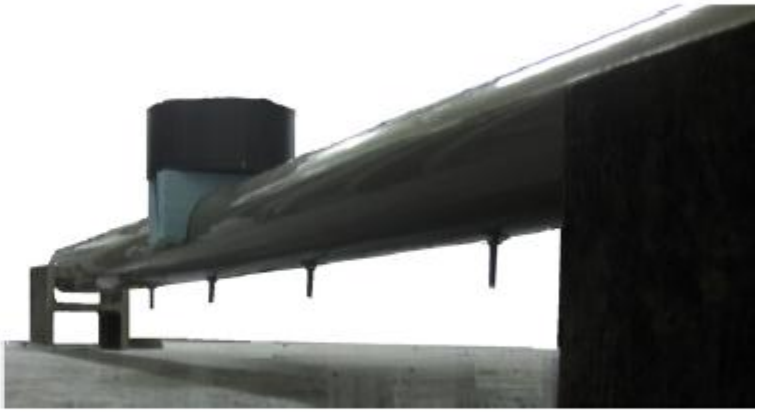

Several drawbacks:

- Difficult to cast;
- Not robust;
- Non reusable mould;
- Very sensitive to contaminations of the environmental noise.

EMM-ARM improvements – test setup

- Beam span reduction and new mould material
- Implementation of new beam supports

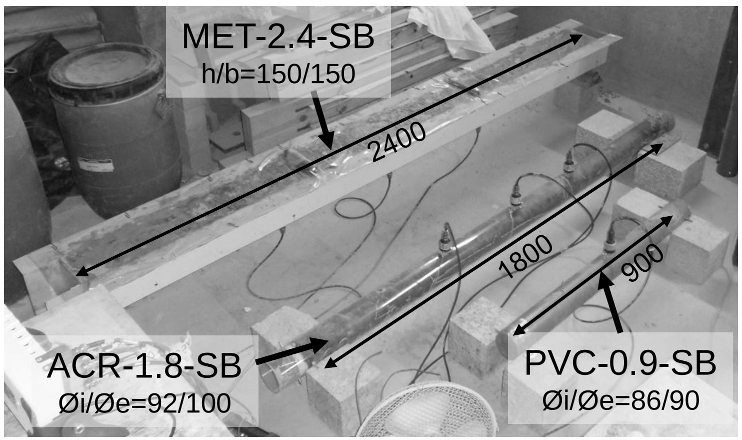

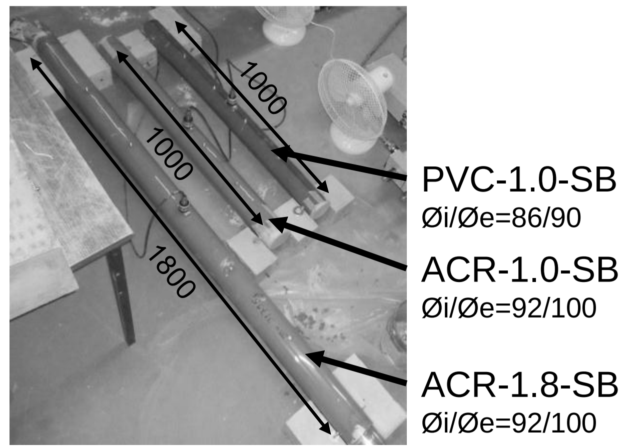

New supports

- Similar results were obtained, thus validating span reduction and changes in both mould material (PVC) and supports.

EMM-ARM improvements – test setup

- New reusable mould

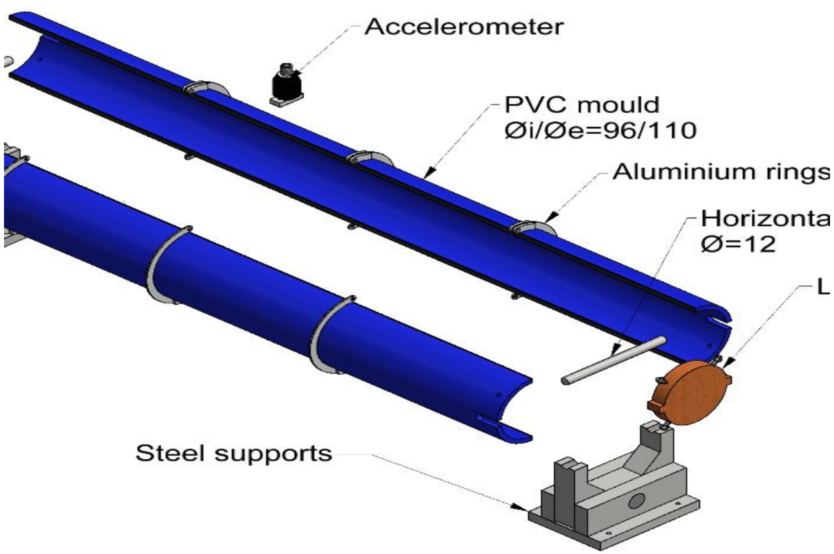

- Two halves of a PVC tube
- Aluminium reinforcement rings
- Wooden lids

- Robust test setup

❑ Similar results were obtained, thus validating the reusable mould

EMM-ARM improvements – Modal analysis technique

- Comparison between ambient vibration and forced vibration tests:
  - Excitation applied through custom non contact electromagnetic actuator.

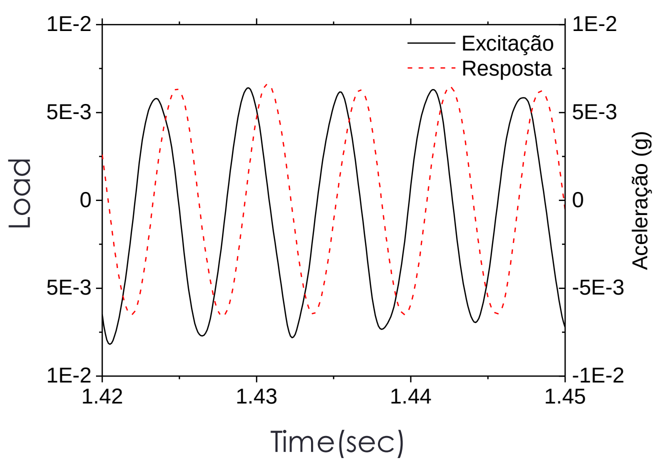

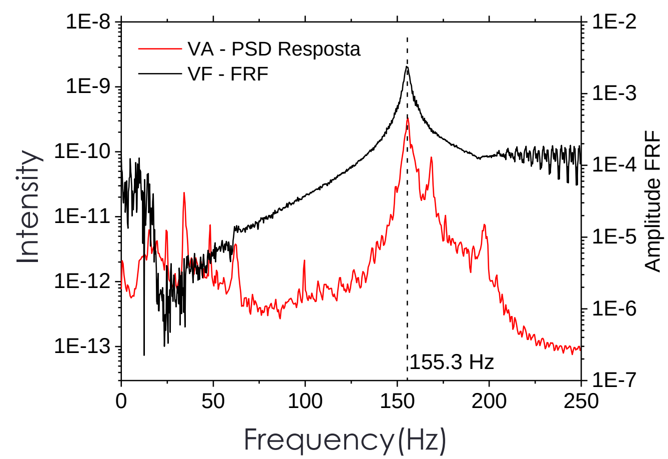

❑ Allows the reduction of the sensitivity to environmental noises

EMM-ARM in-situ aplication: validation

Foz do Dão bridge:

- EMM-ARM implementation to support decision making in pre-stress applications

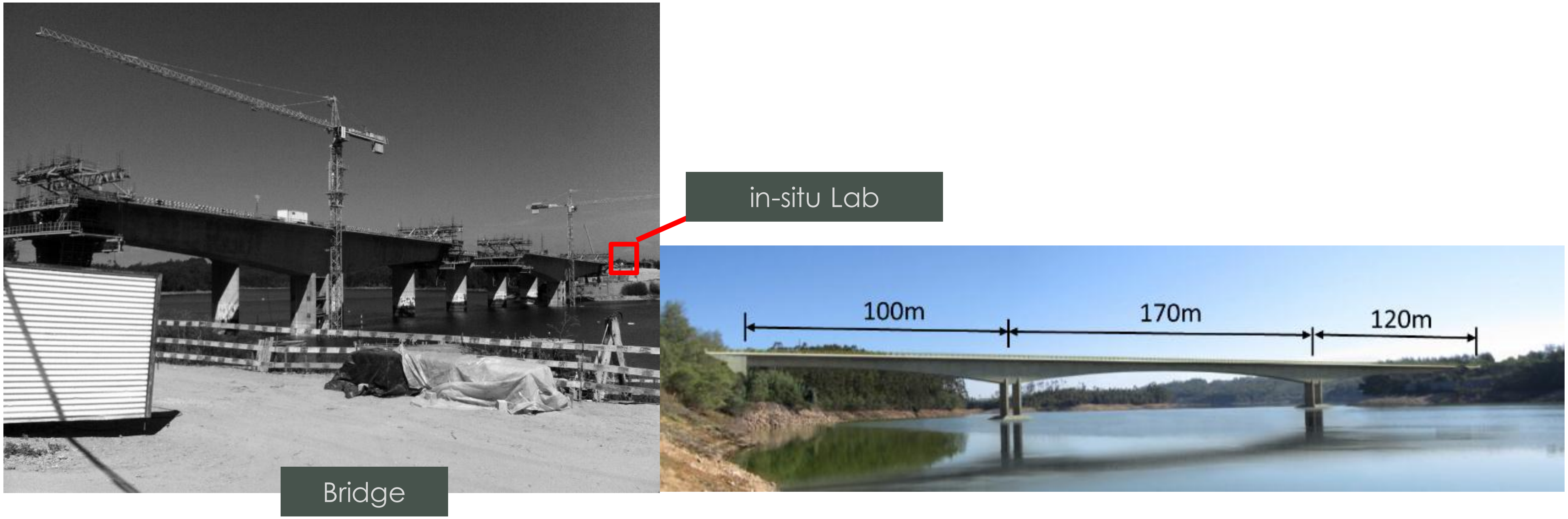

EMM-ARM in-situ aplication: validation

- Extended experimental campaign:
  - Comparison between several types of EMM-ARM beams (reusable, PVC e acrylic);
  - Comparison with classical cyclic compression tests (CC);

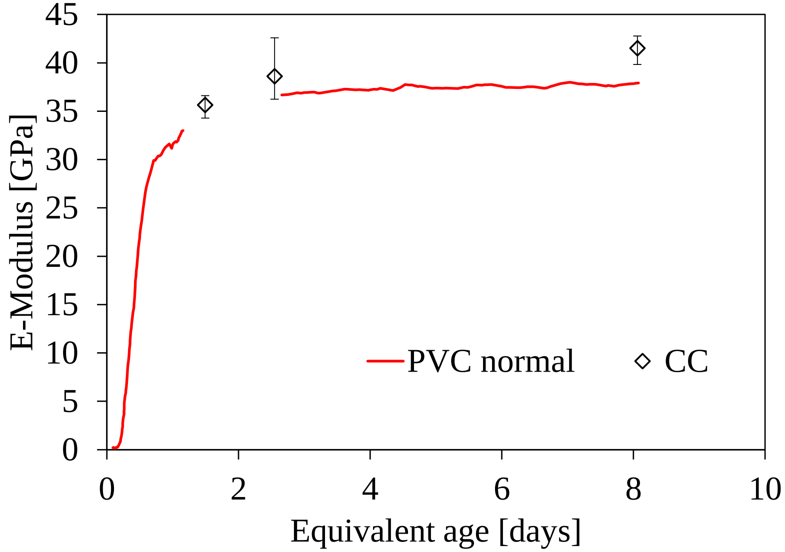

- Good repeatability of the EMM-ARM results
- Excellent coherence between EMM-ARM and CC results

EMM-ARM in-situ application: E vs fcm relationship calibration

- Comparison between results under the same curing conditions:
  - Compressive strength (cubes)
  - E-modulus (EMM-ARM beams)

A	1.887
B	8.228E-3
C	0.353

Fitting to the experimental data

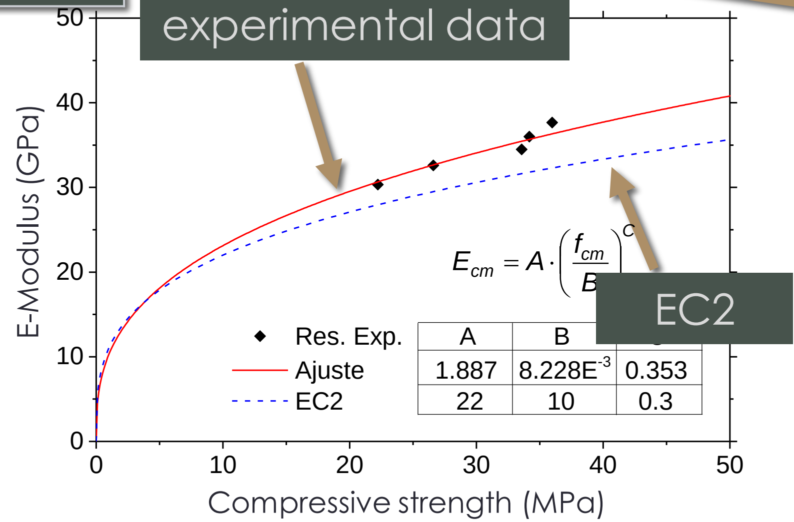

EC2

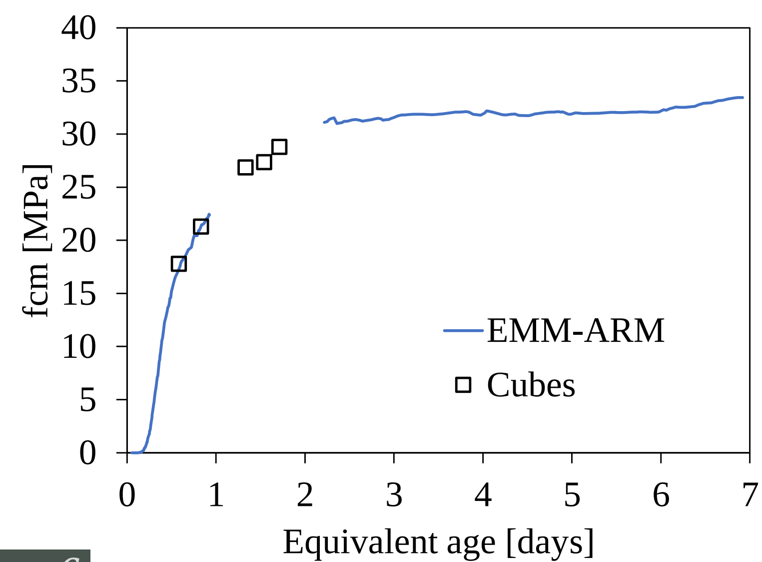

$$E_{cm} = A(f_{cm}/B)^C$$

EMM-ARM in-situ application: *match curing system*

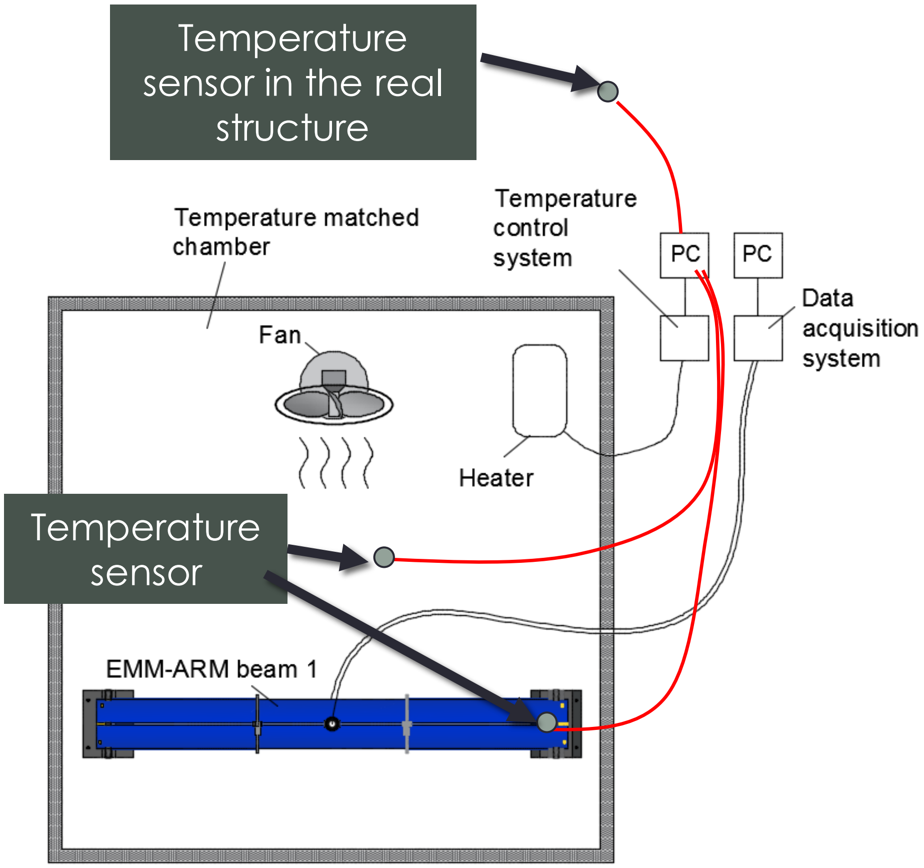

- Preliminary test

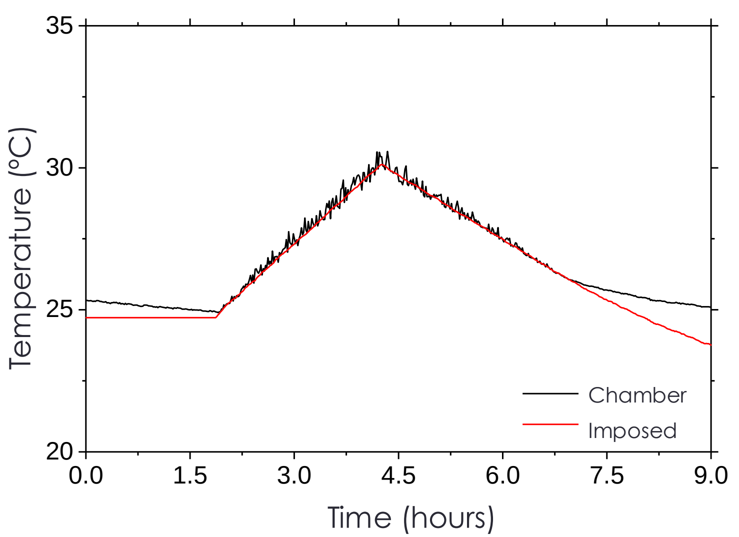

EMM-ARM in-situ application

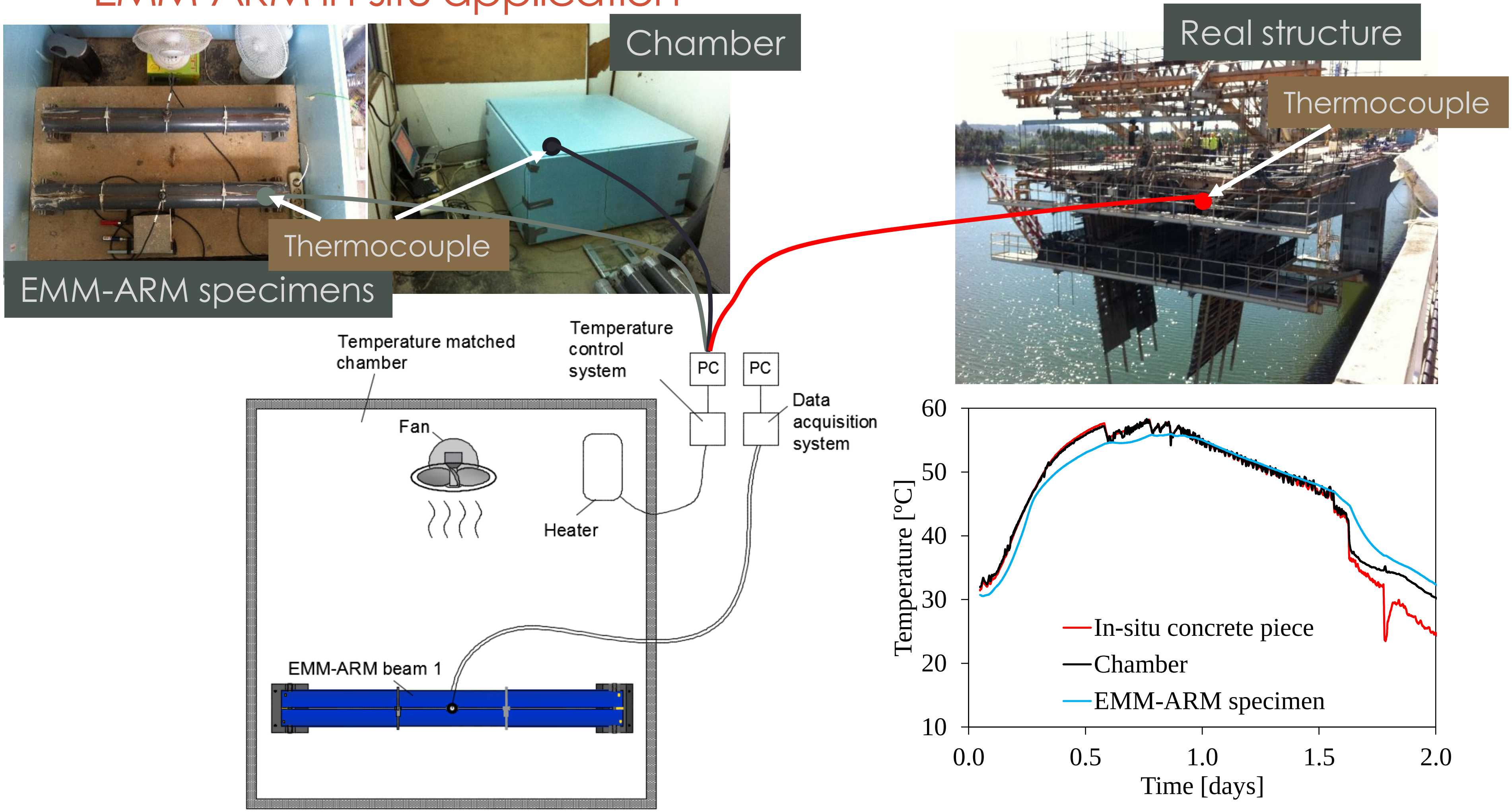

EMM-ARM in-situ application

A	1.887
B	8.228E-3
C	0.353

$$E_{cm} = A(f_{cm}/B)^C$$

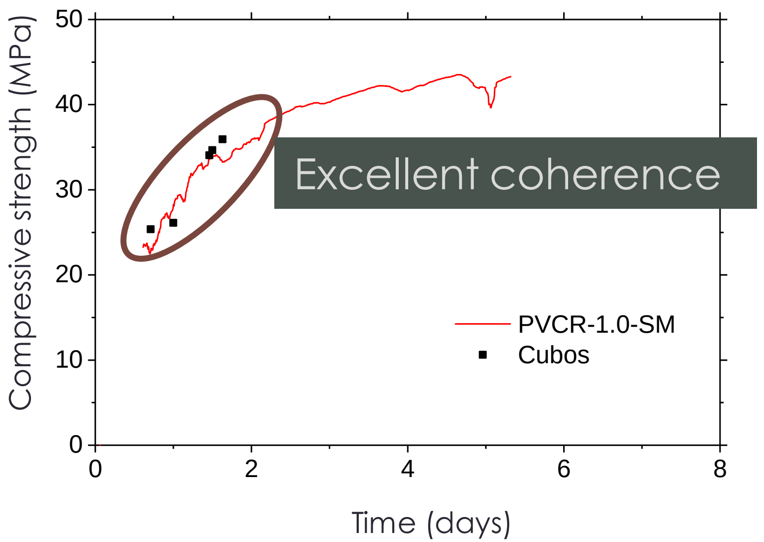

- ❑ Applicability of EMM-ARM under in-situ conditions successfully confirmed.

Other recent works and further ongoing research

of interest for TC-CMS

Other recent works

Application of air cooled pipes for reduction of early age cracking risk in a massive RC wall

Miguel Azenha *, Rodrigo Lameiras, Christoph de Sousa, Joaquim Barros

Engineering Structures 62–63 (2014) 148–163

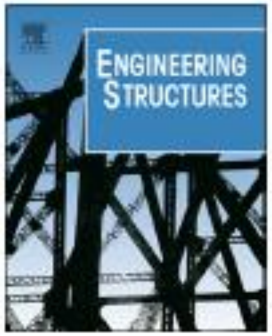

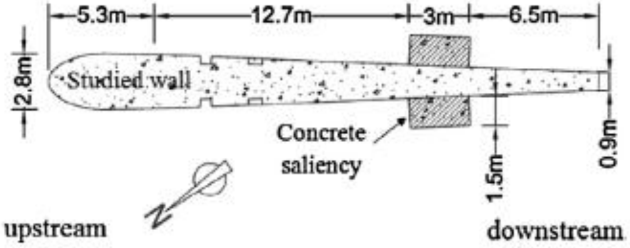

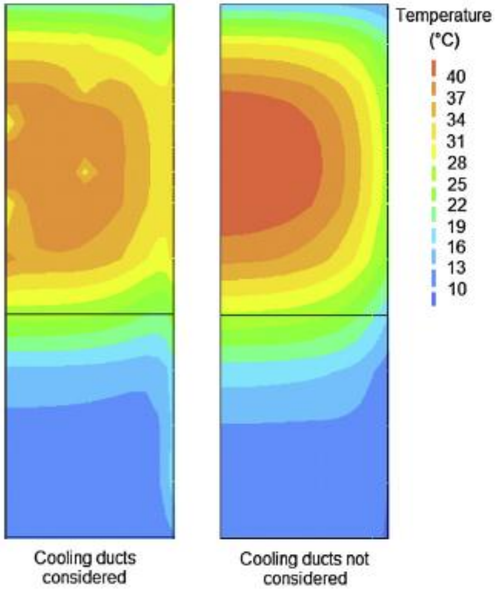

Other recent works

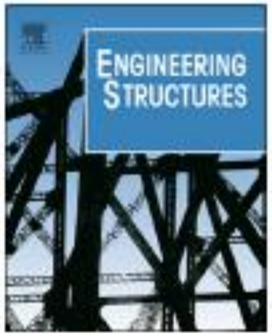

Early-age behaviour of the concrete surrounding a turbine spiral case: Monitoring and thermo-mechanical modelling

José Conceição [a], Rui Faria [a,*], Miguel Azenha [b], Flávio Mamede [c], Flávio Souza [d]

Engineering Structures 81 (2014) 327–340

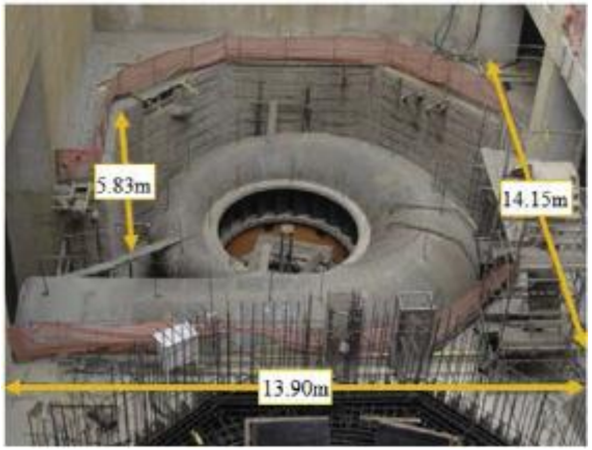

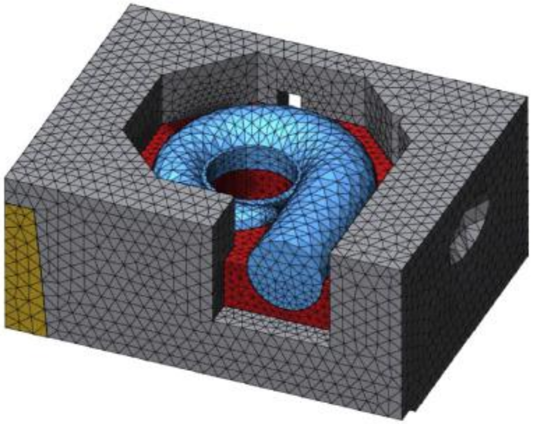

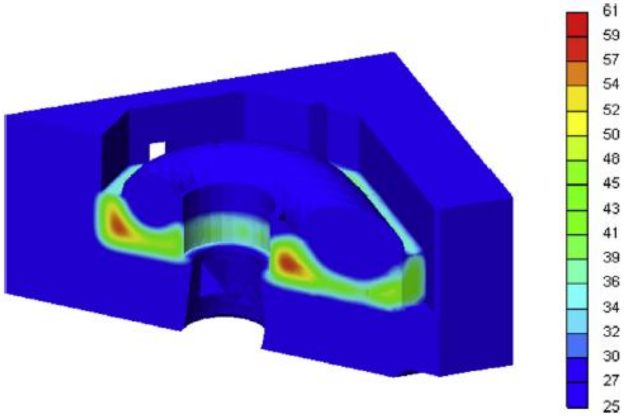

Ongoing research

VisCoDyn Project – FCT - EXPL/ECM-EST/1323/2013

The intent of this work is to explore the possibility of using dynamic approaches to continuously assess viscoelastic properties of concrete, with the proposal of a new methodology termed VisCoDyn. This innovative implementation can be achieved through the submission of a concrete specimen (e.g. a beam) to a known dynamic excitation.

Task 1: Equipment acquisition, training and software development

Task 2: Assembly of the experimental setup and testing

Task 3: Experimental program and round-robin testing

Task 4: Analytical and numerical evaluation of creep data

Task 5: Dissemination of results and connection with industry

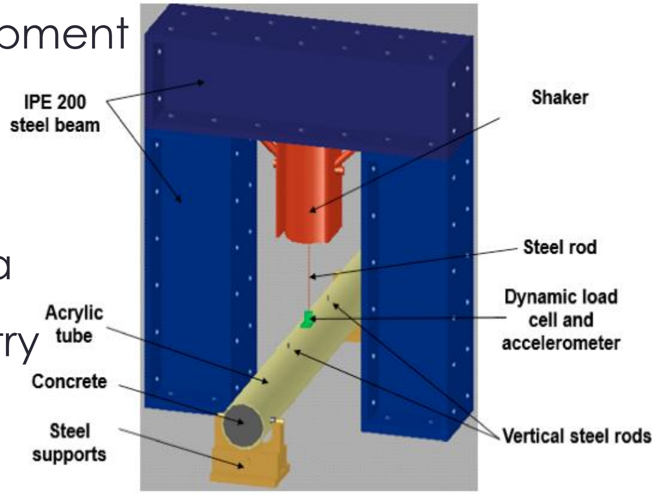

Ongoing research

COST TU1404 – Short Term Scientific Mission – UMinho - EPFL

José Granja, Cyrille Dunant, Miguel Azenha, Arnaud Muller

Cement Paste:

- Chemical composition
- w/c ratio
- PSD of the particles
- Reactions

3D Model

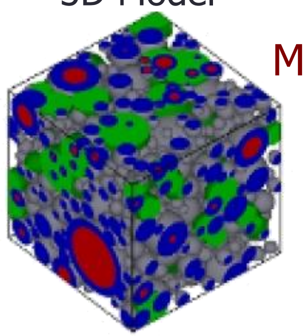

Meshing

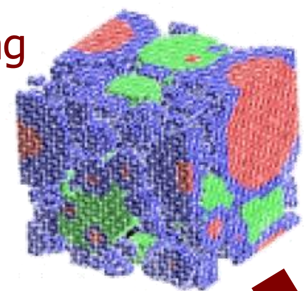

Hydrated and anhydrated phases:

- Mechanical properties

Several unknown properties!

Compare

Back analysis to get the properties

EMM-ARM for cement pastes

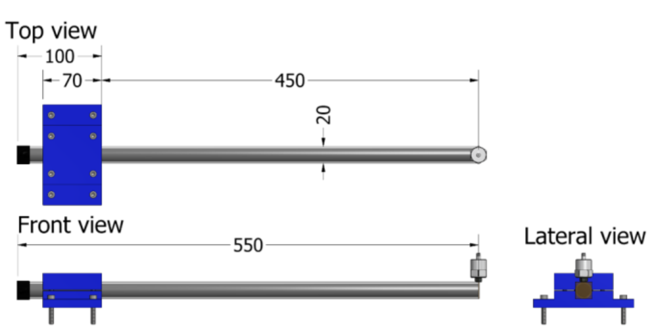

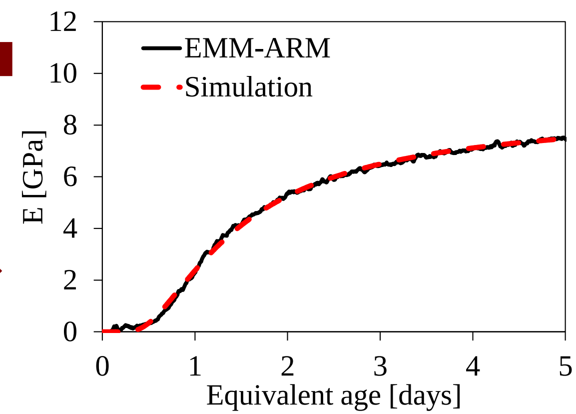

Acknowledgements

- FCT PhD grant SFRH/BD/80682/2011.
- FCT research project VisCoDyn EXPL/ECM-EST/1323/2013.
- COST Action TU1404 (STSM).
- Andreia Silva and Nuno Carvalho for their assistance in the experimental programs.

Shrinkage induced cracking risk of concrete

S. Staquet*, E. Rozière**, R.Cortas, A. Hamami, B. Delsaute, A. Loukili, M.-P. Delplancke-Ogletree

*LGC - Civil Engineering Lab – ULB – Brussels - Belgium

**GeM – Centrale Nantes - France

CMS Workshop “Cracking of massive concrete structures”
Cachan, 17 March 2015

Focus on the influence of the water saturation of aggregates on shrinkage induced cracking risk of concrete

E. Rozière, S. Staquet, R. Cortas, A. Hamami, A. Loukili, M.-P. Delplancke-Ogletree

- **Observations**

Early-age cracking of concrete (before 24 hours) :

Case 1 : Slabs.

Influence of aggregate type.

$Water_{eff}/Cement = 0.5 – 0.6$

Case 2 : Raft slab foundations, walls.

Influence of **aggregate water saturation**, paste volume and W_{eff}/C.

$W_{eff}/C = 0.45$

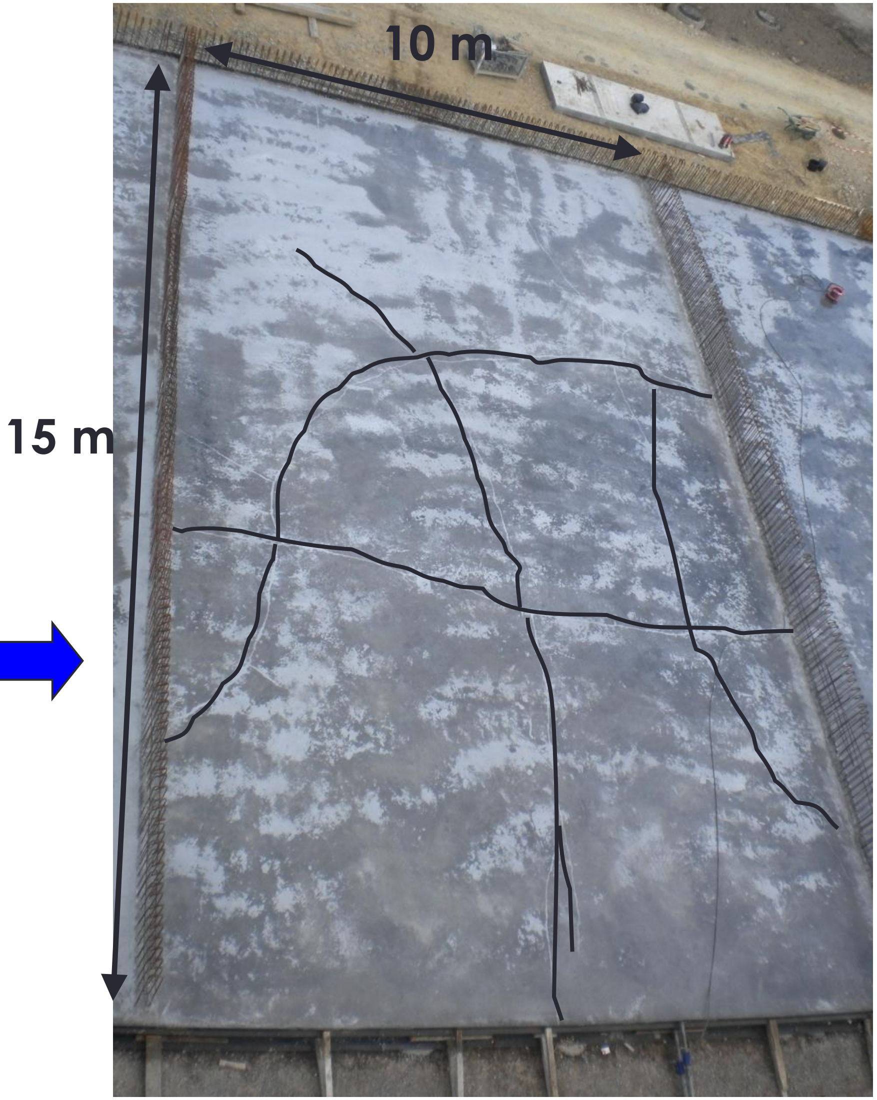

- **Restrained shrinkage caused cracking**

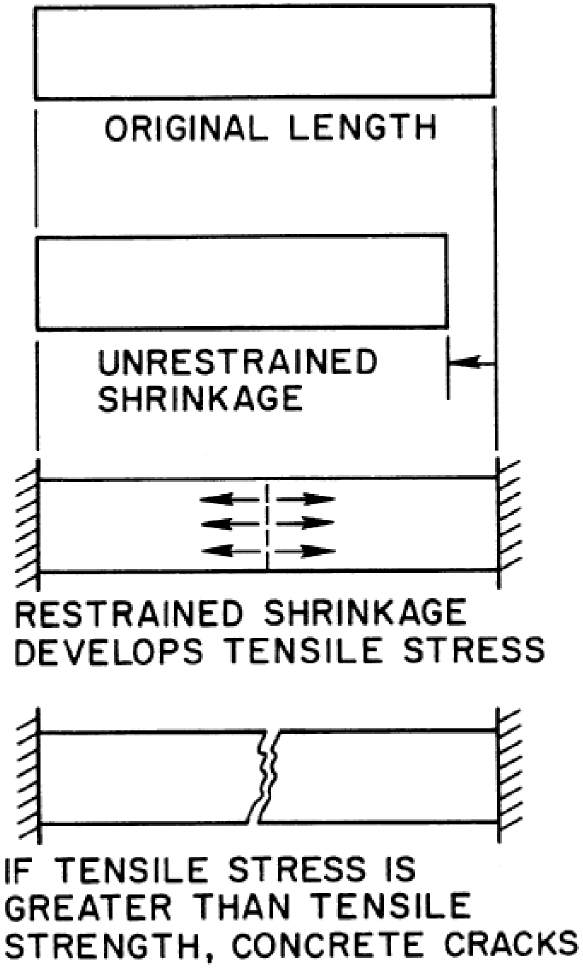

[ACI 224 – 01]

Early-age cracking : experimental approach

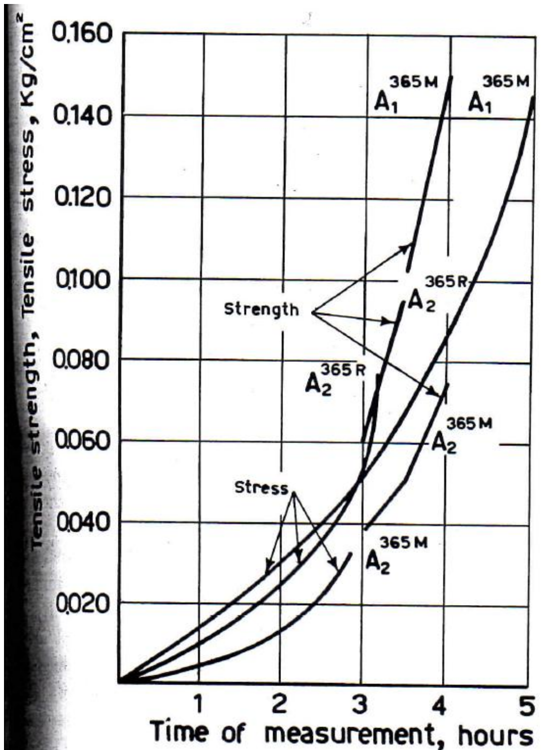

Fig. 13—Tensile stress and strength of semiplastic and plastic mortar made with Cement B (Type I) and cement C (Type V), exposed to climatic conditions E_{20}^{20}

Tensile strength, Tensile stress

Climatic conditions :

20°C, 45% HR, Wind 20 km/h

Ravina & Shalon, ACI, 1968

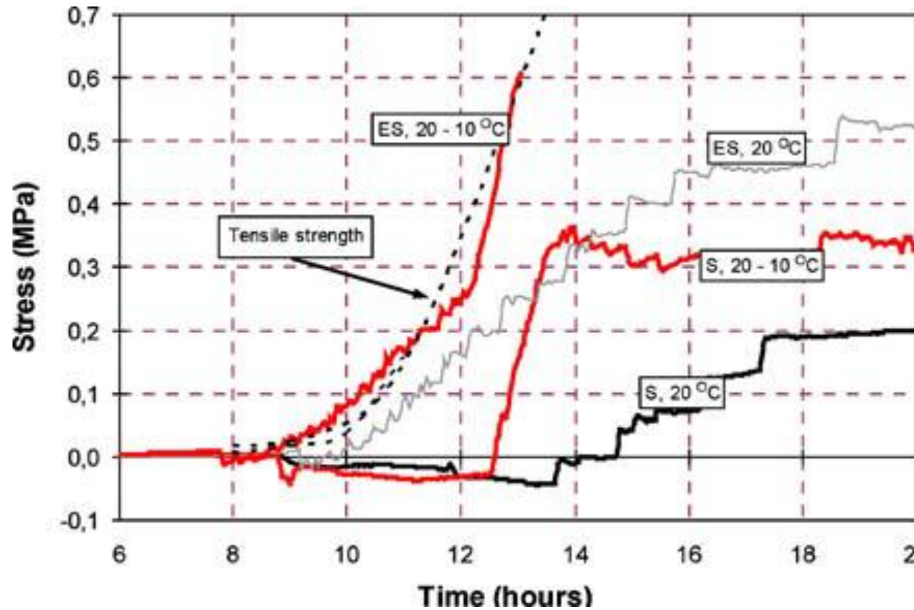

Self generated stress under various exposure conditions, and uniaxial tensile strength :

- Sealed (“S”, 20°C),

- Sealed and cooled (“S, 20–10°C”), exposed to air (“ES, 20°C”)

- Exposed to air and cooled (“ES, 20–10°C”).

Hammer et al., Materials & Structures, 2007

Outline

- **Experimental program**
  - Measurement of early-age shrinkage
  - Mix design
- **Early-age shrinkage**
  - Autogenous and plastic shrinkage
  - Porosity
  - Strength
- **Cracking**
  - Experimental approach
  - Effect of water saturation of aggregates

Experimental procedures

Plastic shrinkage

[TURCRY, 2004]

Autogenous shrinkage

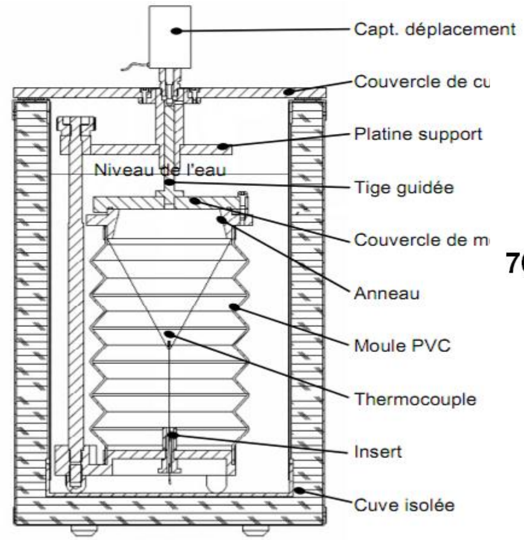

BTJADE
[BOULAY, 06]

Capillary depression

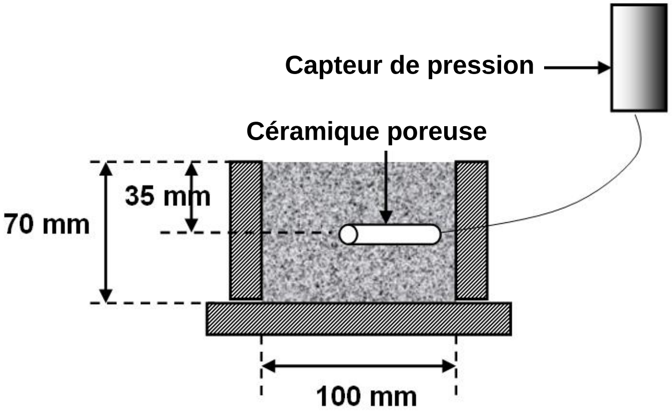

[TURCRY, 2004]

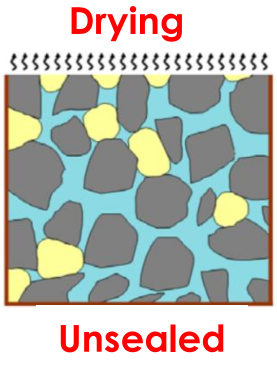

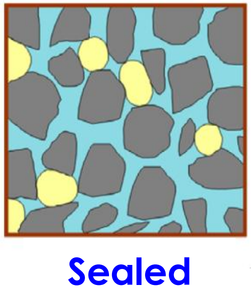

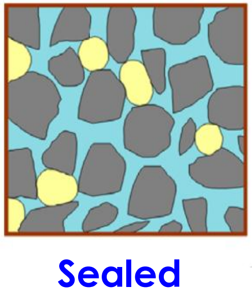

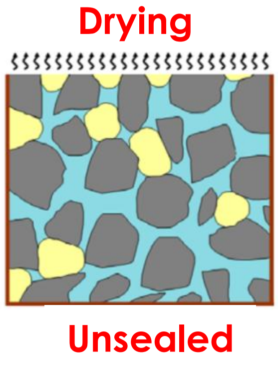

Water in concrete : definitions and experimental choices

Dry aggregates

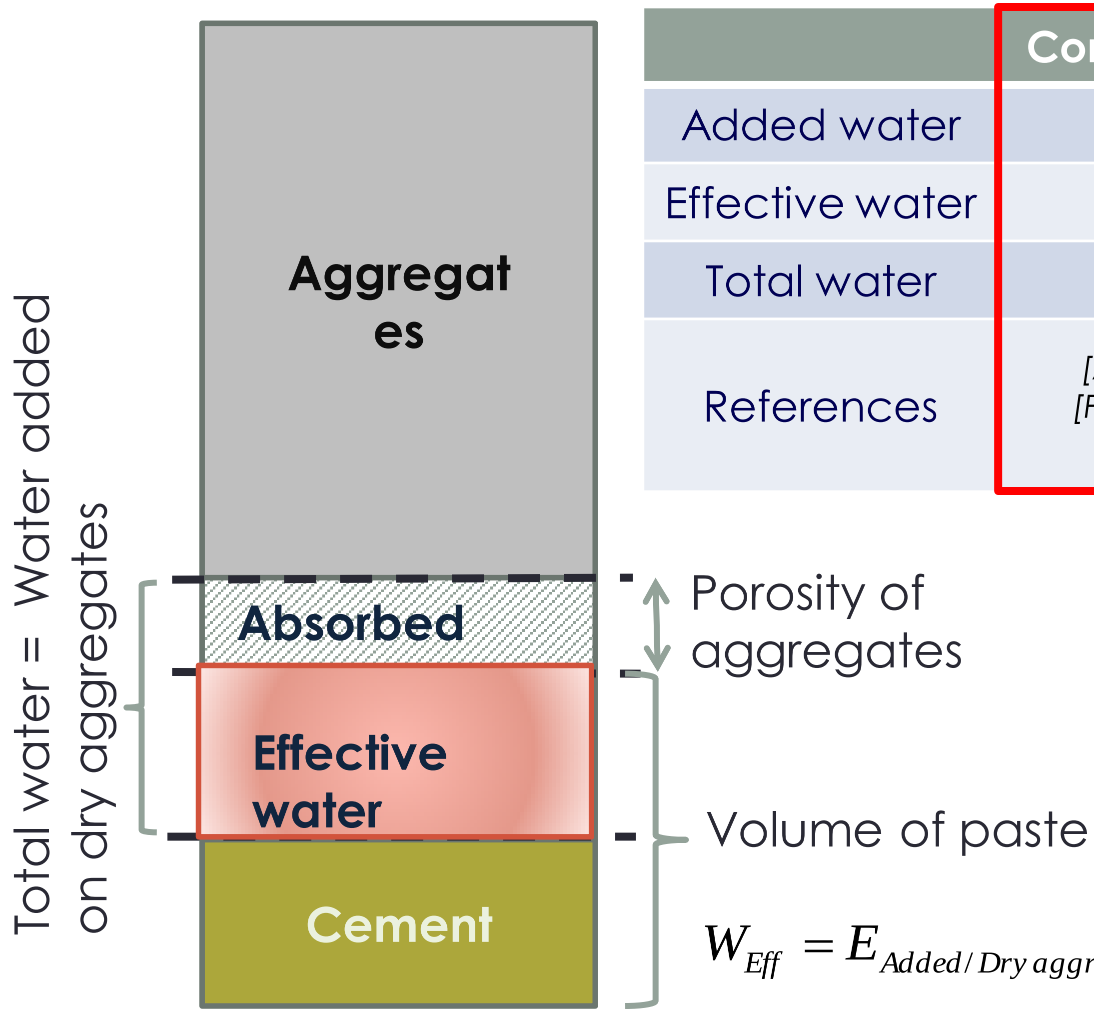

	Constant eff. water	Constant add. water
Added water	Variable	-----
Effective water	-----	Variable
Total water	Constant	Variable
References	*[AL HOZAIMY, 09], [PEREIRA et al., 09], [NF EN 206-1]*	*[TOMA, 99], [KHOON Ng & CHI Ng, 11]*

$$W_{Eff} = E_{Added/Dry\ aggregates} - E_{Absorbed by\ aggregates}$$

Water in concrete : definitions and experimental choices

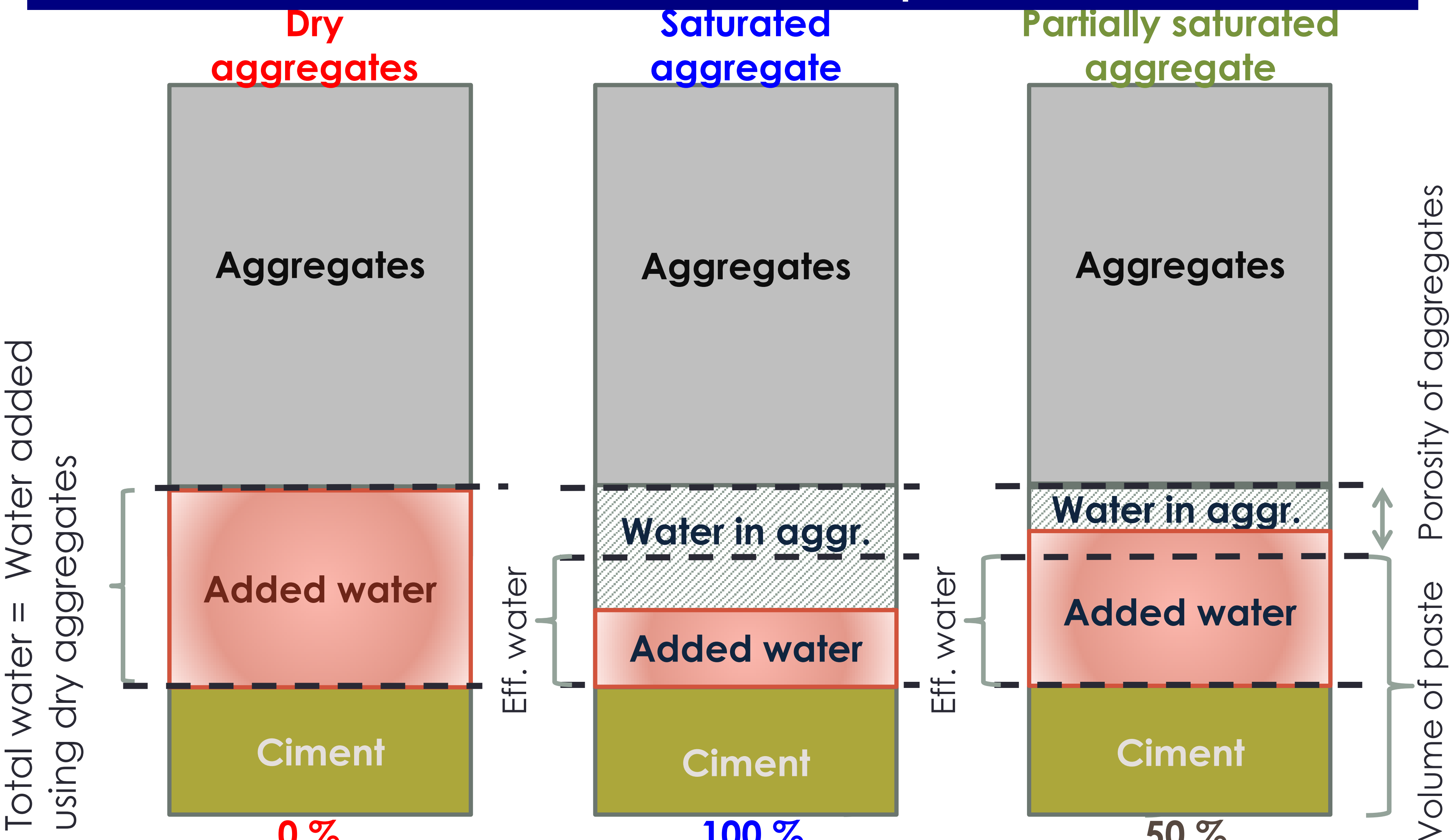

Plastic shrinkage

Concrete mixture BV
Natural limestone gravels Aborption (WA_{24}) 3,2 % *(Standard NF EN 1097-6)*
Initial water saturation : 0%, 50% et 100%
W/C : 0.5 - *E/C : 0.6*
Portland cement CEM I 52,5

Drying :
20 °C – 50 % RH

Same influence of initial water saturation of gravels

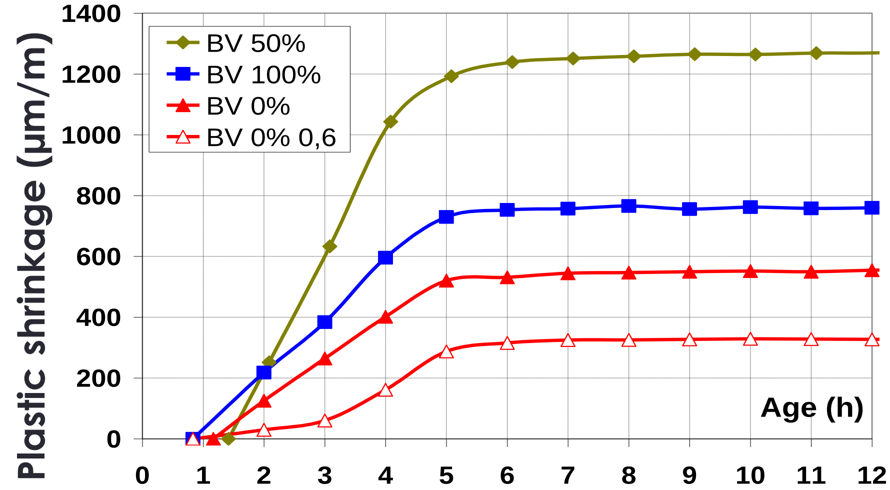

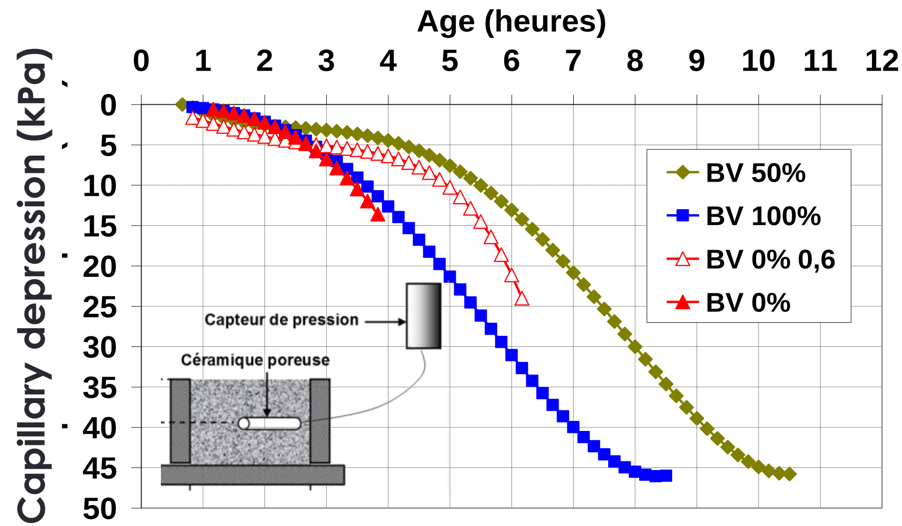

Autogenous shrinkage

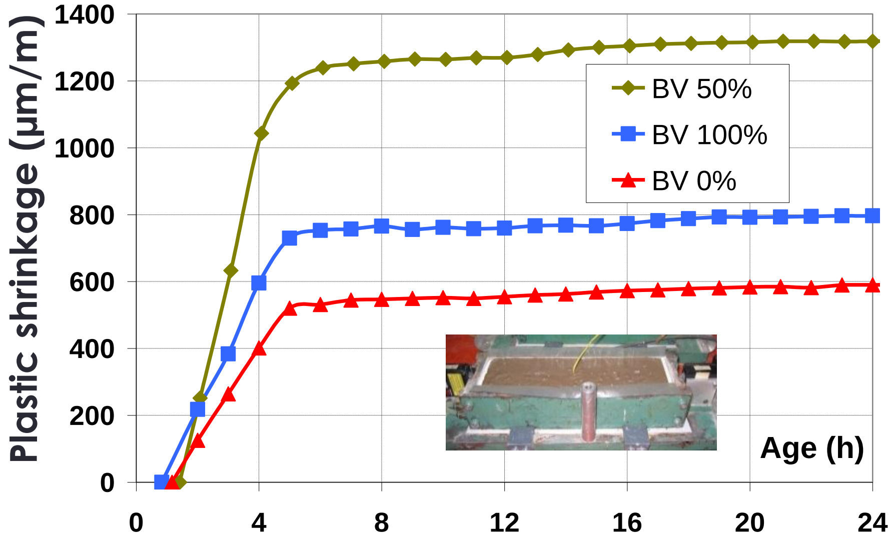

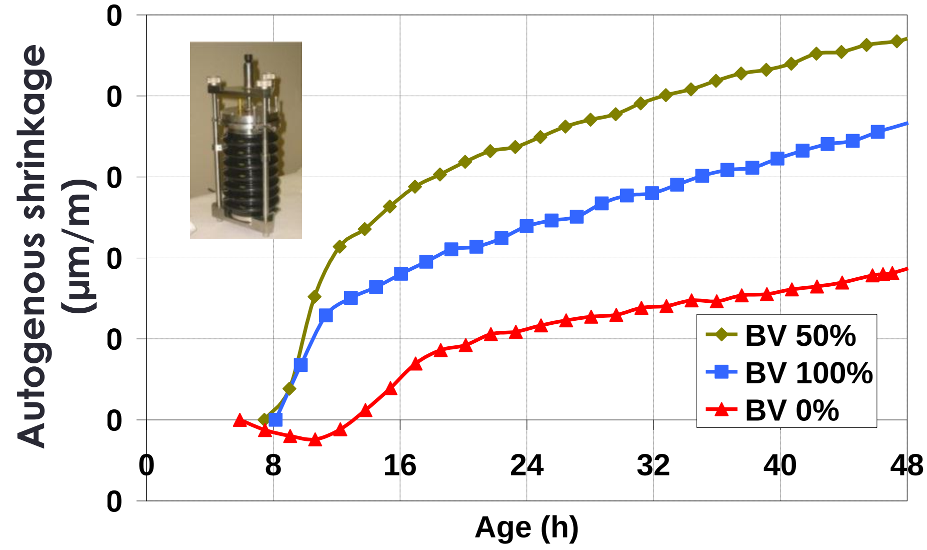

- Relatively low autogenous shrinkage
- Same influence of initial water saturation of gravels : $\text{water}_{\text{paste}}$/cement ratio

Microstructure : evidence of absorption

- Water content of mortar and gravels

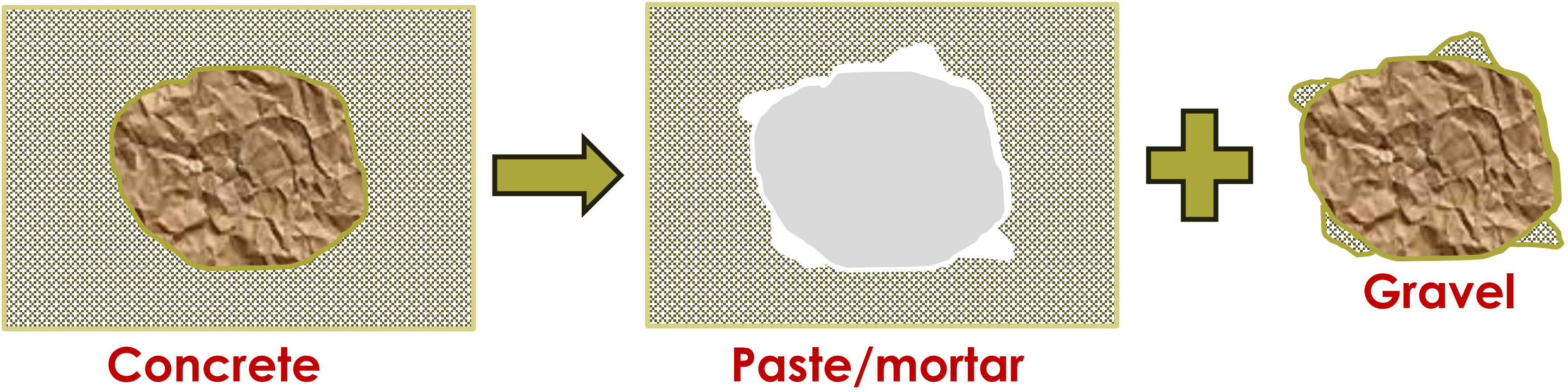

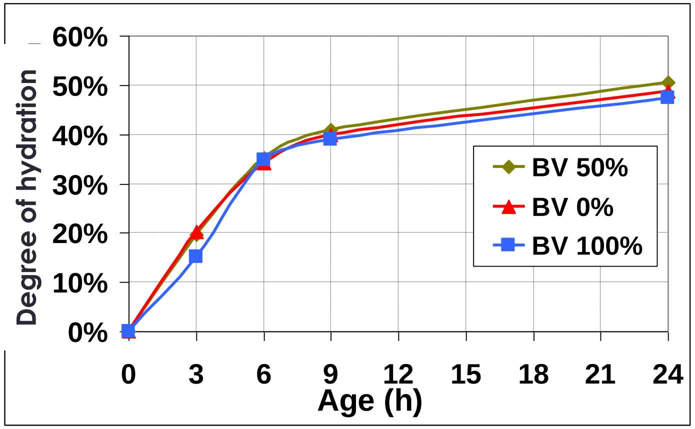

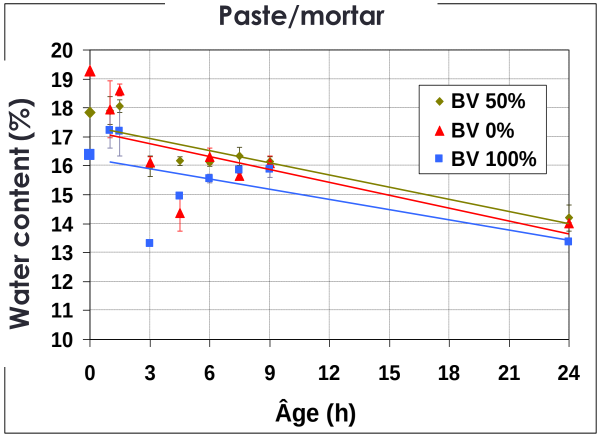

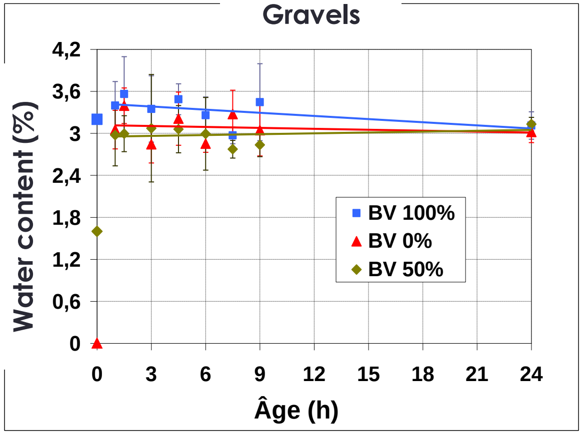

Mercury intrusion porosimetry

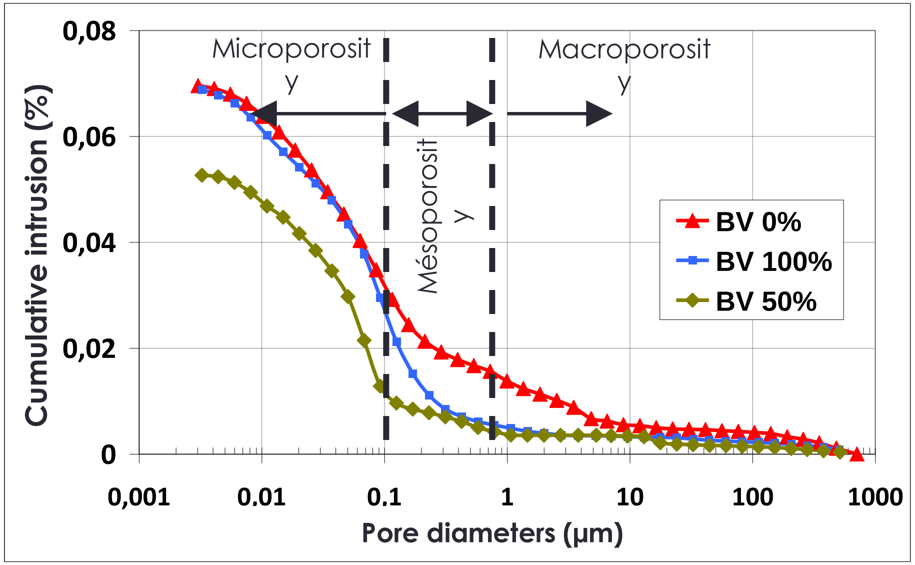

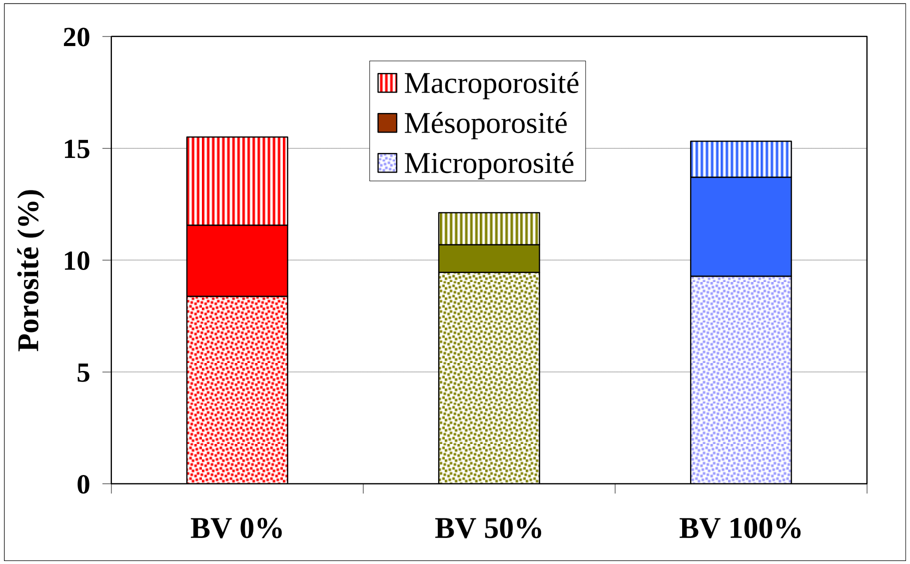

Age : 24 hours

- Porous structure dependent on initial saturation of gravels

Compressive strength

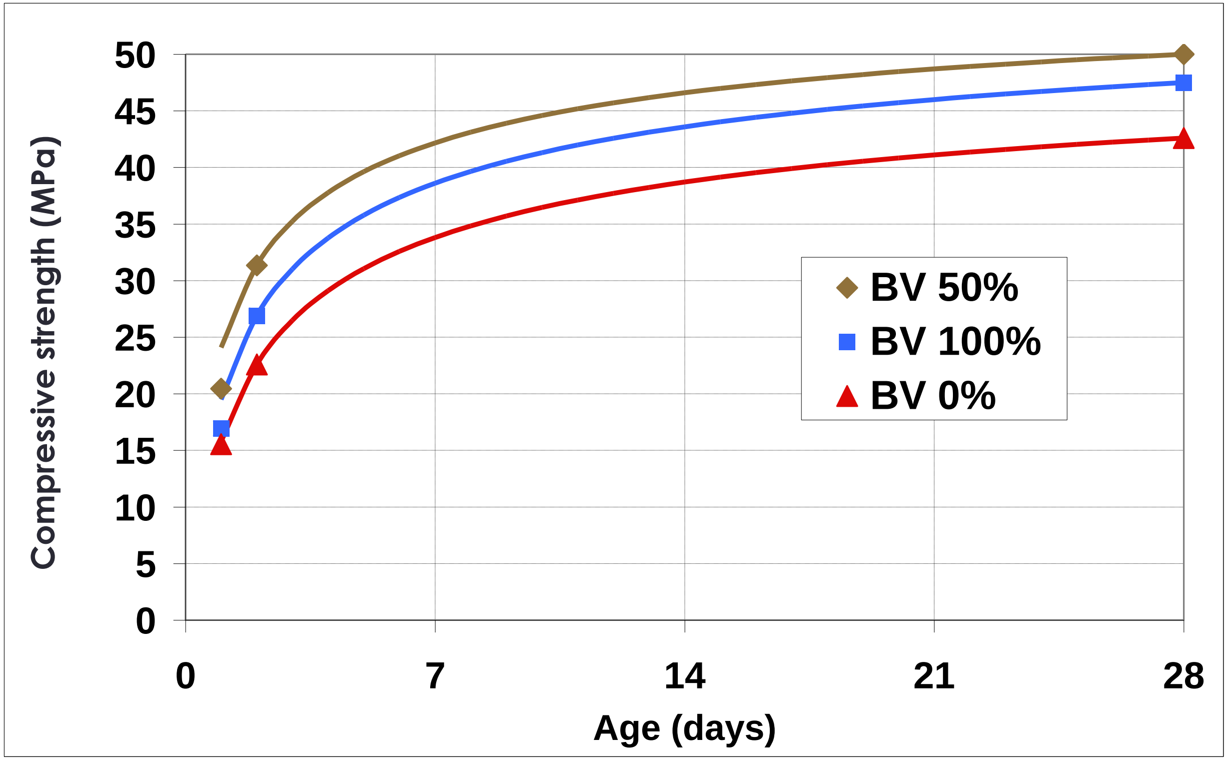

Same influence of initial water saturation of gravels (cf. autogenous and plastic shrinkage) => Influence of added water on macroporosity (evidence) and interfacial transition zone (to be confirmed)

Summary

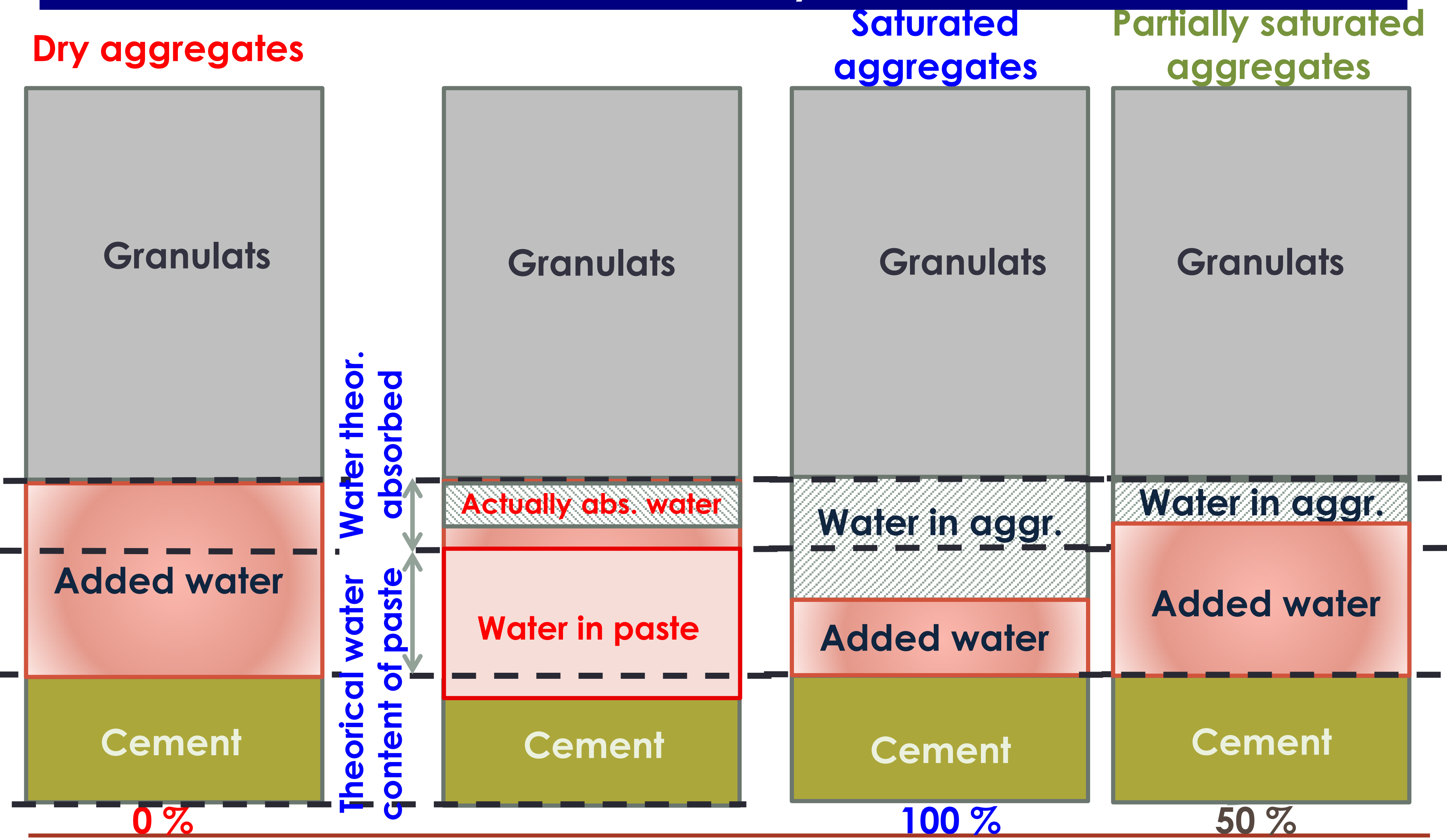
Dry aggregates
Saturated aggregates
Partially saturated aggregates
Granulats
Granulats
Granulats
Granulats
Added water
Water theor. absorbed
Theorical water content of paste
Actually abs. water
Water in paste
Water in aggr.
Added water
Water in aggr.
Added water
Cement
Cement
Cement
Cement
0 %
100 %
50 %

Direct tensile testing rig

New experimental method (Rozière *et al.*, 2012)

Concrete specimen

Spherical pin connection

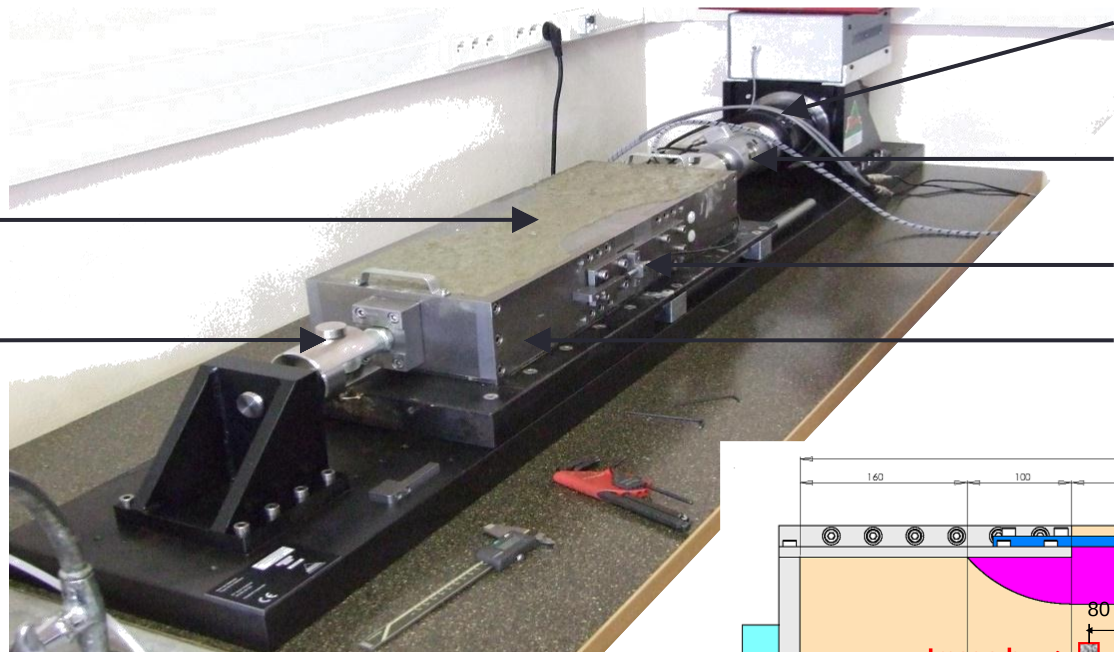

Electric actuator

Load cell

LVDT2

Steel mould :

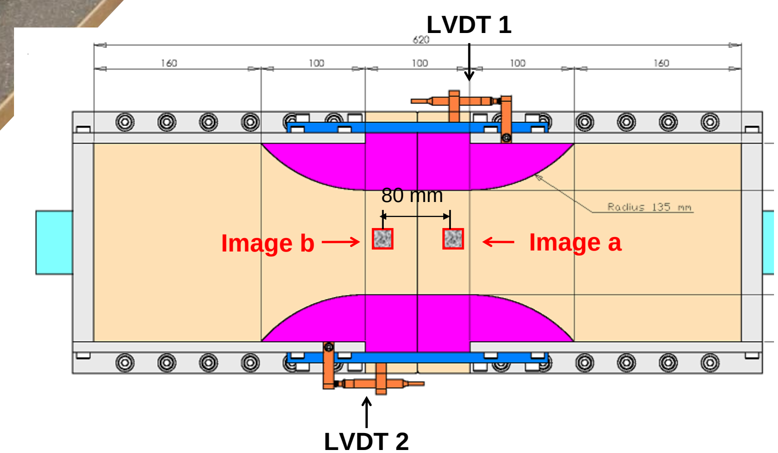

Ultrasonic monitoring of elastic modulus – *FreshCon*

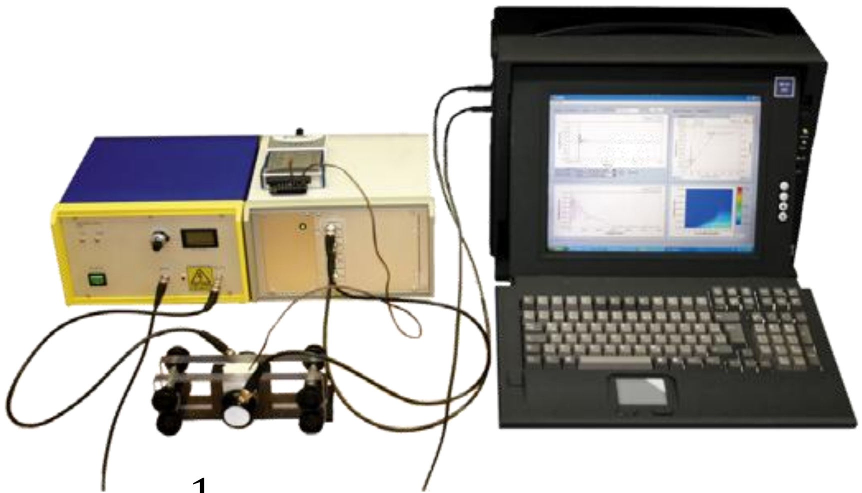

- Poisson ratio : ν_{dyn}
- Elastic modulus : E_{dyn}

$$\upsilon_{dyn} = \frac{\frac{1}{2} \cdot v_p^2 - v_s^2}{v_p^2 - v_s^2}$$

$$E_{dyn} = v_p^2 \cdot \rho_c \cdot \frac{(1+\upsilon_{dyn}) \cdot (1-2\upsilon_{dyn})}{1-\upsilon_{dyn}}$$

- ρ density of fresh concrete,
- v_p compression wave velocity,
- v_s shear wave velocity.

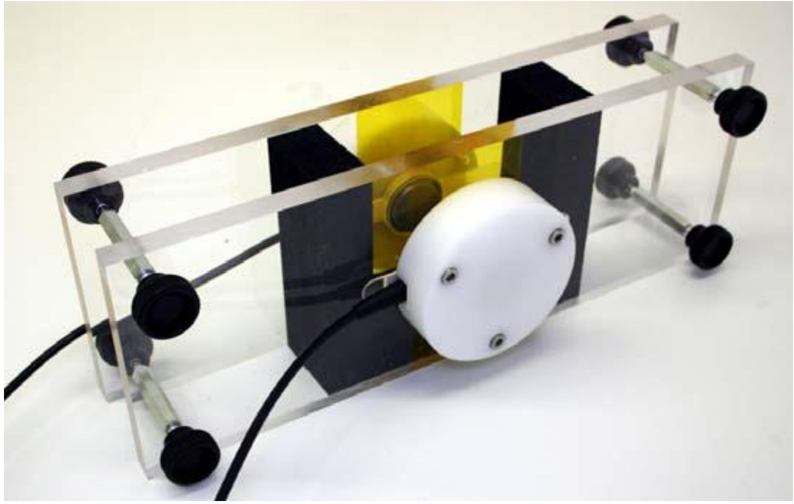

[Reinhardt and Grosse, 2004]

Ultrasonic monitoring of elastic modulus

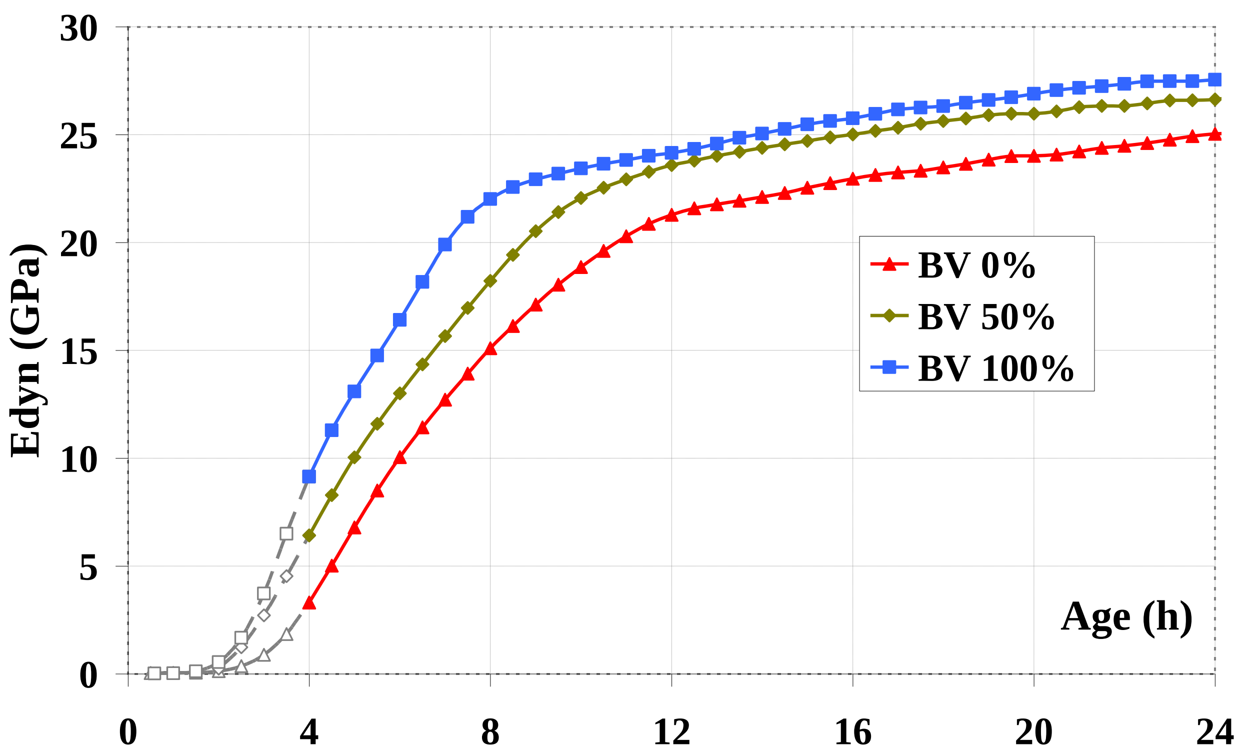

=> Significant influence of water saturation of aggregate on elastic modulus (2-10h).

Assessment of cracking sensitivity due to AUTOGENOUS shrinkage

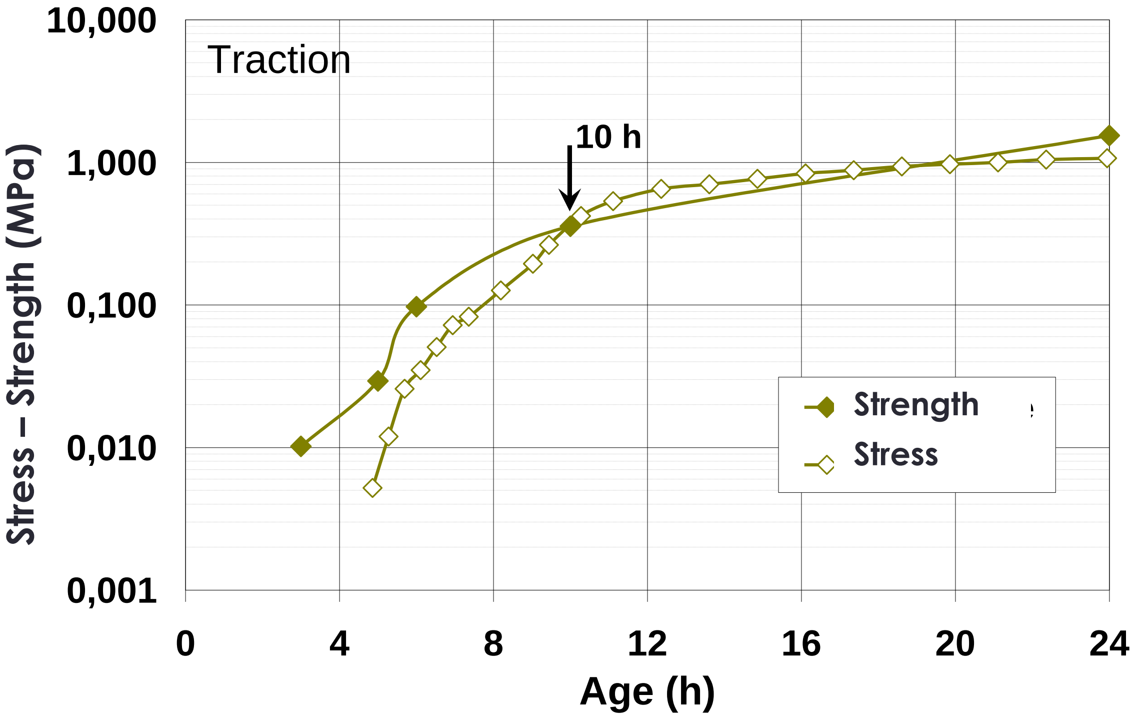

Elastic model :

$$\sigma(t) = \varepsilon(t) \cdot E(t)$$

=> Time period when stresses due to to restrained shrinkage exceed tensile strength.

Influence of water saturation on cracking due to AUTOGENOUS shrinkage

BV 0% | **BV 50%** | **BV 100%**

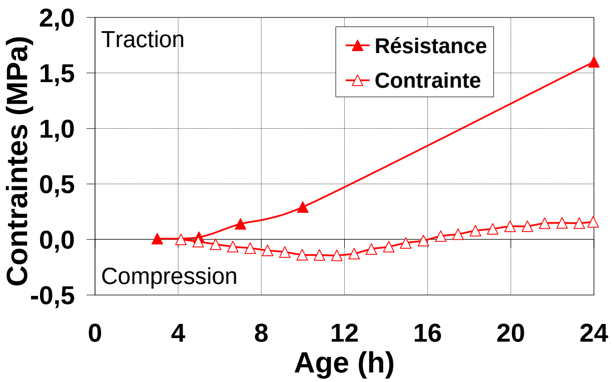

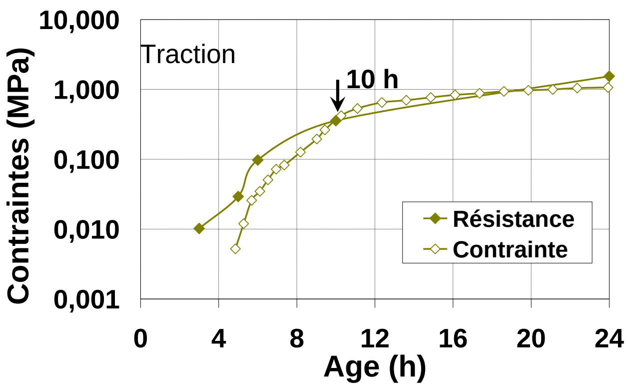

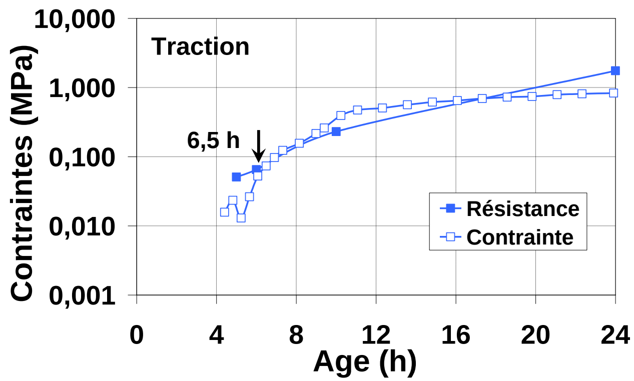

- Limestone gravels (Abs : 3,2%)
- Cement : 350 kg/m^3
- E/C : 0,5

Critical period between 4 and 10 hours

Influence of water saturation on cracking due to PLASTIC shrinkage

TSTM (*Temperature Stress Testing Machine*) :
Restrained shrinkage tests

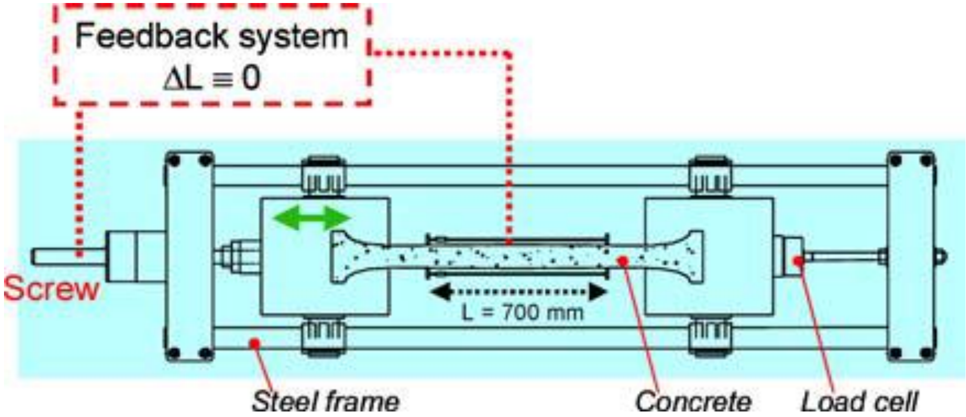

Rig for testing of self generated stress
[Hammer et al., 2007]

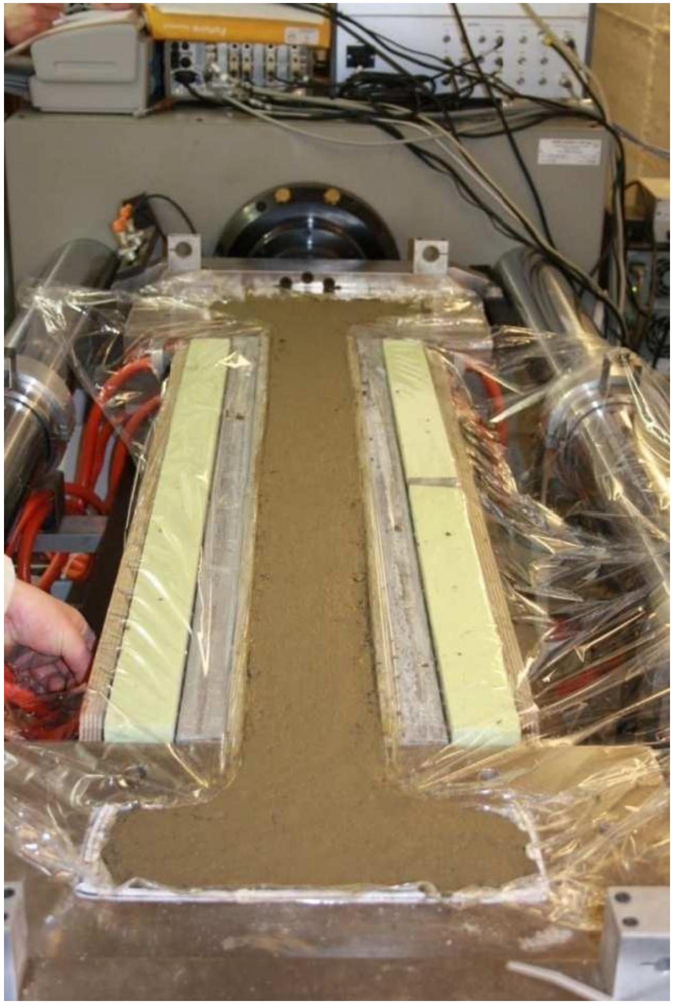

Conclusions

- **An experimental procedure** was designed to investigate the influence of water saturation of gravels of early-age shrinkage (before 24 hours) and cracking sensitivity of concrete.
- **Significant variations** of the plastic shrinkage and early age autogenous deformations were observed.
- Due to the kinetics of absorption of gravels, **the water content remaining in cement paste** was different from the effective water content.
- The evolutions of elastic modulus and tensile strength were experimentally assessed and used to compare the cracking sensitivity of the three studied concretes by **evaluating the self generated stresses**.

Focus on the influence of the type of aggregates on shrinkage induced cracking risk of concrete

S. Staquet, E. Rozière, A. Hamami, B. Delsaute, A. Loukili

Outline

- **Experimental program**
  - Mix design
  - Measurement of thermal expansion coefficient
  - Experimental approach for shrinkage induced cracking

- **Early-age autogenous shrinkage : effect of type of aggregates**
  - Autogenous shrinkage, capillary pressure, thermal expansion coefficient
  - E modulus
  - Autogenous shrinkage induced cracking

- **Early-age drying shrinkage: effect of type of aggregates**
  - Free shrinkage
  - Restraint shrinkage

Properties of aggregates

	Water absorption WA_{24} (%)	Density
Sand 0/4 mm		
Sea sand	0.6	2.58
Limestone sand	0.8	2.65
Gravels 4/20 mm		
Quartz (Q)	0.8	2.59
Dense limestone (DL)	0.74	2.65
Porous limestone (PL)	3.2	2.46

Same water saturation degree (50%) before concrete mixing

Properties of aggregates

	Water absorption WA_{24} (%)	Density
Sand 0/4 mm		
Sea sand	0.6	2.58
Limestone sand	0.8	2.65
Gravels 4/20 mm		
Quartz (Q)	0.8	
Dense limestone (DL)	0.74	
Porous limestone (PL)	3.2	

Same water saturation degree (50%) before concrete mixing

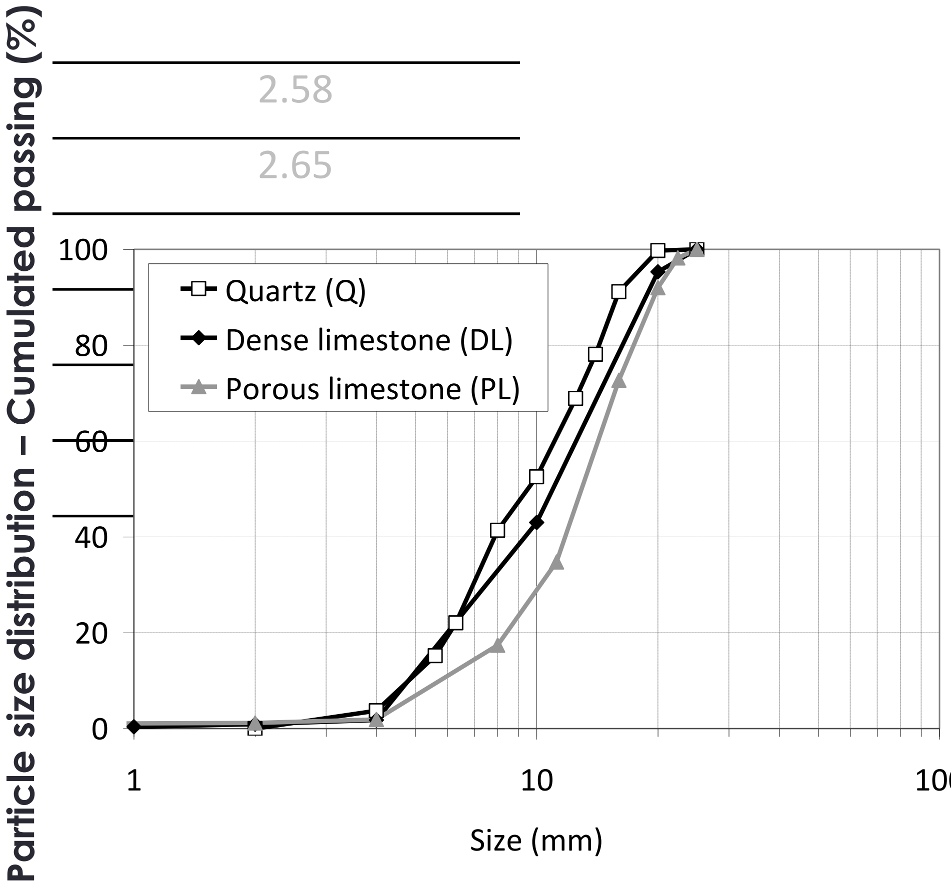

Properties of the studied concretes

	PL	Q	DL
Gravel (kg/m³)	1016	1057	1086
Sea sand (kg/m³)	378	378	378
Limestone sand (kg/m³)	389	389	389
Cement (kg/m³)	350	350	350
Superplasticizer (Sp) (kg/m³)	1.25	1	1
Effective Water: W_{eff} (kg/m³)	**175**	**175**	**175**
Water from superplasticizer (kg/m³)	1	0.8	0.8
Total Water (kg/m³)	211	186	188
Water absorbed by sand: W_{sand} (kg/m³)	23	23	23
Water absorbed by gravels: W_{gravel} (kg/m³)	**16**	**4**	**4**
Added Water: W_{added} (kg/m³)	**172**	**159**	**161**
W_{eff}/C	0.50	0.5	0.5
W_{added}/C	0.49	0.45	0.46
Paste Volume (L/m³)	**288**	**288**	**288**

Same water saturation degree (50%) before concrete mixing

Properties of the studied concretes

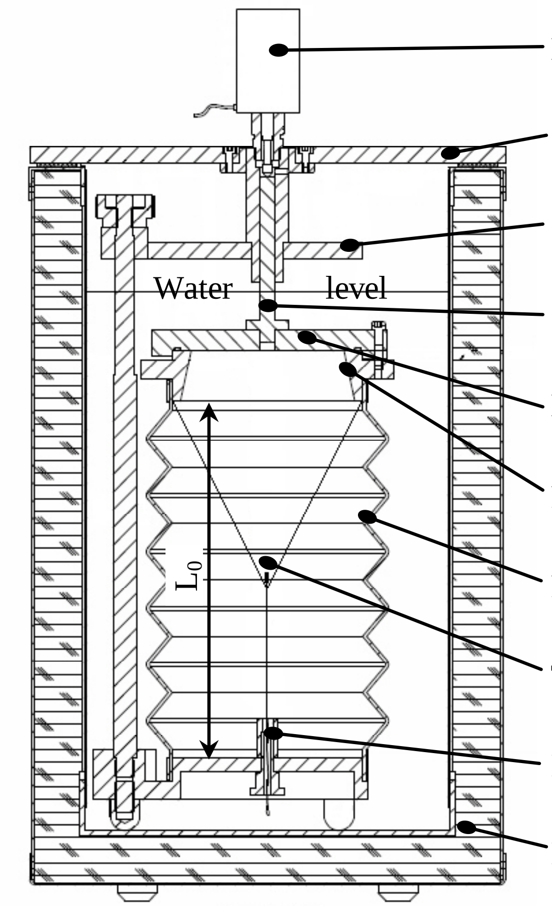

BTJADE
[BOULAY, 06]

Autogenous deformation test device

Properties of the studied concretes

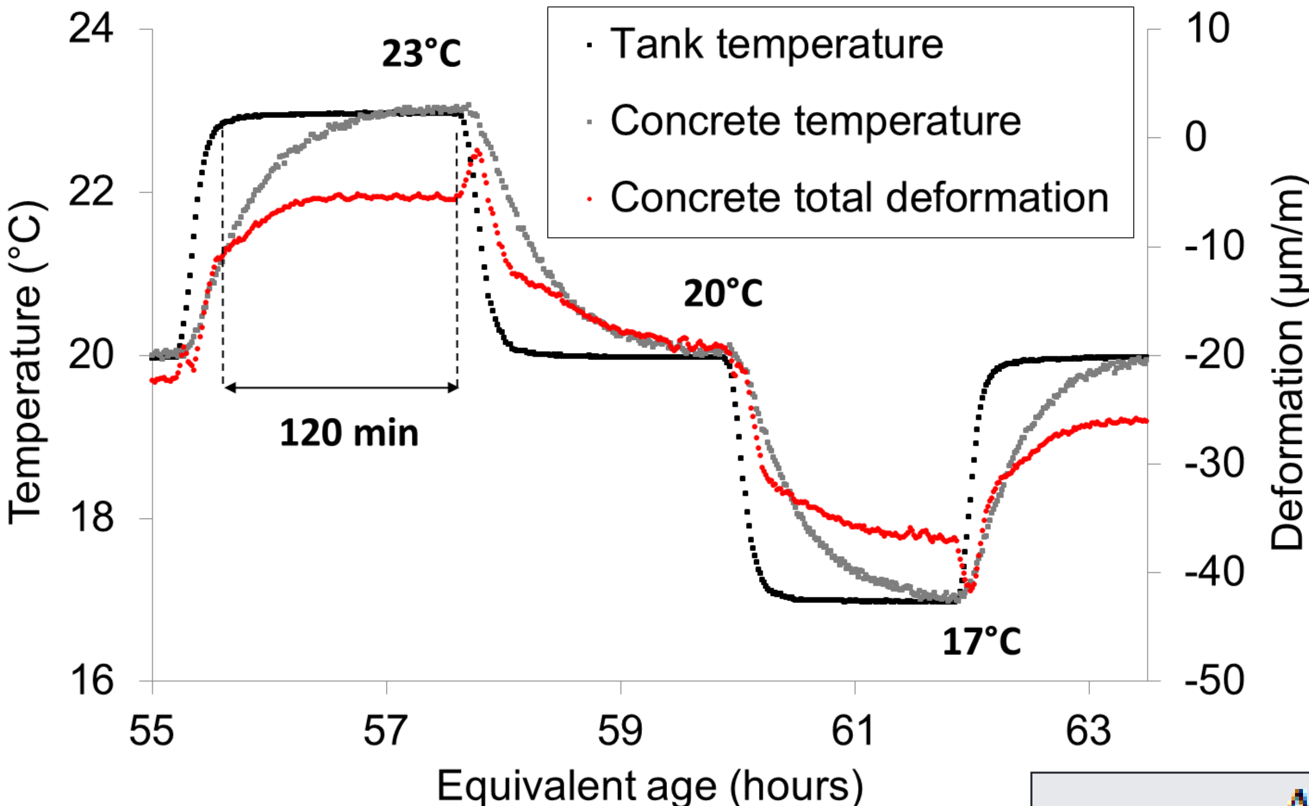

$\Delta\theta_0$: Temperature variation between t and t_0
ΔU_c : Displacement of the concrete.
α_0 : CTE of the concrete sample (α_0)

$$\alpha_0(t_i) = \frac{\dfrac{\Delta U_c(t_{i+1}) - \Delta U_c(t_i)}{L_0}}{\Delta\theta_0(t_{i+1}) - \Delta\theta_0(t_i)}$$

Shrinkage induced cracking

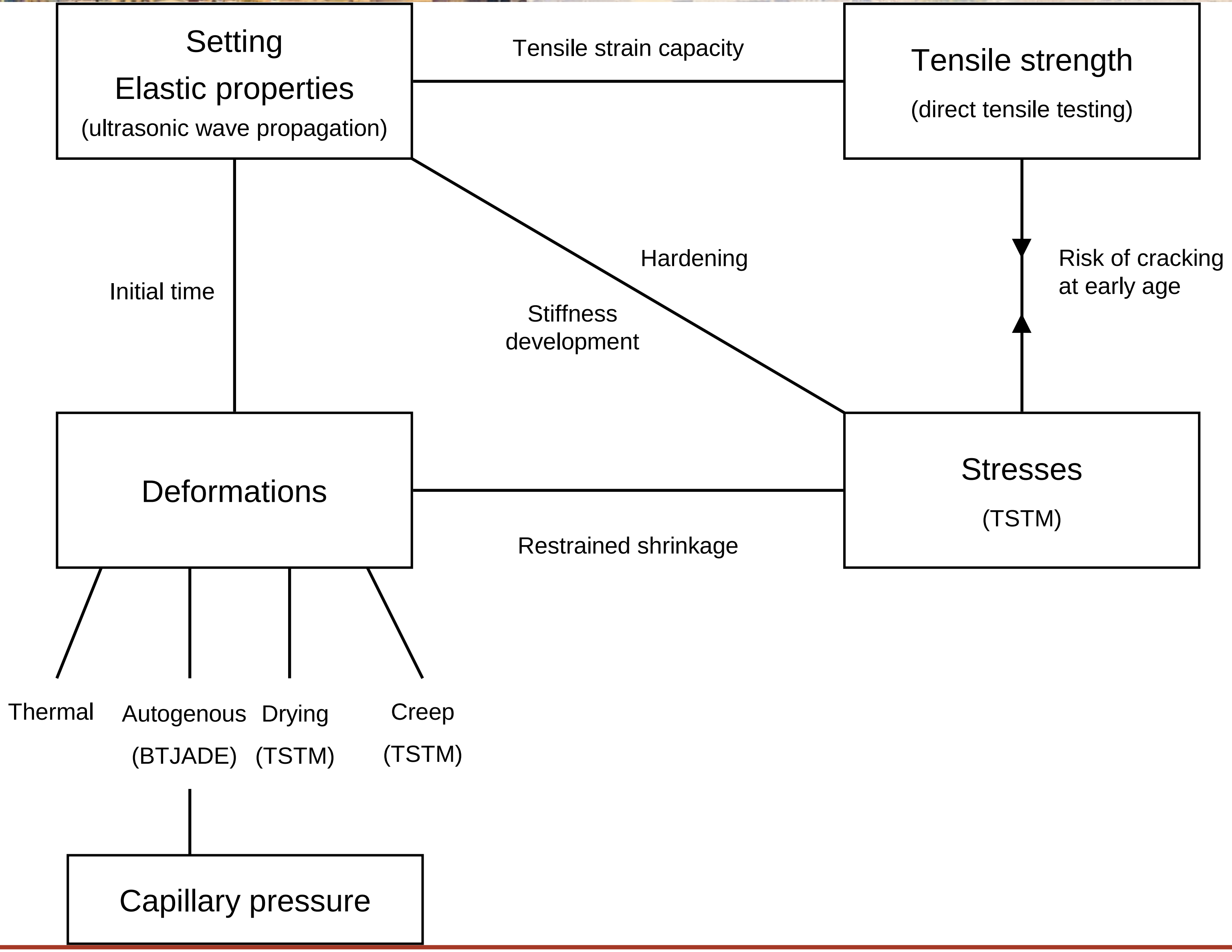

Free and restrained shrinkage, stress development with TSTM

TSTM (Temperature Stress Testing Machine), BATir-LGC

- Linear horizontal device
- 400 kN compression/traction jack
- Computer controlled
- Dog bone shape
  - Length = 1.3 m
  - Section = 100 x100 mm²
- Fixed and mobile heads
- Surrounded by a plastic film
  - Autogenous conditions
- Displacement sensors without contact
  - 75 cm spacing
- Thermal regulation
- Twin mould

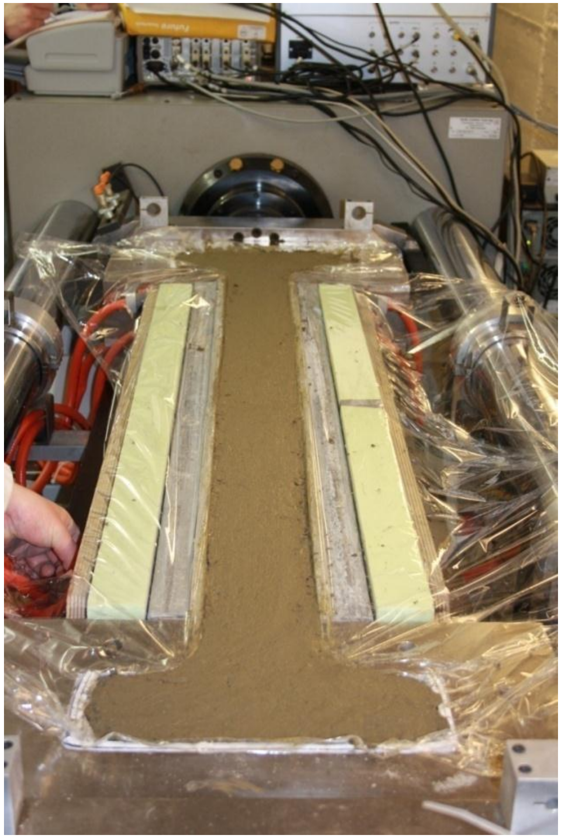

Free and restrained shrinkage, stress development with TSTM

TSTM (Temperature Stress Testing Machine)

- Linear horizontal device
- 400 kN compression/traction jack
- Computer controlled
- Dog bone shape
  - Length = 1.3 m
  - Section = 100 x100 mm²
- Fixed and mobile heads
- Surrounded by a plastic film
  - Autogenous conditions
- Displacement sensors without contact
  - 75 cm spacing
- Thermal regulation
- Twin mould

Fixed head

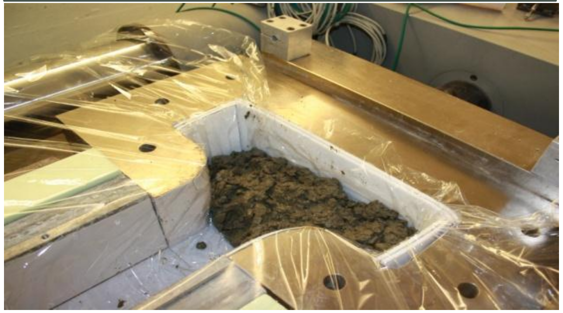

Mobile head

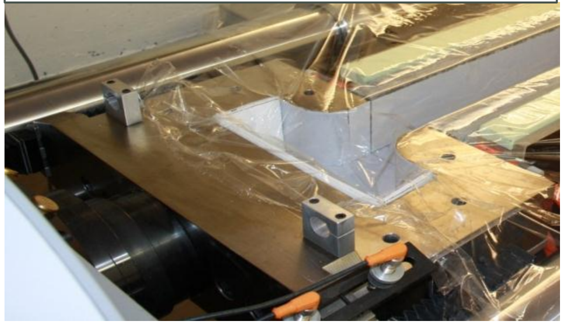

Free and restrained shrinkage, stress development with TSTM

TSTM (Temperature Stress Testing Machine)

- Linear horizontal device
- 400 kN compression/traction jack
- Computer controlled
- Dog bone shape
  - Length = 1.3 m
  - Section = 100 x100 mm²
- Fixed and mobile heads
- Surrounded by a plastic film
  - Autogenous conditions
- Displacement sensors without contact
  - 75 cm spacing
- Thermal regulation
- Twin mould

Free and restrained shrinkage, stress development with TSTM

TSTM (Temperature Stress Testing Machine)

- Linear horizontal device
- 400 kN compression/traction jack
- Computer controlled
- Dog bone shape
  - Length = 1.3 m
  - Section = 100 x100 mm²
- Fixed and mobile heads
- Surrounded by a plastic film
  - Autogenous conditions
- Displacement sensors without contact
  - 75 cm spacing
- Thermal regulation
- Twin mould

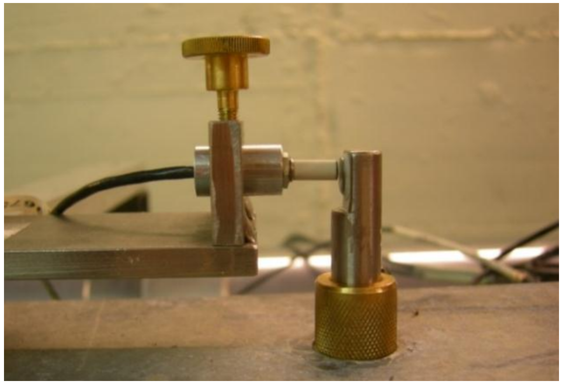

Free and restrained shrinkage, stress development with TSTM

TSTM (Temperature Stress Testing Machine)

- Linear horizontal device
- 400 kN compression/traction jack
- Computer controlled
- Dog bone shape
  - Length = 1.3 m
  - Section = 100 x100 mm²
- Fixed and mobile heads
- Surrounded by a plastic film
  - Autogenous conditions
- Displacement sensors without contact
  - 75 cm spacing
- Thermal regulation
- Twin mould

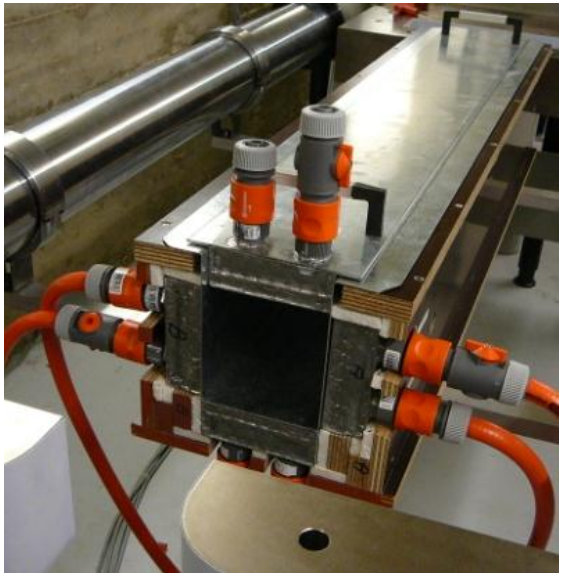

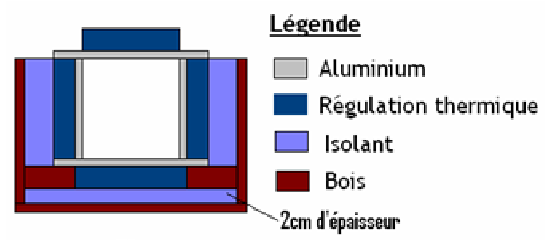

Free and restrained shrinkage, stress development with TSTM

TSTM (Temperature Stress Testing Machine)

- Linear horizontal device
- 400 kN compression/traction jack
- Computer controlled
- Dog bone shape
  - Length = 1.3 m
  - Section = 100 x100 mm²
- Fixed and mobile heads
- Surrounded by a plastic film
  - Autogenous conditions
- Displacement sensors without contact
  - 75 cm spacing
- Thermal regulation
- Twin mould

Fixed head

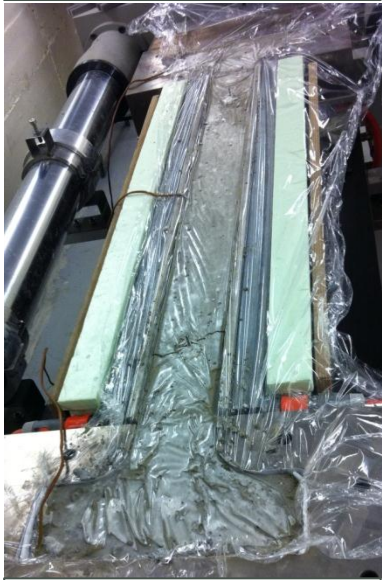

Restrained head

Fixed head

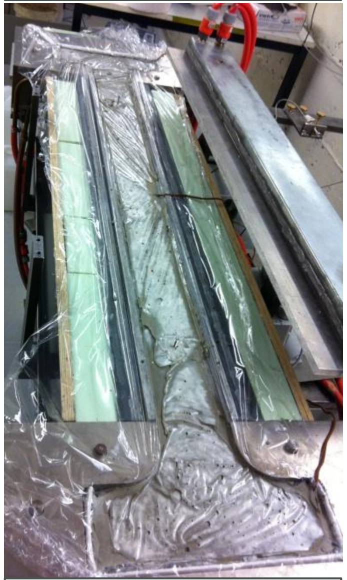

Free head

Free and restrained shrinkage, stress development with TSTM

Free and restrained shrinkage, stress development with TSTM

Free and restrained shrinkage, stress development with TSTM

Free and restrained shrinkage, stress development with TSTM

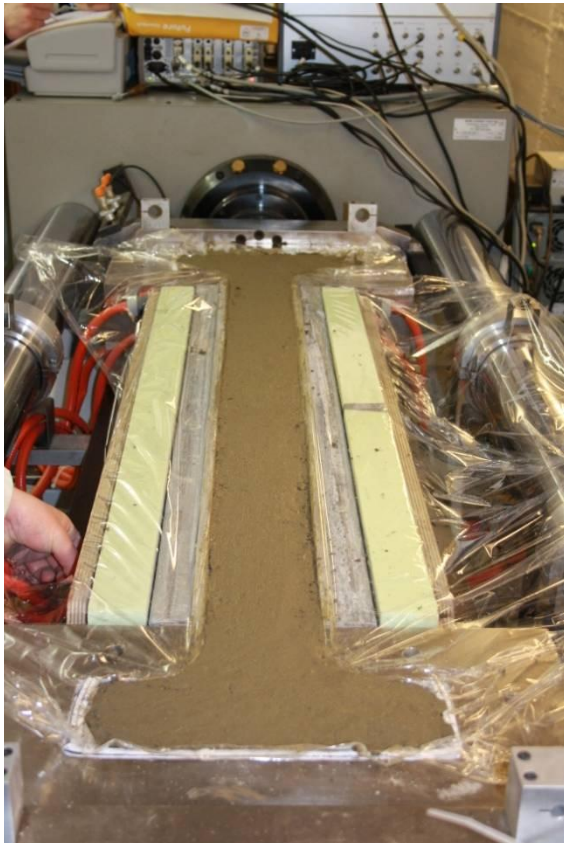

Free and restrained shrinkage, stress development with TSTM

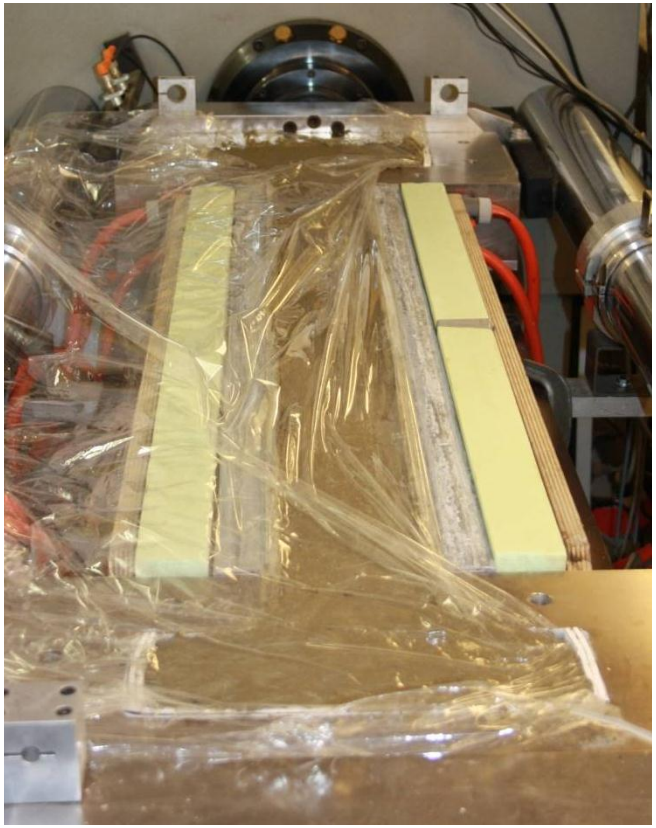

Free and restrained shrinkage, stress development with TSTM

Free and restrained shrinkage, stress development with TSTM

Free and restrained shrinkage, stress development with TSTM

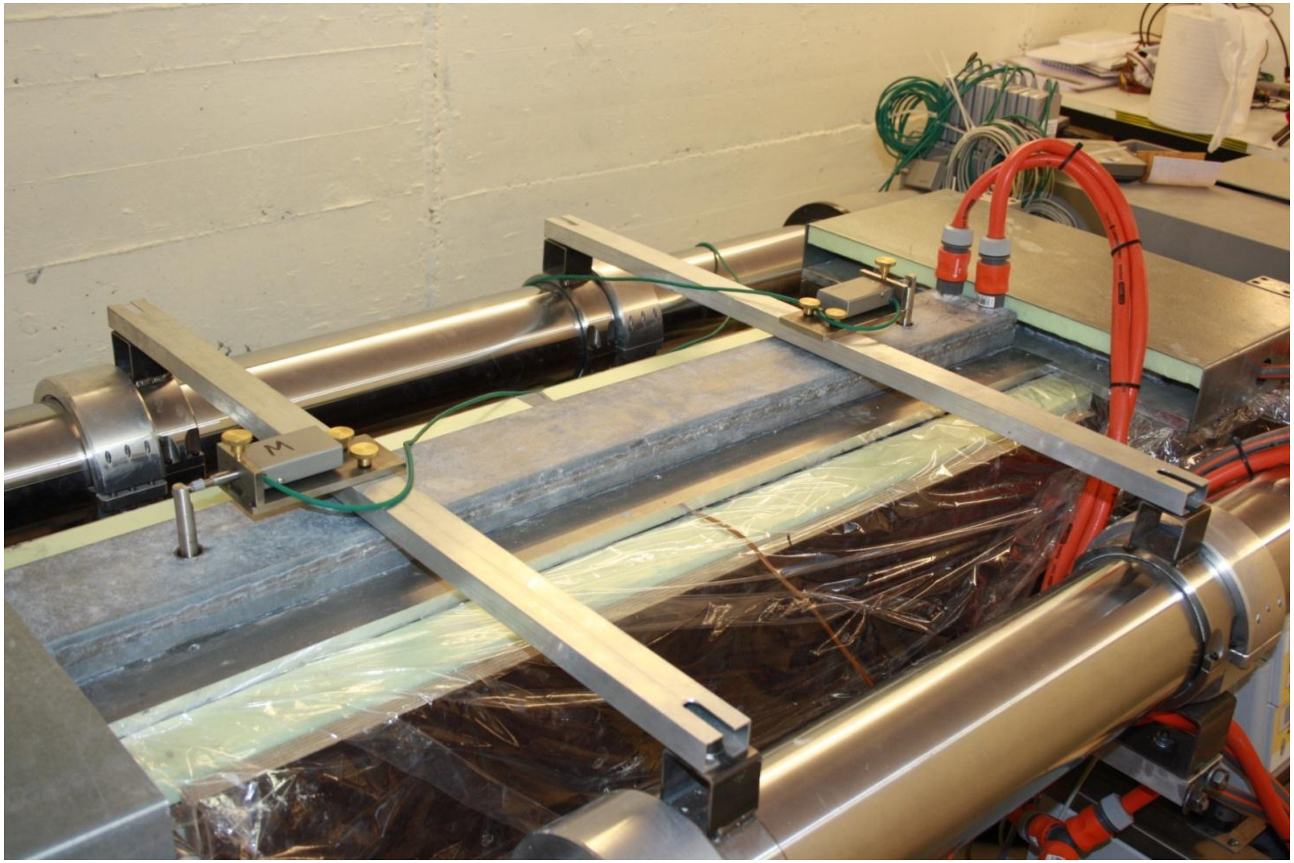

Free and restrained shrinkage, stress development with TSTM

TSTM (Temperature Stress Testing Machine)

- Traction / compression
- Sealed / unsealed conditions
- Force / displacement control
- Various temperature
- Multiple stress levels

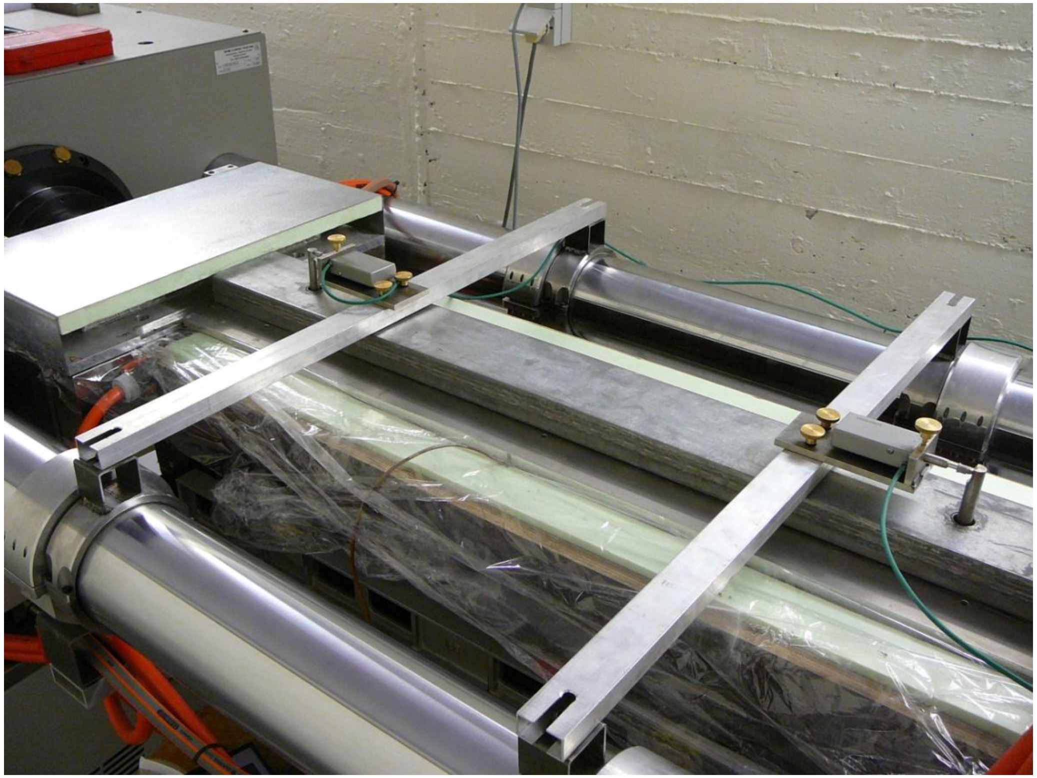

Free and restrained shrinkage, stress development with TSTM

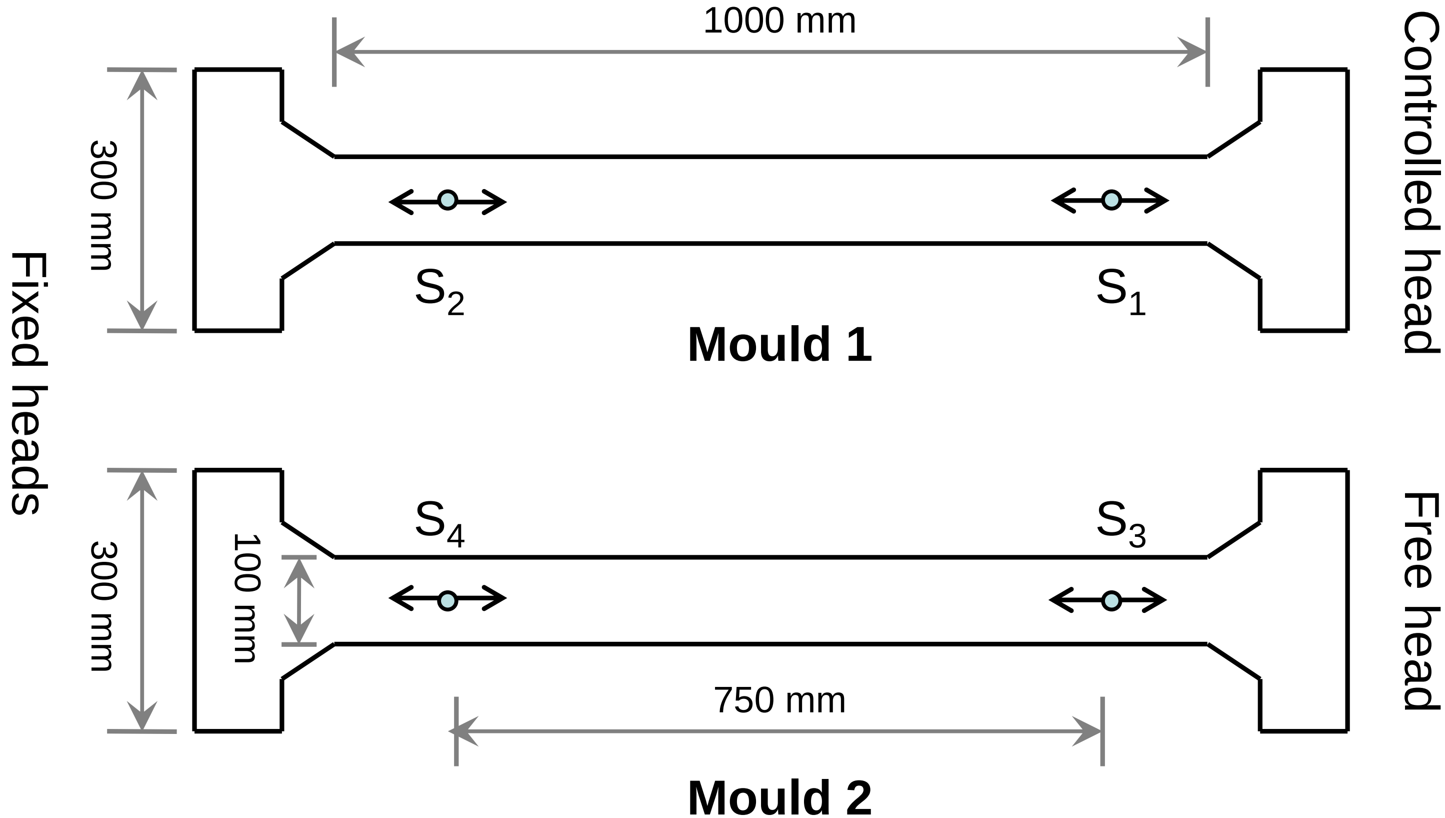

$$\varepsilon_1 = (S_1 + S_2) \times \frac{1000}{750}$$

$$\varepsilon_2 = (S_3 + S_4) \times \frac{1000}{750}$$

Restrained shrinkage, stress development with TSTM

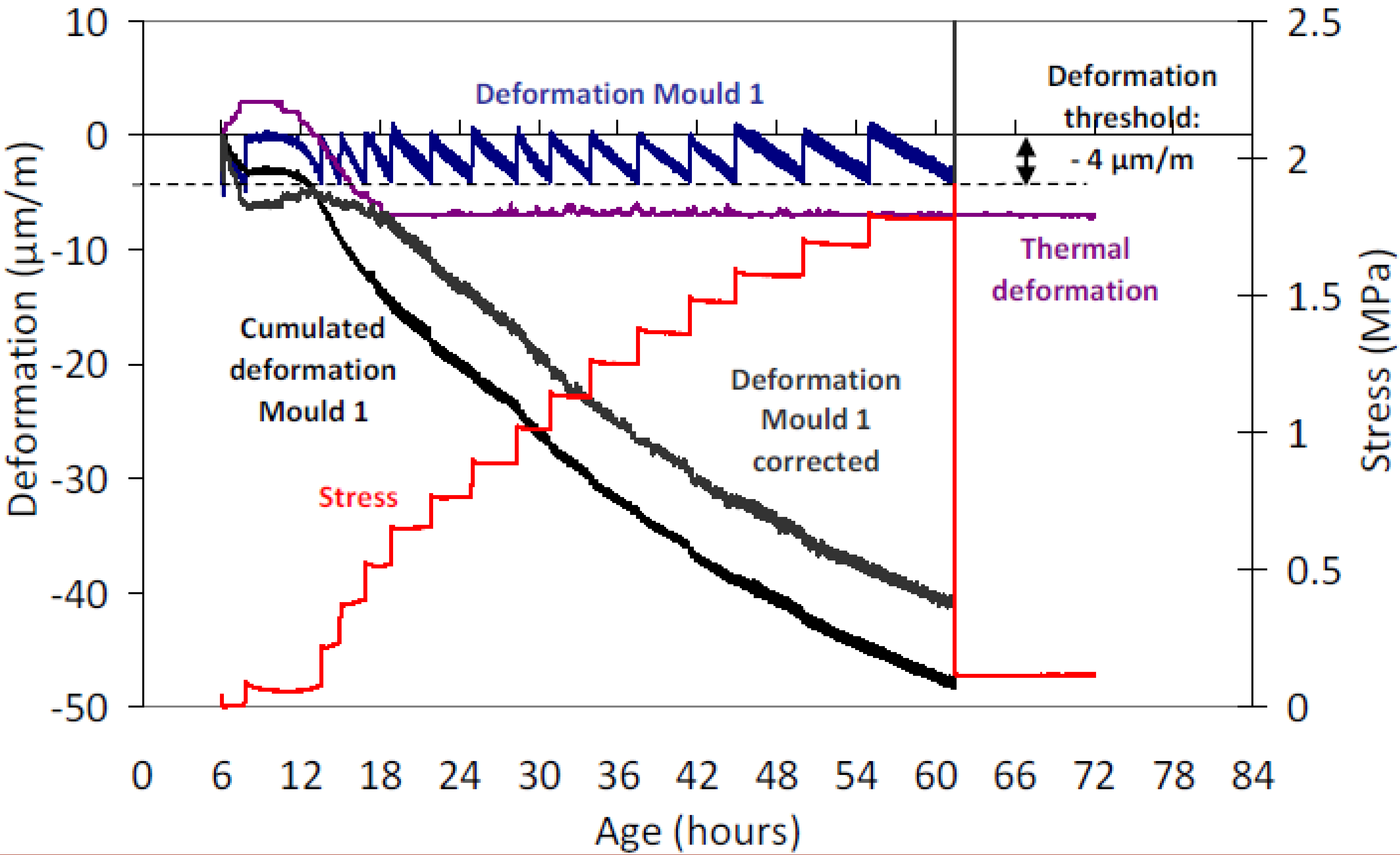

Free shrinkage with TSTM

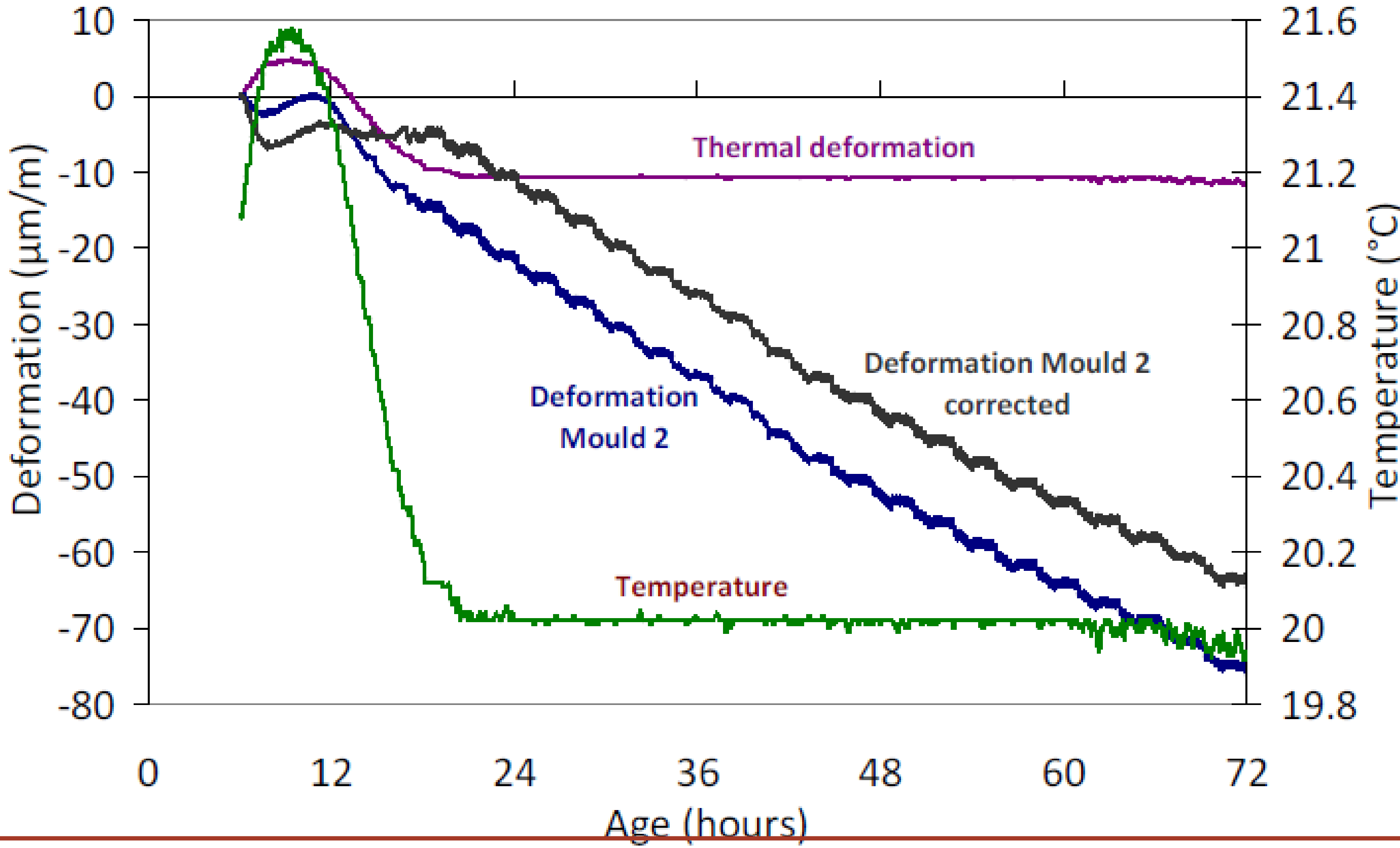

Restrained shrinkage, stress development with TSTM

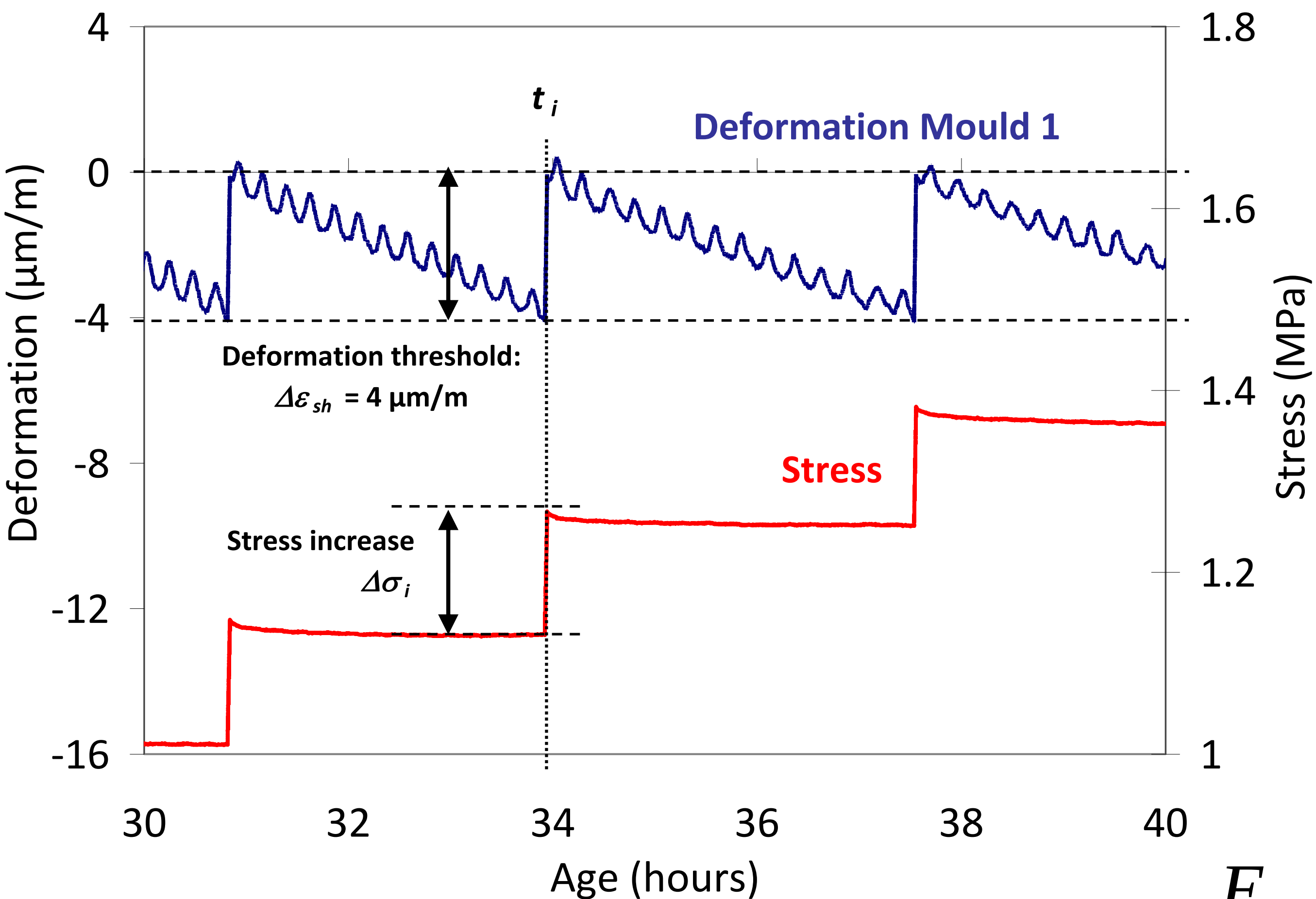

$$E_{TSTM}(t_i) = \frac{\Delta\sigma_i}{\Delta\varepsilon_{sh}}$$

Free and restrained shrinkage, stress development with TSTM

$$\varepsilon_1 = \varepsilon_{el} + \varepsilon_{cr} + \varepsilon_{th} + \varepsilon_{sh}$$

Measured by mold 1 of TSTM
(restraint deformations)

$$\varepsilon_2 = \varepsilon_{th} + \varepsilon_{sh}$$

Measured by mold 2 of TSTM
(free deformations)

$$\varepsilon_1 - \varepsilon_2 = \varepsilon_{el} + \varepsilon_{cr}$$

By knowing the elastic part, creep deformations can be obtained by the difference between deformations measured with the two molds of TSTM

Results and analysis

No clear correlation between autogenous shrinkage and capillary depression

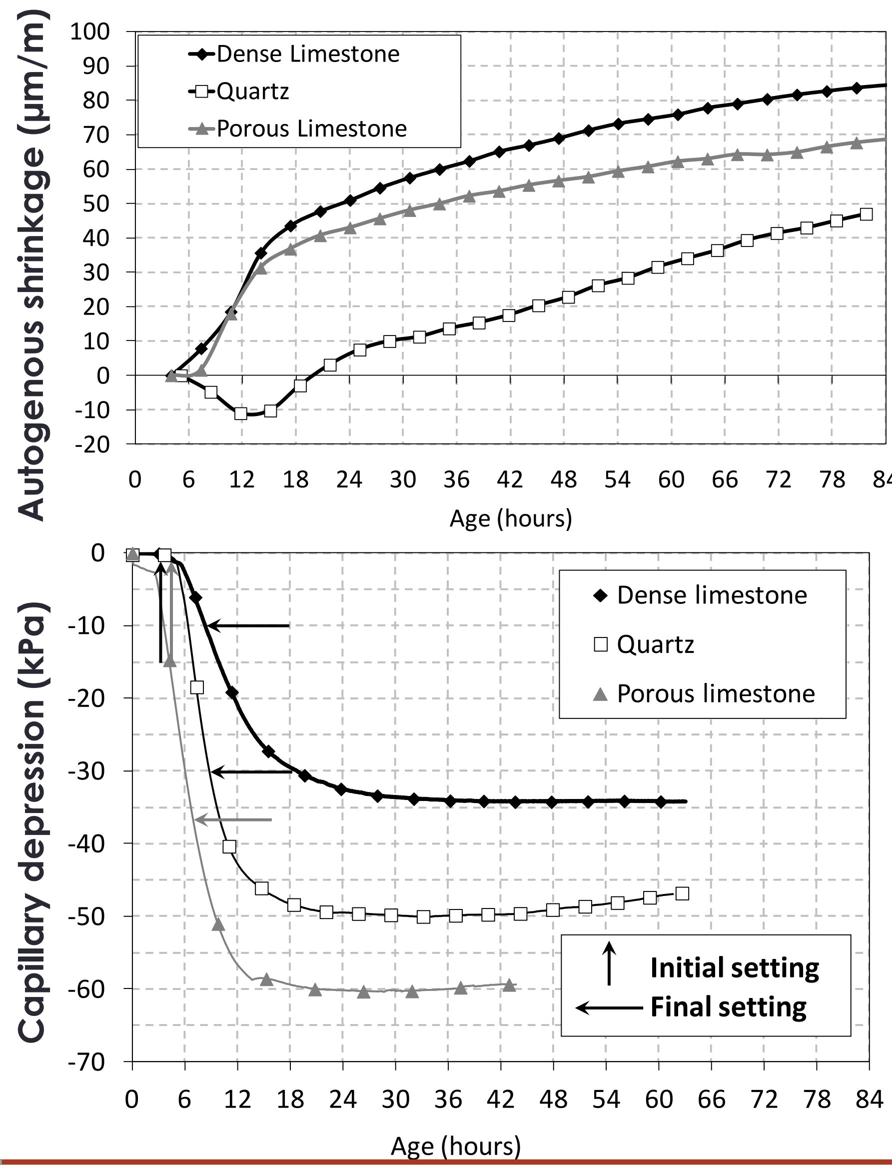

Results and analysis

CTE of quartz gravels is equaled to about twice the CTE of dense and porous limestone gravels

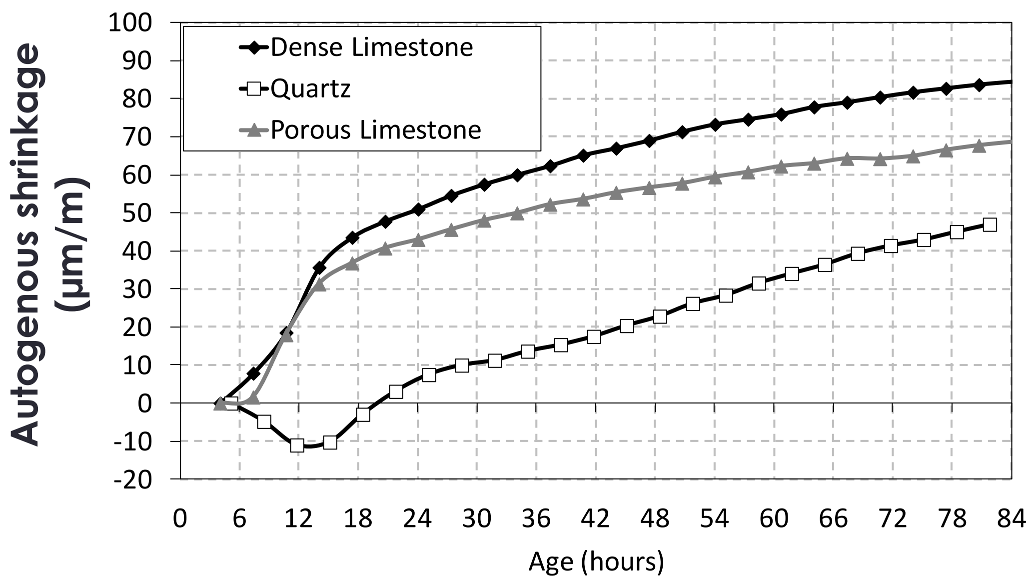

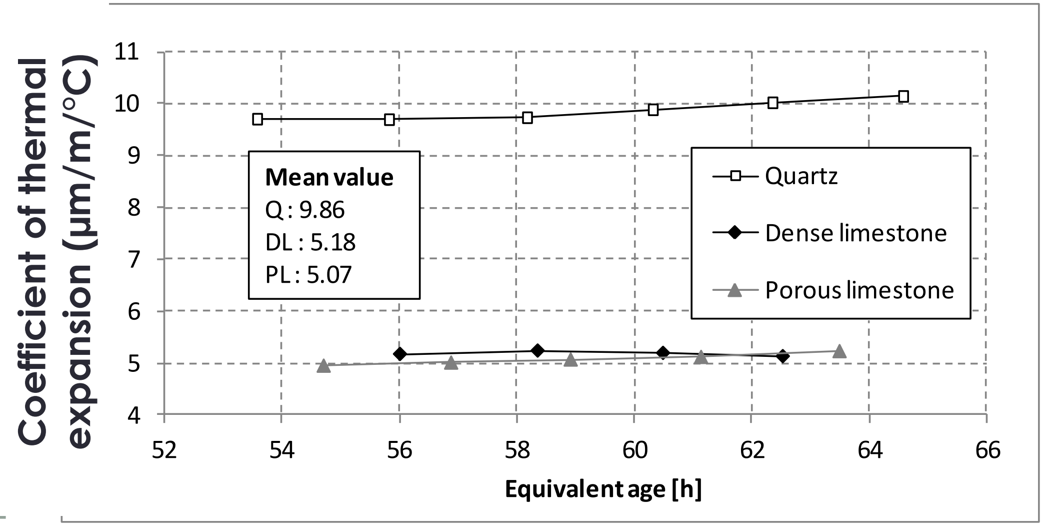

Evolution of dynamic modulus by ultrasound monitoring

Rapid increase of Edyn from 2 to 12-18 hours

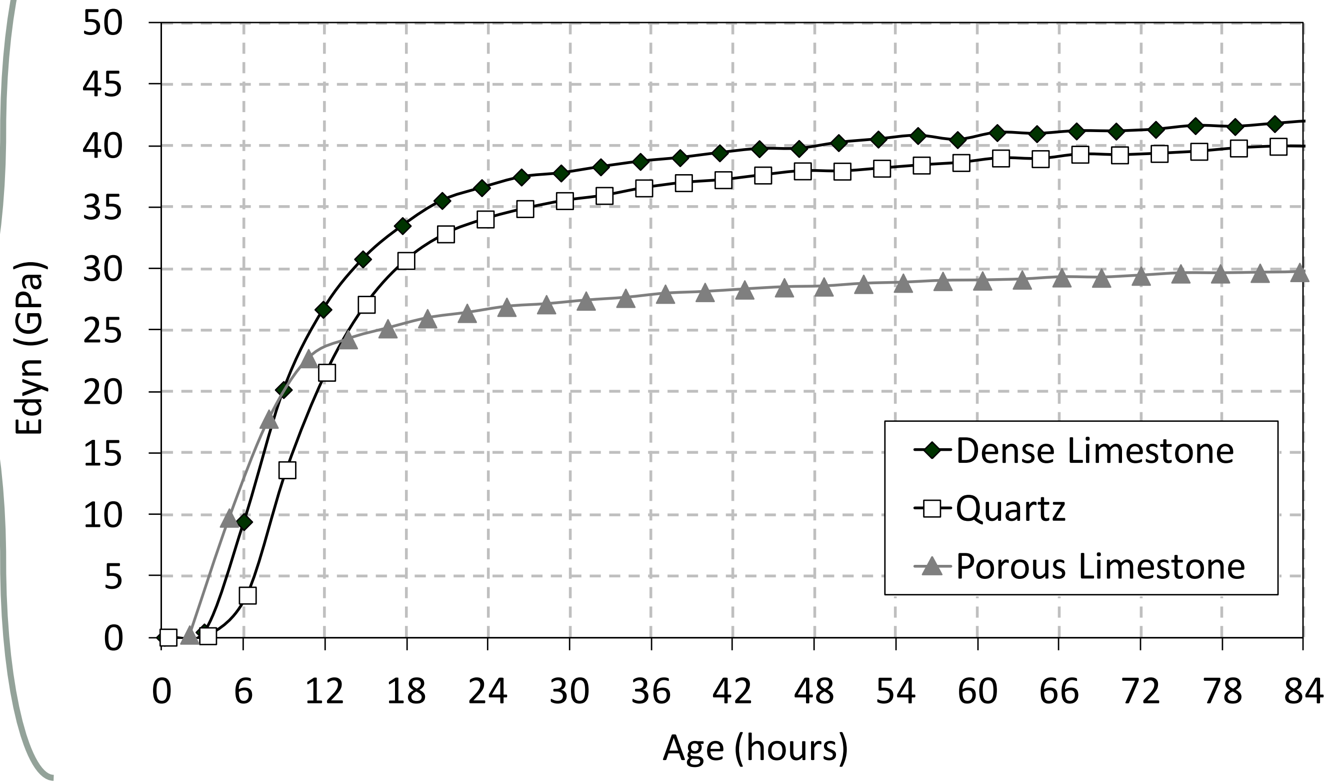

Influence of type of aggregates on cracking due to AUTOGENOUS shrinkage

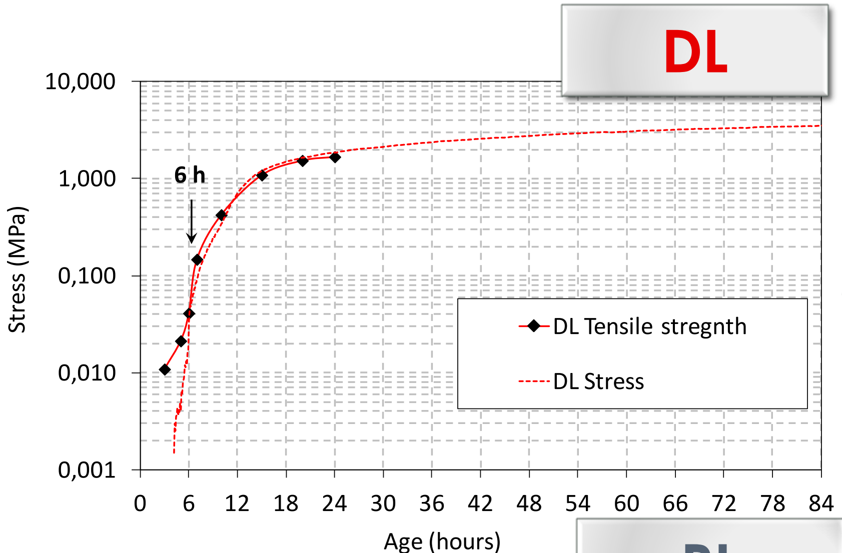

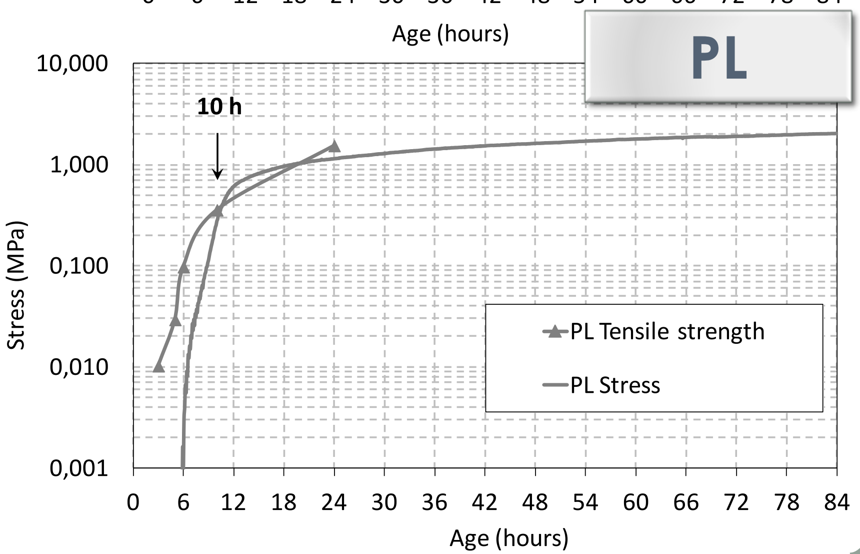

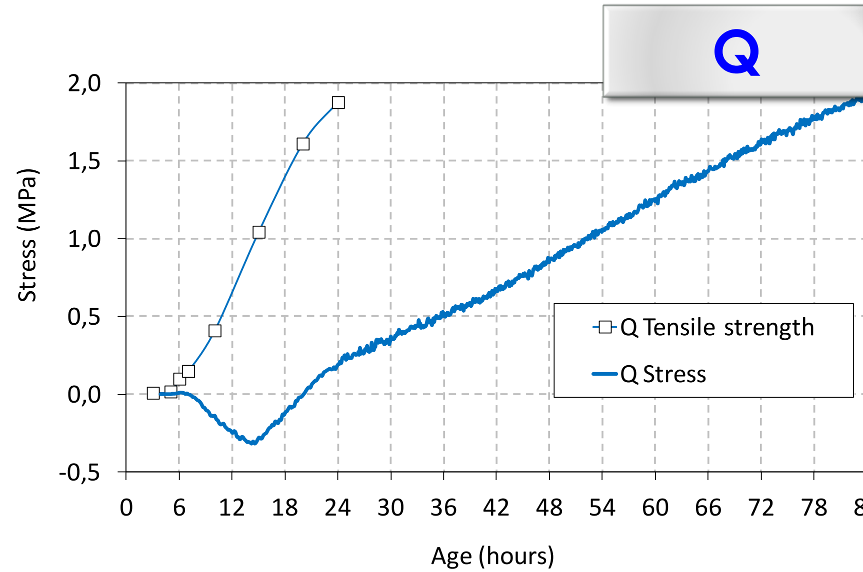

Critical period between 6 and 10 hours

Influence of type of aggregates on cracking due to DRYING shrinkage

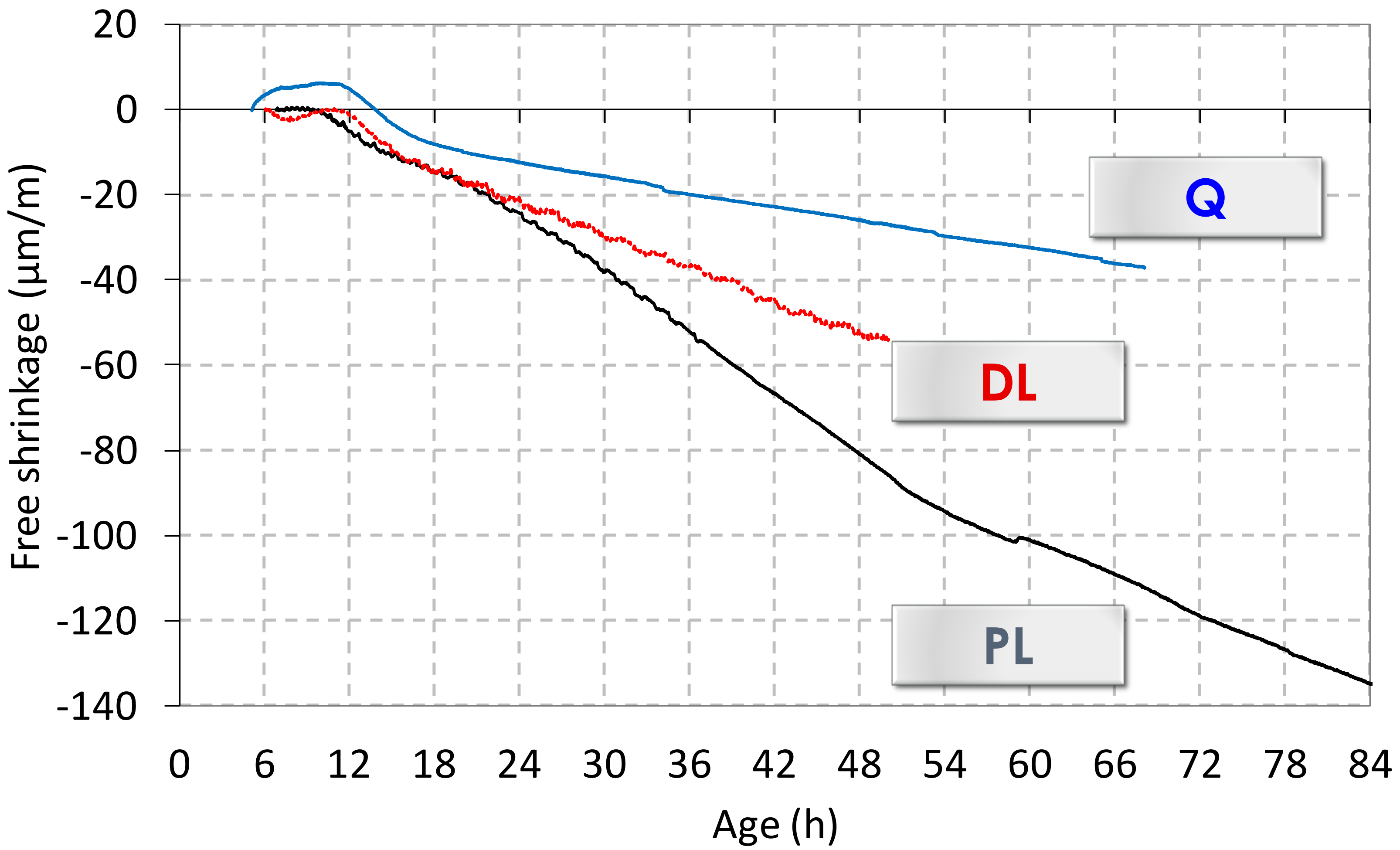

Influence of type of aggregates on cracking due to DRYING shrinkage

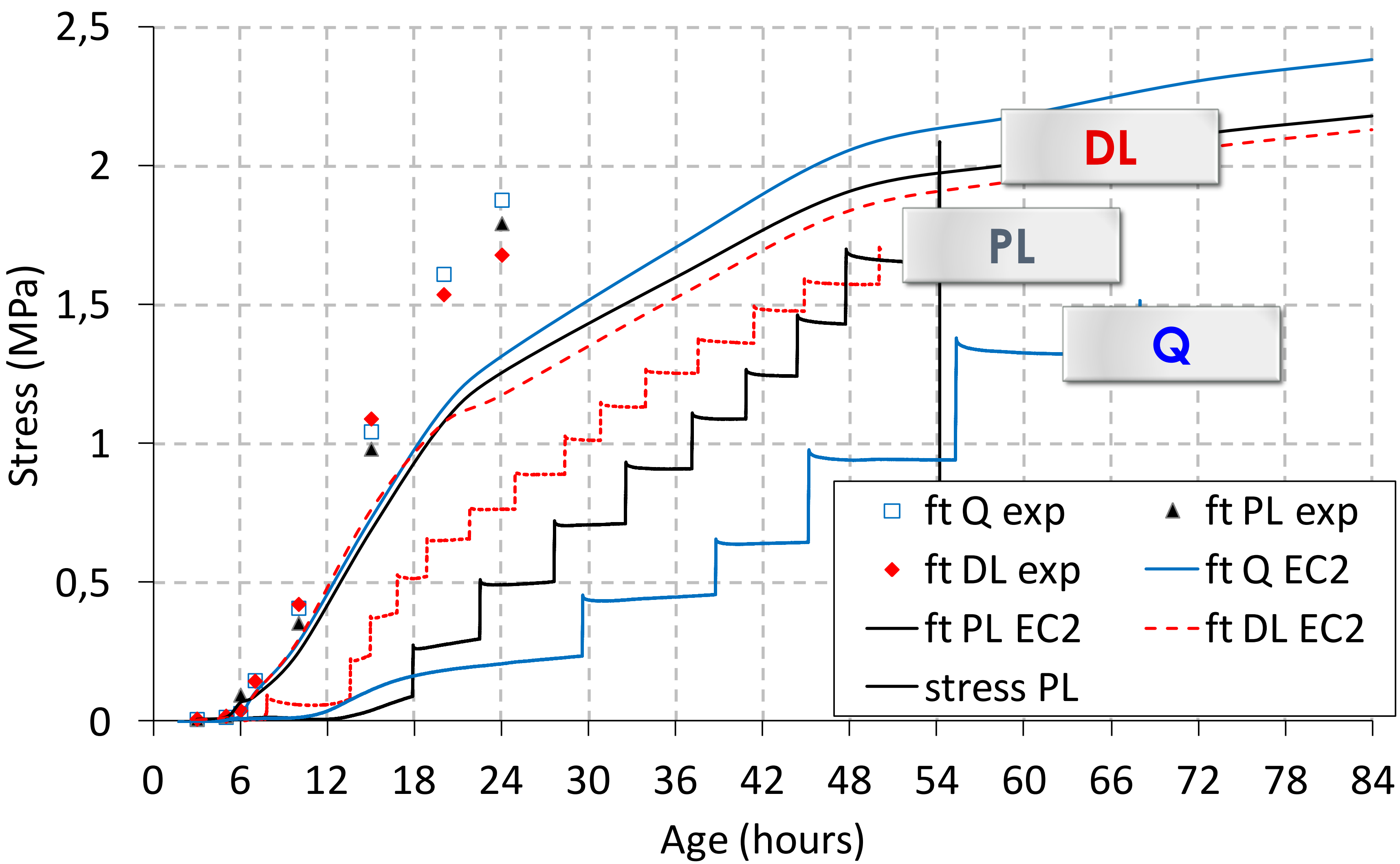

Influence of type of aggregates on cracking due to DRYING shrinkage

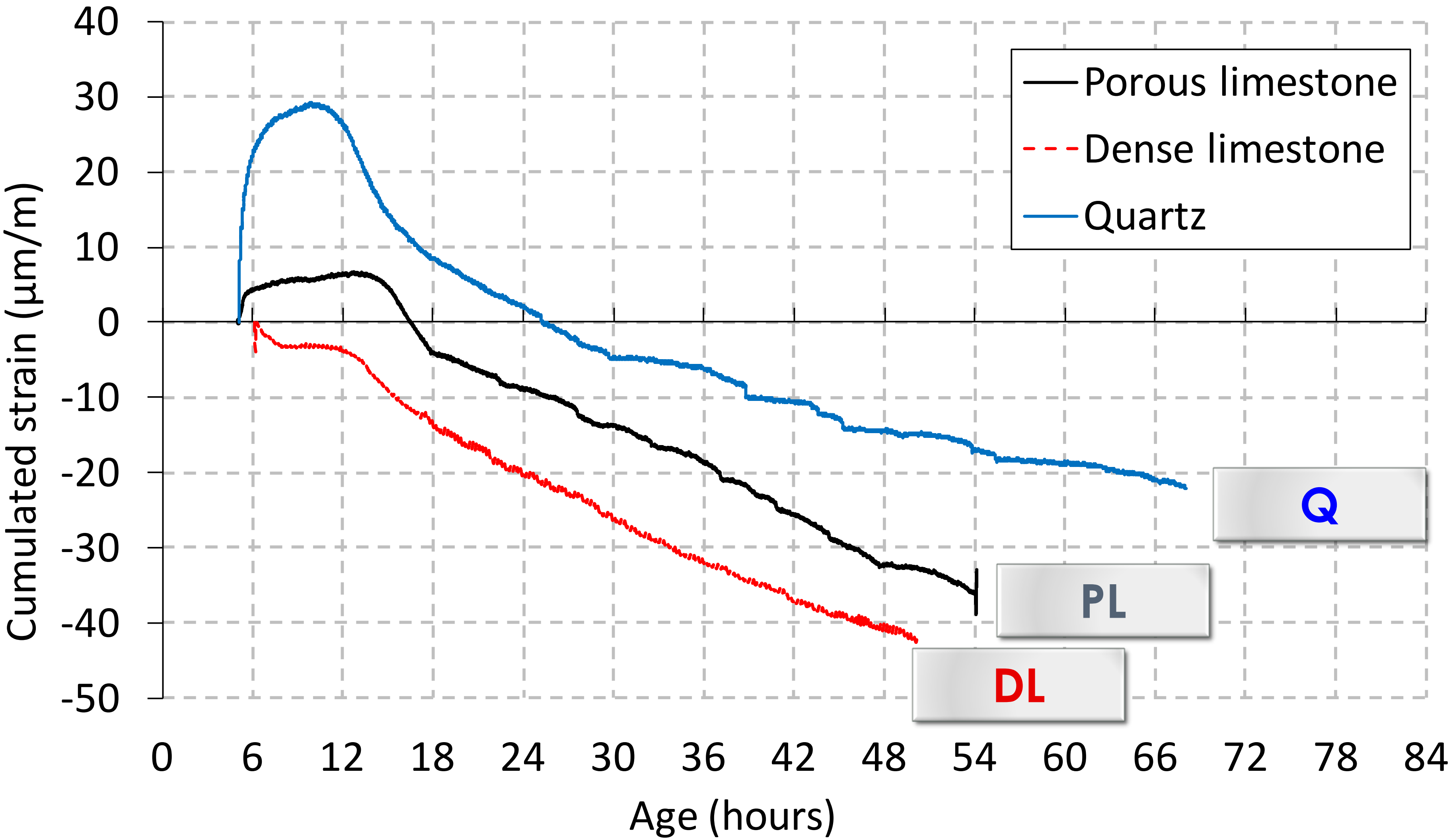

Influence of type of aggregates on cracking due to DRYING shrinkage

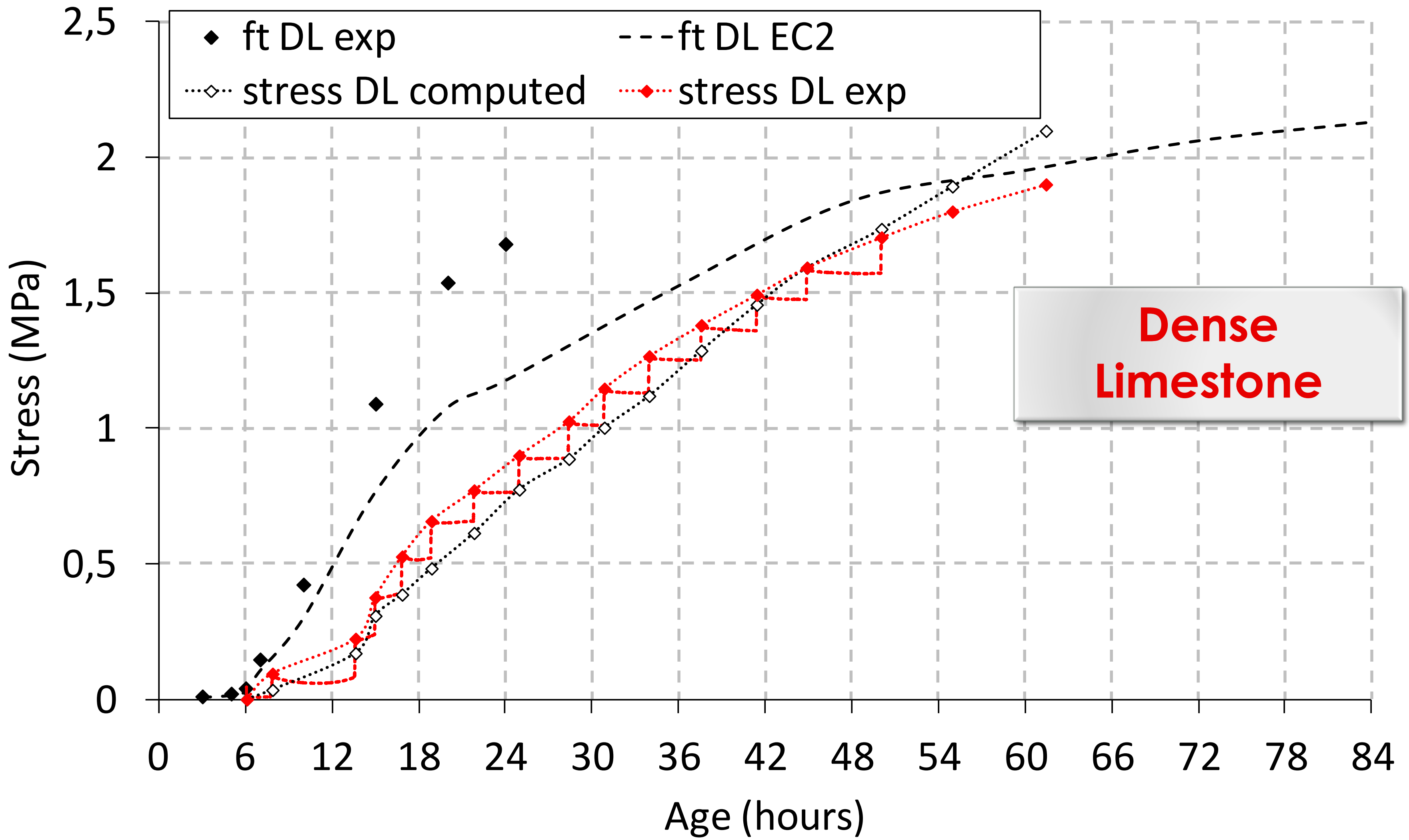

Influence of type of aggregates on cracking due to DRYING shrinkage

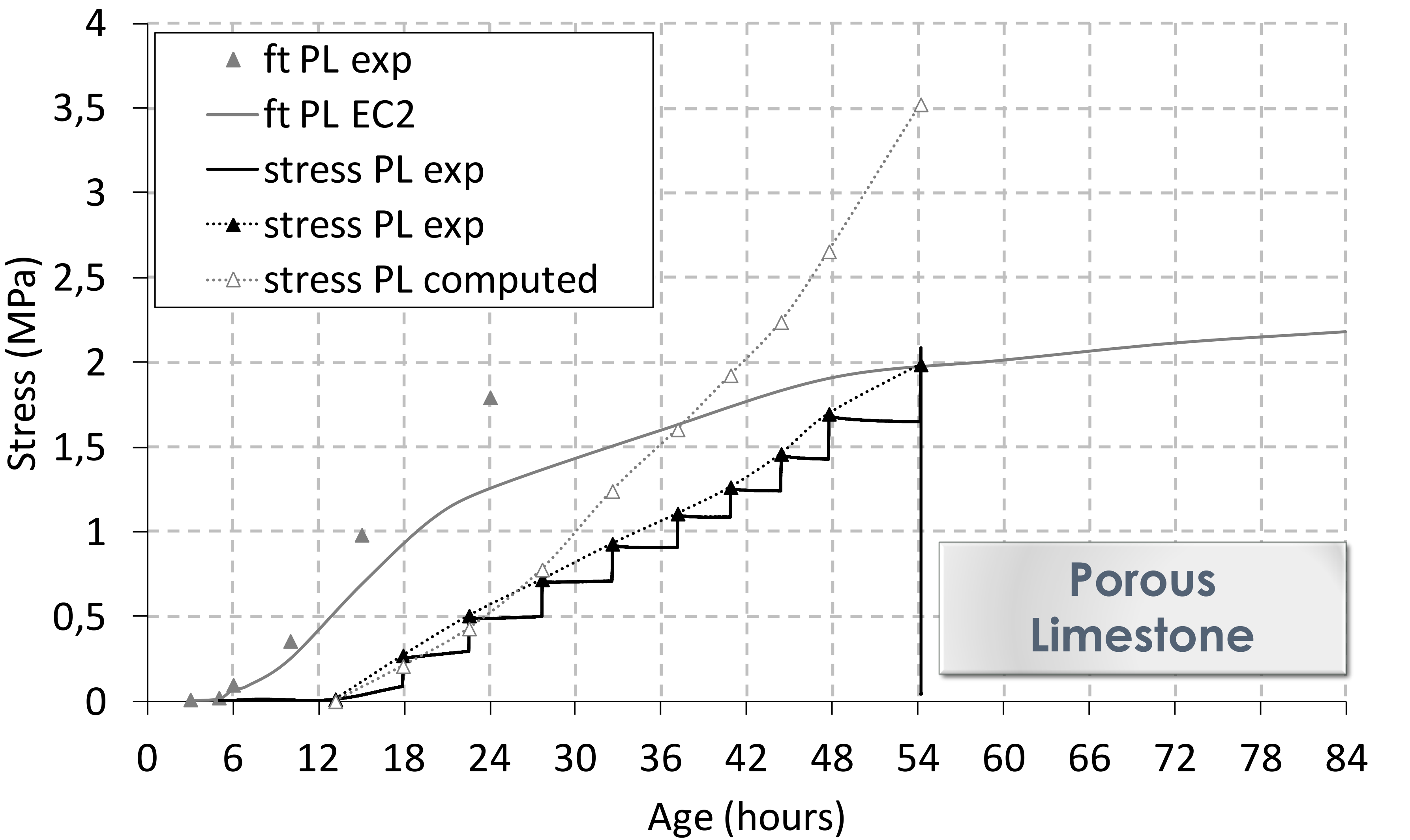

Influence of type of aggregates on cracking due to **DRYING** shrinkage

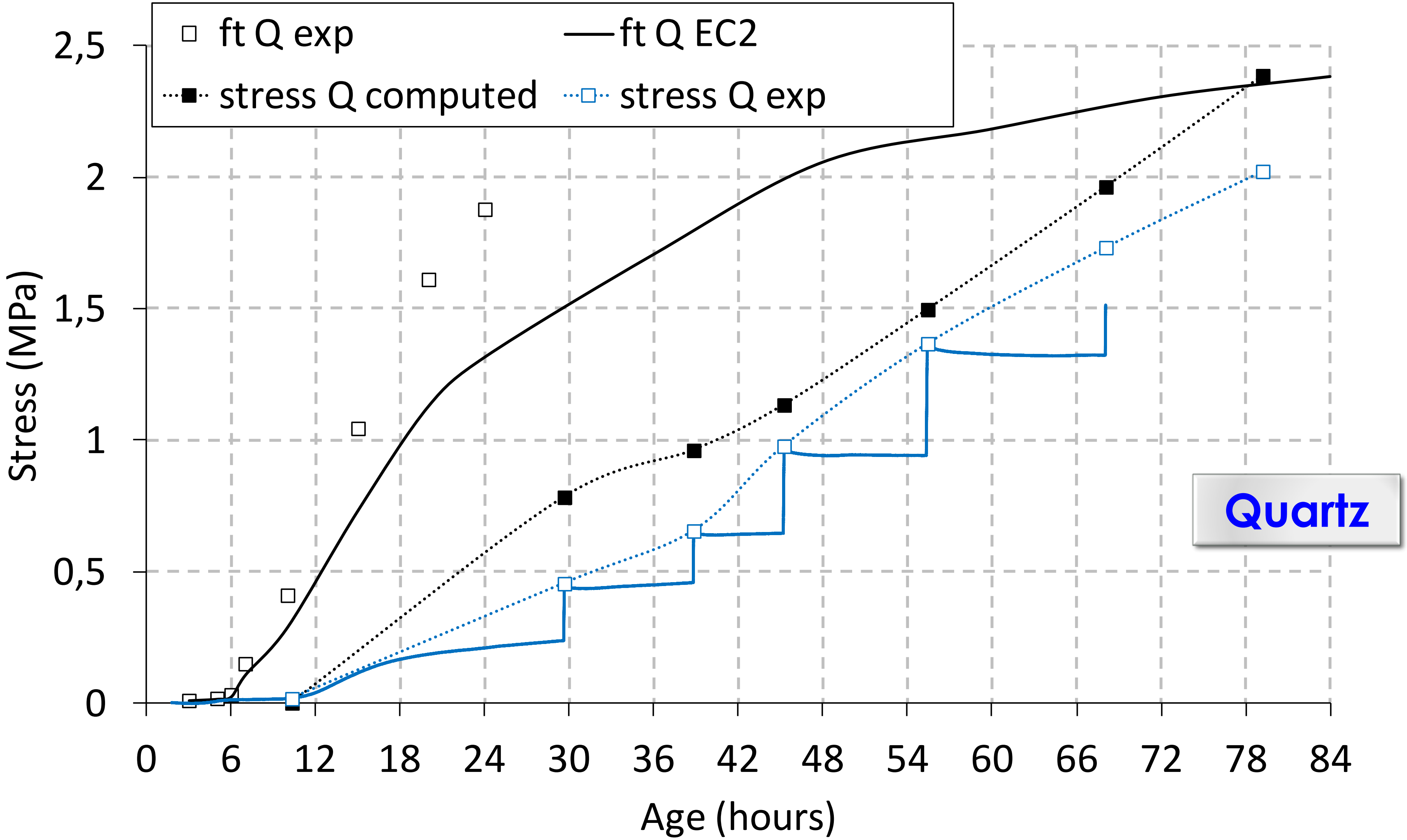

Type of aggregates

Conclusions

- **A comprehensive monitoring** of the main properties of early age concrete was designed with the Temperature Stress Testing Machine to investigate the effect of **dense limestone**, **porous limestone** and **quartzite gravel** on the shrinkage induced cracking sensitivity of concrete.
- **No effect of the type of aggregates** was observed on the setting and the early age development of tensile strength.
- At very early age, until 18 hours, a **very rapid increase** of capillary depression, autogenous deformations, and elastic modulus was observed.
- The results showed that the **risk of cracking was relatively high for dense limestone concrete and porous limestone concrete**, from the ages of 6 and 10 hours respectively.

Type of aggregates

Conclusions

- **TSTM** tests were carried out in **drying conditions**. The three concretes cracked after 54 to 79 hours at similar stress levels. Under restrained conditions, moderate drying shrinkage can result in cracking of normal-strength concrete in isothermal conditions.

- Concrete made with **quartzite gravel** showed delayed risk of cracking thanks to initial expansion, and lower shrinkage magnitude. The **expansion** occurring simultaneously with initial temperature peak was attributed to **thermal deformation**. Quartzite aggregates actually show **higher coefficient of thermal expansion** than limestone aggregates.

CMS Workshop “Cracking of massive concrete structures”
March 17, 2015, ENS-Cachan
Cachan, Île-de-France, FRANCE

Ring test for early cracking sensitivity of FRC: application on tunnel lining

M. Briffaut[1], F. Benboudjema[2] , L. D’Aloia[3]
[1]Laboratoire 3SR (Grenoble)
[2]LMT (Cachan)
[3] CETU(Lyon)

CONTEXT

- Extension Paris subway line No.4
  - Final tunnel lining : 10m formwork (thickness ~50cm)
  - Shotcrete support
- Objectives of the study
  - study the impact of different fibers on the "susceptibility" to cracking at early age (can fiber replace anti cracking girds)
  - Comparison of different types of fiber
    - Polypropylene micro-fiber (PMiF)
    - Polypropylene macro-fiber (PMaF)
    - Metallic fiber (MF)
- Methodology
  - Laboratory test
  - Tunnel lining simulation

Tunnel lining formwork

Cutting machine (support)

CONTEXT

Cracking mechanism: self-restrained shrinkage

- ✓ Gradient of temperature strain and drying shrinkage between the skin and the core of the element

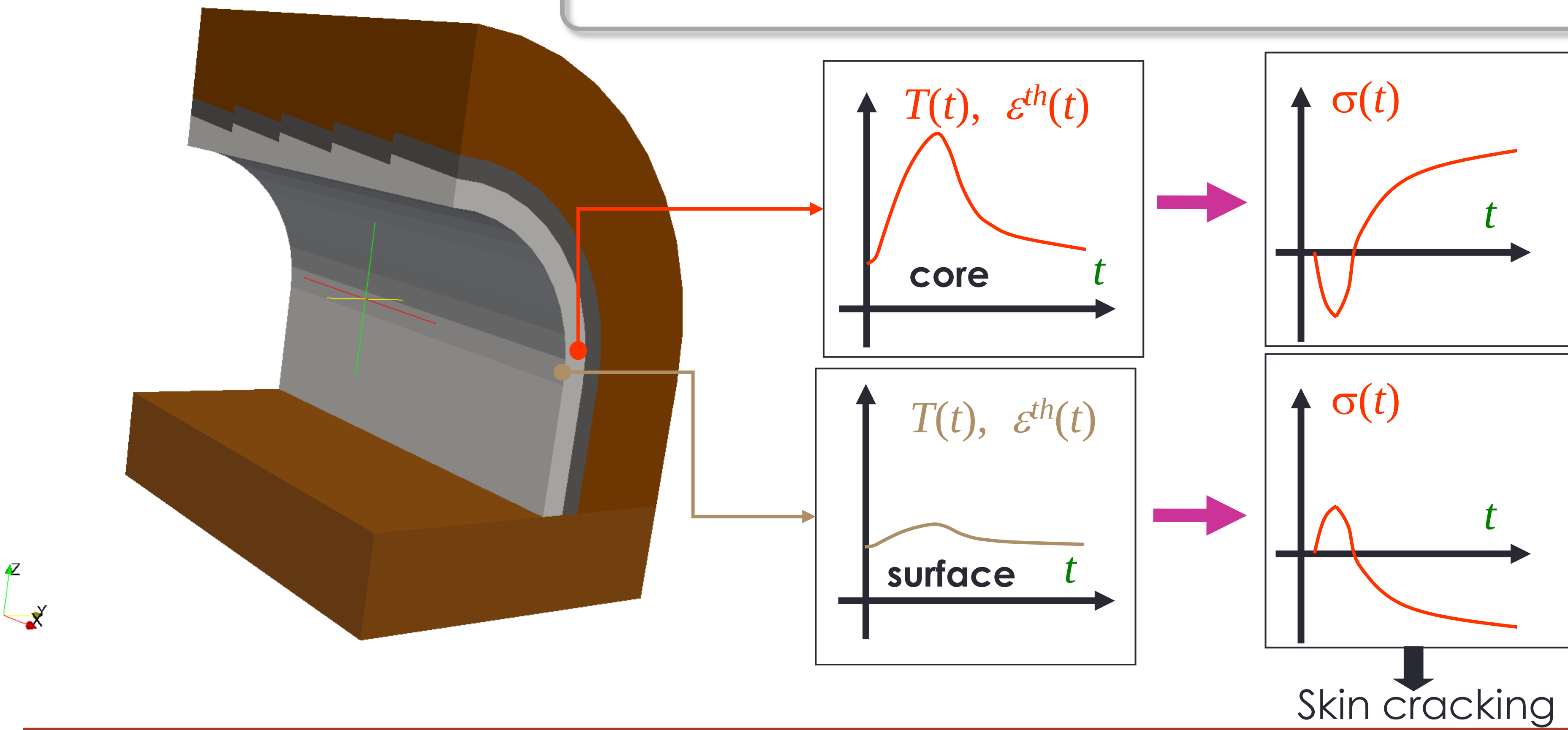

CONTEXT

Cracking mechanism: restrained shrinkage

- ✓ Thermal and autogenous restrained shrinkage

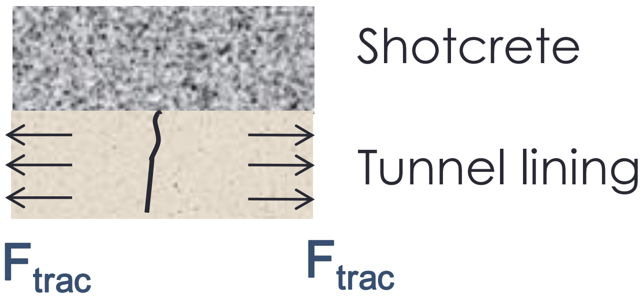

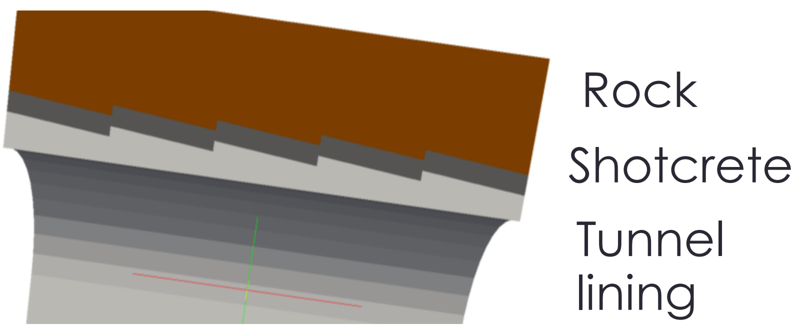

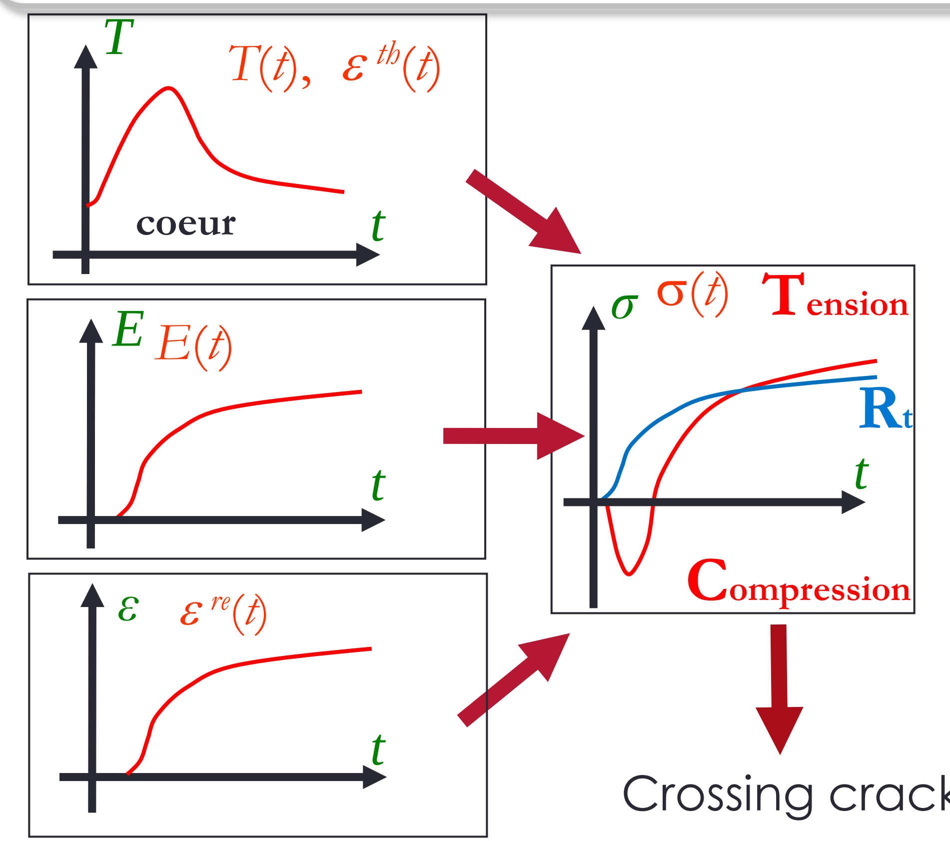

OUTLINE

- Experimental part : Cracking sensivity
  - Presentation of ring tests
  - Classical ring test : drying and autongeneous shrinkage
  - Thermal active ring test : thermal shrinkage
- Simulation of thermal active ring test
  - Brief model presentation
  - Thermal active ring test
- Tunnel lining cracking simulation
  - Influence of each phenomena
  - Influence of reinforcement by fibers

Experimental part: cracking sensivity

Presentation of ring tests

Classical ring test: drying and autongeneous shrinkage

Thermal active ring test: thermal shrinkage

Classical ring test

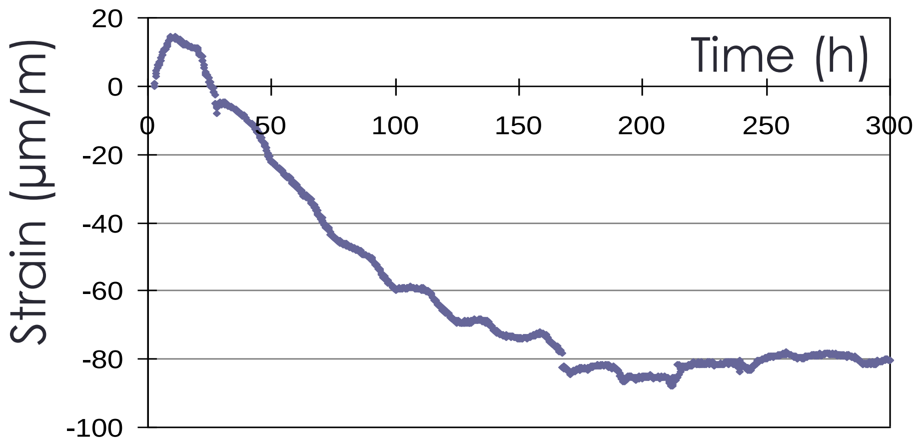

Controlled environment (temp, RH)

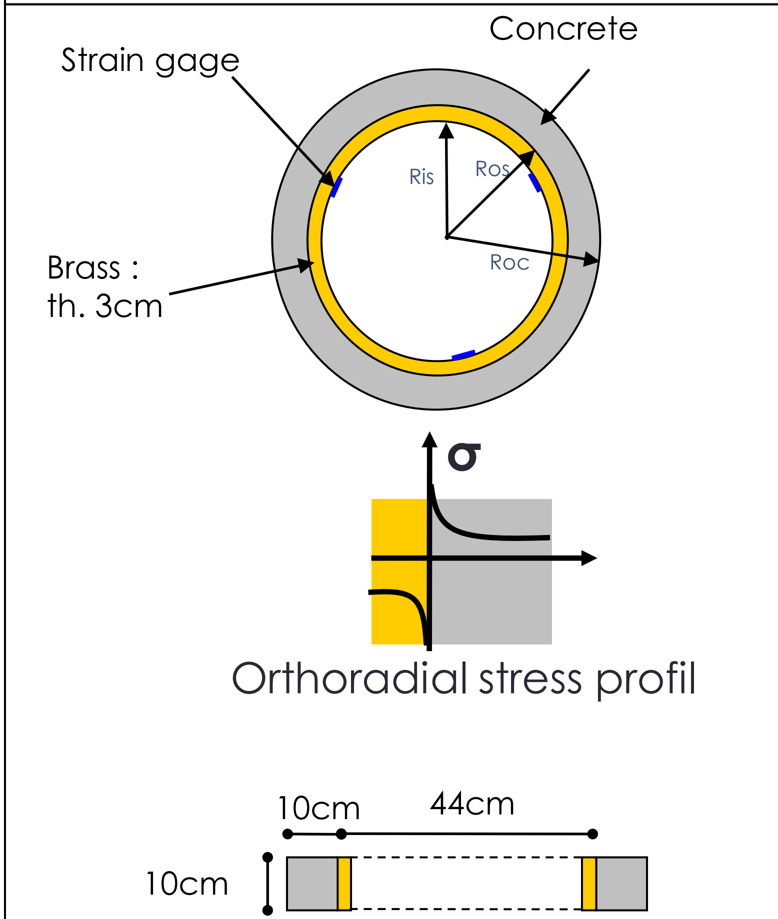

Classical ring test : Passif

- ✓ Thermal shrinkage not taken into account
- ✓ No cracks for concrete with high W/C

Thermal ring test

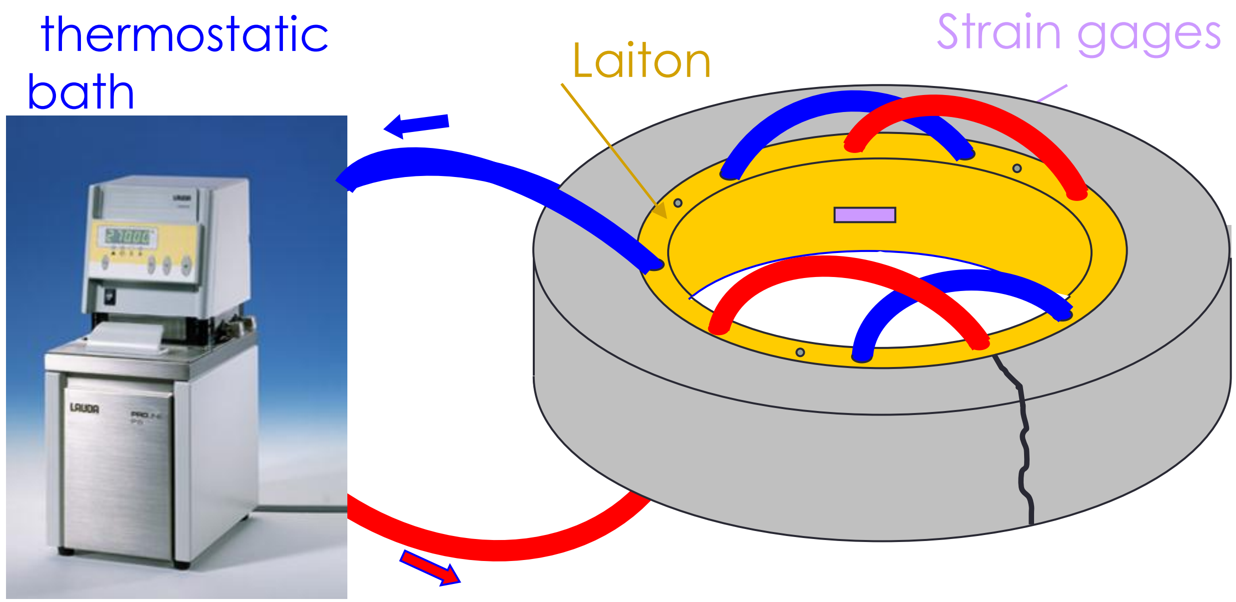

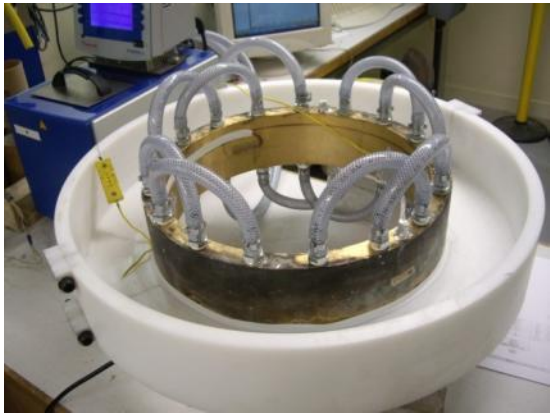

Ring test before casting

Ring test after casting

Thermal ring test : actif

- **Principe:** thermal expansion of metallic ring
- **Advantages:**
  - Axisymmetric geometry
  - Temperature, creep, rupture,…
- **Complex test -> Model benchmarking?**

Thermal ring test : results

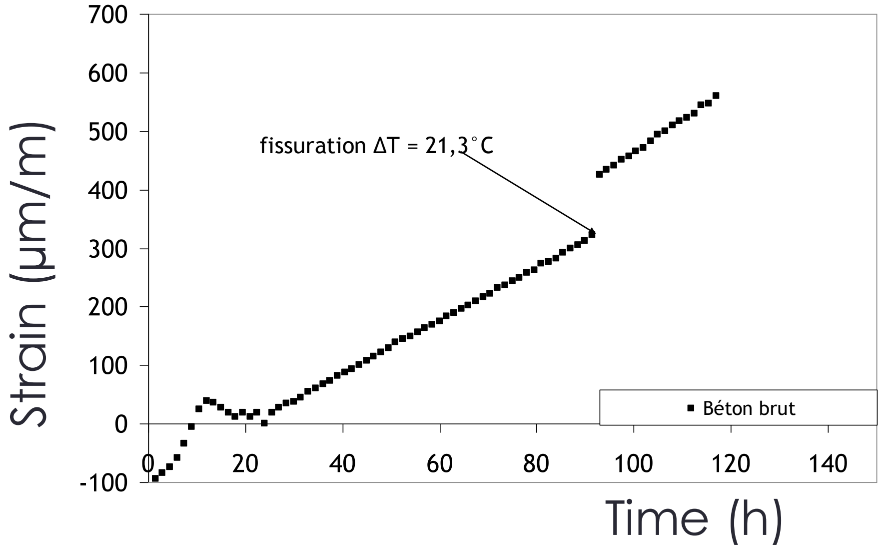

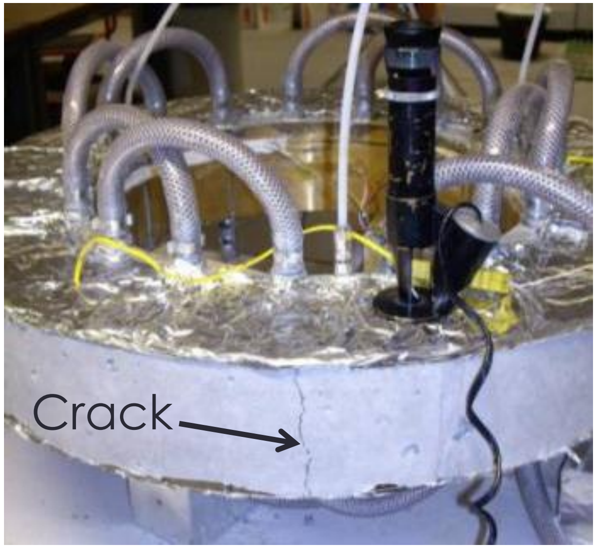

Cracked concrete ring

Experimental results

- ✓ Temperature brass and concrete
- ✓ Deformations measured on the inside radius of brass (low dispersion)
- ✓ **Strain gap: cracking of the concrete ring**
- ✓ Study of rebars, construction joints [Briffaut et al. 11]

FRC : concretes mix

(kg/m^3)	REF (Reference Mix)	FRC-PMiF-0.9 ($0.9\ kg/m^3$)	FRC-PMiF-1.8 ($1.8\ kg/m^3$)	FRC-PMaF	FRC-MF
Sand (0/4)	905	905	905	905	905
Coarse aggregates (4/20)	905	905	905	905	905
Cement	385	385	385	385	385
Total water	170	170	170	170	170
Superplasticizer	4.62	4.62	4.62	5.12	4.62
Fibres (PMiF, PMaF or MF)	0	0.9	1.8	7	43
Slump (mm)	230	225	220	210	218
Entrained air (%)	1.3	2.4	4.4	NM*	NM*

PMaF stands for "polypropylene macrofibres", PMiF for "polypropylene microfibres" and MF for "metal fibres".
**: Not measured.*

Designation	Density	Type	Length (mm)	Tensile strength (MPa)	Young's modulus (GPa)	Fibre content (kg/m^3)
PMaF	0.92	Polypropylene	50	600	5.0	7.0
PMiF	0.91	Polypropylene	12	577	4.2	0.9/1.8
MF	7.85	Steel	50	1,050	210.0	43.0

Classical ring test results

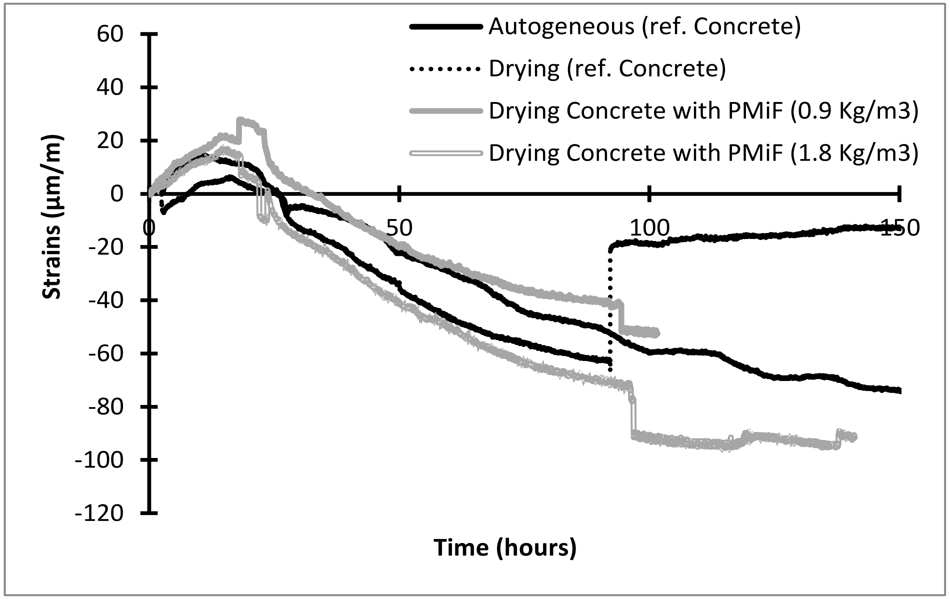

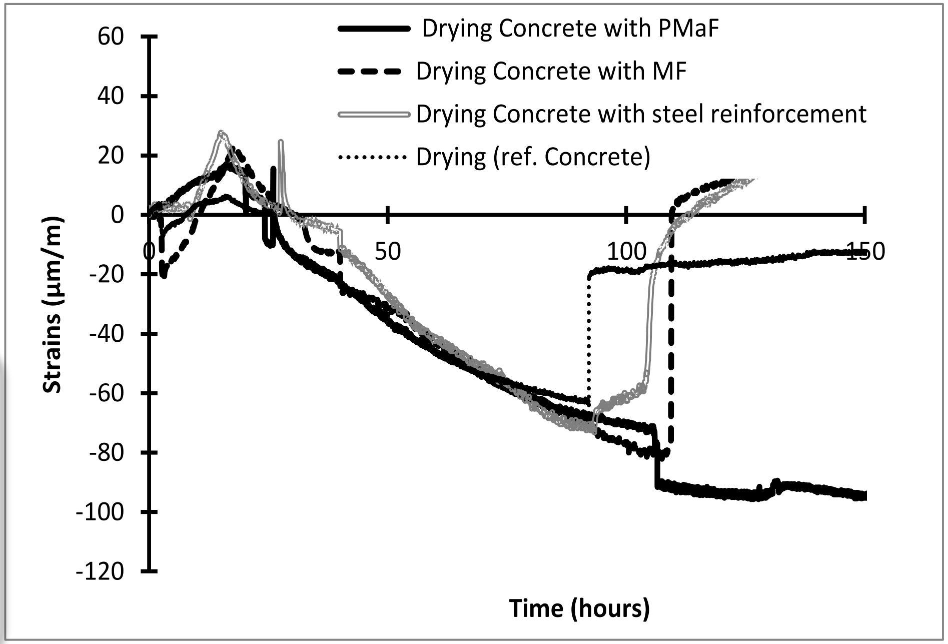

- ✓ No cracks under autogeneous shrinkage
- ✓ Under drying shrinkage :
  - ✓ Micro fiber : slight delay of the crack
  - ✓ Macro fiber and reinforcement : real delay of the crack

Active ring test results

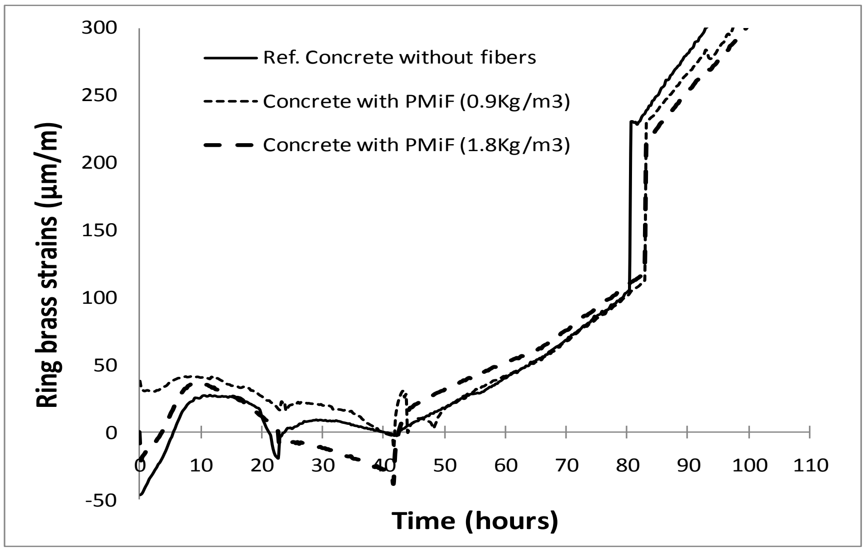

- ✓ Under thermal expansion of the ring:
  - ✓ Micro fiber : slight delay of the crack
  - ✓ Macro fiber and reinforcement : real delay of the crack

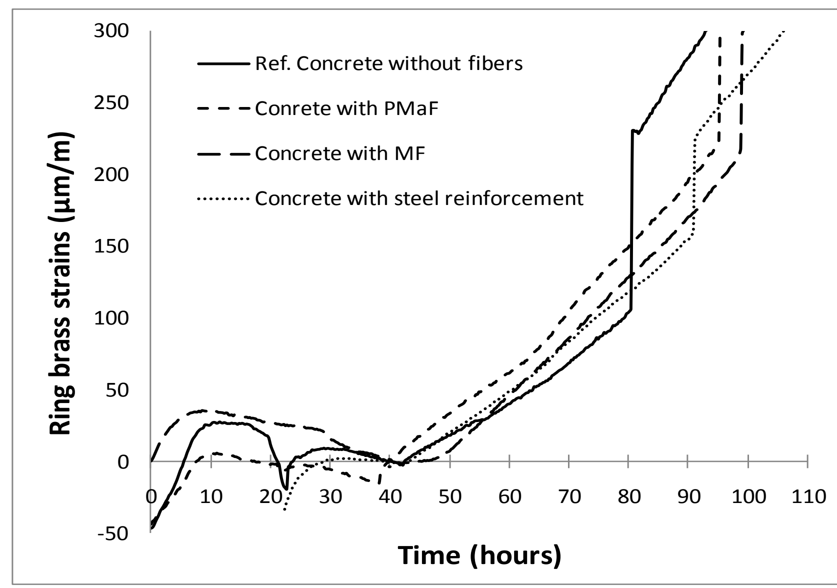

Quantitative ring tests results

Drying shrinkage

	Age of cracking (h)	Fibre content (kg/m^3)	Mean crack opening (µm)
REF	92	0	140
FC-PMiF-0.9	95	0.9	130
FC-PMiF-1.8	96	1.8	130
FC-PMaF	104	7	120
RC-MF	109	43	100
Steel reinforcement (1 rebar ϕ8)	98	0	90

Thermal expansion

	Age of cracking (h)	Fibre content (kg/m^3)	Number of cracks	Crack opening (µm) measured at 50°C
REF	80	0	1	700
FRC-PMiF-0.9	83	0.9	1	550
FRC-PMiF-1.8	83	1.8	1	450
FRC-PMaF	94	7	2	400 and 250
FRC-MF	97	43	2	225 and 150
Steel reinforcement (1 rebar ϕ8)	91	0	2	200 and 150

Simulation of thermal active ring test

Brief model presentation

Thermal active ring test

Focus on coupling between creep and damage

Global strategy

« Standardized » test

Active ring test

Hydration

Creep

Shrinkage

Chemo-thermo-mechanical model

Thermal strains

Mechanical prop. Evol.

Coupling + Representatives boundaries conditions +effect of fibers

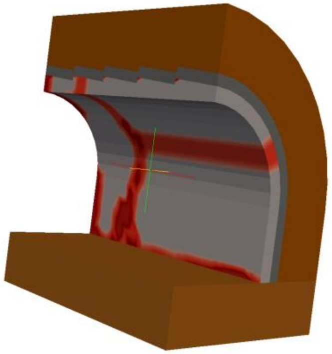

Structures modelling

Example of standardized test

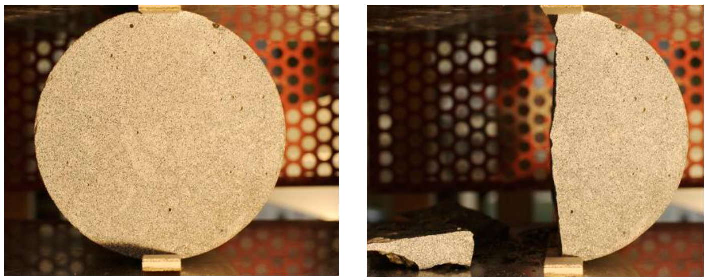

Tensile strength by indirect test

	Tensile strength (MPa)
Without fiber	**3,60**
PMiF [0,9 Kg/M^3]	**3,8**
PMiF [1,8 Kg/M^3]	**3,82**
PMaF [7 Kg/M^3]	**4,07**
Steel [43 Kg/M^3]	**4,78**

Polypro Micro fibers

Polypro Macro fibers

Metallic fibers

Without fibers

Chemo-thermal model

Heat equation with source

$$C\dot{T} = \nabla(k\nabla T) + L\dot{\xi}$$

C = C (ξ, T, concrete mix) = Volumetric thermal capacity
k = k (ξ, T, concrete mix) = Thermal conductivity
L = L (concrete mix) =Total heat release

Hydration degree evolution

[Regourd et al., 80] [Lackner et al., 04] [Ulm et al., 98]

$$\dot{\xi} = \tilde{A}(\xi)\exp\left(-\frac{E_a}{RT}\right)$$

Mechanical parameters evolution[De Schutter et Taerwe, 96]

$$X(\xi) = X_\infty \left(\frac{\xi(t) - \xi_0}{\xi_\infty - \xi_0}\right)^{a_X} \qquad pour\ \xi > \xi_0$$

Autogeneous and thermal strains

[Laplante, 93][Mounanga et al., 06][Ulm et al. 98]

$$\dot{\varepsilon}_{ij}^{au} = \kappa\dot{\xi}\delta_{ij} \quad pour\ \xi > \xi_0 \qquad \dot{\varepsilon}_{ij}^{th} = \alpha\dot{T}\delta_{ij}$$

Creep model

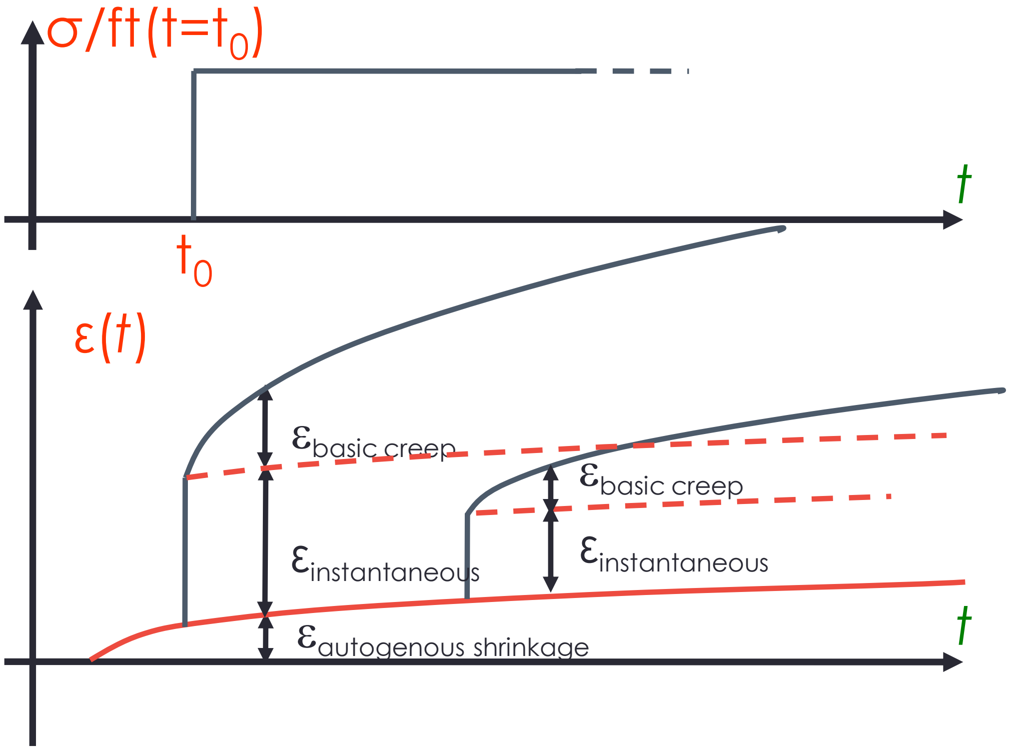

Rheological modelling

- ✓ Kelvin-Voigt chains (KV) :

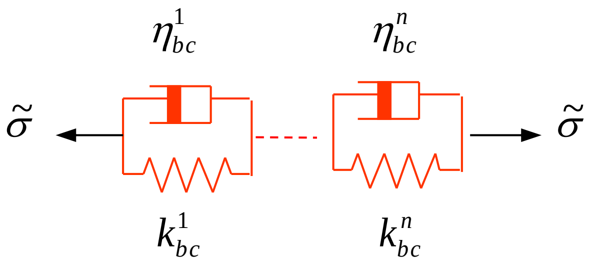

- ✓ Differential equation of one KV:

$$\tau_{bc}^{i}\ddot{\varepsilon}_{bc}^{i}+\left(\tau_{bc}^{i}\frac{\dot{k}_{bc}^{i}(\xi,T)}{k_{bc}^{i}(\xi,T)}+1\right)\dot{\varepsilon}_{bc}^{i}=\frac{\dot{\tilde{\sigma}}}{k_{bc}^{i}(\xi,T)}$$

- ✓ Characteristic time of one KV:

$$\tau_{bc}^{i}=\frac{\eta_{bc}^{i}(\xi)}{k_{bc}^{i}(\xi)}=const$$

Mechanical model

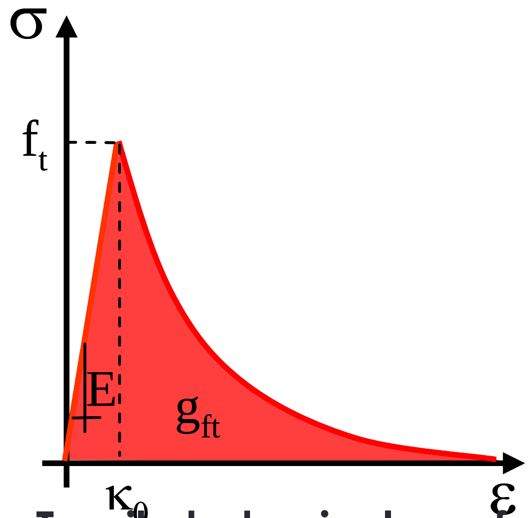

Tensile behavior law of cement paste

Strains decomposition

$$\dot{\tilde{\boldsymbol{\sigma}}} = \mathbf{E}(\xi)\dot{\boldsymbol{\varepsilon}}_{el} = \mathbf{E}(\xi)\left(\dot{\boldsymbol{\varepsilon}}_{tot} - \dot{\boldsymbol{\varepsilon}}_{bc} - \dot{\boldsymbol{\varepsilon}}_{ttc} - \dot{\boldsymbol{\varepsilon}}_{au} - \dot{\boldsymbol{\varepsilon}}_{th}\right)$$

Equivalent strain [Mazars,84] [Mazzoti, 03]

$$\tilde{\varepsilon} = \sqrt{\langle \boldsymbol{\varepsilon}_e \rangle_+ : \langle \boldsymbol{\varepsilon}_e \rangle_+ + \beta \langle \boldsymbol{\varepsilon}_{bc} \rangle_+ : \langle \boldsymbol{\varepsilon}_{bc} \rangle_+}$$

Damage threshold

$$\kappa_0 = \frac{f_{t\infty}}{E_\infty} \cdot \left(\frac{\xi - \xi_0}{\xi_\infty - \xi_0}\right)^{c-a}$$

Damage variable evolution [Nechnech, 00]

$$D_t(\tilde{\varepsilon}) = 1 - \frac{\kappa_0}{\tilde{\varepsilon}}\left[(1 + a_t)\ \exp\left(-b_t\ (\tilde{\varepsilon} - \kappa_0)\right) - a_t\ \exp\left(-2b_t\ (\tilde{\varepsilon} - \kappa_0)\right)\right]$$

Regularization by fracture energy [Hillerborg, 76] [De Schutter, 99]

Fracture energy

- For high fiber content
  - Softening phase -> hardening phase
  - Fracture energy could not be easily determined
- Hypothesis : for low fiber content
  - Concept of fracture energy still relevant

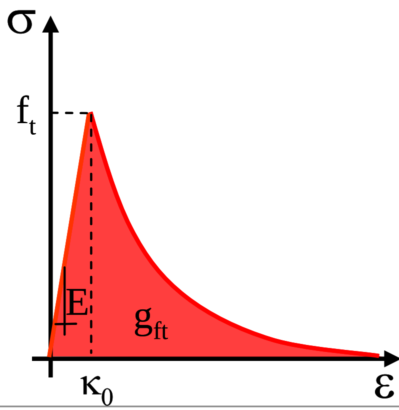

	Fracture energy (J.m⁻²)
REF	100
FRC-PMiF-0.9	230
FRC-PMaF	280
FRC-MF	1,200

Fracture energy values [Bei Xing *et al.*, 04] [Barros and Sena Cruz, 01]

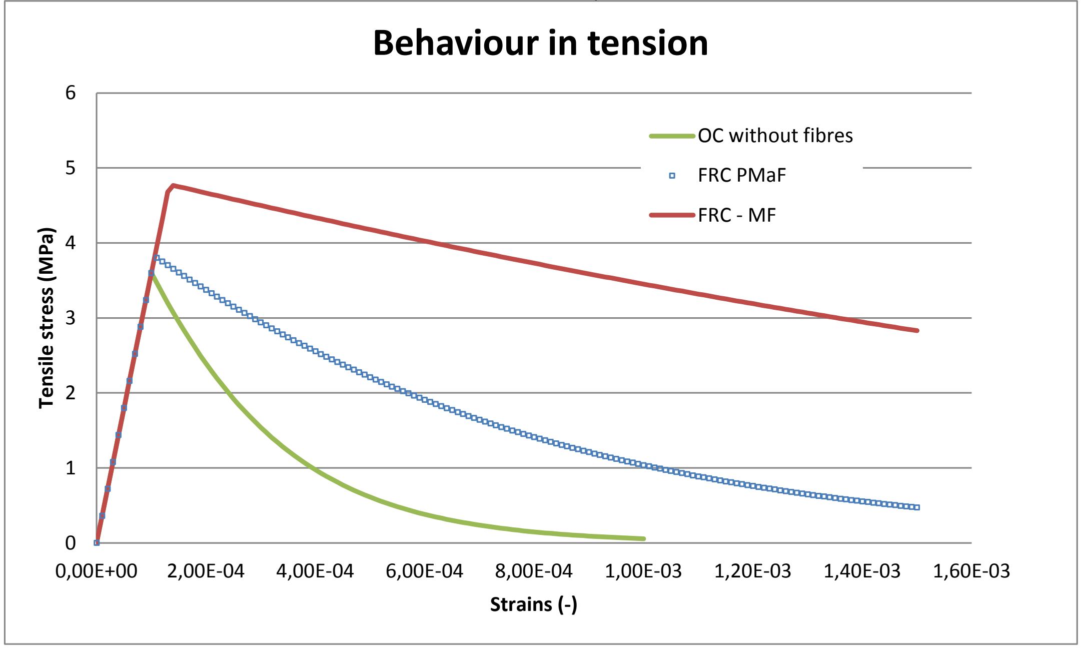

Validation on thermal ring test

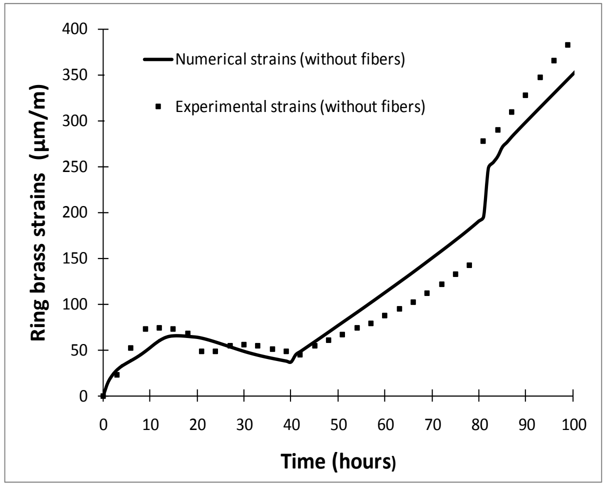

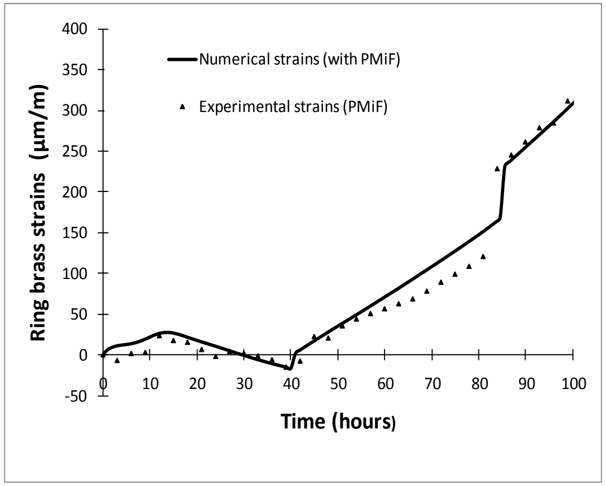

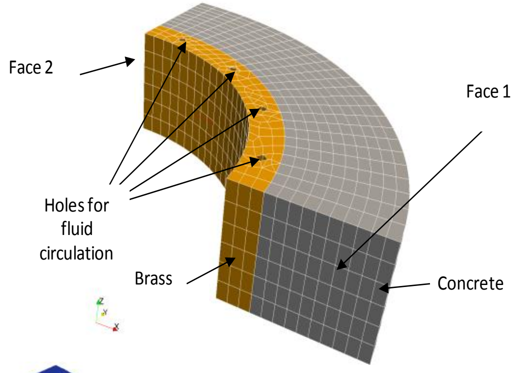

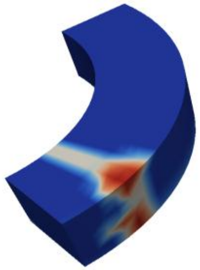

Mesh & Damage pattern

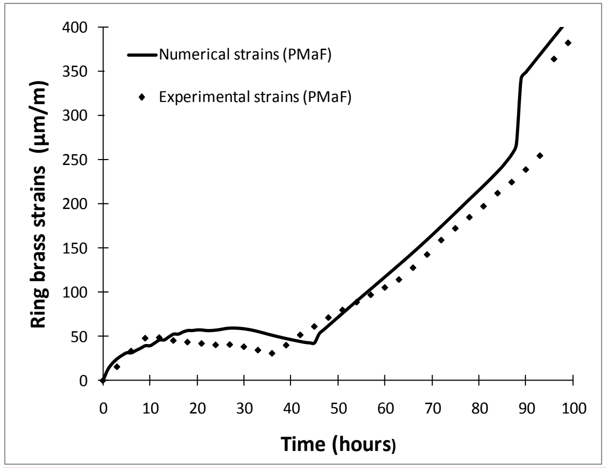

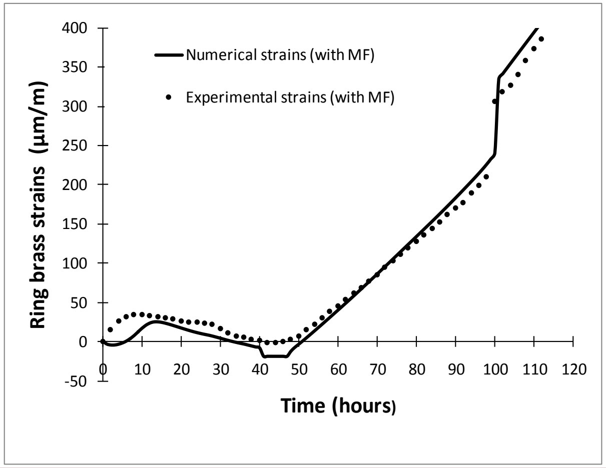

- ✓ Concrete = homogeneous material -> β =0,4
- ✓ Good global agreement between experimental data and simulation
- ✓ No creep increase due to fibers

Tunnel lining cracking simulation

Influence of each phenomena

Influence of reinforcement by fibers

Tunnel lining simulations

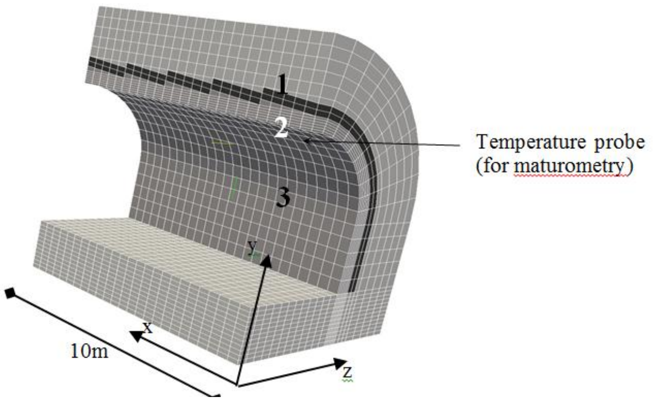

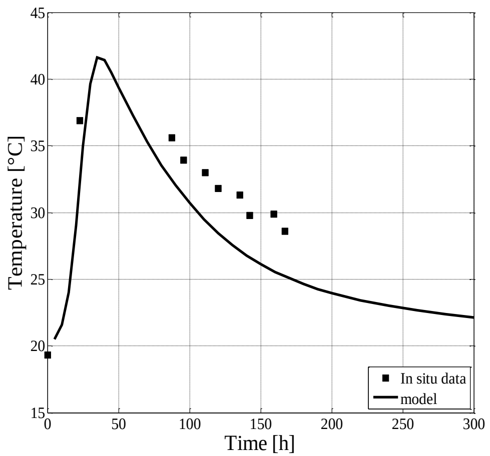

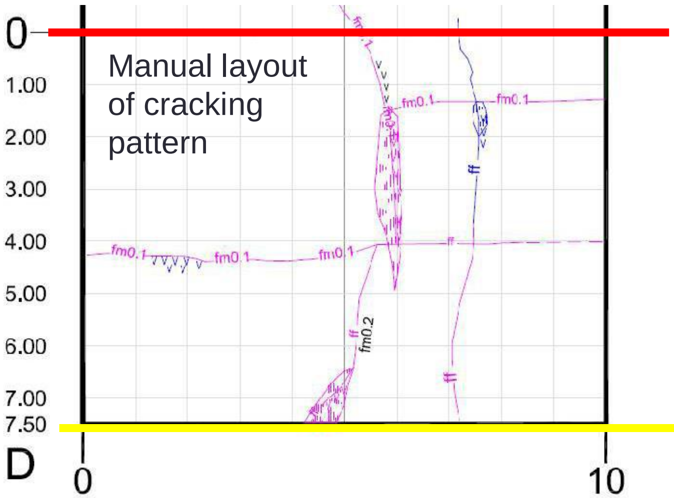

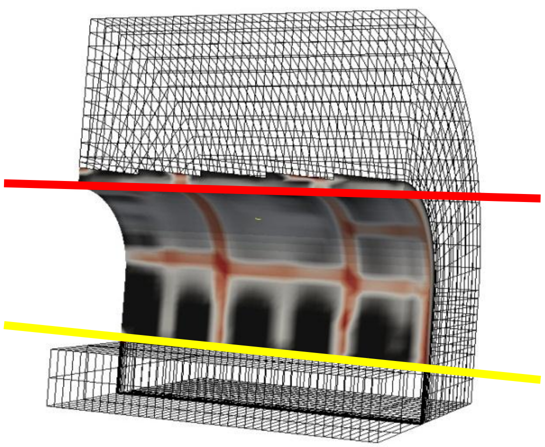

- ✓ Calibration with Temperature in situ
- ✓ **Decrease of tensile strength due to scale effect (40%)** [Van Vliet and Van Mier, 00]: otherwise no crack is predict
- ✓ Coupling coefficient : 0,4
- ✓ Cracking pattern similar to the one observed
  - ✓ Vertical crossing cracks
  - ✓ Horizontal crack

Phenomenon classification

- ✓ High influence of creep (as expected)
- ✓ Main phenomena involve in cracking :
  - ✓ Thermal evolution
- ✓ Drying -> only skin crack

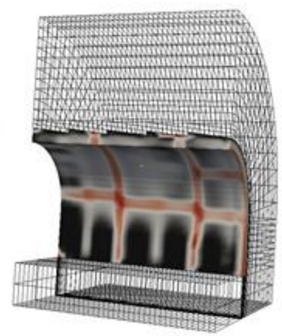

Damage field due to both thermal and autogenous shrinkage after 360 hours (in considering creep)

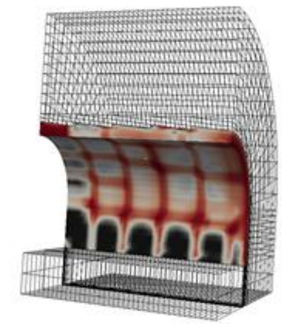

Damage field due to both thermal and autogenous shrinkage after 360 hours (in neglecting creep)

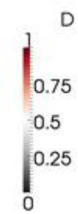

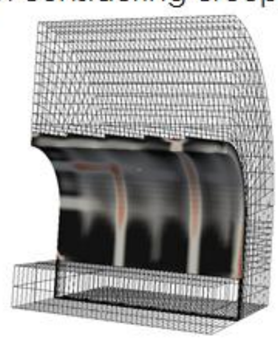

Damage field due to thermal shrinkage after 360 hours

Damage field due to drying shrinkage after 1,000 days

Fibers influence

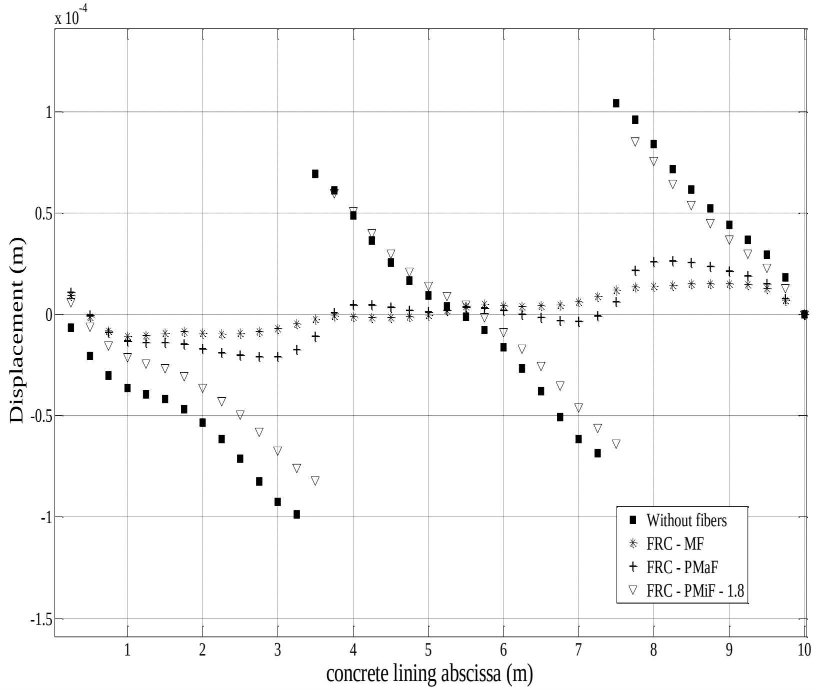

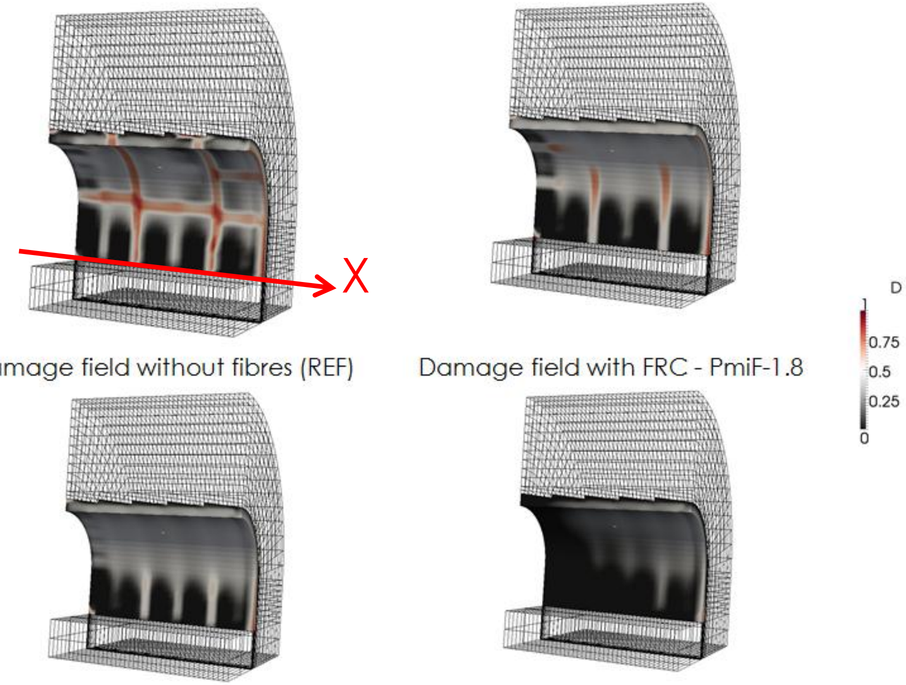

Damage field without fibres (REF)

Damage field with FRC - PmiF-1.8

Damage field with FRC - PMaF

Damage field with FRC - MF

- ✓ Slight reduction of strain gap (cracks) with PMiF
- ✓ No crossing crack predict with macro fibers
- ✓ Decrease of transport properties thought cracks with :
  - ✓ micro fibers : 38%
  - ✓ Macro fibers : 100%!!!! -> take care of pumping consideration

Tunnel lining geometry influence

- Smooth interface
  - Damage and permeability thought cracks decrease (65%)
- Lower thickness
  - Temperature evolution and cracks decrease
  - Permeability decrease 50%

Damage field without fibres (REF)

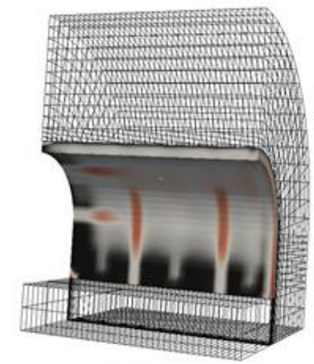

Damage field with a smooth interface between lining and shotcrete

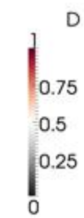

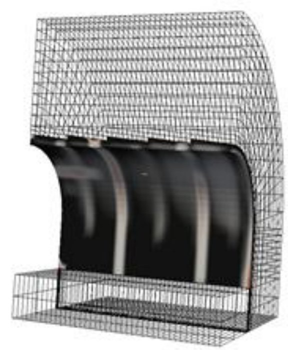

Damage field with a 30-cm concrete thickness

Conclusion

- A global strategy coupling complex and innovative test with chemo-thermo mechanical modelling was used to study the influence of fibers on cracking of massive tunnel lining
- On laboratory test :
  - Use of PMiF does not really delay cracks
  - Use of PMaF delays and distribute cracks
- Coupling coefficient between creep and damage is explained by strains incompatibilities
- Main phenomena involves in tunnel lining cracking is thermal shrinkage
  - Use of PMaF could avoid cracks (at least decrease strongly transport properties)
  - Use of PMiF is useless to prevent early age cracking
  - Decrease tunnel thickness limit temperature shrinkage and reduce crack openings

Avoiding thermal cracks in mass concrete: problems, solutions and doubts

Selmo Kuperman[1,*]
[1]DESEK, São Paulo, Brasil

Types of structures prone to thermal cracks

dams and hydropowerplants

Hydroelectric powerplant under construction in Brazil (2015)

~ 2.900.000 m^3 = CVC + RCC

RCC and CVC being placed in brazilian hydroelectric powerplants

RCC and CVC at Lajeado HPP (1998)

Itaipu powerhouse – 2nd stage construction (2003)

Types of structures prone to thermal cracks

foundation of wind towers

Different types of foundations for wind towers

Wind park Casa Nova (2013) – 436m^3

Wind park Uniao dos Ventos (2012) – 260m^3

Types of structures prone to thermal cracks

foundation blocks – industrial and residential

Pumped concrete for the foundations of industrial and residential buildings

1390m^3

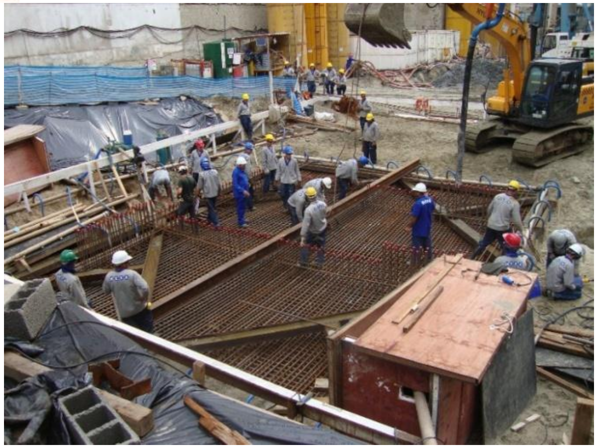

Foundations of residential buildings

390m^3 - SCC

Types of structures prone to thermal cracks

concrete bunkers for radioactive equipments

Concrete bunkers for radioactive equipments

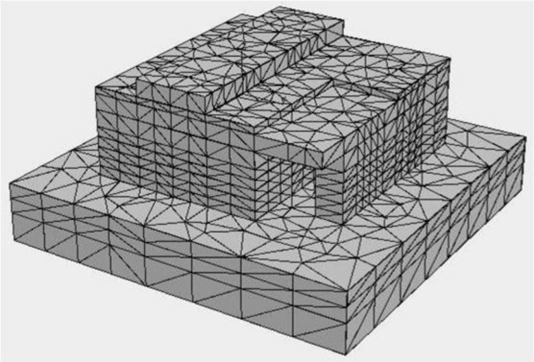

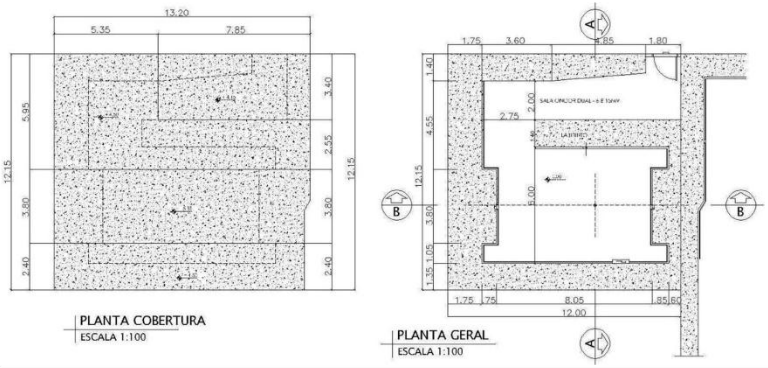

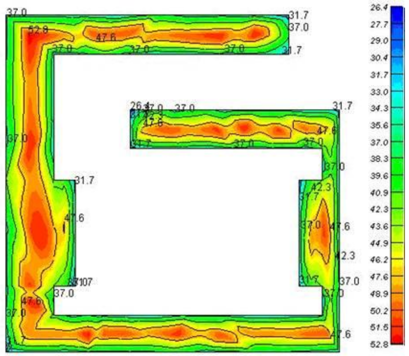

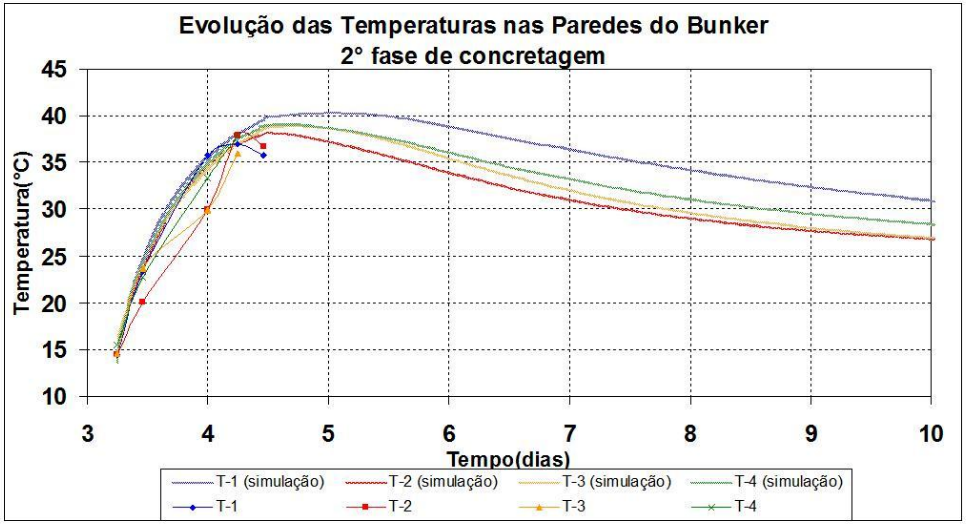

Problems

cracks due to thermal stresses

cracks due to DEF (in most cases together with ASR)

Cracks due to DEF and ASR in foundation blocks of different buildings

ASR + DEF

DEF

ASR + DEF

Cracks due to thermal stresses

Demolition of a concrete foundation block at an industry due to thermal cracking

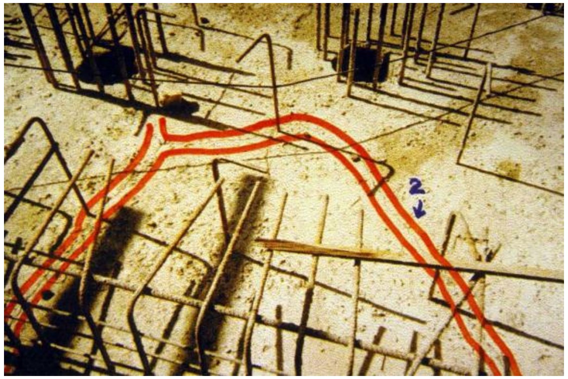

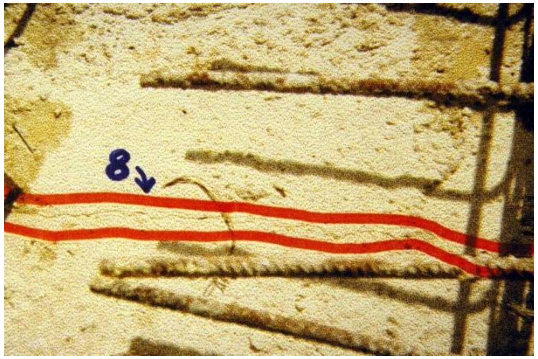

Thermal cracking at Upper Stillwater dam (USA)

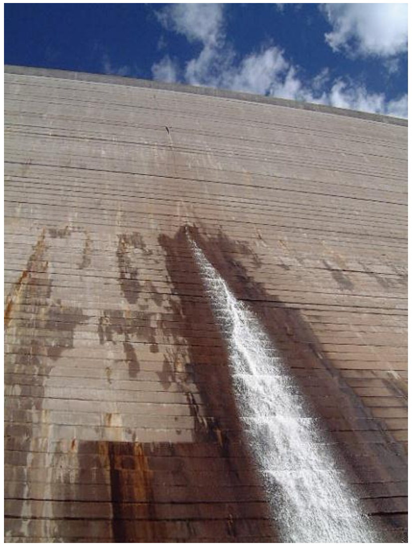

Solutions

thermal stresses analysis – pre-cooling, post-cooling and changes of the construction scheme

Thermal stresses analysis

3D FEM of temperatures coupled with stresses (software B4Cast)

Example: Cracked spillway

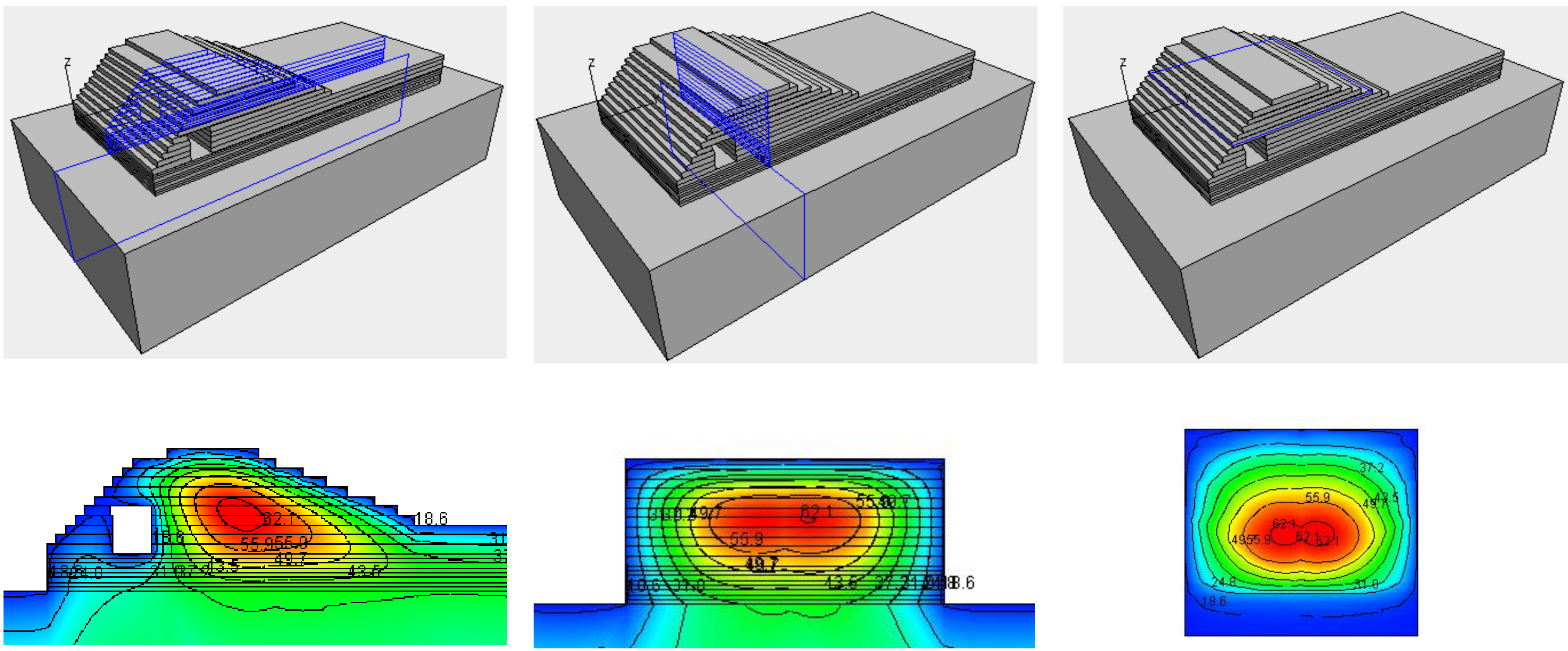

Thermal stresses analysis

3D FEM of temperatures coupled with stresses

Example: Isotherms

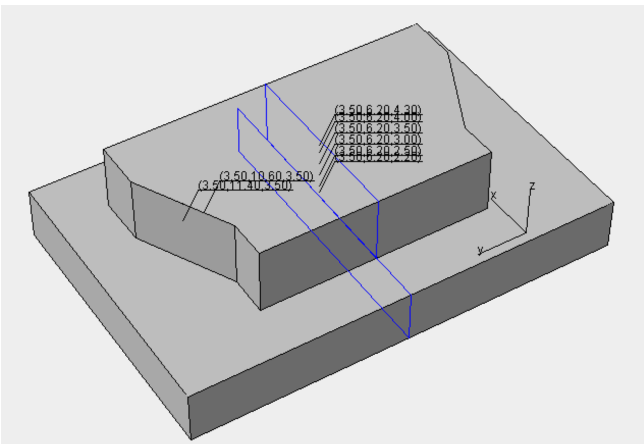

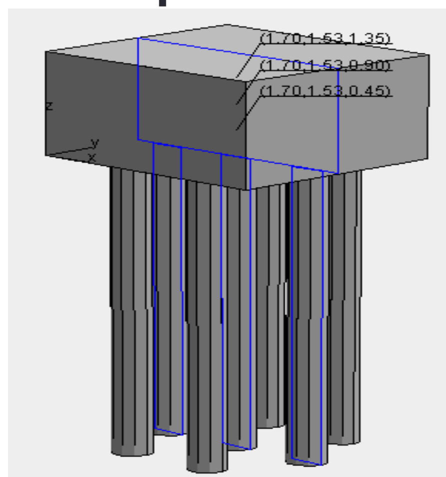

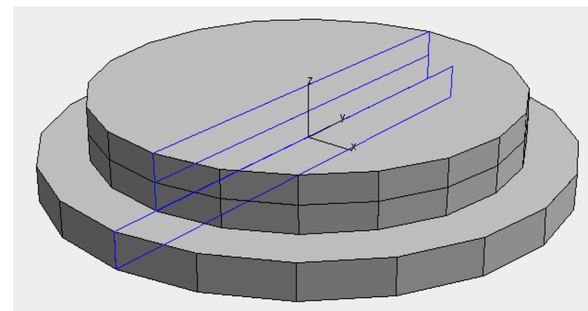

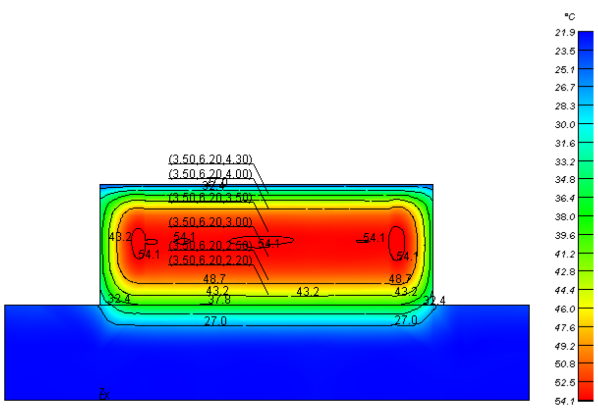

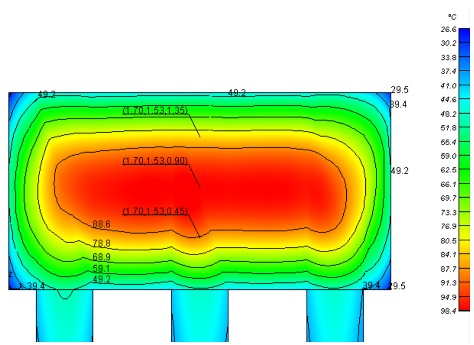

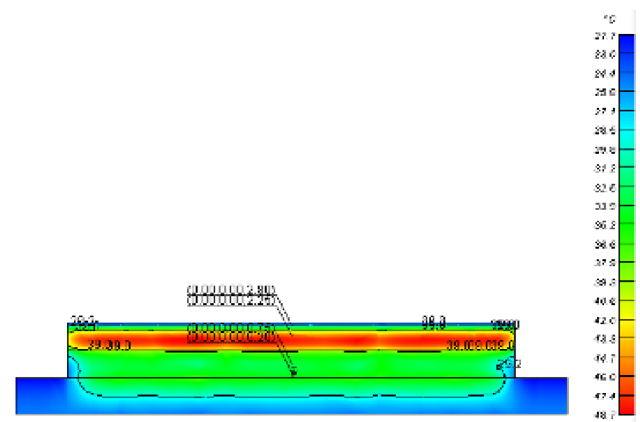

Thermal stresses analysis (B4Cast software)

3D FEM of temperatures coupled with stresses.

Example: Foundation block 17,5m x 9m x 2,75m

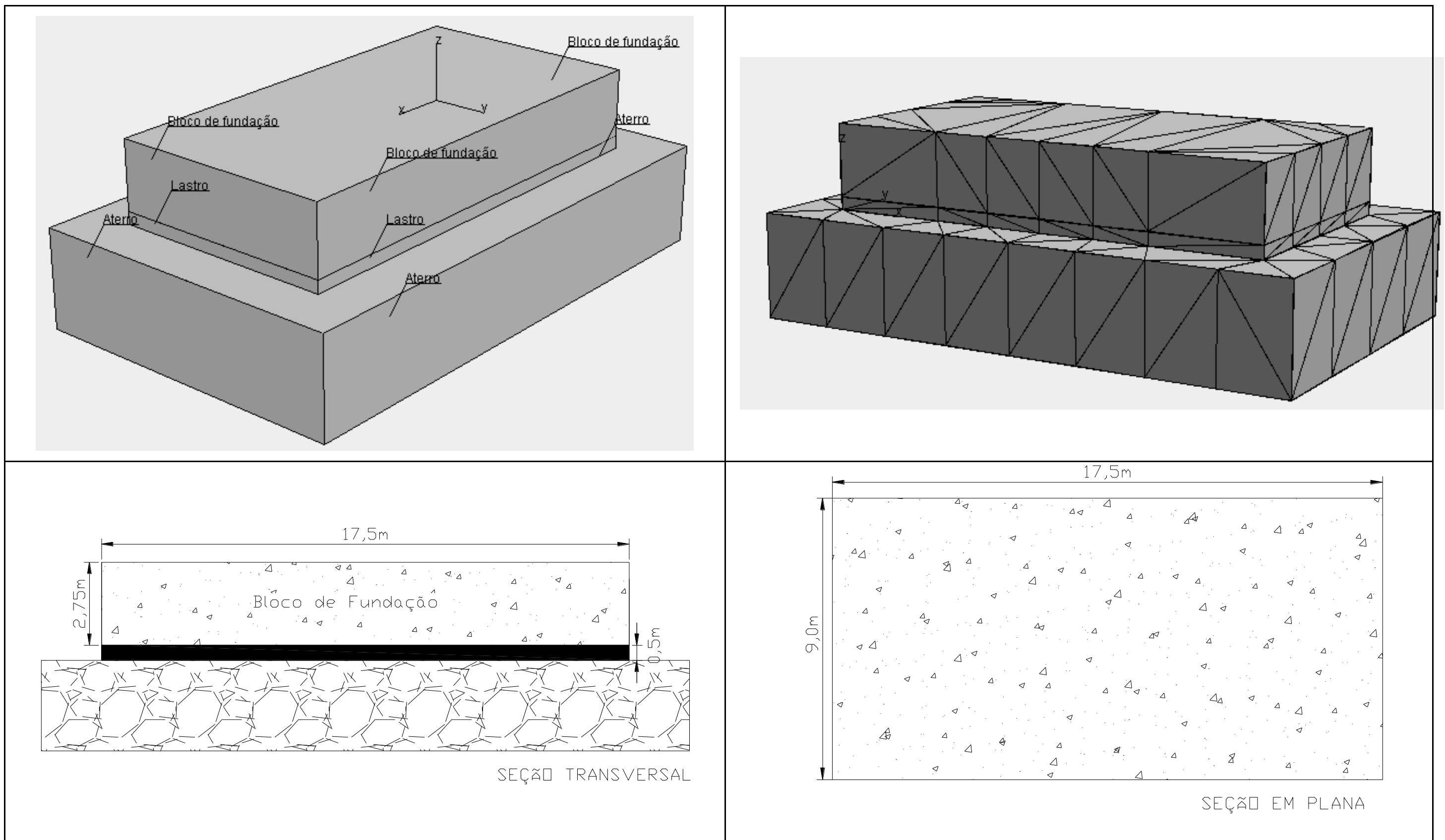

3D FEM thermal stresses analysis
Mix design

TRAÇO A		
Material	**Fornecedor**	**Consumo (kg/m^3)**
Cimento CPIII		420
Areia Fina	Quartzo	480
Pedrisco Misto	Granito	441
Brita 1	Granito	900
Água		165
Aditivo 1		2,100
Aditivo 2 =Policarboxilato		1,302
TRAÇO B		
Material	**Fornecedor**	**Consumo (kg/m^3)**
Cimento CPIII		386
Metacaulim	Metacaulim	34
Areia Fina	Quartzo	493
Pedrisco Misto	Basalto	410
Brita 0	Basalto	100
Brita 1	Basalto	772
Água		48
Gelo		130
Aditivo 1		2,100
Aditivo 2 = Policarboxilato		1,302

Thermal stresses analysis
Concrete properties
Example: Foundation block

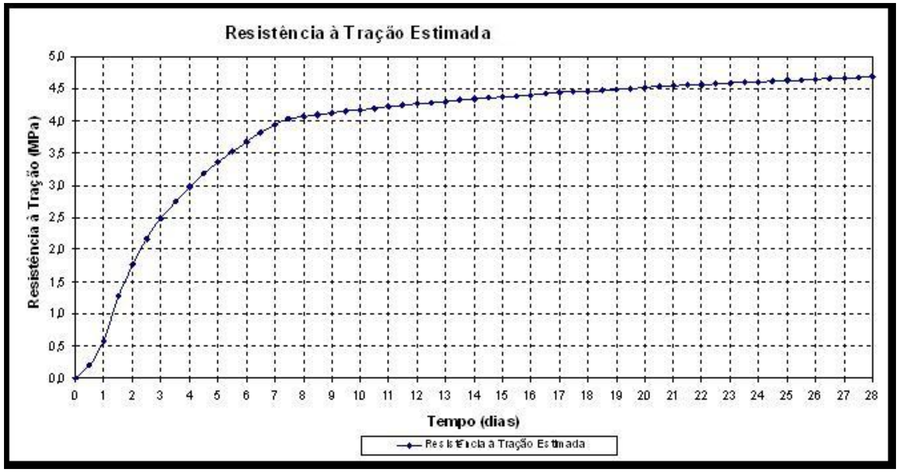

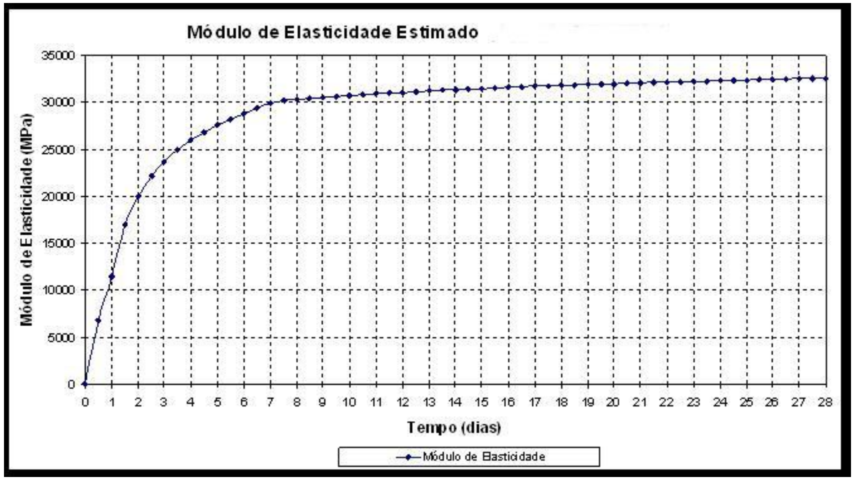

Propriedade térmica	Traço A	Traço B
Calor específico (kJ/kg.°C)	0,97	0,99
Condutividade térmica (kJ/m.h.°C)	8,83	8,77
Coeficiente de dilatação térmica ((10^{-6}/°C)	9,3	9,4

Thermal stresses analysis
3D FEM of temperatures coupled with stresses
Example: Foundation block

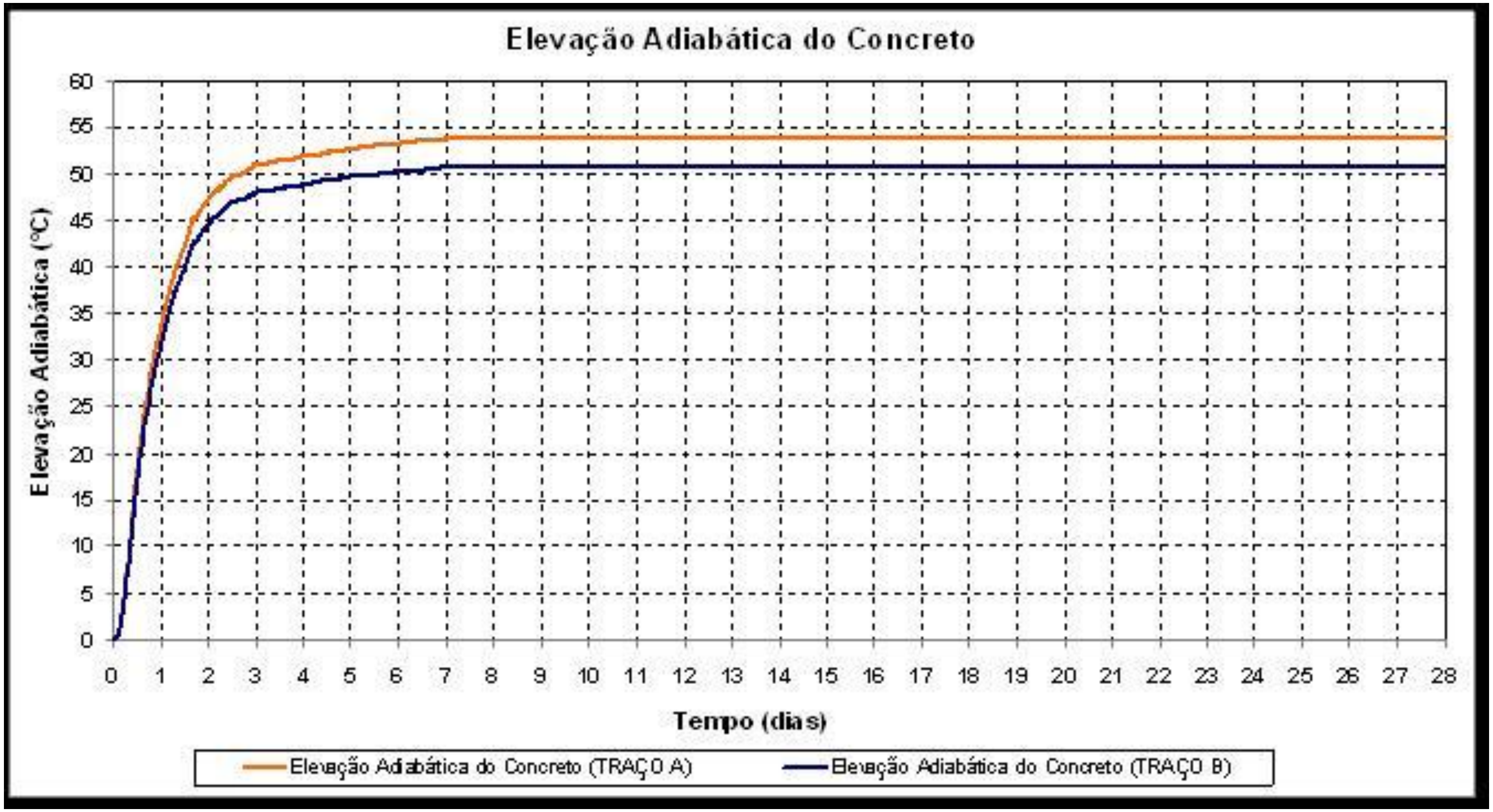

Thermal stresses analysis

Chosen points for monitoring temperatures

Example: Foundation block

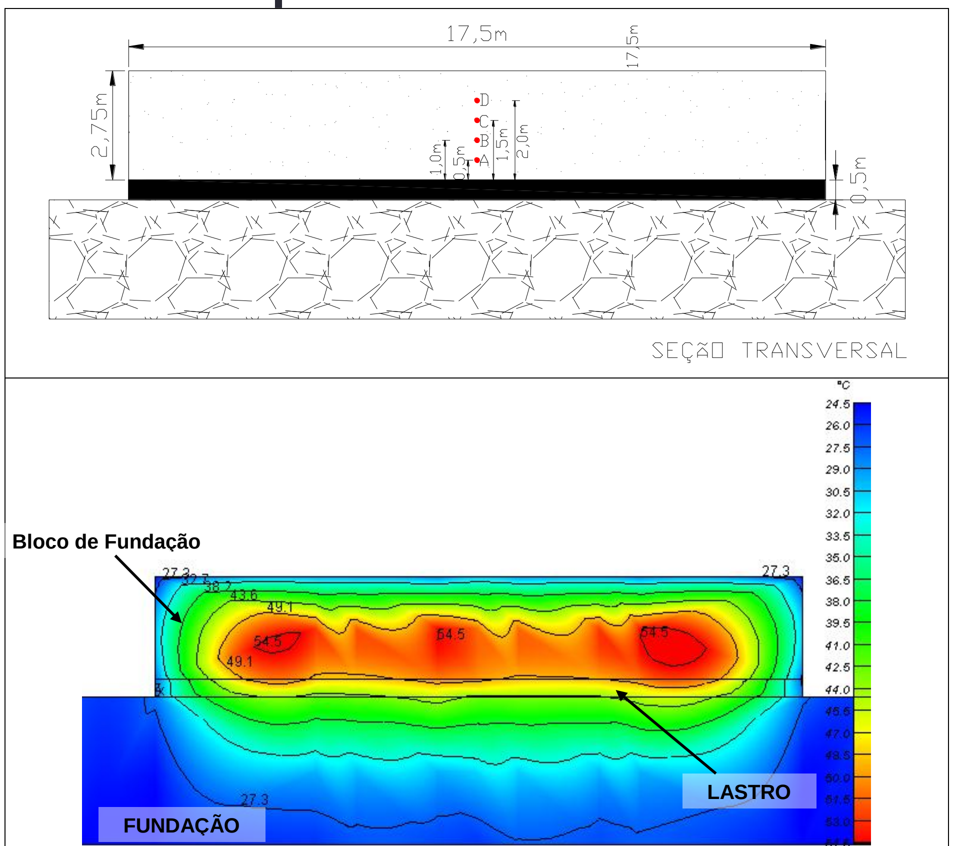

Figura 1 – Localização dos pontos de estudo – Isotermas na direção “x” (152horas)

Thermal stresses analysis

Example: Cases studied for a foundation block

Structure	Case	Mix Design	Placing temperature (ºC)	Lift height (m)
Foundation block	I	A	15	2,75
	II		20	
	III		25	
	IV	B	15	2,75
	V		20	
	VI		25	

Thermal stresses analysis

Example: Cases studied for a foundation block

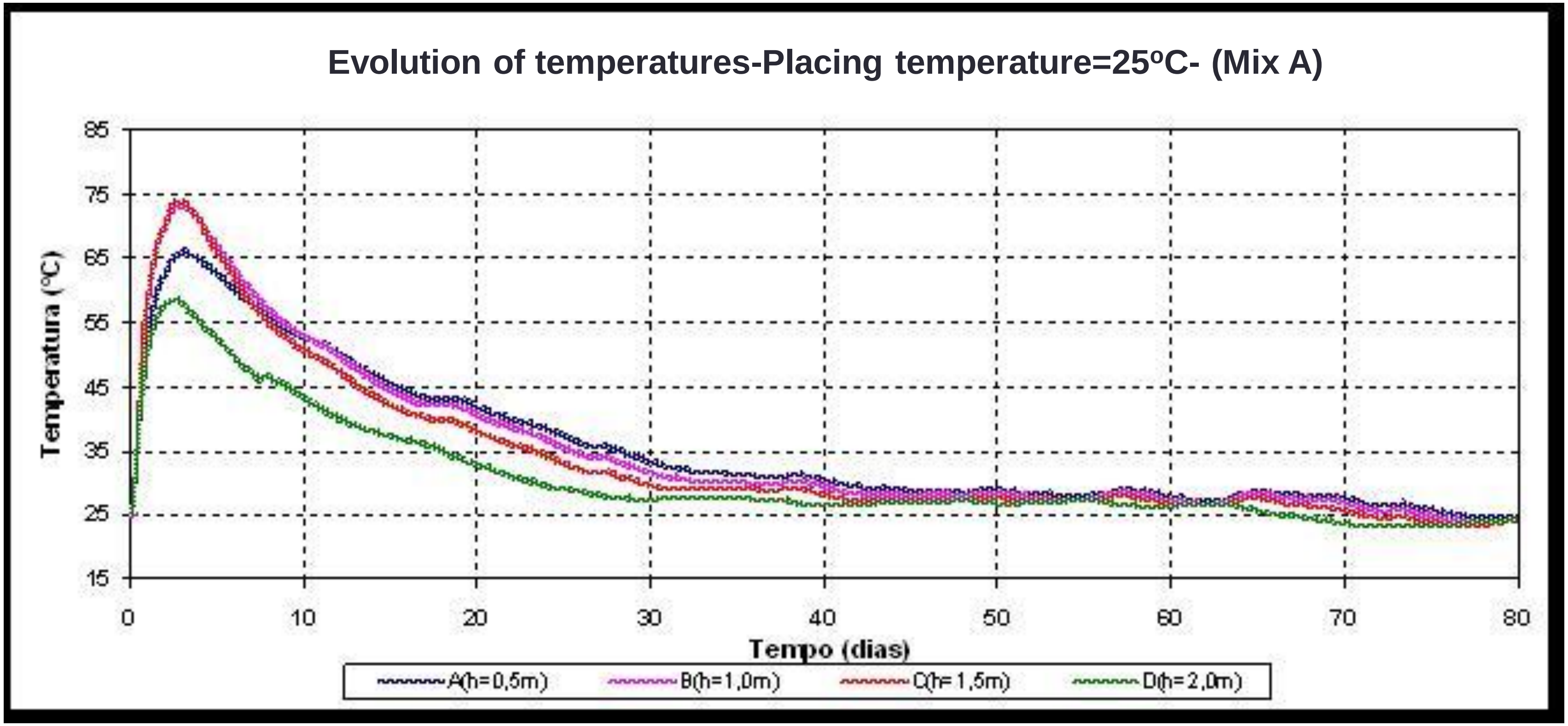

Thermal stresses analysis

Example: Cases studied for a foundation block

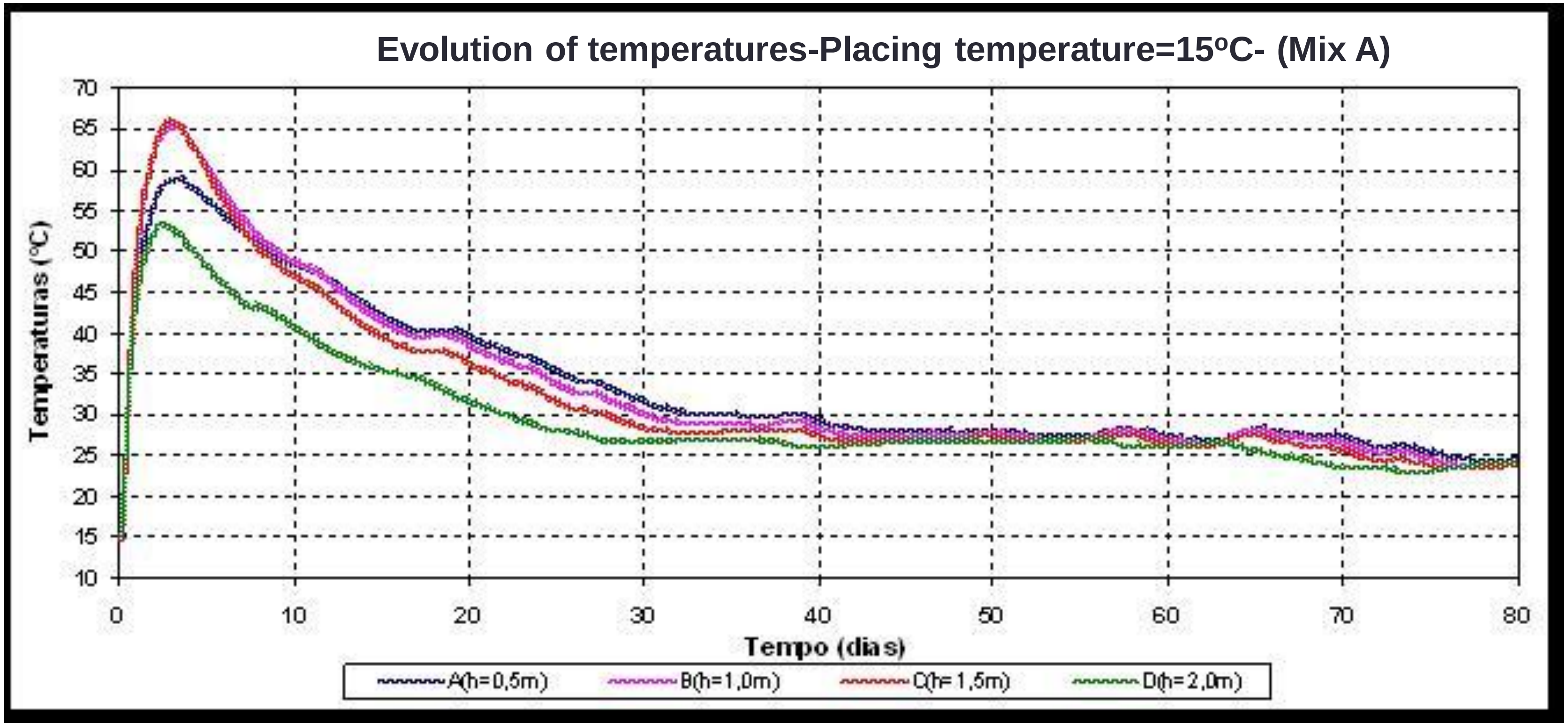

Thermal stresses analysis

Influence of placement temperatures on the maximum temperatures to be reached at the concrete block

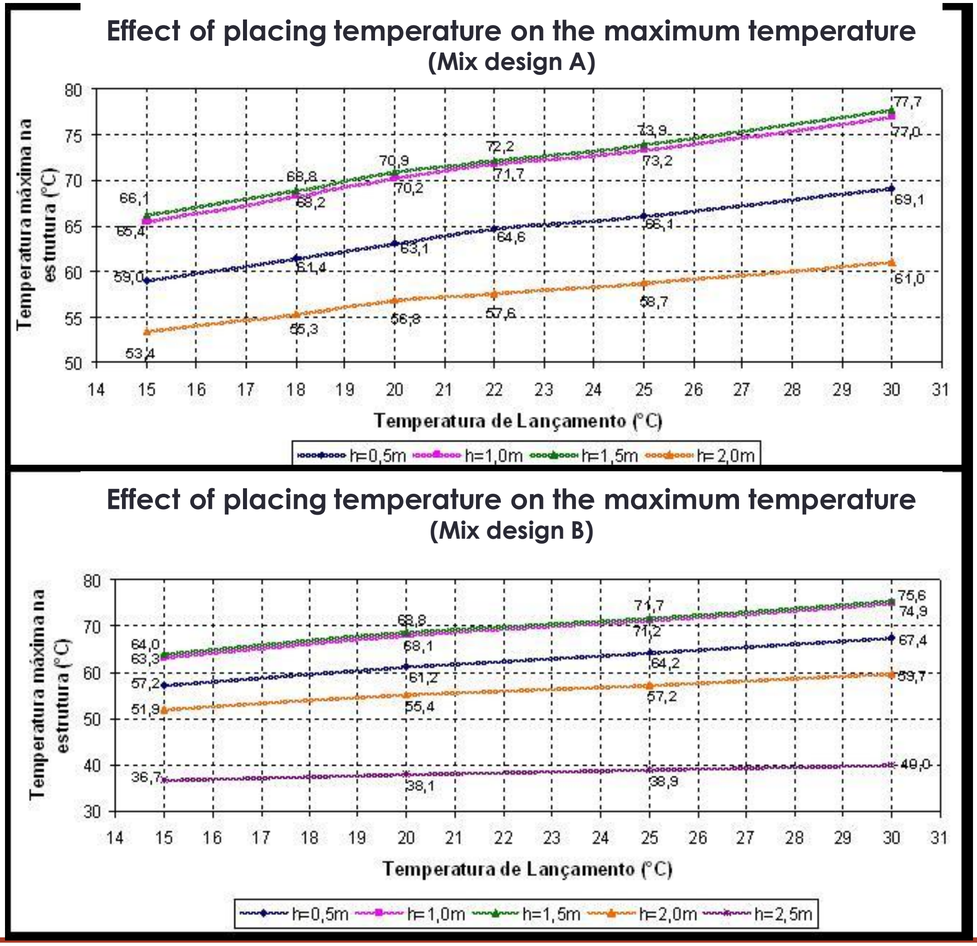

Thermal stresses analysis

Example: Influence of placement temperatures on tensile stresses

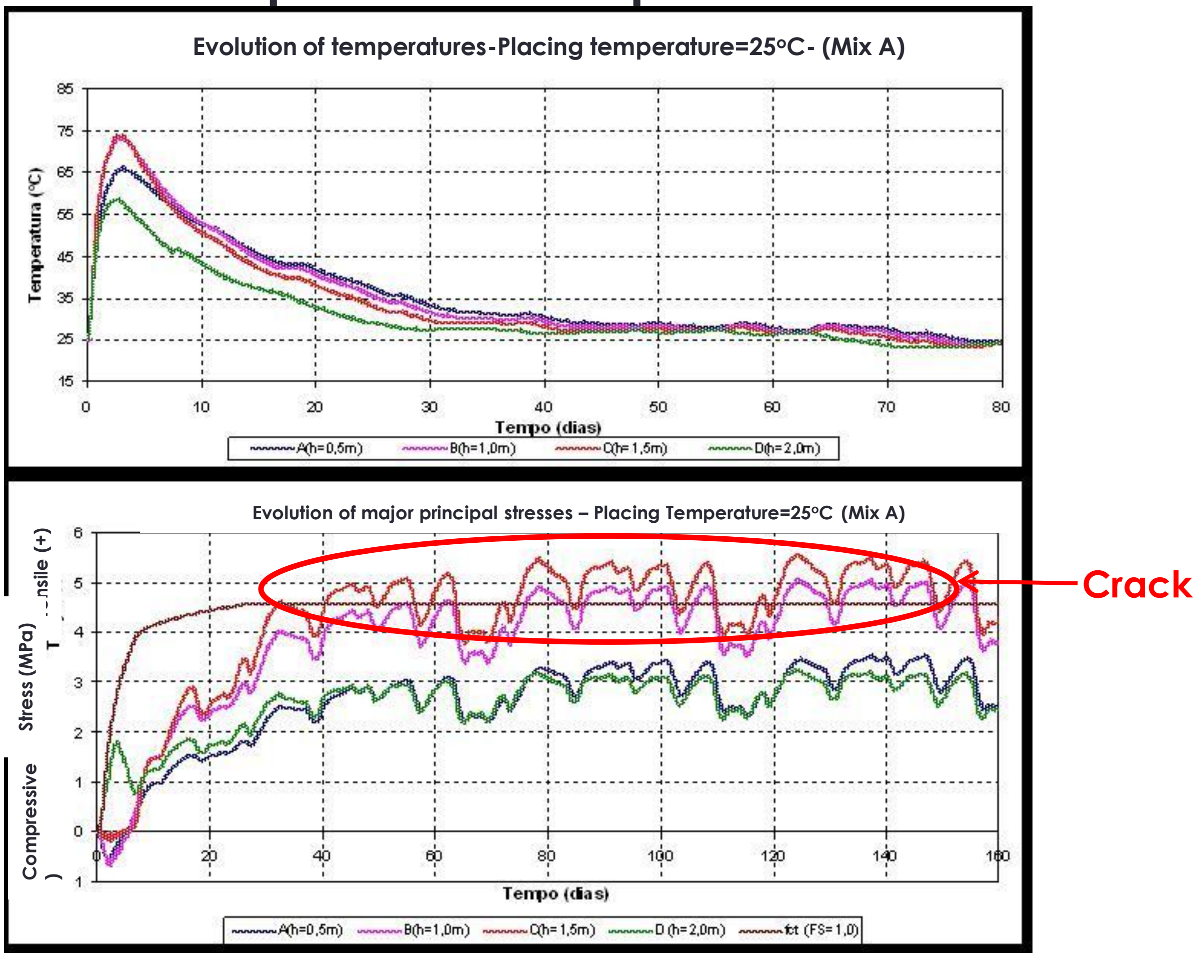

Thermal stresses analysis

Example: Influence of placement temperatures on tensile stresses

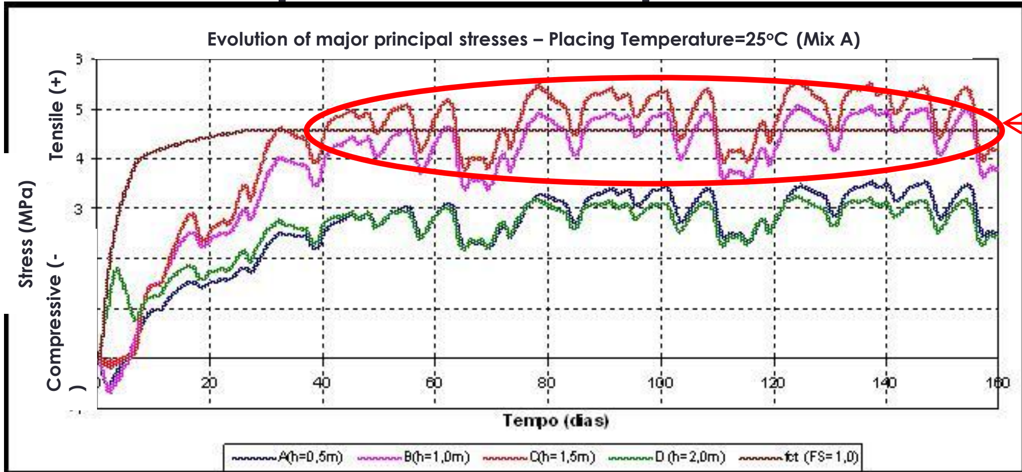

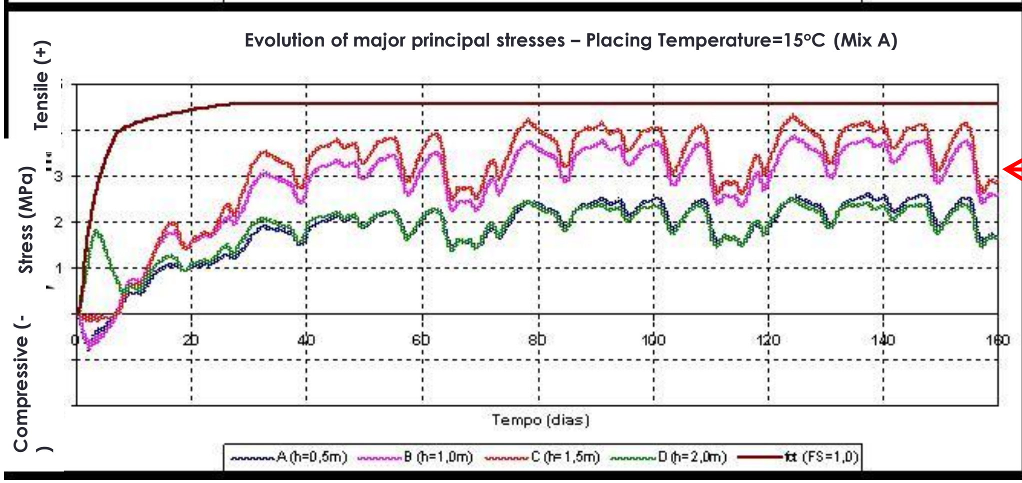

Thermal stresses analysis

Effect of placement temperatures on the maximum tensile stresses

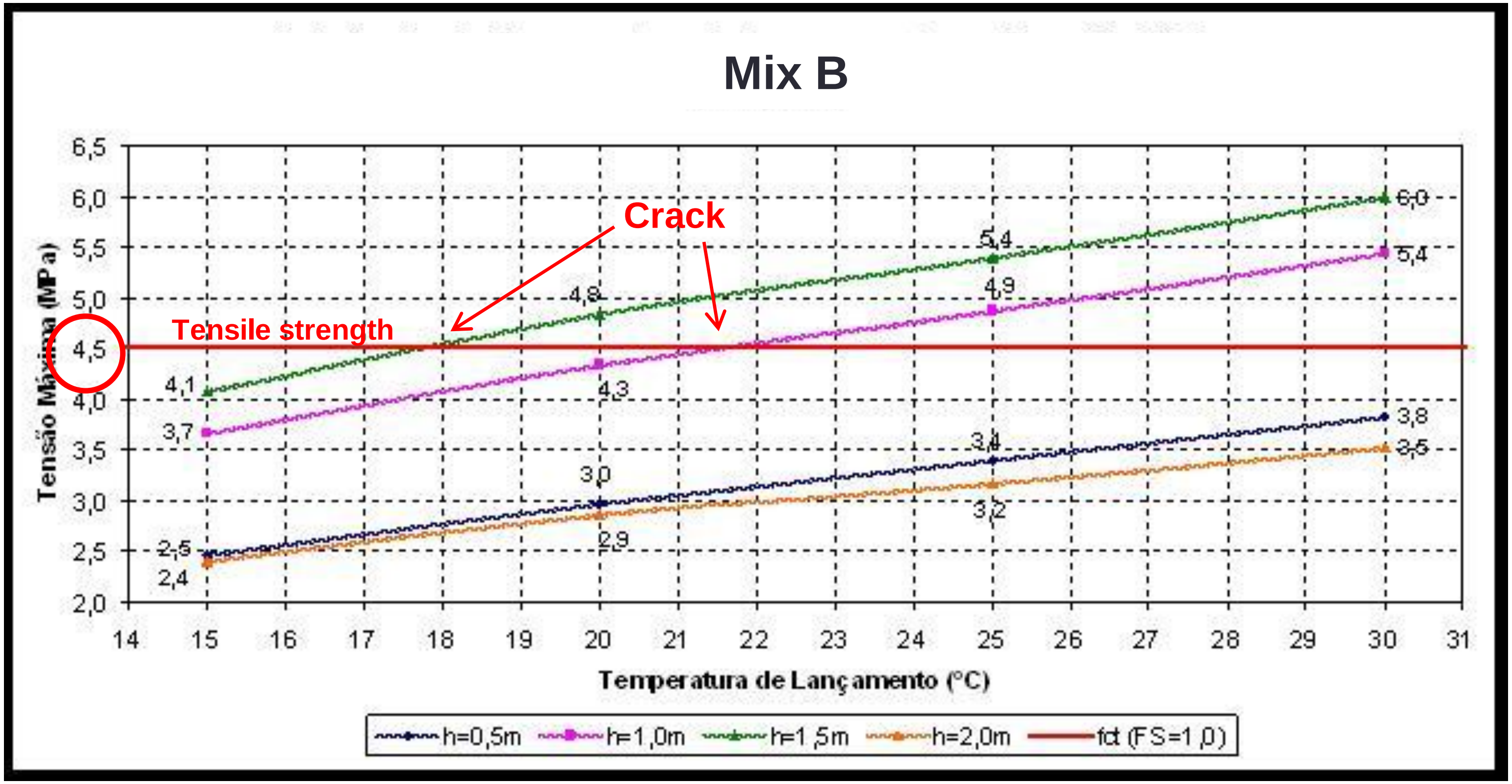

Thermal stresses analysis

Effect of placement temperatures on the maximum tensile stresses at a foundation block

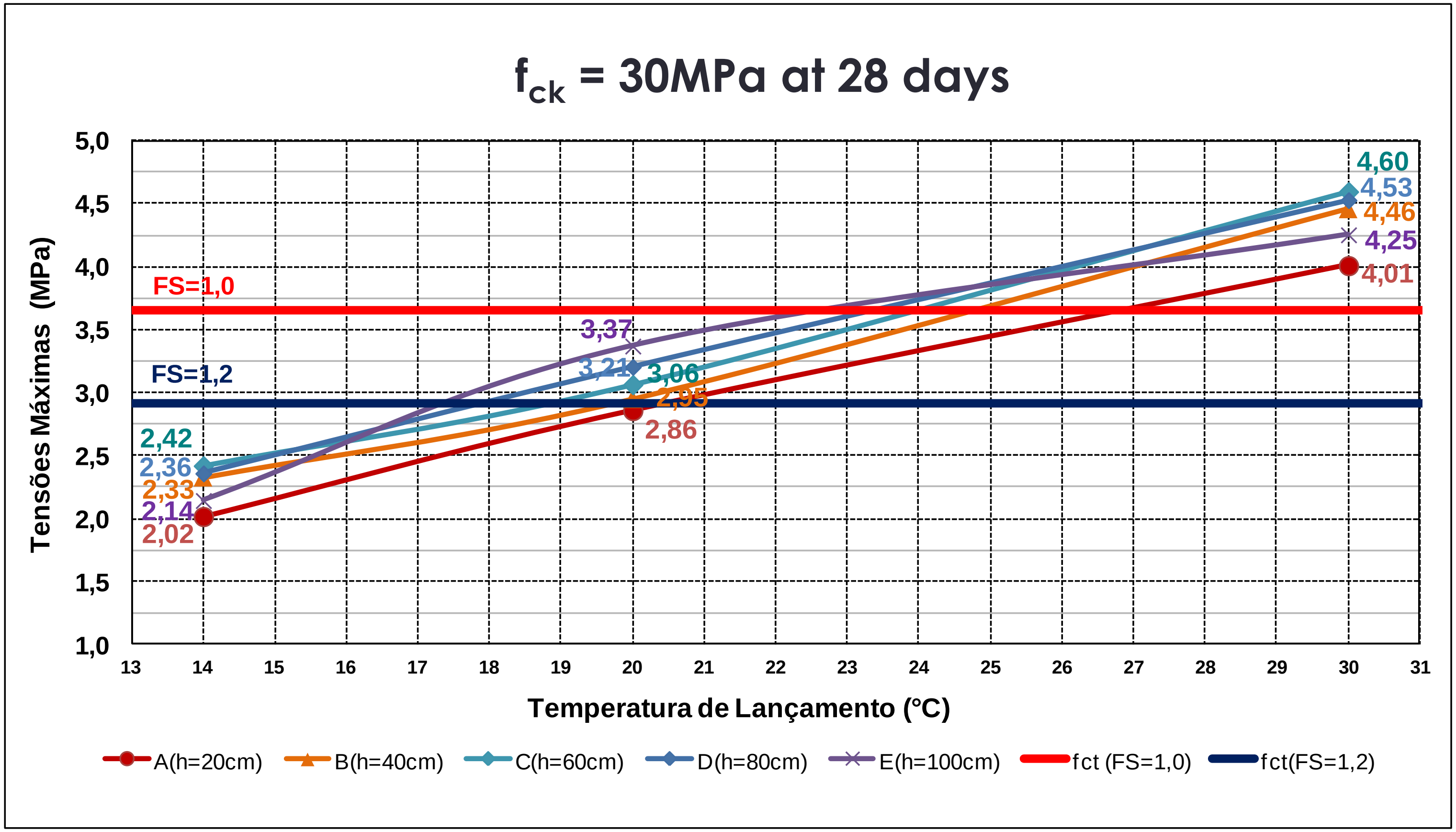

Thermal stresses analysis

Results of a foundation block analysis: pre-cooling the concrete and imposing maximum placement temperatures for different heights

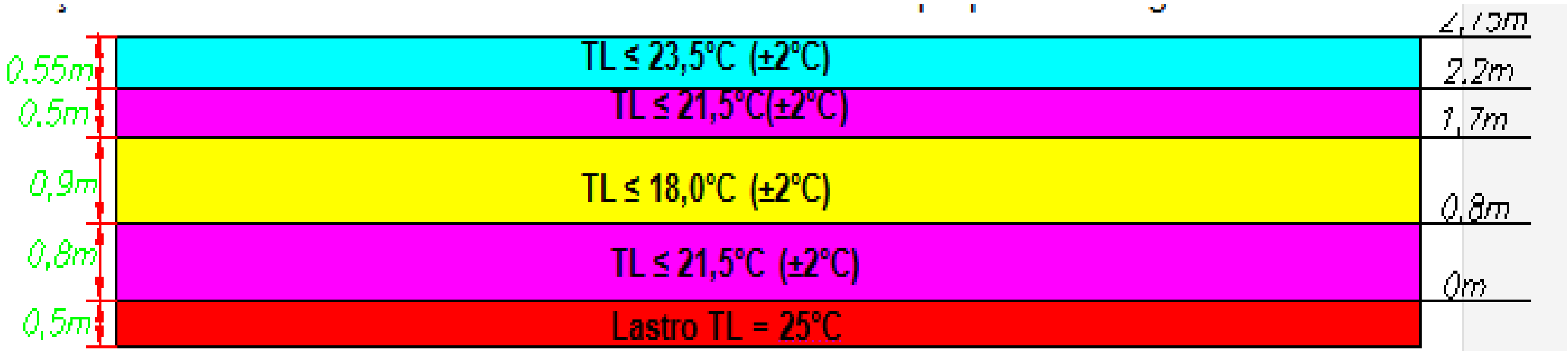

Nota: TL=Temperatura de lançamento do concreto; V_c=Volume de concreto teórico em cada zona de temperatura de lançamento

Thermal stresses analysis

Results of a foundation block analysis: pre-cooling the concrete and imposing maximum placement temperatures for different heights

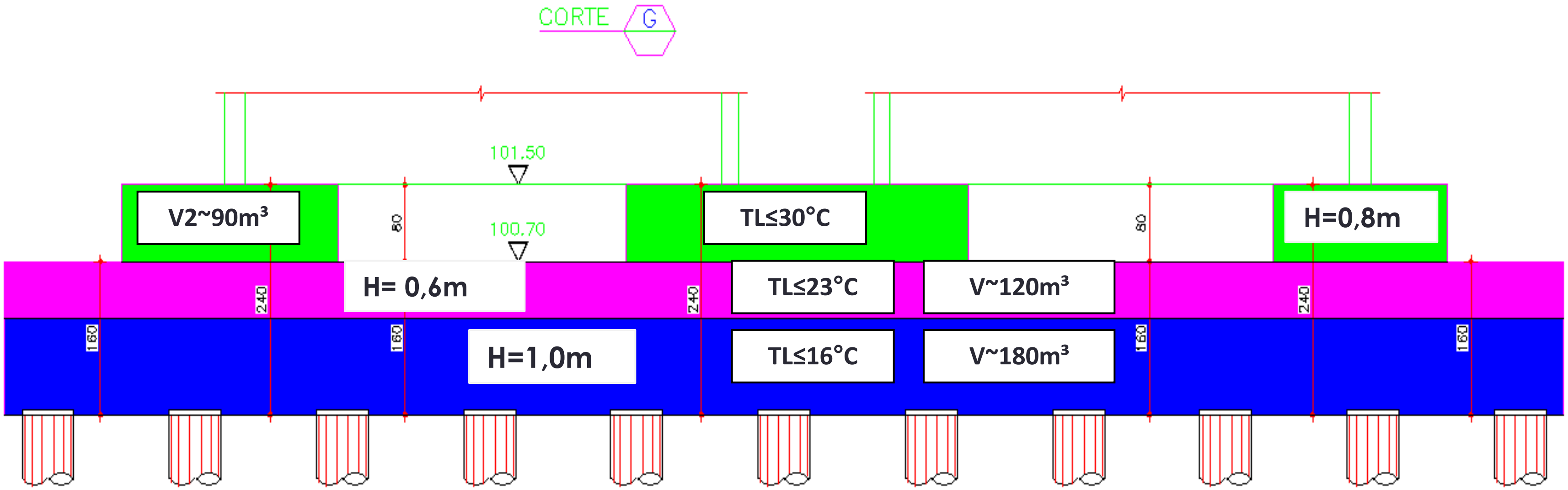

Thermal stresses analysis

Maximum placement temperatures calculated for the Intake of a hydropower plant

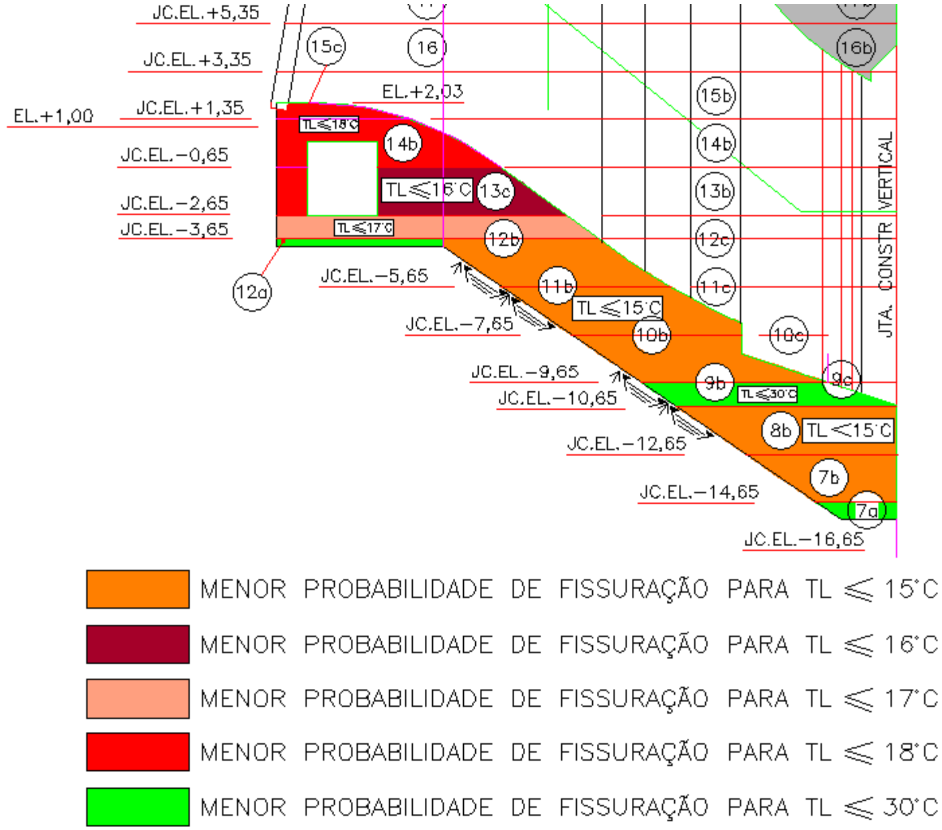

Thermal stresses analysis

Maximum placement temperatures calculated for a foundation block of a commercial building

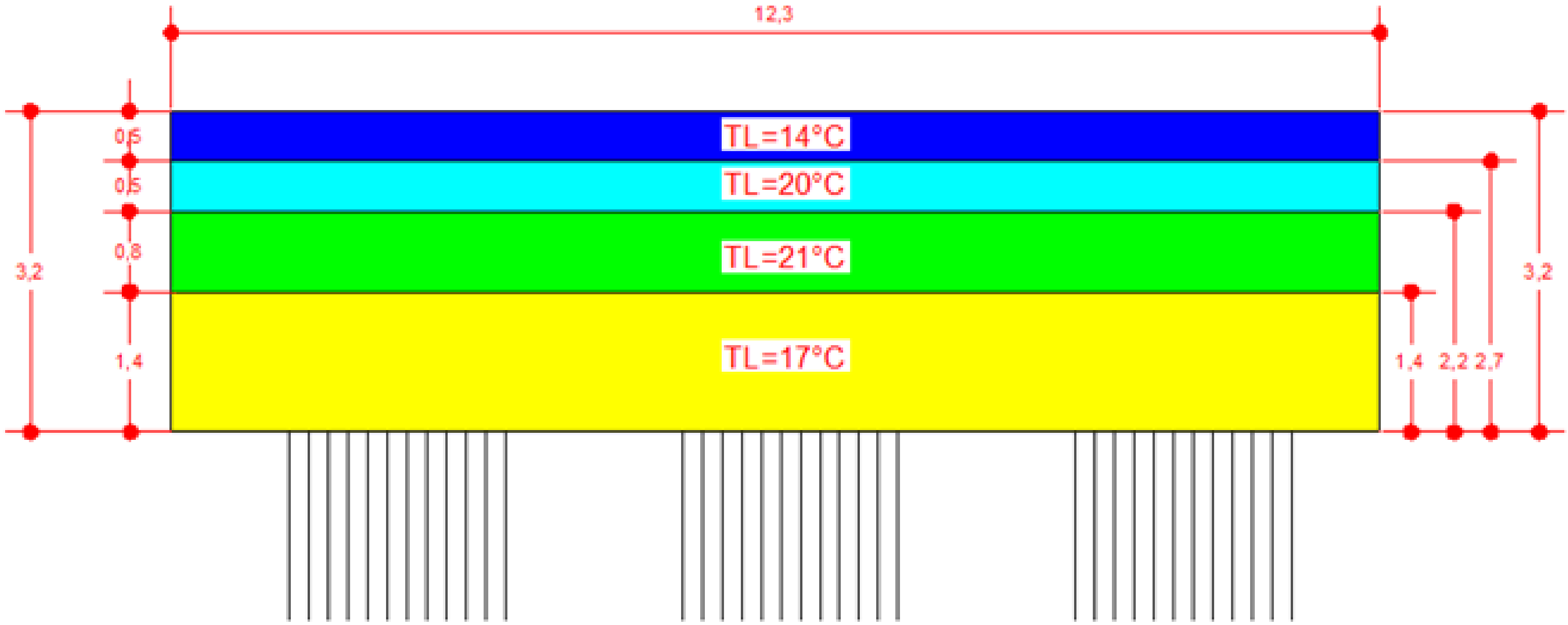

Thermal stresses analysis

Placement temperature of a pre-cooled concrete - Heat balance

BALANÇO TÉRMICO - (30MPa/28d) Refrigerado, bombeado							GELO	82%	
Materiais	Consumo	Calor esp.	q = mc	E	Ti	Tf	Ti - Tf	Quant.Calor	(kcal/m^3)
Mistura	(kg/m^3)	(kcal/kg.C)	(kcal/m^3.C)	(kcal/m^3)	(C)	(C)	(C)	Positivo	Negativo
Cimento	321	0,159	51,04	51,04	**60,0**		60,0	3062,34	
Areia (quartzo)	356	0,191	68,00	68,00	**30,0**		30,0	2039,88	
Areia (granitica)	448	0,176	78,85	78,85	**30,0**		30,0	2365,44	
Brita 0 (granítica)	156	0,176	27,46	27,46	**30,0**		30,0	823,68	
Brita 1 (granítica)	892	0,176	156,99	156,99	**30,0**		30,0	4709,76	
Água	27	1,000	26,83	26,83	**25,0**		25,0	670,77	
Aditivo	2,25	1,000	2,25	2,25	**25,0**		25,0	56,25	
Gelo	121,4	0,500	60,70	60,70	**0,0**	0	0,0	0,00	0,00
Fusão do gelo	121,4	0,000	0,00	0,00	**0,0**	0	0,0	0,00	-9712,75
Gelo/água	121,4	1,000	121,41	121,41	**0,0**	0	0,0	0,00	0,00
Umidade miúdo areia quartzo (5%)	17,8	1,000	17,80	17,80	**30,0**		30,0	534,00	
Umidade miúdo areia granitica (1%)	4,5	1,000	4,48	4,48	**30,0**		30,0	134,40	
Umidade do graúdo(1%)	10,5	1,000	10,48	10,48	**30,0**		30,0	314,40	
Mistura Betoneira	-	-	-	-	-	-	-	2000,00	

Equivalente em água (E=mc.1°C) = 626,29 kcal/m^3

Quantidade total de calor (Q) = 6998,17 kcal/m^3.C

Temperatura de saída do concreto da betoneira (Q / E) =	Tc =	11,2 °C
Ganho de temperatura no transporte até o local de lançamento =	Tt =	2,0 °C
Temperatura de lançamento do concreto =	TL =	13,2 °C

Temperature measurements with thermocouples at a foundation block of a commercial building

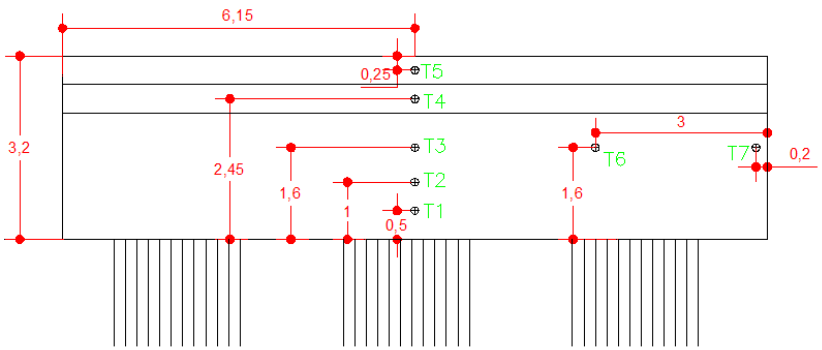

SEÇÃO LONGITUDINAL

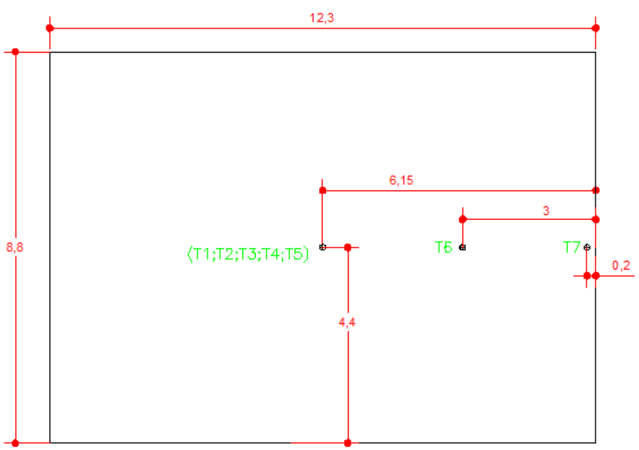

PLANTA

Measured and calculated temperatures of a foundation block

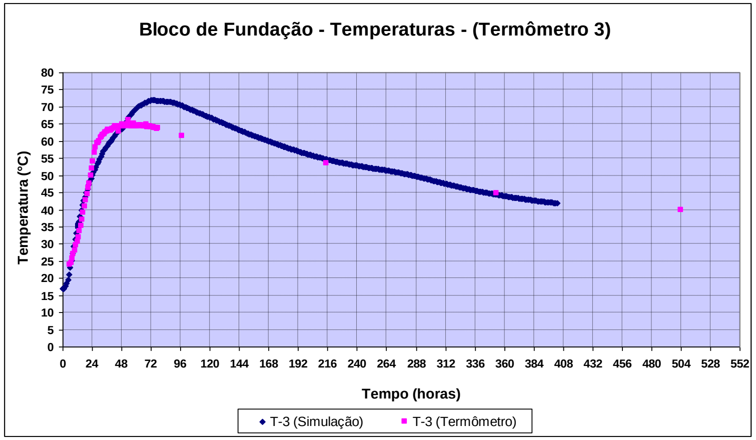

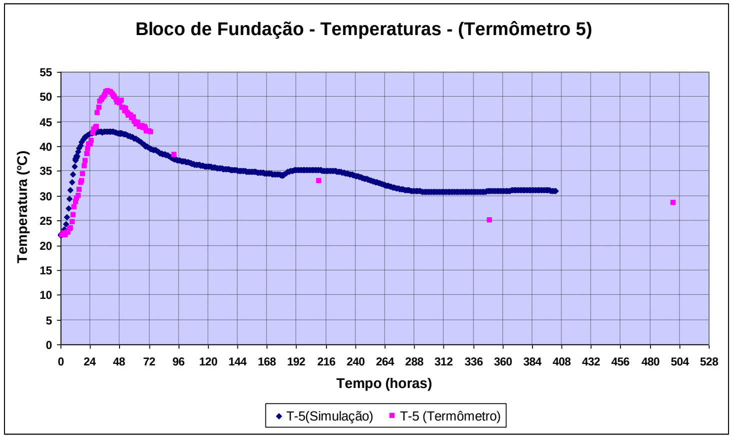

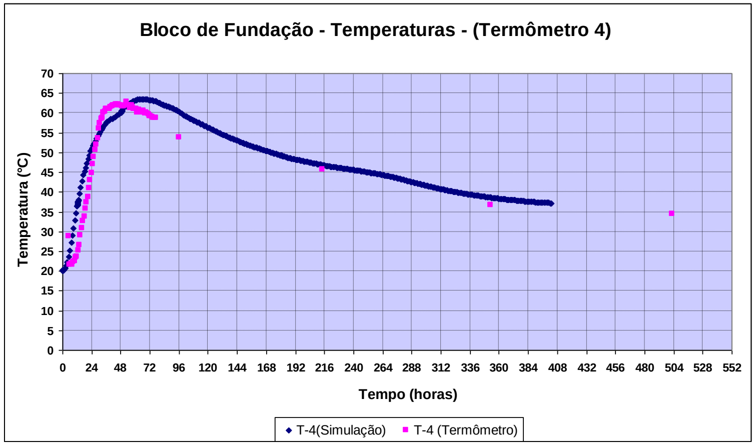

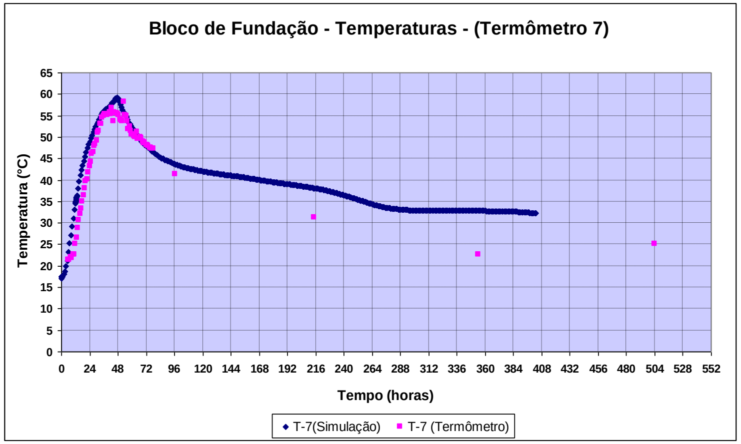

Foundation blocks - Pre-cooling concrete with ice

Pre-cooling of concrete

Steel tubes covered with ice at the 2nd stage Itaipu HPP (2003)

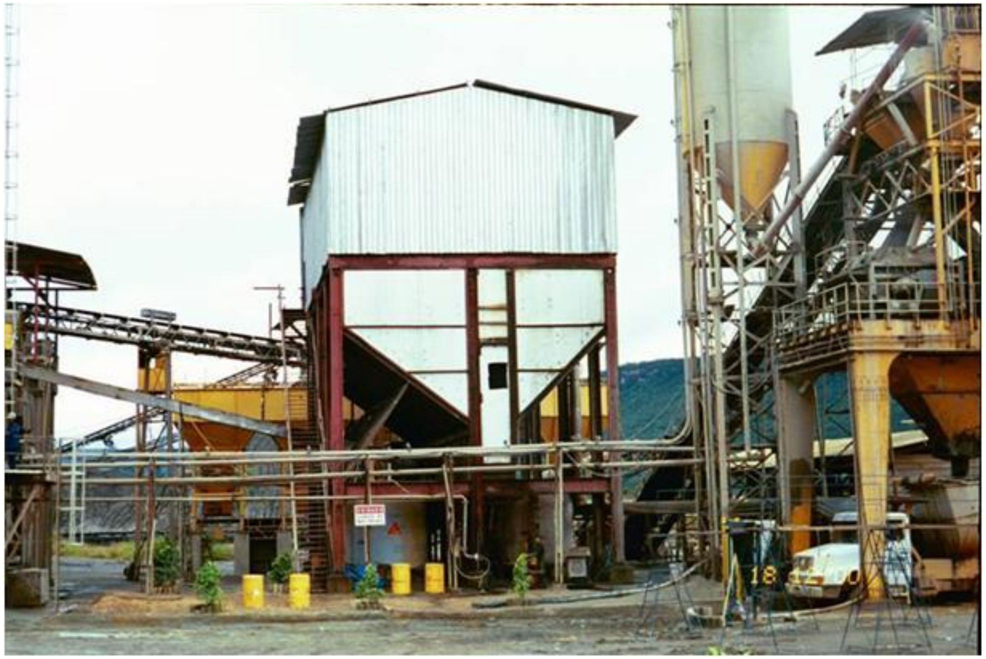

Ice plant at Lajeado HPP (1998)

Production of ice flakes at a hydropowerplant in Brazil (2015)

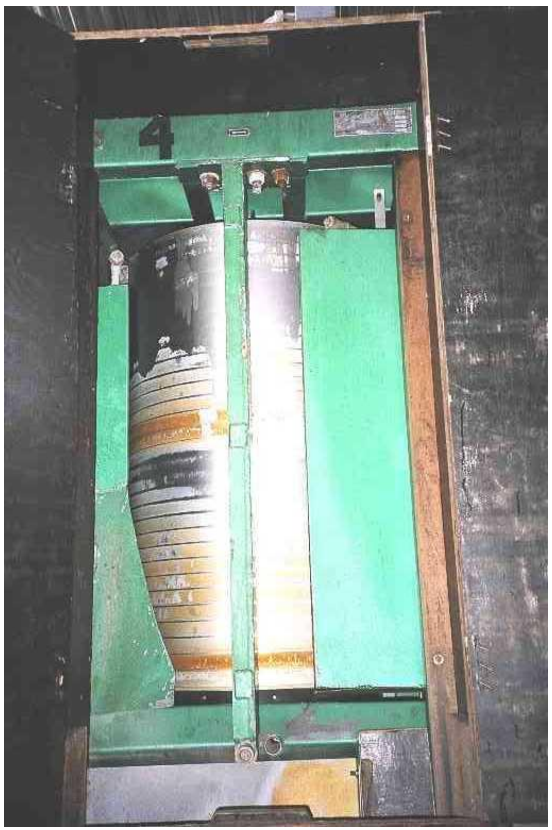

Lift heights at hydropowerplants in Brazil

Conventional concrete (CVC) block construction with 2m lift height and 0,5m high sub lifts (HPP in Brazil).

Sloped lift layer (0,3m) of RCC placement at Lajeado HPP (Brazil).

Doubts

How precise are stresses calculations?

Thermal stresses analysis

Data needed for calculations

Usually available — Sometimes available — Usually unavailable

- Geometry of the structure;
- Concreting plan and construction schedule (mainly placement intervals and lift heights);
- Concrete mix design;
- Concrete properties: compressive strength, tensile strength, modulus of elasticity, Poisson`s ratio, creep, density;
- Thermal properties of concrete and its components: specific heat, thermal conductivity, coefficient of thermal expansion, heat of hydration of cement, adiabatic temperature rise of concrete;
- Mechanical and thermal properties of the restraining members (foundation and walls, such as rock, concrete, soil);
- Ambient conditions of the site (mainly temperatures and wind);
- Curing conditions of the concrete;
- Formwork properties.

Thermal stresses analysis

Which is the accuracy of available data?

✓ Modulus of elasticity *(10%?)*

✓Tensile strength (*Direct test? Splitting test? Strain capacity?)*

✓ Coefficient of thermal expansion of concrete (*can vary between 0,1 and 0,9x10^{-6}/°C? – according to Tanesi, TRB*)

✓Adiabatic temperature rise

✓Heat of hydration

✓ Concrete creep

✓ Restraint conditions (mainly modulus of elasticity) – *try measurements in the structure to check the effects as the height increases and compare with FEM calculations.*

Thermal stresses analysis

Proposition for different Factors of Safety on the calculations of thermal stresses, supposing that all construction details and ambient conditions are available, such as placement intervals, curing conditions, lift heights, construction schedule, etc.

Proposition of Progressive Factors of Safety

- FS = 1,0 = never
- FS = 1,1 = when modulus of elasticity, strengths evolutions with time and thermal properties of concrete are available
- FS = 1,2 = when modulus of elasticity, strengths evolutions with time, heat of hydration of cement and some thermal properties of concrete aggregates are available
- FS = 1,3 = when compressive strength is available

Thermal stresses analysis

Creep: how to consider?

a) Consider modulus of elasticity of concrete only after 1 day or only after the maximum temperature has been attained?

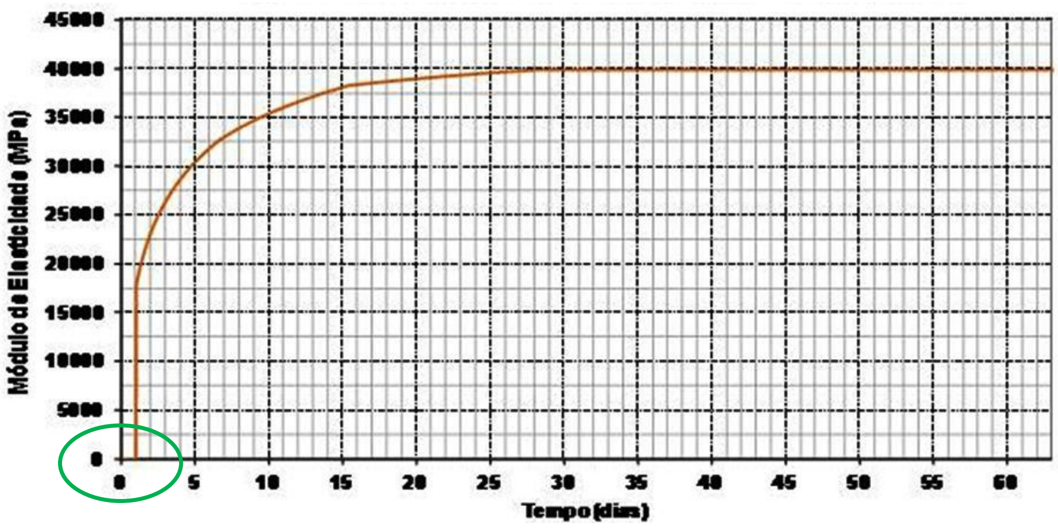

b) Consider creep as either a decrease in the modulus of elasticity or an increase in the tensile strength of concrete?.

New Admixtures to control temperatures: are they useful?

Cement pastes calorimetric tests

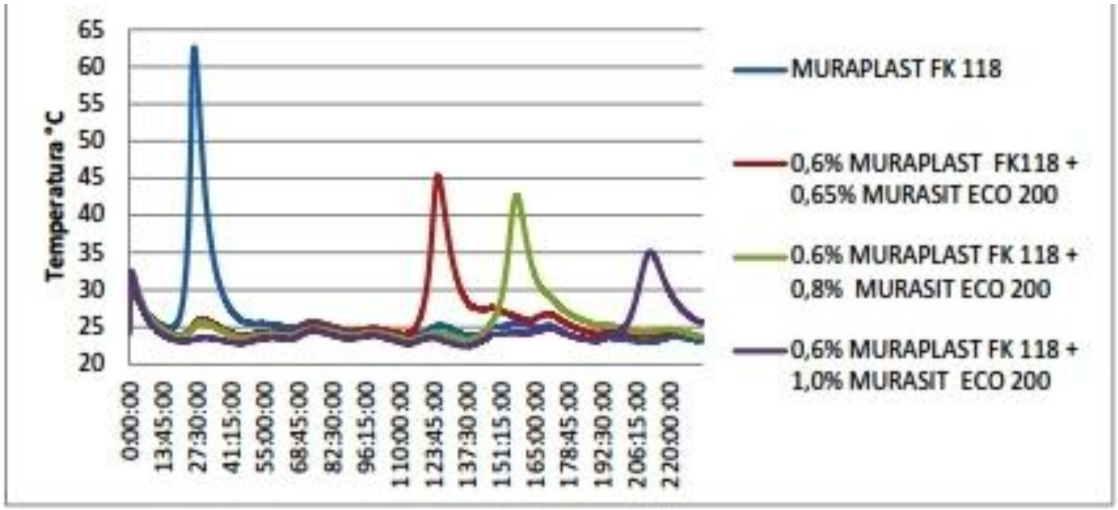

SAMPLES	SETTING TIME (h)		TEMPERATURA FINAL °C
	INICIAL	FINAL	
MURAPLAST FK 118	21:36:00	26:30:00	62,61
0,6% MURAPLAST FK118 + 0,65% MURASIT ECO 200	119:27:00	125:45:00	45,38
0.6% MURAPLAST FK 118 + 0,8% MURASIT ECO 200	152:12:00	157:54:00	42,68
0,6% MURAPLAST FK 118 + 1,0% MURASIT ECO 200	207:27:00	212:18:00	35,05

Issues on modelling cracking of massive concrete structures at early-age

Farid BENBOUDJEMA[1], Aveline DARQUENNES[1] et al.
[1]LMT-Cachan/ENS-Cachan/CNRS/Université Paris Saclay

Mismatch of autogeneous/drying strains and coefficient of thermal expansion

Between agregates and cement paste

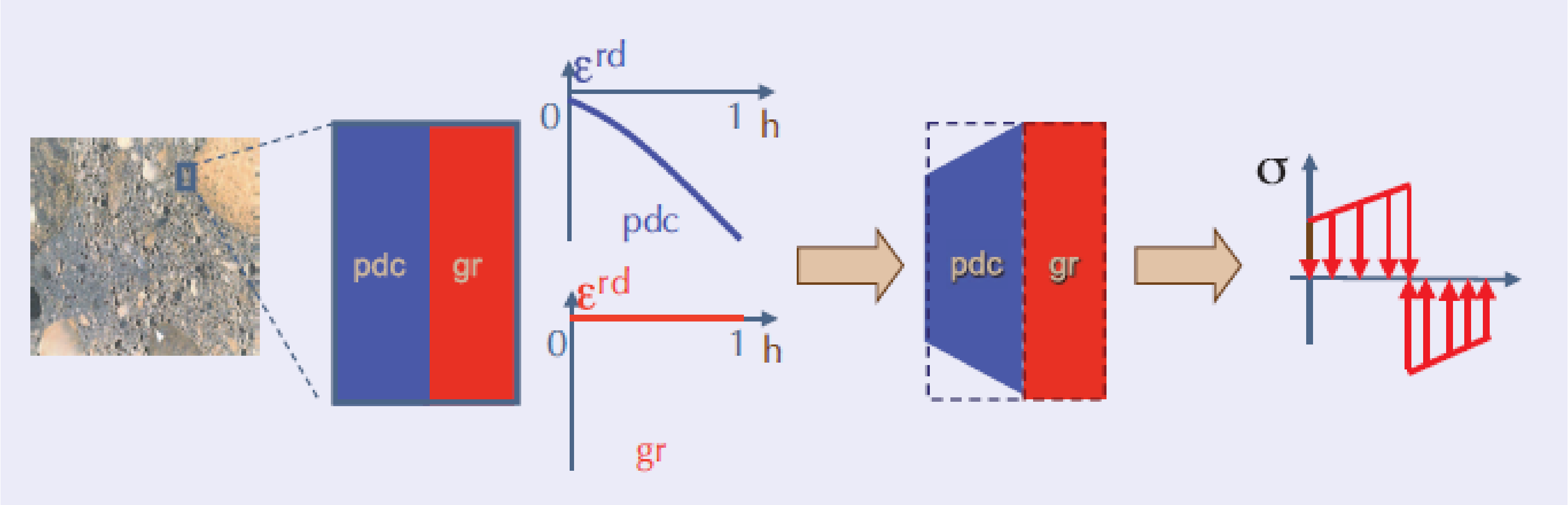

Mismatch of autogeneous/drying strains and coefficient of thermal expansion

Tensile stresses in cement paste / Compressive stresses in Aggregates

4D16

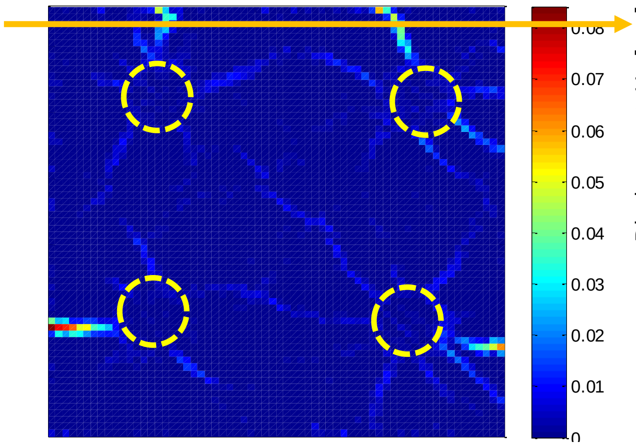

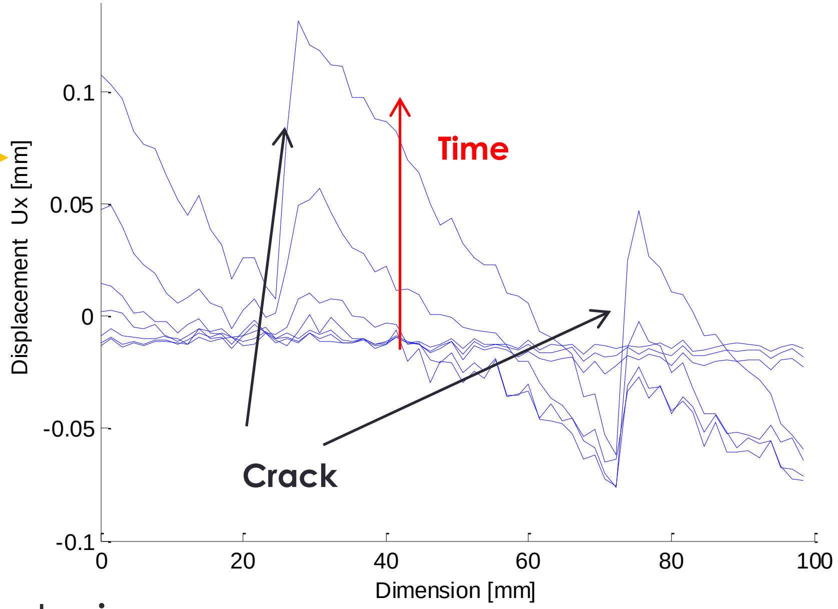

Plot of Mazars equivalent strain

Diffuse cracking? Ambient conditions?, concrete mix, ...?

Stresses generated by self-restraint

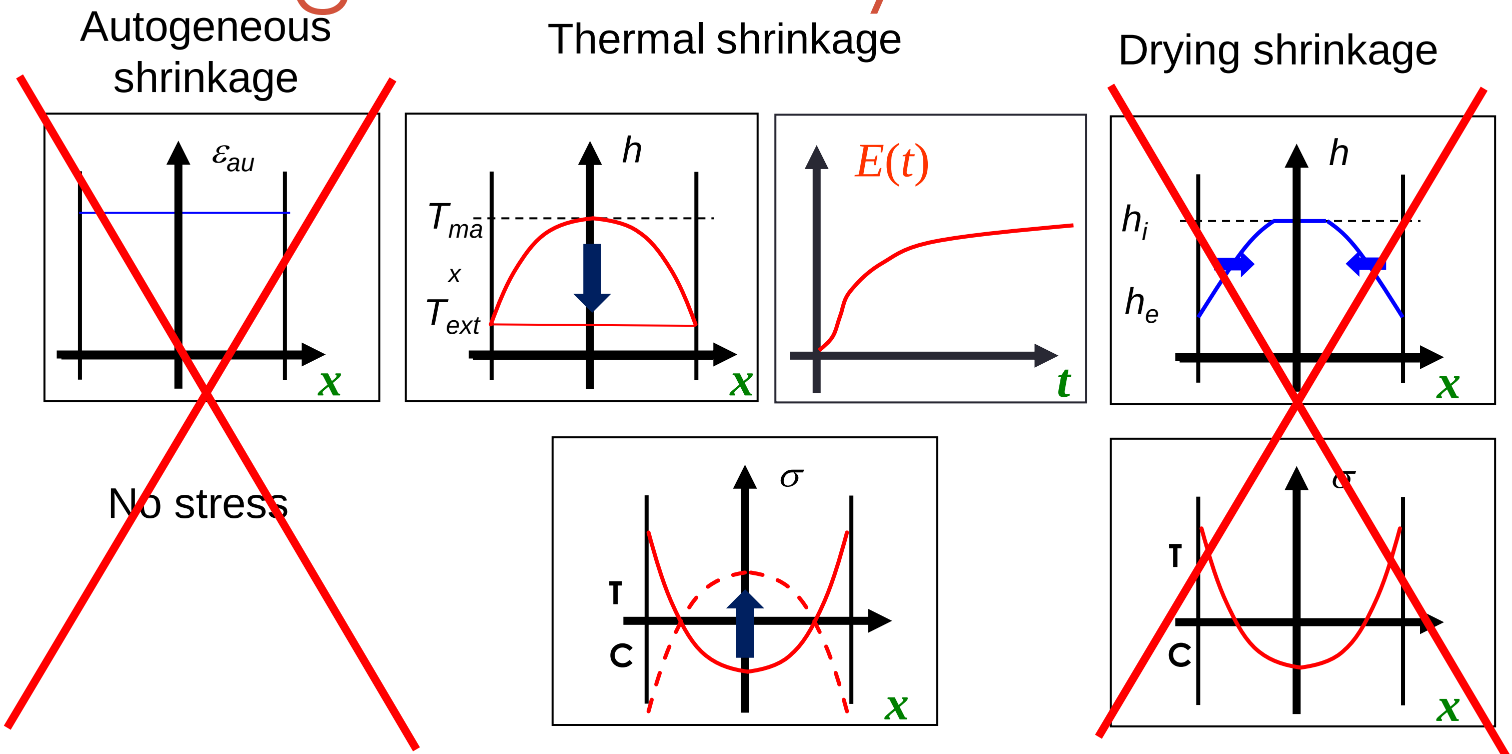

$D_w = 10^{-9}/10^{-12}$ m².s^{-1} / $D_{th} = 10^{-6}$ m².s^{-1}

Superficial cracking mainly driven by gradient of temperature
Ambient conditions, concrete mix, structure size, formwork

Stresses generated by external restraint

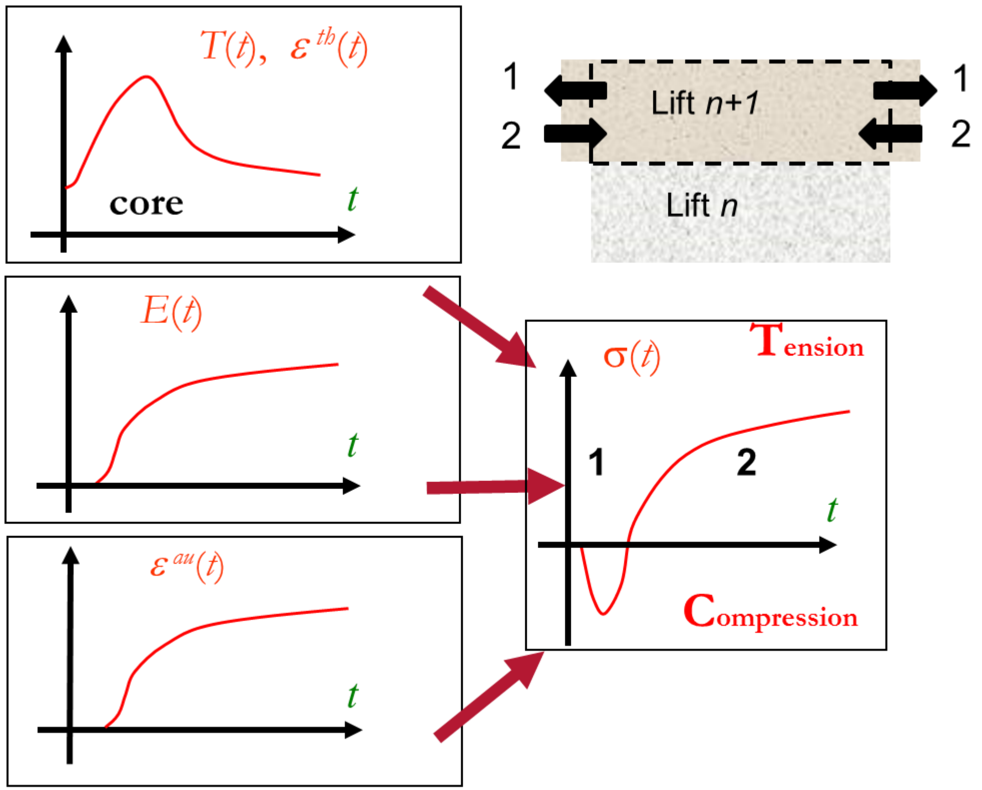

Crossing cracks driven by the maximum reached temperature
Ambient conditions, concrete mix, structure size , formwork

Cracking in massive structures

⇒ **Concrete walls casted during the construction of concrete containments (nuclear powerplant)**

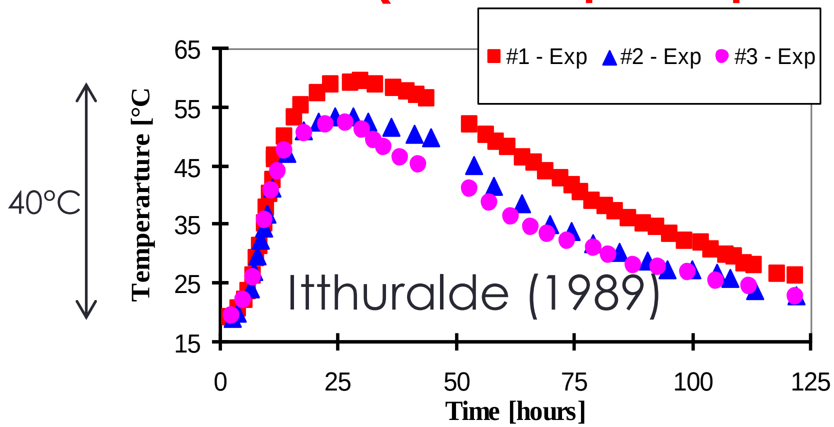

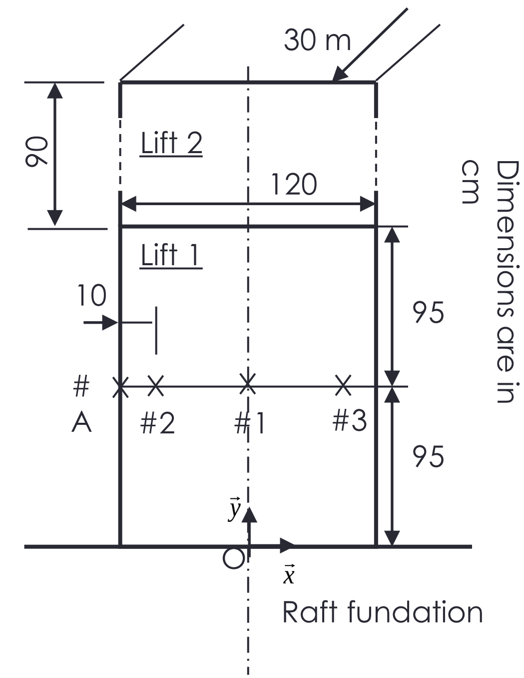

8 cracks, (1×40 µm) + (4×100 µm) + (2×200 µm) + (**1×500 µm**)

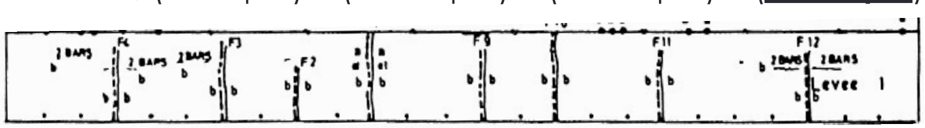

Great reduction
of the tighness

$$Q \approx \frac{w^3\left(p^2 - p_a^2\right)}{24\mu L r T}$$

Design code in Europe

Eurocode EN 1992-1-1
Common building
§ 2.3.3
Deformations of concrete

Consideration should also be given to:

- minimising deformation and cracking due to early-age movement, creep and shrinkage through the composition of the concrete mix;
- if restraints are present, ensuring that their influence is taken into account in design.

No additional information in EN 1992-2 (concrete bridges)

EN 1992-3 (Liquid retaining and containment structures)

Restriction factors, depending on the configuration

Guidelines in Europe (CIRIA …), design code outside Europe (JCI, ACI …)

What we need to predict cracking?

Phenomenological and macroscopic approach

Hydration (thermo-activation)

$$\dot{\xi} = \tilde{A}(\xi)\, e^{-E_a/RT}$$

Heat + exothermy

$$C\frac{\partial T}{\partial t} = \nabla(k\nabla T) + L\dot{\xi}$$

Thermal + Autogeneous shrinkage

$$\dot{\boldsymbol{\varepsilon}}^{th} = \alpha\dot{T}\mathbf{1} \qquad \dot{\boldsymbol{\varepsilon}}^{au} = \kappa\dot{\xi}\mathbf{1}$$

~~**Drying and drying shrinkage**~~

~~$D_w = 10^{-9}/10^{-12}\ m^2.s^{-1}$ / $D_{th} = 10^{-6}\ m^2.s^{-1}$~~

Couplings

$$\dot{\sigma} = E(\xi)(1-D)\left(\dot{\varepsilon} - \dot{\varepsilon}^{th} - \dot{\varepsilon}^{au} - \dot{\varepsilon}^{bc}\right)$$

$$f(\sigma,\xi) \le 0$$

Young modulus and tensile strength vary with hydration degree.

Basic, ~~drying~~ creep …

$$\tau^i_{bc}\ddot{\varepsilon}^i_{bc} + \left(\tau^i_{bc}\frac{\dot{k}^i_{bc}(\xi)}{k^i_{bc}(\xi)} + 1\right)\dot{\varepsilon}^i_{bc} = \frac{\dot{\tilde{\sigma}}}{k^i_{bc}(\xi)} \qquad \tilde{\sigma} = \eta^i_{bc}(\xi)\dot{\varepsilon}^j_{bc}$$

Mechanisms for creep and shrinkage are still not well identified …

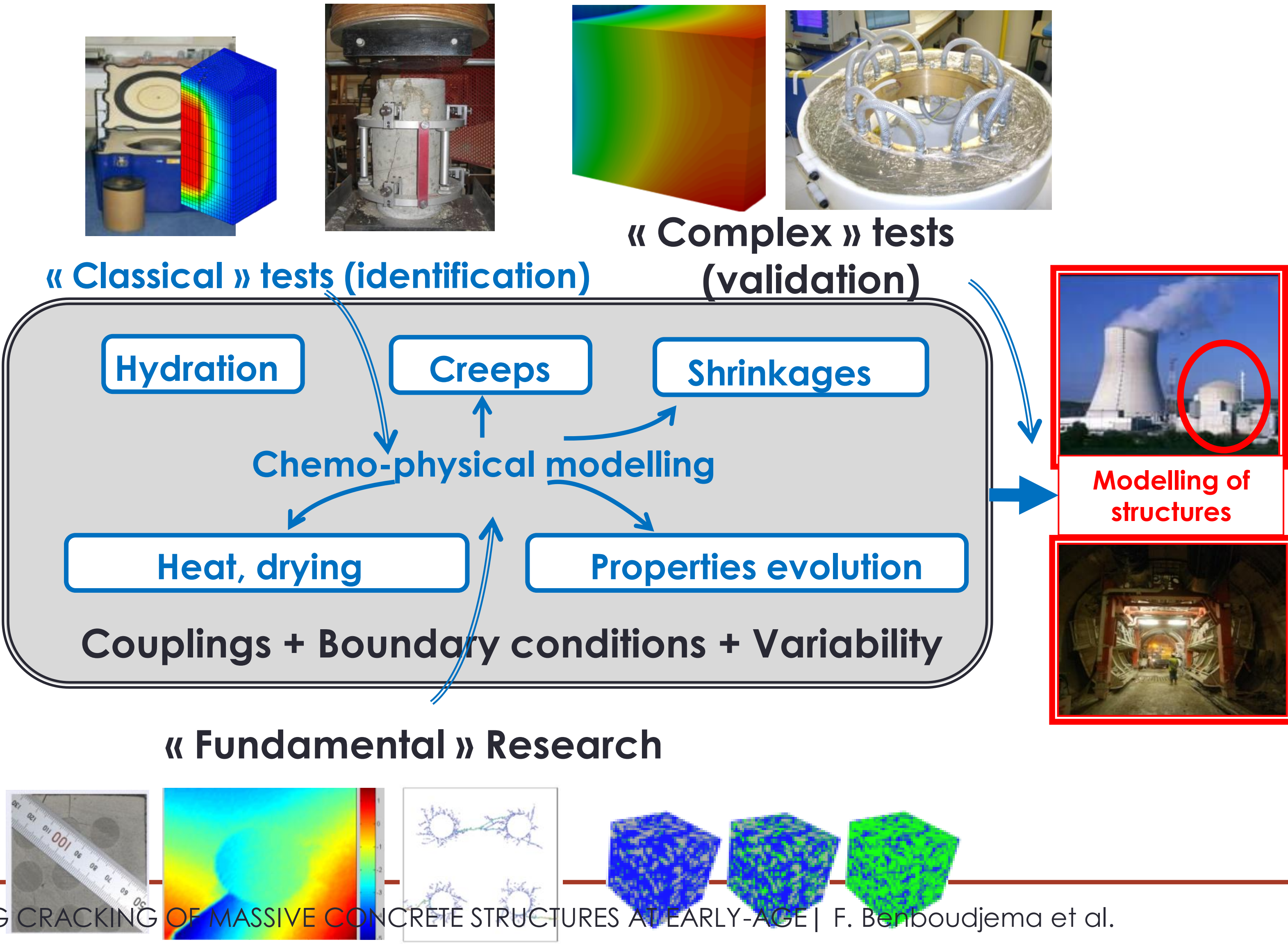
« Classical » tests (identification)
« Complex » tests
(validation)
Hydration
Creeps
Shrinkages
Chemo-physical modelling
Heat, drying
Properties evolution
Couplings + Boundary conditions + Variability
Modelling of
structures
« Fundamental » Research

Some results on structures

Creep and CTE effects

Comparison of basic creep in direct tension and compression

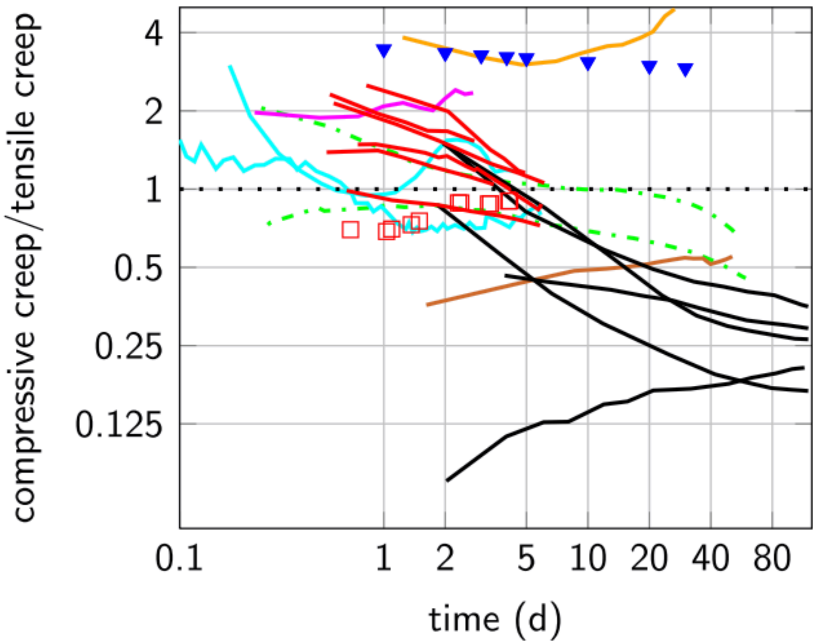

Creep in compression is higher than in tension

Creep in tension is higher than in compression

A. Hilaire PhD thesis

Most of time, data are available in compression
Code models suppose same creep

Influence of creep and its asymmetry

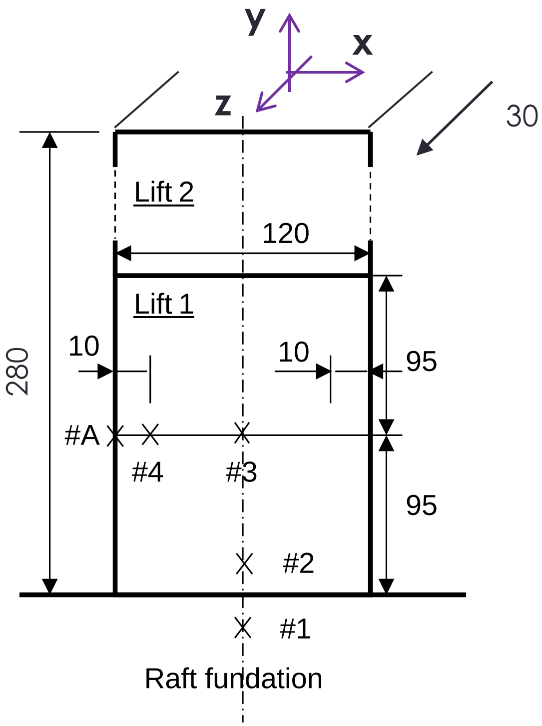

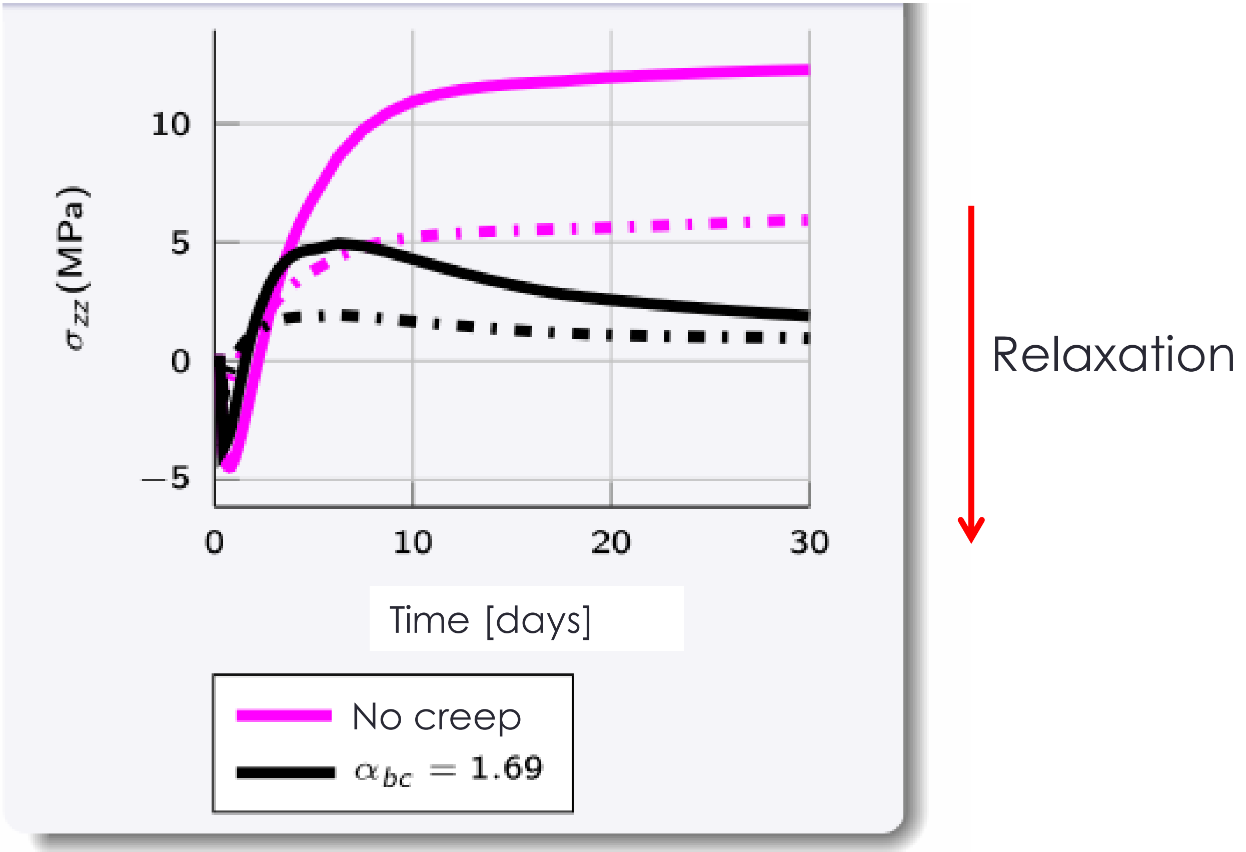

Influence of creep and its asymmetry

$$\alpha = \frac{\text{Creep in tension}}{\text{Creep in compression}}$$

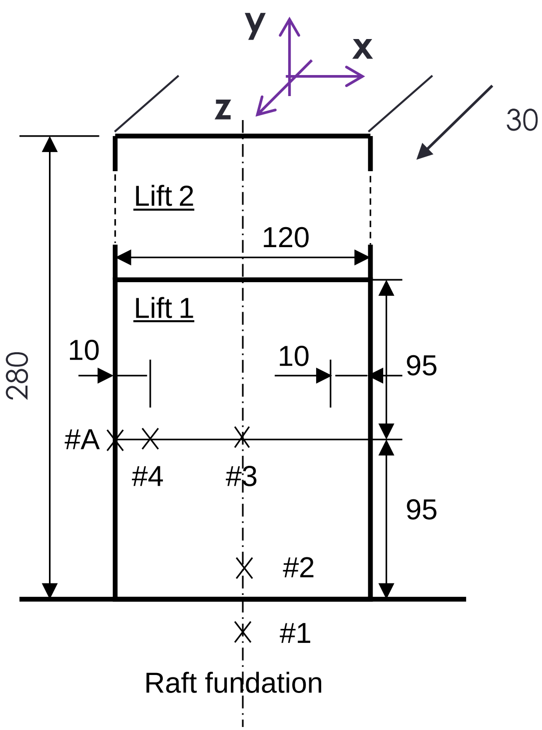

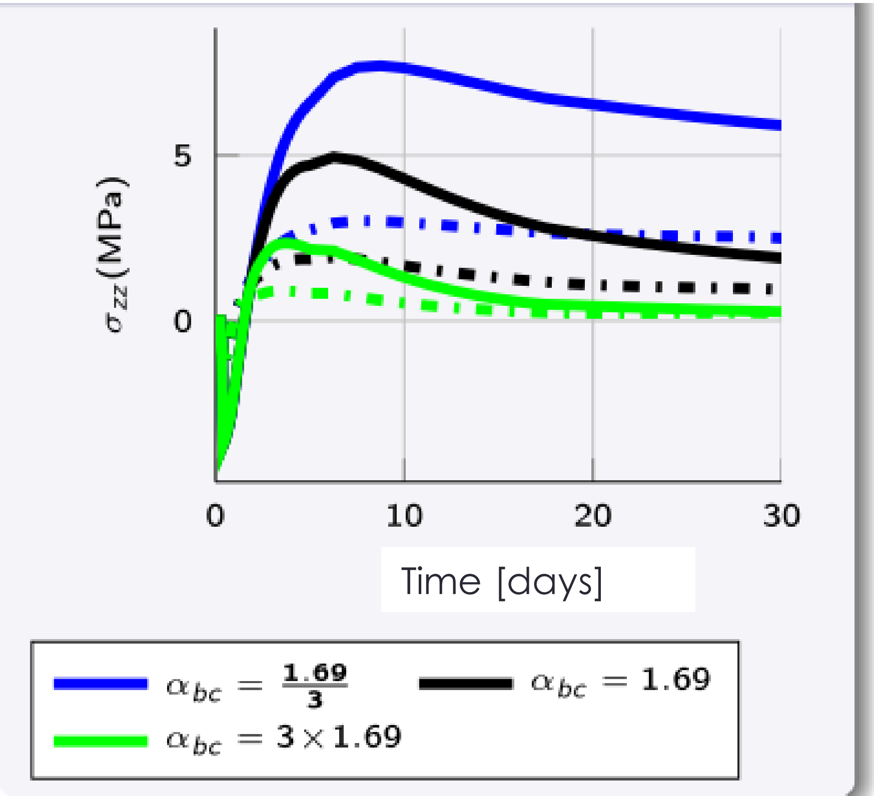

Same effects for other stresses (gradient)

Influence of creep and its asymmetry

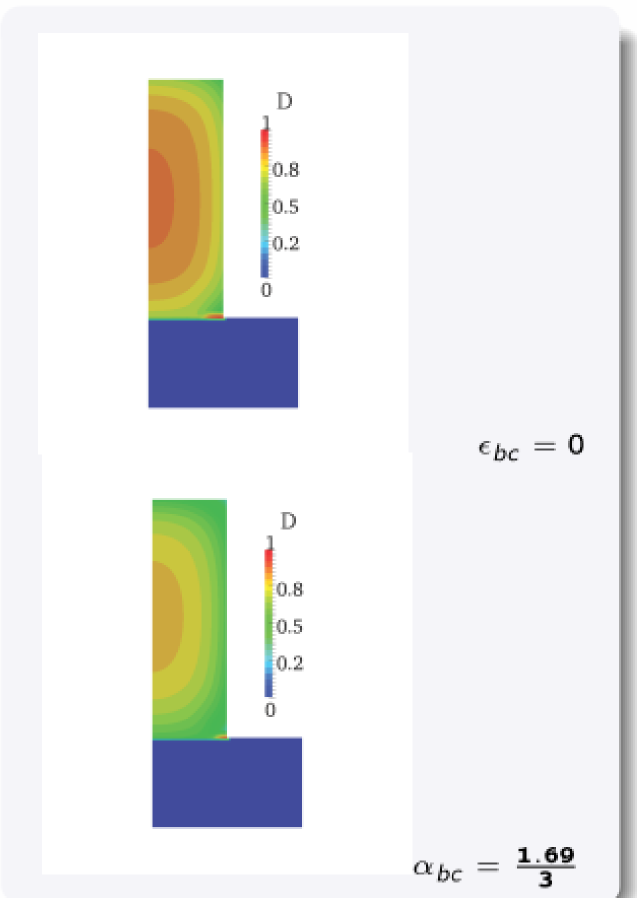

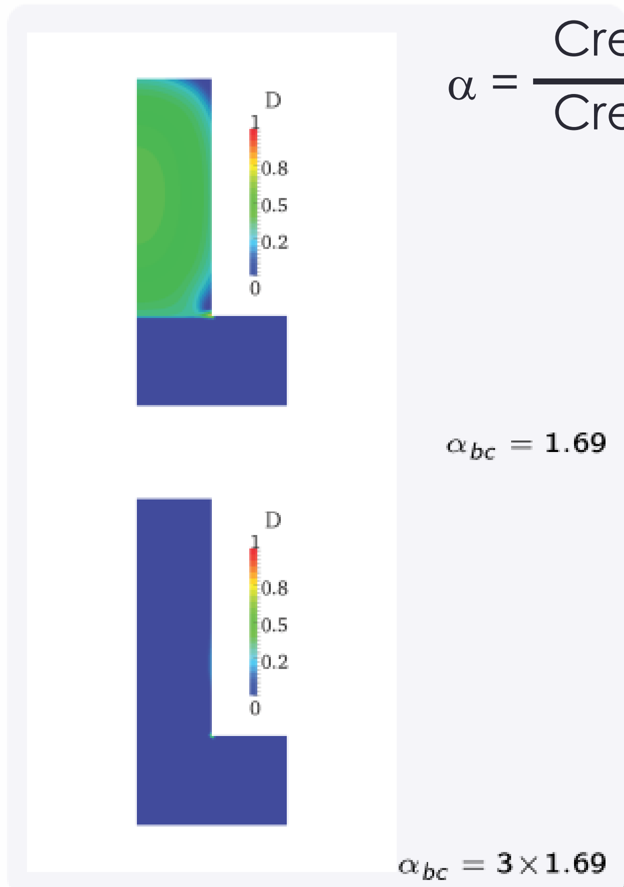

$$\alpha = \frac{\text{Creep in tension}}{\text{Creep in compression}}$$

Damage (cracking) fields

Effect of CTE variations at early age

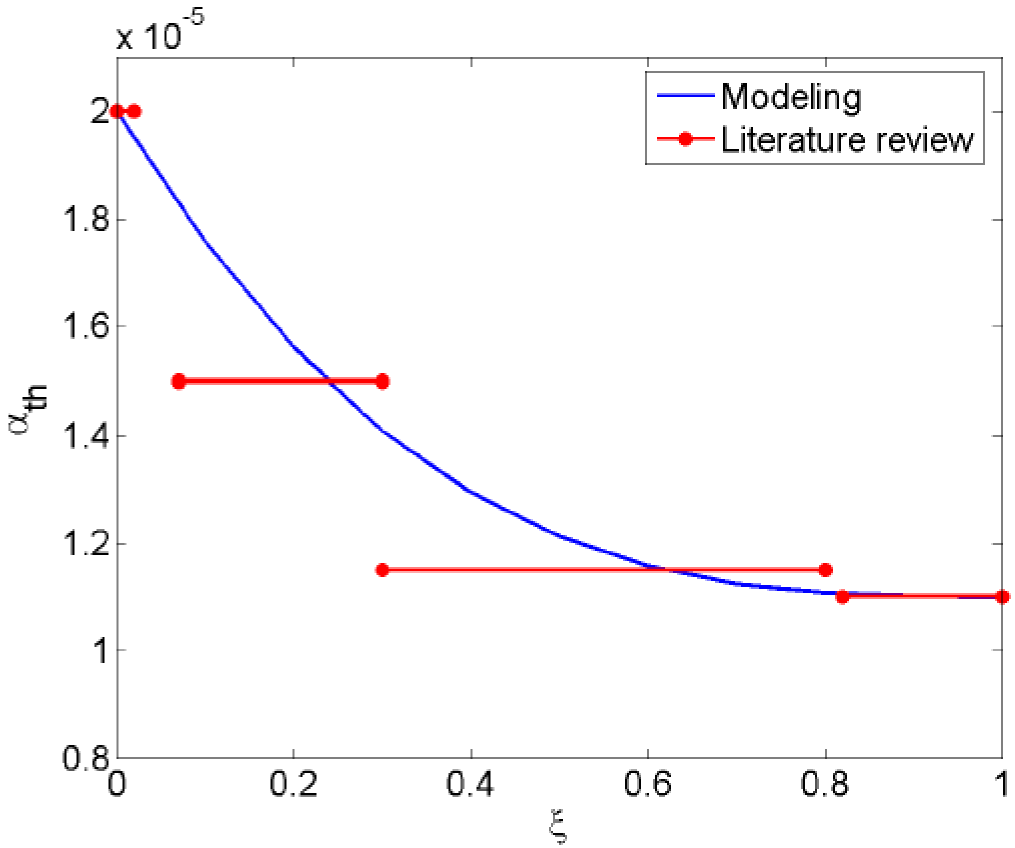

[De Schutter, 1996]

Effect of CTE variations at early age

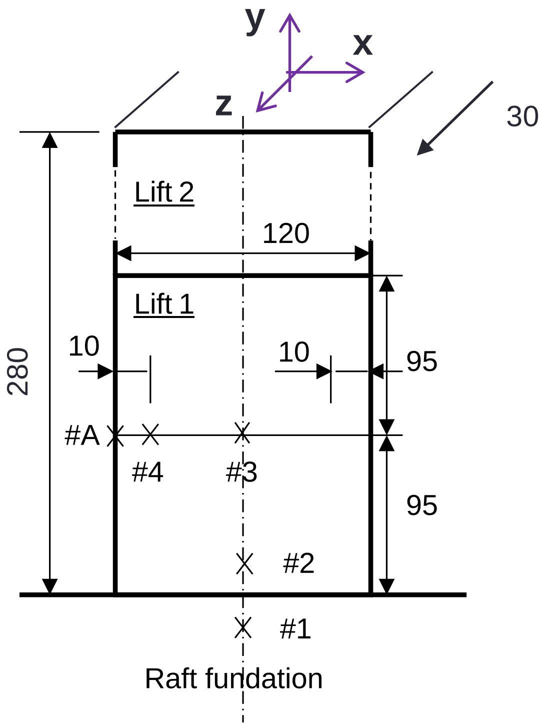

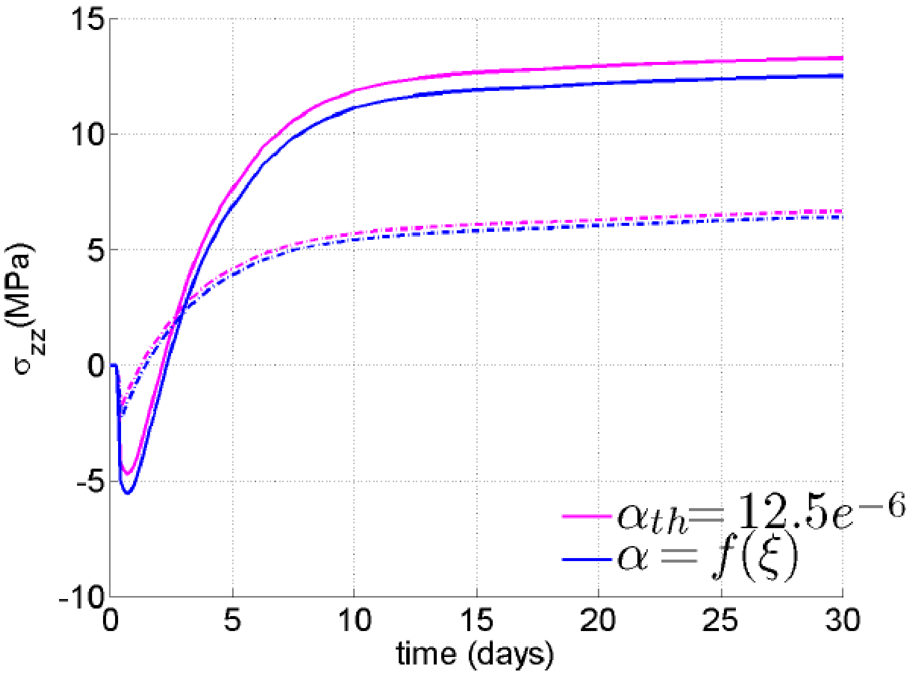

Same effects for other stresses (gradient)

A. Hilaire PhD thesis

Effect of CTE variations at early age

ECOBA mock-up

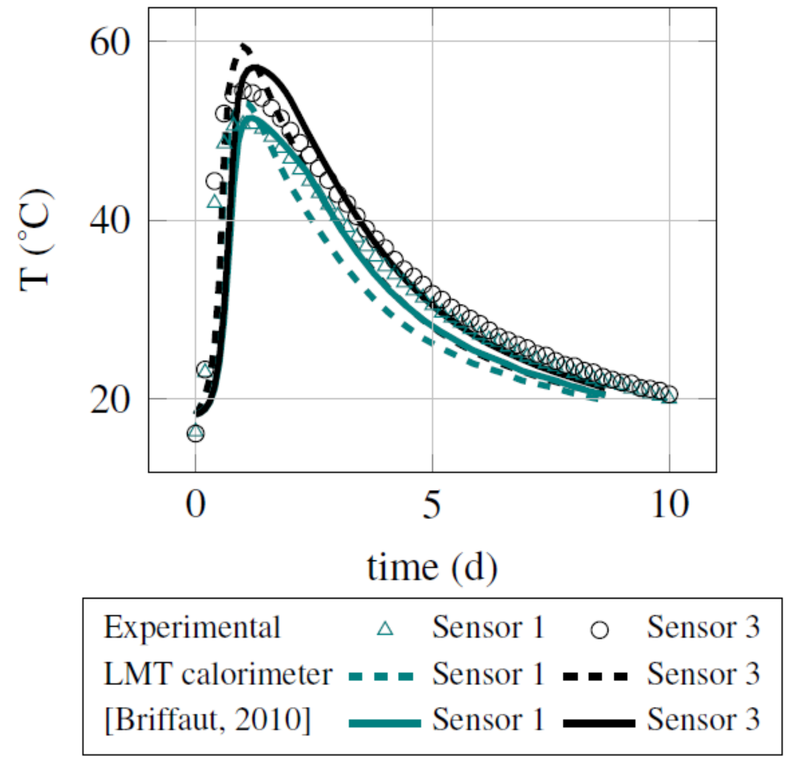

Effect of CTE variations at early age

ECOBA mock-up

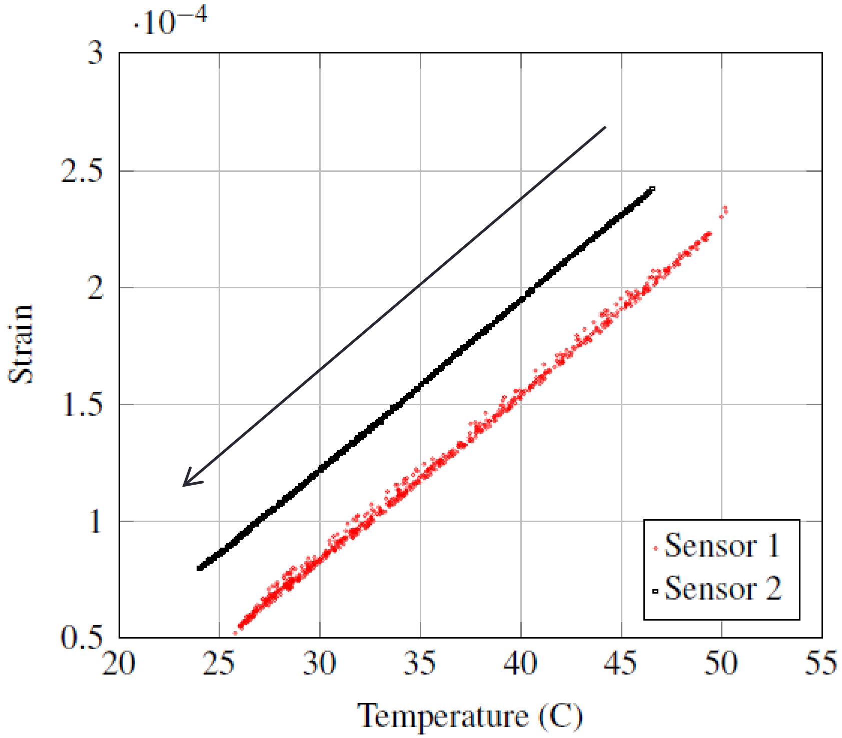

Mismatch of autogeneous/drying shrinkage and coefficient of thermal expansion

On the "structural scale"

Reinforced concrete ties (HA 12)

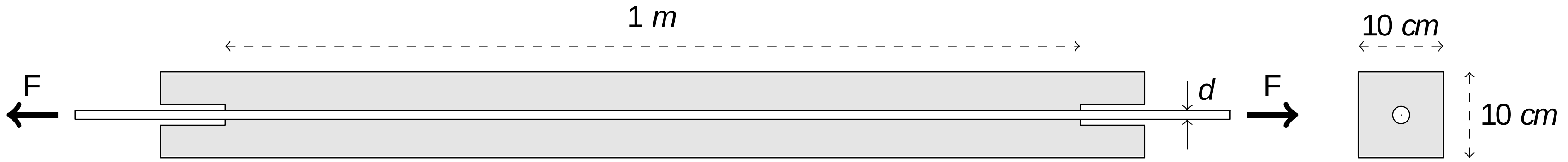

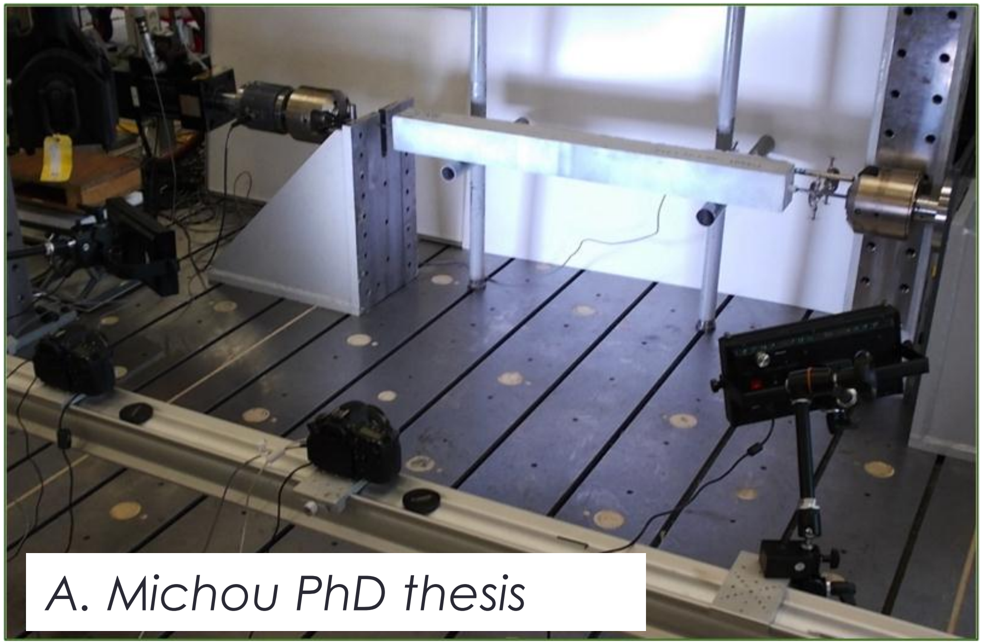

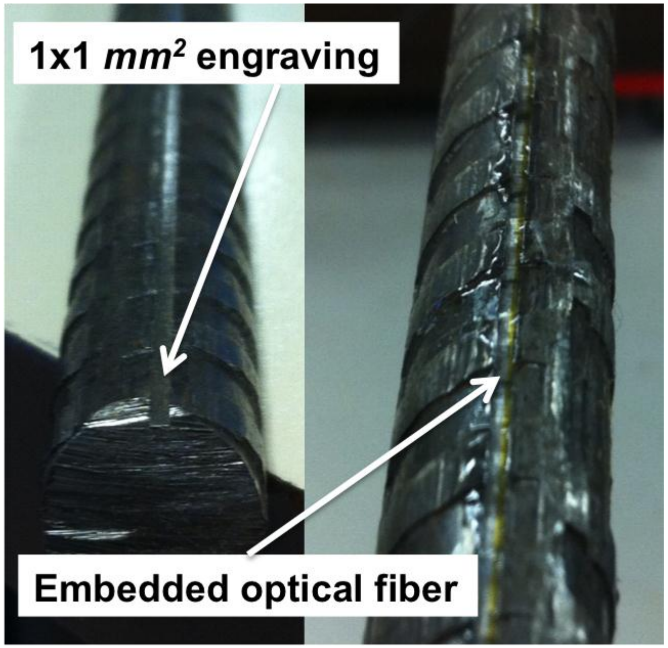

Reinforced concrete ties (HA 12)

Identification of material parameters on compression/tension tests for concrete, steel/concrete interface (pull-out)

↳

Numerical simulations

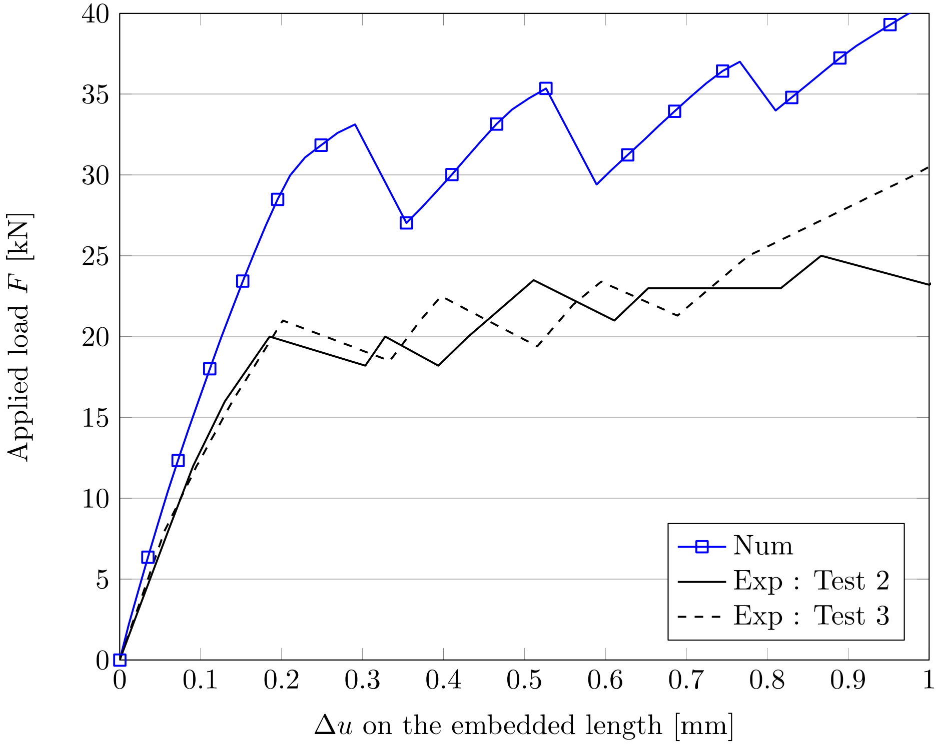

Reinforced concrete ties (HA 12)

$$\epsilon_{tot} = \epsilon_{elas} + \epsilon_{re} + \epsilon_{rd} + \epsilon_{fp} + \epsilon_{fd}$$

Shrinkage tests

Creep tests

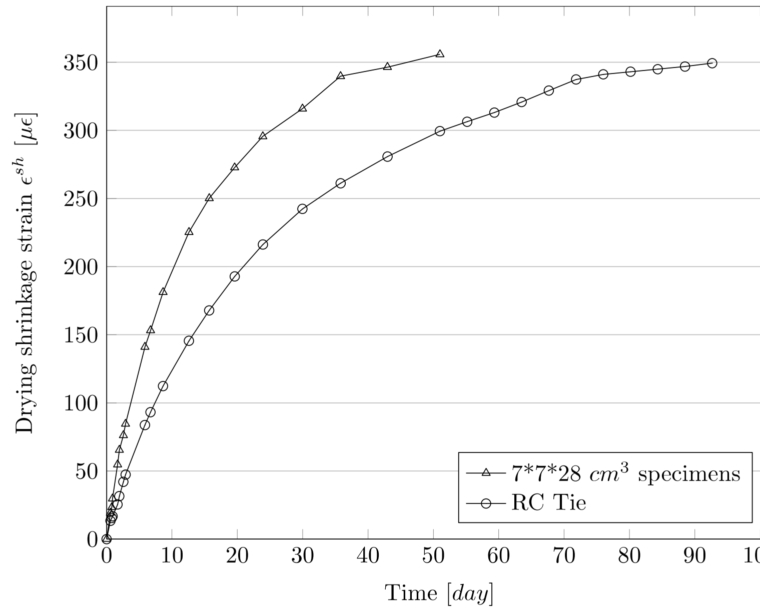

Size effect on shrinkage

Numerical simulations

Reinforced concrete ties (HA 12)

Prior to loading, effect of shrinkage restraint

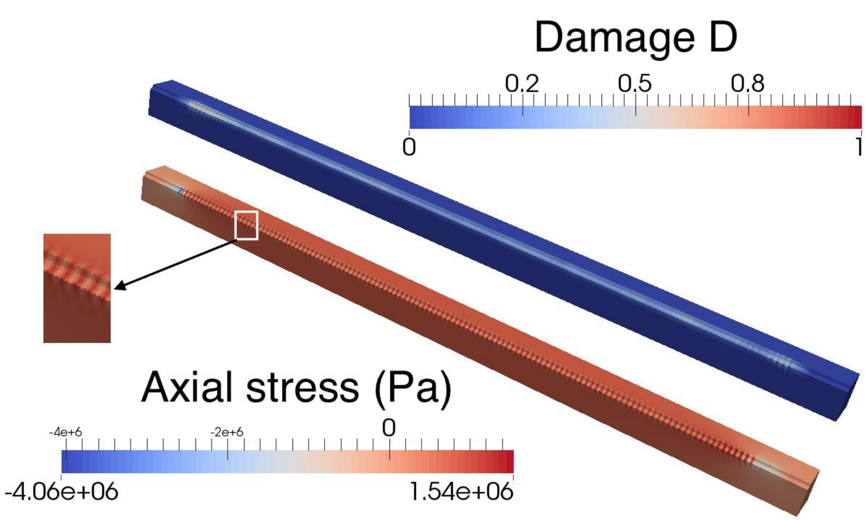

The effect is significant and depends on the reinforcement ratio

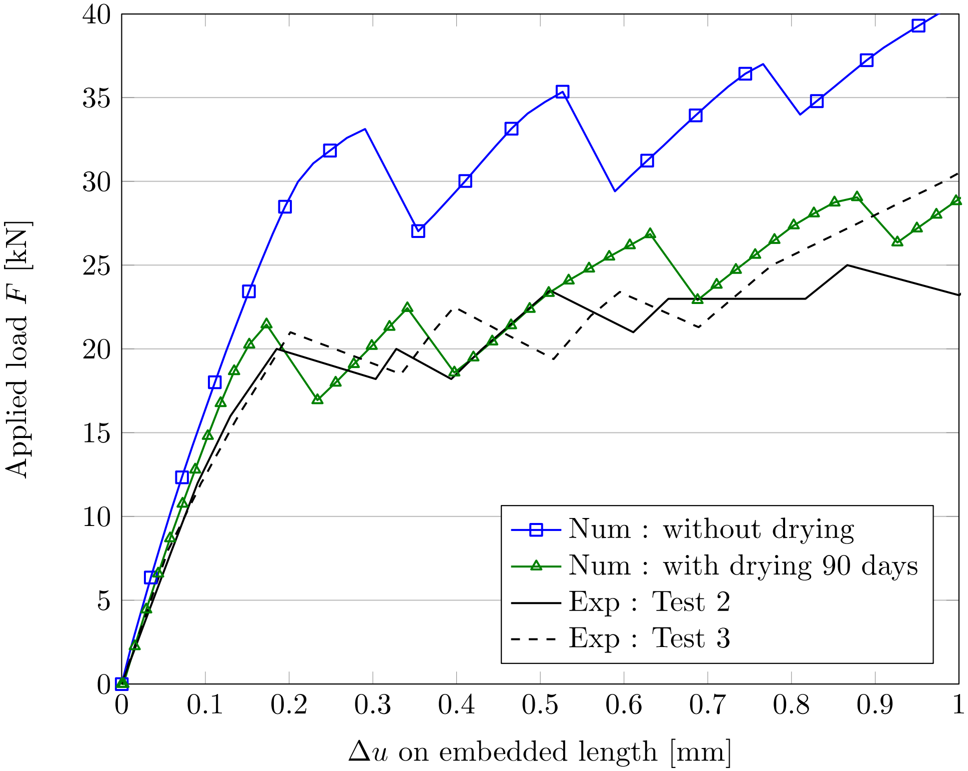

Of course reinforcement has a positive impact !

Mismatch of autogeneous/drying shrinkage and coefficient of thermal expansion

Meso-scale approach

Volumic finite elements

Truss elements

Adapted mesh — Non-adapted mesh (projection of properties on a mesh)

Interface elements — No interface elements — Interface elements

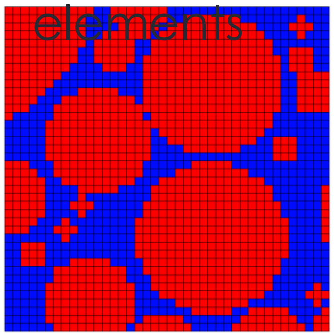

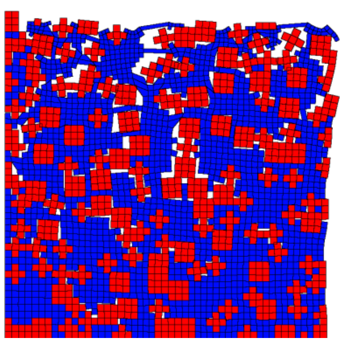

M. Briffaut PhD thesis

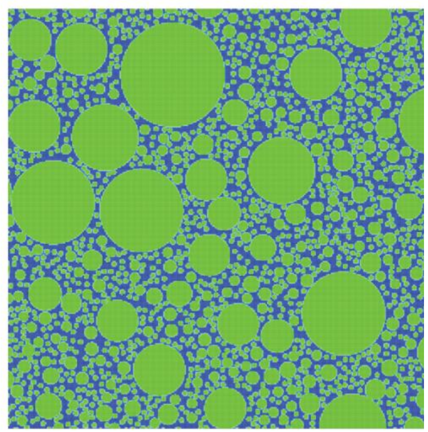

Collaboration with C. Laborderie (Univ. Pau)

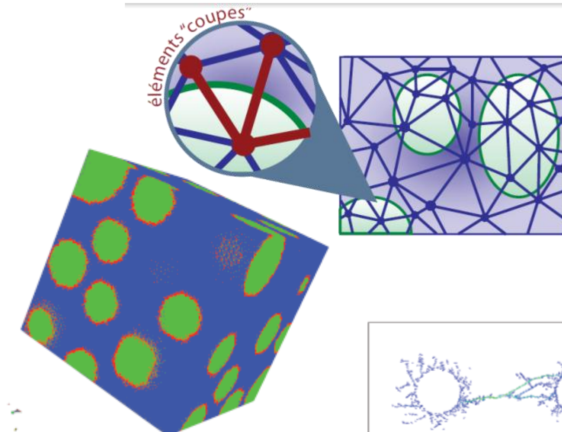

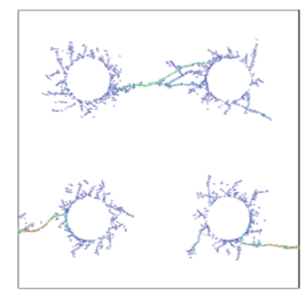

Collaboration with J.-B. Colliat (Univ. Lille)

- ✓ Influence of the concrete mix (ordinary and high performance)
- ✓ Influence of mechanical boundary conditions and temperature evolution

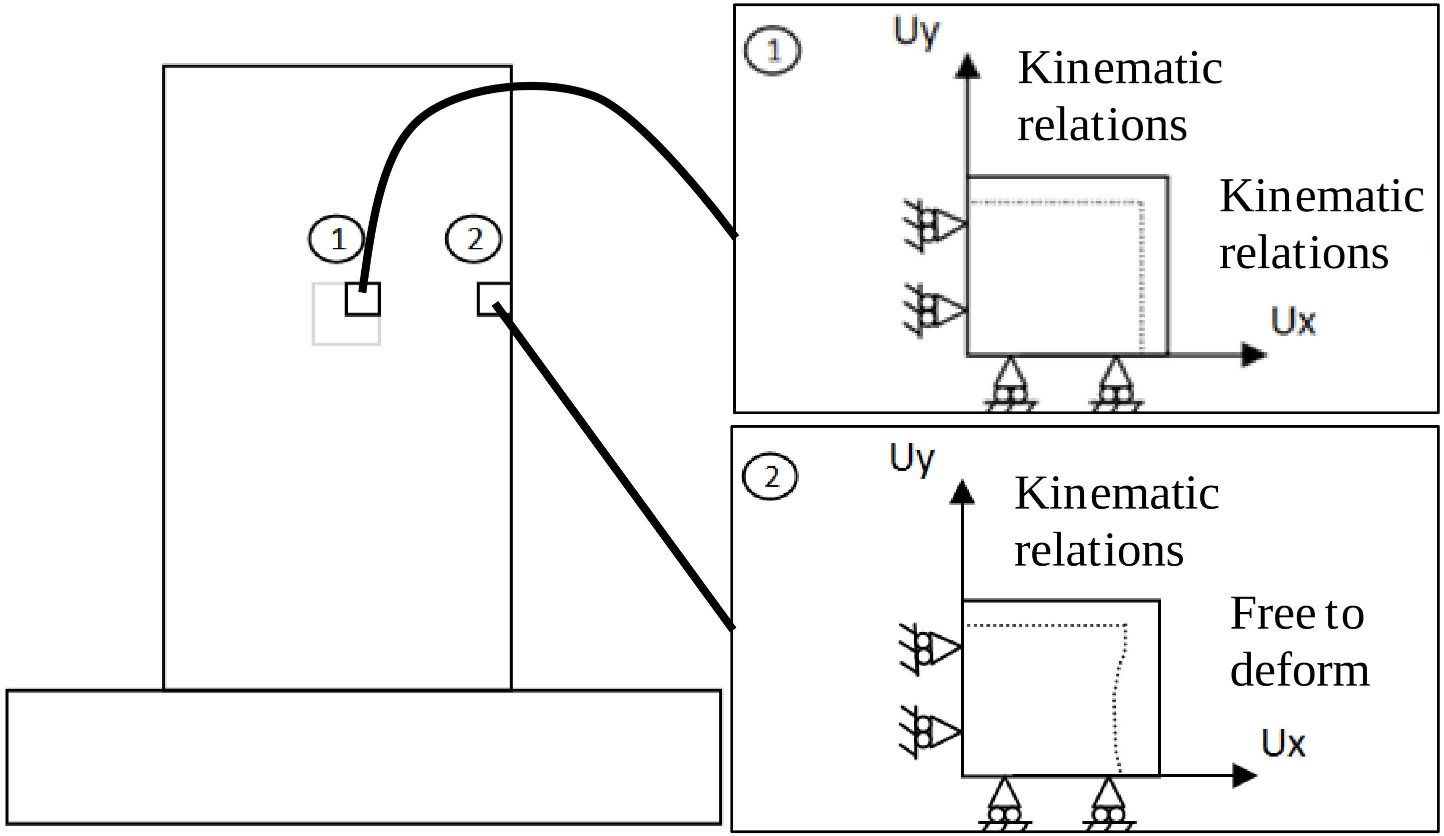

- ✓ Influence of the concrete mix (ordinary and high performance)
- ✓ Influence of mechanical boundary conditions and temperature evolution

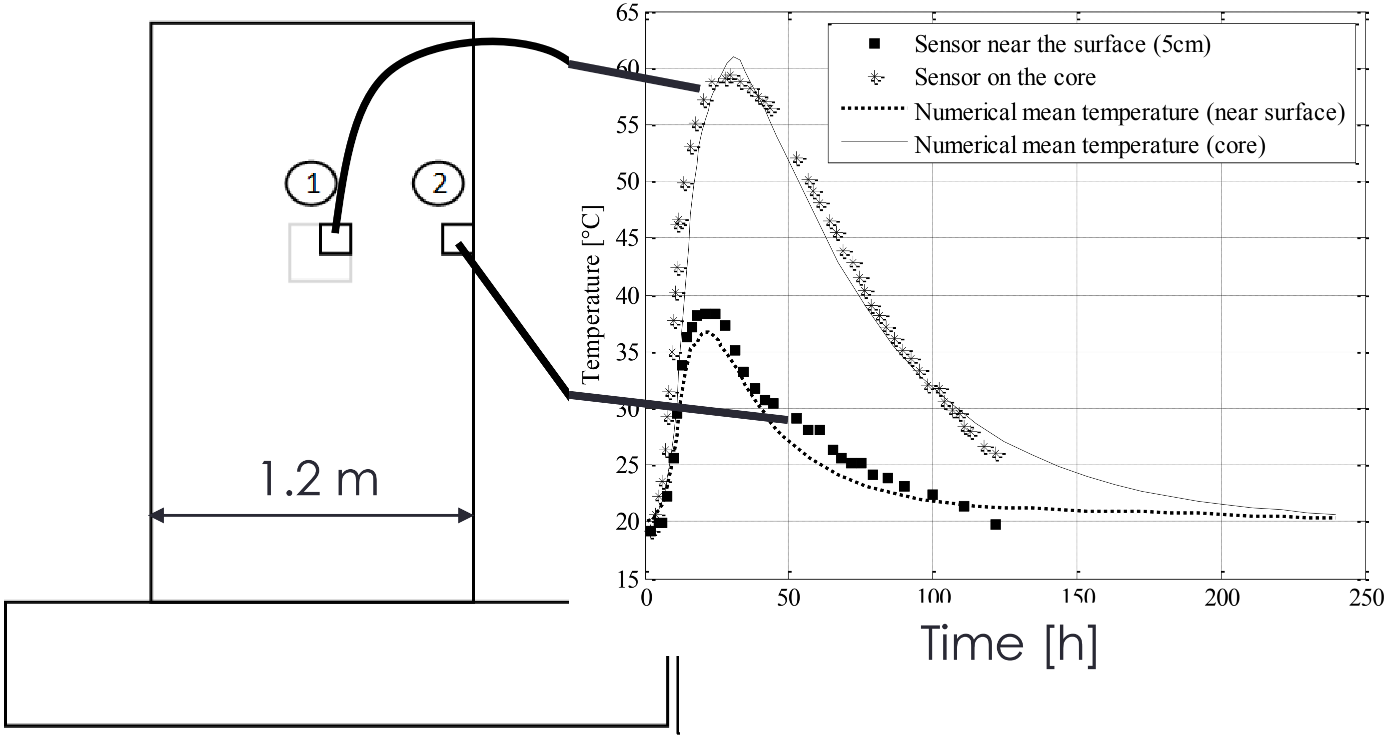

Evolution of the damage field (D) during hydration (in the core)

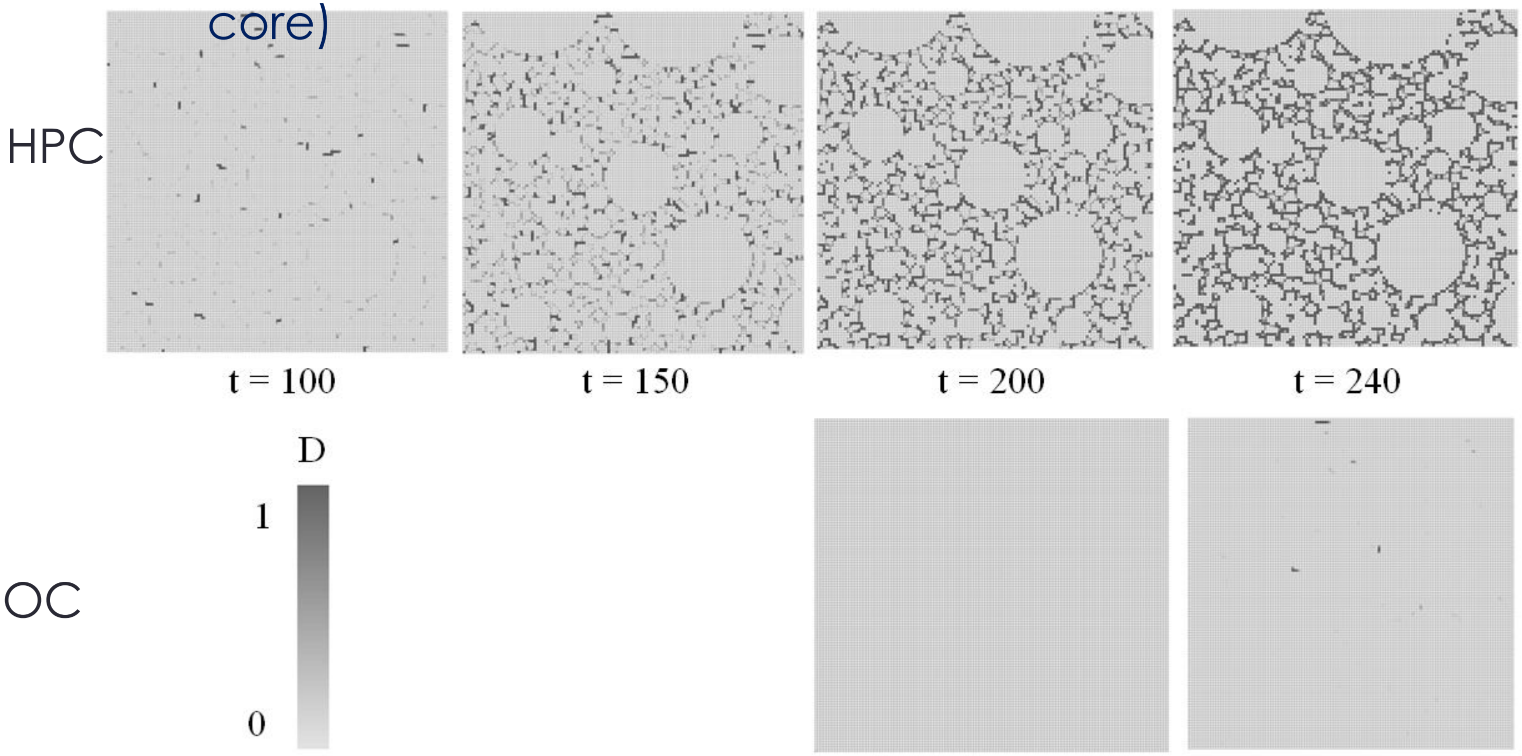

- **Initiation around aggregates**
- **HPC undergoes larger damage since autogeneous shrinkage and temperature increase are larger**

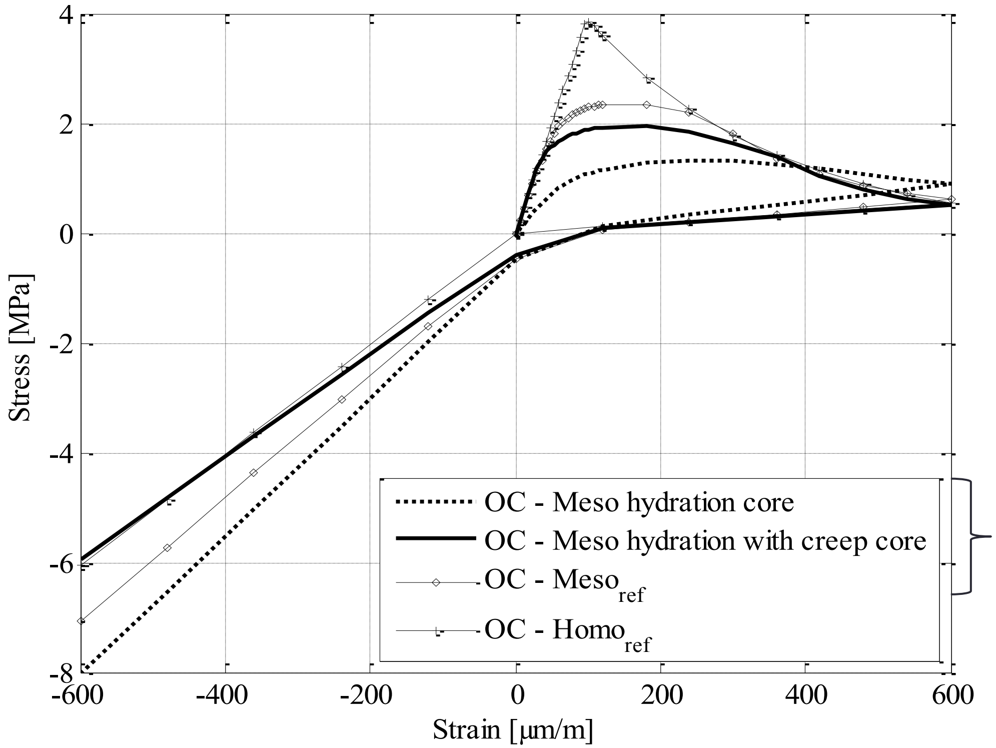

Finite element calculations volumetric mixing law

- Significant decrease of mechanical material parameters and shape of the behavior law, similar to what it is observed at high temperature
- Creep of cement paste has a great positive effect
- Larger (unrealistic) reduction in the case of HPC (*not presented*) : loss of “potentiality” for better properties with a loading in tension ?

Conclusions

- Autogeneous shrinkage induces in an uniform manner damage due to strains incompatibilities between cement paste and aggregates
- Shrinkage restraint of steel rebars can be significant
- Mastering asymmetry of creep in tension/compression is of great importance ! But not CDT evolution at early-age?

Perspectives

- Effect of self-healing?
- Adaptation of the model to mineral admixtures (slag …) with the study of the impact of expansion

CMS Workshop “Cracking of massive concrete structures”

March 17, 2015, ENS-Cachan

Cachan, Île-de-France, FRANCE

Early age modeling of low-pH concrete: Application to the behavior of nuclear waste storage structures

Laurie Buffo-Lacarrière[1], Alain Sellier[1]

[1]Université de Toulouse; UPS, INSA; LMDC (Laboratoire Matériaux et Durabilité des Constructions); 135, avenue de Rangueil; F-31 077 Toulouse Cedex 04, France

Laboratoire Matériaux et Durabilité des Constructions

La maîtrise des déchets radioactifs

Context: Nuclear waste storage structures

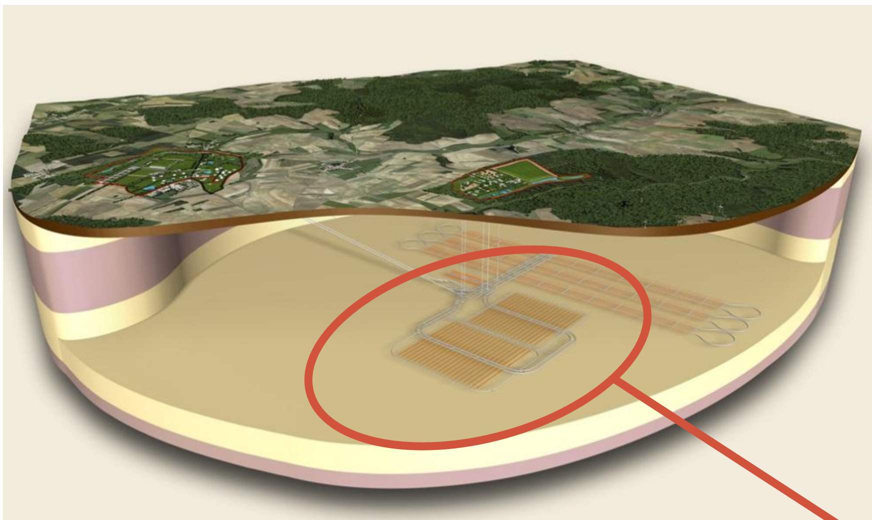

Deep underground repository:

⇒ 500 m underground tunnels

⇒ Callovo-Oxfordian geological formation

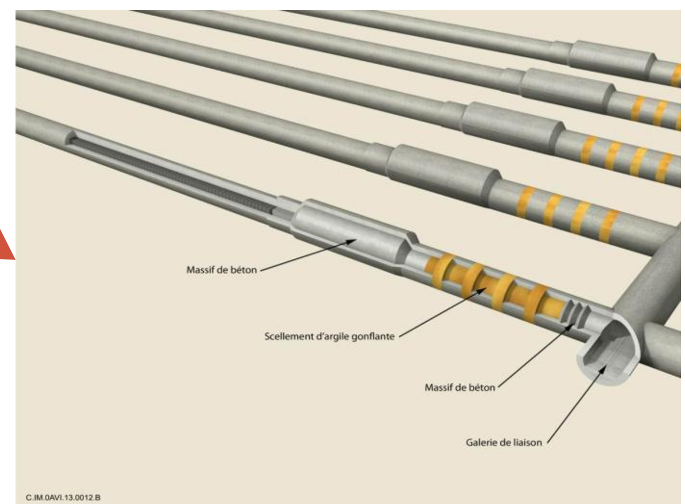

⇒ Rock = barrier for radio-nuclide transport

⇒ Concrete used for the mechanical stability of the storage

- **Tunnels sealing systems**

High-expansion bentonite + Concrete

⇒ Bentonite: barrier for nuclides

⇒ Concrete: bentonite confinement

But: high pH leads bentonite to loose its confinement properties

=> Use of low pH concrete

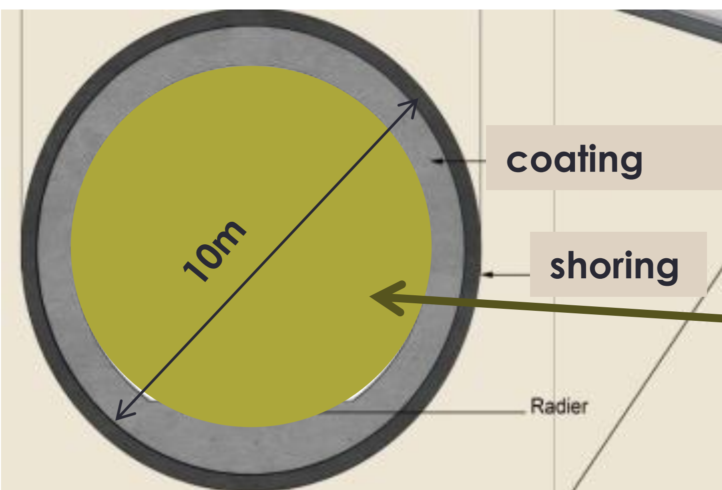

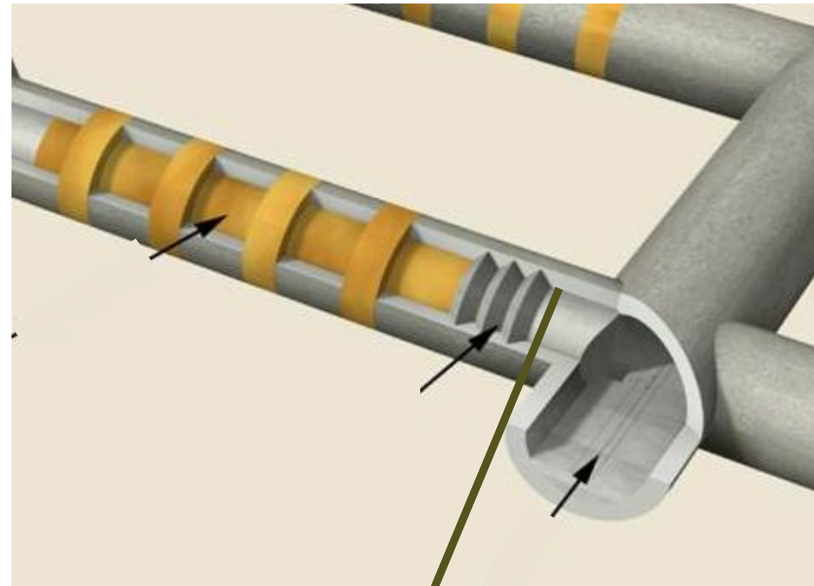

Massive concrete block casted to close the tunnel

- **Tunnels sealing systems**

Low pH concrete:

=> high substitution of cement by mineral additions

(W/C=0,43)	**% in binder**
CEM I	20
Silica Fume	32
Slag	48

Paste composition

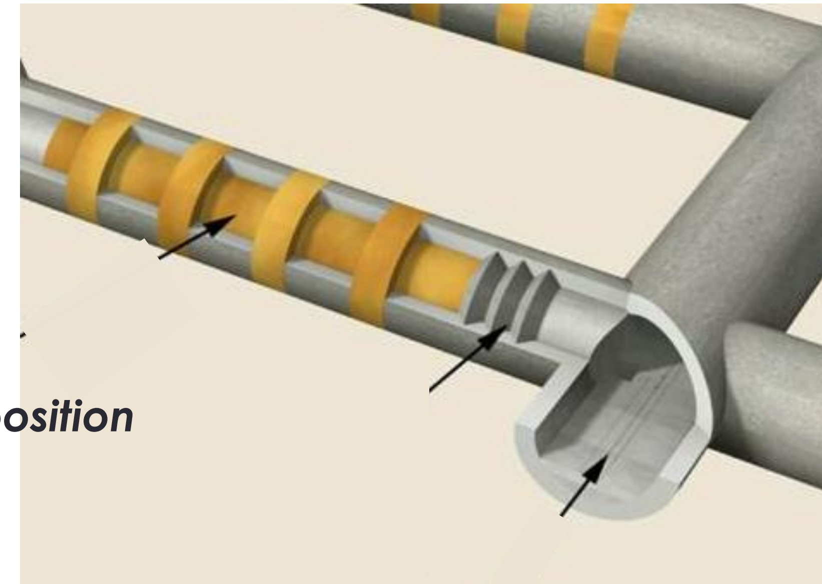

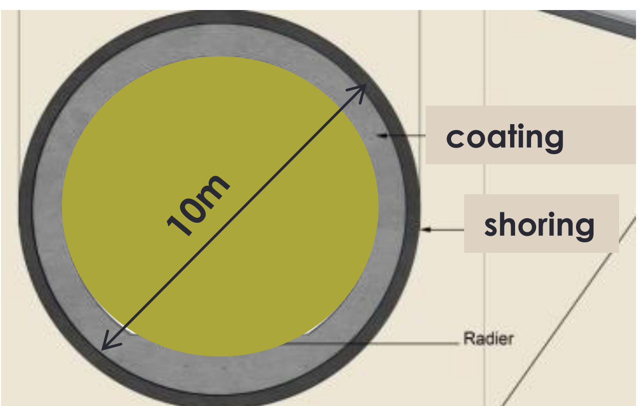

- **Study objectives**

Prediction of paste evolution for low pH concrete

Simulation of the induced early age behaviour in the blocks of sealing system

Early age structure + Restraining = Cracking risk

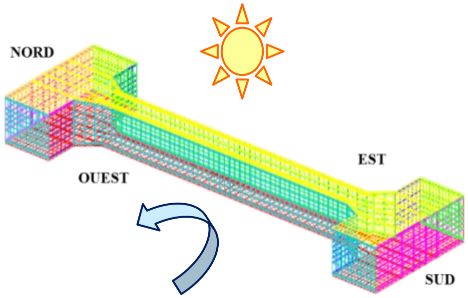

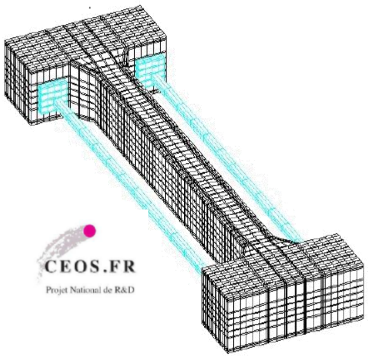

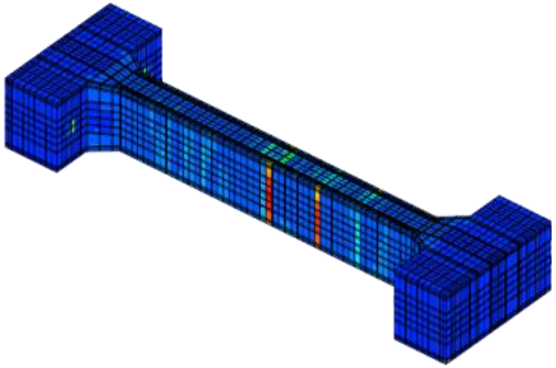

<u>Driving process</u>:
Cement hydration

⇒ Temperature increase
⇒ Water consumption
⇒ Hydrate development

Multiphasic hydration model

Model adapted to low pH cement

<u>Mechanical response</u>:

⇒ Stresses induced by internal or external restraining
⇒ Variation of mechanical properties

Mechanical model with creep + Chemo-mechanical couplings

Outline

- General principle of early age modeling
- Hydration model for composed binder
- Application of the early age THCM model to nuclear waste storage structures

Hydration model for composed binders

Principle of multiphasic model

- **Coupled solving of hydration, temperature and water variations**
  - Strong coupling T/C and H/C

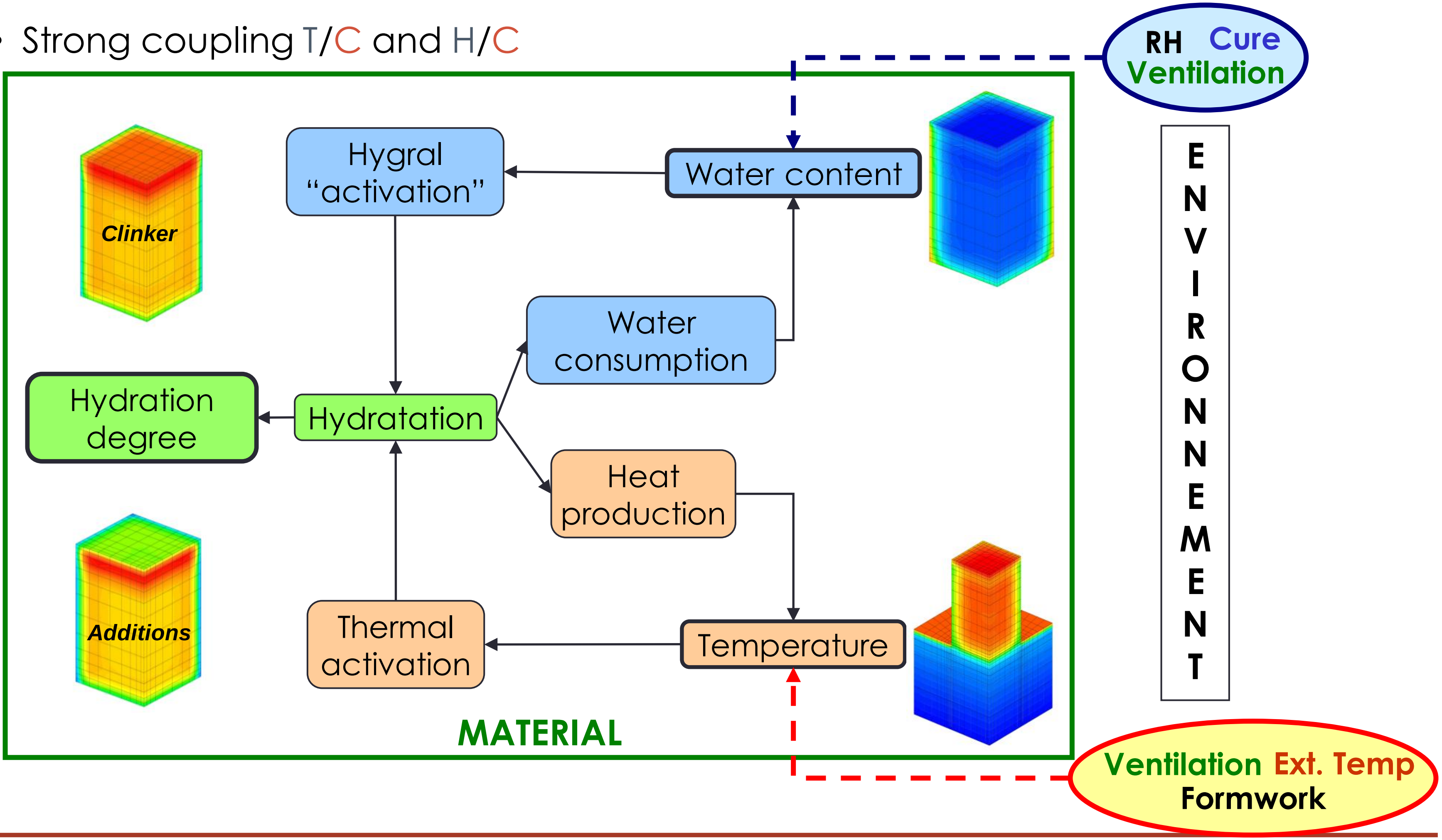

Principle of multiphasic model

- **Coupled solving of hydration, temperature and water variations**
  - Strong coupling T/C and H/C

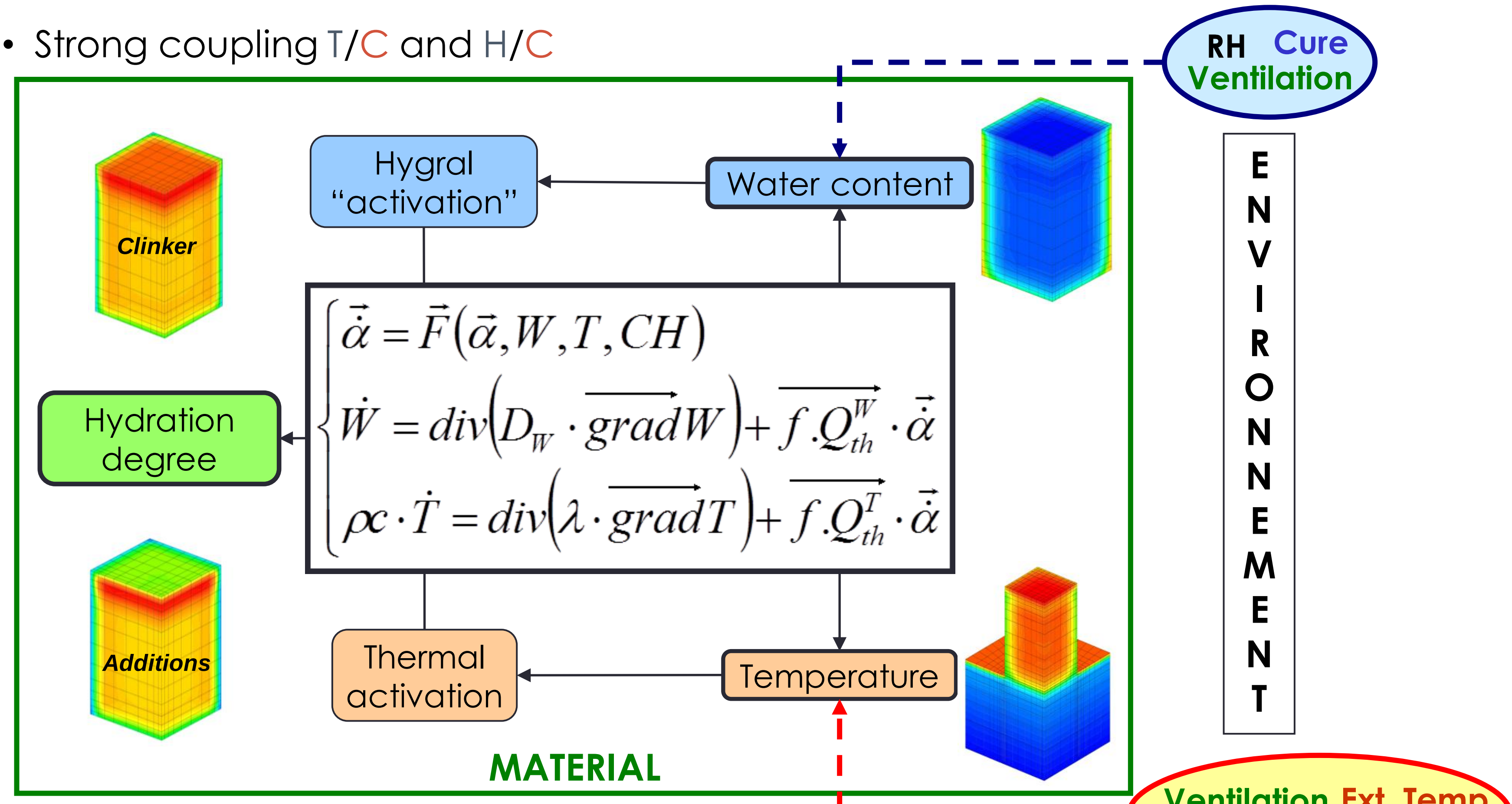

Originality: separate kinetic law for cement and additions

Kinetic law for each anhydrous

- **Individual law needed due to different activation energies**

⇒ Temperature variations have more effects on additions' kinetic

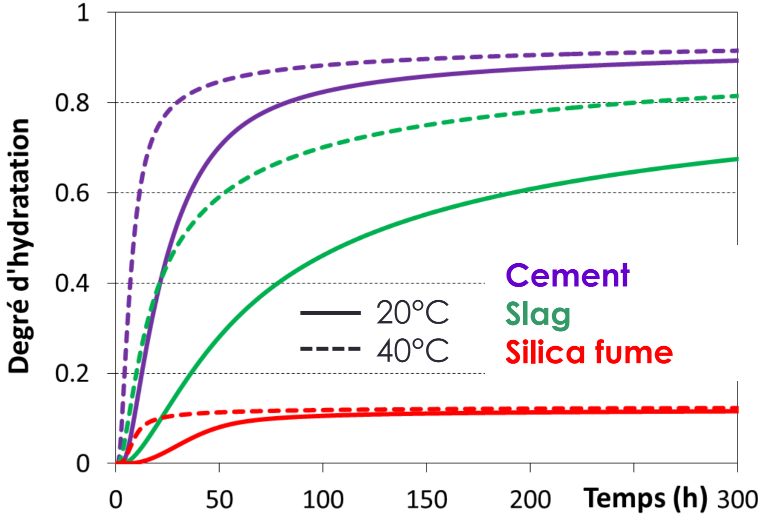

- **Phenomenological law**

$$\dot{\alpha}_i = K_i \cdot g_i(\alpha, W) \cdot \Pi_i(\bar{r}_m) \cdot h_i(T) \cdot s_i(Ca)$$

Chemical activation of dissolution

Activation of precipitation (addition reactions)

Water accessibility to anhydrous

Thermal activation

Interaction clinker/additions

- **Strong coupling between kinetics and T/W balance equation**
  - Reactions influence T and W variations
  - In return T and W variations affect each kinetic law

- **Additional internal variables**
  - Porosity
  - Calcium hydroxide content (effect on additions' kinetic)

Chemical activation of dissolution

Activation of precipitation (addition reactions)

$$\dot{\alpha}_i = K_i \cdot g_i(\alpha, W) \cdot \Pi_i(\bar{r}_m) \cdot h_i(T) \cdot s_i(Ca)$$

Water accessibility to anhydrous

Thermal activation

Specificities of slag blended cement

Calcium needed to produce slag hydrates can come from :
- CaO present in anhydrous slag
- CH produced by cement hydration

Hydrate stoichiometry is affected by portlandite content

➔ Necessity of a scalable stoichiometry of CASH produced by slag

Stoichiometry of slag hydrates

Slag

S, $\bar{S}$, A,F, M, C

$$\frac{\partial C_L}{\partial \alpha_L} = k_L(t)\frac{\partial C_{tot}}{\partial \alpha_L} \qquad \frac{\partial CH}{\partial \alpha_L} = k_C(t)\frac{\partial C_{tot}}{\partial \alpha_L}$$

$C_6A\bar{S}_3H_{32}$, C_4AH_{13}
M_5AH_{13}
$CSAH_L$

$$\frac{C}{S}_L(t) = k_L(t)\frac{C}{S}_{Lp} + k_C(t)\frac{C}{S}_C$$

Cement

C, S, $\bar{S}$, A,F

CSH_C
$C_3(A,F)H_6$
$C_6(A,F)\bar{S}_3H_{32}$
$C_4(A,F)\bar{S}H_{12}$

CH

Higher C/S ratios for CASH with CH

Calcium taken from CH when % of slag decreases

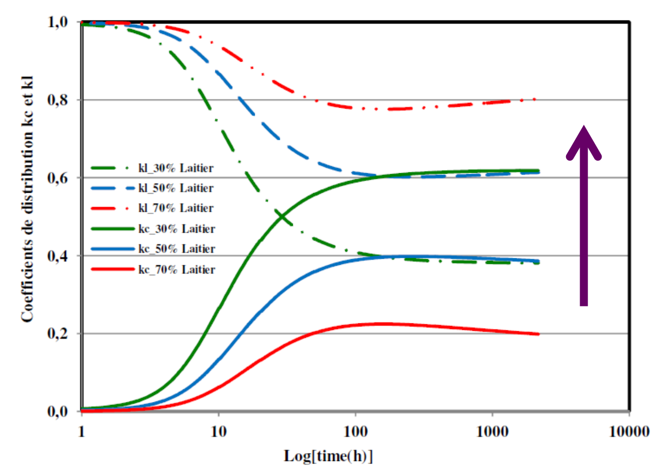

Distribution coefficient function of the probability to encounter CH and CaO

$$\begin{cases} k_C(t) = \dfrac{CH(t)}{CH(t)+C_L(t)} \\ k_L(t) = \dfrac{C_L(t)}{CH(t)+C_L(t)} \end{cases}$$

Validation on experimental results

- **Validation of stoichiometry of slag hydrates**
  - Measurements of C/S ratios for slag blended cement (Richardson 1992)
  - Calculation of the mean C/S ratio of paste from hydration model

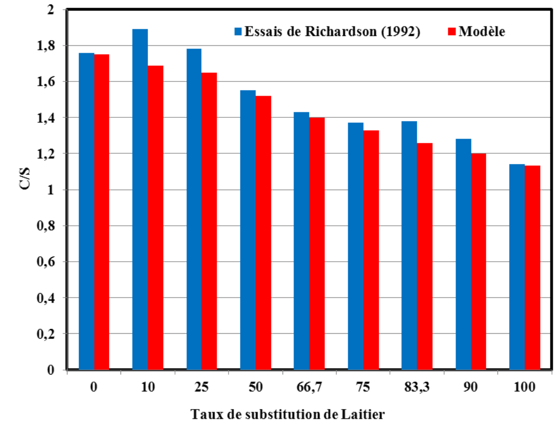

- **Validation of kinetic**
  - Fitting parameters determined using 2 calorimetric test (0% and 70% slag)
  - Prediction without re-fitting of binders with 0%, 30%, 50% and 70% of slag

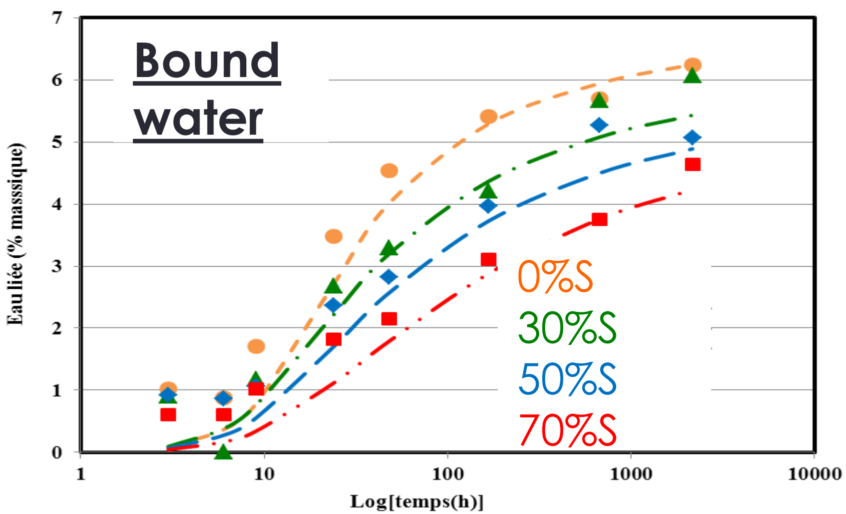

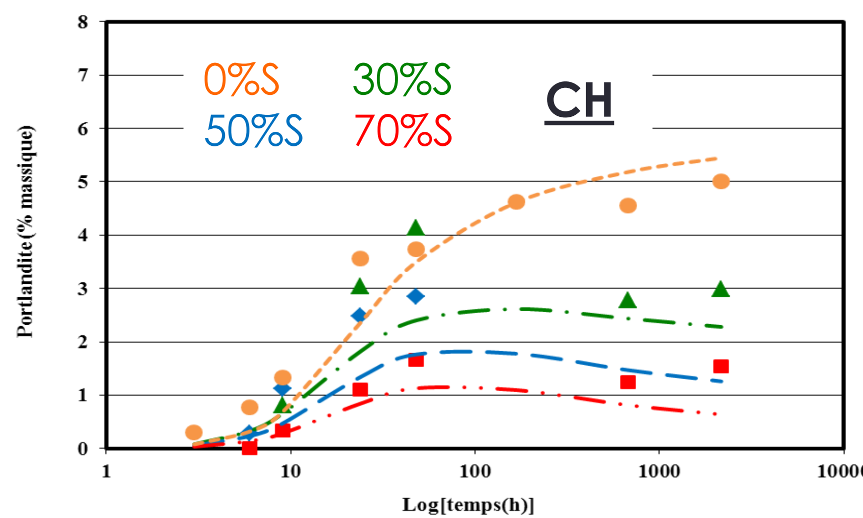

Early age mechanical model

General approach for early age modeling

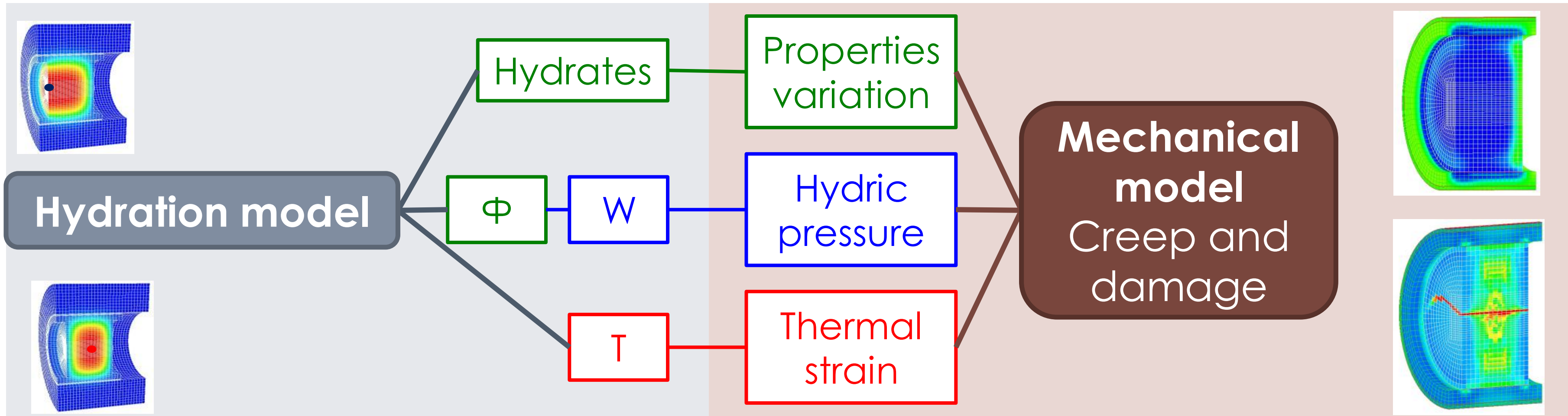

- **Mechanical model needed**
  - Prediction of induced stresses using a rheological model
  - Prediction of crack and damage state using a damage model (*not presented in this presentation*)

  \+ *Adaptation to hardening concrete*

Rheological model

Visco-elastic creep model

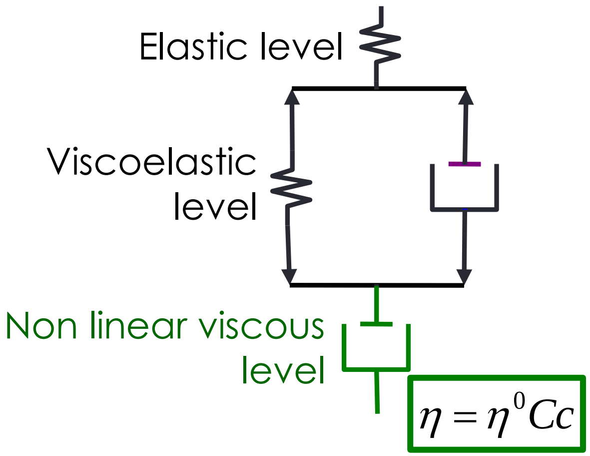

Modification vitesse de fluage par consolidation

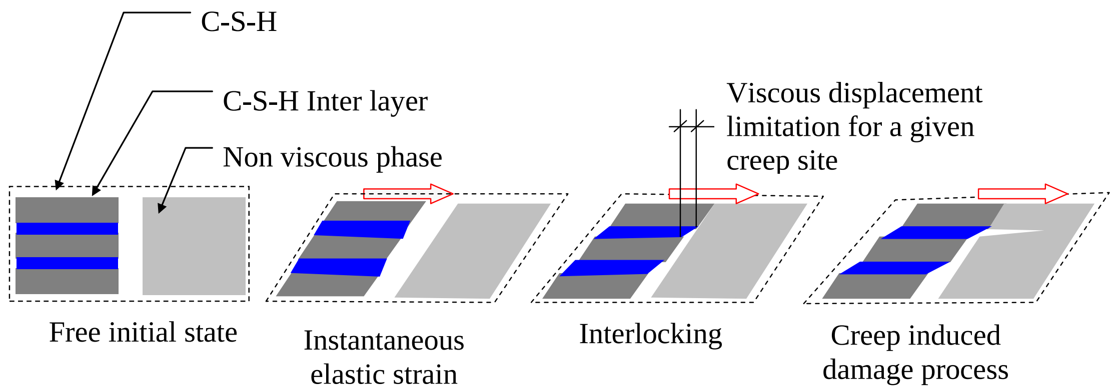

Unified approach for creep and shrinkage

- **shrinkage:** strain induced by the hydric pressure transmission to solid skeleton
- **Pickett's effect:** supplementary shrinkage induced by a better transmission of hydric pressure in the direction of the external load

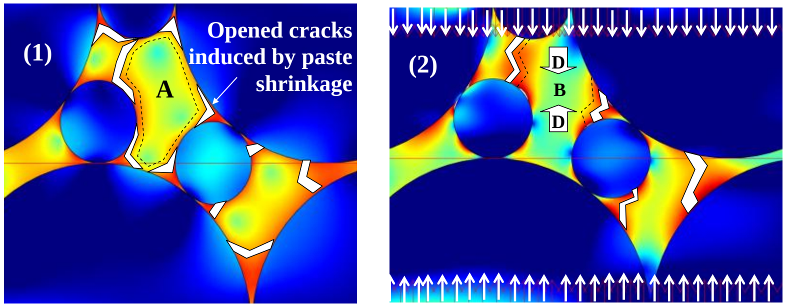

Chemo-mechanical couplings

Numerical adaptation of mechanical model

- Incremental formulation of behavior laws
- Updating of internal variables with hydration development (decrease of damage and consolidation)

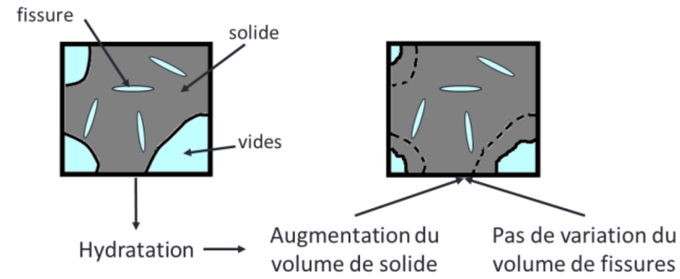

Variation of mechanical properties

Variation laws according to hydration degree

⇒ « Usual » properties : Rc, Rt, E

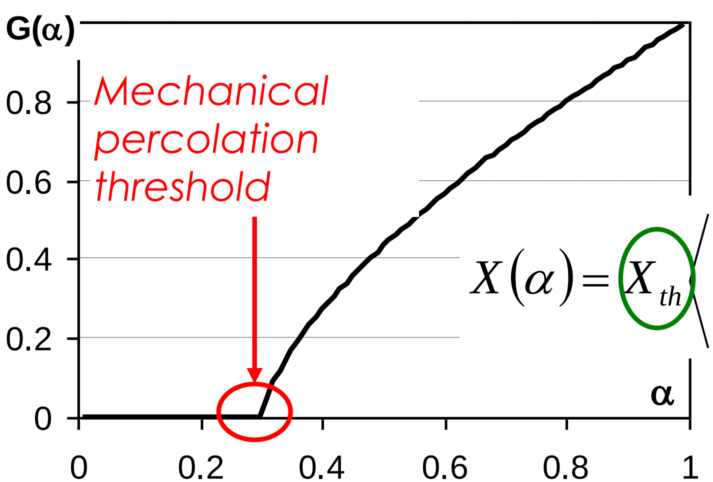

$$X(\alpha) = X_{th}\left\langle \frac{\alpha - \alpha_s}{1 - \alpha_s} \right\rangle^{n}$$

Other properties :

- Fracture energy
- Steel-concrete bond

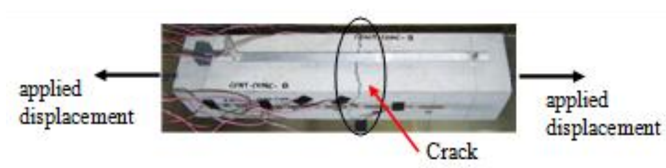

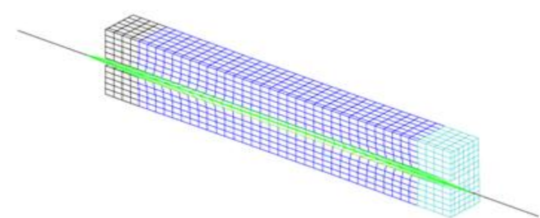

Application to nuclear waste storage structures

Construction stages

- **Simulation of casting**
  - Block 8m diameter and 5 m long
  - Cast in 1 day
  - A layer of 1m is cast every 5 hours

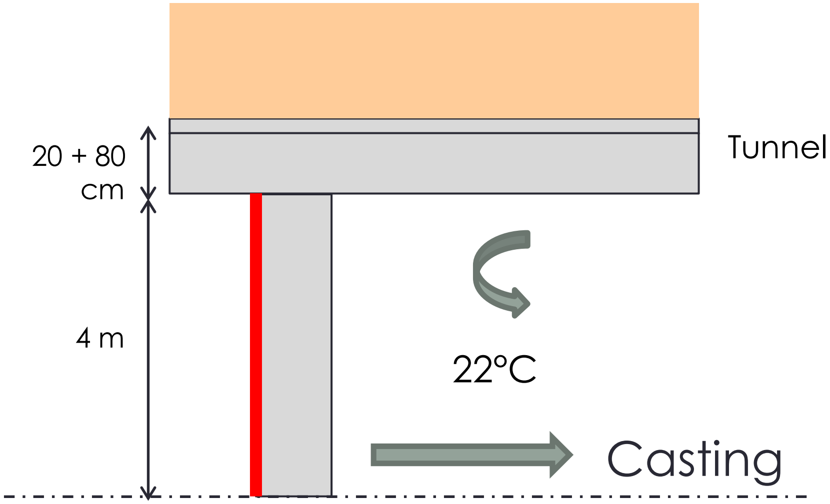

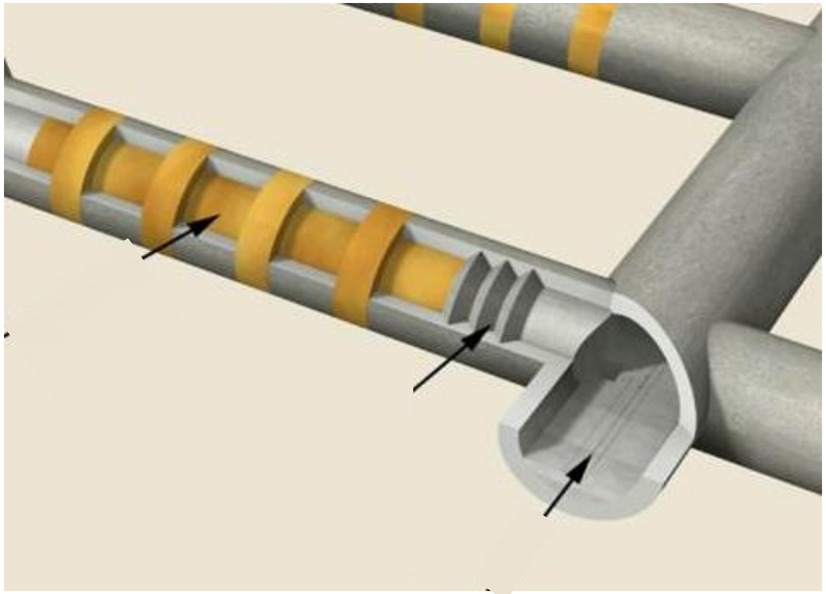

- **2 cases for boundary condition in the red surface**
  - Convection (block in an empty tunnel)
  - Insulated face (block in contact with bentonite)

Comparison of thermal variation

Variation of maximal temperature

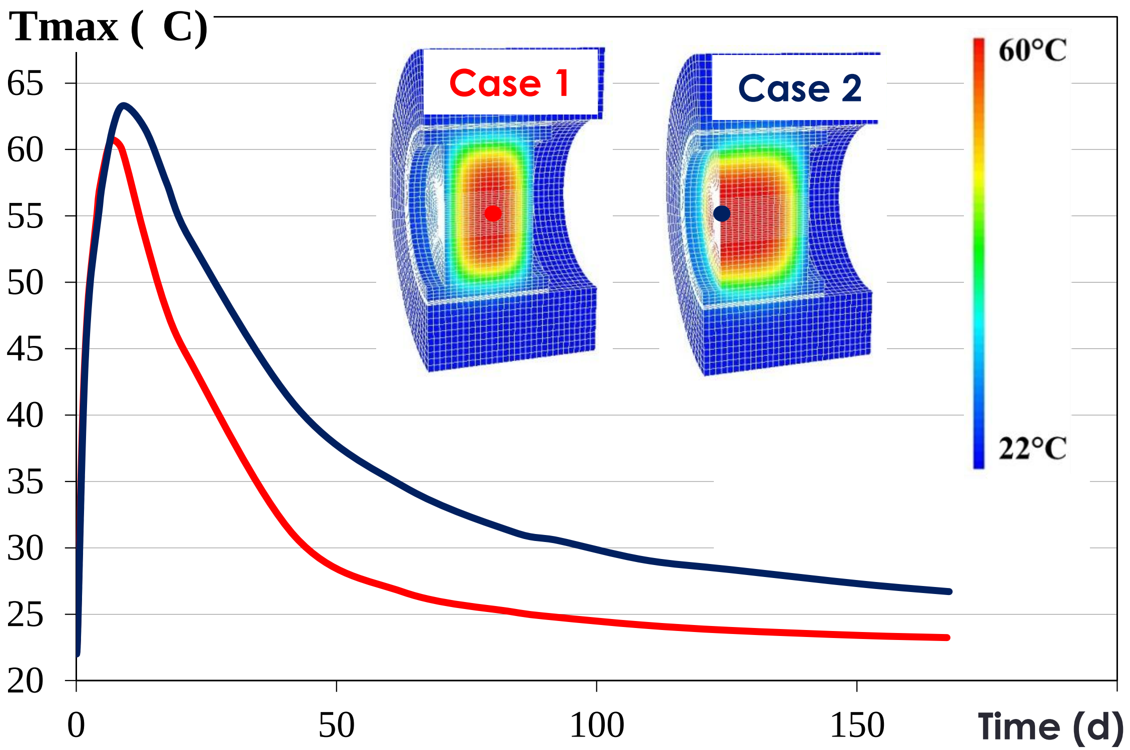

Temperature reaches 60°C

Maximal temperature similar in both cases but cooling rate different

⇒ **What would be the differences in terms of cracking behavior?**

Comparison during heating phase

Stress and damage fields (at the instant of maximal temperature)

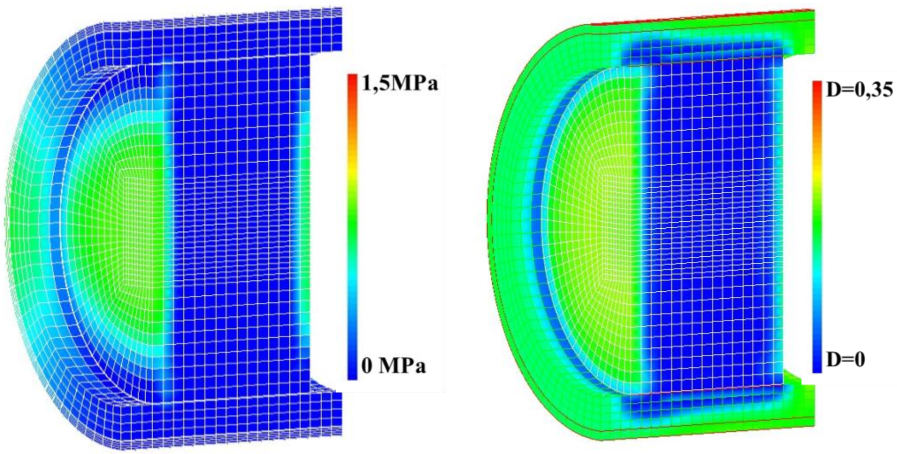

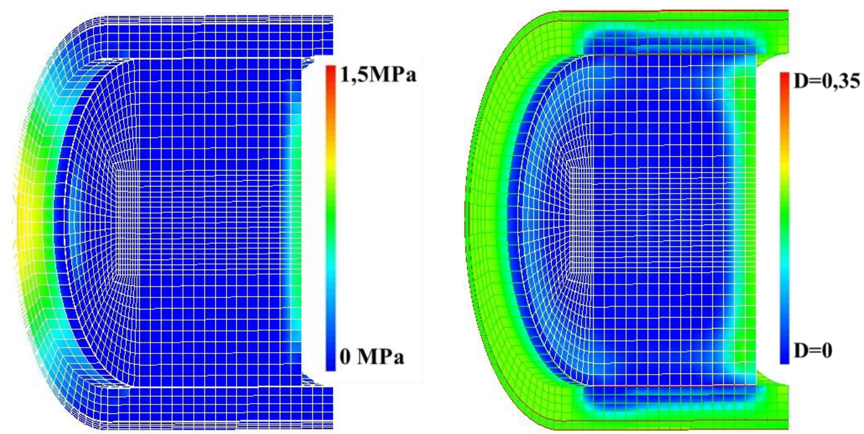

Case 1 (convection on 2 faces)

⇒ Low stresses in the tunnel (due to bloc expansion)

⇒ Convective surface in tension with micro-cracking

Case 2 (convection on 1 face)

⇒ Higher stresses in tunnel (higher expansion of the bloc)

⇒ Micro-cracks on tunnel and on "cold" surface of the bloc

Comparison during cooling phase

Damage and crack pattern 40 days after casting

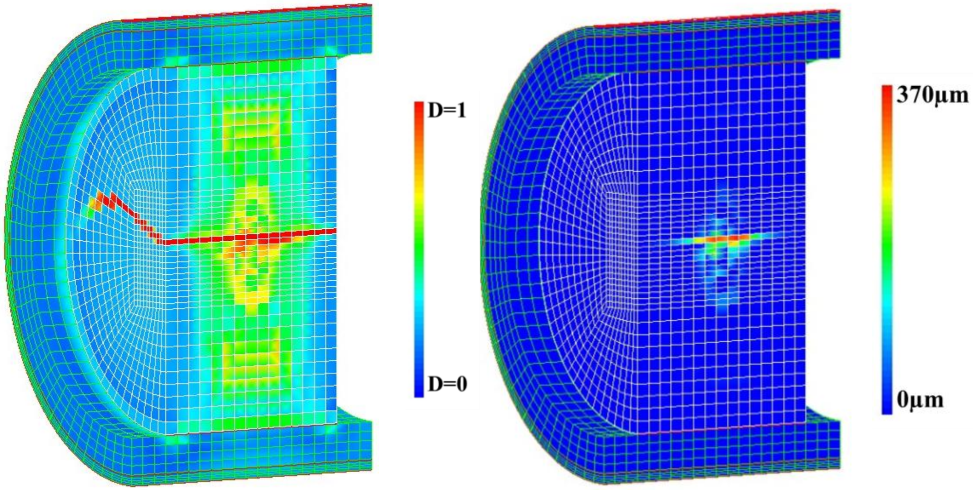

Case 1 (convection on 2 faces)

⇒ Crack at core of the bloc

Case 2 (convection on 1 face)

⇒ Only micro-cracks in the bloc

Comparison

Same mechanical hypothesis on the 2 cases

Differences induced by the thermal boundary conditions

Why the prejudicial case for thermic is not prejudicial for mechanics?

Case 1: Convection on both surfaces

- **Simulation of Case 1**
  - Convection (block in an empty tunnel)
  - Block 8m diameter and 5 m long
  - A layer of 1m is cast every 5 hours

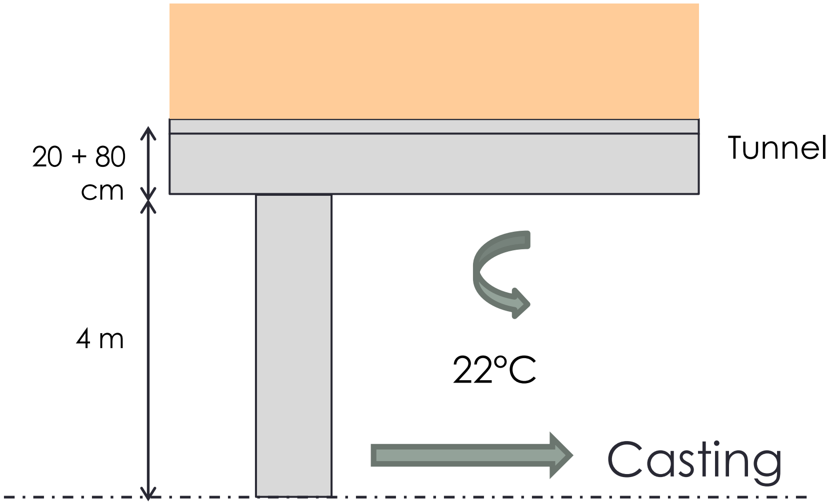

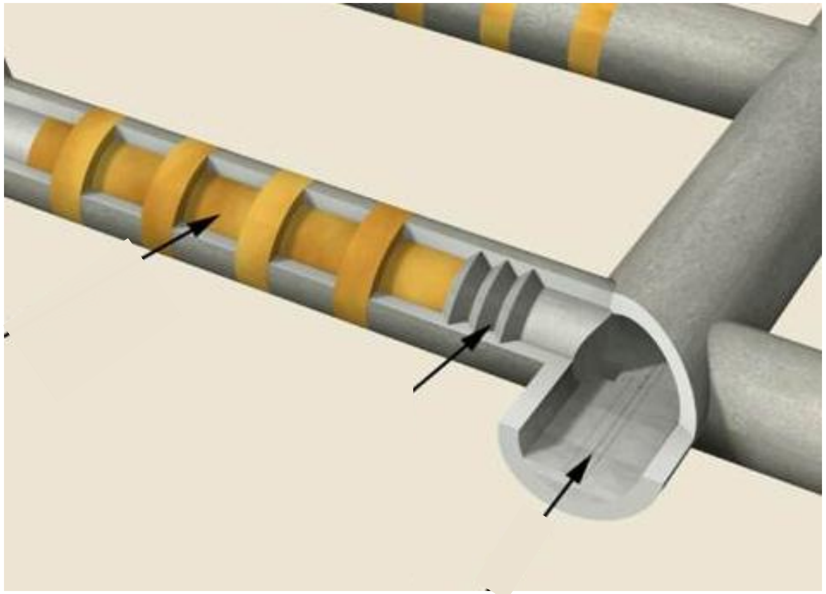

Case 1: Convection on both surfaces

- 1 day after casting of the first layer

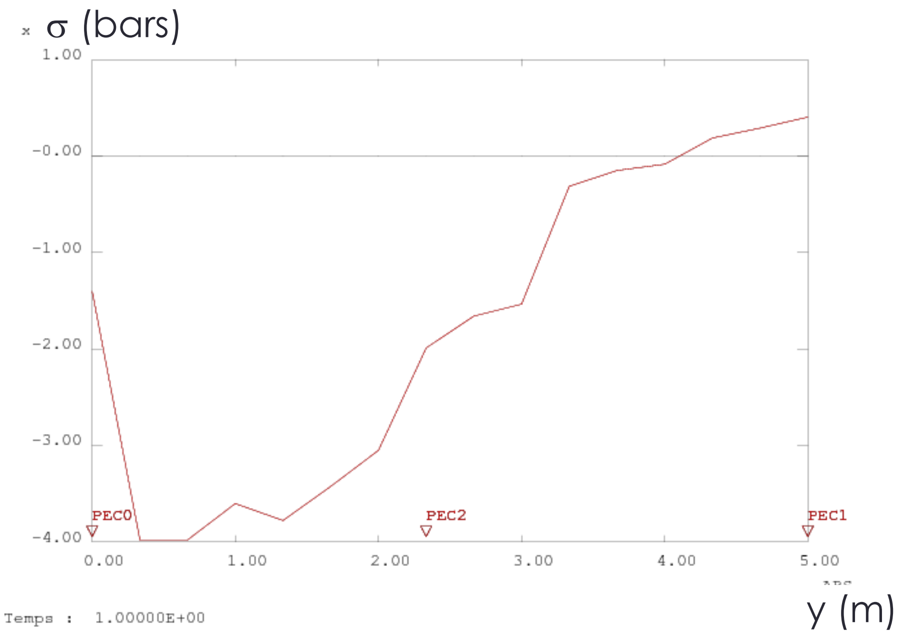

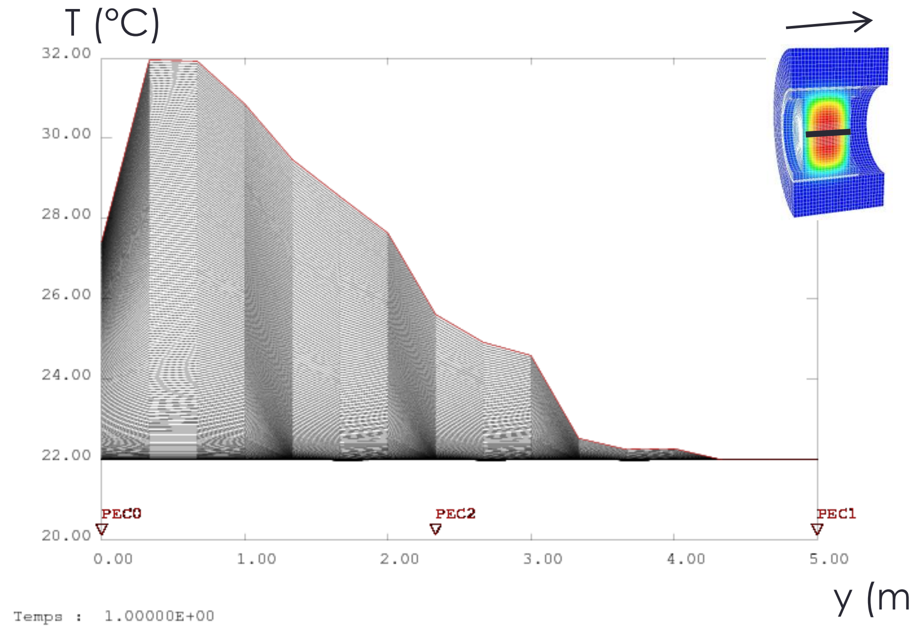

Concreting phasing

⇒ First layers exhibit higher temperature than the last casted

⇒ Cooling on the surface of the 1st layer: lower stress

Case 1: Convection on both surfaces

- **4 days after casting of the first layer**

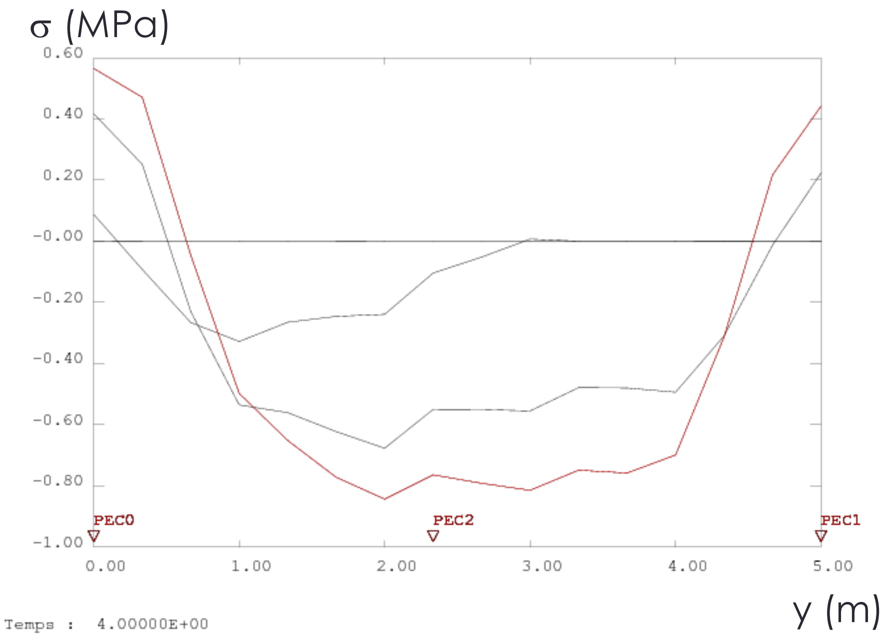

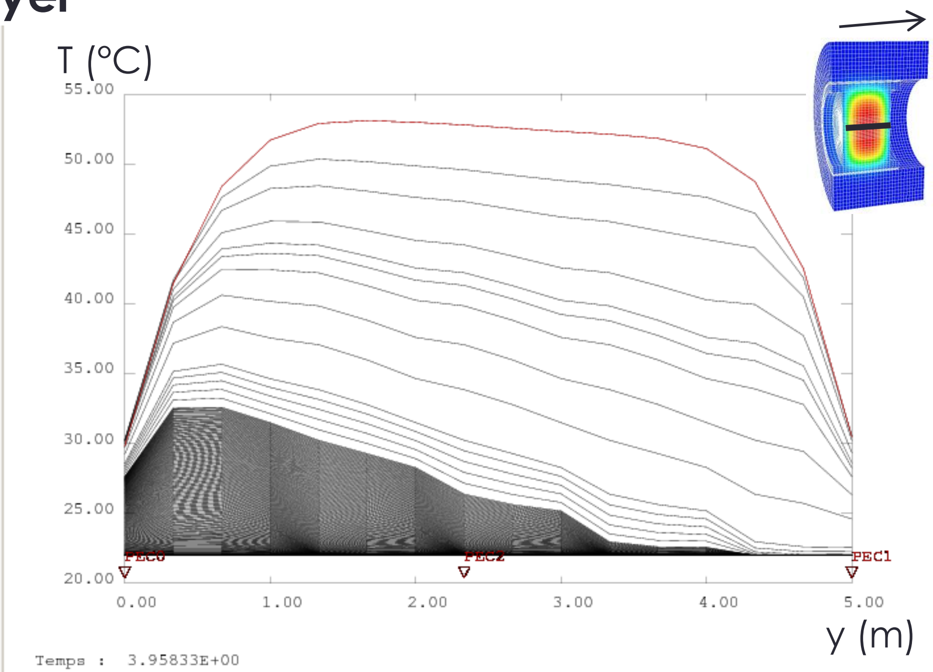

Heating phase: gradient between core and surface

⇒ Compression at core

⇒ Tension on surface

Case 1: Convection on both surfaces

- **7 days after casting of the first layer**

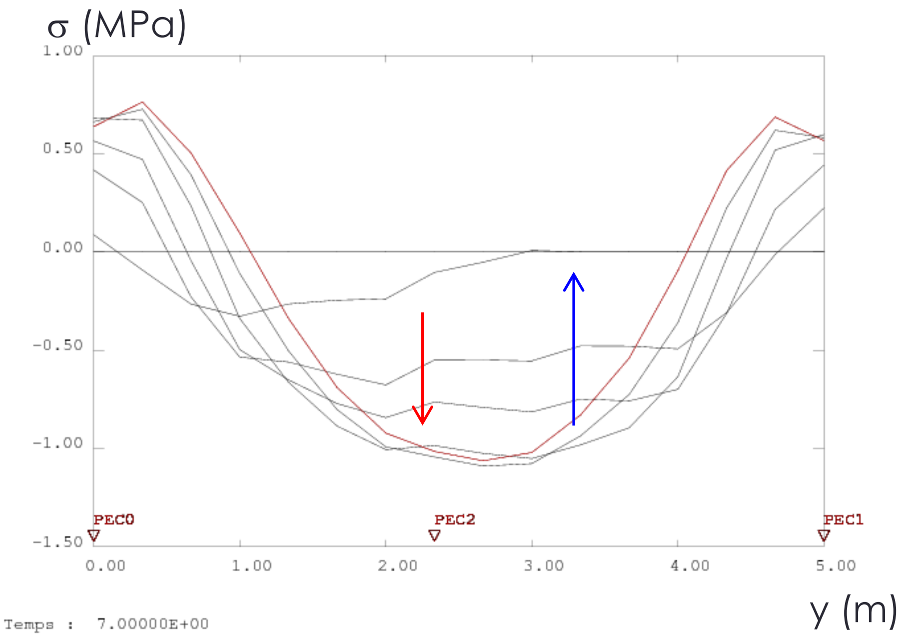

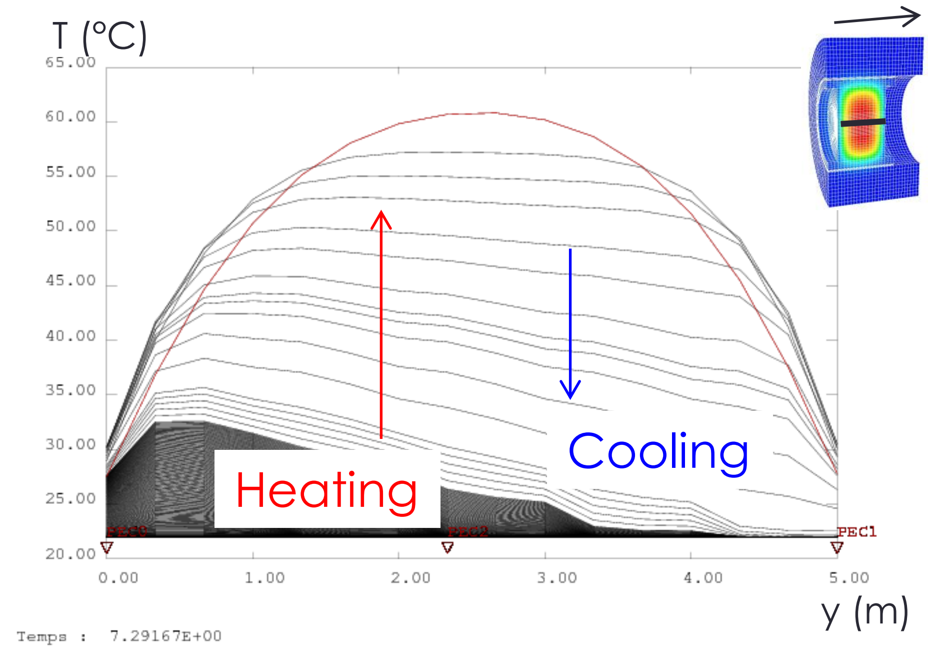

Instant of the temperature maximum

⇒ Thermal gradient between core and surface: micro-cracks in surface

⇒ Beginning of cooling: core stress is going to decrease

Case 1: Convection on both surfaces

- **18 days after casting of the first layer**

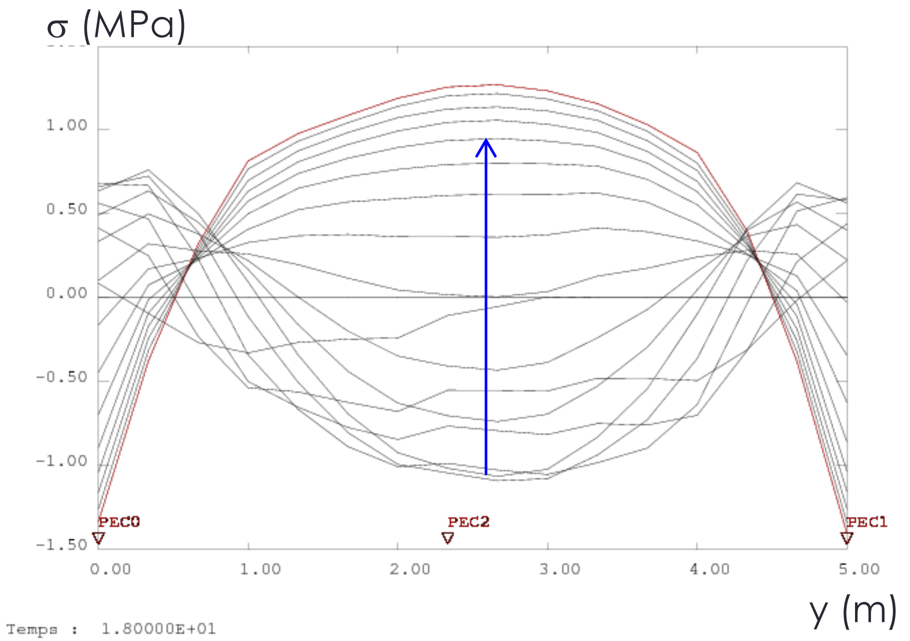

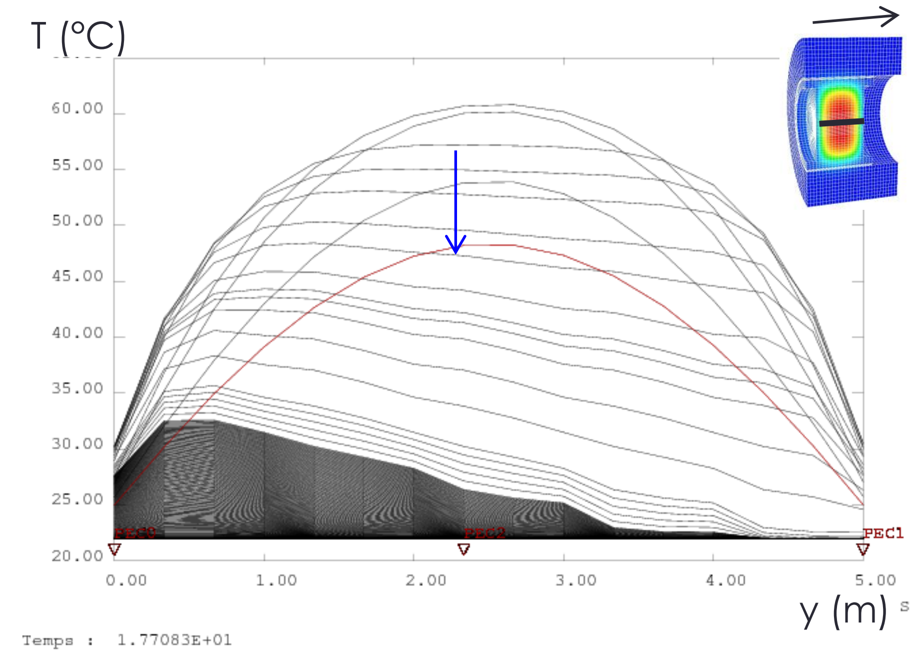

Cooling phase: inversion of stress profile

⇒ Compression in surface (which was colder than core at 7 days)

⇒ Tension at core (maximal value where temperature reached maximum)

Case 1: Convection on both surfaces

- **36 days after casting of the first layer**

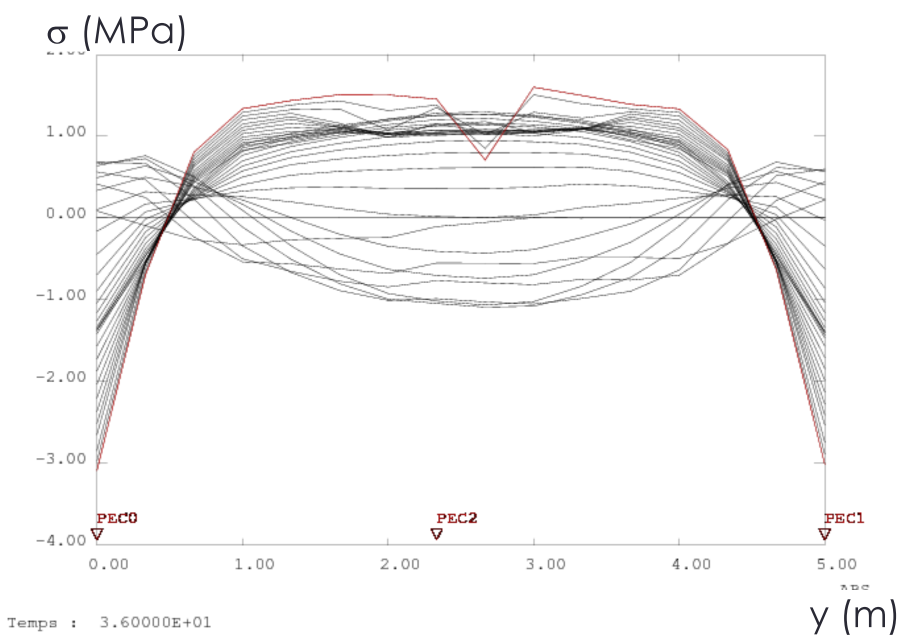

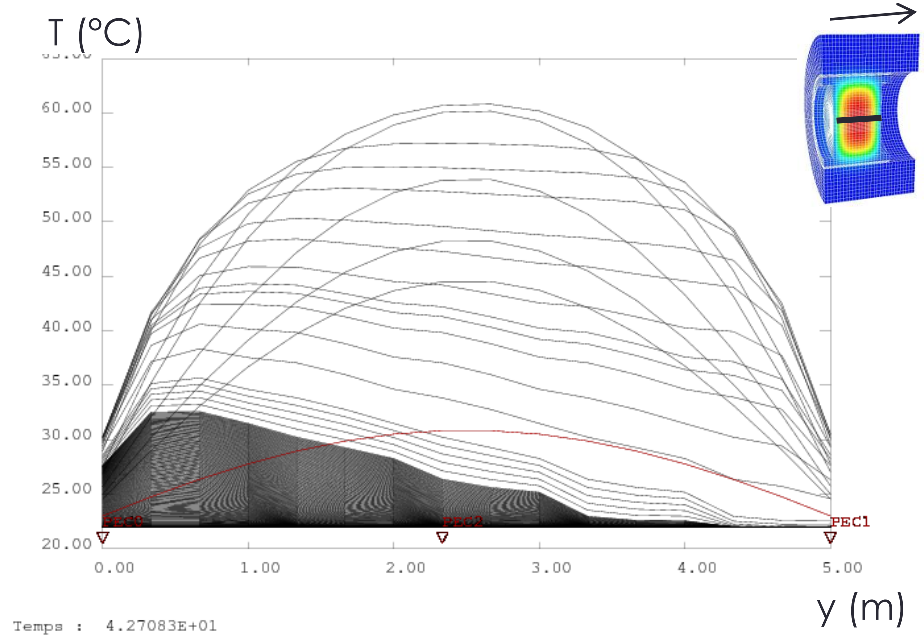

Cooling phase

⇒ Tensile stress at core reaches tensile strength

⇒ Crack at core (which will propagate)

Case 1: Convection on both surfaces

- **40 days after casting of the first layer**

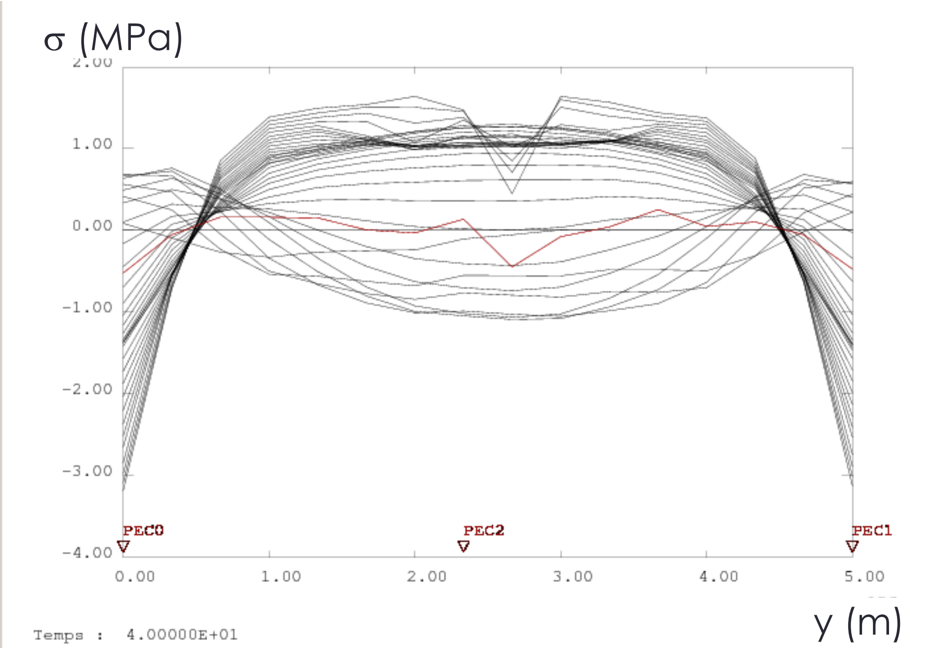

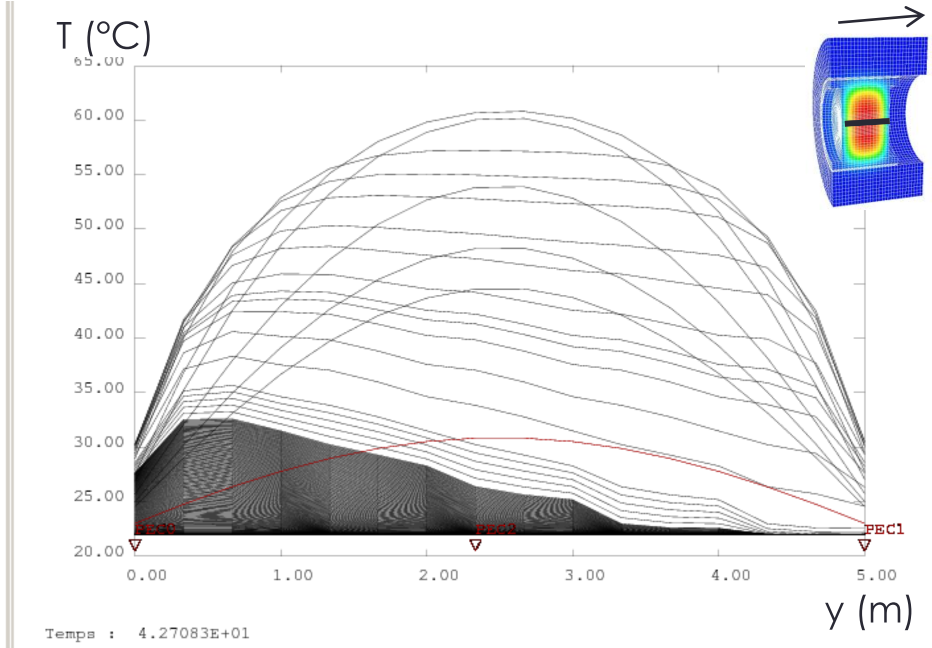

Cooling phase

⇒ Rapid propagation of crack

⇒ Stress tends to zero in a large part of the section

Case 2: Convection on 1 surface only

- **Simulation of Case 2**
  - Insulation on left surface
  - Block 8m diameter and 5 m long
  - A layer of 1m is cast every 5 hours

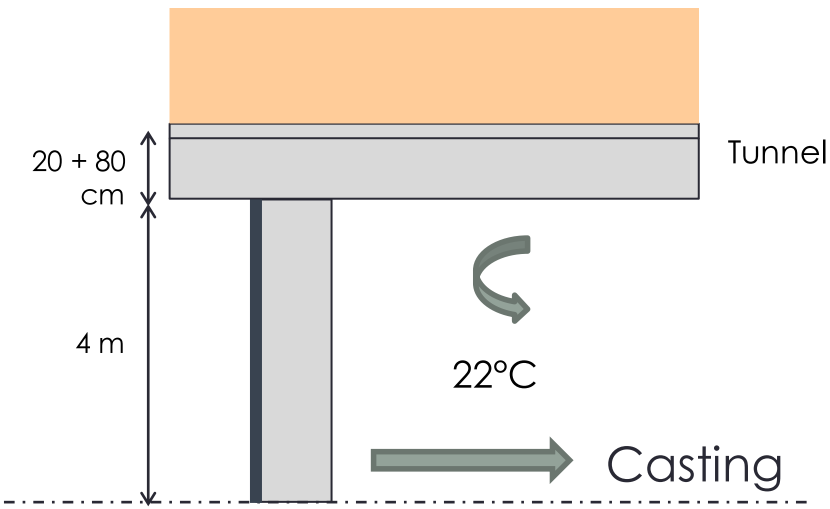

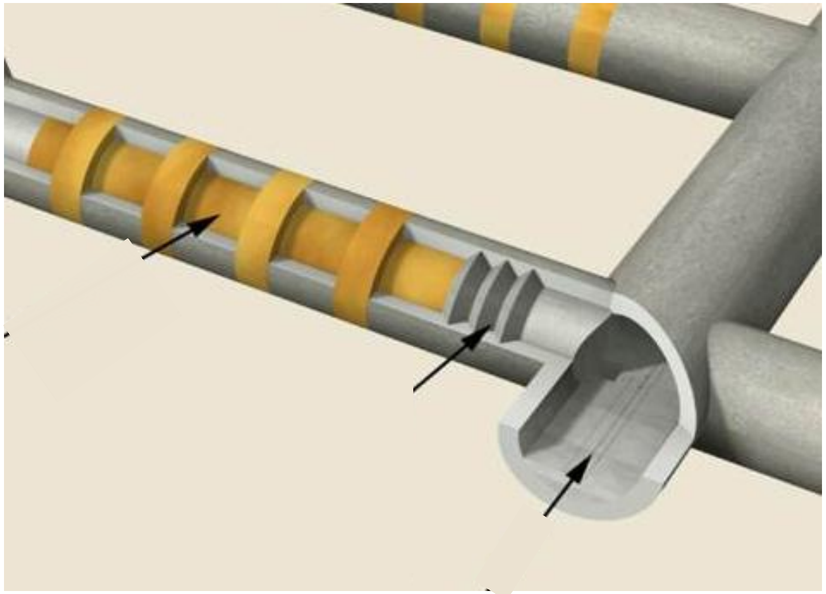

Case 2: Convection on 1 surface only

- **4 days after casting of the first layer**

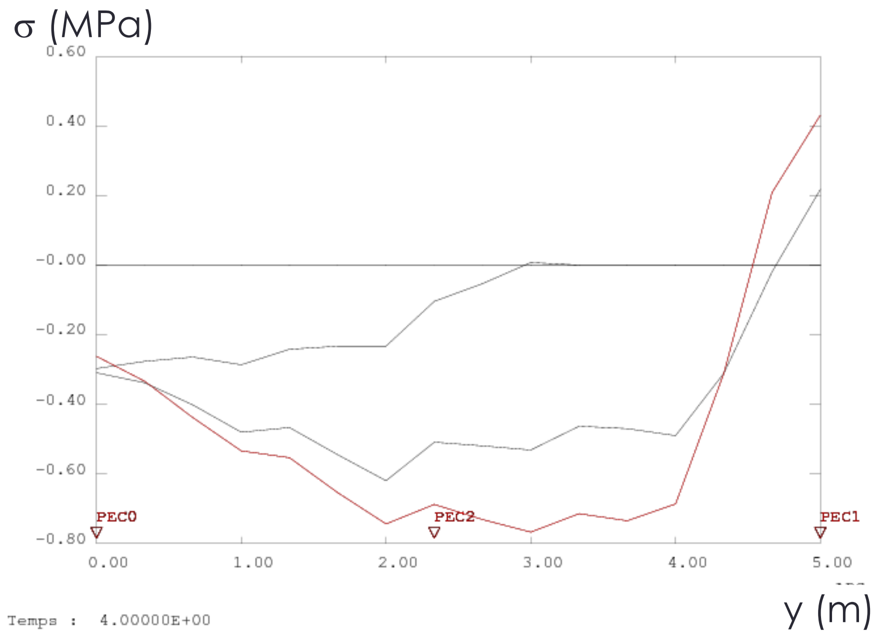

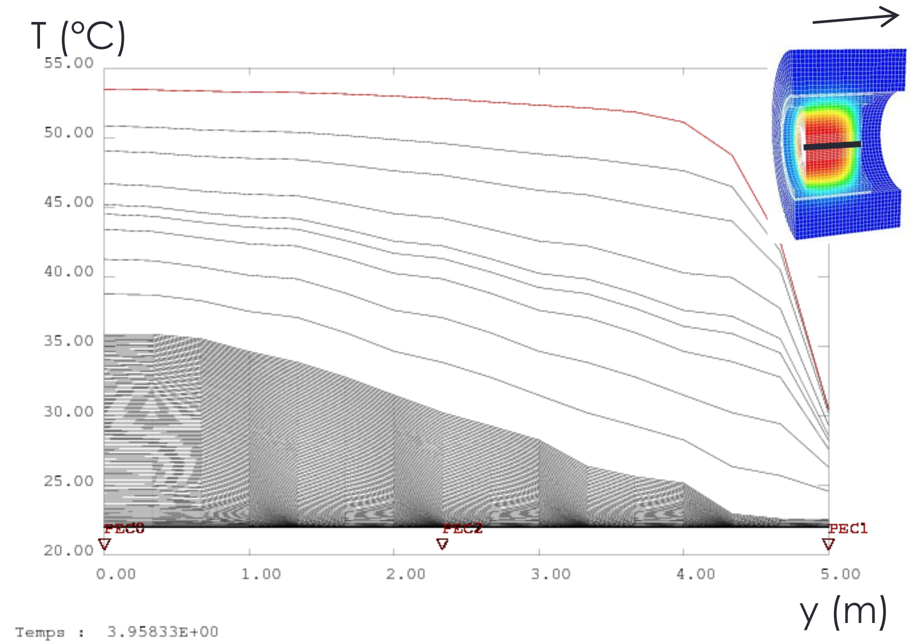

Heating phase: gradient between core and surface

⇒ Compression at core

⇒ Tension on convective surface

Case 2: Convection on 1 surface only

- 9 days after casting of the first layer

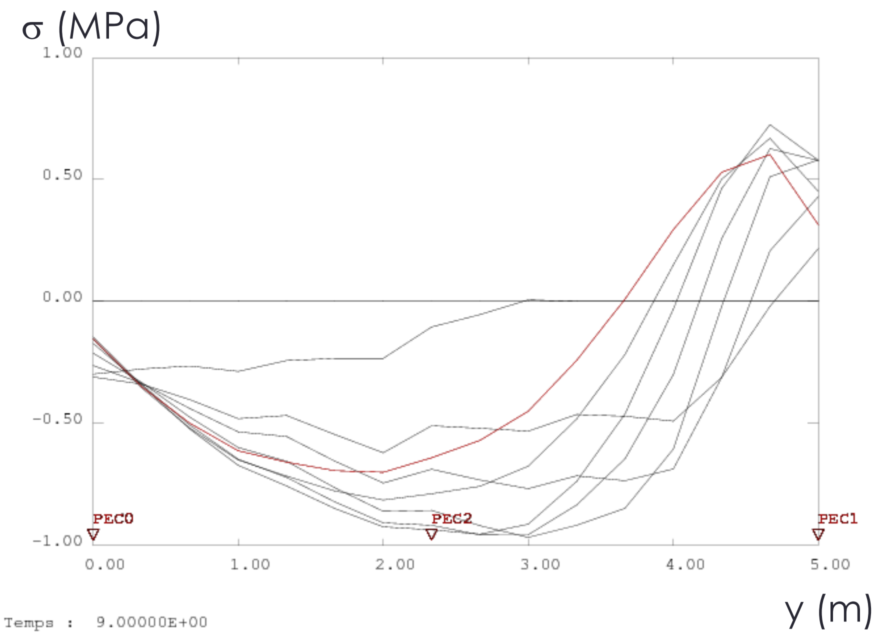

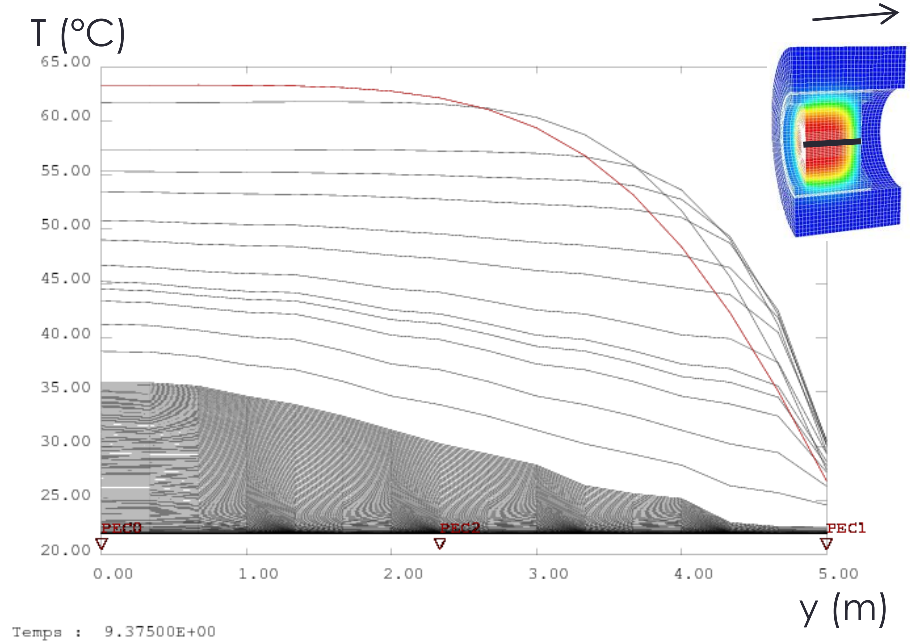

Instant of the temperature maximum

⇒ Thermal gradient between core and surface: micro-cracks in surface

⇒ Beginning of cooling: compressive stress is going to decrease

Case 2: Convection on 1 surface only

- **14 days after casting of the first layer**

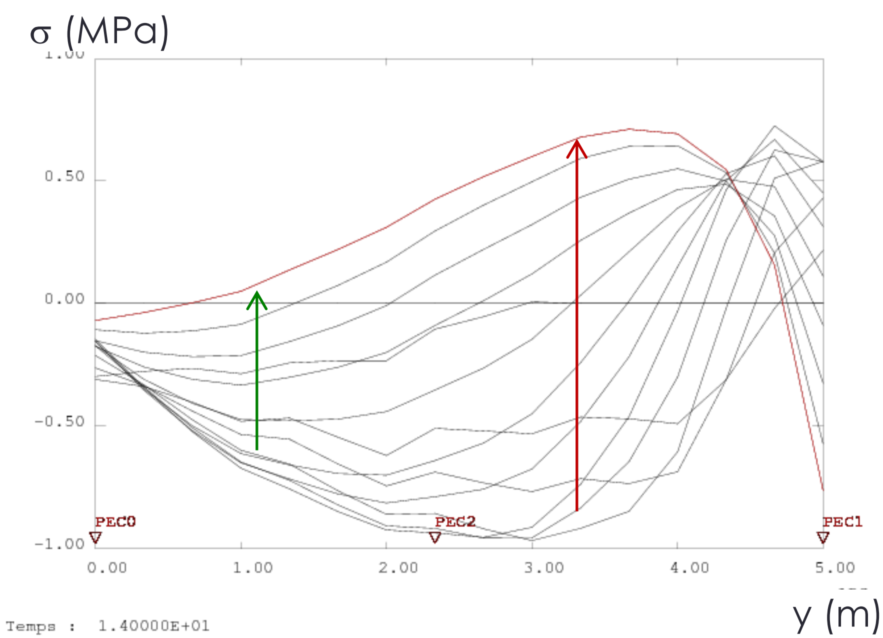

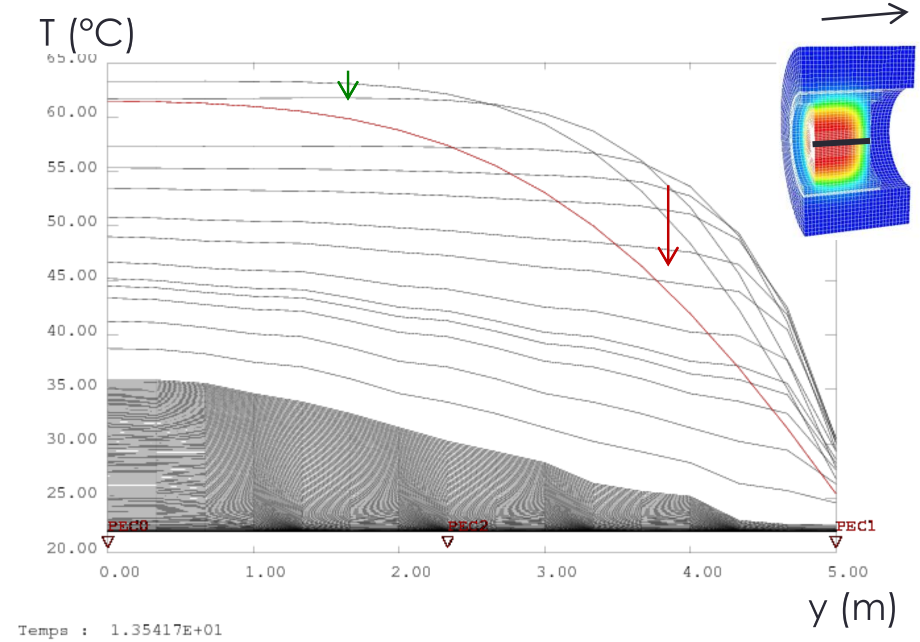

Cooling phase: inversion of stress profile

⇒ Compression in surface (which was colder than core at 7 days)

⇒ On the left face, Tmax but low cooling rate: low "return" of stress

⇒ At core, higher cooling rate and amplitude: tensile stress

Case 2: Convection on 1 surface only

- **42 days after casting of the first layer**

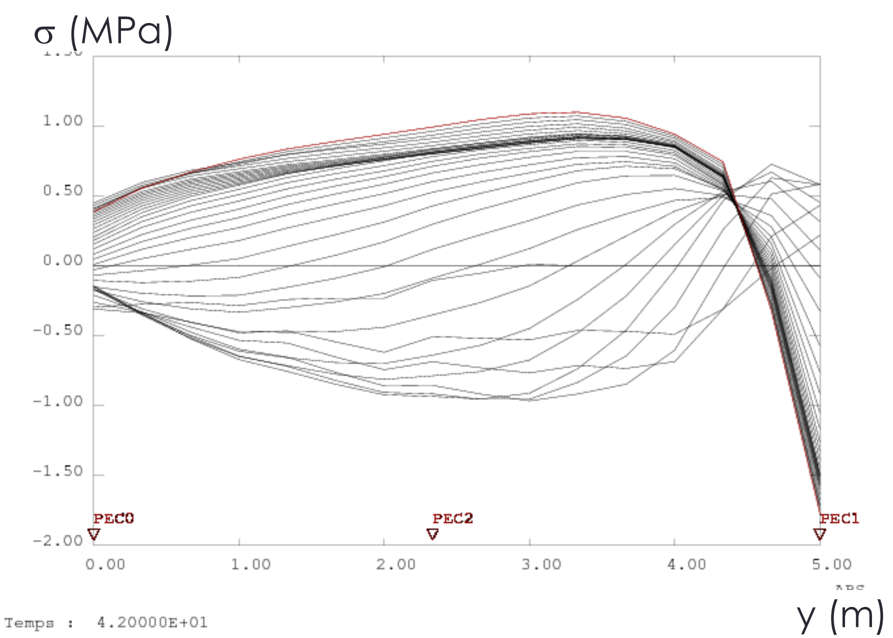

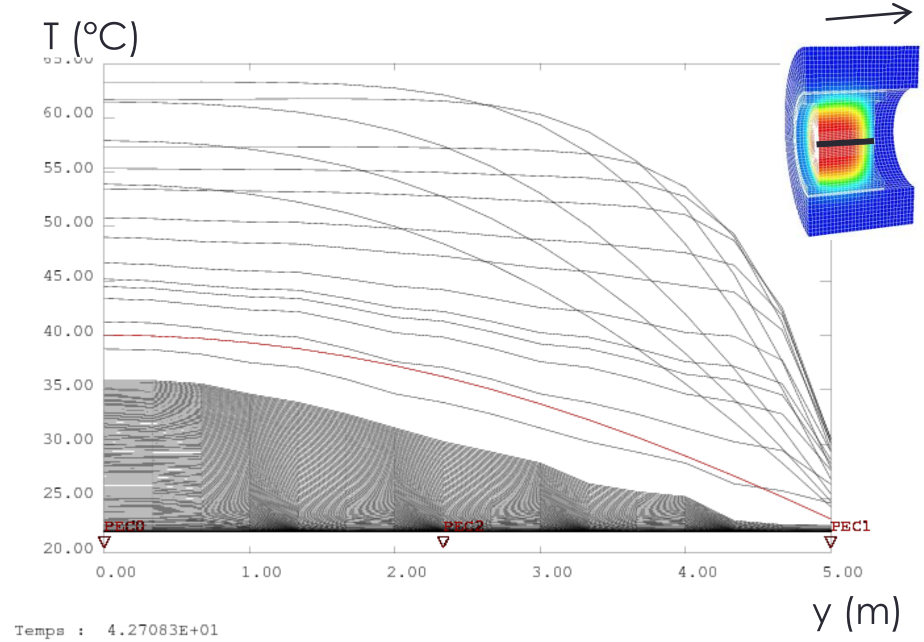

Cooling phase: low cooling rate

⇒ Lower stresses reached (than the one observed in case 1)

⇒ No crack was observed

Conclusion

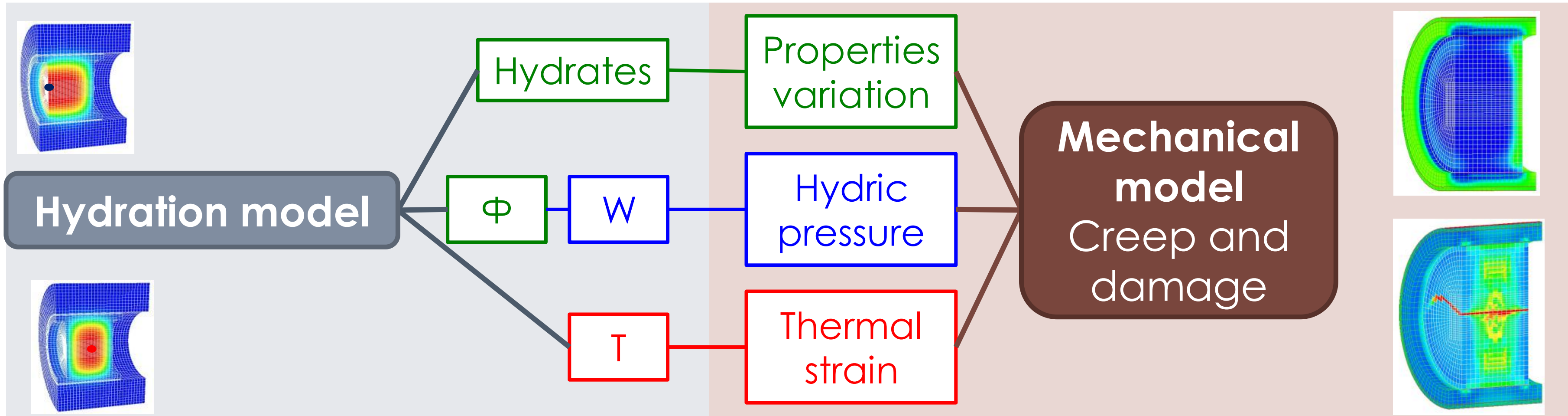

- **Hydration model for composed binder**
  - Kinetic strongly coupled with T/W balance equations
  - Interaction between clinker and additions
  - Stoichiometry of slag-CSH function of CH content at each time step

- **Mechanical simulation**
  - Localized crack for the convective case only
  - Crack at cooling linked with the cooling rate and amplitude at core

References

1. **L. Buffo-Lacarrière**, A. Sellier, B. Kolani, **2014**, *Application of thermo-hydro-chemo-mechanical model for early age behaviour of concrete to experimental massive reinforced structures with strain–restraining system.* European Journal of Environmental and Civil Engineering, Vol. 18, n°7, pp. 814-827
2. B. Kolani, **L. Buffo-Lacarrière,** A. Sellier, G. Escadeillas, L. Boutillon, L. Linger **2012** *Hydration of slag blended cements.* Cement and Concrete Composites, Vol. 34, n°9, pp. 1009-1018
3. **L. Buffo-Lacarrière**, A. Sellier, G. Escadeillas, A. Turatsinze, **2011** *Numerical modelling of hardening concrete mechanical behaviour: application to the prediction of early age cracking risk for massive structures.* Materials and Structures, Vol. 44, n°10, pp. 1821-1835
4. **L. Buffo-Lacarrière**, A. Sellier. , **2011** *Chemo-mechanical modeling requirements for the assessment of concrete structure service life.* ASCE Journal of Engineering Mechanics, Vol. 137, n°9, pp.625-633
5. **L. Buffo-Lacarrière**, A. Sellier, G. Escadeillas, A. Turatsinze, **2007**, *Multiphasic finite element modelling of concrete hydration.* Cement and Concrete Research, Vol. 37, n°2, pp. 131-138

CMS Workshop "Cracking of massive concrete structures"

March 17, 2015, ENS-Cachan

Cachan, Île-de-France, FRANCE

Modelling the mechanical behavior at early-age: influence of the boundary conditions at the structure scale and multiscale estimation of ageing properties

Tulio HONORIO[1,2] ; Benoit BARY[1]; Farid BENBOUDJEMA[2]

[1]CEA, DEN, DPC, SECR, Laboratoire d'Etude du Comportement des Bétons et des Argiles, F-91191 Gif-sur-Yvette, France

[2]LMT (ENS Cachan, CNRS, Université Paris Saclay) 94235 Cachan, France

Concrete at early-age

- Properties evolving at early age (ageing)
- Phenomena taking place at different space and time scales:

[Richardson 2004]

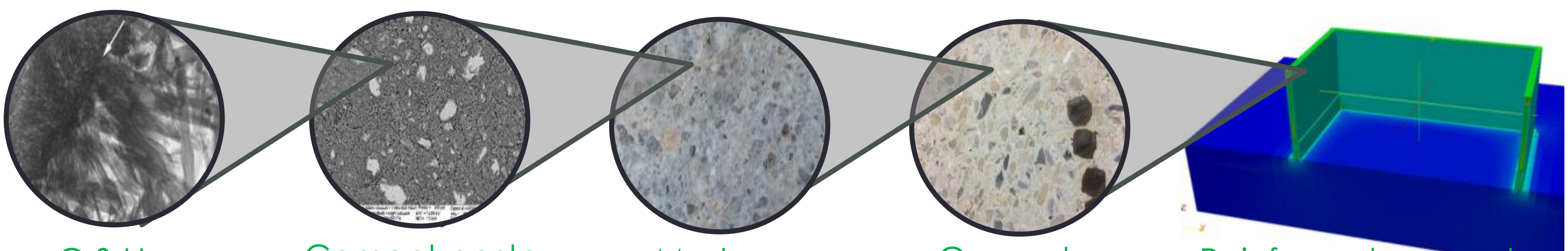

C-S-H | Cement paste | Mortar | Concrete | Reinforced concrete structure

- ITZ
- Solidification
- Creep
- Environmental conditions
- Mismatch of properties of matrix and inclusions
- External restraint
- Shrinkage
- Heterogenous distribution of stress
- Internal restraint

nm | µm | mm | m

Different strategies

- **bottom-up** and **top-down**
- **phenomenological** and **mechanistic** approaches

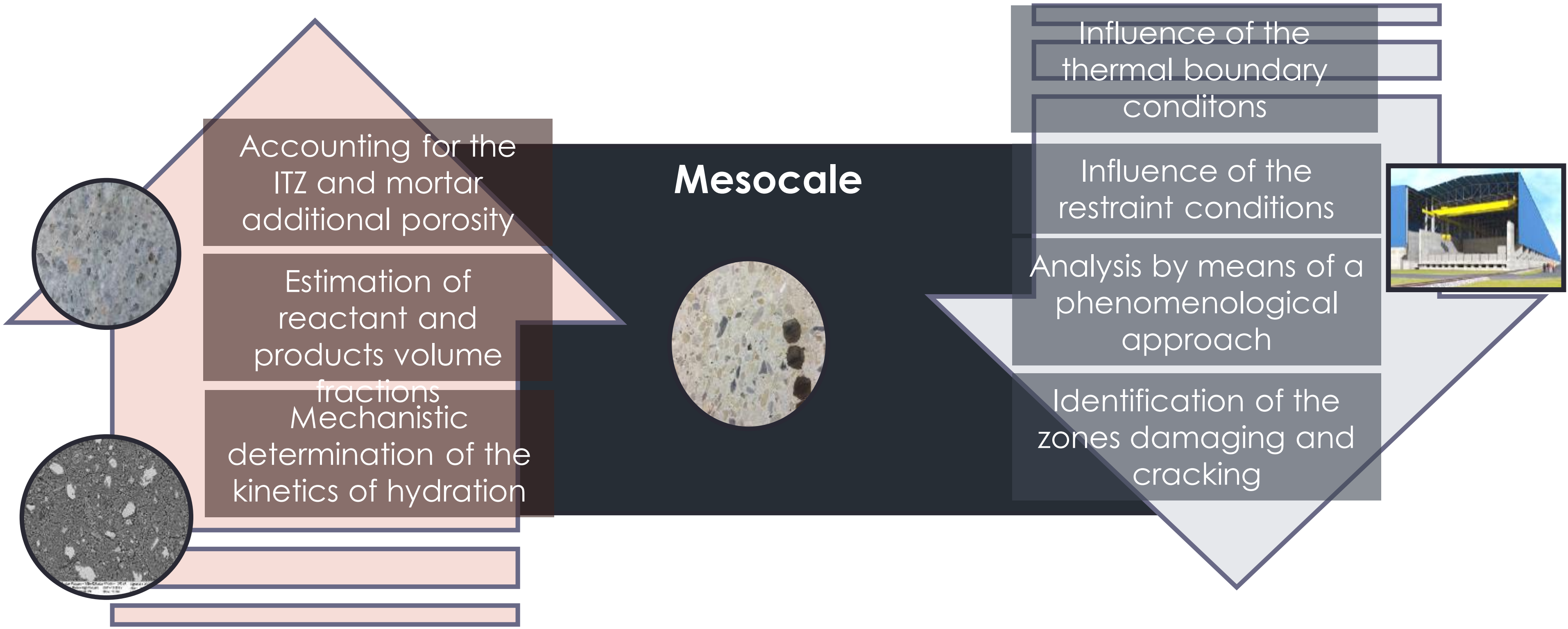

Thermo-chemo-mechanical analysis

A phenomenological approach at the structure level

Chemo-thermal problem

- Heat balance

$$\dot{T}(\mathbf{x},t) = D\,\nabla^2 T(\mathbf{x},t) + Q \qquad \begin{cases} T(\mathbf{x},0) = T_0 & \forall \mathbf{x} \in \boldsymbol{\Omega_c} \\ \lambda\,\nabla T(\mathbf{x},t)\cdot\mathbf{n} - k\,[T(\mathbf{x},t) - T_a] = q_i(t) & \forall \mathbf{x} \in \boldsymbol{\partial\Omega_i} \end{cases}$$

- **Non-homogeneous PDE**
  … with non-homogeneous BC

- Hydration $\quad \dot{\alpha} = A(t)\cdot\exp[-Ea/T]$

- Boundary conditions

$$q_s - q_c - q_r - q_y = 0$$

- q_y: Heat conducted into concrete
- q_r: Re-radiation by concrete
- q_c: Heat loss by convection
- q_s: Radiation absorbed

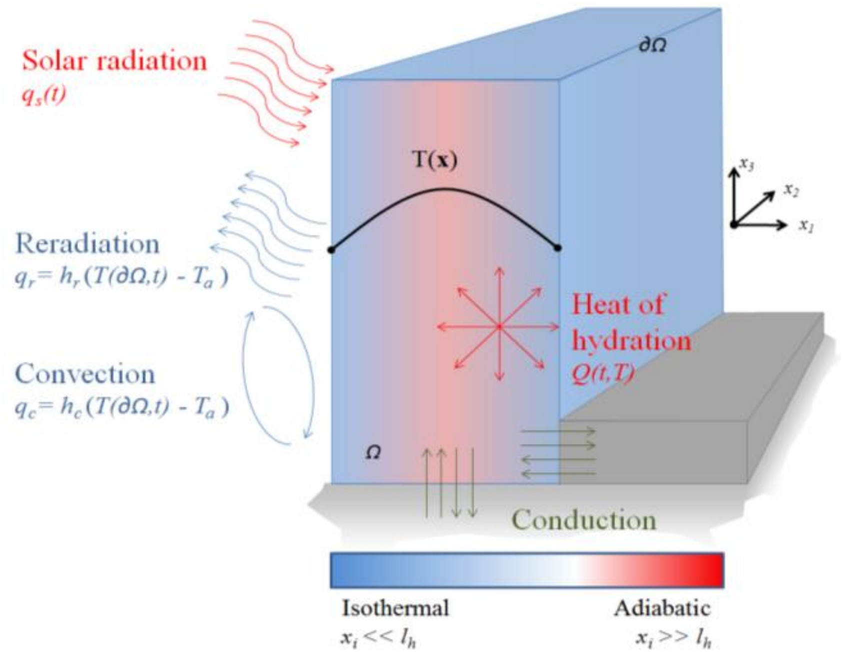

Analytical solutions

Why?

- Elucidates the role of the BC in the chemo-thermal problem
- Validates and allows some extrapolations from the numerical results

$$l_h = \sqrt{\frac{D}{A(\xi)} \exp\left[-\frac{E_a}{R\,T}\right]}$$

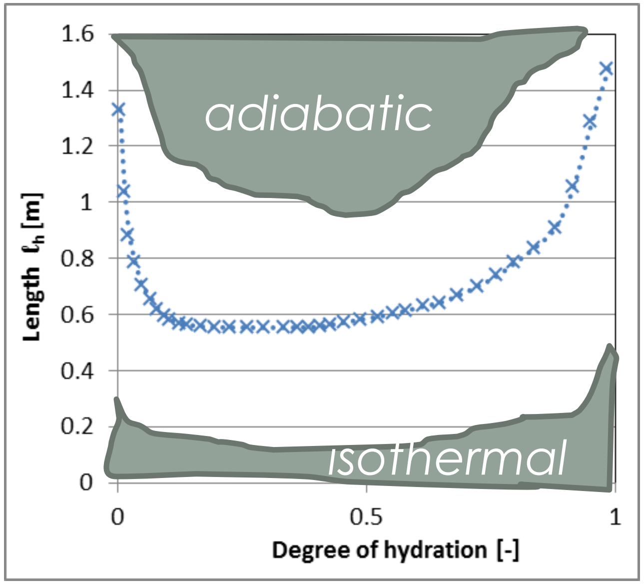

Analytical solutions

- After some hypothesis and simplifications…
  - 1D solution in a semi-infinite domain non-homogeneous PDE with non-homogeneous BC:

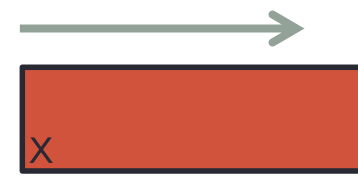

$$T(x,t) \approx T_1(x,t) + T_2(x,t) + T_3(\xi,x,t)$$

$$T_1(x,t) = T_0 \left(1 - \mathrm{erfc}\left[\frac{x}{\sqrt{4\,D\,t}}\right] + \exp\left[\frac{k}{D}(k\,t + x)\right] \mathrm{erfc}\left[\frac{2\ k\,t + x}{\sqrt{4\,D\,t}}\right]\right)$$

Temperature of concrete at placement

$$T_2(x,t) = \left(T_a - \frac{\bar{q}_s}{k}\right)\left(\mathrm{erfc}\left[\frac{x}{\sqrt{4\,D\,t}}\right] - \exp\left[\frac{k}{D}(k\,t + x)\right] \mathrm{erfc}\left[\frac{2\ k\,t + x}{\sqrt{4\,D\,t}}\right]\right)$$

Reradiation and Convection equivalent exchange coeff.

Ambient temperature

Variable flux on boundaries (solar flux)

[Honorio et al. 2014a]

Solar flux

- Convection and reradiaiton
- T_a is kept constant.

- ***Profiles of temperatures at different times →***

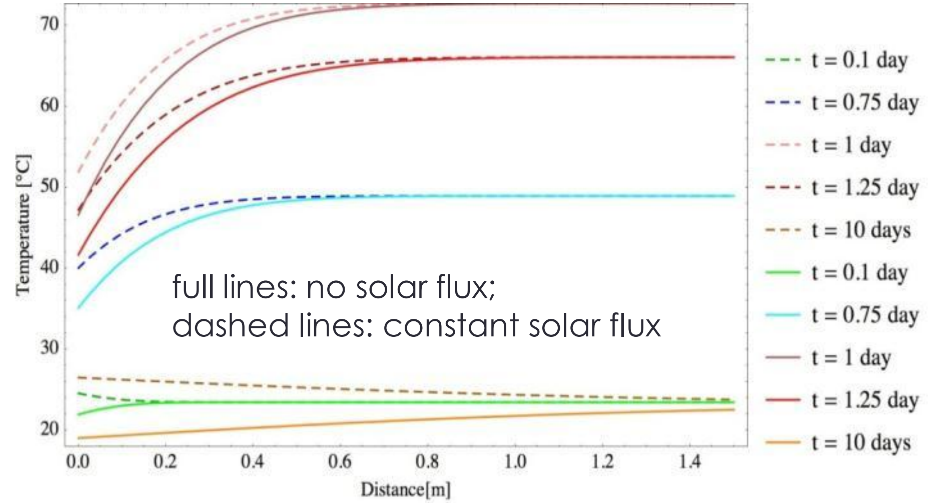

- ***Gradient of temperature ↓***

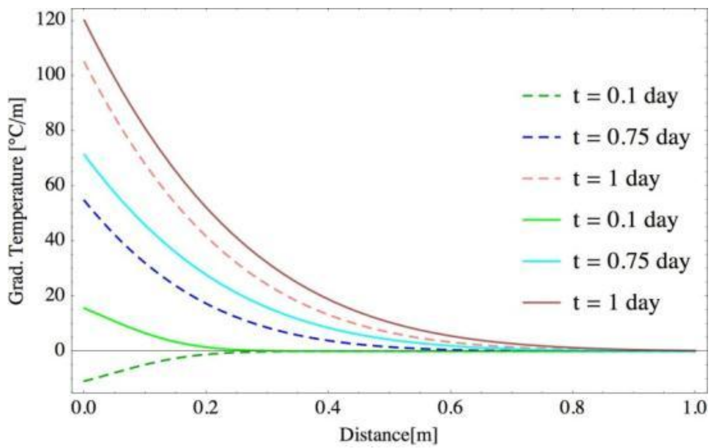

- ***Evolution of the temperatures at different distances from the surface ↓***

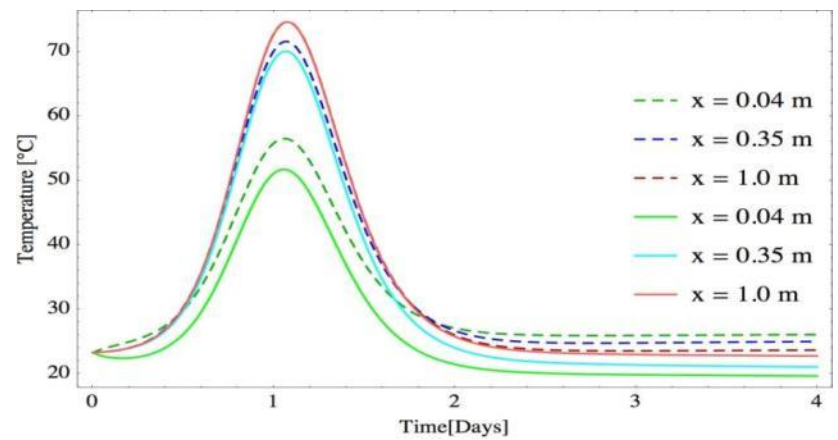

[Honorio et al. 2014a]

FEM analysis

- Goal: Determine concreting temperatures

- Asymmetric thermal loading induced by solar flux
- Test different T scenarios
  - Precooling?

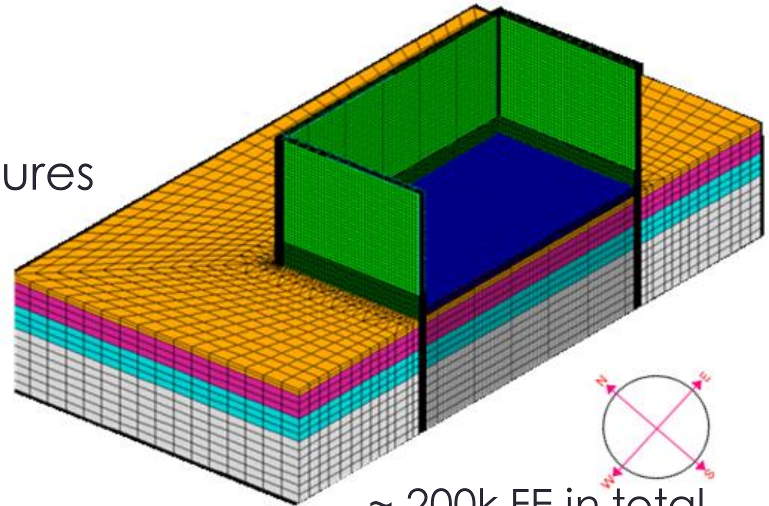

~ 200k FE in total
~ 100k FE for the wall

Solar flux

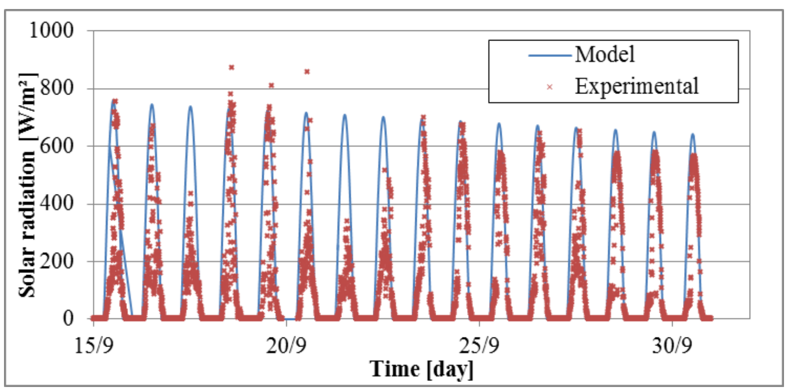

Validation

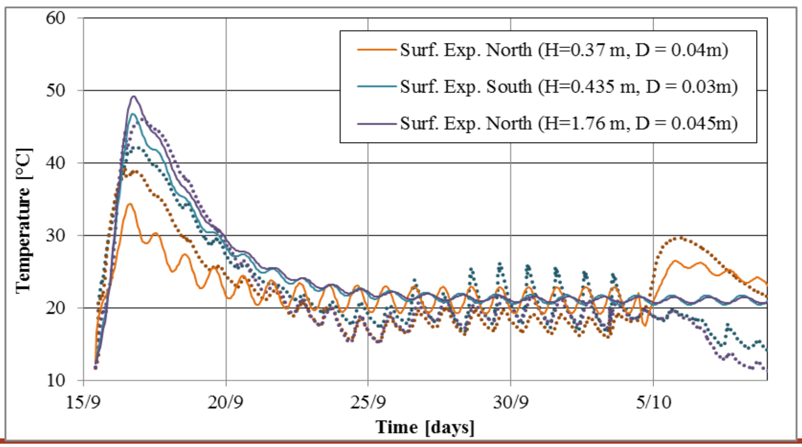

[Honorio et al. 2014a]

Ambient temperature

[Honorio et al. 2014a,b]

- *Maximum T to prevent DEF problems T_{adm}=70°C*
- Maximum temperature reached within the structure varies almost linearly with T_a

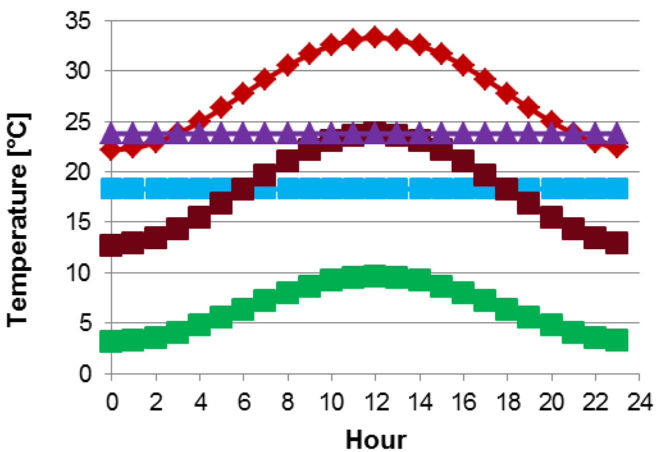

Set of temperatures

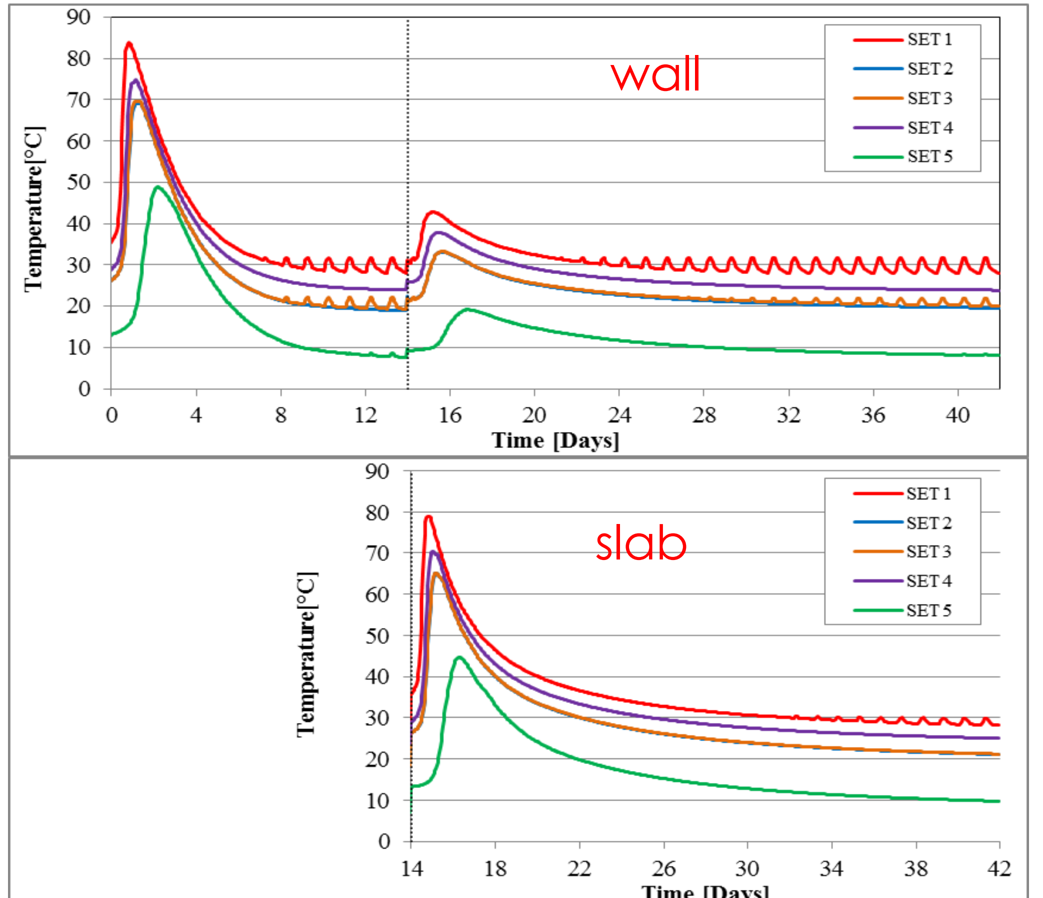

Concreting temperatures

$$T(x,t) \approx T_1(x,t) + T_2(x,t) + T_3(\xi,x,t)$$

$$T_1(x,t) = T_0\,(\ldots) \qquad T_2(x,t) = \left(T_a - \frac{\bar{q}_s}{k}\right)(\ldots)$$

$$T_{max} = c_1\,T_0 + c_2\,T_a + c_3$$

Fitting parameters

[-]	1.28
[-]	0.359
[°C]	34.1

→ $\Delta T_{ad} = 46.62\ °C$

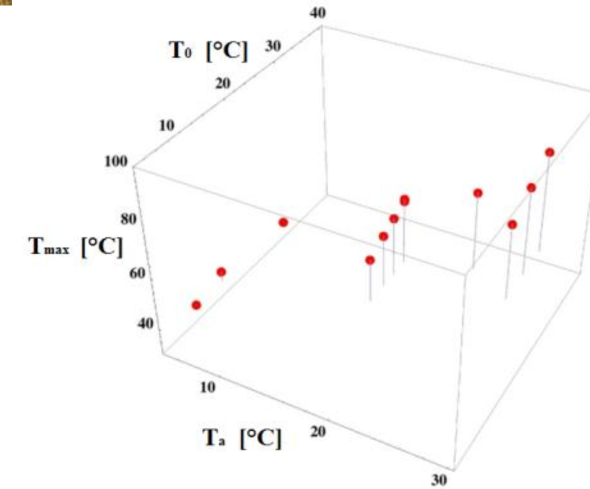

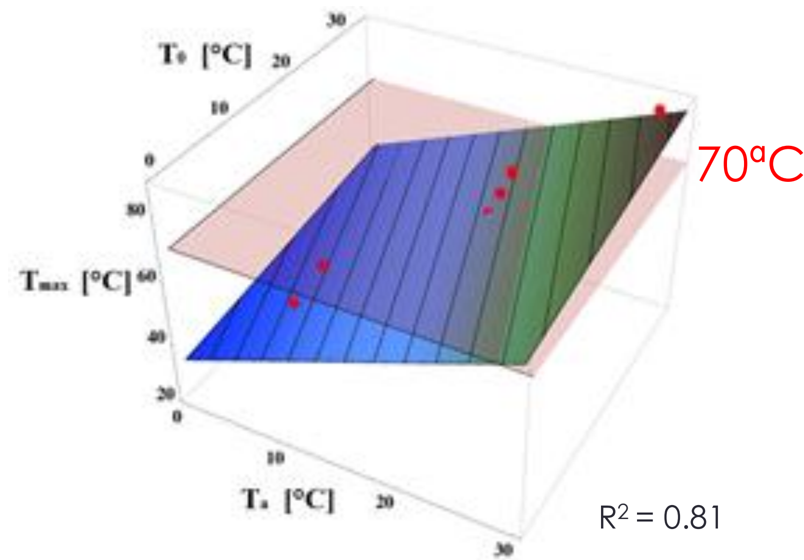

$R^2 = 0.81$

Mechanical model

$$\varepsilon_{in} = \varepsilon_{au} + \varepsilon_{th} + \varepsilon_{cr}$$

- Rheological model

$$\tau^i_{bc}\ddot{\varepsilon}_{bc} + \left(\tau^i_{bc}\frac{\dot{k}^i_{bc}(\xi)}{k^i_{bc}(\xi)} + 1\right)\dot{\varepsilon}^i{}_{bc} = \frac{\tilde{\sigma}}{k^i_{bc}(\xi)}$$

$$\begin{cases} k^i_{bc}(\xi) = k^i_{bc\_\infty}\dfrac{0.473}{2.081-1.608\bar{\xi}}\bar{\xi}^{\psi} e^{\frac{E_{ac}}{R}\left(\frac{1}{T}-\frac{1}{T_0}\right)} \\ \tau^i_{bc} = \dfrac{\eta^i_{bc}(\xi)}{k^i_{bc}(\xi)} \end{cases}$$

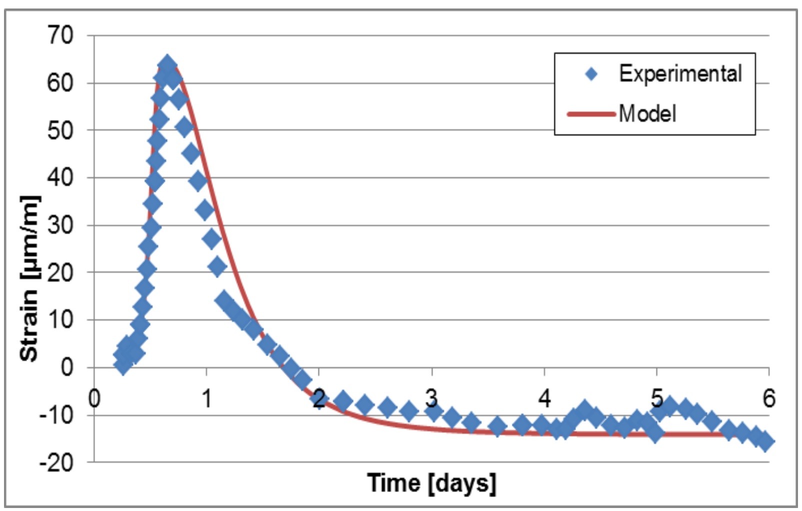

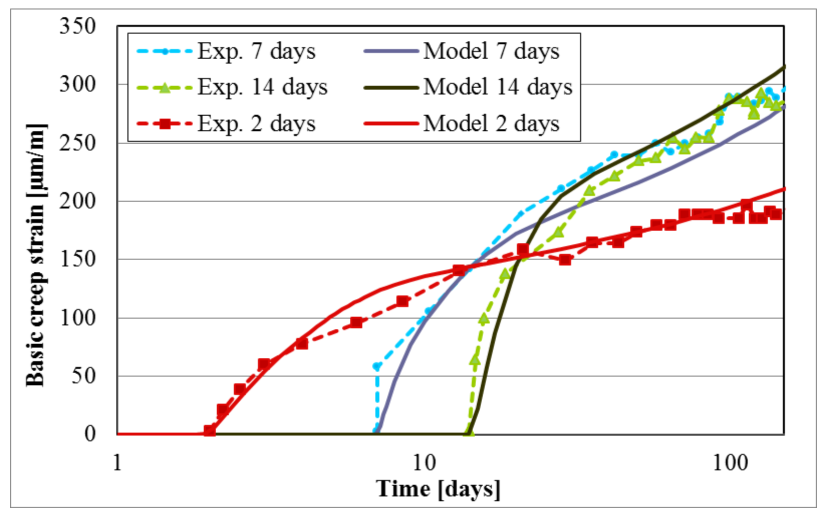

[Honorio et al. under review]

Cracking index

- CI and Probability of cracking as a function of the CI:

$$\mathrm{CI} = \max_{\Omega} \left\langle \frac{\sigma_{ii}(t)}{f_t(t)} \right\rangle_+$$

$$P(CI) = 100 \times \left[1 - \exp\left[-\left(\frac{1}{CI} / 0.92 \right)^{-4.29} \right] \right]$$

The CI obtained from the simulation must be inferior to 54% so that $P(CI) \leq 5\%$

Other criteria existing → B. Craeye (70%); Fairbairn (100%)

[Honorio et al. under review]

Damage model

- Isotropic damage variable D

$$\boldsymbol{\sigma} = (1 - \mathrm{D})\tilde{\boldsymbol{\sigma}}$$

- Equivalent strain

$$\hat{\varepsilon} = \sqrt{\langle \varepsilon_e + \beta \varepsilon_{bc} \rangle_+ : \langle \varepsilon_e + \beta \varepsilon_{bc} \rangle_+}$$

- Coupling between damage and creep

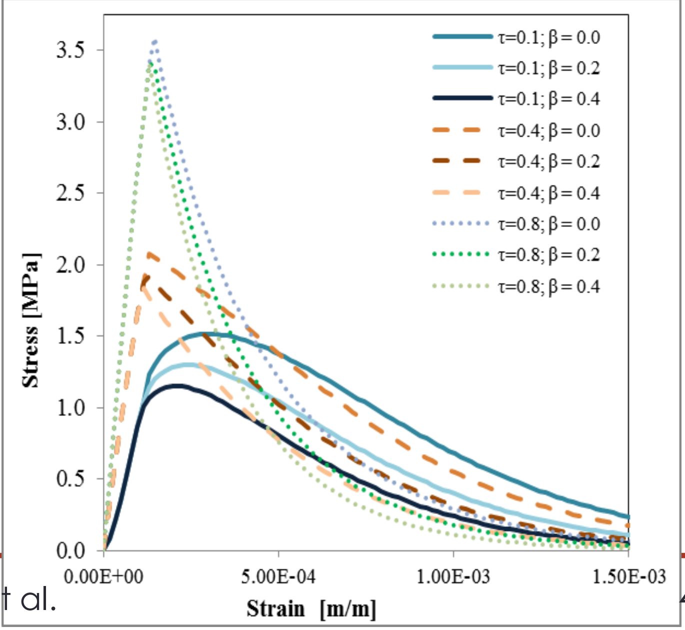

Thermal conditions: Cracking Index

Aug (oscillating) *Aug (constant)* *Nov (oscillating)*

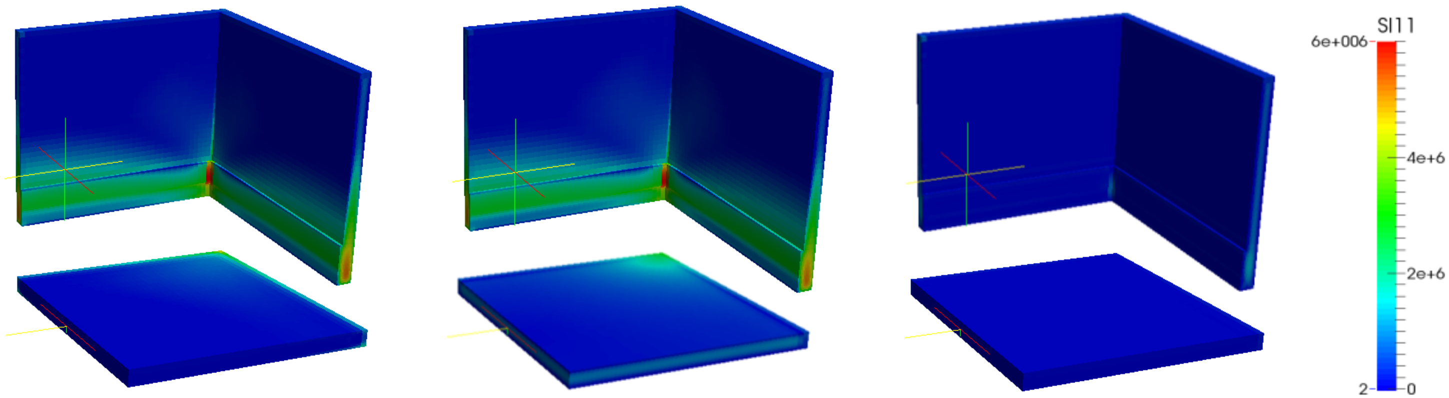

First (maximum) eigenstress according to the 3 thermal boundary conditions

t = 15.08 days

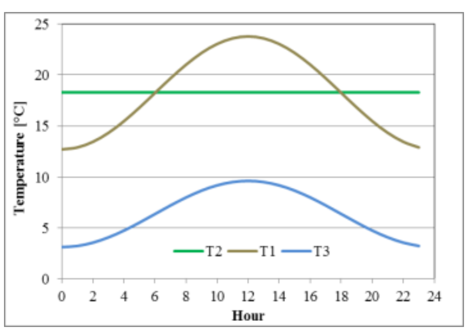

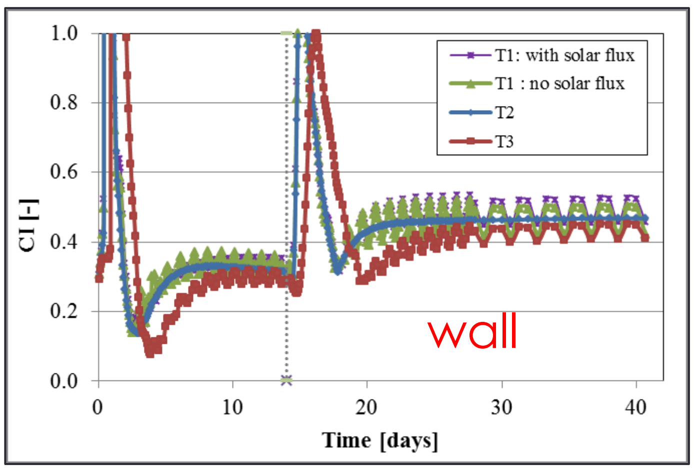

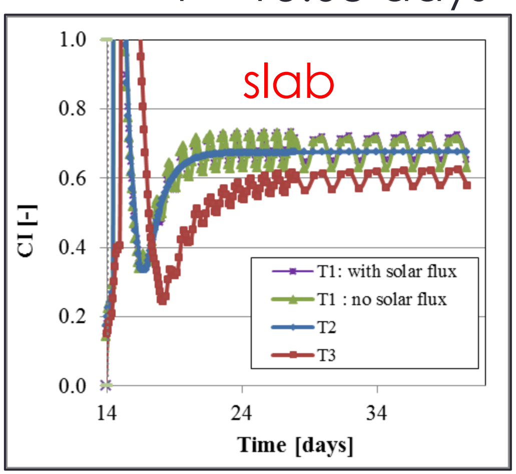

[Honorio et al. under review]

Coupling between creep and damage

August temperatures; t = 15.08 days [Honorio et al. under review]

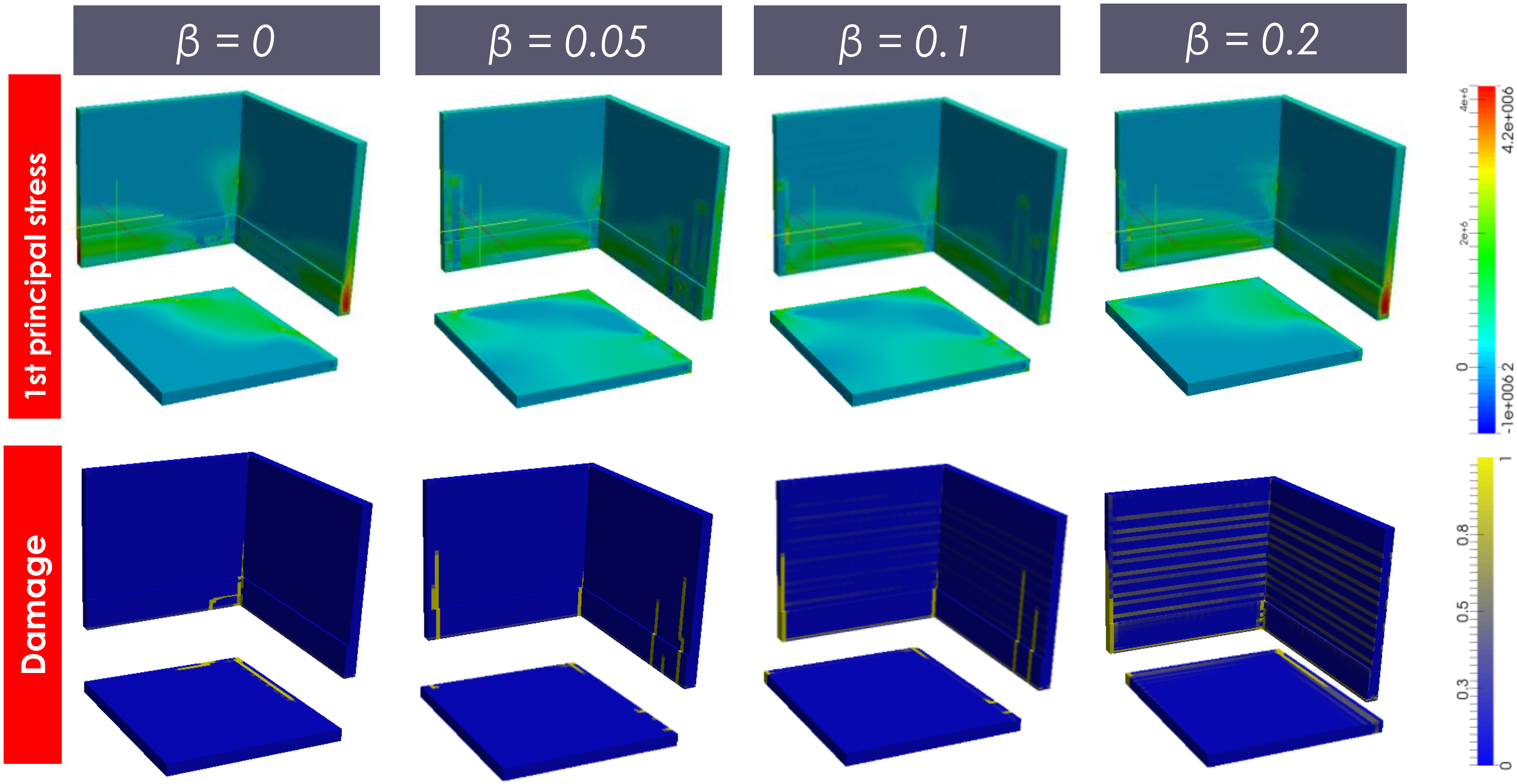

Thermal conditions: Damage and Crack opening

[Mattalah et al. 2009]

Aug (oscillating)

β = 0.1

Damage →

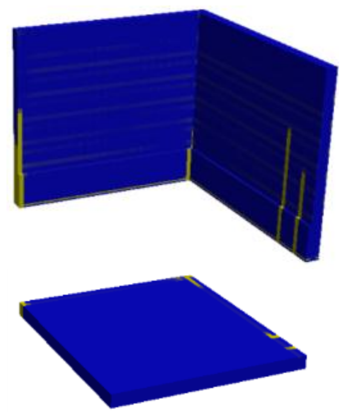

Crack opening

Nov (oscillating)

β = 0.1

Damage →

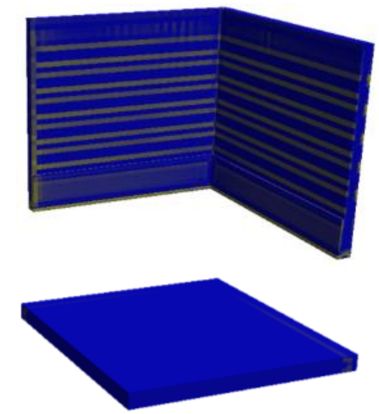

Crack opening

Conclusions

- Phenomenological approaches:
    - It works!
    - *Ad hoc* character: difficult to extrapolate to other scenarios of interest
    - "not very well defined " parameter β
        - Small variations of β can lead to different damage patterns

- Mechanistic approaches to understand the underlying phenomena
    - Justify and improve phenomenological

Multiscale estimation of ageing properties

Concrete at early-age

- Properties evolving at early age (ageing)
- Phenomena taking place at different space and time scales:

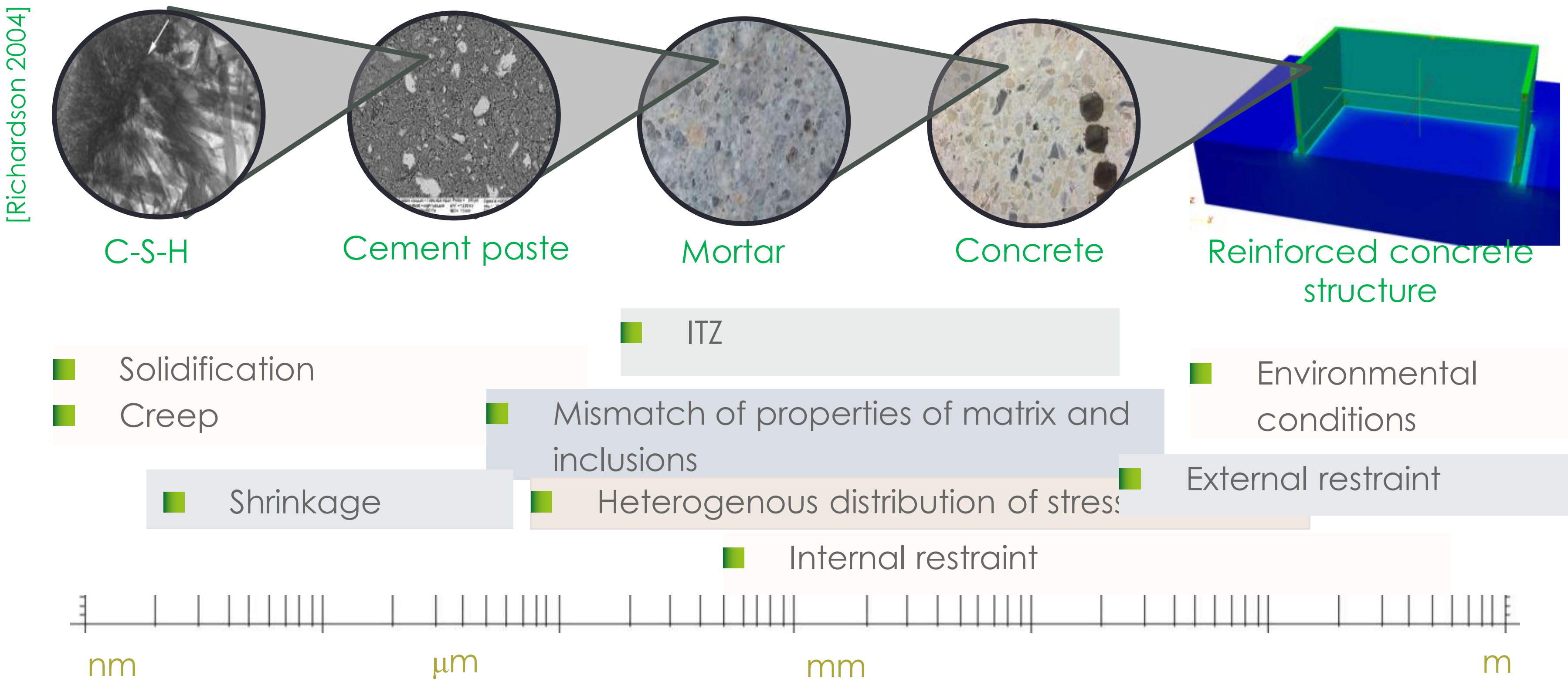

Hydration kinetics

Goals

- Determine the kinetics from the main driving mechanisms
- Estimate the evolution of volume fraction →

Approach

- 2 mechanisms gouverning hydration :
  - **Boundary nucleation and space-filling growth (BNG)**
  - **Diffusion controlled growth (DCG)**

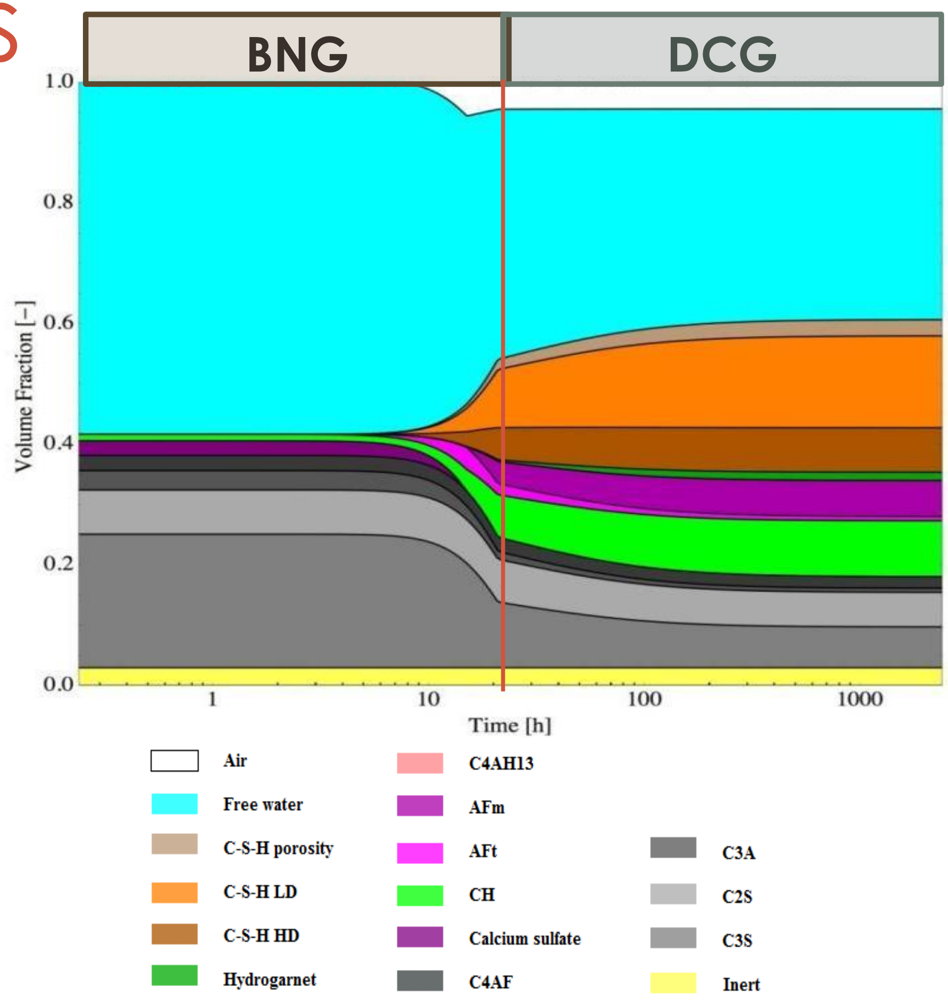

[Honorio et al. 2014c;
Honorio et al. Submitted]

Microstructure representation

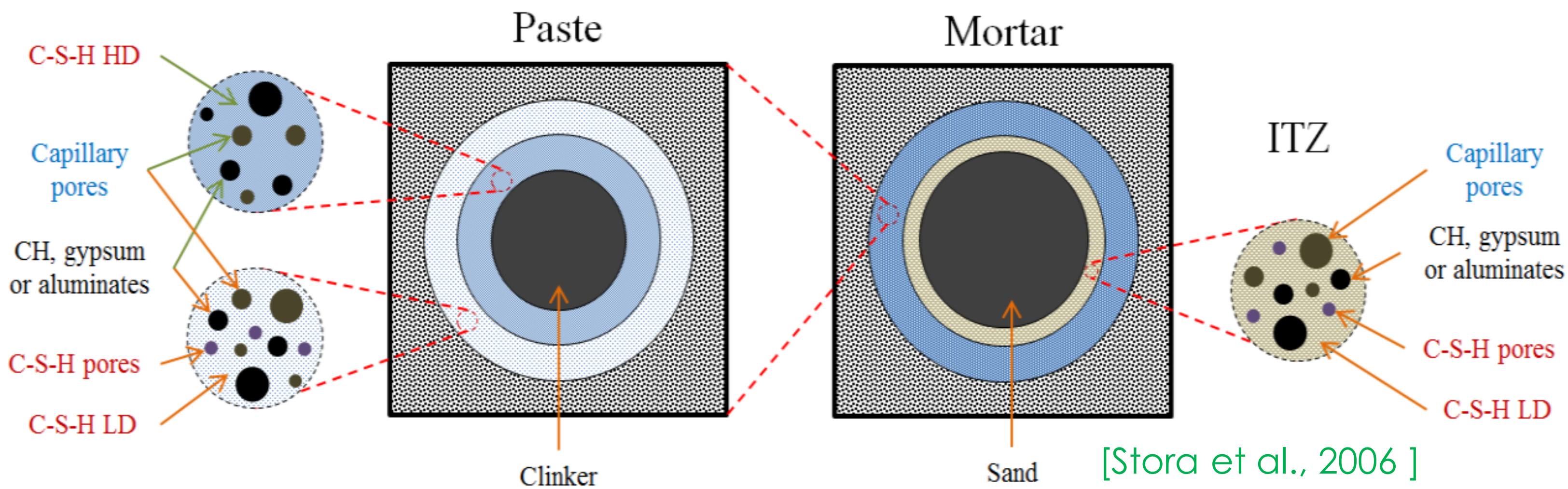

[Stora et al., 2006]

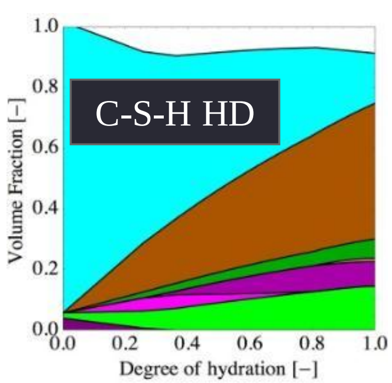

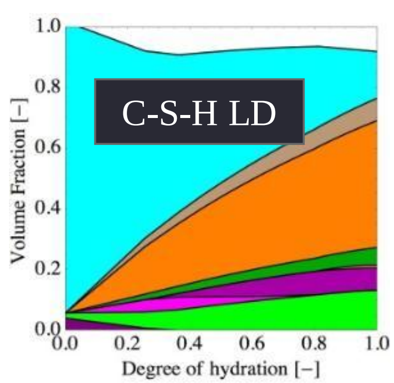

- Repartition of products

[Honorio et al. 2014d]

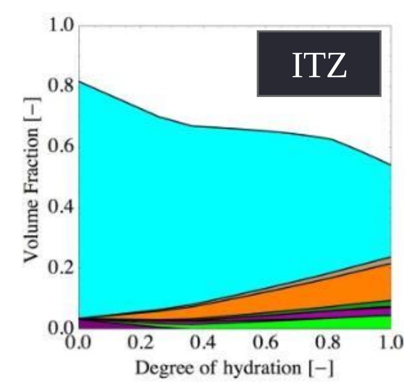

Solutions in elasticity

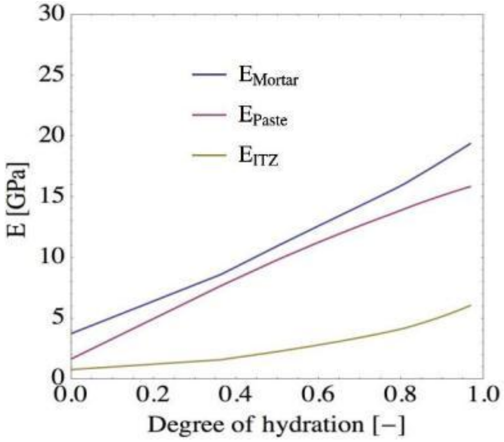

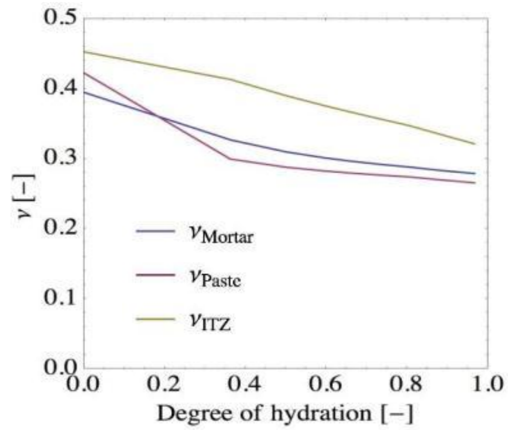

[Honorio et al. 2014d]

Mori-Tanaka

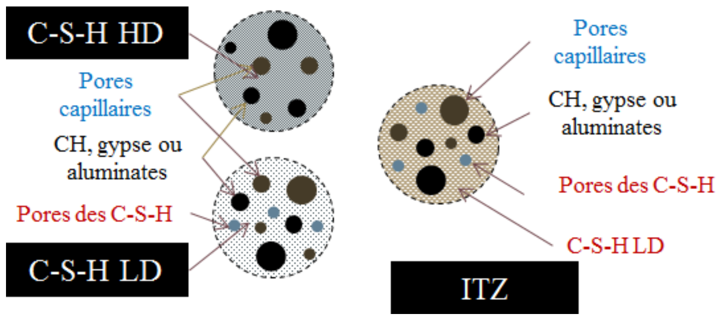

[Mori, Tanaka, 1973]

Generalized Self-Consistent

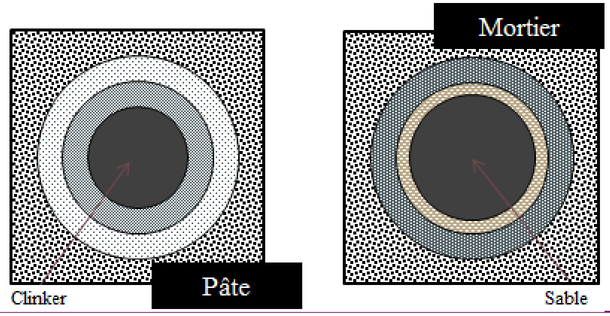

[Christensen, Lo 1979]

Ageing linear viscoelasticity

nanocem

- Volterra Integral operator: → Correspondace principle in a ring (f;+,°)

$$(f \circ g)(t,\tau) \equiv \int_{t'=-\infty}^{t} f(t,t')\, d_{t'} g(t',\tau)$$

[Volterra 1887; Maghous et al. 2003; Sanahuja, 2013]

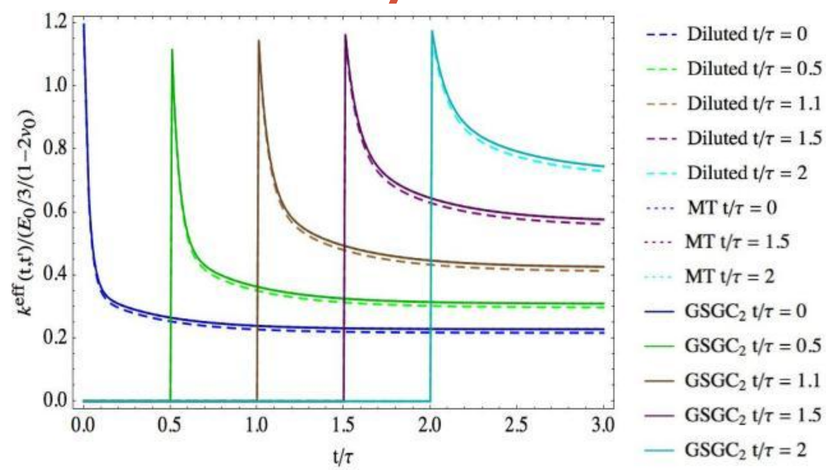

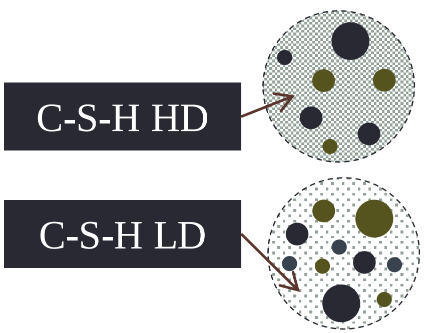

- C-S-H : viscoelastic behavior
  - Intrinsically ageing?
- Solidification → ageing behavior

Mori-Tanaka	Generalized Self-Consistent

Numerical homogeneization

Goals:

- Investigate the influence of the aggregates
- Get local information
- Study more complex microstructures

Elasticité

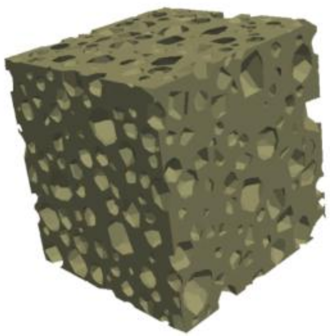

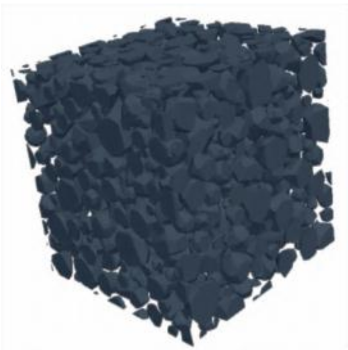

[Bary et al. 2014]

- Matrix : cube (120x120x120)mm^3
- Number of inclusions : 872
    - Equivalent diameters : 8-18 mm

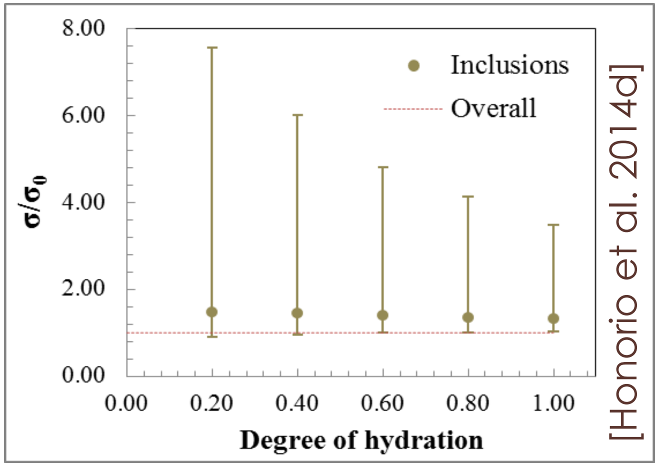

[Honorio et al. 2014d]

Dispersion on stresses within the inclusions

Ageing linear viscoelasticity

Conclusions

- **Different strategies to investigate the behavior at early-age**
  - Mechanistic approach:
    - Some phenomena still need to be better understood (hot point!)
    - Some tools still to be developed

Perspectives

- Contribution to the study of the ageing viscoelastic behavior
  - Influence of the ageing mechanisms at the paste level
  - Influence of the aggregates (shape, PSD, vol. fraction)
  - Mismatch of matrix-inclusions properties
  - Thermal effects

References

Benboudjema F., Torrenti J.M. Early-age behavior of concrete nuclear containments. Nuclear Engineering and Design 2008; 10: 238, p. 12.

Bishnoi, S., Scrivener, K., 2009. Studying nucleation and growth kinetics of alite hydration using µic.pdf. Cem. Concr. Res. 39, 849–860.

Fairbairn, E.M.R., Silvoso, M.M., Toledo Filho, R.D., Alves, J.L.D., Ebecken, N.F.F., 2004. Optimization of mass concrete construction using genetic algorithms. Comput. Struct. 82, 281–299. doi:10.1016/j.compstruc.2003.08.008

Honorio, T. ; Bary, B.; Benboudjema, F. Evaluation of the contribution of boundary and initial conditions in the chemo-thermal analysis of a massive concrete structure. Engineering Structures 80, 2014. [HON14a]

Honorio, T. ; Bary, B.; Benboudjema, F. Factors affecting the thermo-chemo-mechanical behavior of massive concrete structures at early-age: a numerical study. (under review) [HONrev]

Honorio, T. ; Bary, B.; Benboudjema, F; Poyet, S. Modelling hydration kinetics based on boundary nucleation and space-filling growth in a fixed confined zone (submitted) [HONsub]

Honorio, T. ; Bary, B. Benboudjema, F. Estimation of elastic properties of cement based materials at early age based on a combined numerical and analytical multiscale micromechanics approach. CONMOD, Beijing, 2014 [HON14d]

Honorio, T. ; Bary, B. Benboudjema, F. Influence of the particle size distribution on hydration kinetics: a mechanistic analytical approach. CONMOD, Beijing, 2014 [HON14c]

Honorio, T. ; Bary, B. Benboudjema, F. Analysis of the thermo-chemo-mechanical behavior of massive concrete. EURO-C, St Anton am Arlberg, 2014. [HON14b]

Maghous, S., Creus, G.J., 2003. Periodic homogenization in thermoviscoelasticity: case of multilayered media with ageing. Int. J. Solids Struct. 40, 851–870. doi:10.1016/S0020-7683(02)00549-8

Matallah, M., La Borderie, C., Maurel, O., 2010. A practical method to estimate crack openings in concrete structures. Int. J. Numer. Anal. Methods Geomech. 34, 1615–1633. doi:10.1002/nag.876

Sanahuja, J., 2013. Efficient Homogenization of Ageing Creep of Random Media: Application to Solidifying Cementitious Materials. American Society of Civil Engineers, pp. 201–210. doi:10.1061/9780784413111.023

Sanahuja, J., 2013. Effective behavior of ageing linear viscoelastic composites: Homogenization approach. Int. J. Solids Struct. 50, 2846–2856. doi:10.1016/j.ijsolstr.2013.04.023

Stora, E., Bary, B., He, Q.-C., Deville, E., Montarnal, P., 2009. Modelling and simulations of the chemo–mechanical behaviour of leached cement-based materials: Leaching process and induced loss of stiffness. Cem. Concr. Res. 39, 763–772. doi:10.1016/j.cemconres.2009.05.010

Tennis, P.D., Jennings, H.M., 2000. A model for two types of calcium silicate hydrate in the microstructure of Portland cement pastes. Cem. Concr. Res. 30, 855–863.

Ulm F. J., Coussy O., What is a massive concrete structure at early ages. Journal of Engineering Mechanics 2001 ; 35 : 31-2, p.4295-4311.

Van Breugel, K.; Koenders, E:A:B. Solar radiation. Report, Improved Production of Advanced Concrete Structures (IPACS), Luleå University of Technology, ISBN 91-89580-31-1, 2001.

Acknowlegments

This present work has been performed as part of the project on disposal of LILW-SL that is carried out by ONDRAF/NIRAS, the Belgian Agency for Radioactive Waste and enriched Fissile Materials

Is there more risk of cracking with today’s cements than with yesterday’s cements?

Laurent IZORET[1]
[1]ATILH (Technical Association of French Cement Industry)

ATILH
ASSOCIATION TECHNIQUE DE
L'INDUSTRIE DES LIANTS HYDRAULIQUES

- **Short reminder: By itself, cement shrinkage does not implies accidental cracking…**
  - **Influencing factors and trends of variation**
    - ✓ Clinker mineralogy
    - ✓ Fineness of grinding
    - ✓ Nature of main constituant other than clinker
    - ✓ Alcalies
  - **Shrinkage evolution since 25 years**
    - ✓ Since 1986 (1) : ATILH Round Robin test (cement)
    - ✓ Since 1986 (2) : Cement database (manufacturer)
    - ✓ Depuis 2006 (mesures tous les ans)

Cement shrinkage

Influencing factors and trend of variations

Shrinkage measurement

- CEN mortar; w/c = 0.5
- Prisms 4x4x16 cm
- Curing: 20° C/50% H.R.
- R3,7, 14, 28, .. days

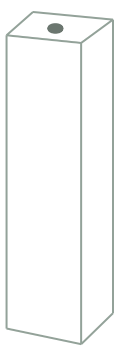

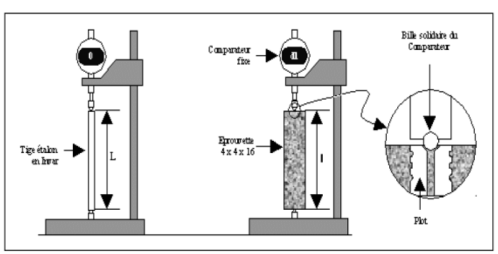

- What do we measure?

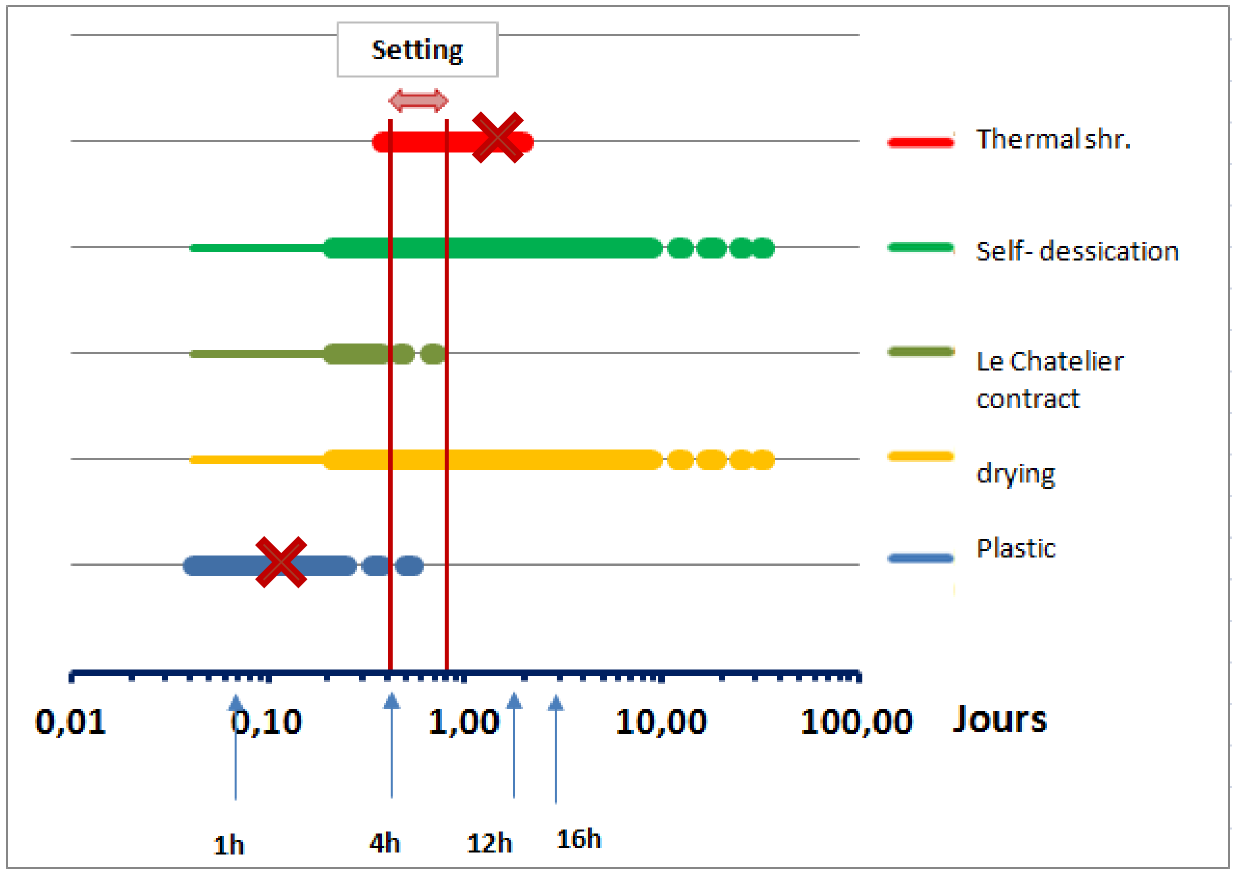

From Venuat (1968)

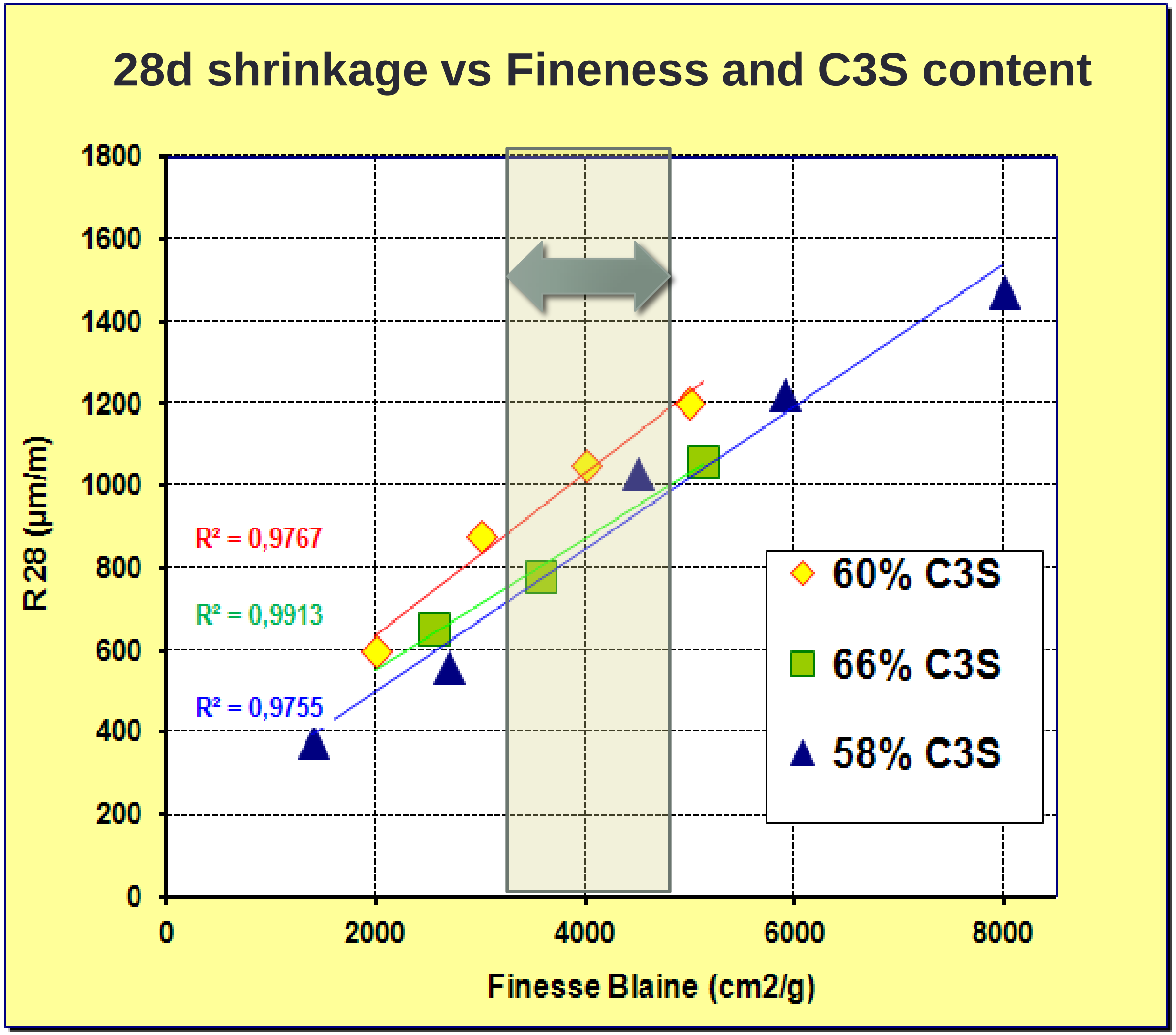

From Cement database (cement manufacturer)

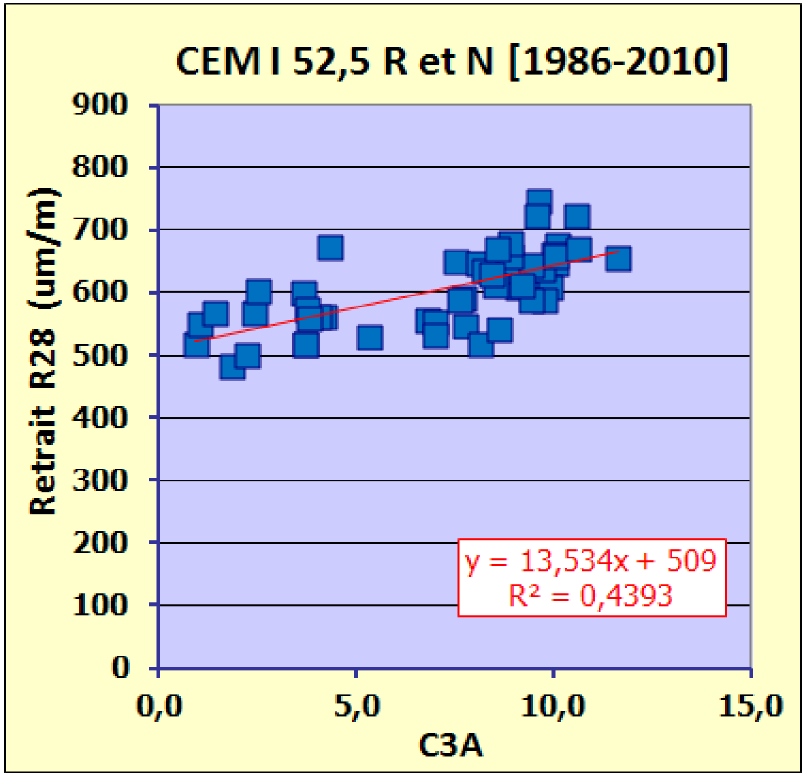

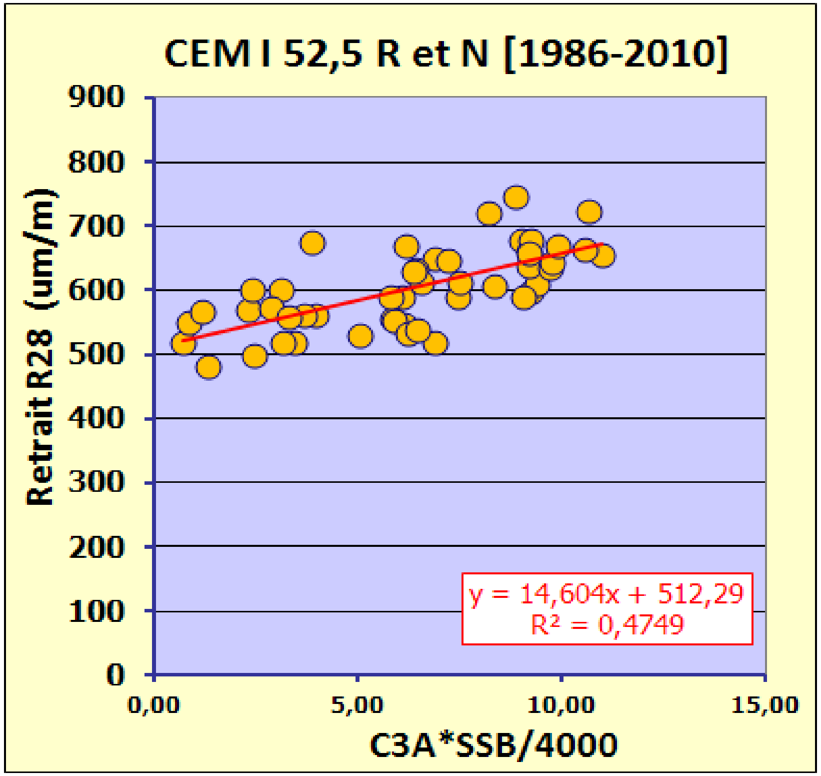

Tentative modelisation

Shrinkage =
- 0,012aC3S(t)*[%C3S] - 0,07aC2S(t)*[%C2S] -2,256aC3A(t)*[%C3A] + 0,859aC4AF(t)*[%C4AF]

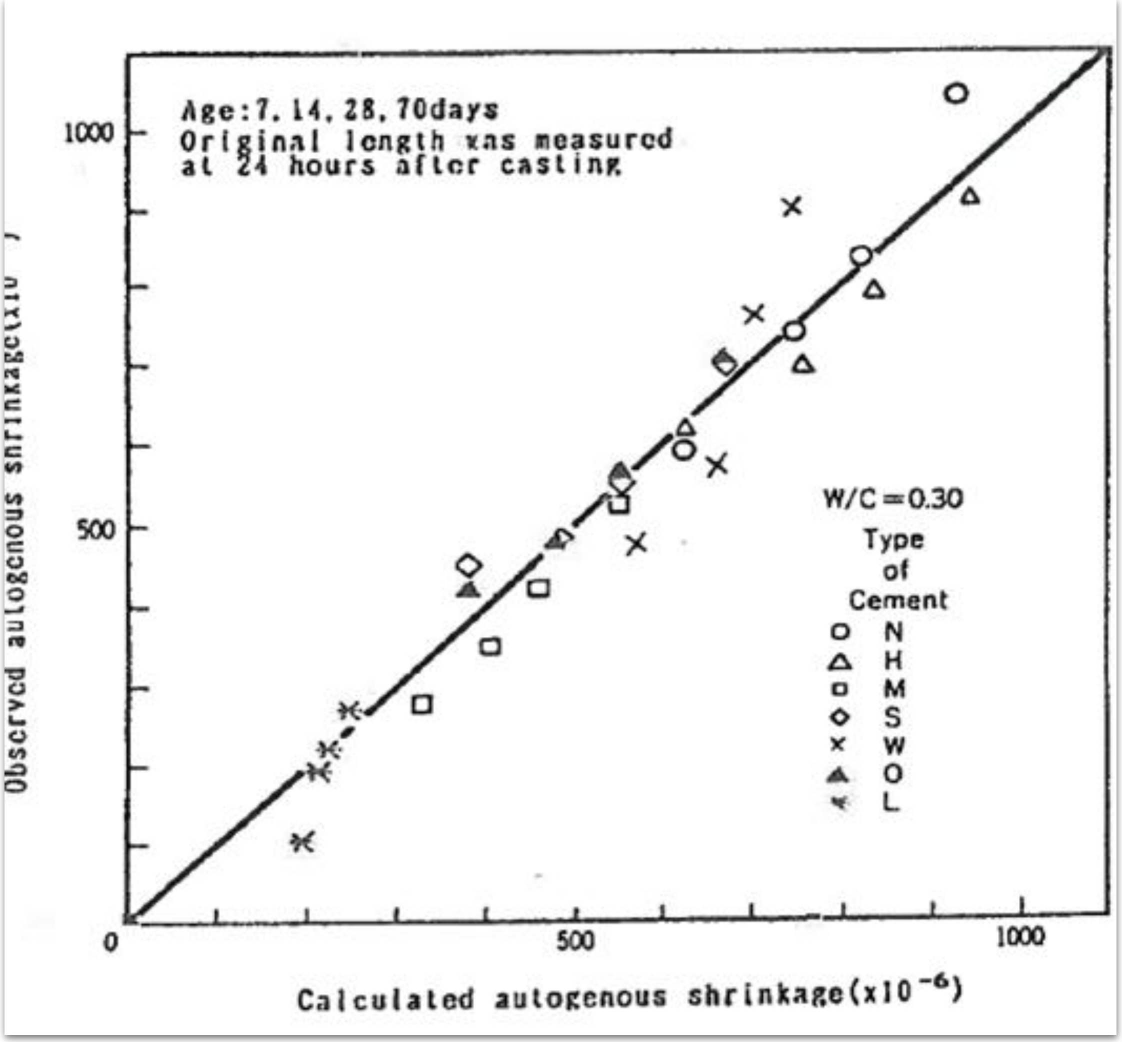

From Venuat (1968)

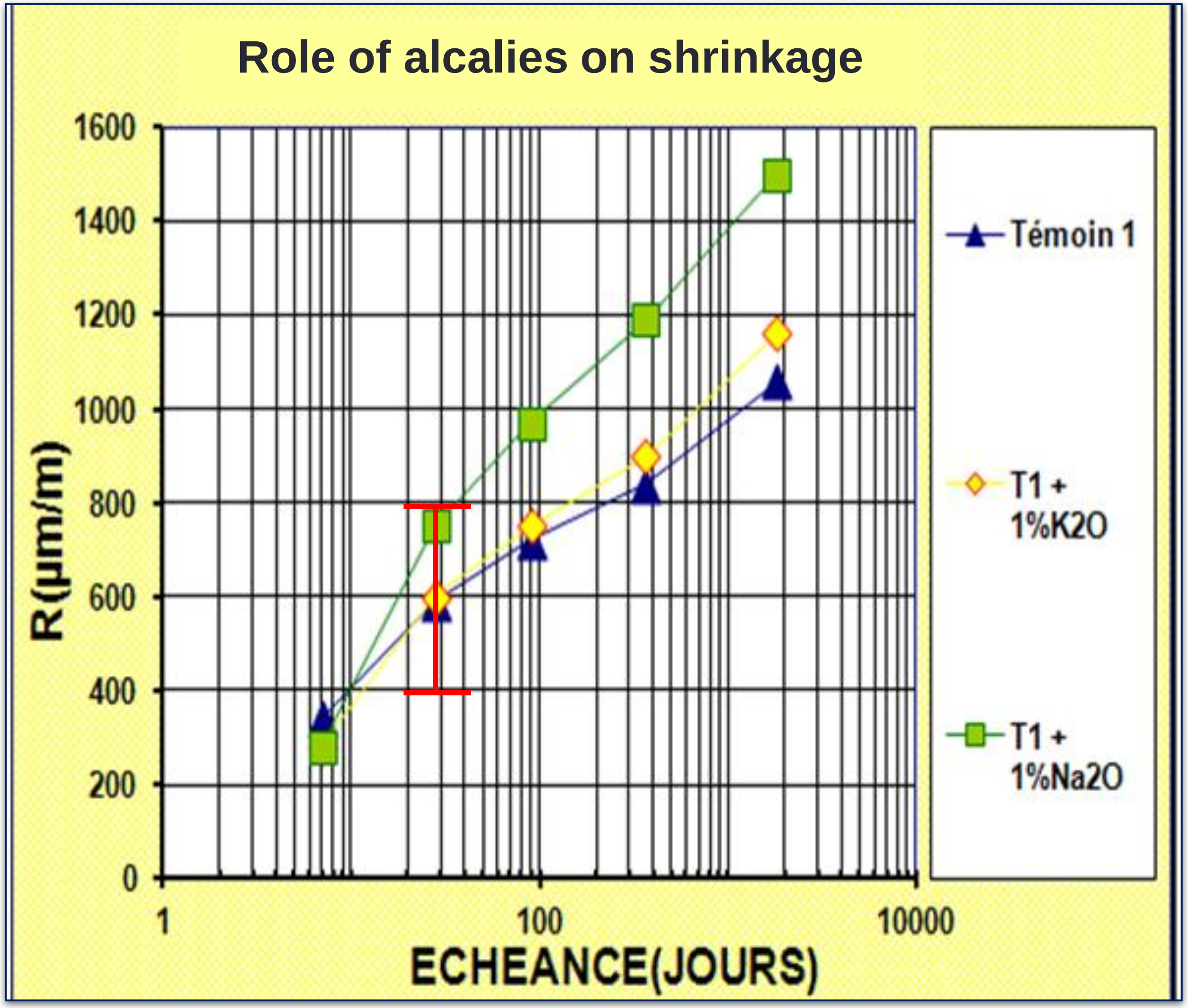

From Venuat (1968)

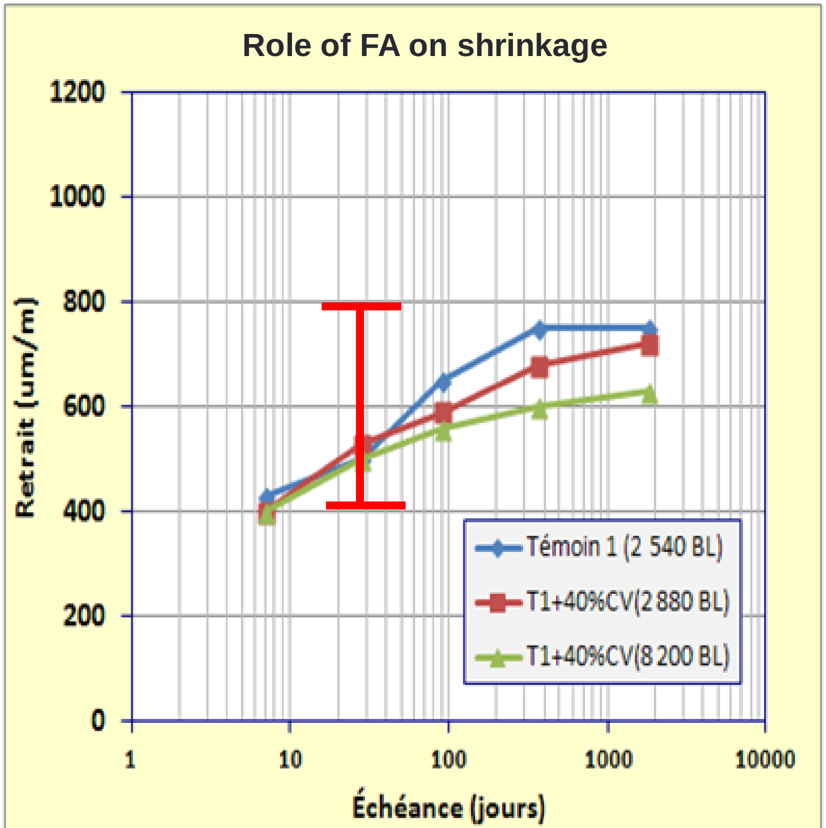

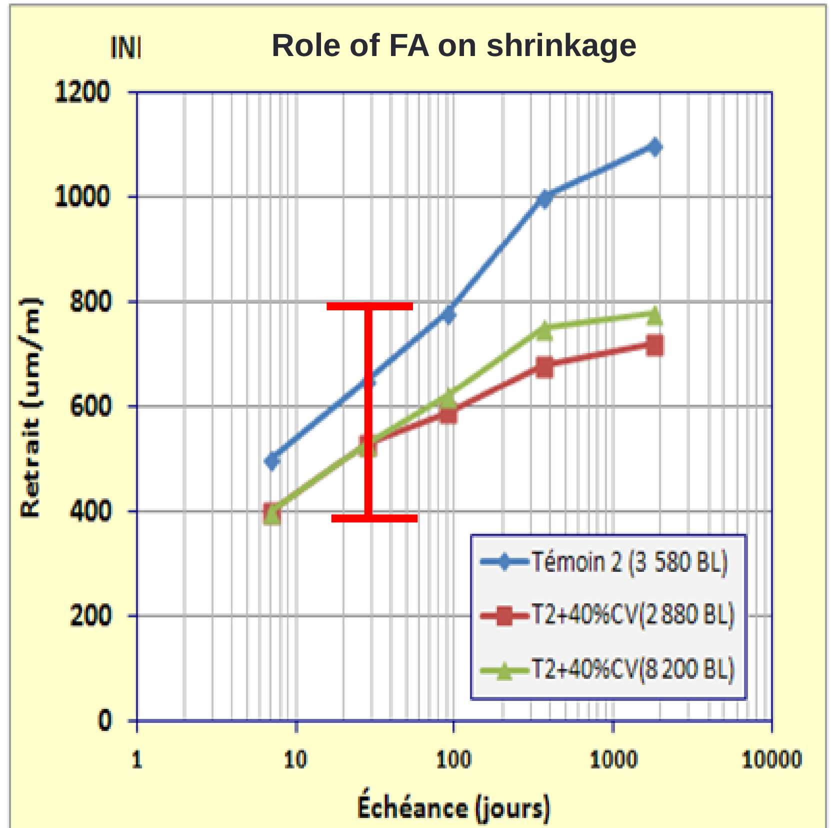

From Cement database (cement manufacturer)

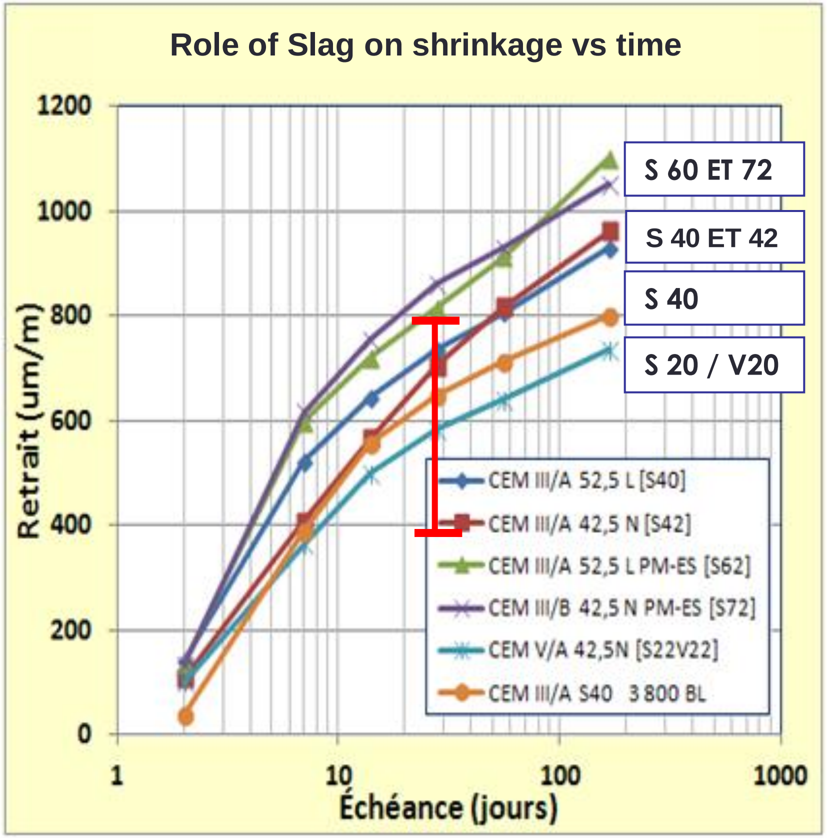

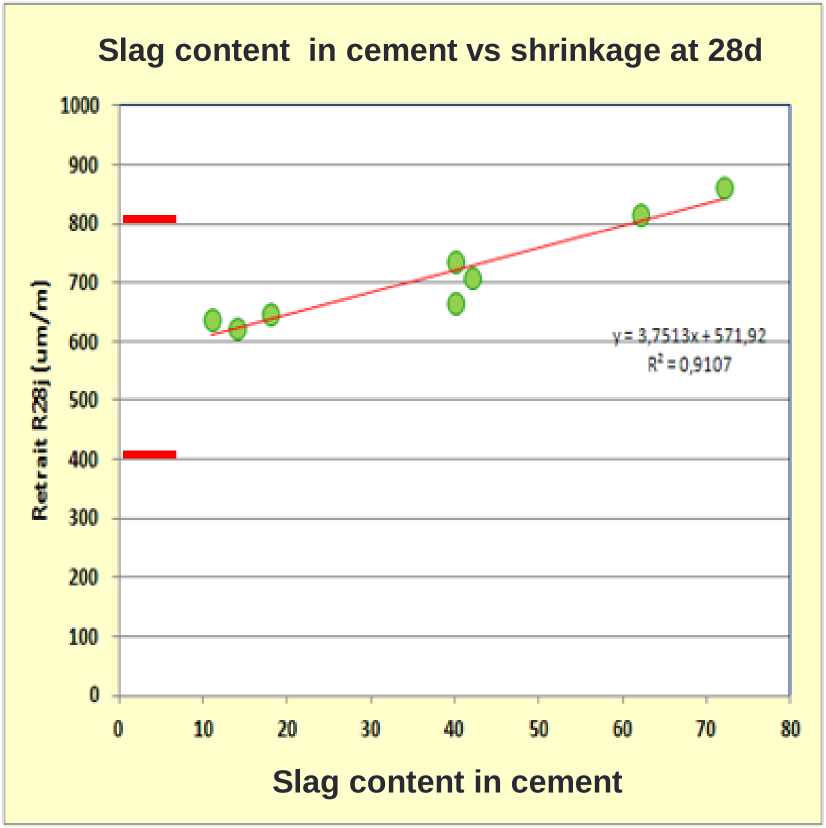

First conclusion

At 28 days, shrinkage remains influenced by the following parameters:

- Cement C3A content and C3S content in a lesser extend
- Fineness of gringing
- Alcalis concentration, e.g. Na2O
- Nature of main constituant other than clinker (Slag requiring the most attention…)
- Range from 400 to 800 µm/m

Are theses characteristics constant over time?

Cement shrinkage

Is there an evolutionary trend?

Is there a correlation with manufacturing conditions?

Alternative Fuels in cement Kilns (F): Evolutionary trend

→Liquids
- Water-solvants
- Used oils

→Solids
- Farines animales
- Old tyres
- Solid Wastes (papers, cartons, plastics, …)

→Trend
- Increasing1986- 2001
- Stability since 2001

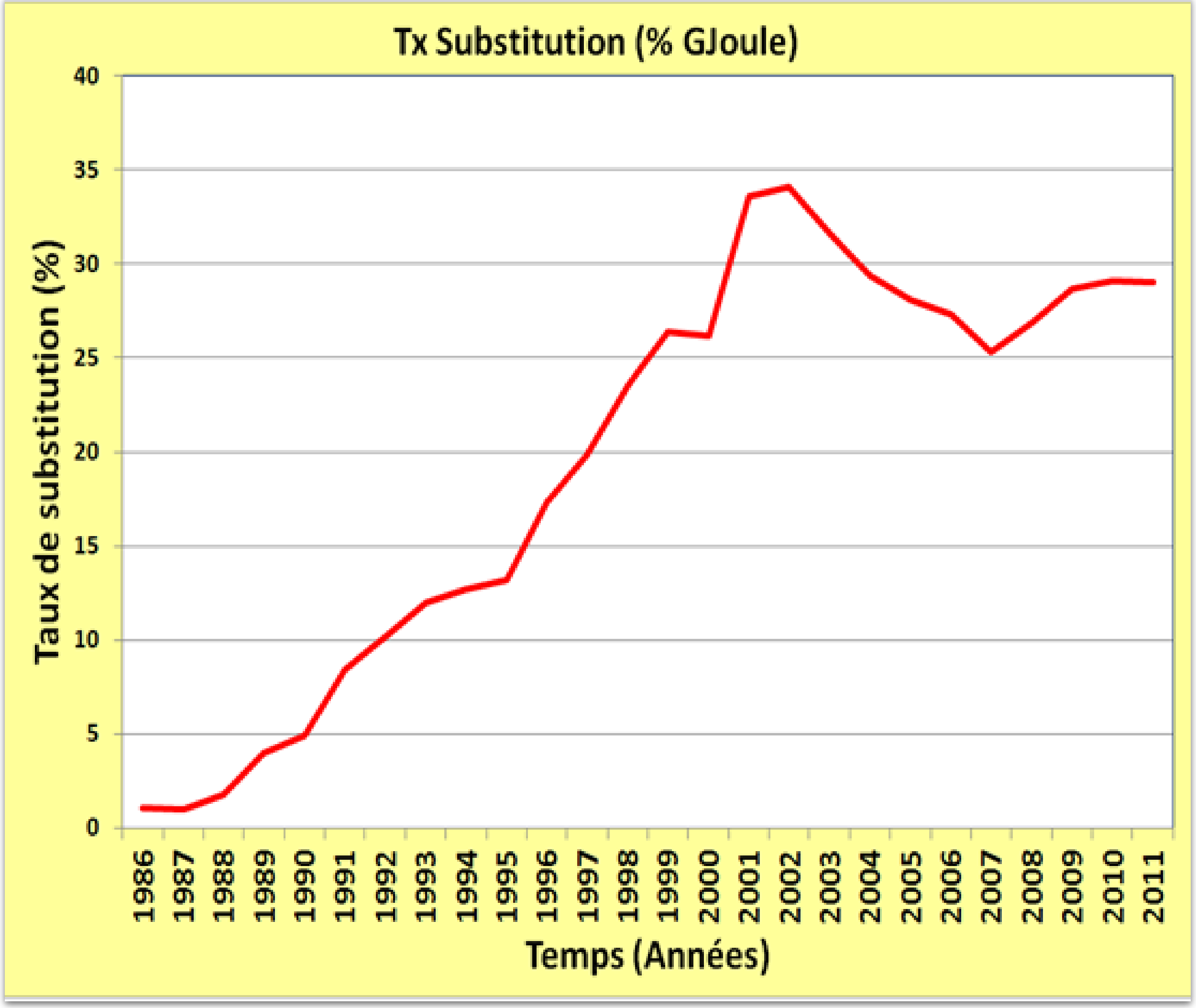

ATILH Data Base Cement Annual Round Robin Test

- Approx 250 Labs over the world
- Between 180 to 220 validated results per year
- 1 Cement type per year

→Flat trend

→No relationship to alternative fuels

→Fluctuations due to cement types

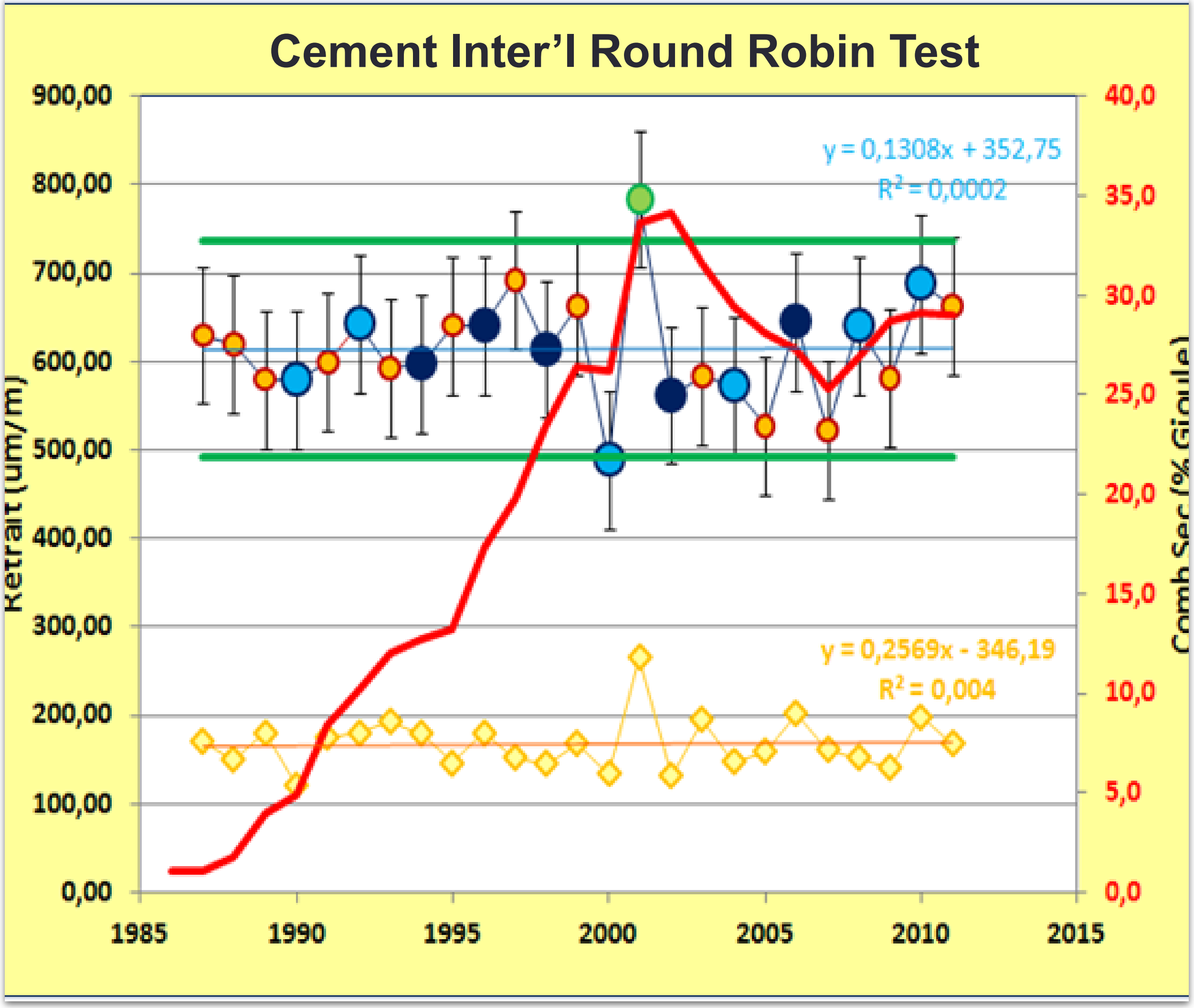

Second conclusion

From one database type:

- 28 days shrinkage ranges from 400 to 800 µm/m depending more on cement type than alternative fuels substtution rate in the cement kilns.
- Early age shrinkage (3d) remains limited between 100 to 200 µm/m with low scattering.
- **Clue**: no trend since 25 years over several cement types

Since 1986 (2): cement data base

From a second database type (cement manufacturer):

- About 8 000 measurements over 25 years
- Two scales of time et two frequences of report
  - √ For a given cement type, between 2 to 6 measurements/ Y.
  - √ 1986-2010 (report frequency every 5 years)
  - √ 2006-2012 (report frequency every year)

Cement Data Base
(Cement Manufacturers)

- Period 986 – 2011
- Report every 5 years
- CEM I 52.5R & N

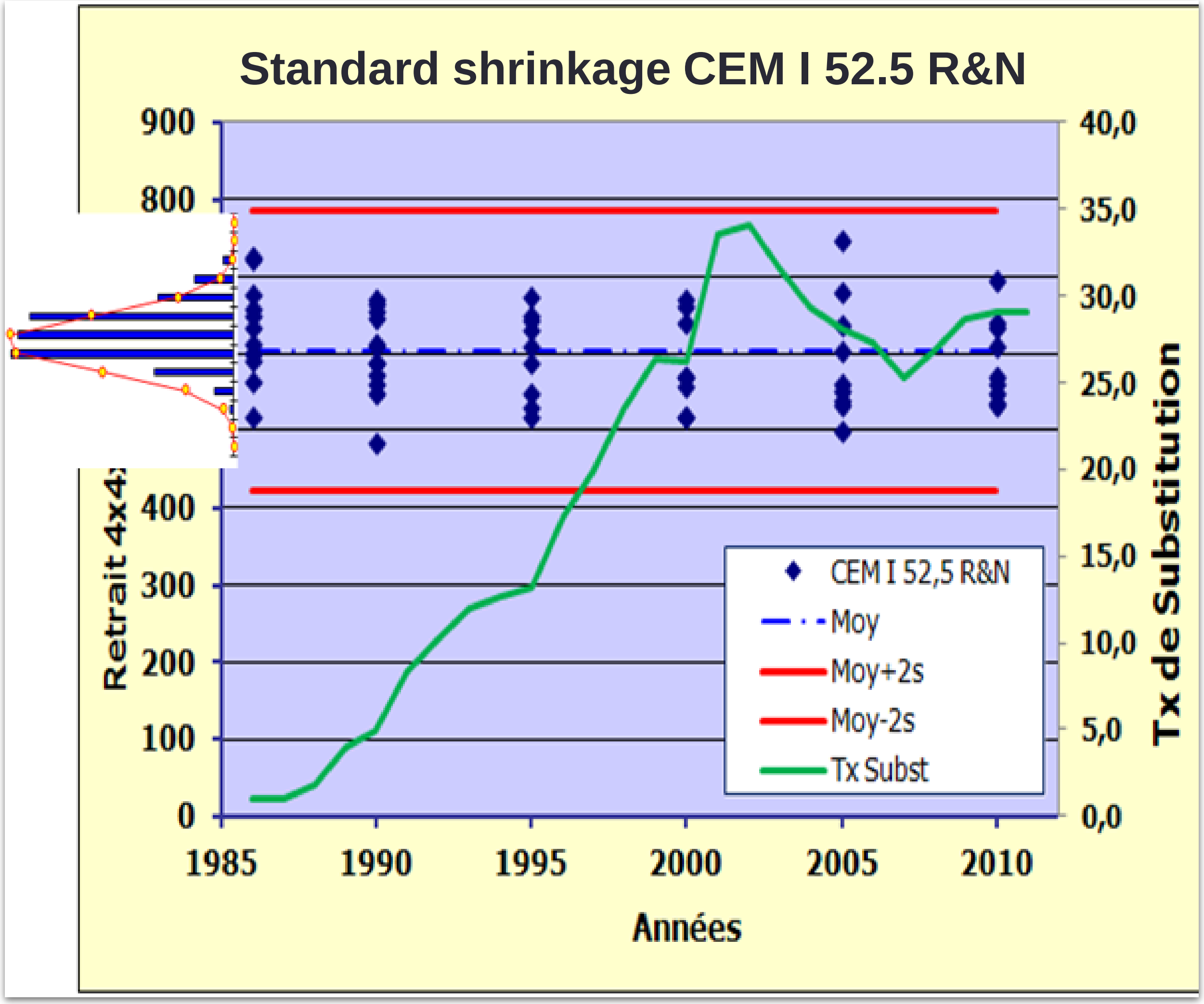

Cement Data Base
(Cement Manufacturers)

- Period 986 – 2011
- Report every 5 years
- CEM I 52.5R & N

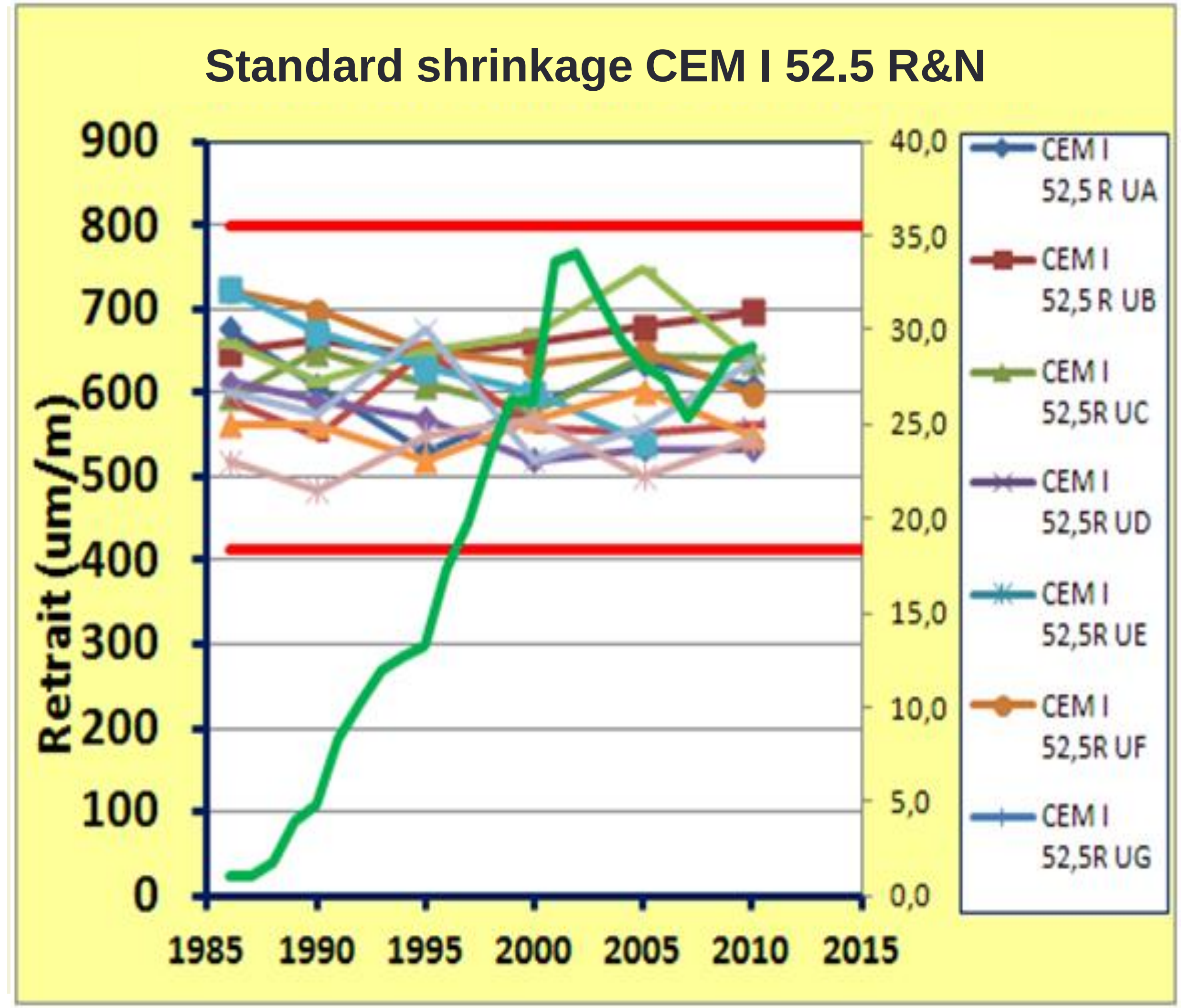

Cement Data Base
(Cement Manufacturers)

- Period 1986 – 2011
- Report every 5 years
- CEM I 52.5R

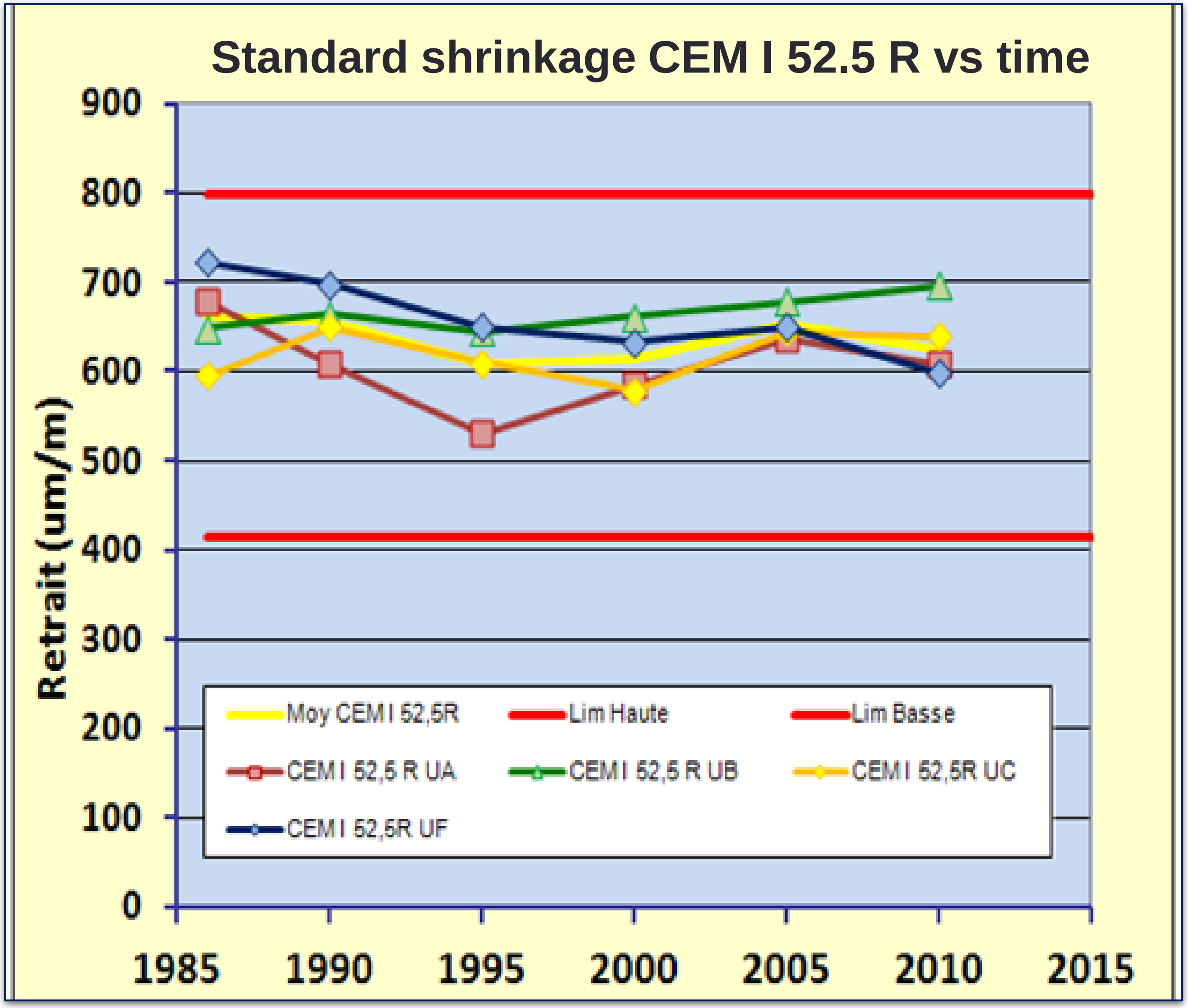

Cement Data Base
(Cement Manufacturers)

- Period 1986 – 2011
- Report every 5 years
- CEM I 52.5R

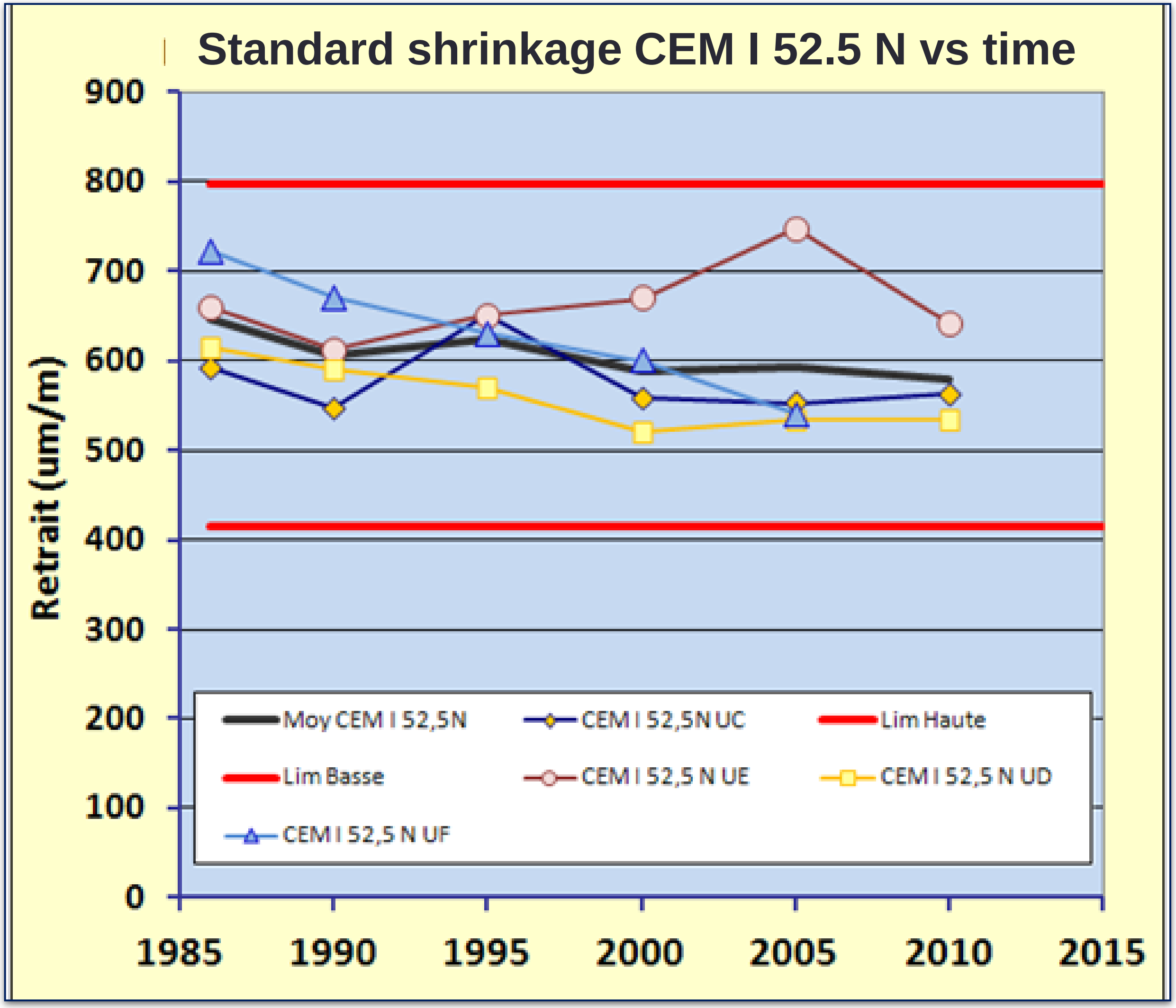

Cement Data Base
(Cement Manufacturers)

- Period 1986 – 2011
- Report every 5 years
- CEM I 52.5 SR

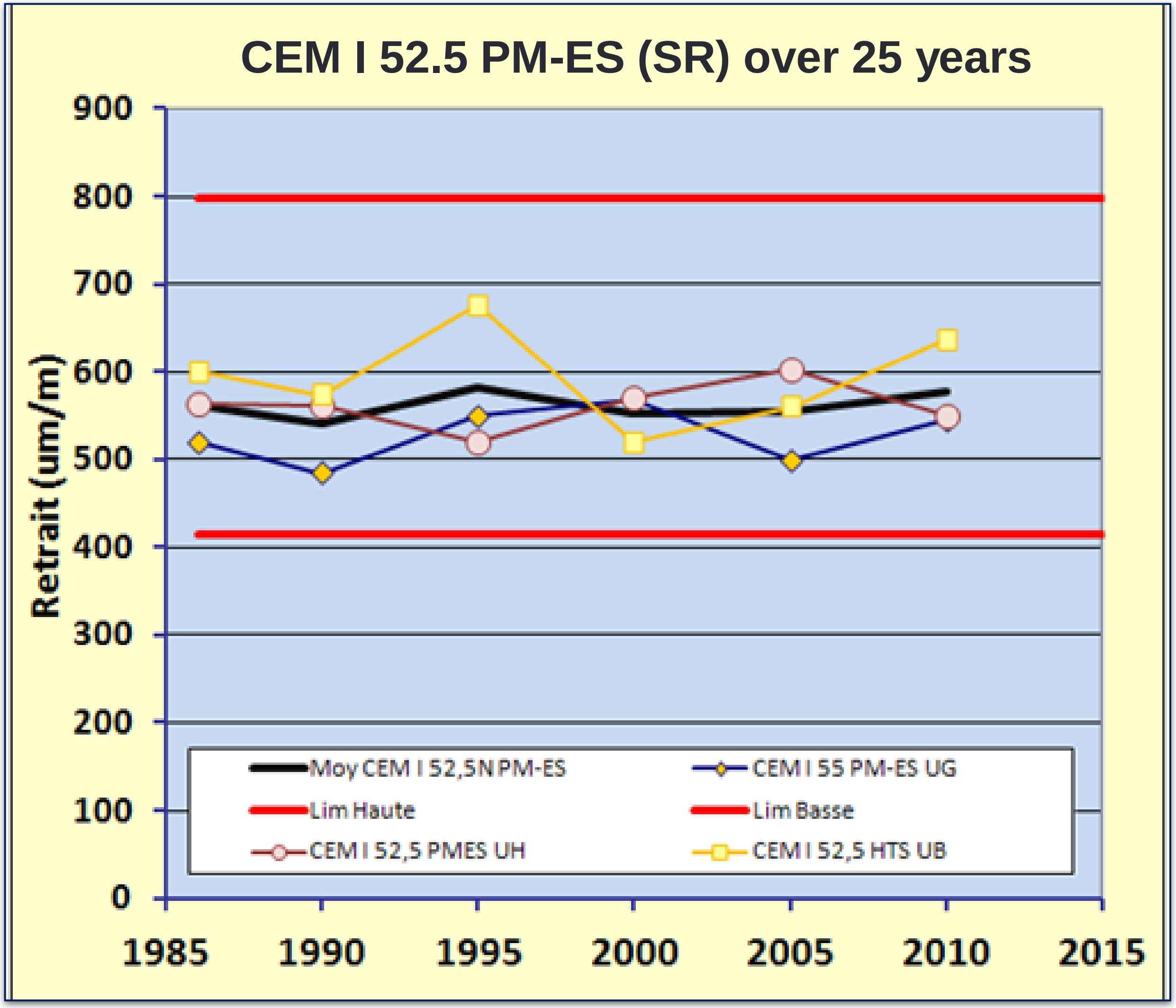

Cement Data Base
(Cement Manufacturers)

- Period 2006-2012
- Report every year
- CEM I 52.5N

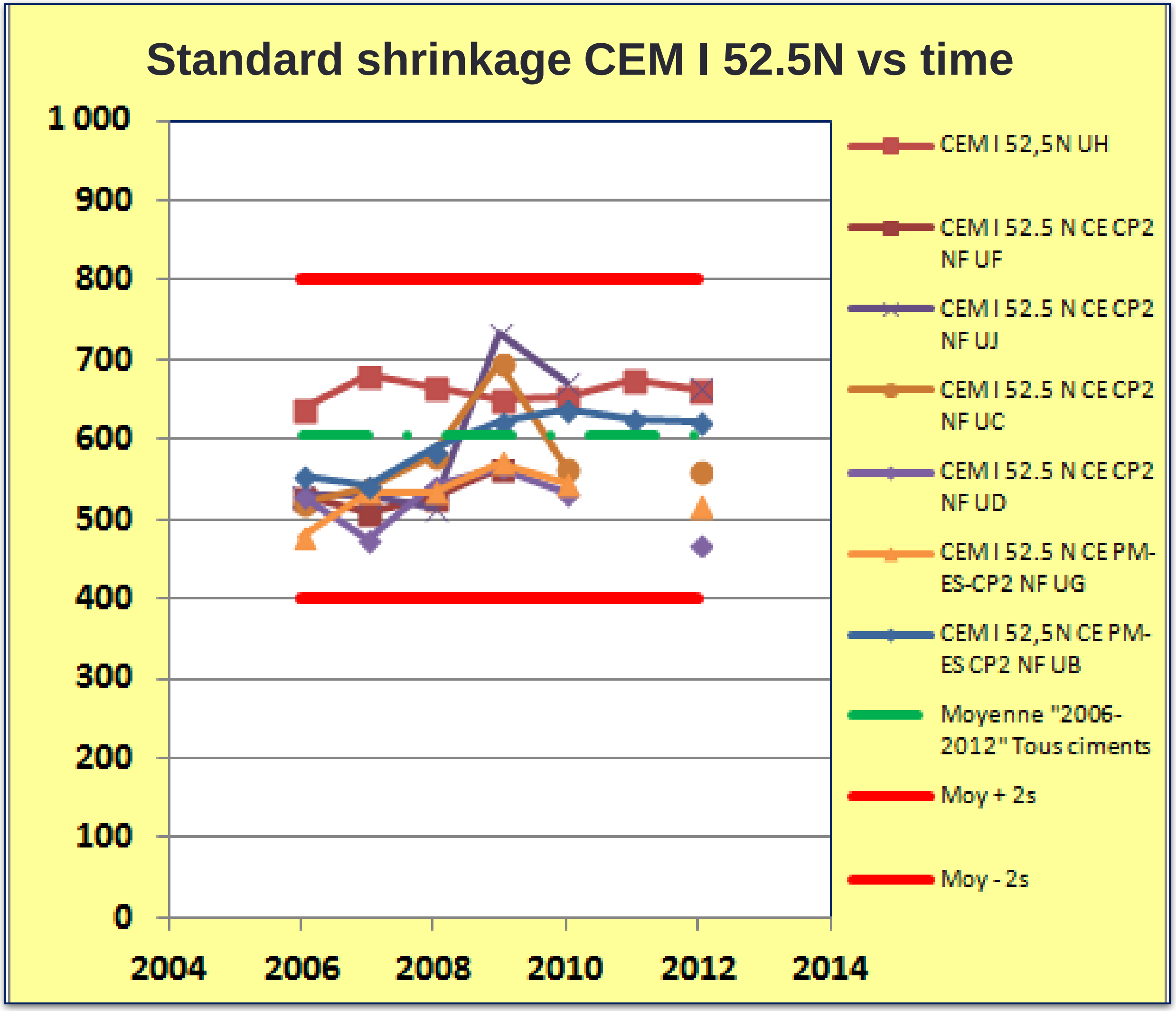

Cement Data Base
(Cement Manufacturers)

- Period 2006-2012
- Report every year
- CEM III/A or B

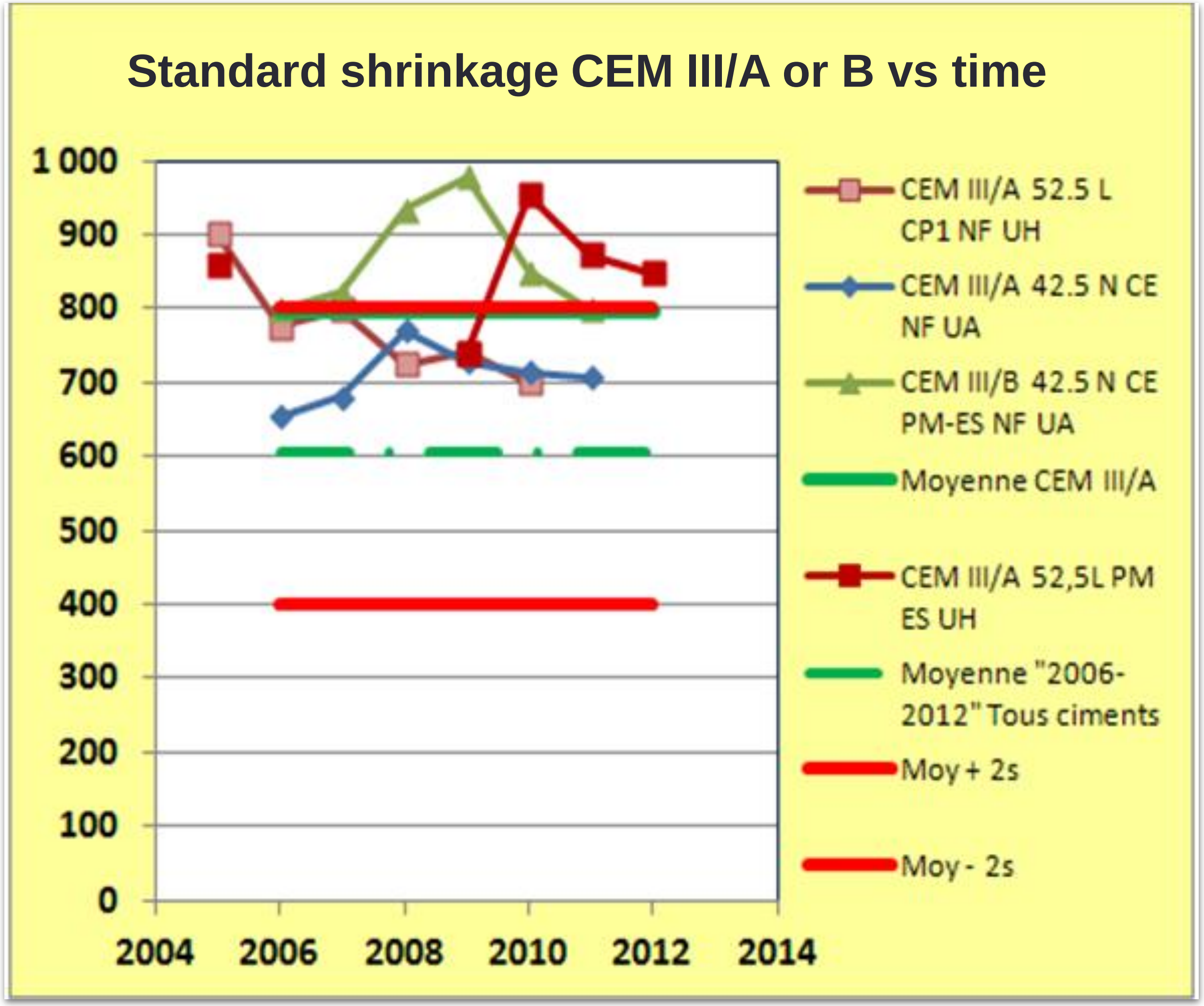

Cement Data Base
(Cement Manufacturers)

- Period 2006-2012
- Report every year
- CEM II/A-S 42.5

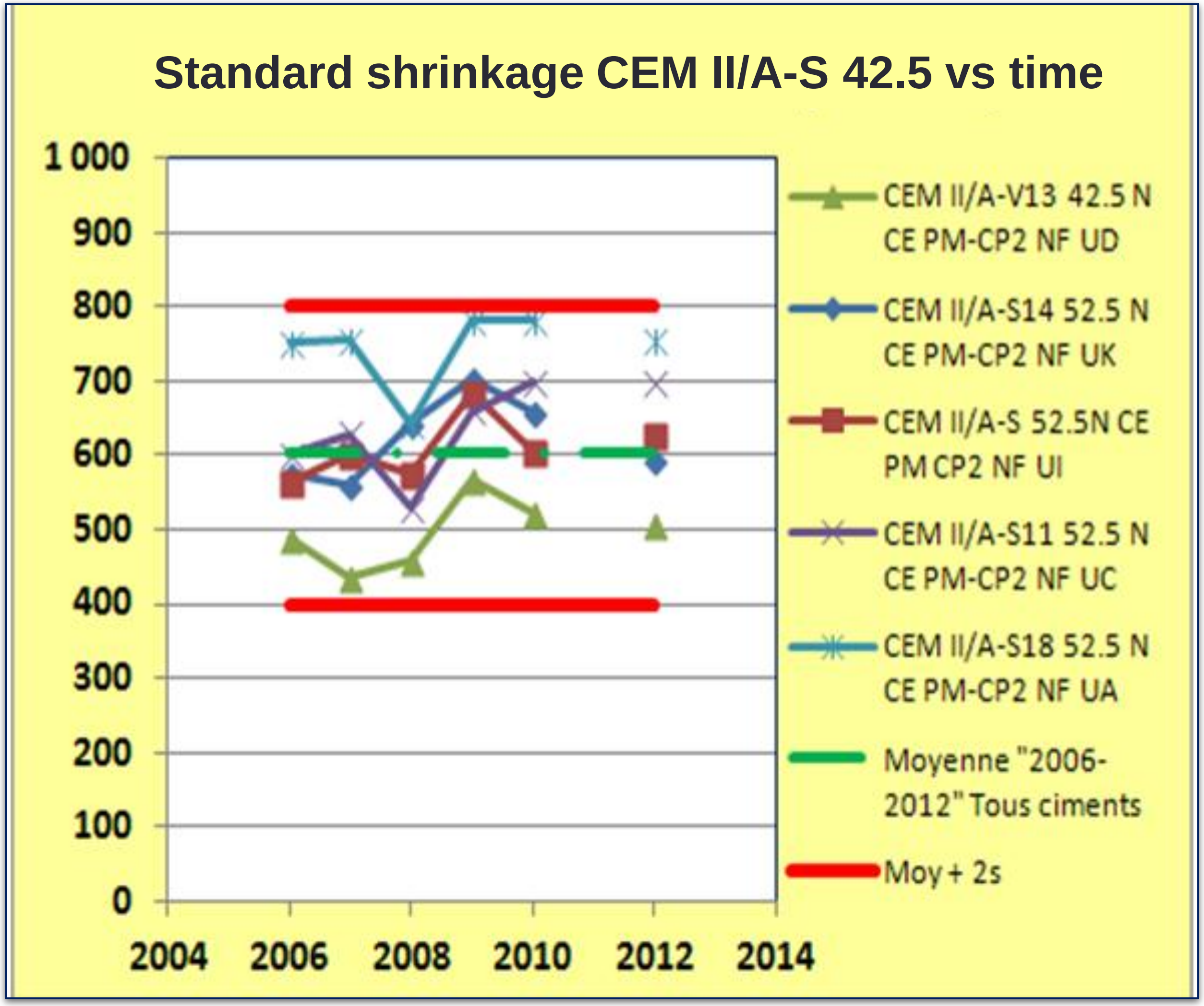

Cement Data Base
(Cement Manufacturers)

- Period 2006-2013
- Report every year
- CEM I 52.5R

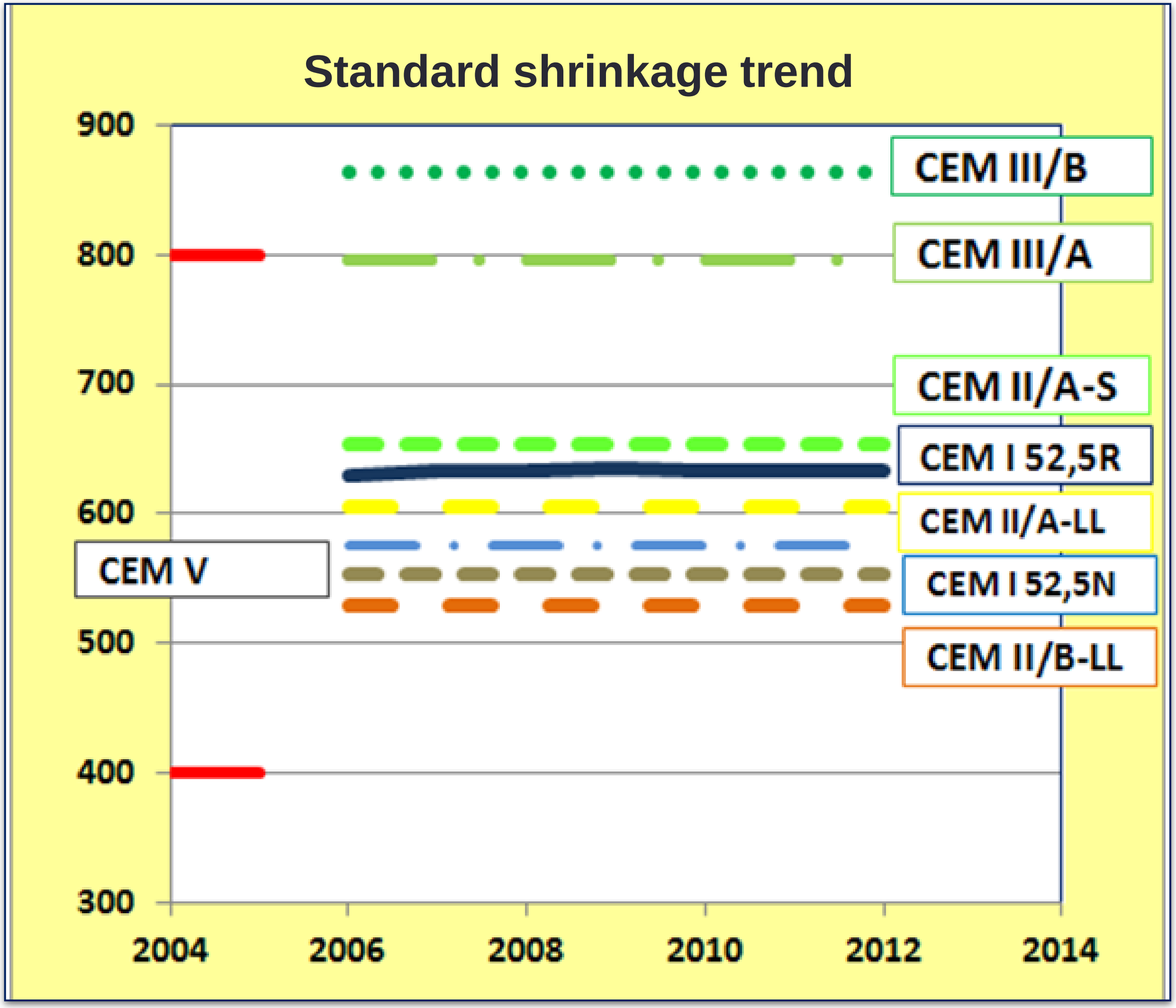

Third and final conclusion

From a second database type (cement manufacturer):

- **All cement types are not equivalent**
  - ✓ by mean of grinding fineness
  - ✓ by mean of the nature of main constituent
    - Low clinker content cements can vary depending on Slag, Fly ash and Limestone
    - Fluctuation in shrinkage may come from main constituent other than clinker e.g. slag
- **Flat trend from shrinkage evolution over 25 years**
- **The risk of cracking due to cement contribution hasn't increased in 25 years**

References

- **Venuat M.**, "Influence du ciment sur le retrait hydraulique après prise". Publication technique du Centre d'étude et de recherches sur les liants hydrauliques (CERILH), n° 189, mai 1968. (in French)